

Sponsored by: The Minerals, Metals and Materials Society, TMS Electronic, Magnetic, and Photonic Materials Division, TMS: Nanomaterials Committee

Program Organizers: Jiyoung Kim, Univ of Texas; David Stollberg, Georgia Tech Research Institute; Seong Jin Koh, University of Texas at Arlington; Nitin Chopra, The University of Alabama; Suveen Mathaudhu, U.S. Army Research Office

Wednesday AM	Room: 8
March 2, 2011	Location: San Diego Conv. Ctr

Session Chair: Suveen Mathaudhu, U.S. Army Research Laboratory

8:30 AM Introductory Comments

8:35 AM Invited

SPD-Processed Nanostructured Metals for Innovative Applications: *Ruslan Valiev*¹; Georgy Raab¹; Maxim Murashkin¹; Nail Zaripov¹; ¹Ufa State Aviation Technical University

Among main requirements for application of nanostructured metals and alloys as advanced functional and structural nanomaterials, one should emphasize their bulk form (rods, wires or sheets) for fabrication of different articles and parts. Secondly, nanometals should possess enhanced properties. In the paper we report new results of our R&D works showing that the use of severe plastic deformation (SPD) techniques allows one to meet these requirements. For this goal equal-channel angular pressing (ECAP) and its recent modifications were used, which allowed to produce rods and wires out of a number of commercial alloys. By changing SPD processing regimes we could also control the nanostructural features of the processed materials. The report also provides examples of successful realization of these principles applied to several commercial Al and Ti alloys and steels for enhancement of their properties. The first pilot articles for innovative applications in medicine and engineering are presented as well.

9:05 AM Invited

Understanding the Role of Interfaces in the Deformation of Lamellar Nanocomposites Fabricated via Severe Plastic Deformation Techniques: *Irene Beyerlein*¹; Jian Wang¹; Ruifeng Zhang¹; Nhon Vo²; Pascal Bellon²; Robert Averback²; Anthony Rollett³; Nathan Mara¹; ¹Los Alamos National Laboratory; ²University of Illinois; ³Carnegie Mellon University

In this work, we study the evolution and role of hetero-phase interfaces in slip and twinning in nanolayered composites during severe plastic deformation. The composite systems studied consisted of two immiscible metals, Ag-Cu or Cu-Nb, wherein the individual phases are submicron to nanometer in scale, and the interfacial content is high. Through a variety of modeling techniques, we have found that changes in the texture and interface crystallography after SPD can be explained based on the predominance of slip in the case of Cu-Nb or the predominance of twinning in the case of Cu-Ag. Polycrystal modeling is employed to predict bulk microstructural properties, such as texture, while atomistic and dislocation-density-based models are applied to study the interactions between the interface and lattice glide and twinning dislocations. Experimental results are interpreted in these models in terms of the influence of interface crystallography on the nucleation of both lattice and twinning dislocations.

9:35 AM

On the Hall-Petch Contribution in a Bulk Nanostructured Al-4Cu Alloy: Shanmugasundaram Thangaraju¹; *Martin Heilmaier*¹; Subramanya Sarma²; B.S. Murty²; ¹Technical University Darmstadt; ²Indian Institute of Technology Madras

Bulk nano-crystalline (NC) materials produced by powder metallurgy show very high strength and follow the Hall-Petch (HP) relation but with both, a higher HP slope and frictional stress as compared to their coarse grained counterparts. In view of this, considering only the experimentally measured yield strength for evaluating the strength-grain size correlations may not be appropriate to determine HP constants for the original mechanism of grain boundary dislocation pile-up. In the present study, Al-4Cu alloys with grain sizes from 47 to 105 nm (synthesized by mechanically alloying followed by vacuum hot pressing at different temperatures) were deformed at room temperature to study the Hall-Petch relation: the analysis revealed a high frictional stress (170 MPa) and a high positive slope (0.13 MPavm) as compared to pure Al. From a detailed evaluation of the different strengthening mechanisms it is inferred that the oxide particles are the likely reason for these high values.

9:50 AM

140th Annual Meeting & Exhibition

Direct Production of Sheet from Alloys of Limited Workability Using Machining-Based Processes: *Wilfredo Moscoso*¹; Mert Efe¹; Dale Compton¹; Kevin Trumble¹; Srinivasan Chandrasekar¹; ¹Purdue University

Large Strain Extrusion Machining (LSEM), a constrained chip formation SPD process, is demonstrated as a method for producing ultrafine grained sheet/foil from alloys of limited workability. By appropriate choice of tool geometry and deformation rate, the hydrostatic pressure, temperature and shear strain in the deformation zone are set, locally, such that metals that would otherwise be difficult to work show significant formability, with minimal or no pre-heating. The process is illustrated using the production of sheet/foil directly from cast alloys (e.g., Cu, brass), and alloys with limited slip systems operative at room temperature (e.g., Mg AZ31). The mechanics underlying the process is also explored both theoretically and experimentally.

10:05 AM Break

10:20 AM Invited

Ductility and Strategies for Improving Ductility of Bulk Nanostructured Materials: Yonghao Zhao¹; *Enrique Lavernia*¹; ¹University of California, Davis

The limited ductility of bulk nanostructured materials has emerged as an important obstacle to widespread application of bulk nanostructured materials, despite their other attributes, such as ultra high strength levels, in some cases. This talk will first analyze the intrinsic and extrinsic reasons for the low ductility of the bulk nanostructured materials, and then summarize effective strategies for improving the poor ductility of bulk nanostructured materials. Finally we report on recent successful results by applying some of these strategies in nanostructured 7075 Al, NiFe, Ni to obtain both high strength and ductility.

10:50 AM

Grain Boundary Segregation of Carbon and Formation of Nanocrystalline Iron-Carbon Alloys by Ball Milling: *Reiner Kirchheim*¹; Yuzeng Chen¹; Andreas Herz¹; ¹University of Goettingen

According to a novel DEFACTANT (DEFect ACTing AgeNT) concept, attractive interaction between solute atoms and defects lowers defect energies which is a generalization of Gibbs Adsorption Isotherm. Thus synthesizing nanocrystalline (NC) material by severe plastic deformation is described by a reduced energy of dislocation and grain boundary (GB) formation in the presence of defactants. The iron-carbon system was chosen as a model system where carbon acts as the defactant. Iron powders mixed with different amount of graphic were ball milled to prepare NC iron-carbon alloys with different carbon concentrations (C0). The microstructures of the powders were examined by means of transmission electron microscopy and X-ray diffraction. The results indicated that once the saturation of GBs is achieved, the grain size of the NC iron-carbon powders will be strongly dependent on C0 described by the assumption of zero grain boundary energy and partitioning of carbon between grains and their boundaries.

11:05 AM

Investigation of Mechanical Properties of Silica/Epoxy Nano-Composites by Molecular Dynamics and Finite Element Modeling: *Bohayra Mortazavi*¹; Julien Bardon¹; Said Ahzi²; David Ruch¹; ¹Centre de Recherche Public Henri Tudor,; ²University of Strasbourg

Materials filled with particles of at least one dimension in the nanosize range are of high interest in numerous areas, such as structural adhesive applications. Inorganic nanoparticles incorporation can impart attractive properties in epoxy matrices by increasing its stiffness and its thermal resistance, among other properties. In this study Molecular Dynamics (MD) and Finite Elements (FE) modeling were performed in order to study the mechanical properties of nano-composites obtained from silica nanoparticles incorporation into an epoxy polymer. To this aim, MD modeling of tensile test was carried out to obtain the elastic modulus and Poisson's ratio of an alfa quartz silica crystal. In a next step, the 3-dimentional FE model of Representative Volume Element (RVE) of the nano-composite was developed by introducing the materials properties of silica obtained by MD simulations. Finally, the validity of the used technique was discussed by comparing the obtained results with experimental measurements.

11:20 AM

Mechanical Properties and Microstructure Evolutions of Ultrafine-Grained Al during Recovery via Annealing: *Yonghao Zhao*¹; Tory Topping¹; John Bingert²; Y. Li¹; Peiling Sun³; Xiaozhou Liao⁴; Yuntian Zhu⁵; Enrique Lavernia¹; ¹University of California, Davis; ²Los Alamos National Laboratory; ³Feng Chia University; ⁴The University of Sydney; ⁵North Carolina State University Raleigh

Ultrafine grained (UFG) metals and alloys usually have mechanical and thermal instabilities which limit their practical engineering applications. Annealing is a simple and effective way to regain strain hardening and stabilize UFG structures. In this work, we systematically investigated the mechanical properties and microstructural evolutions of UFG Al during recovery. In details, we found that low-temperature annealing at 250 C for 20 min increases ultimate strength from 190 to 208 MPa by 10 % and tensile ductility from 4.5 to 6.8 % by 50 % without changing yield strength. Microstructural analyses indicate that upon annealing the average grain size increases from 740 to 840 nm, dislocation density decreases from 5 to 10^{14} m-2, while the GB type was not changed. Moreover, annealing changes statistically stored dislocations to low-energy dislocation wall (subgrain boundaries). The mechanical properties evolution upon annealing was finally rationed based on the microstructural evolutions, fracture and deformation mechanisms.

11:35 AM

Microstructural Evolution of 316L Stainless Steel during ECAP Process: Suk Hoon Kang¹; Hyung-Ha Jin¹; Jinsung Jang¹; Do Hyun Kim²; Kyu Hwan Oh²; Xinghang Zhang³; David Foley³; Karl Hartwig³; ¹Korea Atomic Energy Research Institute; ²Seoul National University; ³Texas A&M University

316L stainless steel samples with 1 x 1 x 6 inch in size were processed by equal channel angular pressing (ECAP) to develop a nano grain microstructure with a higher fraction of coherent site lattice (CSL) boundaries. Two different paths of ECAP were applied, and the corresponding microstructure evolutions were studied using electron backscattered diffraction (EBSD) and transmission electron microscopy (TEM). The results indicate that the shear band has an inclination of about 45 degree from the shear direction; as the more shear deformation is given to the sample material, the shear band width becomes narrower and the grains are more aligned to shear band direction. In the meantime, large amounts of secondary twin boundaries were developed within the shear deformed grains, and the boundaries alignment appeared to have orientation a relationship with the initial twin patterns and also with the shear band direction.

11:50 AM

Microstructure Characterization of Grain Boundaries in Al 5083/B4C Ultrafine Grained Composites: *Ying Li*¹; Zhihui Zhang¹; Rustin Vogt¹; Enrique Lavernia¹; Julie Schoenung¹; ¹University of California Davis

The purpose of this study was to characterize the grain boundaries in Al 5083/B4C ultrafine grained composites fabricated by cryomilling, degassing, cold isostatic pressing and extrusion. The grain boundaries in the ultrafine-grained (UFG) and coarse-grained (CG) Al 5083 regions, and the interfaces between the UFG and CG regions, were investigated by transmission electron microscopy (TEM), high resolution TEM (HRTEM), energy dispersive X-ray spectroscopy (EDX), electron energy loss spectroscopy (EELS) and energy filtered TEM (EFTEM) method. High/low angle grain boundaries, equilibrium and non-equilibrium grain boundaries, elemental segregation and dislocation storage at the grain boundaries were studied in detail. The coincidence site lattice model was also used to analyze the grain boundaries.

12:05 PM Concluding Comments

2nd International Symposium on High-Temperature Metallurgical Processing: Treatment of Metals and Pellets

Sponsored by: The Minerals, Metals and Materials Society, TMS Extraction and Processing Division, TMS: Pyrometallurgy Committee, TMS: Energy Committee Program Organizers: Jiann-Yang Hwang, Michigan Technological

Program Organizers: Jiann-Yang Hwang, Michigan Technological University; Jerome Downey, Montana Tech; Jaroslaw Drelich, Michigan Technological University; Tao Jiang, Central South University; Mark Cooksey, CSIRO

Wednesday AM	Room: 18
March 2, 2011	Location: San Diego Conv. Ctr

Session Chairs: Jeffrey Schoonover, GE Global Research; Stephen Kampe, Michigan Technological University

8:30 AM

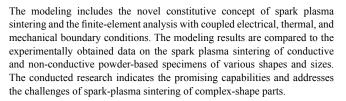
The Production of LaB₆ **by "Hot-Powder" CVD and Subsequent Milling**: *Duygu Agaogullari*¹; Özge Balci¹; Ismail Duman¹; ¹Istanbul Technical University

In this study, LaB_6 were synthesized by a combined method of gas phase reduction of BCl₃ with H₂ on the substrates of fine La grains and high-energy ball milling. An externally heated horizontal quartz tube was used as reactor. Gas mixtures were passed through the reactor at the temperature ranges of 800 to 1000 °C with a 1/4 BCl₃/H₂ molar ratio, where Ar was used as carrier gas. La particles were reacted with deposited boron on their contact surfaces. Subsequently, mechanical alloying was carried out to the coated powder with a duration of 30 minutes. Products were characterized by using X-ray diffraction technique (XRD) and scanning electron microscope (SEM). The purity was determined by Atomic Absorption Spectrometer (AAS). The exhaust gases were analyzed by Fourier Transform Infrared Spectroscopy (FTIR).

8:50 AM

Fundamentals of Spark-Plasma Sintering: Net-Shaping and Size Effects: *Eugene Olevsky*¹; Evan Khaleghi¹; Cristina Garcia¹; William Bradbury¹; Randall German¹; Cnris Haines²; Darold Martin²; Deepak Kapoor²; ¹San Diego State University; ²US Army ARDEC

Spark-plasma sintering is an emerging powder consolidating technique which provides significant advantages to the processing of materials into configurations previously unattainable. Net-shaping capabilities and size effects on spark-plasma sintering are analysed both theoretically and experimentally. Modeling and experimentation are conducted for cylindrical, prismatic, and complex powder specimen shapes. The impact of the shape and size factors on the non-uniformity of electric current density, temperature, relative density, and grain size spatial distributions is analysed.



9:10 AM

Microwave Brazing of Gas Turbine Components: *Jeffrey Schoonover*¹; Laurent Cretegny¹; 'GE Global Research

Microwave heating was investigated for braze repair of gas turbine components such as shrouds and nozzles. A novel process using a ceramic susceptor and a locally-generated plasma was developed to selectively heat and melt the braze material while keeping the component relatively cool. Epitaxial growth of braze metal on a monocrystalline substrate was demonstrated. An advantage of this energy efficient process over conventional brazing is that parent or near-parent braze compositions may be locally melted to fill a crack while the component remains below the recrystallization temperature, resulting in improved braze joint properties.

9:30 AM

Spark Plasma Sintering of Tantalum Carbide: *Evan Khaleghi*¹; ¹San Diego State University

A tantalum carbide powder was consolidated by spark plasma sintering. The specimens were processed under various temperature and pressure conditions and characterized in terms of relative density, grain size, hardness, and rupture strength (measured using a novel measurement technique). The results are compared to hot pressing conducted under similar settings. It is shown that high densification is accompanied by substantial grain growth. Carbon nanotubes were added to mitigate grain growth; however, while significantly increasing specimens' rupture strength and final density, they had little effect on grain growth.

9:50 AM

Heats of Reaction in the Formation of TiB₂ Reinforced Titanium Aluminide Composites: *Andrew Baker*¹; Stephen Kampe¹; Tony Zahrah²; ¹Michigan Tech; ²Matsys Inc.

Reaction synthesis is a technique to produce ceramics, intermetallics, and in-situ composite materials. The technique, and the resulting microstructures of the product, rely upon a large enthalpy reduction during the reaction, and also the relatively high temperatures that are characteristic of the process. This research presents experimental heats of reaction for the formation of various volume relative proportions of TiB₂-reinforced titanium aluminide composites utilizing bomb calorimetry. To overcome the kinetic constraints and achieve ignition in these formulations, a boron (B)/potassium nitrate (KNO₃) initiation aid was incorporated within the blended reactant compact. The heat contribution from the initiation aid was regressed to provide estimates of the heat of reaction of the nominal formulations. Powder x-ray differences between the predicted equilibrium products from formulation and the actual products.

10:10 AM

A Path Planning Study of Multi-pass Heat Treatment using High Power Direct Diode Laser: *Soundarapandian Santhanakrishnan*¹; Radovan Kovacevic¹; ¹Southern Methodist University

This study is focused on the development of a coupled finite element (FE) thermo-kinetic (TK) phase transformation model to minimize tempering effect of multi-pass laser heat treatment (MPLHT) process. The model predicts the temperature history, phase transformations, and the hardness of MPLHT process. A 2-kW high power direct diode laser (HPDDL) of 808 nm in wavelength is used to heat treat the tool steel AISI S7 by changing the laser power and scanning speeds while keeping a constant size of overlap. The tempering effect of the MPLHT process is studied for different lengths of scan. The numerical results are experimentally evaluated to study the

effect of length of scans on the variation of tempering temperature, phase transformations and the change of hardness.

10:30 AM

140th Annual Meeting & Exhibition

Hot Workability of 1.2690 Ledeburitic Tool Steel and Development Of Microstructure: *Milan Tercelj*¹; Goran Kugler¹; ¹University of Ljubljana, NTF-OMM

The 1.2690 high alloyed tool steel is usually applied for cold working and is alloyed with carbide-forming elements Cr, V, W and Mo. It exhibits very poor hot deformability. Since there is no enough available data in literature for elucidation of this problem, hot workability and development of microstructure during hot deformation was studied. Hot compression tests were carried out in temperature range 850-1200°C and strain rates range 0.001-6s⁻¹. SEM and OM were used for observation of microstructure. Results revealed very complex precipitation of carbides that depends on deformation temperature as well as on strain rate. It was found that especially at lower temperatures of hot working range the precipitation of carbides strongly depends on strain rate. Three different hot deformation behaviours were observed depending on temperature and strain rate range.

10:50 AM

Effect of TiO2 on the Conduction Heat Transfer of Mold Flux: Xuemei Qing¹; *Bing Xie*¹; Jiang Diao¹; ¹Chongqing University

Based on non-stationary hot wire method, a testing device was stablished, and the lattice conductivities of the mold fluxes which have different integration basicity (0.9, 1.1, 1.3) and different TiO2 content (0~8%) were measured at different temperatures (400~1300°C) by this mechanism.The results showed that when the TiO2 content was held constant, the lattice conductivities of the mold fluxes increased with the basicity increased, and when the basicity remained constant, the lattice conductivities of the mold fluxes decreased with the increase of the content of TiO2. At the same time, the lattice conductivities of all the mold fluxes increased firstly and decreased afterward with increasing the temperature from 400°C to 1300°C, and the peak value always appeared at 700°C to 800°C. XRD results showed that CaTiO3, Ca(Si1.5Ti0.5)O5, Ca2Ti5O12 were precipitated after adding TiO2, and these phases will decrease the conduction heat transfer ability of the mold flux in various degree.

11:10 AM

Flow Stress and Microstructural Evolution during Single and Double Hit Isothermal Forging of Waspaloy: *Ahmad Chamanfar*¹; Mohammad Jahazi¹; Javad Gholipour²; Priti Wanjara²; Stephen Yue³; ¹AMTC-IAR-NRC and McGill University; ²AMTC-IAR-NRC; ³McGill University

The high temperature deformation behavior of the nickel-base superalloy, Waspaloy, using single and double hit isothermal compression testing was investigated at 1373 K (1100°C), above the γ ' solvus, and constant strain rate of 0.01 s -1. For single hit deformation, the applied strain was 0.84 and for double hit compression, the strain per pass and inter pass time were respectively 0.42 and 60 seconds. Flow softening and microstructure investigation indicated that dynamic recrystallization (DRX) took place during deformation in the single hit compression and each pass of the double hit compression. Furthermore, about 15% flow stress relaxation was observed in the second pass of the double hit compression because metadynamic recrystallization (MDRX), static recrystallization (SRX) and grain growth occurred during the inter pass time. The solution heat treatment at 1373 K for 15 minutes conducted before starting the deformation, resulted in full dissolution of γ precipitates and grain growth from 10 μ m to 173 μ m. The incidences of MDRX, SRX and grain growth during inter pass time in the double hit deformation led to an increase of the DRX grain size from 24 μm to 60 μm.

11:30 AM

Effects of Binders on Oxidized Pellets Preparation from Vanadium/ Titanium-Bearing Magnetite: Guihong Han¹; Yuanbo Zhang¹; Yanfang Huang¹; Zengqing Sun¹; Guanghui Li¹; *Tao Jiang*¹; ¹School of Minerals Processing & Bioengineering, Central South University

Because of small specific surface area and poor ballability, vanadium/ titanium-bearing magnetite is difficult for production of oxidized pellet. A novel organic copolymer binder, modified humic acid (MHA), has been authorized recently in China. Effects of the novel MHA binder on the quality of V/Ti-bearing magnetite pellets are studied in this research. Experimental results show the MHA binder can obviously improve the strength of green pellet. Because of better heat endurance, the MHA binder pellet has a higher strength than Peridur pellet under the same preheating conditions. Moreover, TFe grade of pellet with the MHA binder is much higher than that of the bentonite pellet. The strength of preheated pellet containing MHA binder of 0.25%~1.0% meets the requirements of oxidized pellet production by gratekiln process. Comparatively, MHA is a promising orgainc binder for iron ore pellets, the price of which is only one tenth as that of Peridum and about 3 times as that of bentonite.

11:50 AM

Constituents and Porosity of Lead Concentrate Pellets Produced in the Trepce Plant: *Ahmet Haxhiaj*¹; Jaroslaw Drelich²; ¹University of Pristina; ²Michigan Technological University

Porosity of pellets is one of the main parameters in reductive melting process in water-jacket furnace during the roasting of sulfide lead concentrate in a smelter located in Trepçë. Roasting is done at about 900°C, for pellets which are composed of PbS, $CaCO_3$, Fe_2O_3 , and SiO_2 . In order to facilitate the formation of slag in the reductive melting, the pellets must have proper content of CaO, SiO_2 , and FeO, and porosity. Pellets with porosity of 18% do not melt adequately in the water-jacket furnace. The optimal porosity for pellets melting was found to be 35-55% and is achieved with loading of pellets with more than 10 wt.% CaO. The pellets with less than 10% CaO have not enough pores for the gasses to penetrate their entire structure. The composition of the pellets must satisfy the ratio of CaO : SiO_2 : FeO = 1 : 1.2 : 1.8.

12:10 PM

Experimental Research on Increasing Hematite Concentrate Proportion in Oxide Pellet: *Xiaohui Fan*¹; Lishun Yuan¹; Yi Wang¹; Luben Xie¹; ¹Central South University

Effect of 3 inorganic bentonite, 5 composite bentonite, as well as hematite proportion on pelletizing and induration are studied in this paper. The results show that on the premise of small range adjusting and guaranteed pellet quality, the proportion of hematite concentrate can be increased to 50%.

12:30 PM

Oxidized Pellet Preparation from Refractory Specularite Concentrates Using Modified Humic Acid (MHA) Binders: Guohua Bai¹; Daoyuan Zhang¹; *Yuanbo Zhang*¹; Guihong Han¹; Zijian Su¹; Guanghui Li¹; ¹School of Minerals Processing & Bioengineering, Central South University

Specularite concentrates have poor hydrophilicity and ballability as well as bad high-temperature reactivity, which restrict the large-scale application of them in the pelletizing and sintering production. Modified humic acid (MHA) organic binders are firstly used for pellet preparation from specularite in this paper. The results show when using 1.0% MHA binder, the drop strength of green pellets is 3.7 times/0.5m and compression strength is 12.5 N/P. Under the optimal experimental conditions of preheating temperature 980 \square , preheating time 12 min, roasting temperature 1280 \square and roasting time 10 min, the preheated pellets have the compression strength of more than 400 N/P, and that of roasted pellets is 2747 N/P. The strength of finished pellets meet the requirements of blast furnace iron-making. MHA is a kind of more effective organic binder for specularite pellets compared with the inorganic bentonite.

Advances in Mechanics of One-Dimensional Micro/ Nano Materials: Nanomechanics: Pillars and Wires

Sponsored by: The Minerals, Metals and Materials Society, TMS Materials Processing and Manufacturing Division, TMS Electronic, Magnetic, and Photonic Materials Division, TMS: Nanomechanical Materials Behavior Committee

Program Organizers: Reza Shahbazian-Yassar, Michigan Technological University; Seung Min Han, Korea Advanced Institute of Science and Technology; Katerina Aifantis, Aristotle University

Wednesday AM March 2, 2011 Room: 1B Location: San Diego Conv. Ctr

Session Chairs: Reza Shahbazian Yassar, Michigan Technological University; Katerina Aifantis, Aristotle University

8:30 AM Invited

Deformation and Failure of Phosphide- and Boride-Based Nanofilaments: Melisa Steighner¹; Humberto Gutierrez¹; *Christopher Muhlstein*¹; ¹The Pennsylvania State University

Theoretical predictions of unique physical and mechanical properties for compound nanofilaments with novel morphologies have motivated countless nanomaterials research programs. However, in some case empirical confirmations of the predictions have been elusive, either due to the difficulty to synthesize the predicted nanostructures or due to the complexity of the experiments needed to unambiguously demonstrate their physical properties. In this presentation we explore the structural and mechanical properties of phosphide- and boride-based nanofilaments that were synthesized using chemical vapor deposition techniques. Their deformation and fracture behaviors were evaluated using a micromachined loadframe and correlated one-to-one with their structure, morphology and chemical composition studied by transmission electron microscopy. Combining micro-Raman spectroscopy and direct stress measurements, we studied the mechanical behavior of nanofilaments in the presence of strain. These experiments provided insight into when and how nanoscale size effects are observed.

8:55 AM Invited

The Brittleness Transition in 1-D Pillars: *William W. Gerberich*¹; A. Beaber¹; ¹University of Minnesota

A transition-state modeling effort has been recently posed for dislocation nucleation. Parallel to that, several experimental efforts have been mounted to measure the yield and fracture characteristics of 1-D structures, in our laboratories emphasizing silicon. We conclude that both yield and flow stresses as well as fracture toughness are length scale dependent and plan to illustrate how a transition-state model might be applied to the brittle to ductile transition in strain-rate sensitive materials. Some in-situ transmission electron studies of the flow stress in nanopillars will illustrate the progress towards this goal.

9:20 AM Invited

Deformations in Nano-Sized Pillars of Metallic Glasses: *Jeff De Hosson*¹; Alexey Kuzmin¹; ChangQiang Chen¹; YuTao Pei¹; ¹Univ of Groningen

Size effect, or the lack thereof, during deformation of nano-sized metallic glassy objects has recently drawn great attention. It is not only of fundamental interest when scrutinizing shear localization processes, but also of practical significance for the incorporation of small size components in micro-/nano- electromechanical systems. An intriguing question is why and how nucleation and propagation of these shear bands (SBs) are affected by the size of the system, and would it be possible to suppress brittleness and enhance ductility by changing the size of the samples? Therefore, we have carried out quantitative in-situ TEM compression and bending experiments of metallic glass pillars with diameters ranging from 50 nm to 500 nm. A micromechanical model based on quantitative description of shear banding events explains the size-dependent deformation behavior and a statistical analysis of strength reveals the physical picture defined by the interactions between stress fields of flow defects.



9:45 AM

Elastic and Plastic Deformation of Nano- and Micro- Pillars: Katerina Aifantis¹; ¹Aristotle University

Experimental evidence will be presented on the deformation of polymeric and metallic nano-cones and nano-pillars, through atomic force microscopy indentation and nanoindentation. It will be shown that gradient plasticity can capture the deformation of such nanoscale configurations and estimates will be provided for the key material parameters, namely the elastic modulus and the internal length, that come into play in elasticity and gradient plasticity.

10:00 AM Invited

Dislocation Sources in Micro-Pillars: Wei Cai1; 1Stanford University

The size-dependent yield stress observed in recent experiments of submicrometer metallic pillars provides a unique opportunity in which the predictions from defect dynamics simulations can be directly compared with mechanical strength measurements. The balance between the dislocation multiplication rate and depletion rate (at the surface) may be the key to understand the observed size effect in flow stress. Here we report two counterintuitive observations concerning dislocation multiplication in small volumes from Molecular Dynamics and Dislocation Dynamics simulations. In body-centered-cubic (BCC) metals, the surface itself can induce dislocation multiplication as a single dislocation moves across the pillar. In face-centered-cubic (FCC) metal pillars and thin films, however, even jogs of the Lomer-Cottrell type are not strong enough pinning points to act as permanent dislocation Dynamics models against the more fundamental atomistic models.

10:25 AM

Numerical Study of Fracture of Si-NWs Subjected to Lithiation/ Delithiation: *Ill Ryu*¹; William Nix¹; ¹Stanford University

There is currently a great amount work devoted to the development of electrodes for Li-ion batteries. Silicon is one of the most promising candidates, because it shows high charge capacity and low discharging rates. However, silicon experiences a huge volume expansion about 400% during the lithiation/delithiation process. As shown recently, silicon nano-wires are attractive candidates for electrodes because they provide less constraint on the volume changes that occur during Li charging. In the present study, we have tried to estimate the critical size below which fracture does not occur in silicon nano-wires.

10:40 AM Break

11:05 AM Invited

Deformation Mechanisms In Single Crystalline fcc Nanowhiskers: *Daniel Gianola*¹; Andreas Sedlmayr²; Lisa Chen¹; Gunther Richter³; Reiner Mönig²; Oliver Kraft²; ¹University of Pennsylvania; ²Karlsruhe Institute of Technology; ³Max Planck Institute for Metals Research

The emerging picture in the size-dependent deformation of small-scale fcc metals suggests that the relationships between density and character of defects, discrete source statistics, and free surface/defect interactions, governs the mechanical response. Theoretical and simulation results also predict a shift in the rate-controlling mechanisms at small specimen size towards deformation modes that require thermal activation. We present results from quantitative in situ experiments on near defect-free fcc nanowhiskers in electron microscopes. Cu and Au nanowhiskers endure stresses near the limit of their ideal strength during tensile straining and the resulting deformation behavior suggests a lack of conventional dislocation-dislocation interactions. Transient and non-ambient temperature nanomechanical experiments are employed to extract activation parameters for plastic deformation. These results will be discussed in the context of thermal activation of nanoscale plastic deformation, which has recently been predicted to be important in ultra-strength materials.

11:30 AM

Mechanics of Nanotubes/Nanowires: In Situ Microscopy: *Reza Shahbazian-Yassar*¹; Kasra Momeni¹; Hessam Ghassemi¹; Anjana Asthana¹; Yoke Yap¹; ¹Michigan Technological University

The correct estimation of mechanical properties in nanotubes and nanowires has been a challenging task due to complexity of stress state and end-support boundary conditions. Here we utilized simple beam formulations and buckling theories to explain the deformation and mechanics of boron nitride (BN) nanotubes and zinc oxide (ZnO) nanowires. Size scale effects were observed in ZnO nanowires and were explained by the modification of atomic structure at the nanowire surface. In addition, the rippling and bifurcation of multiwalled BN nanotubes were observed upon buckling and were quantified in terms of number of walls and nanotube's diameter.

11:45 AM Invited

Structure-ElasticPropertyRelationsinOne-DimensionalNanostructures:GheorgheStan¹;RobertCook¹;¹NationalInstitute ofStandards and Technology

Nanoscale mechanical property measurements enable the link between atomistic simulations and micromechanical models to be defined and established. In this talk discussion will focus on the applicability of contact-resonance atomic force microscopy (CR-AFM) for quantitative measurements of the elastic modulus of one-dimensional nanostructures. By using CR-AFM we have systematically investigated the size-dependence of the elastic modulus of various nanowires and nanotubes: ZnO nanowires, Te nanowires, and AlN nanotubes. The observed increases in elastic moduli with reduction in nanowire diameter directly proved the stiffening enhancement that occurs in the outer layers of nanowires of reduced diameter. A distinctive CR-AFM application of enhanced compositional sensitivity has been demonstrated in measuring the mechanics of nonplanar subsurface Si-SiO2 interfaces in partially oxidized Si nanowires. Such examples demonstrate the unique spatial resolution and compositional sensitivity of CR-AFM in investigating structure-mechanical property relationships at the nanoscale.

12:10 PM

A Study of the Mechanical Properties of Nanowires Using Nanoindentation: *Gang Feng*¹; Davood Askari²; ¹Villanova University; ²University of Texas at Brownsville and Texas Southmost College

A nanoindenter with scanning capabilities was used to perform nanoindentations on several nanowires with radii in the range of 20–500 nm, positioned on a substrate. Since the geometry of indentation of a nanowire differs significantly from the indentation of a half-space, a two interface contact model has been developed for the nanoindentation of a nanowire on a flat substrate, with the two interfaces, indenter/nanowire and nanowire/substrate, being in a series. The model has been used to analyze the nanoindentation data for several types of nanowires. Furthermore, to evaluate the analytical model, 3-dimensional finite element analysis (FEA) is performed, indicating significant nanowire-receding, a large deformation at the nanowire/substrate contact, and the insignificance of the adhesion at the contact. We also find that the sphere (indenter)/cylinder contact cannot be well approximated by a Hertzian elliptical contact.

12:25 PM

Mechanical Behavior of the Ag Nanowires for Transparent Electrode Application: *Chansun Park*¹; Hui Wu²; Yi Cui²; Seung Min Han¹; ¹KAIST; ²Stanford University

In this study, we utilized nanoindentation to study the mechanical behavior of both single crystalline and polycrystalline Ag nanowires synthesized using a solution based synthesis and an electrospinning method, respectively. The solution synthesis method involves a poly reduction reaction, which is a common method of producing colloidal particles of metal elements, then selective growth of single crystalline nanowires along the (100) orientation. The electrospinning method involves using polymer based solutions with Ag precursors, then extracting out the fibers that are removed the polymer and therefore produce polycrystalline Ag nanowires. Both synthesis methods are tuned to fabricate wires of different diameters, and their hardnesses were determined using the Hysitron Ti-750 nanoindenter. Instead of using Oliver and Pharr method for indentation hardness, we utilized a method where is calculated by utilizing the measured stiffness that was reported by Feng et al.1.1. G. Feng et al, Journal of Applied Physics 99, 74304(2006).

Alumina and Bauxite: Precipitation, Calcination and Properties

Sponsored by: The Minerals, Metals and Materials Society, TMS Light Metals Division, TMS: Aluminum Committee, TMS: Aluminum Processing Committee

Program Örganizers: James Metson, University of Auckland; Carlos Suarez, Hatch Associates Consultants Inc

Wednesday AM	Room: 17A
March 2, 2011	Location: San Diego Conv. Ctr

Session Chair: To Be Announced

8:30 AM Introductory Comments

8:35 AM

Effect of Technological Parameters on PSD of Aluminum Tri-Hydroxide from Seed Precipitation in Seeded Sodium Aluminate Solution: Yusheng Wu¹; Li Mingchun¹; Qu Yanping¹; ¹shenyang university of technoloy

Abstract: Periodical attenuation of particles, which interferes seriously with the normal alumina production, exists in Bayer process. In order to construct A mathematical model of total number of particles and particle size distribution (PSD) which is helpful to broadcast and control the PSD of aluminum tri-hydroxide for alumina refinery, the PSD of aluminum tri-hydroxide for alumina refinery, the PSD of aluminum tri-hydroxide from seeded precipitation process in deferent technological parameters has been investigated under industrial conditions modeled in laboratory. The results show that PSD of the direction of translation to the small particle size with the initial precipitation temperature decreasing and molecule ratio of Na2O/Al2O3 increasing. The volume fraction of particles below 44μ m first increased and then decreased With the initial concentration of Na2O increasing. The PSD has a opposite variation tendency in different initial seed amount compared with the initial concentration of Na2O.Keywords: Bayer process, Sodium aluminate solution, Periodically attenuating, Particle size distribution, Aluminum tri-hydroxide

9:00 AM

Methods to Reduce Operating Costs in Circulating Fluidized Bed Calcination: Cornelis Klett¹; Michael Missalla¹; Bernd Reeb¹; Hans Schmidt¹; ¹Outotec GmbH

Calcination of Gibbsite or Hydrate to Alumina needs approximately 30% of the energy input to an alumina refinery. Over the years Circulating Fluidized Bed (CFB) Calciners by Outotec (formerly Lurgi) have reduced energy consumption for calcination significantly. Until 1961 rotary kilns were standard technology for calcination of alumina. Since 1961 CFB technology reduced fuel consumption up to 30%. Since then, CFB calciners have been constantly improved and methods have been developed to reduce fuel consumption further. Some of these methods have resulted in increasing process complexity and operator and maintenance demand. However, also a lot of measures have been introduced to mitigate the negative effects of the increased process complexity and to improve operability and maintainability even beyond. In this paper different options and methods for reduction of fuel consumption, but also increase of operability and maintainability are compared and evaluated in their effects on installation costs and operating costs.

9:25 AM

Pressure Calcination Revisited: Fred Williams¹; C Misra²; ¹CMIS Corp; ²AluminaTech

Twenty-five years ago at the TMS 100tth anniversary meeting of the Hall-Heroult Process, two Alcoa scientists, S. W. Sucech and the co-author of this paper, C. Misra presented a paper on an improvement to the alumina calcination process – pressure calcination. The improved process offered an

opportunity for a net energy reduction in fluid flash calciners of 1.6 GJ/ton alumina (and the subsequent green house gas reductions). The improved process could be retrofitted into existing fluid flash calciners and produce an alumina meeting smelting requirements with the added advantage of high attrition resistance and thus low dust generation. The question is: Why hasn't this improvement been incorporated into today's alumina plants?Technical data in the previous paper will be reviewed and updated in the present paper.

9:50 AM

Dynamic Simulation of Gas Suspension Calciner (GSC) for Alumina: *Benny Raahauge*¹; Susanne Wind¹; Mengzhe Wu¹; Torsten Jensen¹; ¹FLSmidth

Training of plant operational personnel is becoming more important today than ever, to sustain high availability and productivity of high capacity equipment. The Gas Suspension Calcination process for production of Smelter Grade Alumina is very easy to operate and control regardless of calcining capacity. But increasing calcining capacity of single GSC units exceeding 4500 tpd of SGA makes it increasingly costly to loose operating time. The process dynamics of GSC units are very fast with some true response times in fraction of seconds. To train GSC operators, FLSmidth has developed a dynamic Calciner Simulator which serves the primary purpose of training both new operators, as well as maintaining the skills of experienced ones. The dynamic Calciner Simulator has been developed from supply of more than 75 Pyro process simulators by FLSmidth to the global cement. The first Calciner Simulator for Alumina will be commissioned in Australia later this year.

10:15 AM Break

10:25 AM

Physical Simulation and Numerical Simulation of Mixing Performance in the Seed Precipitation Tank with a Improved Intermig Impeller: *Zhang Ting-an*¹; Liu Yan¹; Wang Shuchan¹; Zhao Hongliang¹; Zhang Chao¹; Zhao Qiuyue¹; Dou Zhihe¹; Lv Guozhi¹; ¹Northeastern University

The C6D fiber optic reflection probe was used to measure the local solid concentration distributions in the seed precipitation tank with a new-style impeller—Improved intermig impeller and the commercial software FLUNET 12.0 was used to simulate numerically its flow fields. The physical simulation results show that the high rotation and viscosity high-speed particles are more conducive to uniform distribution. When \Box =3.50cp \Box n=172rpm, the multiple relationships of the average value of the practice and theory is1.011 times. The numerical simulation results show that the too longer or shorter impeller off-bottom clearance height(C) is not conducive to the suspending of Al(OH)3 particles. Enlarging the blade diameter is good for the suspending of Al(OH)3 particles. The blade diameter need the more power consumption. The physical simulation results compare well with the numerical simulation ones.

10:50 AM

Two Perspectives on the Evolution and Future of Alumina: *Linus Perander*¹; James Metson¹; Cornelis Klett²; ¹Light Metals Research Centre; ²Outotec GmbH

Over the 125 year history there have been a number of step-changes in the Hall-Heroult process, despite a remarkable adherence to the original concepts of the invertors. In addition to the steady increment in scale, most noteworthy perhaps have been the introduction and impending disappearance of Soderberg technology, the introduction of magnetically compensated cell design, changes in dynamics of alumina feeding and the introduction of dry-scrubbers for HF control and fluoride recovery. The Bayer process has also seen some significant advances, driven by the demands of energy and environmental imperatives and the steadily narrowing window of product specifications, driven in turn by refinements in the Hall-Heroult process. Demands for coarser particle size distribution and higher specific surface areas have been accompanied by changes in precipitation strategy and conversion to more energy efficient stationary calcination processes. The properties of a "typical" metallurgical alumina have thus changed. Indeed



the term "alumina" is now more indicative of stoichiometry than it is of structure, and even in this, it is less than precise. In this paper we discuss how new scientific tools and insights are changing the way we define (and perhaps should specify) this material.

11:15 AM

Significant Improvement of Energy Efficiency at Alunorte's Calcination Facility: *Michael Missalla*¹; Hans Schmidt¹; Joaquim Ribeiro²; Reiner Wischnewski³; ¹Outotec GmbH; ²Alunorte-Alumina do Norte do Brasil S.A.; ³Hydro Aluminium AS

The Alunorte refinery produces 6.3 million t/a of alumina with seven Circulating Fluid Bed (CFB) calciners. The calcination facility only needs about one third of the total energy for the refinery. The CFB calcination system has implemented several preheating and cooling stages with cyclones for the separation of gas and solids. If the cyclones were more efficient, it would lead to an increase in heat recovery thus decreasing energy consumption. The paper presents a process to improve efficiency of these cyclones and the solid dust load significantly by using new method of simulation technology. With the optimised process considerably lower energy consumption figures are achieved. Results of these improvements regarding fuel and electrical energy consumption as well as return on investment are presented. Alunorte has already installed the improvements at two of their seven calciners and has received the energy efficiency award 2010 from the German Energy Agency.

11:40 AM

Attrition of Alumina in Smelter Handling and Scrubbing Systems: Stephen Lindsay¹; ¹Alcoa, Inc.

Smelting customers place various levels of importance upon the Attrition Index of Smelter Grade Alumina, SGA. Concerns are generally associated with the content of alumina fines in fluorinated alumina as it arrives to the reduction cell. In this paper the author discusses factors of importance related to the design and operation of the alumina handling systems. Examples will be given in which the attrition of alumina particles has been minimal. Discussion will include techniques on how to estimate the contribution of fine particles of bath evolved by the pots from attrition of alumina particles.

Aluminum Alloys: Fabrication, Characterization and Applications: Materials Characterization

Sponsored by: The Minerals, Metals and Materials Society, TMS Light Metals Division, TMS: Aluminum Processing Committee *Program Organizers:* Subodh Das, Phinix LLC; Zhengdong Long, Kaiser Aluminum; Tongguang Zhai, University of Kentucky

Wednesday AM	Room: 14A
March 2, 2011	Location: San Diego Conv. Ctr

Session Chair: Tongguang Zhai, University of Kentucky

8:30 AM

N

Transmission Electron Microscopic Investigations of Grain Boundary Beta Phase Precipitation in Al-5083: *Ramasis Goswami*¹; Peter Pao²; Ronald Holtz²; ¹SAIC/Naval Research Laboratory; ²Naval Research Laboratory

The fine scale microstructure of Al-5083 sensitized at 70, 100 and 175°C and at ambient temperature for different durations has been investigated using transmission electron microscopy (TEM) to study the evolution of the β phase (Al3Mg2) at grain boundaries. TEM observations showed that, at 100°C, the grain boundary precipitation of β -phase was discrete between 3 to 14 days of aging, and no segregation of Mg at the grain boundary was observed between two discrete β islands. Considerable portion of grain boundaries were fully covered by the β -phase after 30 to 45 days of aging at 100°C. Grain boundaries were also observed to be migrated by diffusion induced grain boundary migration (DIGM) after aging for 90 days at 100°C. The nucleation and growth of β -phase at grain boundaries at different

temperatures, 70, 100, 175 $^{\rm o}{\rm C}$ and ambient temperature, will be discussed in detail.

8:50 AM

Effect of Ultrasonic Impact Treatment on a 5456 Aluminum Alloy Characterized through Micro-Specimen Testing and X-Ray Tomography: *Caroline Scheck*¹; Kim Tran²; Christopher Cheng¹; Marc Zupan¹; ¹University of Maryland, Baltimore County; ²Naval Surface Warfare Center, Carderock Division

Ultrasonic impact treat (UIT) is a surface treatment that causes uniform, but severe, plastic deformation. UIT gives excellent parameter control and has a high energy efficiency, unlike similar processes such as shot peening. The objective of this work is to show the measured hardness, strength, and void properties of an ultrasonically impacted 5456-H116 aluminum. Micro-indentation is used to map the hardness properties while microsample specimens directly measure tensile mechanical properties. The micro species (3mm in length by 1mm wide with a gage section of 250 mm square) are made at varying distances from the UIT treated surface and tested to characterize the Young's modulus and yield strength. Voids in the gage section of the micro specimens are analyzed before and after testing using a novel X-ray topography. These void characteristics are linked to the yield and plastic deformation behavior of the material.

9:10 AM

Effect of Extrusion Microstructure on the Corrosion Behavior of AA6005A Aluminum Alloy: *Dan Seguin*¹; Calvin White¹; Richard Dickson²; ¹Michigan Technological University; ²Hydro Aluminum

Extrusions of AA6005A alloy have a duplex grain structure consisting of a thin recrystallized layer near the extrusion surface and a fibrous layer at the core. The recrystallized layer in underaged AA6005A is known to be susceptible to intergranular corrosion when containing more than about 0.12% Cu. No study on the corrosion behavior of the fibrous core structure exists to date. For the present work, specimens of thin-walled AA6005A extrusion with a range of thermal and surface treatments were prepared and exposed to an accelerated corrosion solution. Within the fibrous structure, surfaces cut normal to the extrusion direction were found to be much more susceptible to pitting attack than surfaces cut parallel to the extrusion direction.

9:30 AM

Failure Loads and Deformation in 6061-T6 Aluminum Alloy Spot Welds: *Radu Florea*¹; Kiran Solanki¹; Douglas Bammann¹; Brian Jordon¹; Matt Castanier¹; ¹Mississippi State University

Failure loads and deformation in 6061-T6 aluminum alloy resistance spot welded joints were experimentally investigated. The welding experiments were carried out using different process parameters such as electrode forces, welding times, and currents. Nugget and microstructure characteristics were quantified using laser beam profilometry, electron back scatter diffraction technique (EBSD), and quasi-static shear tests. Mechanical tests were used to characterize the failure forces in spot welded specimens to elucidate the influence of process parameters. Finally, the microstructure of the weld nugget was discussed based on the process parameters, and the modeling results were compared with measurements obtained by electron back scatter diffraction mapping.

9:50 AM

Magnesium Diffusivity Measurement in AA5083 Alloys: Soumya Kar¹; Michael Free¹; ¹University of Utah

AA5083 alloys are widely used for marine application. However, these alloys are susceptible to intergranular corrosion after prolonged exposure at moderate temperature. Formation of Mg rich beta phase is the primary concern in this type of material degradation. We investigated Mg diffusion behavior to quantify the amount of beta phase formation. AA5083 alloy was investigated with O and H131 temper. 5456-H116 alloys were also investigated for comparative study. High resolution scanning electron microscopy images were taken to identify the beta phase. Beta phase thickness was estimated from the etch trench thickness distribution profile. The model was developed

based on the fundamental assumption that increase of Mg along the grain boundary is due to the depletion of Mg from the bulk. Solving a mass balance equation, the model can provide beta phase thickness for a range of thermal exposure time and temperature. Mg diffusivity parameters can be estimated from this information.

10:10 AM Break

10:25 AM

Surface Energy, Electronic Structure, and Complexity of Al-Based Intermetallics: *Jean-Marie Dubois*¹; Esther Belin-Ferré²; ¹Institut Jean Lamour, CNRS; ²LCPMR, CNRS

Many compounds based on aluminum alloyed with transition elements or simple metals contain a large number of atoms in their crystal unit cell. As a consequence of the resulting complexity, their properties depart significantly from the ones of the elemental constituents. In this paper, we will examine one such important property, namely surface energy, which we will assess based on friction experiments against steel in vacuum. We will show how it correlates to partial densities of electronic states deduced from soft x-ray emission spectroscopy. Complexity will be shown to play the key role, via Hume-Rothery and hybridization effects.

10:45 AM

Measurement of Resistivity/Conductivity of Aluminium Oxide-Film by Electrochemical Impedance Spectroscopy (EIS): *Khaled Habib*¹; ¹KISR

The technique of Electrochemical Impedance Spectroscopy (EIS) is widely used in laboratories and industries for materials evaluation. The aim of this investigation is to measure ,for the first time, the resistivity/ conductivity of the anodized (oxide) aluminium sheets (samples) by using the EIS in a laboratory in 0-10 % sulphuric acid. In order to achieve such task, the alternating current (AC)impedance and the thickness of the anodized (oxide) aluminium samples will be measured at low frequency in 0-10 % sulphuric acid.In other words, the absolute value of the AC impedance will be equivalent to the direct current resistance of the anodized (oxide) aluminium samples. As a result, the resistivity/conductivity of the anodized (oxide) aluminium samples can be determined by knowing the resistance and the thickness of the samples in 0-10 % sulphuric acid.

11:05 AM

Effect of Conical and Cylindrical Tool with Grooves Pin Profiles on Tensile Strength in Friction Stir Welding Process: C. N. Suresha¹; B. M. Rajaprakash¹; Sarala Upadhya¹; ¹Bangalore University

Friction stir welding (FSW) is an innovative solid-state material joining method invented by The Welding Institute (TWI). It has evolved into a process focused on joining arc weldable (5xxx and 6xxx) and unweldable (2xxx and 7xxx) aluminum alloys where it can be implemented by the aerospace and automotive industries for their joining needs. The present study has aimed to investigate the influence of tool profile on tensile strength and joint efficiency of welded joints of AA 7075-T6 Aluminum alloy by FSW process. Tool profiles like conical and cylindrical with grooves are used in this study. Experiments were carried to find contribution of the main welding parameters, such as tool rotational speed, weld traverse speed and plunge depth on tensile strength of welded joint. It has been observed that the use of tool having conical grooved profile has resulted better results than the tool having cylindrical grooved profile.

Aluminum Reduction Technology: Cells Technology, Development and Sustainability

Sponsored by: The Minerals, Metals and Materials Society, TMS Light Metals Division, TMS: Aluminum Committee, TMS: Aluminum Processing Committee

Program Organizers: Mohd Mahmood, Aluminium Bahrain; Abdulla Ahmed, Aluminium Bahrain (Alba); Charles Mark Read, Bechtel Corporation; Stephen Lindsay, Alcoa, Inc.

Wednesday AM	Room: 17B
March 2, 2011	Location: San Diego Conv. Ctr

Session Chair: Gilles Dufour, Aluminerie de Deschambault

8:30 AM

High Amperage Operation of AP18 pots at Karmøy: Marvin Bugge¹; Haakon Haakonsen¹; Ove Kobbeltvedt¹; Knut Paulsen¹; ¹Hydro Aluminium

The AP18 potline at Karmøy has increased the amperage to 230 kA. This has increased the productivity and reduced the specific production costs. The operation showed some lack of performance at high amperage for the old pots designed for lower amperage. The old pots had too high heat input resulting in thin ledge and higher Si content in the metal. To improve the heat balance the pot voltage had to be reduced for the old pots, and this resulted in reduced CE. The cathode life was reduced to ~2250 days due to use of graphitized cathode blocks and the increased amperage. The new cathodes designed for 230 kA show good operational results. The young pots show 94-94.5% current efficiency and 13.1 kWh/kg Al energy consumption. Due to less bath volume in the new pots it has been a challenge to reduce the anode effect frequency.

8:50 AM

Aluminium Smelter Manufacturing Simulation – Can These Bring Real Cost Savings?: Maarten Meijer¹; ¹Hencon

Incorporating logistics tools at the smelter design stage: implications for capex and opex Optimising interaction between smelter units and processes for additional cost savings The use of simulation in achieving "lean thinking" in new smelters or upgrades

9:10 AM

Simultaneous Preheating and Fast Re-Start of 50 Aluminium Reduction Cells in an Idled Pot Line- A New Soft Re-Start Technique for a Pot Line: Albert Mulder¹; Anita Folkers¹; *Marco Stam*¹; Mark Taylor²; ¹Aluminium Delfzijl; ²The Light Metals Research Centre

Due to the global economical crisis a significant amount of primary aluminium production capacity has been shut-down. A number of different strategies to restart idled aluminium reduction cells have been discussed in the literature. This paper describes the successful development and execution of the start-up of 50 cells simultaneously in one pot line. The procedure is based on restarting reduction cells using a cold metal plate. Contrary to electrical preheating of new cells with use of cokes or graphite, these cells have been prepared with anodes positioned in direct contact and on top of the cold metal plate. The rate of preheating of the cells and associated melting of metal is controlled by a gradual line current increase. The actual start-up of the cells is performed sequentially by the addition of liquid electrolyte and moving the anode beam upwards. In this respect 50 cells have been started in 8 days.

9:30 AM

SWOT Perspectives of Mid-age Prebaked Aluminium Smelter: *Pradip Choudhury*¹; Arun Sharma¹; ¹National Aluminium Company Ltd.

Aluminium smelters in nineties witnessed radical changes in technology of electrolysis, carbon manufacturing and casting. The pace of transformation in Aluminium industries posed different challenges specifically to the midage smelters operating with relatively lower amperage. Enduring needs to match the demands of evolving technology, socio-cultural and environment issues forced mid-age Smelters to adopt appropriate strategies as long-



term business imperatives. With structured approach, the threat perception could be turned into vast opportunities of innovation and improvements. Energy conservation, waste management, recycling, emission control and customer orientation remained specific focus areas to enhance productivity and retain profitability in the backdrop of global economic recession. Process optimization and system upgradation through customised solutions, motivating and retaining high employee morale became the order of the day. The paper is a case study on the sustainable achievements of the state owned Indian Aluminium major, NALCO, through well-coined strategies and pragmatic investment.

9:50 AM Break

10:00 AM

Integrated Approach for Safe and Efficient Plant Layout Development: *Rafael Pires*¹; Robert Baxter¹; Laszlo Tikasz¹; Robert McCulloch¹; ¹Bechtel

Aluminium complex layout development usually involves dealing with an intricate mix of operations (e.g. smelter, refinery, rolling mill, port). The choice of a layout can significantly impact the success of the envisaged operation, in terms of safety, life-cycle cost and environmental impact. This paper is a continuation of last year's publication, exploring the application of safety by design and lean manufacturing methods on the layout design of a fully integrated aluminium complex. An innovative approach, derived from lessons learnt to assist plant layout development and resource analysis, is presented. This approach is able to quickly and effectively assess safety and efficiency in a proposed layout. The dynamic feature of this approach provides the capability of closely mimicking the future traffic operation, allowing to monitor how the traffic evolves in time.Throughout this paper, the design of access roads, choice of transportation modes, and planning of resource are discussed.

10:20 AM

Improving Current Efficiency of Aged Reduction Lines at Aluminium Bahrain (Alba): *Abdulla Ahmed*¹; Ragahavendra K.S.R¹; Hasanain Hassan¹; ¹Aluminium Bahrain (Alba)

The side worked end-on-end pre-bake anode technologies install during 1970's at Alba achieved a current efficiency of 90%. During the early nineties, the potlines were retrofitted from side break to point fed cell arrangement, along with an increase of 7% and 10% in line current. The retrofits included anode gas collection system, a changed anode setting pattern, and installation of alumina and aluminium fluoride feeders controlled using individual cell controller, which increased the current efficiency to 92.5%. During the last 6 years, improvements done in the alumina feeding control, thermal control and stability of cell operations has increased the current efficiency to 94.5%. Close monitoring and follow up of quality of work and key parameters on daily basis by the new employees forum introduced at Alba in 2004 called SMART Centres (See My Actions Reflect Targets) has also contributed towards this improvement and maintaining it.

10:40 AM

Current Efficiency for Aluminium Deposition from Molten Cryolite-Alumina Electrolytes in a Laboratory Cell: *Geir Martin Haarberg*¹; Joseph Armoo¹; Henrik Gudbrandsen²; Egil Skybakmoen²; Asbjørn Solheim²; Trond Eirik Jentoftsen³; ¹Norwegian University of Science and Technology; ²SINTEF; ³Hydro Aluminium

The current efficiency with respect to aluminium can be as high as 96 % in modern Hall-Heroult cells. The loss in current efficiency is strongly linked to the fact that aluminium is soluble in the electrolyte. In addition the presence of dissolved sodium must be considered. The back reaction between dissolved metals and the anode product is responsible for the major loss in current efficiency. The rate of the reaction is controlled by diffusion of dissolved metals (Al and Na) through the diffusion layer. A laboratory cell was used to determine the current efficiency for aluminium during constant current electrolysis. Standard conditions were NaF/AlF3 (CR=2.5), Al2O3 (sat), 5 wt% CaF2 at 980°C and 0.85 A/cm2. Current efficiencies ranging from ~90 - 97 % were obtained. The current efficiency was found to increase

slightly by increasing cathodic current density. Increasing excess AIF3 gave higher current efficiencies.

11:00 AM

New Progress on Application of NEUI400kA Family High Energy Efficiency Aluminum Reduction Pot ("HEEP") Technology: Dingxiong Lv¹; Xiquan Qi¹; Junman Qin¹; Zijin Ai¹; *Yungang Ban*¹; ¹Northeastern University Engineering & Research Institute Co. Ltd

China's first 400kA class potline was put into operation in August 2008 with NEUI400(I) cell technology. The annual design production capacity of the potline is 230kt. The present amperage is 420kA, average working voltage is less than 3.88V, DC energy consumption is less than 12.8 kW•h/kg-Al, and the anode effect frequency is below 0.015.Based on the successful application and testing results of NEUI400(I) cells, further research work was carried out on the structural optimization, energy saving and environment protection. The improved NEUI400 (II~IV) cells were successfully applied in the potlines of LinFeng, NanShan and JinNing smelters, and the annual design production capacity is 250kt, 250kt and 300kt respectively. All the NEUI400 potlines amperage reached 430~450kA after start-up. Excellent technical-economic indexes were obtained after the cells putting into operation three months, such as average working voltage is less than 3.85V, DC energy consumption is less than 12.5 kW•h/kg-Al, anode effect frequency is well below 0.01.

11:20 AM

Development of NEUI500kA Family High Energy Efficiency Aluminum Reduction Pot ("HEEP") Technology: Dingxiong Lv¹; *Yungang Ban*¹; Xiquan Qi¹; Jingxiong Liu¹; 'Northeastern University Engineering & Research Institute Co. Ltd

Based on the successful development and commercial application experience of NEUI400kA class reduction cells, also combined with testing results and proprietary numerical simulation softwares, NEUI developed NEUI500kA class high-efficient reduction cell technology, and successfully resolved the problems with increasing of amperage capacity, current density and cell span. Compared with NEUI400kA class cell technology, better simulation results were obtained. The economic and security of busbar is more better; and the cell current deviation of two sides is less than 0.5%, cathode busbar voltage is lower than 200mV, |Bz|ave is less than 3.14Gs, and vertical magnetic gradient is less than 3.1Gs. Interface deformation is more smaller, and MHD stability is further improved. Ideal thermal balance and uniform pressure distribution of the cell were obtained. Furthermore, more greater intensity and economical tube truss superstructure was adopted.

11:40 AM

An Innovative Approach to Improving the Operational Performance of Aluminum Smelters: Nelson Dubé¹; Thiago Heitling¹; ¹SNC-Lavalin

The efficient operation of an aluminum smelter necessitates that all production activities have to be executed perfectly to ensure an optimum operation. In today's competitive environment, all aluminum smelters need to continually look for improvement opportunities in order to achieve better profitability and market position. The innovative Plant Optimization Services, developed by SNC-Lavalin, is aimed at assisting aluminum smelter personnel in their plant operational debottlenecking and performance improvement processes. The methodology takes an integrated approach - combining the elements of process management, production process analysis, and equipment management. This paper presents the methodology, the analysis outputs, and the implementation of changes.

Battery Recycling: Session I

Sponsored by: The Minerals, Metals and Materials Society, TMS Extraction and Processing Division, TMS Light Metals Division, TMS Electronic, Magnetic, and Photonic Materials Division, TMS: Recycling and Environmental Technologies Committee, TMS: Energy Conversion and Storage Committee *Program Organizers:* Gregory Krumdick, Argonne National Laboratory; Linda Gaines, Argonne National Laboratory

Wednesday AM	Room: 12
March 2, 2011	Location: San Diego Conv. Ctr

Session Chairs: Gregory Krumdick, Argonne National Laboratory; Linda Gaines, Argonne National Laboratory

8:30 AM Introductory Comments

8:35 AM

Taking a Life Cycle Approach to Battery Management: *Mira Inbar*¹; ¹Dow Kokam

The end of a battery's life is a topic of much interest and debate. Will batteries be recycled or reused after they have reached 80% capacity in vehicles? We argue that the end of a battery's life must be conceived in the early design of the battery system and implemented throughout the battery's life cycle. Inherent in good battery design is a deep understanding of the environmental tradeoffs involved in a battery life cycle: from material sourcing, to manufacturing, to use, to end-of-life management. Dow Kokam is undertaking a Life Cycle Analysis, using the GaBi software, to quantify the environmental impacts and benefits (greenhouse gases, water, particulates, etc) from cradle to grave. This analysis will give us a detailed understanding of the "hot spots" in the environmental profile of our battery systems and how certain parameters in battery production influence the environmental profile.

8:55 AM

Role of Recycling in the Life Cycle of Batteries: John Sullivan¹; Linda Gaines¹; Andrew Burnham¹; ¹Argonne National Laboratory

Over the last few decades, rechargeable battery production has increased substantially. Applications including phones, computers, power tools, power storage, and partially to fully electric vehicles are either commonplace or will be in the next decade or so. Because advanced rechargeable batteries, like nickel metal hydride or lithium ion systems, consist of less-plentiful and comparatively expensive materials (e.g., nickel, cobalt, cadmium, misch metal) that often require considerable energy to be formed into battery components, battery recycling has the potential to significantly reduce the burdens associated with the life cycle of batteries. The key issue is, therefore, to determine the most practical type of recycling. Is it feasible to recover such components as anodes, cathodes, and electrolytes, or should the elements be recovered? Estimates of the impacts of battery recycling are given.

9:15 AM

Treatment or Recycling End-Of-Life (H)EV Battery Packs: Mark Caffarey¹; ¹Umicore USA

To understand the processing options for an end-of-life (H)EV battery pack, it is important to compare the Treatment process as it is known today with the Umicore UHT process. The Ultra High Temperature process allows for maximum recycling while allowing minimal air emissions and waste generation. The UHT process is the only process that returns the metals contained to their elemental phase thus allowing for a recycled battery material equal to primary material. A description of the new Umicore facility is given (7,000 tons of batteries per year) with its inputs and outputs as well as a Life Cycle Analysis illustrating process benefits on the short and long term for the battery industry and society as a whole. Opportunities to build on the UHT process with additional recycling options such as for Lithium and Rare Earths show that this can serve as a building block for further recycling improvements

9:35 AM

Evaluation of Environmental Tradeoffs in Portable Battery Recycling: *Elsa Olivetti*¹; Gabrielle Gaustad²; Randolph Kirchain¹; ¹Massachusetts Institute of Technology; ²Rochester Institute of Technology

Approximately 80% of portable batteries manufactured in the US are primary alkaline batteries with a global annual production >10 billion. The majority of these batteries go to landfills at end-of-life (EOL). An increased focus on environmental issues related to disposal combined with recently implemented EOL directives in the EU and Canada, has intensified interest in quantifying optimal EOL routes for both primary and secondary batteries. Careful evaluation of the environmental impacts of battery recycling is critical to determining the conditions under which recycling is most beneficial. The magnitude of portable batteries that are retired each year, variation in material composition between different battery types, and the broad dispersion of those batteries makes the logistics of efficient battery collection challenging. This research investigates environmental tradeoffs within collection and recycling systems for the recovery of materials in EOL batteries. Analysis compares alkaline battery recycling challenges to other chemistries, including rechargeable Li-ion systems.

9:55 AM

Managing Hybrid Electric Batteries at End of Life: *Todd Coy*¹; ¹Kinsbursky Brothers / Toxco

Hybrid systems are commonplace with a variety of models available from different manufacturers. As these vehicles start to age, the management of the battery system has surpassed the contingency planning stage and is now a reality that the auto manufacturer, dealership service centers, must take into consideration when replacing older hybrid battery systems. Automotive Dismantlers must also be aware of the hazards that these batteries present if batteries are not removed prior to their receipt at a dismantlers facility. The recovery and proper handling of batteries is a complicated task for persons not aware of the regulatory requirements for managing hazardous materials. This is true for companies located in California, as California maintains one of the strictest regulatory code systems in the United States. Navigating these environmental regulations, as they pertain to the proper management and disposal of end of life batteries can be an arduous undertaking.

10:15 AM Break

10:25 AM

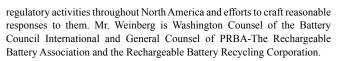
The 10 Obstacles to a Successful Battery Recycling Program: The North American Experience: Lisa Pollack¹; *Carl Smith*¹; ¹Call2Recycle

Battery recycling in North America has reached adolescence. Retailers are demanding collection programs that can be incorporated into overall corporate sustainability programs. Consumer education is difficult to track and expensive. Municipalities are slow to take action, but require worldclass results. There are no uniform success metrics. Furthermore, the effort required to indulge politicians, corporate sustainability executives, manufacturers, consumers and environmentalists isn't paying off in collection results. How can battery recyclers overcome the obstacles of "puberty" and ensure a successful, long-term program? Carl Smith, CEO of Call2Recycle®, will offer an overview of the battery recycling industry's evolving landscape including: how recent legislation in North America will affect international battery recycling initiatives; why product stewards must work together to develop measurement standards; why the latest battery chemistry advancements aren't as exciting as they seem; and how battery industry stakeholders can help lift the burden from manufacturers and share end-of-life responsibilities.

10:45 AM

Product Stewardship Pressures on the Lead and Motive Power Battery Industries: *David Weinberg*¹; ¹Wiley Rein LLP

This presentation will address challenges to the world's most successful recycling programs – those related to lead acid batteries – and the quickly expanding realm of EV, HEV and other motive power batteries that arise from the uniformed fervor of "product stewardship" advocates and outdated hazardous materials transportation regulations. It will cover legislative and



140th Annual Meeting & Exhibition

11:05 AM

A Preliminary Investigation for Spent LIBs Recycling: Mengjun Chen¹; Fu-shen Zhang²; Jianxin Zhu²; ¹Southwest University of Science and Technology; ²Research Center for Eco-Environmental Sciences, Chinese Academy of Sciences

Spent lithium-ion secondary battery (LIB) is one important kind of waste electric and electronic equipment (WEEE). At present, technologies available for spent LIBs recycling include chemical deposition, solvent extraction, Etoile-Rebatt process, electrodeposition, floatation and ion-exchanging. In this paper, a novel vacuum-aided pyro-metallurgical process for recovery metallic Co directly from waste LIBs was presented. The experiment results showed that 1) the decomposition and reduction rates of LiCoO2 increased with the increase of experiment temperature; and 2) metallic Co can be recovered successfully when the experiment temperature was higher than 700° and the system pressure was maintained at 10 Pa. XRD and SEM results obtained at different temperatures showed that, in this paper, LiCoO2 was first reduced to CoO at a lower temperature and then it was reduced to metallic Co as the increase of temperature. This vacuum-aided pyrometallurgical process might be a promising one for spent LIBs recycling.

11:25 AM

Recovery of Metal Values from Waste Cathode Active Material Using Organic Acid as Leachant and Its Application to Synthesis of LiCoO2: *Hyun-Jong Kim*¹; Seong Ho Son¹; Chi Ho Shin¹; Howard Lee²; ¹Korea Institute of Industrial Technology; ²OSC Co., Ltd.

Since lithium ion batteries (LIBs) consist of heavy metals, organic chemicals and plastics, the recovery of major spent cell components is beneficial in terms of environmental protection and also for the provision of raw materials. In this study, environmentally benign organic acids were used to recover the cobalt and lithium from cathode materials of LIBs. Various organic acids, including acetic acid, citric acid, and taurine, etc., were tested as a function of leachant/reductant concentration and temperature. As a heating process, autoclave could highly improve the leaching efficiency up to over 90%. In a view point of the LiCoO2 synthesis, acetic acid was favorable since the metal acetate could be easily used in sol-gel reaction. The leached cobalt acetate solution was directly supplied to prepare the LiCoO2 powder. Battery charge-discharge experiments showed very promising results for the recycle of LIBs.

11:45 AM Concluding Comments

Sponsored by: The Minerals, Metals and Materials Society, TMS Electronic, Magnetic, and Photonic Materials Division, TMS Structural Materials Division, TMS: Biomaterials Committee *Program Organizers:* Jamie Kruzic, Oregon State University; Nima Rahbar, University of Massachusetts, Dartmouth; Po-Yu Chen, University of California, San Diego; Candan Tamerler, University of Washington

Wednesday AM	Room: 15A
March 2, 2011	Location: San Diego Conv. Ctr

Session Chairs: Po-Yu Chen, University of California, San Diego; David Kisailus, University of California, Riverside

8:30 AM Keynote

Turning Weakness into Strength: Explaining the Great Strength and Extensibility of Spider Silk: *Markus Buehler*¹; ¹Massachusetts Institute of Technology

Biology creates hierarchical structures, where initiated at nano scales, are exhibited in physiologically materials to provide structural support, force generation, catalytic properties or energy conversion. Spider silk is one of the strongest, most extensible and toughest biological materials, exceeding the properties of many engineered materials including steel. The issue is particularly puzzling since despite its great strength, spider silk is made of weak hydrogen bonds. We discovered that the great strength and extensibility of spider silk can be explained based on the particular structural makeup of the material, which involves several hierarchical levels from the nano- to the macro-scale. Our work unveils the material design strategy that enables silks to achieve superior material performance despite simple and inferior material constituents. This concept could lead to a new materials design paradigm, where enhanced functionality is not achieved using complex building blocks but rather through the utilization of simple repetitive constitutive elements.

9:10 AM Invited

Biomechanics of Cancer Cells: Chwee Teck Lim¹; ¹National University of Singapore

During the onset of a disease, a cell may experience alterations in both the composition and organization of its cellular structures. These alterations may eventually manifest as changes in the mechanical properties such as cell deformability and cell adhesion. With the recent advancements in micro/ nanotechnology and biophysical techniques, we can now probe and study mechanical property changes in individual cells and even proteins. In fact, knowing the effect of mechanical forces acting on cells can reveal ways by which diseased cells differ from healthy ones. This can help us better understand and establish possible connections between change in mechanical properties of cells and the onset and progression of human diseases. Here, we will highlight studies on cancer using techniques such as atomic force microscopy, microfluidics, cell migration and cell adhesion assays among others. It is hoped that from these studies, new and effective diagnostics for disease detection may be developed.

9:40 AM

On the Structure and Mechanical Behavior of Scales from Cyprinus Carpio: Adriana Garrano¹; *Dwayne Arola*²; ¹University of Catania; ²University of Maryland Baltimore County

In this investigation the microstructure and mechanical behavior of scales from Cyprinus Carpio (i.e. the common freshwater carp) were evaluated. Uniaxial tensile specimens were prepared from extracted scales and the constitutive behavior was characterized in the hydrated and dehydrated conditions and as a function of anatomic position (i.e. from head to tail). Dehydration was achieved using selected polar solvents. In the hydrated condition the scales exhibited an average tangent modulus of E < 0.5 GPa, ultimate strength of suts $^{\circ}60$ MPa and strain to failure of emax $^{\circ}12\%$. Though dehydration caused significant changes in the elastic modulus (factor of 2

or more), the change in strength and strain to fracture was less substantial. There was some variation in the properties as a function of location, which appeared to correlate with the microstructure. Fish scales may provide a new model for compliant material designs requiring toughness and penetration resistance.

10:00 AM

Mechanical Properties and Laminate Structure of Arapaimas Gigas Scale: Yen-Shan Lin¹; *Marc.A Meyers*¹; Eugene.A Olevsky¹; ¹UCSD

The Arapaimas is one of the largest freshwater fish with a length of more than 2m, living in Amazon river. Their armor-like scales with laminate structure protects them from being attacked by the piranha. The scales are made by collagen and composed of highly mineralized external layer and soft internal layers. In this study, the mechanical properties and structure were investigated. The micro-hardness value of the external layer (550MPa) is higher than internal layer (200MPa) due to the higher mineral content in external layer. Tensile strength is higher in dry condition (53MPa) than in wet condition showing that hydration plays an important role in mechanical properties of the scales. The fracture surface investigated by SEM indicates that the pull-out collagen fibers is the main fracture mechanism. The structure of the demineralized scale exhibits 67-nm periodicity on the collagen fiber. And the deproteinated scale shows randomly orientation plate with 10nm thickness.

10:20 AM Break

10:30 AM Invited

Biological Materials: A Materials Science Approach: *Marc Meyers*¹; Po-Yu Chen¹; Maria Lopez¹; Yasuaki Seki¹; Albert Lin¹; Joanna McKittrick¹; ¹University of California, San Diego

The approach used by Materials Science and Engineering is revealing new aspects in the structure and properties of biological materials. The integration of advanced characterization, mechanical testing, and modeling methods can rationalize heretofore unexplained aspects of these structures. As an illustration of the power of this methodology, we apply it to biomineralized shells, avian beaks and feathers, and fish scales. We discuss removable attachment devices, focusing on the gecko, the abalone, and the Brazilian tree frog. We also present a few selected bioinspired applications: Velcro, an Al2O3-PMMA composite inspired on the abalone shell, and synthetic attachment devices inspired by the gecko. Research is supported by the NSF Grant DMR 1006931.

11:00 AM

Dynamic Mechanical Behavior of Shark Tessellated Skeleton: *Xiaoxi Liu*¹; Hamed Youssefpour¹; Mason Dean²; Adam Summers³; James Earthman¹; ¹University of California, Irvine; ²Max Planck Institute of Colloids and Interfaces; ³University of Washington

Much of the skeleton of sharks is characterized by a tessellated structure, comprised of mineralized tiles of hydroxyapatite called tesserae covering a soft hyaline cartilage core. The significance of this skeletal tissue type has not been well understood, particularly with regard to any mechanical advantages provided by the tiled structure. In the present work, dynamic mechanical behavior of blue shark tessellated cartilage was studied by performing both stress relaxation and percussion tests. Results from these tests indicate that tessellation strongly influences the dynamic stiffness and damping capacity of shark cartilage under loading that is parallel to the tessellated layer, while it has little effect on either of these properties under normal loading or impact. These findings reveal plausible advantages of shark tessellated skeletons: 1) allowing efficient movement and feeding activity; 2) reducing the risk of failure by lowering impact forces normal to the surface and effectively dissipating impact energy.

11:20 AM

Structure and Mechanical Behavior of Saxidomus Purpuratus Shells: Wen Yang¹; Marc Meyers¹; Guang-Ping Zhang²; Xiao-Wu Li³; ¹University of California, San Diego; ²Institute of Metal Research, Chinese Academy of Sciences; ³College of Sciences, Northeastern University

The structure and mechanical behaviour of Saxidomus purpuratus bivalve shell were investigated. The inner and middle layers have a cross-lamellar structure, while the outer layer has porosity and does not have tiles, but 'blocky' regions. That leads to structure-dependent hardness. The hardness of outer layer decreases significantly compared with those of inner and outer layers, especially in the plane view. The compressive strength along the three different loading directions exhibits a significant difference. The cracking paths were found to be closely related to the loading direction. The Weibull strength at 50% of the probability of failure, with the loading direction perpendicular to the surface of the shell is much less than those in the other two orientations in shell plane loading. These differences are interpreted in terms of the anisotropic structures. Moreover, high cycle fatigue behavior was also be investigated by three point bending testing through gradually increasing load method.

11:40 AM

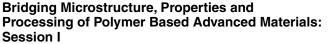
Unveiling the Deformation and Toughening Mechanisms of Nacre – Lessons from Nature: Xiaodong Li¹; ¹University of South Carolina

Nacre is a natural nanocomposite with superior mechanical strength and toughness. What is the secret recipe that Mother Nature uses to fabricate nacre? What roles do the nanoscale structures play in the inelasticity and toughening of nacre? Can we learn from this to produce nacre-like nanocomposites? The recent discovery of nanoparticles in nacre is summarized, and the role these nanoparticles play in nacre's toughness is elucidated. It was found that rotation and deformation of aragonite nanoparticles are the two prominent mechanisms contributing to energy dissipation in nacre. The biopolymer spacing between nanoparticles facilitates the particle rotation process. Individual aragonite nanoparticles are deformable. Stacking fault and dislocation formation together with deformation twinning were found to play an important role in the plastic deformation of individual nanoparticles. This talk also presents future challenges in the study of nacre's nanoscale structure and mechanical properties.

12:00 PM

On the Growth and Mechanical Behavior of Abalone Nacre: Role of Organic Constituent: *Maria Lopez*¹; Po-Yu Chen¹; Laura Connelly¹; Ratnesh Lal¹; Joanna McKittrick¹; Marc Meyers¹; ¹UCSD

Characterization of the growth surfaces removed from red abalone (Haliotis rufescens) shells is performed. Abalone shell is demineralized exposing the chitin matrix and its structural and mechanical components are analyzed. The details of the mineral and organic layer surface are revealed by atomic force microscopy (AFM) and scanning electron microscopy. AFM pull-off and nanoindentation experiments are performed on the organic interlayer. Indentation of the organic layer provides a force-deflection curve that can be expressed as tension on a centrally-loaded membrane. The effect of hydration of organic layer is revealed. Results allow insight to the biomineralization mechanism, further explaining the influence of the organic component in the process.



Sponsored by: The Minerals, Metals and Materials Society, TMS Extraction and Processing Division, TMS Materials Processing and Manufacturing Division, TMS: Materials Characterization Committee, TMS: Shaping and Forming Committee, ASM-MSCTS: Texture and Anisotrophy Committee

Program Organizers: Dongsheng Li, Pacific Northwest National Laboratory; Said Ahzi, University of Strasburg; Moe Kahleel, Pacific Northwest National Laboratory

Wednesday AM	Room: 32B
March 2, 2011	Location: San Diego Conv. Ctr

Session Chair: Said Ahzi, University Louis Pasteur, Strasbourg

8:30 AM Introductory Comments

8:35 AM Keynote

Constitutive Modeling of Deformation Behaviour of Semicrystalline Polymers under Small Strains: Stanislav Patlazhan¹; Yves Remond²; ¹Russian Academy of Sciences; ²University of Strasbourg

The constitutive modelling of tensile deformation behaviour of semicrystalline polymers under small strains is discussed. The heterogeneous materials are treated within the two-phase model comprised of the crystalline elastoplastic component imbedded into the soft amorphous domain. Structural transformations between the hard and soft components are assumed to obey thermofluctuation mechanisms. The plastic flow is supposed to occur within the hard component due to the inter- and intralamellar sliding. One-dimensional basic structural-mechanical element (BSME) as the structure-sensitive model of the deformed material is analysed in the limits of linear and nonlinear dependences on the applied stresses. Our analysis and results suggest that instead of a single element, the spectrum of the interacting BSME of different structural-mechanical properties reflecting strong heterogeneity of semicrystalline polymers should be considered. This approach is shown to provide the best fitting of tensile behaviour of iPP at different strain rates below the yield point.

9:05 AM

Molecular Dynamics Simulation of Diffusion of Atmospheric Penetrates in Polydimethylsiloxane based Nanocomposites: Alexander Sudibjo¹; Varun Ullal¹; *Douglas Spearot*¹; ¹University of Arkansas

Molecular dynamics (MD) simulations are used to study the nanoscale mechanisms associated with diffusion of small atmospheric penetrates in polydimethylsiloxane (PDMS) based nanocomposites with metallic inclusions. PDMS is modeled within the MD framework using a hybrid coarse-grained interatomic potential which retains atomic distinction along the siloxane backbone but models the methyl side groups as united atoms. In a novel contribution, crosslinking is incorporated into the nanocomposite model via the introduction of tetra(dimethylsiloxy)silane crosslinking agents combined with silanol-termined PDMS chains. Diffusion-related material properties are extracted over a range of temperatures for both N2 and O2 penetrates, allowing for the calculation of diffusion constants and activation energies using an Arrhenius style equation. Ultimately, these calculations are motivated by the need to calibrate a recently developed PDMS-based sensor, where metallic nanoparticles are embedded within a PDMS matrix.

9:25 AM

Nanostructuration of Polymers for Energy, Drug Delivery and Bio-Implant Systems: *Frédéric Addiego*¹; Marc Michel¹; Valérie Toniazzo¹; David Ruch¹; ¹CRP Henri Tudor

The search for a method to design nanostructures from a variety of materials is of growing interest. As the commercialization of nanotechnology continues to expand, the ability to translate design methods from a laboratory to applications is of increasing significance. In our Institute, we examine several of the most readily scalable bottom-up methods for the fabrication of such structures made of particles and polymers. In this frame, we propose to employ versatile and straightforward methods of processing (layer-by-layer, plasma polymerization and extrusion) allowing to fabricate materials whose architectures and properties make them suitable for energy, drug delivery and bio-implants development.

9:45 AM

140th Annual Meeting & Exhibition

A Bilinear Semi-Empirical Constitutive Model for an Orthotropic Material: Edmond Saliklis¹; Jorien Baza¹; ¹California Polytechnic State University

This study developed a nonlinear constitutive model for a sustainable orthotropic material. The model is semi-empirical in that it is grounded in mechanics principles but it was slightly modified to capture the behavior of a specific nonlinear material. The material is an extruded composite made of a recycled polypropylene homopolymer reinforced with the agricultural fiber kenaf. Fifty-six tension tests were performed to solve for Young's modulus at various angles to the primary axis of the material. These experimentally obtained values formed the basis of the body of data used to create the new constitutive model. The new constitutive model simplified the nonlinear stress-strain relationships into bilinear stress-strain curves. The "break" in the bilinear curve is based on strain energy principles. The proposed constitutive model captures the modulus of elasticity through any angle from the primary extruded axis and comparisons of the model to experimental data will be shown.

10:05 AM Break

10:20 AM

FabricationandCharacterizationofSuperStrongCelluloseNanowhiskerPaper:DongshengLi¹;HamidGarmestani²;¹PacificNorthwestNational Laboratory;²Georgia Institute of TechnologyPacific

Effective property prediction is the cornerstone for performance evaluation of materials applied under irradiation condition. Phase field model and molecular dynamics model are used to predict the microstructure and local properties. Different methods have been developed to bridge low scale models with polycrystalline level models. Finite Element Analysis (FEA), microstructure informed FEA, self consistent models, Taylor models, Sachs models and statistical continuum mechanics are evaluated. Cost, efficiency and accuracy were compared for these methods. Pros and cons, depending on the problems studied, are discussed. While open to discussion, general recommendation on bridging methodology is presented based on different scenarios.

10:40 AM

Fully Recoverable High Strain Shape Memory Polymers: *Walter Voit*¹; Taylor Ware¹; Ken Gall²; ¹UT Dallas; ²Georgia Tech

Shape-memory polymers (SMPs) with recoverable strains of more than 800%, twice the previously published literature value, are demonstrated. SMPs are self-adjusting, smart materials in which shape changes are controlled at specific, tailored temperatures. We adjust the glass transition temperature (Tg) between 28 °C and 55 °C through synthesis of copolymers of methyl acrylate, methyl methacrylate and isobornyl acrylate. SMPs with both crosslinker densities and photoinitiator concentrations optimized at fractions of a mole percent, demonstrate fully recoverable strains at 807% for a Tg of 28 °C, at 663% for a Tg of 37 °C and at 553% for a Tg of 55 °C. We synthesized a novel compound, 4,4'-di(acryloyloxy)benzyl, polymerized it into acrylate SMPs and characterized the resulting polymer which yielded fully recoverable strains above 500%. These materials are intended to enable future applications where recoverable high strain capacity and the ability to accurately and independently position Tg are required.

11:00 AM

Hydroxyapatite Reinforced Polymer Biocomposites with Tailored Mechanical Properties through Microstructure Design: *Ryan Roeder*¹; Timothy Conrad¹; Jeffrey Vitter¹; Justin Deuerling¹; ¹University of Notre Dame

Hydroxyapatite (HA) reinforced polymers were first conceived as a bone-analog biomaterial enabling mechanical properties to be tailored to mimic those of bone tissue, but have generally fallen short of bone tissue at comparable levels of porosity and HA content. Recently, dense or porous HA whisker reinforced polyaryletherketone (PAEK) biocomposites have been engineered to mimic the elastic properties human bone tissue. Novel powder processing and compression molding methods enabled the dispersion of high volume fractions of HA reinforcements. Single crystal HA whiskers enabled improved load-transfer from the matrix to reinforcement, resulting in significantly improved static and fatigue properties when directly compared to equiaxed powder reinforcements. A multiscale, micromechanical model was also developed to accurately predict the anisotropic elastic constants from the HA whisker volume fraction, aspect ratio distribution, and orientation distribution.

11:20 AM

Computer-Aided Design, Processing and Characterization of Polymer-Matrix Magnetic Composites: *Tianle Cheng*¹; Jie Zhou¹; Yu Wang¹; ¹Michigan Technological University

Diffuse interface field models of magnetic particle self-assembly and polymer-matrix magnetic composites are developed to study the processingmicrostructure-property relationships and the underlying mechanisms. Ferro-colloidal processing under external magnetic field is investigated as a fabrication route to particle-matrix microstructure control. Directed self-assembly of dipolar interacting particles in uncured polymer matrix is simulated to understand the mechanisms responsible for controlled formation of particulate microstructures. The simulated evolution of particle microstructures during composite fabrication process is seamlessly incorporated into the magnetic composite model to perform in-situ property characterization, which provides a way for real-time monitoring of microstructure optimization. It is shown that, with the gradual formation of aligned particles into fibrous microstructures along external field direction from randomly-dispersed initial state, the effective composite properties develop strong magnetic anisotropy. The effects of composite microstructures on the effective magnetic properties are discussed.

11:40 AM

Effects of Filler Microstructures on Effective Properties of Magnetic Composites: Phase Field Modeling and Simulation: *Jie Zhou*¹; Tian-Le Cheng¹; Yu Wang¹; ¹Michigan Technological University

Phase field model is developed to calculate heterogeneous distributions of magnetization and magnetic field and effective susceptibility of magnetic composites with arbitrary multi-component microstructures, where interphase boundary conditions are automatically satisfied without explicitly tracking inter-phase interfaces in the composites. Computer simulation is performed to study the relationships between filler microstructures and effective properties of magnetic composites. Composites composed of paramagnetic, superparamagnetic and non-magnetic (diamagnetic) constituent components are considered. Various factors associated with filler microstructures are investigated, including particle size, shape, orientation, volume fraction, spatial arrangement and directional alignment. It is found that dipole (and multipole) interactions among high-susceptibility fillers and the resultant effective demagnetization factors of filler ensembles play critical roles in determining the composite properties, which sensitively depend on filler arrangement and, especially, directional alignment into fibrous microstructures (chains). Such microstructurally engineered composites, whose fillers are not randomly dispersed, exhibit strong magnetic anisotropy despite all constituent components are isotropic.

Bulk Metallic Glasses VIII: Fatigue and Corrosion *Sponsored by:* The Minerals, Metals and Materials Society, TMS Structural Materials Division, TMS/ASM: Mechanical Behavior of Materials Committee

Program Organizers: Gongyao Wang, University of Tennessee; Peter Liaw, Univ of Tennessee; Hahn Choo, Univ of Tennessee; Yanfei Gao, Univ of Tennessee

Wednesday AM	Room: 6D
March 2, 2011	Location: San Diego Conv. Ctr

Session Chairs: Y. Yokoyama, Institute for Materials Research; Jamie Kruzic, Oregon State University

8:30 AM Invited

Fracture and Fatigue in Monolithic and Composite Metallic Glasses: *Robert Ritchie*¹; Maximillien Launey²; Douglas Hofmann³; William Johnson³; ¹University of California Berkeley; ²Lawrence Berkeley National Laboratory; ³California Institute of Technology

The mechanical properties of bulk metallic glasses (BMG) are often plagued by low fracture and fatigue resistance. Correspondingly, much effort in recent years has been devoted to improving their damage tolerance properties, either through compositional changes or by introducing some degree of microstructure. By matching the microstructural length scales (of a second phase) to mechanical crack-length scales, metallic glass matrix composites can demonstrate strongly improved tensile ductility, toughness, and fatigue resistance. These improvements are explained by the effect of the mechanically soft and ductile second phase, which acts stabilizing against shear localization and critical crack propagation; it results in extensive plastic shielding, which further stabilizes crack growth. In this talk, the fracture and fatigue behavior of semi-solidly processed Zr- and Tibased BMG matrix composites with in-situ dendritic phase were examined. Specifically resistance-curve, fatigue crack-growth, and stress-life behavior are here presented in light of the relevant toughening and fatigue mechanisms involved.

8:50 AM

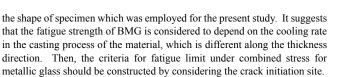
Zr-Based Glass-Forming Film for Fatigue-Property Improvements of 316L Stainless Steel: Annealing Effects: Jinn P. Chu¹; *Cheng-Min Lee*¹; R. T. Huang²; Jia-Hong Zhu¹; Peter. K. Liaw³; ¹Nation Taiwan University of Science and Technology; ²National Taiwan Ocean University; ³The University of Tennessee

When annealed in the supercooled liquid region (\Box T), $Zr_{53}Cu_{29}Al_{12}Ni_6$ metallic glass thin film exhibits a uniform structure relative to the metastable as-deposited film because of the annihilation of the columnar structure. Microstructure became condensed due to the structure relaxation and free volume equilibrated in the annealed film. Therefore, it is expected that the annealed Zr-based glass-forming film would improve mechanical properties such as high strength, enhanced ductility, and smooth surface, along with good adhesion to the substrate. These properties are considered to be key factors that will improve the fatigue resistance of materials. A fatigue test of coated 316L stainless steel was carried out. Under a stress of 750 MPa, the fatigue life was improved from 4.4 x 10⁵ cycles of the uncoated sample by ~10 times to 4.5 x 10⁶ cycles, and further improved by more than 22 times to 10⁷ cycles when the annealing was applied.

9:00 AM Invited

Fatigue of Zr-Based Bulk Metallic Glass under Cyclic Shear Stress: Yoshikazu Nakai¹; Kenich Nakagawa¹; Kohei Mikami¹; ¹Kobe University

Fatigue strength of Zr-based bulk metallic glass plate with rectangular cross-section was conducted under cyclic torsion to reconcile the applicability of fracture criteria. A computer-controlled direct drive motor driven fatigue testing machine was developed for the tests. The stress ratio, R, was -1 and the loading frequency was 10 Hz. It was found that fatigue cracks initiated from the center of the side surface although the maximum shear stress was higher at the center of plate surface than that at the center of side surface for



9:20 AM Invited

Fatigue Crack Growth in Zr-Based Bulk Metallic Glasses: Jamie Kruzic¹; Sarah Philo¹; Maximilien Launey²; ¹Oregon State University; ²Lawrence Berkeley National Laboratory

Fatigue crack growth rates were measured for $Zr_{44}Ti_{11}Ni_{10}Cu_{10}Be_{25}$ and $Zr_{58,5}Nb_{2,8}Cu_{15,6}Ni_{12,8}Al_{10,3}$ bulk metallic glasses (BMGs). Growth rate data overlapped considerably for both. The former BMG was tested in different initial free volume states, different residual stress states, and in both ambient air and dry nitrogen environments. Fatigue crack growth rates were relatively unaffected by the initial free volume state. This was attributed to the formation of a fatigue transformation zone of increased local free volume at the fatigue crack tip. When residual stresses were not annealed out, it was found that the fatigue threshold and fracture toughness increased due to residual compressive stresses at the sample surfaces. Finally, it was observed that testing in a dry nitrogen environment significantly increased the fatigue threshold, suggesting a corrosion fatigue mechanism in ambient air. A similar environmental effect was observed for the Zr-Nb-Cu-Ni-Al BMG in ambient air, but at very different growth rates.

9:40 AM

The Effect of Structural Ordering on Active, Passive and Localized Corrosion in an Amorphous Cu75Hf20Dy05 Alloy: Derek Horton¹; John Scully¹; ¹University of Virginia

The role of structural change on the corrosion properties of amorphous alloys is unclear. An amorphous material that undergoes devitrification without changing composition is an ideal specimen to reveal the effect of structural ordering on corrosion properties in the absence of an accompanying chemical partitioning. This study focuses on the Cu75Hf20Dy05 amorphous alloy systems which undergoes single phase devitrification to a stoichiometrically equivalent solid solution. The global corrosion behavior of this system was studied during active, passive, and passive/pitting conditions. The results indicate that the ordered crystal structure plays a dominant role in the corrosion behavior due to the periodic presence of beneficial solute atoms which can enhance (a) oxide formation, (b) impeded dissolution, (c) and alter surface diffusion.

9:50 AM Invited

Why Can't The Excellent Corrosion Resistance of Amorphous and Amorphous-Nanocrystalline Melt Spun Alloys be Achieved in Thermally Sprayed Coatings?: *J.R. Scully*¹; N. Tailleart¹; T. Aburada¹; D. Horton¹; R. Huang¹; A. Lucente¹; ¹University of Virginia

We have previously investigated the corrosion resistance of selected aluminum, transition metal, rare earth metallic glass alloys(Al-Co-Ce,Al-Fe-Gd, Al-Ni-Y)in the form of ribbons spun from the molten state. These have been analyzed in the as-spun amorphous, relaxed amorphous, amorphous +nano-crystalline,and fully crystalline states. Results suggest that certain structural and/or chemical non-uniformities strongly affect corrosion resistance while other defects are not detrimental at certain length scales. These findings were compared to results on low porosity Al-Co-Ce metallic coatings applied to various substrates deposited using a pulsed thermal spray(PTS) process.Coating thicknesses ranged from 100 to 500 □m. Coatings were characterized using a variety of metallurgical and corrosion methods. The localized corrosion properties of the PTS applied coating samples were inferior to those of compositionally equivalent fully amorphous melt spun ribbons even when synthesized using the same feedstock powders. The inferior corrosion behavior in coatings was traced to presence of certain metallurgical and physical defects but not others.

10:10 AM Break

10:20 AM

140th Annual Meeting & Exhibition

Investigation of the Corrosion Behavior of a Zr-Based Bulk Metallic Glass: *Courtney Harmon*¹; Mary Cavanaugh¹; Katharine Flores¹; Rudolph Buchheit¹; ¹The Ohio State University

While research has proven the exceptional mechanical properties of bulk metallic glasses (BMG's), little is known about the corrosion properties of Zr-based BMG's. The corrosion behavior of a $Zr_{58,5}Nb_{2,8}Cu_{15,6}Ni_{12,8}AI_{10,3}$ BMG exposed to dilute chloride solutions with pH values ranging from 2 to 12 was characterized by cyclic polarization. Results showed that the glass is spontaneously passive across this pH range exhibiting passive current densities less than 1 μ A/cm² between pH 2 and 10, and only slightly greater at pH 12. Passive film breakdown occurred during anodic polarization with breakdown potentials ranging from -0.05 to -0.15 V_{see} from pH 2 to 10 with a significant increase to +0.45 Vsce at pH 12. Repassivation occurred at about -0.20 V_{see} and did not appear to vary with solution pH. Additionally, free corrosion exposure experiments were performed to characterize corrosion mode and morphology as a function of pH and results are to follow.

10:30 AM Invited

Characterization of Shear Bands Induced by Three-Point Bending Fatigue Test in Zr-Cu-Al Bulk Metallic Glass: *Pei-Ling Sun*¹; Gongyao Wang²; Peter Liaw²; ¹Feng Chia University; ²University of Tennessee

Zr50Cu40Al10 bulk metallic glass was deformed by three-point bending fatigue test. Shear bands appeared on the tension and compression sides after deformation. Characterization of these shear bands by scanning electron microscopy (SEM) reveals the presence of different fracture modes: river pattern and smooth fracture path. Cross sections of the shear bands were then cut by focused ion beam (FIB) for transmission electron microscopy (TEM) observation. The microstructure of the shear bands will be investigated in detail and the deformation mechanism will be discussed.

10:50 AM

Four-Point-Bending Fatigue Study on a Tough Fe-Based Bulk-Metallic Glass: *Gongyao Wang*¹; Marios Demetriou²; Peter Liaw¹; William Johnson²; ¹University of Tennessee; ²Keck Laboratory

Amorphous steel alloys of Fe-(Mo,Ni,Cr)-(C,B)-P have recently been developed. These Fe-based bulk metallic glasses exhibit low shear moduli, high toughness, and good glass-forming ability. In the current investigation, Fe70Mo5Ni5C5B2.5P12.5 glassy rods with 3 mm in diameter were fabricated and then polished to $2 \times 2 \times 25$ mm3 rectangular beam samples. Four-point-bending fatigue experiments are performed on these Fe70Mo5Ni5C5B2.5P12.5 beam samples in air. The applied stress versus cycles to failure (S-N) curve will be presented. Moreover, a mechanistic insight into the mechanism governing the fatigue failure in a low-shearmodulus high-toughness Fe-based bulk-metallic glasses will be proposed. Acknowledgement: This work is financially supported by the US National Science Foundation, under CMMI-0900271 and DMR-0909037, with Drs. C. V. Cooper, Dr. D. Finotello, and Dr. A. Ardell as contract monitors.

11:00 AM Invited

Compression-Compression Fatigue Behaviour of Zr-Based Bulk Metallic Glass (BMG): The Effects on the Near-Surface Residual-Stresses: *Bartlomiej Winiarski*¹; Gongyao Wang²; Yoshihiko Yokoyama³; Peter Liaw²; Philip Withers¹; ¹University of Manchester; ²The University of Tennessee; ³Tohoku University

The influence of compression-compression fatigue conditions on evaluation of near-surface residual stresses (RS) in rod-like $Zr_{50}Cu_{30}Al_{10}Ni_{10}$ bulk metallic glass (BMG) was studied. The fatigue tests were conducted at ambient temperature, with a maximum stress of 1525 MPa. After the fatigue experiment residual-stresses were inferred locally, in volumes about 20 × 20 × 5 µm³, by applying a focused ion beam (FIB)–based micro-slotting semidestructive mechanical relaxation method. The results show that the compression-compression fatigue increases beneficial compressive residual-stresses depending on the maximum fatigue stress, and mapped locations on the sample. The compressive residual stress elevates with higher fatigue

stress and reaches its maximum near the sample grips. Wheras, in the middle of the sample, the compressive RS experience minor improvement.

11:20 AM

Effects of Frequency on Fatigue Behavior of Zr-Base Bulk Metallic Glasses: *Qingming Feng*¹; Gongyao Wang¹; Lu Huang²; Peter Liaw¹; ¹University of Tennessee; ²Beijing University of Aeronautics & Astronautics

Fatigue tests were conducted on Zr-base Bulk Metallic Glasses (BMGs) using a state-of-the-art high-frequency, 1000-Hz, material test system. Fatigue experiments were conducted at high (1000 Hz), mid-high (100 Hz) and conventional (10 Hz) frequencies in air at room temperature. The effects of the test frequency, and temperature increase during fatigue are discussed. Following the completion of fatigue tests, the samples were examined by scanning electron microscopy (SEM) to identify the failure mechanisms and transition regions, several possible explanations are presented to explain the observed frequency effects. Acknowledgement: G. Y. Wang and P. K. Liaw very much appreciate the financial support of the US National Science Foundation, under DMR-0909037, and CMMI-0900271, with Drs. A. Ardell, Dr. D. Finotello, and Dr. C. V. Cooper as contract monitors. Q. M. Feng wishes to gratefully acknowledge the financial support provided for this study by the National Science Foundation.

11:30 AM Invited

Investigating the Effects of Fatigue on Annealed and As-Quenched Zr-Based Bulk Metallic Glasses: *Peng Tong*¹; Despina Louca¹; Peter Liaw²; Gongyao Wang²; Yoshihiko Yokoyama³; ¹University of Virginia; ²University of Tennessee; ³Tohoku University

Bulk metallic glasses (BMGs) exhibit unique physical properties and understanding their mechanical response is central to their application as engineering materials. In order to look for a structural signature resulting from changes brought upon by fatigue, the local atomic structures of Zr-glasses Zr50Cu40Al10 (Zr541) and Zr60Cu30Al10 (Zr631) were investigated via the pair density function analysis of synchrotron X-ray diffraction data. A comparison of the local atomic configuration of as-quenched and annealed alloys indicated that annealing induces some local ordering in the structure of Zr631. For Zr541, a weaker change on the local structure from annealing was observed. However, the local structure changes after cyclic loading are more dramatically observed in the annealed sample than in the as-quenched one. Our results indicate that the physical properties of BMGs following fatigue loading conditions may be influenced by structural relaxation, with annealing leading to observable differences at the atomic level under fatigue.

11:50 AM

Interpreting Temperature Change in Shear Bands of a Bulk-Metallic Glass Using Spatial-Temporal Analysis: *Jiajia Luo*¹; Gongyao Wang¹; Hairong Qi¹; Yoshihiko Yokoyama²; Peter Liaw¹; Akihisa Inoue²; ¹University of Tennessee; ²Institute for Materials Research

Infrared imaging represents an innovative sensing modality to study interior structure of metallic glasses such that hidden defects like fracture can be identified and handled in a controlled way. However, how to interpret the temperature change from infrared images across the entire glass over certain period of time remains a challenging problem. This paper formulates the temperature evolution over time across spatial domain using a linear mixing model and presents robust unsupervised unmixing algorithm such that joint effects of hidden (or source) events (or defects) can be identified, providing prevailing support to the understanding of IR image of Bulk-Metallic Glass. Besides characterizing the internal structural change under pressure, the proposed unmixing algorithm also has the potential to reveal depth information of the defect, which is a breakthrough to functional infrared imaging.

12:00 PM Invited

Fatigue and Fracture Behavior of a Ca-Based Bulk-Metallic Glass: Julian Raphael¹; Gongyao Wang²; Peter Liaw²; Oleg Senkov³; Dan Miracle³; ¹J R Technical Services, LLC; ²University of Tennessee; ³Air Force Research Laboratory

The compression and fatigue behavior of a Ca65Mg15Zn20 bulk-metallic glass (BMG) was studied in air at room temperature. During the preparation of cubical samples of the Ca65Mg15Zn20 for compression and fatigue investigations, small spherical cavities were found. Under both monotonic and cyclic compression loadings of the samples, fractures initiated atthese cavities and propagated in a direction generally parallel to the loading axis. Finite-element analysis (FEA) was used to model the fracture behavior. The FEA of a centrally located spherical void showed that under compression loading, large tensile stresses evolved in the cavities. The orientation of the maximum principal stress (P1) was found to be normal to the direction of crack propagation, which is consistent with the experimental finding. Stresses in deeply embedded adjacent voids and those in superficial voids were also studied. The influence of the void location in the cubical sample on the fracture behavior was quantitatively discussed.

12:20 PM

Studying Fatigue-Crack-Propagation Behavior of Zr-Based Bulk-Metallic Glasses: *Gongyao Wang*¹; P. Liaw¹; Y. Yokoyama²; Q. Feng¹; T Toll¹; A. Inoue²; ¹University of Tennessee; ²Institute for Materials Research

The fatigue-crack-propagation behavior is very critical for predicting the fatigue life of structural materials. Various compositions of zirconium (Zr)-based bulk-metallic glasses (BMGs) were fabricated by an arc-melt tiltcasting technique. The casting rods were cut into disk-shaped compact-tension specimens. Fatigue-crack-growth-rate experiments were performed on these BMG samples in air. The experiments were conducted at a frequency of 10 Hz, using an electrodynamic test instrument with an R ratio of 0.1, where R = $\frac{963\min.}{963max.}$, $\frac{963min.}{963max}$ are the applied minimum and maximum absolute stresses, respectively. The crack-growth rates of Zrbased BMGs with different compositions will be presented. A mechanistic understanding of the fatigue behavior of these Zr-based BMGs is suggested. Acknowledgement: This work is financially supported by the US National Science Foundation, under CMMI-0900271 and DMR-0909037, with Drs. C. V. Cooper, Dr. D. Finotello, and Dr. A. Ardell as contract monitors.

Cast Shop for Aluminum Production: Melt Quality Control

Sponsored by: The Minerals, Metals and Materials Society, TMS Light Metals Division, TMS: Aluminum Committee, TMS: Aluminum Processing Committee

Program Organizers: Geoffrey Brooks, Swinburne University of Technology; John Grandfield, Grandfield Technology Pty Ltd

Wednesday AM	Room: 16A
March 2, 2011	Location: San Diego Conv. Ctr

Session Chairs: Claude Dupuis, Rio Tinto Alcan; Steinar Benum, Aloca Norway

8:30 AM Introductory Comments

8:35 AM

In-Line Salt-ACD[™]:

A Chlorine–Free Technology for Metal Treatment: *Patrice Robichaud*¹; Claude Dupuis¹; Alain Mathis²; Pascal Coté³; Bruno Maltais³; ¹Rio Tinto Alcan, Arvida Research & Development Centre; ²Rio Tinto Alcan, Aluval; ³STAS

A new generation of the Alcan Compact Degasser (ACDTM), the Salt-ACDTM, based on the utilization of salt fluxes in replacement of chlorine gas, was introduced to the aluminum industry [1]. This unique technology has been developed by Rio Tinto Alcan (RTA) since 2003 and in collaboration



with La Société des Technologies de l'Aluminium du Saguenay (STAS). Its utilization in combination with the Rotary Flux Injector (RFI^{TM}) for furnace preparation and/or the Treatment of Aluminum in Crucible (TAC^{TM}) for aluminum pre treatment eliminates the use of chlorine in casthouses. The Salt-ACDTM technology has been successfully implemented and operated in RTA casthouses. It supports the objective of eliminating chlorine from the casthouse for health, safety and environmental reasons. This paper presents recent developments in terms of equipment, key components and retrofittability to existing ACDTM units. The operating experience and metallurgical performance are reviewed.

9:00 AM

The Effect of TiB2 Granules on Metal Quality: Maryam Al Jallaf¹; Margaret Hyland²; Barry Welch³; Ali Al Zarouni¹; Fahimi Abdullah¹; ¹DUBAL; ²University of Auckland; ³Welbank Consulting

TiB2 granules were added to a fully graphitized electrolytic cell in a trial to provide a barrier coating on the carbon cathode to prolong cathode life. The consequential impact on metal cleanliness was evaluated by a detailed metallographic analysis using the PoDFA technique. Metal produced from the test cell was mixed with regular potline metal and cast into billets. Samples were taken from different locations in the process stream and also for three different types of metal charged into the furnace, namely regular potline metal, 10 tons of metal from test cell mixed with regular potline metal, and 20 tons of metal from test cell mixed with regular metal. The PoDFA analysis shows that samples containing metal from test cell had more grain refiner inclusions than regular potline metal but fewer carbide inclusions. However, there was no overall significant negative impact on the specified requirements of metal cleanliness.

9:25 AM

Thermodynamic Analysis of Ti, Zr, V and Cr Impurities in Aluminium Melt: *Abdul Khaliq*¹; Muhammad Rhamdhani¹; Geoffrey Brooks¹; 'Swinburne University of Technology

Aluminium has been considered as an alternative for copper conductor applications. Metal impurities in particular Ti, Zr, V and Cr in the solution affect the electrical conductivity of aluminium significantly. Industrially boron treatment has been used to remove these impurities through the formation of borides. However solution thermodynamics and reaction mechanics of the borides formation in an aluminium melt are not well understood. In the present study, thermodynamic analysis has been carried out to investigate and elaborate the formation of various borides in aluminium melt. It has been shown in this study that diborides (MB2) were the most thermodynamically stable boride compounds of these impurities in the given working conditions. The ZrB2, TiB2 and VB2 particles were more stable compared to AlB2 and CrB2 hence did not dissolve readily. It is also shown that the relative stability of boride particles has been affected by the presence of other metal diborides.

9:50 AM

Current Technologies for the Removal of Iron from Aluminum Alloys: *Lifeng Zhang*¹; Jianwei Gao²; ¹Missouri University of Science and Technology; ²Shanghai Jiao Tong University

In the current paper, the Fe-rich phases in and their detrimental effect on aluminum alloys are summarized. The use of high cooling rate, solution heat treatment and addition of elements such as Mn, Cr, Co, Be and Sr are reported to modify the platelet Fe-rich phases in aluminum alloys. Technologies to remove iron from aluminum are extensively reviewed, including gravitational separation, electromagnetic separation, and centrifuge. Other methods include electrolysis, electro-slag refining, fractional solidification, fluxing refining, and three-layer cell electrolysis process.

10:15 AM Break

10:25 AM

Electromagnetically Enhanced Filtration of Aluminum Melts: Mark Kennedy¹; *Shahid Akhtar*¹; Ragnhild Aune¹; Jon Bakken¹; ¹Norwegian University of Science and Technology

The major drawback of the use of Ceramic Foam Filters (CFF) for purification of aluminum is their low efficiency for particles in the range of 10-30 μ m. The application of electromagnetic force from an induction coil in combination with a filter can cause back mixing and recirculation through the filter media. In the present work an experimental set-up has been designed, built and verified by studying the meniscus behavior of molten aluminum under varying magnetic field strength. Batch type filtration experiments with 30 ppi CFF were also conducted with and without a magnetic field using an A356 aluminum alloy containing 20% anodized and lacquered plates, as well as 20% composite material (A356 base and 15% SiC particles with size range 10-50 μ m). The presence of a magnetic field has proven to have both an effect on the build up of the filter cake, as well as on the re-distribution of particles within the filter.

10:50 AM

A Review of the Development of New Filter Technologies Based on the Principle of Multi Stage Filtration with Grain Refiner Added in the Intermediate Stage: John Courtenay¹; Stephen Instone²; Frank Reusch³; ¹MQP Limited; ²Hydro Aluminium Deutschland GmbH; ³Drache Umwelttechnik GmbH

Recent developments in filtration technology based on the principle of using a three stage process where a ceramic foam filter is operated in cake mode in the first stage; grain refiner is added in a second chamber and a further filtration means is used in the third stage to remove oxide inclusions or agglomerates originating from the grain refiner addition are reviewed. The first development – the XC Filter, was presented by Instone et al in 2005 and described a system where a small deep bed filter (DBF) was successfully applied in the third chamber. A second prototype multi stage filter was described at TMS 2008 based on the same principle but with a cyclone deployed in the final chamber. An industrial prototype was constructed based on water modeling work and plant trials were undertaken. The current stage of development of each system and their relative merits are evaluated.

11:15 AM

Wettability of Aluminium with Sic and Graphite in Aluminium Filtration: Sarina Bao¹; Anne Kvithyld²; Thorvald Engh¹; Merete Tangstad¹; ¹NTNU; ²SINTEF

The aim of aluminium filtration is to remove inclusions such as Al3C4. For inclusions to be removed they have to come in close contact with the filter walls composed of Al2O3 or SiC. It is therefore important that the molten aluminium has close contact with the filter wall. In addition to wetting properties between inclusions (Al4C3) and molten aluminium, the wettability of the filter (SiC) by aluminium is determined in sessile drop studies in the temperature range 1000-1300°C. Wettability changes with time in three successive steps and improves with time. To describe wettability at filtration temperatures employed in the industry of around 700°C, the results will be extrapolated to this temperature in future work.

11:40 AM

Study of Microporosity Formation under Different Pouring Conditions in A356 Aluminum Alloy Castings: Lu Yao¹; Steve Cockcroft¹; Daan Maijer¹; Jindong Zhu¹; Carl Reilly¹; ¹University of British Columbia

In this work, the formation of microporosity has been examined under different casting conditions aimed at manipulating the tendency to form and entrain oxide films in small directionally cast A356 samples. Porous disc filtration analysis (PoDFA) was used to assess the melt cleanliness and identify the inclusions in the castings. The porosity volume fraction and size distribution were measured using X-ray micro-tomography (XMT) analysis. By fitting a pore formation model to the experimental results, an estimate of the pore nucleation population has been made. The results from the model predictions indicate that increasing the tendency to form and entrain oxide films not only increases the number of nucleation sites but also reduces the supersaturation necessary for pore nucleation in A356 castings.

Characterization of Minerals, Metals and Materials: Structural Characterization

Sponsored by: The Minerals, Metals and Materials Society, TMS Extraction and Processing Division, TMS/ASM: Composite Materials Committee, TMS: Materials Characterization Committee *Program Organizer:* Sergio Monteiro, State University of the Northern Rio de Janeiro - UENF

Wednesday AM	Room: 14B
March 2, 2011	Location: San Diego Conv. Ctr

Session Chairs: Jiann-Yang Hwang, Michigan Technological University; Jeongguk Kim, Korea Railroad Research Institute

8:30 AM

Micro-Computerized Tomography of Ti-5111 Friction Stir Welded Microsamples: *Christopher Cheng*¹; Jennifer Wolk²; Marc Zupan¹; ¹University of Maryland Baltimore County; ²Naval Surface Warfare Center, Carderock Division

The use of Ti and Ti alloys in marine applications can deliver improved mechanical, physical, and corrosion properties. These material performance gains when put into service can be significantly reduced by the difficulties of conventional welding of joints. Friction stir welding (FSW) is an alternate welding process that overcomes some of the difficulties, but localized mechanical characterization of the various regimes of FSW joints are still immature. Previous measurements of the mechanical properties of the weld, transition, and base regimes of friction stir welded Ti-5111 microsamples showed significant differences in stiffness, yield strength, and ultimate tensile strength. Micro-Computerized Tomography (micro-CT) is utilized to document the internal gage structure of the microsample before and after tensile testing. The micro-CT information is linked to fractography of the failure surfaces, the microstructural textural information, and crystallographic slip which are used to explain the variations in the different FSW zone mechanical properties.

8:45 AM

Application of Novel Techniques to the Three-Dimensional Characterization of Microstructural Features in a+β Titanium Alloys: John Sosa¹; Santhosh Koduri¹; Vikas Dixit¹; Peter Collins²; Stephen Niezgoda³; Surya Kalidindi³; Hamish Fraser¹; ¹The Ohio State University; ²University of North Texas; ³Drexel University

Advanced three-dimensional data collection techniques such as Robo. Met-3DTM have permitted rapid acquisition of robust datasets on optical length scales. Implementation of such datasets may improve the accuracy of neural networks and phase-field models. However, the accurate statistical representation of three-dimensional microstructural features is challenging, requiring continual improvement to analytical methods. This work addresses the serial two-dimensional collection, three-dimensional processing, and analysis of datasets containing microstructural features such as equiaxed-a and colony-a in a+B titanium alloys. In regards to equiaxed-a, rigorous dataset collection, along with novel 3-D feature-find and separation algorithms have allowed for robust three-dimensional quantification that was subsequently compared to 2-D stereological measurements, providing new insights into their validity. With regard to colony-a, collaboration with Dr. Surya Kalidindi's group at Drexel University has led to advanced automated colony segmentation permitting 3-D visualization of their interpenetrating morphology and three-dimensional quantification. Crystallographic information has been incorporated using electron backscatter diffraction (EBSD).

9:00 AM

Application of Conical Beam X-Ray Tomography to Multi-Phase Materials: Jason Wolf¹; Anthony Rollett¹; Marc De Graef¹; ¹Carnegie Mellon University

We report on the use of a new, custom-designed conical x-ray tomography instrument, consisting of a Phoenix 160 kV multi-focal x-ray source, a 3056x3056 fiber optically coupled CCD camera with 12 micron pixel size and a GdOS poly-crystalline scintillator, with optimal operation around 40 kV. This setup, mounted inside a lead sarcophagus on an air-bearing table, is capable of a resolution of about 400 nm. Tomographic reconstructions are carried out using the SnapCT tomography code (Digisens) on a multi-GPU platform; the reconstruction occurs in near real time. The system employs a cylindrical or rod-shaped sample with a diameter of 1-2 mm, mounted on a five-axis precision stage. We will report on a number of material data sets, ranging from carbon foams to biological materials to two-phase alloy systems. We will also discuss a number of segmentation methods used for post-processing of the tomographic reconstructions.

9:15 AM

High Temperature X-ray Diffraction Characterization of Thermal Energy Storage Materials – The Binary Phase Diagram Study: *Wen-Ming Chien*¹; Vamsi Kamisetty¹; Ivan Gantan¹; Prathyusha Mekala¹; Anjali Talekar¹; Dhanesh Chandra¹; ¹University of Nevada, Reno

Thermal energy storage materials (organic crystalline materials) undergo a solid-solid phase transition before melting which will store large amounts of thermal energy. Three materials [tris(hydroxymethyl)aminomethane(TRIS) and 2-Amino-2-methyl-1, 3-propanediol(AMPL) and Pentaglycerol(PG)] were used for this study. High temperature X-ray diffraction characterization and differential scanning calorimetric (DSC) methods were used to develop the binary AMPL-TRIS and AMPL-PG phase diagrams. The high temperature solid-state phases of AMPL and TRIS were characterized as a disordered BCC structure, and PG was characterized as FCC. Lattice and volume expansion calculations on single phase of AMPL, TRIS and PG have been performed. Calculate the AMPL-TRIS and AMPL-PG binary phase diagrams by using the Thermal-Calc software. The detail of the thermal properties and excess Gibbs energies will present.

9:30 AM

Non-Invasive X-Ray Imaging of Paint Layers in Old Master Paintings: *Peter Reischig*¹; Lukas Helfen²; Tilo Baumbach²; Arie Wallert³, Joris Dik¹; ¹Delft University of Technology; ²Institute for Synchrotron Radiation, Karlsruhe Institute of Technology; ³Rijksmuseum Amsterdam

To develop conservation procedures for a certain type of painting, as well as for a thorough art historical study or conservation of a specific work of art, it is of crucial importance to look under the surface and visualize its paint stratigraphy. We propose synchrotron based x-ray laminography to explore the fine details of the microstructure, which are hard to detect by conventional (non-destructive) techniques. The method can provide threedimensional high-resolution local maps of the paint layers without the need of invasive sample removal. The rotation axis is perpendicular to the sample surface and inclined to the incident beam, enabling scanning of whole paintings. For the reconstruction, filtered backprojection algorithms are used, based on radiographs that exhibit absorption contrast (from local variations in density) and/or phase contrast (from interfaces). The technique enables visualization of fine structure (pigment particles, voids, cracks) in underlying paint layers and the substrate.

9:45 AM

Characterization of Residual Stress Distributions and Microstructural Changes in Laser Shock Peened Ti-6Al-4V Alloy: *Yixiang Zhao*¹; Ulrich Lienert²; Jon Almer²; Yang Ren²; David Lahrman³; Dong Qian¹; S. Mannava¹; Vijay Vasudevan¹; ¹University of Cincinnati; ²Advanced Photo Source, Argonne National Laboratory; ³LSP Technologies, Inc.,

Laser shock peening (LSP) is a novel surface treatment process that generates deep compressive residual stresses and microstructural changes and thereby dramatically improves fatigue strength of critical metal



aircraft engine parts. The present study was undertaken to develop a basic understanding of the effects of LSP parameters on the residual stress distributions and microstructural changes in Ti-6Al-4V alloy. Coupons of the alloy with and without a sacrificial/ablative layer were LSP-treated using the LSP systems at GE Aviation and LSP Technologies, Inc. Depth-resolved characterization of the macro residual strains and stresses was achieved using high-energy synchrotron x-ray diffraction, as well as by conventional XRD. The near-surface and through-the-depth changes in strain, texture and microstructure were studied using EBSD/OIM and by TEM. Local property changes were examined using microhardness and nanoindentation. The results showing the relationship between LSP processing parameters, microstructure, residual stress distributions and hardness are presented and discussed.

10:00 AM Break

10:15 AM Invited

In Situ Tomographic Characterization of Single Cavity-Growth during High-Temperature Creep of Metallic Materials: *Augusta Isaac*¹; Federico Sket²; Krzysztof Dzieciol³; Andras Borbely³; ¹Laboratório Nacional de Luz Síncrotron; ²Madrid Institute for Advanced Studies of Materials; ³École Nationale Supérieure des Mines de Saint-Étienne

The service lifetime of metallic components for high temperature applications is usually controlled by creep damage consisting of nucleation, growth and coalescence of grain boundary voids. This work presents a conceptually new approach to void growth characterization based on synchrotron microtomographic measurements performed in-situ during creep. We show that the average growth rates of voids in leaded brass and copper are larger by a factor of about 25 and 46 than predicted by the continuum theory, respectively. The distorted shape of voids reconstructed by nanotomography suggests that the enhanced growth rate is related to the crystallographic nature of creep deformation.

10:45 AM

EBSD Analysis Strategies for Quantitative Characterization of 'Multi-Phase' Steel Microstructures: *Eric Payton*¹; Shenja Dziaszyk¹; Gunther Eggeler¹; ¹Ruhr-Universitaet Bochum

Quantitative characterization of the volume fractions, sizes, and spatial arrangements of major microstructural components is necessary for further development of advanced low-alloy steels, such as TRIP steels, which are important in automotive manufacturing. Automated EBSD is capable of producing data that can be used to simultaneously characterize the crystallographic texture as well as the volume fraction and size of grains of ferrite and retained austenite. However, several challenges remain in distinguishing martensite, bainite, ferrite, and the local state of recrystallization by EBSD. To assess the quality of EBSD data analysis strategies suggested by various authors for identifying these microstructural components, EBSD, nanoindentation, and other characterization techniques were performed on the same regions of several 'multi-phase' steels. EBSD simulations were used to EBSD-based characterization of microstructural evolution during processing of many engineering alloys.

11:00 AM

EBSD Ferrite Fraction in Austenitic Welds: *Carl Necker*¹; John Milewski¹; John Elmer²; ¹Los Alamos National Laboratory; ²Lawrence Livermore National Laboratory

In this study we test the potential of electron backscatter diffraction (EBSD) as a delta ferrite quantification technique in austenitic stainless steel welds. Quantification of ferrite in welds presents issues as existing techniques (magnetic permeability, ferrite scopes, x-ray diffraction) sample volumes larger than the welds. EBSD sub-micron resolution and millimeter scan sizes overcome the volumetric averaging issues. Optical image analysis allows for local analysis but relies on sufficient differential phase contrast. With proper surface preparation EBSD should clearly differentiate austenite from ferrite. Centrifugally cast stainless steel weld ferrite secondary standards were used in this study. EBSD results were compared to optical image analysis, ferrite

scope, and the standard's Magne Gage ferrite numbers. EBSD results were lower than the other characterization techniques. Although EBSD clearly differentiated austenite and ferrite, it was clear that surface topography, total area scanned and scan step size play significant roles in properly capturing the ferrite morphology.

11:15 AM

Characterization of Twin Boundaries in Twinning-Induced Plasticity Steels Using Electron Backscatter Diffraction Electron Microscopy: Erin Diedrich¹; David Field¹; ¹Washington State University

This experiment uses electron backscatter diffraction (EBSD) performed in a field emission scanning electron microscope (FESEM) to characterize and quantify twin boundaries in mechanically deformed TWIP steel samples in order to relate the presence of twins to the mechanical properties of the material. EBSD scans were performed at magnifications of 2,400x and 20,000x on samples that were mechanically deformed to 3%, 9% strain and to failure, as well as a specimen of as-received material. The twin fractions within the low-strain value specimens remained relatively constant, however this fraction increased from 1.4% in the as-received material to 3.6% in the sample pulled to failure at 34% true strain. However, the suspected presence of bundles of nano-scale twins that behave as lattice defects resulted in poor diffraction patterns and it was determined that these percentages are not an accurate representation of the twin fraction.

11:30 AM

EBSD Detail Extraction for Greater Spatial and Angular Resolution in Material Characterization: Jay Basinger¹; David Fullwood¹; Brent Adams¹; ¹Brigham Young University

Orientation imaging methods have been a mainstay of characterization efforts for crystalline materials for nearly two decades. Electron backscatter diffraction images provide statistical data regarding atomic alignment to create relatively large scale (up to several mm) orientation maps in crystalline and polycrystalline materials. However, recent work has highlighted that the information in such images has generally been under-used. Advances in high-resolution strain measurement, dislocation densities, and defect detection have begun to utilize this often ignored detail. This paper presents a review of recent developments in detail extraction from EBSD, including new developments in pattern center determination (a critical enabling technique that facilitates many other high-resolution techniques) and image separation methods as a basis for improved spatial resolution in material characterization.

11:45 AM

Segmentation of Three-Dimensional EBSD Data through Fast Multiscale Clustering: *Cullen McMahon*¹; Cassandra George¹; Md. Zakaria Quadir²; Michael Ferry²; Lori Bassman¹; ¹Harvey Mudd College; ²University of New South Wales

Complete and accurate analysis of subgrain microstructural features must include three-dimensional information. Three-dimensional electron backscatter diffraction (EBSD) data can be used to characterize these features, however their boundaries first must be determined. This cannot be accomplished simply with pixel-to-pixel misorientation thresholding because many of the boundaries are gradual transitions in crystallographic orientation. Fast Multiscale Clustering (FMC) is an established image processing technique that we have combined with quaternion representation of orientation to segment this kind of data. Segmentation algorithms often have issues handling images with both distinct and subtle boundaries. Our implementation of FMC addresses this by using a novel distance function and statistical analysis to take into account the variance in orientation of each feature. Although FMC was originally a two-dimensional image processing algorithm we have extended it to analyze three-dimensional data sets. As an example, a segmentation of microbands in cold-rolled aluminum will be presented.

12:00 PM

Characterization and Processing Ultramafic Nickel Ore after Acid Attack to Disintegrate Fibres: *Salah Uddin*¹; Mitra Mirnezami¹; Ram Rao¹; James Finch¹; ¹McGill University

Ultramafic ores are a potential major resource of nickel. The primary processing challenge is posed by fibrous minerals such as chrysotile. These minerals create physical entanglement which increases pulp viscosity and hinders selectivity in flotation. The proposal in this paper is to disintegrate the fibres by adapting technology pursued in CO2 sequestration. The concept is to release Mg by acid attack (the Mg is reacted with CO2 in the sequestration process) which destabilizes the fibres enabling them to be broken by grinding. Structural changes in the ore due to combined acid (H2SO4) and grinding treatment was characterized using SEM-EDAX, XRD, Micro-Raman and FT-IR. Based on the analysis, a possible mechanism of fibre disintegration and consequent change in slurry rheology is proposed. The possibility of collectorless flotation through the use of H2SO4 and elimination of frother due to the high ionic strength liquor produced (due to released Mg ions) is demonstrated. Significant improvement in Ni grade-recovery with higher MgO rejection was achieved compared to untreated ore. The process has environmental attractions: the H2SO4 can be derived from SO2 smelter offgas and the tailings are candidates for CO2 sequestration.

12:15 PM

Microwave Sintering of CaO Stabilized Nature Baddeleyite: Li Jing¹; Peng Jinhui¹; *Guo Shenghui*¹; Li Wei¹; Zhang Libo¹; ¹Faculty of Metallurgy and Energy Engineering, Kunming University of Science and Technology

Partially stabilized zirconia ceramics (PSZ) were prepared by microwave sintering using natural baddeleyite which was obtained by flotation of baddeleyite ore as starting materials. Because of using natural baddeleyite as raw and the process producing no waste, it realized shorter process, energy saving, environmentally-friendly and non- damage processing. In this work natural baddeleyite stabilized with 3.8 wt.% CaO were sintered at 1300 \Box for 60 min in a multi-mode 2.45 GHz microwave furnace. Microwave sintering could fast heating and sintering. Besides that, microwave sintering could heat materials wholly, low the sintering temperature, improve the materials properties and save energy. X-ray spectrum displayed the product composed by the tetragonal phase and monoclinic phase that also showed the product through scanning electron microscopy. PSZ which was with high density was confirmed by the method of the Archimedes technique.

Coatings for Structural, Biological, and Electronic Applications II: Process-Property-Performance Correlations - I; Metallic Coatings

Sponsored by: The Minerals, Metals and Materials Society, TMS Electronic, Magnetic, and Photonic Materials Division, TMS: Thin Films and Interfaces Committee

Program Organizers: Nuggehalli Ravindra, New Jersey Institute of Technology; Choong Kim, University of Texas at Arlington; Nancy Michael, University of Texas at Arlington; Gregory Krumdick, Argonne National Laboratory; Roger Narayan, Univ of North Carolina & North Carolina State Univ

Wednesday AM	
March 2, 2011	

Room: 6E Location: San Diego Conv. Ctr

Session Chairs: Nuggehalli Ravindra, New Jersey Institute of Technology; Nancy Michael, University of Texas at Arlington

8:30 AM Symposium Overview

8:35 AM Invited

Improved Mechanical Properties of Coatings and Bulk Components as a Function of Grain Size: *Robert Gansert*¹; Chris Melnyk²; David Grant²; David Lugan²; Brian Weinstein²; ¹Advanced Materials & Technology Services, Inc.; ²California Nanotechnologies, Inc.

Thermal sprayed coatings produced from nano- and near-nano grained powders provide improved properties as compared to conventional powders. These nano- and near-nano grained materials show great potential for applications in the aerospace, energy, and many other industries. A study is proposed to investigate the influence of grain size on mechanical properties by examining nano-, near-nano, and micro-grained materials. Powders, coatings and consolidated components of tungsten carbide based materials (WC-Co-Cr, WC-Co) will be examined. Thermal spray coatings will be produced of carbides of various grain sizes, from nano to micron sized grains. An examination of consolidated forms will be performed using these materials. Spark Plasma Sintering (SPS) will be used to provide consolidated forms of these materials. A comparison will be made of the influence of grain size in thermal spray coatings to that of bulk consolidated materials using these materials.

9:00 AM Invited

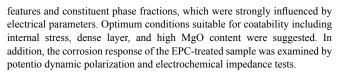
Residual Stresses in Coatings Measured at Micro Scale: Jeff De Hosson¹; Vasek Ocelik¹; Ivan Furar¹; ¹Univ of Groningen

In this contribution we demonstrate a novel approach of measuring internal stresses at the micron scale in coatings scale. The new method is based on applying of dual beam microscopy like imaging-milling semidestructive instrument to realize mechanical relaxation for measuring internal stress. Focused Ion Beam is used as a knife to release the local strain induced by internal stresses. Surface relaxation in the vicinity of such cut is mapped by the Digital Image Correlation of scanning electron microscope images and released stresses are calculated on the base of displacement maps. Measurements were performed on laser clad coatings with different thicknesses. 3.3 kW IPG fiber laser was used to create different metallic coatings. Numerical and statistical methods are used to calculate the stress components inside the laser treated coatings.

9:25 AM Invited

Factors Influencing the Formation of Oxide Layer on AZ91 Mg Alloy Coated by Electrochemical Plasma Coating: *Dong H. Shin*¹; In Jun Hwang¹; Kang Min Lee¹; Young Gun Ko²; ¹Hanyang University; ²Yeungnam University

A study was made to study the formation of oxide layer on AZ91 Mg alloy coated by electrochemical plasma coating (EPC) process as functions of various electrical parameters such as frequency, wave form, and current density. The formation of coating layer was characterized by scanning electron microscope and X-ray photoelectron spectroscopy for their structural



9:50 AM Invited

Phase Stability and Surface Rumpling during Cyclic Oxidation of Pd/ Pt-Modified Ni-Al Bond Coats at 1150°C: Raghavendra Adharapurapu¹; Jun Zhu¹; Don Lipkin²; Voramon Dheeradhada²; Tresa Pollock³; ¹University of Michigan; ²General Electric Global Research Center; ³University of California Santa Barbara

Phase stability, surface rumpling and interdiffusion behavior of Pd/Ptmodified Ni-Al-Hf-Cr bond coats were investigated during cyclic oxidation via a combinatorial approach. Bond coats with compositions in the range of Ni-(33-39)Al-5Cr-(1-8)Pd/Pt were deposited on RenéN5 substrates and subjected to both short-term and long-term cyclic oxidation experiments at 1150°C. The Pt- and Pd-modified overlay coatings exhibited comparable oxidation kinetics with intermediate Pt/Pd+Hf additions exhibiting the best cyclic oxidation properties. The oxidation lives of the Pd-modified overlays exceeded those of Pd-modified diffusion aluminides with a positive synergistic effects between Pd/Pt and Hf+Cr additions. Transformations from B2-phase->3R+7R-martensites->y'->y+y' occurred in both Pd- and Pt-modified coatings due to Al depletion to substrate and surface oxide. Rumpling or surface roughening occurred for all the coating compositions at 1150°C. A greater depletion of Pd to the substrate compared to Pt was also observed; the interdiffusion coefficients were consistent with those measured in NiAl-NiAl+Pt/Pd diffusion couples.

10:15 AM Break

10:25 AM Invited

The Benefits of the Thermal Properties and Durability of Alodine EC2 Coated Aluminum in the Heat Transfer Industry: *Jianhui Shang*¹; Ryan Brune¹; Wesley Sprague¹; Larry Wilkerson¹; Steve Hatkevich¹; ¹American Trim LLC

The heat exchanger industry currently employs the high thermal conductivity of aluminum to produce efficient coils at a low cost. These systems often deteriorate over time as the aluminum coils oxidize or their protective coating wears away, leading to a decreased effectiveness for transferring heat. Recently, Henkel Corporation developed a new coating for aluminum that increases the thermal transfer capability and prevents surface oxidation and abrasive damage. This coating, called Alodine EC2TM, will allow for the replacement of expensive copper coil systems with low cost aluminum coils, and the increased thermal properties will allow for smaller heat exchangers to be constructed that exhibit the same heat transfer capabilities as larger traditional systems. This will result in systems with lower cost and decreased weight. This paper presents the thermal properties of Alodine EC2TM to validate the potential applications to the heat transfer industry.

10:50 AM

Characterization of Electroless Ni-B Coating for Tribological Application: *Soupitak Pal*¹; Nisha Verma¹; Vikram Jayaram¹; Sanjay Biswas¹; Yancy Riddle²; ¹Indian Institute of Science; ²UCT Coatings. Inc

The crystalline counterpart of amorphous electroless Ni-B coatings are generally regarded as low friction and wear resistant materials in which the major crystalline phases are Ni₃B and Ni₂B whose evolution occurs through a multi-stage crystallization process due to the presence of composition fluctuation in the as deposited coating induced by the deposition process. This study mainly focuses on the role of individual crystalline phases on the overall tribological behaviour of the coating. Microstructural developments are carefully probed in conjunction with heat treatments. Ball (alumina, steel) on disk tribometer has been used to evaluate the overall tribological properties while the response of individual phases has been analyzed through lateral force microscopy using a silicon nitride cantilever. Though scaling of contact area and the nature of the counterface influence the results, it is found that increase in the ratio of $\rm Ni_2B$ to $\rm Ni_3B$ leads to a decrease in coefficient of friction.

11:05 AM

140th Annual Meeting & Exhibition

Improving High Temperature Performance of Aluminum Foams by Nickel Coating: Zhuokun Cao¹; Huan Liu¹; *Yihan Liu*¹; Guangchun Yao¹; 'Northeastern University, China

To meet the application of aluminum foams as high temperature acoustic absorbers, nickel coating was formed on the surface of aluminum foams by direct electroplating. Microstructure of the pretreated and nickel coated specimens was observed by SEM, and influences of pretreatment, current density, operating time and additives on the property of coating were discussed. Flat and smooth coating was obtained by electroplating for 2 hours at a current density of 0.02A/m2 with certain additives. Compressive tests were performed on the specimens both with and without nickel coating at room temperature and at 540, 660 and 700 °C. The results show the fact that nickel coating can effectively improve the compressive property of aluminum foams, especially at high temperature near and beyond the melting point of aluminum.

11:20 AM

Studies on Ni-Ti Thin Films Grown by Bias Assisted Magnetron Sputtering: *B Geetha Priyadarshini*¹; Shampa Aich¹; Madhusudan Chakraborty²; ¹Indian Institute of technology (IIT),Kharagpr; ²Indian Institute of technology (IIT), Bhubaneswar

Co-sputtering from Ni and Ti elemental targets was employed to deposit Ni-Ti thin films on Si (100) substrates. The influence of energetic particle bombardment on the microstructure of sputtered deposited Ni-Ti alloy films has not been well understood by the researchers. Attempts are made here to investigate the microstructural and structural evolution taking place during the ion-bombardment on Ni-Ti thin films using Field Emission Scanning Electron Microscopy (FE-SEM), High Resolution Transmission Electron microscopy (HR-TEM) and Grazing Incidence X-ray diffraction (GIXRD). Films deposited at -100 V substrate bias, were amorphous exhibiting smooth and continuous microstructure. At 600 °C annealing temperature, the films were polycrystalline with grain size of 15-25 nm containing mixture of B19' and B2 phases.

Commonality of Phenomena in Composite Materials II: Development of New Composite Materials

Sponsored by: The Minerals, Metals and Materials Society, ASM International, TMS Structural Materials Division, TMS/ASM: Composite Materials Committee *Program Organizers:* Meisha Shofner, Georgia Institute of Technology; Carl Boehlert, Michigan State University

Wednesday AM	Room: 6A
March 2, 2011	Location: San Diego Conv. Ctr

Session Chair: Nik Chawla, Arizona State University

8:30 AM Invited

Tuning the Properties of Nanocrystalline Semiconductors: Producing Bulk Sized Nanocomposites Using Electric Currents: J. Alaniz¹; J. Morales¹; C. Dames¹; J. Garay¹; ¹UC Riverside

Improving the performance of devices such as thermoelectric power generators often hinge producing materials with a precise blend of properties. Nanocrystalline oxides and semiconductors offer a route for attaining new functionalities, yet their direct application in products has been hindered by the difficulty in producing them reliably. One reason is that consolidation of nanocrystalline powders usually results in grain growth and therefore loss of enhanced nanocrystalline properties. Recently, the versatile material processing technique of current activated pressure assisted densification has proven effective in overcoming the grain growth challenge; it is now possible to efficiently produce materials large enough to be viable nanocrystalline parts. The materials produced have very different properties than traditional materials including improved tailorable conductivity, and magnetic coupling and can be used for energy scavenging, cooling and magnetic sensing. The results will be discussed in terms of crystal length scale effects and proximity of nanoscale phases.

9:10 AM

Initial Characterization of an Aluminum Based Syntactic Foam: Oliver Strbik¹; Satyendra Kumar¹; Chris Smith¹; *Todd Osborn*¹; Joe Cochran²; Thomas Sanders²; Naresh Thadhani²; Laura Cerully²; Tammy McCoy²; Liang Quan²; Vincent Hammond³; Kyu Cho³; ¹Deep Springs Technology; ²Georgia Tech; ³Army Research Lab

Continued progress in the development of metallic, high-strength, hollow spheres has generated renewed interest in syntactic metal foams. These foams, when composed of hollow spheres in a lightweight metallic matrix, possess low density, high specific stiffness, high strength to weight ratios, and greatly increased energy absorbing capabilities. As a result, they are of interest for applications ranging from ballistic armor to aircraft structures to automotive structural components and crumple-zones. Recently, a metallic foam composed of AA5083 filled with 60% (Vol) of M350 spheres has been produced using conventional casting methods. Following fabrication, the foam microstructure was characterized using both optical and electron microscopy. Quasi-static compression and microhardness testing was performed to determine the change in properties resulting from the incorporation of the spheres. Finally, limited ballistic testing has been performed to determine the ability of the foam to provide protection against low caliber threats.

9:30 AM

Machinable Aluminum Matrix Composite: William Harrigan¹; ¹Gamma Technology

One of the impediments to widespread us of aluminum matrix composites has been the difficulties in machining parts at an acceptable cost. Gamma Technology has refined the production of spherical aluminum oxide particles and has incorporated the new particles into aluminum matrix composites. These composites have mechanical and physical properties similar to the SiC or B4C reinforced composites made for the past 20 years by powder metallurgy techniques. This new composite has the ability to be machined with carbide inserts. This paper will discuss the mechanical properties of several composites containing the spherical aluminum at temperatures up to 350°C. Another composite has yield strength properties greater than 650 MPa at room temperature. The microstructure of these composites and the fracture surfaces will be presented to demonstrate the role of the spherical particles in developing the mechanical properties.

9:50 AM

Stability and Lithium Adsorption Property of LiMn2O4-LiSbO3 Composite in Aqueous Medium: *Li-Wen Ma*¹; Xi-Chang Shi¹; Bai-Zhen Chen¹; Kun Zhang¹; ¹School of Metallurgical Science and Engineering

LiMn2O4-LiSbO3 composite with the molar ratio Mn/Sb=3 was obtained by solid state reaction. The synthesis process of the LiMn2O4-LiSbO3 composite was analyzed by TG-DSC. The structure, stability and Li+ extraction/adsorption properties of the composites obtained at various temperatures were characterized by X-ray diffraction (XRD), scanning electron microscopy (SEM) and atomic absorption spectrophotometer (AAS). The results show that the LiMn2O4-LiSbO3 composite has a combined structure of LiMn2O4 (spinel) and LiSbO3 (perovskite) in which manganese and antimony ions diffuse mutually into perovskite and spinel to form complex solid solutions. The lithium in the LiMn2O4-LiSbO3 composite can be extracted from its framework with the structure and morphology maintained during acid treatment. After acid treatment the composite can adsorb Li+ from an aqueous lithium solution, which demonstrates that it can be used as lithium inorganic adsorbent.

10:10 AM Break

10:30 AM Invited

Nanotube Based Composites: A Matrix of Understanding: Enrique Barrera¹; 'Rice University

Inventing nanotube-based nanocomposites can take on several pathways. These pathways are further enabled when a matrix of understanding is established and the properties of nanotubes in broad array of materials are considered. Certainly, advancement of nanosystems is fostered by the knowledge base created in completely different materials. The leveraging of new ideas for polymer-based nanocomposites is an attractive approach for producing metal matrix nanocomposites. Likewise, the ability to advance nanoceramics is not far removed from the advancement of polymeric or metal matrix nanocomposites. In this presentation, the philosophy, design considerations, approaches, and achievements of nanocomposites will be overviewed and the use of a matrix of understanding will be identified that has fostered a broad range of nanotechnology advances.

11:10 AM

Impact Damage Sensing of Multiscale Glass/Epoxy Composite Structures: Luciana Arronche¹; Valeria La Saponara¹; ¹University of California, Davis

Carbon nanotubes provide increased conductivity to polymer matrix composites, and have been the object of much attention. Changes of conductivity offer a method to monitor structural health. This work investigates the effect of impact damage on the electrical properties of composite samples prepared with epoxy resin, multi-walled carbon nanotubes (MWCNT), and glass fiber woven reinforcement. The current work follows an investigation of counter-intuitive results (Yesil et al., Surfactant-modified multiscale composites for improved tensile fatigue and impact damage sensing, accepted by Materials Science and Engineering A, July 2010): higher resistivity changes were measured on the impacted surface, while damage occurs close to the opposite surface. The effects of manufacturing and resistance measurement methods are studied: a) variability between impacted and bottom surfaces and between batches; b) difference between 2 and 4 points probe methods. Moreover, the damage sensing performance of specimens with as-received MWCNT or with treated MWCNT are discussed.

11:30 AM

Temperature-Sensitive Shape Memory Polymer Based Acoustic Metamaterials: *Brayden Ware*¹; Walter Voit¹; ¹University of Texas at Dallas

Shape-memory polymer (SMP) acoustic metamaterials are dynamic composites containing local sonic resonators with variable stiffness coatings that change controllably as a function of temperature. The resonators absorb incident sound waves in specific frequency ranges. Modeling: we use multiple scattering theory to describe viscoelastic wave propagation through the composites to demonstrate negative effective mass density and a frequency band gap that moves with changing temperature. Sound transmission through the material is an order of magnitude less than predicted by the conventional mass-density law. Experimental: we synthesize several versatile acrylic SMP coatings around 5 to 15 mm lead and tungsten balls to create materials with tunable resonant frequencies. We can adjust the glass transition temperature (between about -20°C and 80°C) and stiffness in the rubbery regime (between about 300 KPa and 20 MPa). Dynamic mechanical analysis and impedance tube tests are used to confirm the predicted temperature-sensitive sound attenuation.

11:50 AM

Reinforced Steel/Polymer/Steel Sandwich Composites with Improved Properties: *Heinz Palkowski*¹; Olga Sokolova¹; Adele Carradó²; ¹TU Clausthal; ²Institut de Physique et Chimie des Matériaux de Strasbourg

Composite parts as sandwich structures are specifically used in applications for automotive, aerospace and vehicle industries. 316L/PP-PE/316L composites were investigated because of high stiffness and strength, good forming behaviour and damping properties. For thermal and mechanical joining additionally local plate reinforcing elements (RE) in the polymer core of the sandwich were placed and their forming behaviour and limits



were studied by deep drawing and bending processes. The experimental and theoretical analyses of failure mechanisms of sandwich plates without and with various RE were also investigated. Due to the material, size, shape and position of the local inlays the forming behaviour of the sandwich composites by deep drawing is strongly influenced. The position of local inlays e.g. in head, edge or flange regions of sandwich cup after deep drawing strongly influences the forming and flow behaviour of RE as well as sandwich composite areas. Results will be given.

12:10 PM

Fatigue Damage Identification in Glass/Epoxy Composite Structures through Embedded Piezoelectrics and Wavelet Transforms: Valeria La Saponara¹; Wahyu Lestari²; Charles Winkelmann¹; Luciana Arronche¹; ¹University of California, Davis; ²Embry-Riddle Aeronautical University

This work investigates signal processing and interpretation of waveforms acquired from cross-ply woven fiberglass/epoxy specimens with surfacemounted and embedded piezoelectric (PZT) transducers. The specimens are loaded under axial tensile fatigue in load control. The PZTs' pitch-catch signals are recorded at set intervals while the specimens are loaded at the mean stress in the testing machine, at low ultrasonic frequencies. Therefore, the waveform captures cumulative global damage of the specimens. In some samples, edge replications were taken concurrently to the waveforms. We discuss a signal processing technique based on wavelet transforms, where the denoised signal is processed with Gabor wavelet transforms, and the area of one of its contours is measured at set fatigue intervals, throughout the specimens' life. Results seem to indicate the presence of a steady-state condition which may be correlated to the characteristic damage state typical of cross-ply composites, and to the nonlinear accumulation of transverse cracks.

Computational Plasticity: Continuum Computational Plasticity

Sponsored by: The Minerals, Metals and Materials Society, TMS Materials Processing and Manufacturing Division, TMS Structural Materials Division, TMS/ASM: Computational Materials Science and Engineering Committee, TMS: High Temperature Alloys Committee *Program Organizers:* Remi Dingreville, Polytechnic Institute of NYU; Koen Janssens, Paul Scherrer Institute

Wednesday AMRoom: 1AMarch 2, 2011Location: San Diego Conv. Ctr

Session Chair: To Be Announced

8:30 AM Invited

Microstructural Evolution and Its Effect on Plastic Flow and Strain Localization: John Bassani¹; ¹University of Pennsylavnia

We consider a class of elastic-plastic materials possessing local orthotropic symmetries that evolve with deformation. Microstructural spin, i.e. the spin of the orthotropic axes, is defined to be the difference between the material spin and plastic spin. At finite strain, flow rules are defined in the intermediate configuration in terms of a thermodynamically-consistent non-symmetric stress and two second-order orientation tensors. A fundamental relationship between plastic stretching and spin is derived utilizing representation theory for tensor-valued functions, and that result is the basis of phenomenological constitutive relations for plastic spin which have been implemented in finite element simulations. Significant effects of microstructural evolution on limits to ductility are predicted from analyses of necking and shear banding. Comparisons with experimental data for textured polycrystals under both uniaxial tension and shear are very promising.

9:00 AM Invited

Advances in the Constitutive Equation Parameter Identification Procedure: Why Experiments Should Discuss With Numerical Simulations: Jerôme Crépin¹; Eva Héripré²; Arjen Roos³; Dominique Geoffroy³; ¹MinesParistech; ²Ecole Polytechnique; ³ONERA

The topic of this talk concerns a methodology for identifying mechanical parameters of constitutive equations thanks to an optimization procedure based on multiscale coupling between microstructure characterizations (morphology, crystallographic texture, chemical composition, etc...), mechanical strain field analysis obtained during in situ or ex situ tests and finite element simulations. Special interest is given to the effects of different boundary conditions (homogeneous strain, homogeneous stress, experimental strain field) applied to the finite element mesh and in particular the sensitivity of these simulations on the optimum set of parameters. Moreover, global 3D simulations performed on an RVE will be compared to the results of 2D extruded mesh from experimental characterization. Discussions about recent tools dedicated to virtual 3D microstructures in respect to real microstructure will be introduced.

9:30 AM

On the Origin of Plastic Instability of Al-Mg Alloy 5052 during Stress Rate Change Test: Chen-Ming Kuo¹; Chi-Ho Tso¹; ¹I-Shou University

Plastic instability or Portevin-Le Chetelier effect is observed during stress rate change test of Al-Mg alloy 5052 at room temperature. In the stress rate change experiments, strain retardation and plastic instability are observed between the initial and final stress levels, that is, although the applied stress rate changes from the initial stress level, plastic strain is insignificant until the plastic instability occurs. By gradually increasing the final stress level from initial stress level at fixed applied stress rate, plastic instability is also observed and could be modeled by the typical plastic deformation mechanism, that is, thermally activated kinetic flow theory of dislocations coupled with structural evolution law. By changing the values of suitable parameters to simulate the microstructure change of instability, the origin of plastic instability could be understood.

9:50 AM Invited

Probabilistic Simulation of Incubation and Nucleation of Fatigue Cracks in AA 7075-T651: *Anthony Ingraffea*¹; Jacob Hochhalter²; Michael Veilleux¹; Jeffrey Bozek¹; ¹Cornell University; ²NASA

Microstructurally small fatigue cracking in AA 7075-T651 includes incubation, nucleation, and microstructurally small propagation stages. The first part of this work addresses incubation through identification of particles prone to cracking, and predicting particle cracking frequency, given a distribution of particles and crystallographic texture.For the nucleation event, it is hypothesized that nucleation can be predicted by computing a non-local metric near the crack front. The hypothesis is tested by experimentation and 3D finite element modeling. Slip- and energy-based nucleation metrics are tested for validity. Each metric is derived from a continuum crystal plasticity formulation. Good agreement is found between the predicted frequency of particle cracking and two preliminary validation experiments. For nucleation, it is found that a continuum crystal plasticity model and a nonlocal nucleation metric can be used to predict the nucleation event. However, nucleation metric threshold values that correspond to various nucleationgoverning mechanisms must be calibrated.

10:20 AM

A Stochastic-Based Modified Gurson Model for Modeling Void Growth in Metallic Alloys: Huiyang Fei¹; Kyle Yazzie¹; Nikhilesh Chawla¹; *Hanqing Jiang*¹; ¹Arizona State University

The Modified Gurson Model, also known as Gurson-Tvergaard-Needleman Model, is widely used to study ductile fracture in metallic materials where microvoid formation is prevalent. In Gurson's theory, the void volume fraction (VVF) is the only parameter representing a void, while the size of void is ignored. In the FEA package ABAQUS, the initial VVF is an average value assigned to an area. In this talk, we developed a stochastic method that could generate a random distribution of VVF as the initial configuration for FEA simulation. The numerical simulations were conducted with ABAQUS/Standard using Gurson parameters obtained from experiments. This stochastic enhancement method better characterizes the real distribution of microvoids in porous metals, and better predicts the failure than non-randomized Modified Gurson Model in ABAQUS, compared to the experiments. Moreover, this stochastic enhancement can also be applied to other Gurson parameters, such as nucleation strain, critical failure VVF, etc..

10:35 AM Break

10:55 AM Invited

Approaching Statistically Significant Correlations through Reduced Modeling of Initial Yielding Behavior: Siddiq Qidwai¹; Alexis Lewis²; Andrew Geltmacher²; ¹SAIC; ²Naval Research Laboratory

Image-based 3D modeling techniques have been used to examine the role of microstructure on the initial yielding behavior of a beta titanium alloy. The determination of statistically significant microstructure-property correlations among the many measured parameters require analysis of data from large 3D microstructural reconstructions, and in many cases, these analyses exceed the computational power of the available hardware and software. In this paper, two techniques are examined to increase computational efficiency by decreasing image-based model sizes. The first technique involves the evaluation of reduced-parameter constitutive relationships. The second technique involves the use of 2-point cross-correlation method based on crystal orientation probability function to identify smaller sub-volume sets within the large sample that when properly weighted are statistically representative of the entire microstructure. It was found that each of these approaches was effective in reducing the computational resources necessary to analyze statistically significant volumes of material.

11:25 AM Invited

Deformation and Microrotation in the Vicinity of Grain Boundaries: Continuum Analysis of Atomistic Simulations: Garritt Tucker¹; *Jonathan Zimmerman*²; David McDowell¹; ¹Georgia Institute of Technology; ²Sandia National Laboratories

Grain boundaries and their deformation accommodation mechanisms impact the mechanical behavior of polycrystalline materials, particularly when grain size is at the nanometer scale. Some commonly observed processes in nanocrystalline metals include heterogeneous dislocation nucleation, grain boundary sliding, and migration. Here, we apply metrics from continuum mechanics to atomistic simulations to develop a theoretical understanding of deformation mechanisms in grain boundaries. Expressions for deformation gradient and vorticity are evaluated for simulations of 3-dimensional symmetric tilt grain boundaries of Cu subject to uniaxial tension and simple shear loading conditions. Numerous grain boundary orientations are analyzed with respect to deformation mechanisms and our metrics for deformation and microrotation. Our analysis also compares how the microrotation varies with distance from the grain boundary and with increasing applied strain. Sandia is a multiprogram laboratory operated by Sandia Corporation, a Lockheed-Martin Company, for the United States Department of Energy's National Nuclear Security Administration under contract DE-AC04-94AL85000.

11:55 AM

An Attempt to Express Isotropic Yield Functions of Metals Based on the Invariants of Stress Tensor: *Mohammad Habibi Parsa*¹; Kamal Azimi¹; Payam Matin²; ¹University of Tehran; ²Sciences University of Maryland

Different yield functions have been proposed for describing metals yield points and there are many kind of yield function that is used for different types of metals. Many of proposed yield function have been originated from extensive experiments and curve fitting of resulted data. Few theoretical based yield functions have been also suggested. Such different yield functions are source of confusion for applicant of these functions for predicting of yield phenomena. In the present work, it has been tried to describe yield function of metals using stress tensor invariants in order to describe all different kind of yield functions by one equation. Based on mentioned idea, general form of polynomial yield function based on the stress tensor invariants has been developed and then using geometrical tool and existing experimental results, a general polynomial yield function has been proposed that can express all of existing yield functions.

12:15 PM

Three Dimensional Visualization and Microstructure-Based Modeling of Plasticity

and Void Growth in Pb-Free Solder Alloys: Vaidehi Jakkali¹; Ling Jiang¹; Jason Williams¹; Nikhilesh Chawla¹; M Pacheco²; V Novitski²; S Lau³; Luke Hunter³; ¹Arizona State University; ²Intel; ³Xradia

Pb-free interconnects are being used extensively in Electronic Packaging. One of the significant defects introduced during processing of the solder joints is voids. The presence of porosity affects the mechanical performance of solder joints. 3D X-Ray Tomography is an effective non destructive technique of characterizing the nature of porosity in Solder joints. In this study, 3D X-Ray Tomography was used to visualize and re-construct the microstructure of Sn-3.9Ag-0.7Cu/Cu solder joints. This reconstructed micro-structure was incorporated into a Finite Element Model, using Modified Gurson criterion to simulate shear deformation and eventual failure of the joint due to void nucleation, growth, and coalescence. The effectiveness of this technique in understanding the effect of size, shape, and distribution of pores on local and global plasticity of the solder joints will be discussed.

Computational Thermodynamics and Kinetics: Microstructual Evolution

Sponsored by: The Minerals, Metals and Materials Society, ASM International, TMS Electronic, Magnetic, and Photonic Materials Division, TMS Materials Processing and Manufacturing Division, TMS: Alloy Phases Committee, TMS: Chemistry and Physics of Materials Committee, TMS/ASM: Computational Materials Science and Engineering Committee, ASM: Alloy Phase Diagrams Committee *Program Organizers*: Raymundo Arroyave, Texas A & M University; James Morris, Oak Ridge National Laboratory; Mikko Haataja, Princeton University; Jeff Hoyt, McMaster University; Vidvuds Ozolins, University of California, Los Angeles; Xun-Li Wang, Oak Ridge National Laboratory

Wednesday AM	Room: 9
March 2, 2011	Location: San Diego Conv.

Session Chairs: Min Soo Park, Texas A&M University; Nele Moelans, Katholieke Universiteit Leuven

Ctr

8:30 AM Invited

Role of Elastostatic Interaction in Domain Processes of Magnetic Shape Memory Alloys: *Yongmei Jin*¹; ¹Michigan Technological University

A phase field micromagnetic microelastic model is employed to study the role of elastostatic interaction in magnetic domain evolution and field-induced deformation of magnetic shape memory alloys. The model explicitly treats magnetic and elastic domain microstructures and takes into account multiple thermodynamic driving forces, including magnetostatic, elastostatic, magnetocrystalline, exchange, chemical, and applied magnetic and mechanical loadings. Computer simulations reveal details of coupled magnetic and elastic domain evolutions, and show that the competition between elastostatic and magnetostatic interactions governs domain processes and the resultant field-induced strain behaviors in magnetic shape memory alloys. The different contributions from twin shear strain and magnetostrictive strain to elastostatic interactions are analyzed. The effects of twin boundary mobility on domain processes are discussed.

9:00 AM Invited

Phase-field Modeling of Deformation Twinning: Taewook Heo¹; Yi Wang¹; Saswata Bhattacharya¹; Xin Sun²; Shenyang Hu²; *Long Qing Chen*¹; ¹Pennsylvania State University; ²Pacific Northwest National Lab

We propose a phase-field model for modeling microstructure evolution during deformation twinning. Using a face-centered cubic aluminum as an



example, the deformation energy as a function of shear strain is obtained using first-principle calculations. The gradient energy coefficients are fitted to the twin boundary energies along the twinning planes and to the dislocation core energies along the directions that are perpendicular to the twinning planes. The elastic strain energy of a twinned structure is included using the Khachaturyan's elastic theory. We simulated the twinning process and microstructure evolution under a number of fixed deformation magnitudes and predicted the twinning plane orientations and microstructures. It is shown that twinning may take place through either nucleation and growth or spinodal mechanism, and the relative volume fractions of twin variants has approximate linear dependence on the magnitude of deformation strain.

9:30 AM

Microstructure Evolution and Analysis of Single Crystal Nickel-Based Superalloy During Compression Creep: Shu Zhang¹; Sugui Tian¹; ¹ Shenyang University of Technology

Through creep property test and microstructure observation, the microstructure evolution of [001] orientation single crystal nickel-based superalloy during compressive creep is identified as the cubical \947' phase being transformed into the rafted structure along the direction parallel to the applied stress axis. By the calculation of von Mises stress distribution of the \947' phase with the three-dimensional stress-strain finite element method, it indicates that the applied compressive stress may change the stress distribution of the cubical \947'/\947 phases, and the coarsening orientation of \947' phase is closely related to the von Mises stress distribution of the \947 matrix channel. Under the action of the applied compressive stress, the bigger von Mises stress is produced on (001) crystal plane of the cubical \947' phase, which is the main reason for microstructure evolution. The driving forces of the elements diffusion and directional coarsening of \947' phase during compressive creep are further discussed.

9:45 AM

Combining Phase-Field and CALPHAD for Systems Containing Intermediate Phases with Low Solubility: *Nele Moelans*¹; Bo Sundman²; ¹K.U. Leuven, Belgium; ²INSTN, CEA, France

Reactive growth of intermediate phases with low solubility is important for many applications, for example IMC growth in solder joints, growth of silicide layers and oxidation. Gibbs energies developed according to the CALPHAD approach, using a regular solution model, can be combined with the phase-field technique to study microstructure evolution in multicomponent systems. Phases with low solubility, however, are usually modeled as stoichiometric or using a sublattice model defined for a restricted composition range. This format is not directly compatible with the free energies used in a phase-field model. We have compared 3 approaches to combine CALPHAD thermodynamic descriptions of multi-component systems with the phase-field technique, applicable for systems containing phases with limited solubility. The methodologies are illustrated for binary and ternary systems.

10:00 AM Break

10:10 AM Invited

Modeling of Crystal Defects and Interactions at Diffusive Time Scales: Jon Dantzig¹; ¹University of Illinois

Many important aspects of the mechanical behavior of materials are manifested at the atomic length scale, but at diffusive time scales. This combination makes these phenomena inaccesible to both molecular dynamics and continuum approaches. The phase-field crystal (PFC) method is able to capture this portion of parameter space using a coninuous function to represent density resolved at the atomic length scale, coarse-grained in time to diffusivescales. Modifications to the original PFC model that stabilize vacancies are described, and the mechanical response of defected structures under mechanical loading will be presented.

10:40 AM

Free Energy Functionals for Efficient Phase Field Crystal Modeling of Structural Phase Transformations: *Michael Greenwood*¹; Nikolas Provatas²; Joerg Rottler¹; ¹University of British Columbia; ²McMaster University

The phase field crystal (PFC) method is a promising technique for modeling materials with atomic resolution on mesoscopic time scales. While numerically more efficient than classical density functional theory (CDFT), its single mode free energy limits the complexity of structural transformation that can be simulated. We introduce a new PFC model inspired by CDFT, which uses a systematic construction of two-particle correlation functions that allows for a broad class of structural transformations, including bcc, fcc and hcp lattices. Our approach allows for control and parameterization of temperature effects and anisotropy of the surface energy and elastic coefficients of the material.

10:55 AM

Control of Domain Configurations and Sizes in Crystallographically Engineered Ferroelectric Single Crystals: Phase Field Modeling: *Jie Zhou*¹; Tian-Le Cheng¹; Ke-Wei Xiao²; Wei-Feng Rao²; Yu Wang¹; ¹Michigan Tech.Univ.; ²Virginia Tech

Phase field modeling and simulation is performed to study the mechanisms of crystallographic domain engineering technique for ferroelectrics. It is found that both domain configurations and domain sizes in ferroelectric single crystals can be controlled through sophisticated thermal and electrical conditions imposed on the materials during ferroelectric phase transformations. The simulations reveal that minimal domain sizes and highest domain wall densities are obtained with intermediate magnitude of electric field applied along non-polar axis of ferroelectric crystals, while lower and higher fields produce coarser domains and lower domain wall densities. It is found that temperature also plays an important role in domain size control. The simulations show that selection of polar domain variants by external electric field during nucleation stage of ferroelectric phase transition significantly affects subsequent domain growth and evolution kinetics and controls the formation and sizes of twin-related lamellar domains. This technique can be used to develop high-performance piezoelectrics.

11:10 AM

Phase Field Modeling of Nanoparticles for Medical Applications: Jonathan Guyer¹; David Saylor²; James Warren¹; ¹NIST; ²FDA

Nano-particulate silver systems are widely used in wound dressings, surgical masks, and catheter coatings as anti-microbial agents. We have shown that a phase field model of the electrochemical interface captures behaviors including electrocapillary phenomena, differential capacitance curves that resemble experimental measurements, and non-linear kinetics consistent with the empirical Butler-Volmer relation. Although numerical constraints limit the applicability of this model to dimensions of a few nanometers, the model is capable of making predictions at precisely the spatial and temporal scale that we are interested in for studying medical applications of silver nano-particles. We will discuss the impact of particle size, solution concentration, and particle aggregation on ion release and surface charge, which not only impact the anti-microbial efficacy and system stability, but may also affect biocompatibility. Finally, we will discuss our efforts to extend the length and time scales of the model.

11:25 AM

Phase-Field Crystal Modeling of Compositional Domain Formation in Ultrathin Films: *Srevatsan Muralidharan*¹; Raika Khodada²; Mikko Haataja¹; ¹Princeton University; ²California State University Northridge

Bulk-immiscible binary systems often form stress-induced miscible alloy phases when deposited on a substrate. Both alloying and surface dislocation formation lead to the decrease of the elastic strain energy, and the competition between these two strain-relaxation mechanisms leads to the emergence of compositional nanoscale domains. We develop a phase-field crystal model for compositional domain formation of binary metallic systems. We demonstrate that the model naturally incorporates the competition between alloying and misfit dislocations, and quantify the effects of misfit and line tension on equilibrium domain size. Then, we quantitatively relate the parameters of the PFC model to a specific system, CoAg/Ru(0001), and demonstrate that the simulations capture experimentally observed morphologies. We find that a Co rich system is pseudomorphic with the underlying substrate, while in an Ag rich system, the excess Ag phase displays dislocations and stacking faults that is in equilibrium with the 50-50 pseudomorphic alloy phase.

11:40 AM

Quantitative Phase-Field Predictions of β " Precipitate Size Distribution as a Function of Heat Treatment Conditions and Alloying Composition in AA6111: Junsheng Wang¹; Shiyao Huang¹; Ruijie Zhang¹; William Donlon¹; Mei Li¹; Long-Qing Chen²; John Allison³; ¹Ford Research and Advanced Engineering Lab, Ford Motor Company; ²Department of Materials Science and Engineering, Penn State University; ³Department of Materials Science and Engineering, The University of Michigan

A phase-field model was used to simulate precipitate nucleation and growth during the heat treatment of AA6111 (Al-Mg-Si) alloys. The influence of forming prior to heat treatment is also included in this analysis. After the forming process, the dislocation density is calculated which is then related to the nucleation density of precipitation. The distribution of critical β " precipitate nuclei in AA6111 alloys were stochastically assigned and the potential for nucleation was calculated as a function of local supersaturation. Therefore, we calculate the nucleation and growth kinetics of β " precipitate during age hardening of AA6111 alloys. We studied the effects of initial Mg and Si concentrations on the β " size distribution. In addition, both aging time and temperature alter the precipitate size and thus affect the final yield strength of AA6111 components. Transmission electron microscopy was performed to quantify the size and number density of precipitates for model development and validation.

11:55 AM

Phase-Field Simulations of Bainitic Phase Transformation in 100Cr6: *Wenwen Song*¹; Ulrich Prahl¹; Wolfgang Bleck¹; Krishnendu Mukherjee¹; ¹RWTH Aachen University

Bainite structure is of considerable importance in the design of high strength steels which contribute a lot in automotive industry. In order to better understand the mechanisms of bainite structure formation and its microstructure evolution controlling parameters, 2D phase-field simulations of the bainitic phase transformation are performed coupling with CALPHAD method. In the present work, high carbon bearing steel EN DIN 100Cr6 is used to investigate the bainite transformation and the bainitic growth mode is considered to be faceted in the phase-field simulations. The results show the bainitic microstructure evolution and its growth kinetics. Carbon diffusion as well as the interfacial mobility during bainitic phase transformation is stressed. The phase-field predicted phase fraction and microstructure evolution results are compared against the dilatometry and HRTEM experimental results. The isothermal bainitic phase transformation kinetics is successfully modeled.

12:10 PM

Transmission Electron Microscopy and Modeling of Carbide Precipitation in Tempered Martensitic Steels: *Peter Hedström*¹; Joakim Odqvist¹; Fredrik Lindberg²; ¹KTH - Royal Institute of Technology; ²Swerea KIMAB AB

Carbide precipitation during tempering of martensite has a significant effect on the final mechanical properties of alloyed steels. Hence, detailed knowledge of carbide precipitation sequences, element partitioning and size distribution evolution is essential. The recent advancement in modelling strategies has opened up the possibility to perform modeling of carbide precipitation with predictive capability, but more detailed experimental work is required to assess the necessary thermodynamic and kinetic data for the relevant alloy systems. The purpose of this work is to provide such an experimental assessment for some selected model and industrial alloys. The experimental results from transmission electron microscopy and atom probe are used to evaluate modeling of carbide precipitation using a Langer-Schwartz approach.

David Pope Honorary Symposium on Fundamentals of Deformation and Fracture of Advanced Metallic Materials: Deformation, Fracture, and Advanced Characterization Techniques

Sponsored by: The Minerals, Metals and Materials Society, TMS Materials Processing and Manufacturing Division, TMS Structural Materials Division, TMS: High Temperature Alloys Committee, TMS/ASM: Mechanical Behavior of Materials Committee, TMS: Nanomechanical Materials Behavior Committee *Program Organizers:* E. P. George, Oak Ridge National Laboratory; Haruyuki Inui, Kyoto University; C. T. Liu, The Hong Kong Polytechnic University

Wednesday AM	Room: 32A
March 2, 2011	Location: San Diego Conv. Ctr

Session Chairs: Tresa Pollock, University of California Santa Barbara; Erland Schulson, Dartmouth College

8:30 AM Invited

Forensic Applications of Materials Science-An Overview: Michael Smith¹; ¹Federal Bureau of Investigation

Forensic science serves as an umbrella term for a broad range of technical activities that also entail a legal element. While many are familiar with such disciplines as DNA analysis and latent fingerprints, the role of materials science in the legal system is relatively less known. Nevertheless, materials issues commonly arise in both civil and criminal legal proceedings. To illustrate this, a range of examples will be presented along with an explanation of how the information provided by the forensic analysis of materials is used in investigative and judicial settings.

9:00 AM Invited

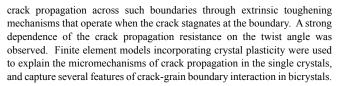
Investigations of Zirconium Alloy Deformation and Fracture: Jake Ballard¹; John Sutliff¹; Tom Angeliu¹; *Robert Mulford*¹; Joseph Pyle¹; ¹Knolls Atomic Power Lab

Zirconium-based alloys have been the backbone of commercial nuclear power generation for over half a century, but unexpected behaviors are still observed during service. Fundamental understanding of zirconium alloy deformation and fracture, especially during power transients is growing in its importance to better predicting long-term performance and minimizing testing and post irradiation examination costs. The complexity of events controlling deformation and fracture require both mechanical and chemistry focused studies. For example, one hypothesis attributes fuel rod failure to fission product release from cracked fuel promoting iodine stress corrosion cracking. Results from several fundamental studies will be presented, including Zircaloy fracture mechanism maps, atomistic modeling of iodine at grain boundaries and surfaces, and electron backscattered diffraction analysis of iodine SCC crack tips and fracture surfaces. A goal of these studies is to better guide development of modeling tools to enhance prediction capabilities and better guide future testing.

9:30 AM Invited

Crack Growth on Basal Planes in Zn Single and Bicrystals: Experiments and Computations: *Sharvan Kumar*¹; Dhiraj Catoor²; ¹Brown University; ²Dassault Systèmes Simulia Corp

Crack propagation on the basal planes in zinc was examined by means of in-situ fracture testing of pre-cracked single crystals, with attention paid to the fracture mechanism. Crack propagation occurred in bursts of dynamic extension followed by periods of arrests, the latter accompanied by plastic deformation. The crystallographic orientation of the crack growth direction on the basal plane influenced the fracture load and deformation at the crack-tip, producing noticeably different fracture surfaces. Insitu crack propagation experiments across grain boundaries of controlled "twist misorientation" in bicrystals confirmed significant resistance to



10:00 AM Invited

JIM INTERNATIONAL SCHOLAR AWARD WINNER: Crack Tip Dislocations and the Sequential Multiplication Process of Dislocation Sources along the Crack Front Revealed by HVEM-Tomography: *Masaki Tanaka*¹; S. Sadamatsu¹; G.S. Liu²; H. Nakamura¹; K. Higashida¹; I.M. Robertson²; ¹Kyushu University; ²University of Illinois

Previous investigations have revealed that the brittle-to-ductile transition (BDT) behavior often exhibited in metals is influenced by the activity of crack tip dislocations—but the exact processes governing dislocation multiplication at the crack tip remains experimentally ambiguous. This study elucidates the three-dimensional structure of crack tip dislocations via a novel combined approach of high-voltage electron microscopy and tomography (HVEM-tomography) in single crystal silicon. It was revealed that dislocations cross-slipped proximal to the crack tip even in the initial stages of plastic deformation. The local stress intensity factor along the crack front was calculated, taking into account the experimentally determined dislocation character. Based on these results, a model to account for the sequential multiplication of dislocation sources along the crack front is proposed.

10:30 AM Invited

Improving Surfboards through the Adaptation of Metallic Honeycomb Sandwich Structure Technology: *Edison Conner*¹; ¹N/A

Edison Conner was a Materials Science undergraduate student of Dr. Pope, graduating from the University of Pennsylvania in 2005. Mr. Conner's senior project proposed fundamental design changes that could dramatically improve the performance of surfboards. Traditional surfboard construction techniques were developed in the 1960's and do not employ many of the major technological advances that have occurred in the advanced composites industry over the past half-century. Mr. Conner's talk will discuss a hypothesis for creating a higher-performance surfboard followed by a discussion of how his newly-developed aluminum honeycomb core surfboards have met those needs.

11:00 AM Invited

Fundamental Research to Discover Amazing Metals through the "Nano-Metallurgy": Kenji Abiko¹; ¹Tohoku University

Recently, due to the remarkable technological progress in industries, the demand for the development of higher performance metals has been accelerated. It is, however, not easy to discover such metals of desirable properties. Fortunately, we know the incredible properties and phenomena of metals appear sometimes by the ultra-purification. After our investigation of such facts, I proposed the new concept of "Nano-Metallurgy" in the UHPM International Conference at Helsinki, 2000, to discover amazing metals. The properties of conventional metals are strongly affected by the impurity atoms. After the removal of the impurity effects by ultra-purification, the incredible properties are revealed as the inherent properties. After the nanocontrol of beneficial elements by doping to the ultra-purified matrix and then the nano-control of structure by heat treatment, amazing metals of very interesting properties will be born. In my talk, the development of innovative stainless alloys will be present through the concept of "Neno-Metallurgy".

11:30 AM

Subsonic Edge Dislocation near Interface Solved with Discrete Image Edge Dislocation Components: Johannes Weertman¹; ¹Northwestern University

The use of ordinary image edge dislocations to solve the problem of an edge dislocation near an interface is thwarted because of the impossibility of simultaneously satisfying the two traction continuity conditions. However, using only discrete edge image dislocations components (some dependent

on the shear wave velocity and others on the longitudinal wave velocity) the problem is solved of an edge dislocation moving near a welded interface separating material of different elastic constants or moving near a free surface.

11:45 AM

140th Annual Meeting & Exhibition

Fundamentals of Fatigue Crack Initiation and Propagation: Chandra Pande¹; ¹Naval Research Laboratory

A basic understanding of the fundamental nature of fatigue crack initiation and growth in metals has long been a major scientific challenge starting with the first dislocation model of fatigue crack growth of Bilby et al. (1963). Understanding the process of emission of dislocations from cracks, and determining precise expressions for the size of the plastic zone size, the crack-tip opening displacement and the energy release rate of the crack are some of the major technical issues for this purpose. We summarize briefly some of the significant results obtained in our investigations towards this goal.

12:00 PM

Intelligent Microscopy for the Study of Fracture and Fatigue: David Fullwood¹; Brent Adams¹; Travis Rampton¹; Ali Khosravani¹; ¹Brigham Young University

A fundamental goal in the investigation of fracture and fatigue mechanisms is the development of methods for recording critical event inception. The development of in-situ test equipment, and high-resolution microscopy techniques (such as high-resolution orientation imaging microscopy, HROIM) have placed invaluable tools into the hands of researchers. Nevertheless, practical considerations limit the volume of material that can be carefully monitored during a given testing regime. Machine learning techniques offer a promising framework for enhancing efficiency in the search for critical events. This paper presents initial efforts to develop an intelligent microscopy environment for the study of fracture and fatigue, based upon machine learning methods, in general, and reinforcement learning, in particular. The test bed for the study will include ductility studies in magnesium, exploiting recent advances by the authors in the area of HROIM.

Deformation, Damage, and Fracture of Light Metals and Alloys: Session III

Sponsored by: The Minerals, Metals and Materials Society, MS&T Organization, TMS Light Metals Division, TMS: Chemistry and Physics of Materials Committee, TMS/ASM: Mechanical Behavior of Materials Committee

Program Organizers: Qizhen Li, University of Nevada, Reno; Xun-Li Wang, Oak Ridge National Laboratory; Yanyao Jiang, University of Nevada, Reno

Wednesday AM	Room: 13
March 2, 2011	Location: San Diego Conv. Ctr

Session Chair: Qizhen Li, University of Nevada, Reno

8:30 AM Invited

Confining Shear Bands and Fracture to Improve Plasticity in an Amorphous Mg Alloy Reinforced with Mo Particles: *Taigang Nieh*¹; Jason Jang²; Jacob Huang³; ¹University of Tennessee; ²National Central University; ³National Sun Yat-Sen University

Amorphous alloys are intrinsically brittle because of the formation of plastically instable shear bands. By adding ductile crystalline phase to arrest shear bands is an effective method to improve plasticity. We synthesized amorphous Mg alloy (Mg58Cu28.5Gd11Ag2.5) reinforced with porous Mo particles with different volume fractions and particle sizes by casting technique. It was found that the presence of porous Mo particles (20-50 μ m) could effectively block/deflect shear band propagation. For a given volume fraction of Mo particles, smaller particles or more volume fraction would lead to shorter inter-particle spacings, thus smaller confinement zone sizes

for shear band, and consequently the improvement of compression plasticity (up to 27%). We will also discuss the criterion and mechanism for plasticity improvement in amorphous alloys.

9:00 AM

Formability of Wrought Magnesium Sheet for Various Temperatures and Strain Conditions: Michael Miles¹; David Fullwood¹; Brent Adams¹; *Jonathan Scott*¹; Ali Khosravani¹; ¹Brigham Young University

Formability of wrought magnesium alloys at or near room temperature is not favorable. The hexagonal close packed structure of Mg has few active slip systems at lower forming temperatures, limiting ductility. Much greater levels of ductility can be reached at higher temperatures but this is expensive and inconvenient for a high-volume production environment. A series of forming experiments will be conducted at room temperature and at slightly elevated temperatures, up to 150°C. Limit strains will be measured in uniaxial tension, plane strain, and biaxial tension. Microstructure evaluation will be performed on samples formed at different temperatures and strain paths, in order to determine how twinning and dislocation density are correlated localization and failure under these forming conditions. Highresolution EBSD will be used to generate data on twinning and dislocation density in order to find links between forming conditions, initial texture, and forming ductility.

9:15 AM

Utilizing HR-OIM and In-Situ Tensile Tests for Studying Crack Initiation in AZ31 Magnesium Alloys: *Ali Khosravani*¹; Brent L. Adams¹; David T. Fullwood¹; Mike Miles¹; Stuart Rogers¹; Jonathan Scott¹; ¹Brigham Young University

The magnesium alloys, including AZ31 alloys, are being increasingly used in structural applications. However, poor ductility of the hcp materials due to limited numbers of slip systems is a major issue preventing faster deployment of AZ31 alloy. Several parameters, collectively known as FIPs, failure initiation parameters, have been reported as the main reasons for the nucleation of cracks within the microstructure. These FIPs often include tensile, compression, and double twinning, triple junction, grain boundary sliding, and their intersections. The objective of this paper is to clarify the importance of each FIP in crack initiation using HR-OIM. By utilizing in-situ tensile test in the SEM and applying different levels of strain up to failure, the stress and dislocation maps of the microstructure can be obtained at each step. The dislocation maps can further be refined to consider basal slip and non-basal slip maps which can help us in the investigation.

9:30 AM

Stress Intensity Factor Solutions for Friction Stir Spot Welds of Magnesium AZ31 Alloy: *Tian Tang*¹; Mark F. Horstemeyer¹; Brian Jordan¹; Paul Wang¹; ¹Mississippi State University

The focus of the present study is to investigate the stress intensity solutions for friction stir spot welds of magnesium AZ31 alloy using finite element method. Three dimensional finite element models are constructed to thoroughly analyze the distribution of stress intensity factors including both global and local values. For the local stress intensity factors, we considered two cases, namely, infinitesimal kinked crack and finite length kinked crack. The local stress intensity factors at the critical points of infinitesimal length kinked crack are determined using the global stress intensity factors and analytical expressions of Cotterell and Rice (1980). In comparison to the stress intensity factor solutions of resistant spot welds with respect to the faying face cause the distribution of stress intensity factors significantly different from those of resistant spot welds with symmetric structure.

9:45 AM

Deformation Induced Phase Transformation during Machining of Ti-5Al-5Mo-5V-3Cr: *David Yan*¹; Guy Littlefair¹; Tim Pasang¹; ¹AUT University

Ti-5553 is a relatively new titanium alloy with applications particularly in the aerospace industry for such key structural components as landing gear. However, during machining of Ti-5553, the elevated temperature and high strain at the tool-workpiece interface may alter workpiece microstructure and result in β to a phase transformation. During phase transformation, some intermediated phase such as ω phase may form which is brittle and hard to machine, and it could reduce the fatigue life of machined components. The aim of this research work is to optimize the machining condition for Ti-5553, in which the β to a phase transformation could be fully understood. Analysis of variables such as micrographs of phase components and cutting zone temperature demonstrates that the cutting temperature governs the formation of final phase components and to some extent this variation has been quantified to allow for further and more detailed investigation.

10:00 AM Break

10:15 AM Invited

Fatigue Modeling in Nickel-Base Superalloys: Bradley Fromm¹; Chen Shen¹; Timothy Hanlon¹; Yan Gao¹; *Liang Jiang*¹; ¹GE Global Research

Fatigue is a leading cause of damage in gas turbine components. Tremendous progress has been made in understanding fundamental mechanisms of fatigue and in methods for fatigue life prediction and damage tolerant design of engineering components. Recent advances in threedimensional microstructural characterization, e.g., serial sectioning and highenergy x-ray, and in microstructure-based fatigue modeling are enabling a more mechanistic understanding of the fatigue process. These techniques are demonstrated here in nickel-base superalloys, a key class of materials within the hot-section of aero and land-based gas turbines. Discussed herein are the characterization techniques used to interrogate the fatigue initiation process, the microstructure-based fatigue modeling approach, and the key challenges involved in modeling and mechanistic understanding of fatigue behavior.

10:45 AM Invited

Fatigue Deformation of Nanocrystalline NiFe Alloy: Sheng Cheng¹; Yonghao Zhao²; Xun-Li Wang³; Sooyeol Lee¹; Li Li¹; Jon Almer⁴; Peter Liaw¹; Enrique Lavernia²; ¹University of Tennessee, Knoxville; ²University of California, Davis; ³Oak Ridge National Laboratory; ⁴Argonne National Laboratory

Materials fatigue is one of the fundamental problems in application, and has remained an active research subject for decades. As a group of emerging materials, the fatigue deformation of nanocrystalline materials has been poorly understood. Recently, we have conducted a series of studies on fatigue deformation of nanocrystalline NiFe alloy. Advanced characterization using both electron transmission microscopy and in-situ high-energy X-ray diffraction has been performed to study the structure stability during fatigue crack propagation. It is found that significant grain growth can be induced by the local plastic deformation around crack tip. The in-situ diffraction technique further demonstrates the internal strain distribution, and correlates it with the microstructure variation near crack tip. Our study indicates that the crack propagation behavior in nanocrystalline materials is not only different from that in conventional materials, but also different from these computer predictions.

11:15 AM

Mechanical Properties and Deformation Mechanisms of Ultrafine Grained Al and Ti: Yonghao Zhao¹; Troy Topping¹; Y. Li¹; Peiling Sun²; Ruslan Valiev³; ¹University of California, Davis, CA 95616, USA; ²Feng Chia University, Taichung 40724, Taiwan; ³Ufa State Aviation Technical University, Ufa 450000, Russia

The high strength of ultrafine grained (UFG) materials is particularly attractive for light-weight structural materials such as Al, Mg and Ti alloys used in aerospace, transportation and biomedical industries. However, UFG metals and alloys usually have mechanical and thermal instabilities, due to a high density of lattice defects, which limit their practical engineering applications. Annealing is a simple and effective way to regain strain hardening/ductility and stabilize UFG structures. In this work, we systematically investigated the mechanical properties and microstructural evolutions of UFG Al and Ti during annealing. The UFG Al and Ti were prepared by equal-channel-angular pressing (ECAP). Annealing formed multi-modal grain structure in UFG Ti and polygenized dislocation walls



in UFG Al. Mechanical results indicate that both structures improved the combination of strength and ductility. The improved mechanical properties were finally rationed based on the microstructures, fracture and deformation mechanisms.

11:30 AM

Investigation of the Fatigue Crack Growth Behavior of Wrought and Cast Light Metals: *Anastasios Gavras*¹; Brendan Chenelle¹; Diana Lados¹; ¹Worcester Polytechnic Institute

The response of light metals under fatigue crack growth conditions was investigated. Fatigue crack growth experiments were conducted on cast and wrought aluminum alloys (A535 and 6061),wrought titanium alloys(Ti-6Al-4V),and alloys processed by novel techniques (6061 aluminum alloys processed by cold spray and friction stir welding).Microstructural effects on the resistance to fatigue crack propagation within each class of materials were evaluated by altering the microstructure through heat treatment, chemistry, and processing. In addition, initial crack size effects were studied for each material under various stress ratios (R=0.1, R=0.5, and R=0.7). The mechanisms of fatigue crack growth at the microstructural scale were identified and will be discussed. The differences in the behavior and controlling crack growth mechanisms between long and small cracks, in the near-threshold regime, and their importance in design are also discussed. Recommendations for integrating materials knowledge into a new design approach for fatigue crack growth resistance are provided.

11:45 AM

An Experimental Study on Cyclic Deformation and Fatigue of Extruded ZK60 Magnesium Alloy: *Qin Yu*¹; Jixi Zhang¹; Yanyao Jiang¹; Qizhen Li²; ¹Department of Mechanical Engineering, University of Nevada, Reno; ²Department of Chemical and Metallurgical Engineering, University of Nevada, Reno

Cyclic deformation and low-cycle fatigue properties of extruded ZK60 Mg alloy were experimentally investigated by conducting fully reversed strain-controlled fatigue experiments along the extrusion direction. The material shows marginal cyclic hardening. Under larger strain amplitudes (>0.52%), asymmetric hysteresis loop and significant tensile mean stress develop. With an immediate strain amplitude $(0.45\% \sim 0.52\%)$, asymmetric hysteresis loop evolves with loading cycles to become symmetric at about 10% fatigue life, accompanied by moderate saturated mean tensile stresses. Symmetric hysteresis shape without mean stress is observed for lower strain amplitudes (<0.45%). The strain-life curve shows a kinking plateau at the strain amplitude of 0.52%. Tensile cracking is exhibited and the SWT fatigue parameter is appropriate to describe the mean stress effect. The fatiguefractured surfaces and the residual twins were microscopically observed. The microscopic features strongly depend on the strain amplitudes and are discussed with respect to the possible crack initiation and propagation mechanisms.

12:00 PM

Effect of Strain Ratio on Cyclic Deformation and Fatigue of Extruded Magnesium Alloy AZ61A: *Jixi Zhang*¹; Qin Yu¹; Yanyao Jiang¹; Qizhen Li¹; ¹Department of Mechanical Engineering, University of Nevada, Reno

Strain-controlled fatigue tests at a variety of strain amplitudes combined with three levels of strain ratio (R=0, -1, -8) were conducted on an extruded magnesium alloy AZ61A using smooth tubular specimens. As the strain ratio decreased, stronger cyclic hardening rate, more asymmetric hysteresis loop, smaller stress amplitude, and lower mean stress were observed. This is considered to be associated with the twinning-detwinning processes during cyclic deformation and the accumulation of residual twins with the number of loading cycles. At the same strain amplitude, fatigue life increased with decreasing strain ratio. The strain-fatigue life curves exhibited a distinguishable kink at the strain ratios of -1 and -8, but the kink disappeared at the strain ratio of 0. Fatigue crack initiation was dependent on strain amplitude and strain ratio, while fatigue crack propagation was dominated by mechanical twins.

Dynamic Behavior of Materials V: Dynamic Deformation

Sponsored by: The Minerals, Metals and Materials Society, TMS Structural Materials Division, TMS/ASM: Mechanical Behavior of Materials Committee

Program Organizers: Marc Meyers, UCSD; Naresh Thadhani, Georgia Institute of Technology; George Gray, Los Alamos National Laboratory

Wednesday AM	Room: 5A
March 2, 2011	Location: San Diego Conv. Ctr

Session Chair: William Proud, U. Cambridge

8:30 AM Invited

A New Paradigm for Lowering the Ductile-to-Brittle Transformation Temperature in Steels: *Morris Fine*¹; Semyon Vaynman¹; Dieter Isheim¹; Yip-Wah Chung¹; Shrikant Bhat²; ¹Northwestern University; ²ArcelorMittal

Inspired by the early work of Weertman, we will present results of a theoretical study on the effect of slightly misfitting nanoscale precipitates on dislocation configurations in metals. The study shows that coherent and coplanar precipitates can twist nearby screw dislocations to locally reduce the Peierls stress, giving rise to improved dislocation mobility at low temperatures. Experimental results will be presented on copper precipitation-strengthened low-carbon steels that have remarkably high Charpy impact fracture energies at cryogenic temperatures. These results suggest a new paradigm for markedly reducing the ductile-to-brittle transformation temperatures in materials.

9:00 AM

Deformation Twinning in Tantalum: *Changqiang Chen*¹; Kaliat Ramesh¹; Kevin Hemker¹; Mukul Kumar²; Jeffrey Florando²; ¹Johns Hopkins University; ²Lawrence Livermore National Laboratory

The competition between deformation twinning and dislocation slip in bcc metals, such as tantalum, has been a long standing issue. The conditions under which twinning occurs are not clearly understood. In this work, we use transmission electron microscopy (TEM) and atomic scale high resolution microscopy (HREM) to characterize deformation twins in tantalum deformed under a wide range of loading conditions (quasistatic, dynamic and shock loading) and temperatures (down to 77k). The competition between dislocation slip and mechanical twinning is analyzed from both the micromechanical and crystallographic points of view, and possible twinning criteria are discussed.

9:15 AM

Dynamic Deformation Response of High-Strength Ni-Containing Steels: *Ratnesh Gupta*¹; Sharvan Kumar¹; ¹Brown University

In this study, the effect of Ni content and heat treatment on microstructure and mechanical properties of Fe-xNi (x=2.5%-10%)-(0.1C/no Cu or 0.04C+1.2Cu)-Cr,Mo,V/Nb steels were examined. Plates were heat-treated to achieve high quasi-static yield strengths varying from 860 to 1100 MPa. The dynamic deformation behavior of these steels was examined in compression in the strain rate regime 2000 s-1 to 3000 s-1 using a split-Hopkinson bar. Optical microscopy of deformed specimens confirmed shear localization to varying extents in these steels, the extent depending on the quasi-static yield strength. Thus, under comparable deformation conditions, whereas a 3.5%Ni steel did not show shear localization, the 10%Ni steel showed fully developed shear band(s) with microcracks within the shear band. Transmission electron microscopy characterization of specimens extracted from within the shear band and without, enabled a recognition of the microstructure evolution within the band. These observations will be presented and implications discussed.

9:30 AM

Dynamic Properties of Ultrafine-Grained Magnesium Alloys: *Bin Li*¹; ¹Center for Advanced Vehicular Systems

Dynamic testing was performed on ultrafine-grained (UFG) Mg alloys (ZK60 and AZ31B) processed by severe plastic deformation with grain size ranging from tens of microns to 250 nm, at strain rates from quasi-static (0.0001/s) to dynamic(10000/s). The dynamic properties of hcp Mg alloys present a strong rate dependence. At quasi-static rates, the deformation was dominated by dislocation slip with a moderate strain hardening, whereas at high strain rates, a sharp increase in strain hardening was observed, indicative of a transition from dislocation slip at quasi-static rates to twinning at dynamic rates. The dislocation structure of the UFG Mg alloys was analyzed by transmission electron microscopy (TEM) before and after testing.

9:45 AM Break

10:00 AM Invited

Lighter, Stronger, Faster: Materials for an Insecure Future: *K Ramesh*¹; ¹Johns Hopkins University

In a near future dominated by energy insufficiency and global insecurity, structural materials are increasingly being required to be strong as well as light and to survive dynamic loads as a consequence of impact, explosions, and high-speed transportation. In this talk we explore the behavior of lightweight materials (in particular, metals and ceramics) subjected to dynamic loads. The dynamic behaviors of these materials are discussed in terms of the inertia associated with mass transport, the inertia associated with failure processes, and the inertia associated with deformation mechanisms. We develop specific insights through a combination of careful high strain rate experiments, transmission electron microscopy and high-resolution electron microscopy and fundamental analytical modeling of the deformation and failure processes. As specific examples, we examine the dynamic behavior of nanostructured aluminum alloys and of aluminum nitride.

10:30 AM Invited

Small Scale Experiments to Support Strength and Damage Modeling: *Ellen Cerreta*¹; Darcie Koller¹; George Gray¹; Curt Bronkhorst¹; Carl Trujillo¹; Juan Escobedo¹; Alex Bergquist¹; Benjamin Hansen¹; Davis Tonks¹; Ricardo Lebensohn¹; ¹Los Alamos National Laboratory

The limited understanding of the stochastic way in which polycrystalline materials fail prevents accurate prediction of their performance. Understanding these processes allows for prediction of their response in service and can lead to the design of more failure resistant materials. Characterization of these processes can be difficult, particularly within the dynamic strain rate regime due to limitations in experimental platforms, in-situ diagnostics, and understanding of path dependent processes. In this talk, current studies to investigate dynamic damage evolution in bulk metals will be discussed. Through the use of novel wave shock wave shaping experiments and combinations of dynamic test platforms (gas guns, laser shock and direct high explosive drive), the kinetic and spatial effects on dynamic damage can be examined. Soft recovery of these specimens enables post mortem characterization. In this way, relationships between dynamic loading conditions and deterministic damage processes are revealed.

11:00 AM

Influence of Cryogenic Processing on Dynamic Tensile Response of High-Purity Copper: *Joel House*¹; Michael Nixon¹; Philip Flater¹; James O'Brien²; William Hosford³; Robert De Angelis⁴; ¹Air Force Research Laboratory; ²O'Brien & Associates; ³University of Michigan; ⁴University of Florida, REEF

It was demonstrated in the work by Wang et al (2002) that cryogenic temperature processing could be used to increase the overall toughness of high-purity copper. Increased material toughness was attributed to coherent twin boundaries introduced via the cryogenic processing and retained by low temperature recrystallization annealing, Ma et al (2004). The current research seeks to extend that characterization by processing high-purity copper using severe plastic deformation at cryogenic temperatures. The severe plastic deformation was introduced by equal channel angular pressing. A series of experiments to characterize the mechanical properties were conducted using a commercially available copper as a baseline for comparison with cryogenic ECAP copper. The Dynamic Tensile Extrusion experiment, see Gray et al (2005), was the principle source of data. Optical microscopy, scanning electron microscopy, and electron backscattered diffraction were used to characterize the grain morphology and the texture evolution.

11:15 AM

High Plasticity and Substantial Deformation in Nanocrystalline NiFe Alloys under Dynamic Loading: *Yonghao Zhao*¹; Sheng Cheng²; Yazhou Guo³; Ying Li¹; Qiuming Wei³; Xun-Li Wang⁴; Yang Ren⁵; Peter Liaw²; Enrique Lavernia¹; ¹University of California, Davis; ²university of tennessee; ³University of North Carolina, Charlotte; ⁴Oak Ridge National Laboratory; ⁵Argonne National Laboratory

High strength of bulk nanocrystalline materials (with an average grain size < 100 nm) has been widely reported, but their plasticity is disappointingly low. In this paper, by dynamically deforming a nanocrystalline NiFe alloy, we achieved a highly improved plasticity (from 8% deformation strain under quasi-static deformation to a maximum strain of ~22%) accompanied by a much enhanced yield strength (33% enhancement compared with quasi-static deformation). Microstructure investigation indicates that the high plasticity was mainly resulted from dynamic deformation induced significant grain coarsening due to grain rotation and grain boundary sliding. In addition, detwinning (e.g. a great reduction of twin density) occurred driven by dynamic loading. Both grain coarsening and de-twinning led to a unique texture as compared to conventional deformation texture. Our work demonstrates ways of improving plasticity of nanocrystalline materials and their potential technological applications in dynamic loading atmosphere (Adv. Mater. 21, 2009, 5001).

11:30 AM

Micromechanical Modelling of the Dynamic Behavior of Amorphous and Crystalline Polymers: Said Ahzi¹; Nadia Bahlouli¹; ¹University of Strasbourg

In a first part of this work, we will discuss the cooperative model for the yield behavior of amorphous polymers as well as the micromechanically based extension of this model to semi-crystalline polymers. This model is valid for a wide range of strain rates (from quasi-static to dynamic) and temperatures. Applications and comparison of predicted results to experimental ones from the literature will be shown and discussed. The second part of this work describes the experimental characterization and the modeling of the thermomechanical behavior of two thermoplastics polyolefins: a polypropylene and an impact polypropylene. Several dynamic strain rates and temperatures were considered. The effect of the adiabatic heating on the flow stress is analyzed and discussed in terms of molecular motion. The micromechanically-based cooperative model was then used to model the yield behavior and the large deformation response. A good correlation between our tests results and the model was obtained.

11:45 AM

High-Strain Rate Behavior of Nanostructured Niobium Processed by Severe Plastic Deformation to Very Large Strains: *Suveen Mathaudhu*¹; Zhiliang Pan²; Weihua Ying²; Laszlo Kecskes¹; Quiming Wei²; ¹U.S. Army Research Laboratory; ²University of North Carolina - Charlotte

We have investigated the high-strain rate, uni-axial compressive behavior of nanostructured niobium (Nb), a refractory metal with bodycentered cubic lattice structure. The material was processed by equal channel angular extrusion (route C) to a maximum number of passes of 24. The microstructure of the processed billets was analyzed using electron back-scattering diffraction (EBSD). We have performed mechanical testing within a wide range of strain rates: from quasi-static loading to high-rate (strain rate >103 /s) loading. It was found that nanostructured Nb exhibits reduced strain rate sensitivity (~0.02) in comparison with the coarse-grained counterpart (~0.04). Unlike many other nanostructured bcc metals such as Fe and W, nanostructured Nb exhibits homogeneous plastic flow under high-rate uni-axial compression. Flow softening is primarily caused by uniform adiabatic temperature rise of the whole specimen.



12:00 PM

Strain-Rate and Temperature Dependent Tensile Behavior of Pb-Sn and Sn-Ag-Cu Solder Alloys: *Brad Boyce*¹; Mike Neilsen¹; Luke Brewer²; ¹Sandia National Labs; ²Naval Postgraduate School

The present study examines the thermomechanical strain-rate sensitivity of eutectic 63Sn-37Pb and Pb-free 95.5Sn-3.9Ag-0.6Cu solder over a broad range of strain rates from 0.0002/s to 200/s at temperatures ranging from -60°C to +100°C. A recently developed servohydraulic tensile method enabled this span of 6-orders of magnitude in strain-rate with a single technique, thereby eliminating ambiguity caused by evaluation across multiple experimental methods. As expected, the tensile behavior of both alloys exhibited strong temperature and strain-rate sensitivity. Microstructural characterization using backscatter electron imaging and electron backscatter diffraction revealed very little intragranular rotation after deformation, suggesting the dominance of a grain boundary sliding deformation mechanism. Finally, a unified-creep-plasticity (UCP) constitutive model for solder deformation has been developed to describe the observed behavior with much higher fidelity than the common Johnson-Cook model.

12:15 PM

Deformation and Failure Behavior of Al/Si Nanocomposites at Atomic Scales: *Avinash Dongare*¹; B. LaMattina²; A.M. Rajendran³; M.A. Zikry⁴; D.W. Brenner⁵; ¹North Carolina State University, Department of Materials Science and Engineering, Department of Mechanical and Aerospace Engineering; ²University of Mississippi, Department of Mechanical Engineering; ³U. S. Army Research Office; ⁴North Carolina State University, Department of Mechanical and Aerospace Engineering; ⁵North Carolina State University, Department of Materials Science and Engineering; ⁵North Carolina State University, Department of Materials Science and Engineering; ⁶North Carolina State University, Department of Materials Science and Engineering

Nanostructured composites materials comprised of metal/ceramic interfaces show significant promise for use in energy, defense, and nuclear applications. Functionally graded ceramic particle reinforced composites are an emerging class of materials for protective structures and are often referred to as blast and penetration resistant materials. The improved damage mitigation is attributed to the compositional gradients introduced through the variation of the concentration of the reinforcing ceramic particles in the matrix. Nanolayered metal-ceramic composities have also shown superior mechanical properties as compared to the conventional-engineered materials. The design and optimization of these composites for extreme environments requires a fundamental understanding of the links between the atomic scale microstructure and mechanical behavior under dynamic loading conditions. Large scale molecular dynamics simulations are used to understand the micro-mechanisms related to deformation and failure of Al/Si interfaces at high strain rates and impact loading conditions. The effect of microstructure (grain size, layer thickness, distribution, etc.) and loading conditions on the strengthening and failure behavior of metal-ceramic composites will be discussed.

Electrode Technology for Aluminium Production: Anode Quality and Rodding Processes

Sponsored by: The Minerals, Metals and Materials Society, TMS Light Metals Division, TMS: Aluminum Committee Program Organizers: Alan Tomsett, Rio Tinto Alcan; Ketil Rye, Alcoa Mosjøen; Barry Sadler, Net Carbon Consulting Pty Ltd

Wednesday AM	Room: 16B
March 2, 2011	Location: San Diego Conv. Ctr

Session Chair: Nigel Backhouse, Rio Tinto Alcan

8:30 AM Introductory Comments

8:35 AM

Multivariate Monitoring of the Baked Anode Manufacturing Process: Julien Lauzon-Gauthier¹; Carl Duchesne¹; Jayson Tessier²; Katie Cantin³; Isabelle Petit³; ¹Aluminium Research Centre – REGAL; ²STAS; ³Alcoa

Producing consistent high quality baked anodes is important for improving performance of the Hall-Heroult aluminum reduction process. Reducing variability is, however, challenging □ variations are introduced by both the raw materials and the plant itself, the former constantly fluctuate (supplier transitions, natural variability), and little feedback on anode quality is available before their use in reduction cells since lab quality assessment is destructive, time consuming and costly. Partial Least Squares (PLS) regression was used for developing a plant-wide monitoring scheme for the baked anode manufacturing process. Relationships are established between raw material properties, process conditions, and baked anode quality attributes. The model was built using weekly averaged data available at the Alcoa Deschambault smelter. Good prediction results and traceability were obtained for several anode properties. Model interpretation based on carbon plant knowledge will be discussed, and its intended use for plant monitoring, troubleshooting and decision making will be illustrated.

9:00 AM

Characterization of a Full Scale Pre-Baked Carbon Anode Using X-Ray Computerized Tomograph: Donald Picard¹; Houshang Alamdari¹; Donald Ziegler²; Pierre-Olivier St-Arnaud¹; Mario Fafard¹; ¹NSERC/ Alcoa Industrial Research Chair MACE3 and Aluminium Research Centre-REGAL, Laval University; ²Alcoa Canada Primary Metals

In the conventional Hall-Héroult electrolysis process, the carbon anode is formed either by compaction or vibro-compaction. The final properties of an anode are influenced by many parameters such as the raw material properties, which may change from day to day. To minimize the effects of the raw materials property variation on the final product, one may want to model numerically the forming process. However, it is imperative that information on real anodes is gathered in order to calibrate those models. Some of the most valuable information is the density and porosity distribution of a full scale baked anode obtained with the computed tomography method. To test the method, three cored samples of 300 mm diameter were taken from a real anode and scanned with a Somatom Sensation 64. Calibrations standards were also used to fit the CT scan results with the experimental results.

9:25 AM

FEM Analysis of the Anode Connection in Aluminium Reduction Cells: *Susann Beier*¹; John J. J. Chen¹; Mario Fafard²; ¹University of Auckland; ²University of Laval

Achieving voltage savings over the anode assembly in an aluminium reduction cell, particularly at the anode connection, is a worthwhile approach within a wider programme of improvement in energy efficiency. Experiments carried out using operating cells are very difficult and expensive, however finite element method (FEM) simulations as used in this study are a cost efficient and accurate method to understand the behaviour of the anode connection, and to identify the constraints to voltage savings. This study investigates the impacts of stub deterioration and yoke stiffness on the anode connection and hence the performance of the anode assembly. An ideal stub diameter for the investigated configuration was found, and the increased voltage drops for various level of stub deterioration were identified. The results show that a yoke cross-bar with reduced height and hence reduced stiffness decreases the tensile stress developed in the anode carbon, which lowers the risk of anode cracks. A limit for stub service life is suggested, showing a potential saving of US\$0.8m annually. A limit for a stub service life was suggested, showing a potential saving of US\$1m annually.

9:50 AM

Development of Industrial Benchmark FEA Model to Study Energy Efficient Electrical Connections for Primary Aluminium Smelters: David Molenaar¹; Kan Ding²; Ajay Kapoor²; ¹CSIRO; ²Swinburne University of Technology

Process improvements of 5MW per plant (50,000tCO2e pa for coal based electricity) are possible through optimisation of the complex cast iron to carbon contacts within aluminium smelter anode and cathode assemblies. Finite element analysis is considered the tool of choice within industry for assessing potential improvements; however there are limitations with existing models regarding handling of contact resistance and carbon stress state. A study has been undertaken using thermo-electrical-mechanical finite element analysis of the cast iron to carbon contact for an anode assembly. The contact pressure and electrical resistance and its dependence on temperature have been derived from data available in the public domain. This paper presents development of the benchmark model including results. The benchmark model will be used as the reference point for the development of more advanced models in ongoing studies to assist primary aluminium smelters achieve these substantial savings in energy efficiency and reduced greenhouse gasses.

10:15 AM Break

10:25 AM

Real Time Temperature Distribution during Sealing Process and Room Temperature Air Gap Measurements of a Hall-Héroult Cell Anode: *Olivier Trempe*¹; Daniel Larouche¹; Donald Ziegler²; Michel Guillot¹; Mario Fafard¹; ¹Université Laval; ²Alcoa

An experimental investigation of the sealing process of an anode assembly used in electrolysis cells has been performed to better define the thermal and mechanical aspects of the cast iron thimble solidification between the steel stub and carbon hole. Three holes of a baked anode have been thoroughly measured with a Coordinate Measuring Machine (CMM) to obtain a high precision three-dimensional map of the carbon interface. These measurements were then compared to the outer surface of the frozen thimbles to obtain a room temperature air gap dimension. Thirty-nine thermocouples, placed in a strategic configuration, allowed the reconstruction of the temperature field in the steel stub, carbon block and solidifying cast iron thimble from the pouring to room temperature. Hence, heat transfer coefficients can be evaluated at the carbon/cast iron and steel/cast iron interfaces with a thermal model. Metallographic analysis is matched with the cooling curves.

10:50 AM

Effects of High Temperatures and Pressures on Cathode and Anode Interfaces in a Hall-Heroult Electrolytic Cell: *Lyne St-Georges*¹; Laszlo I. Kiss¹; Jens Bouchard¹; Mathieu Rouleau¹; Daniel Marceau¹; ¹UQAC

This paper deals with the physical modifications occurring at high temperatures and pressures at the interfaces found in the anode and cathode of a Hall-Heroult electrolytic cell. The anode and the cathode are fabricated with carbon blocks, were steel bars are inserted and sealed with cast iron. Consequently, their interfaces are composed of cast-iron and steel and of cast-iron and carbon. For the investigation presented here, an experimental setup was build to heat and load anodic and cathodic samples. A specific attention was put on the samples preparation, to reproduce real cathode/ anode sealing conditions. During the heating and the loading of the samples, fluctuations of electrical and thermal contact resistances are observed and related to physical transformations at the interfaces. These transformations could explain the fluctuations of electrical and thermal contact resistances observed and potentially the non-homogeneities of voltage and current distribution occurring in a Hall-Heroult electrolytic cell.

11:15 AM

New Apparatus for Characterizing Electrical Contact Resistance and Thermal Contact Conductance: Nedeltcho Kandev¹; *Hugues Fortin*¹; Sylvain Chénard¹; Guillaume Gauvin²; Marie-Hélène Martin²; Mario Fafard²; ¹Hydro-Quebec; ²Laval University

A new apparatus for characterizing the electrical contact resistance and the thermal contact conductivity of connections has been developed and tested. Samples have been heated by induction heating of a stainless steel billet, which creates a powerful heat generator, instead of the commonly used convection furnace. With this apparatus, the thermo-electro-mechanical (TEM) behavior of metal-carbon and metal-metal interfaces can be reproduced. Using a controlled inert gas environment, temperature up to 1000°C and mechanical pressure up to 2 MPa can be achieved. A major advantage is that the temperature equilibrium of the samples can be reached quickly (within 2 or 3 hours) while precisely controlling the heat flux. Recent experimental results performed on steel-carbon samples showed that this concept is feasible and very efficient. This apparatus will be used to establish the constitutive laws of interfaces to support numerical modeling of the aluminium reduction cell.

11:40 AM

Carbon Anode Modeling for Electric Energy Savings in the Aluminium Reduction Cell: *Dag Herman Andersen*¹; Z. L. Zhang²; ¹Hydro Primary Metal Technology; ²Norwegian University of Science and Technology (NTNU)

The carbon anode geometrical design influences the energy consumption in aluminium production. A 2D finite element model (FEM) of an anode immersed in an aluminium reduction cell has been developed to study how the anode geometry affects the variation in the anode to cathode distance (ACD). Large variation in ACD will prevent a systematic reduction of the average ACD and thereby hindering a reduction of electrical power loss in the bath. Another modelling example focuses on the large amount of energy loss occurring at the anode-cast iron interface due to the roughness-induced contact resistance. An analytical equation for the real contact area has been established to link the electrical power loss from the contact resistance with the pressure-dependent interface properties. The proposed contact model can be implemented in a full scale electrical FEM analysis of an anode, and used to optimize energy savings.

Fatigue and Corrosion Damage in Metallic Materials: Fundamentals, Modeling and Prevention: Materials Corrosion and Prevention

Sponsored by: The Minerals, Metals and Materials Society, TMS Structural Materials Division

Program Organizers: Tongguang Zhai, University of Kentucky; Zhengdong Long, Kaiser Aluminum; Peter Liaw, University of Tennessee

Wednesday AM	Room: 31C
March 2, 2011	Location: San Diego Conv. Ctr

Session Chairs: Yoshiki Yamada, Ohio Aerospace Institute; Zhefeng Zhang, Institute of Metal Research, Chinese Academy of Sciences

8:30 AM

The Zinagizado Processes as New Electrochemical Alternative to Prevent the Corrosion: S. R. Casolco¹; A. Zanatta A.¹; H. Castañeda²; S. Valdez³; ¹ITESM-Campus-Puebla; ²Battelle, Applied Energy Systems; ³Instituto de Ciencias Físicas-UNAM

The corrosion is the principal cause of metallic deteriorates. Corrosion originates the fracture, pitting, crack by the oxidation and weakening of the surface. For all this, several anticorrosive processes have been developed



to prevent corrosion. In the present work, is described the electrochemical deposition process called Zinagizado, which is based in to add a thin layer of Zn-Al-Ag alloy, previously called ZINAG. This alloy has been studied for their excellent mechanical properties, additionally is been proposed as an alternative of anticorrosive material. Due to the Zinag is consumed first, such as a sacrificial anode. The deposition of Zinag provides the environmental protection against the corrosion and could be used to covering all kind of steel metallic materials in contact with corrosive medium. The anticorrosive properties, has been obtained by the corrosion resistance of zinc achieve by the aluminium and silver addition, which is cathodically respect to the iron and steel.

8:50 AM

Corrosion Control by Natural Alkaloids in Silicone Coatings on Mild Steel in Simulated Seawater: Sandy Tran¹; James Earthman¹; ¹University of California, Irvine

Protective coatings are typically applied to improve corrosive and fouling resistance but often fail to satisfactorily prevent corrosive damage, especially in aqueous settings where microbiologically influenced corrosion (MIC) is common. MIC and fouling are often coupled mechanisms that involve the settlement of microorganisms that attach and grow on immersed surfaces. Alkaloids are chemicals used by plants for defensive purposes, but which exhibit properties favorable for MIC inhibition, such as anti-microbial and chemisorption properties. Immersion testing with nicotine in a simulated seawater solution was performed to evaluate the potential effectiveness of natural alkaloids for reducing corrosion rate. Nicotine was also incorporated into two silicone coatings that were evaluated for corrosion resistance. Relative to a control sample of a coated mild steel, a coated sample in the presence of nicotine in seawater decreased the corrosion rate by over eightfold. Electrochemical impedance spectroscopy and electrochemical noise analysis are being performed to confirm results.

9:10 AM

Electrochemical Evaluation of Martensitic-Austenitic Stainless Steel in Sulfuric Acid Solutions: Mosaad Sadawy¹; ¹University of Technology

The electrochemical behavior of martensitic-austenitic stainless steel has been evaluated in sulfuric acid solution by weight loss and electrochemical techniques. The results indicated that, increasing sulfuric acid concentration leads to increasing the corrosion rate and decreasing the passive region. Also the results showed that solution heat treated at 1050 0C and as-received specimens gave the highest corrosion resistance, while the tempering process has an adverse effect on martensitic-austenitic stainless steel, showing that the corrosion current increased by increasing tempered temperature.

9:30 AM

The Preparation of Imidazoline Corrosion Inhibitor: Daowu Yang¹; Yunyun Zhang¹; Zhuo Ren¹; ¹ChangSha University of Science & Technology

2 - phenyl-imidazoline was improved to enhance its water solubility and inhibition efficiency, and then composite corrosion inhibitor was manufactured with 2 - phenyl-imidazoline quaternary ammonium salt, potassium iodide, triethanolamine, polyoxyethylene nonylphenyl ether and peregal. An efficient, environmentally friendly Hydrochloric acid composite corrosion inhibitor was selected by orthogonal gravimetric measurements. The static corrosion rate of the composite inhibitor is less than 0.5 g $/(m2 \cdot h)$, and the inhibition efficiency steel reached above 95%, which can increase by 1.1% compared with imidazoline inhibitor. The corrosion inhibition effect of the composite inhibitor have been investigated by weight loss measurements, Tafel polarization curve methods and electrochemical impedance spectroscopy (EIS). The result shows that the composite corrosion inhibitor efficiency is high in process temperature range of Hydrochloric acid cleaning; The composite corrosion inhibitor restrain the process of cathode and anode, which belongs to cathode control-oriented and charge transfercontrolled.

9:50 AM

Effect of Temperature on The Loss of Ductility of S-135 Grade Drill Pipe Steel and Characterization of Corrosion Products in CO₂ Containing Environment: Arshad Bajvani Gavanluei¹; Brajendra Mishra¹; David Olson¹; ¹Colardo School of Mines

Evaluation of loss of ductility of the API S-135 grade drill pipe steel was studied at different temperatures from 25 - 175 °C in CO_2 containing solution using constant extension rate test in connection with a high temperature/high pressure autoclave. Besides, the effect of temperature on the composition and morphology of corrosion product layers of this steel were investigated using X-ray diffraction (XRD), scanning electron microscopy (SEM). Results indicated the change of loss of ductility with temperature and the maximum was observed at 175 °C. XRD studies of the specimens revealed the formation of iron carbonate on the surface. SEM study of surface of the specimens showed a rhombohedric crystalline iron carbonate layer above 100 °C while no FeCO₃ was detected at temperatures below 100 °C. Compactness of films increased with temperature.

10:10 AM Break

10:20 AM

Corrosion Behavior and Galvanic Corrosion Studies of Ti-6Al-4V Alloy GTA Weldment in HCl Solution: M. Atapour¹; *E. Zahrani*¹; M. Shamanian¹; M. H. Fathi¹; ¹Isfahan University of Technology

The corrosion behavior and galvanic coupling of Ti-6Al-4V alloy in its welded and unwelded conditions were investigated in 5% HCl solution. Welded samples were fabricated using the conventional continuous current gas-tungsten arc welding process. Open circuit potential and potentiodynamic polarization tests were used for corrosion examinations. In addition, open circuit conditions in a zero-resistance ammeter were used to examine the galvanic corrosion behavior of the base metal – weld metal pair. The results indicated that the welded sample exhibited higher corrosion rate compared to the base metal. The galvanic corrosion evaluations showed that the welded sample was the anode of the base metal – weld metal pair. The inferior corrosion behavior of the weld sample is attributed to the coarse prior β grains and acicular a/ β microstructure.

10:40 AM

Comparative Study of Hot Corrosion Behavior of Plasma Sprayed Yttria and Ceria Stabilized Zirconia Thermal Barrier Coatings in Na2SO4+V2O5 at 1050 °C: Mohammad Sadegh Mahdipoor¹; Mohammad Reza Rahimipour¹; *Mohammad hamed Habibi*²; ¹Materials and Energy Research Center; ²University of Tehran

Thermal Barrier Coatings are subjected to spallation and destabilization due to hot corrosion. Ceria Stabilized Zirconia (CSZ)-based TBCs have been intensively investigated for the YSZ replacement because CSZ has a much lower thermal conductivity and a higher expected thermal expansion coefficient than those of YSZ. In this research, Yttria stabilized zirconia (YSZ) and ceria stabilized zirconia (ZrO2 25CeO2 2.5Y2O3) TBCs were fabricated, followed by hot corrosion tests with a Na2SO4+V2O5 salt at 1050 °C. The treated samples were characterized using XRD and SEM equipped with EDS. From studies on microscopic failure behavior, the formation of YVO4 crystals and the amount of phase transformations of tetragonal ZrO2 to monoclinic lead to degradation of coatings. Results revealed that CSZ TBCs were better resistant to hot corrosion than YSZ TBCs. The amount of YVO4 crystals and monoclinic ZrO2 in YSZ are much more than CSZ which leads sooner degradation of YSZ than CSZ.

11:00 AM

The Effect of Temperature on the Corrosion Behavior of 625 Superalloy in PbSO4-Pb3O5-PbCl-ZnO Molten Salt System with 10 wt. % CdO: *E. Zahrani*¹; A. M. Alfantazi¹; ¹The University of British Columbia

Corrosion behavior of 625 supperalloy under 47.288PbSO4 -12.776 Pb3O5 -6.844 PbCl -23.108 ZnO -10 CdO (wt.%) molten salt mixture and dynamic air atmosphere were studied at 600, 700 and 800°C. Electrochemical impedance spectroscopy(EIS), open circuit potential measurements and potentiodynamic polarization technique were used to evaluate the degradation mechanisms and characterize the corrosion behavior of the alloy. Morphology, chemical composition and phase structure of the corrosion products and surface layer of the corroded specimens were studied by SEM/EDX and x-ray map analyses. Results confirmed that during the exposure of the alloy to the molten salt, Cr was mainly dissolved through an active oxidation process as CrO3, Cr2O3 and CrNbO4 while Ni dissolved only as NiO in the system. Formation of a porous and non-protective oxide layer with decreased resistance should be responsible for the weak protective properties of the barrier layer at high temperatures of 700 and 800°C.

Friction Stir Welding and Processing VI: Friction Stir Processing

Sponsored by: The Minerals, Metals and Materials Society, TMS Materials Processing and Manufacturing Division, TMS: Shaping and Forming Committee

Program Organizers: Rajiv Mishra, Missouri University of Science and Technology; Murray Mahoney, Retired from Rockwell Scientific; Yutaka Sato, Tohoku University; Yuri Hovanski, Pacific Northwest National Laboratory; Ravi Verma, General Motors

Wednesday AM	Room: 5B
March 2, 2011	Location: San Diego Conv. Ctr

Session Chair: Ravi Verma, General Motors

8:30 AM Invited

Friction Stir Processing to Enable High Peak Combustion Pressures in Mid-sized and Heavy Duty Diesel Engines: *Glenn Grant*¹; Saumyadeep Jana¹; Mark Veliz²; Brad Beardsley²; ¹Pacific Northwest National Laboratory; ²Caterpillar Technical Center

As the internal combustion engine has gained efficiency, peak combustion pressures (PCP) have been steadily rising. Since 2003, however, PCP has plateaued around 190 to 200 bar because above this, conventional engine materials in pistons, cylinder liners, and heads will be beyond strength and fatigue limits. In order to increase engine efficiency further, either unconventional expensive materials must be used, or conventional materials must be modified in a way that increases their durability. This presentation describes efforts to develop Friction Stir Processing (FSP) as a method of surface modification for better durability. Data will be presented showing that FSP can produce up to 15 times fatigue life improvement and up to 80% improvement in fatigue strength. This work, a partnership between the US-DOE and Caterpillar, Inc., is developing the FSP process required to engineer the surface of engine components for improved properties, and fabricating prototype parts for testing in-engine.

8:55 AM Invited

Mechanical Properties of Friction Stir Processed, Friction Stir Welded, and Gas Metal Arc Welded AA5083 Aluminum Plate: *Christopher Smith*¹; Murray Mahoney²; Rajiv Mishra³; ¹Friction Stir Link; ²Consultant; ³Missouri University of Science and Technology

Friction Stir Processing (FSP) can be used to locally modify material properties of aluminum, such as room temperature ductility. Ductility is increased due to the resulting fine grain microstructure and localized surface annealing. This allows FSP to locally improve the formability of aluminum, normally limited, without altering the properties of the bulk of the structure. Typically, forming of aluminum is restricted, with most aluminum fabrications composed primarily of flat components and excessive joining. Alternatively, FSP can enable the forming of complex shapes, reducing the number of detail parts and the subsequent joining steps. One such example is the fabrication of angles or C-channels. This paper will describe the results of a qualification program of FSP on 5083-H116 aluminum to form angles or C-channels. Static and dynamic material property test results on FSP'ed material, base material, and GMAW'ed material in both formed and unformed conditions will be presented.

9:20 AM Invited

Friction Stir Powder Processing (FSPP) in Al/Cu and Fe/C Systems: *Hidetoshi Fujii*¹; Koji Inada¹; YuFeng Sun¹; Yoshiaki Morisada²; ¹Osaka University; ²Osaka Municipal Technical Research Institute

Friction Stir Powder Processing (FSPP) has been developed, based on the principle of FSW (friction stir welding). The FSPP is a method to design the properties of the welded area as well as to prevent the defect formation, by performing FSW after powder with a controlled composition is placed in the gap between two plates. AA1050 was used as the plates and pure Al powder (89µm average grain diameter) and pure Cu powder (106µm average grain diameter) were used as the powder. When using pure Al powder as the filler material, the formation of defects is prevented. When using pure Cu powder, Al2Cu precipitates were formed in the stir zone, and consequently, the hardness significantly increased. In addition, when carbon powder is added into a steel plate, stirring and diffusion of carbon and the transformation occur simultaneously, leading to significantly harden the FSPPed area.

9:45 AM

Mechanical Interlock of Thin Metallic Wire Using Friction Stir Forming: *Koshi Yamamura*¹; Kazuya Torikai²; Tadashi Nishihara²; ¹Yamamua Mfg. Co., Ltd.; ²Kokushikan University

Friction Stir welding (FSW) is attracting attention as solid-state joining process using friction heating. In recent author's study, noting excellent fluidity of aluminum alloy at FSW, micro-forging and its application to mechanical interlocking were investigated. We call this new process friction stir forming (FSF). In this study, a novel method of mechanical interlock of a thin metallic wire using FSF is proposed. The FSF process uses the friction heat and plastic deformation generated between a rotating tool and the material being forged. Trial with friction stir interlocking of aluminum alloys and various thin wires were carried out using a modified milling machine. The results were discussed in terms of pulling out characteristics. We concluded that a thin metallic wire has been successfully interlocked with aluminum alloy by friction stir technique.

10:05 AM

Friction Stir Fabrication - An Additive Friction Stir Technology: Jeffrey Schultz¹; Peter Ferek¹; ¹Schultz-Creehan, LLC

Friction stir fabrication (FSF) is an additive solid state, friction stir coating and joining method being developed at Schultz-Creehan, LLC (Blacksburg, VA, www.schultz-creehan.com). The FSF process uses shear-induced interfacial heating and plastic deformation to deposit wrought metal and metal matrix composite (MMC) coatings onto metal and MMC substrates. In this process, the coating alloy (in rod or powder form) is forced through a rotating spindle onto the substrate surface. Frictional heating occurs at the filler-rod/substrate interface due to the rotational motion of the filler rod and the downward force applied. The mechanical shearing that occurs at the interface acts to disperse any oxides or boundary layers, resulting in a metallurgical bond between the substrate and coating. As the substrate moves, the coating is extruded under the rotating shoulder of the stirring tool at the nose of the spindle.

10:25 AM

Friction Consolidation of Aluminum Chips: *Wei Tang*¹; Anthony Reynolds¹; ¹University of South Carolina

In this paper, friction consolidation was applied on various aluminum chips (2xxx, 5xxx, 6xxx, and 7xxx series) with a rotating die and a stationary 'billet' chamber. For consolidation aluminum, both components were made with H13 tool steel, and the die had a scroll pattern on the working end: similar to a 0° friction stir welding tool shoulder. In the friction consolidation process, the Z axis force was remained constant and different rotational speeds were applied from 100 rpm to 400 rpm, and solid aluminum disks were obtained. The consolidation quality was evaluated from the cross section after grinding, polishing and etching processes, and micro-hardness testing was performed along the mid-plane of the cross section. The die rotation rate, consolidating time cost, consolidating torque and power, consolidating quality, grain size, micro-hardness distribution, and relationship among those factors were discussed in this paper.



10:45 AM

Friction Stir Processing as a Base Metal Preparation Technique for Modification of Fusion Weld Microstructures: *Jeff Rodelas*¹; John Lippold¹; James Rule¹; Jason Livingston¹; ¹The Ohio State University

Friction stir processing was applied as a technique to modify the base metal microstructure of Ni-base Alloy 600 prior to fusion welding. Following FSP, autogenous gas tungsten arc welds were placed atop the stir-processed region. The resulting weld microstructure was characterized using various techniques. Grain refinement produced from FSP increased the extent of expitaxial nucleation and led to grain refinement of the weld metal. Grain size within the heat affected zone was also reduced by a factor of 3 near the fusion boundary relative to unprocessed base metal. The combination of fusion zone and heat affected zone grain refinement is a unique characteristic of friction stir processing and is not otherwise achievable using conventional weld microstructure refinement methods.

11:05 AM Break

11:15 AM

Thermal Stability of Friction Stir Processed Ultrafine Grained Al-Mg-Sc Alloy: *Nilesh Kumar*¹; Rajiv Mishra¹; ¹Missouri University of Science & Technology

Friction stir processing of coarse grained (initial average grain size ~ 50 μ m) Al-Mg-Sc resulted into ultrafine grained alloy (average grain size ~ 0.4 μ m). This alloy was subjected to annealing heat treatment at varying temperatures from 200 °C – 600 °C for 1 h duration at each temperature to study the stability of ultrafine grained microstructure. To understand the role of Al₃Sc precipitates in this alloy, another Al-Mg alloy was friction stir processed using the same processing parameters and subjected to identical annealing conditions. EBSD and TEM were employed to investigate the grain growth and precipitate coarsening as a result of annealing heat treatment.

11:35 AM

Effect of Friction Stir Processing on Constituent Particles in a Commercial 2024Al: Somayeh Pasebani¹; Indrajit Charit¹; Rajiv Mishra²; ¹University of Idaho; ²Missouri University of Science and Technology

Almost all commercial aluminum alloys have primary constituent particles that are often harmful to their mechanical properties. Friction stir processing (FSP) leads to substantial changes in the constituent particle size and distribution, lessening the deleterious effects of the constituent particles. FSP was carried out on AA 2024Al alloy with a combination of different parameters (tool rotation speed of 200-1000 rpm and traverse speed of ~25-152 mm/min). Backscattered Electron (BSE) imaging mode was used to detect and analyze the relevant constituent particles in 2024 Al. Energy Dispersive X-ray Spectrometry (EDXS) experiments were conducted in the SEM to characterize the chemical identity of the constituent particles. It has been observed that the insoluble constituent particles (Al-Cu-Mn-Fe) were fragmented into particles of smaller sizes and more rounded shapes. Conversely, the soluble particles (Al-Cu-Mg) in most cases went into solution during FSP. Different possible mechanisms are proposed to explain the phenomenon behind these changes.

11:55 AM

Obtaining Sub-Micron Grain Size in AM60 Magnesium Alloy Using Friction Stir Processing: *Daniel Gesto*¹; David Verdera¹; Paz Miniño²; Pilar Rey¹; Gloria Pena²; ¹AIMEN Technology Centre; ²Universidad de Vigo

Friction Stir Processing has gained importance in recent years as a very useful tool to produce UFG microstructures in cast and wrought magnesium and aluminum alloys, achieving superplastic behaviour. In this work, the influence of initial material condition and cooling rate on microstructure (in particular in the final grain size) of an AM60-6 mm thick magnesium alloy was carried out. A MP159 fix pin tool for 3 mm butt joints was used. FSP tests were conducted on as-cast and solubilized plates. Particular attention was paid to the level of grain refinement when a cooper backing plate and a cooling agent are used. A clearly homogenized structure and sub-micron grain sizes were obtained when these vigorous cooling systems were employed.

12:15 PM

Effect of Friction Stir Processing on Corrosion Behavior of AA5083 Aluminum Alloy: *Gaurav Argade*¹; Rajiv Mishra¹; Chris Smith²; Murray Mahoney³; ¹Missouri University of Science and Technology; ²Friction Stir Link; ³Consultant

The corrosion behavior of AA5083 depends on microstructural features such as matrix grain size, second phase size, and distribution of (β-Al3Mg2) and the nature of Al-Fe-Mn complex dispersoids. In the present work, the effect of grain size on the corrosion behavior of the alloy was studied in a 3.5 wt% NaCl solution. The grain size was varied via friction stir processing (FSP) by adopting different combinations of tool rotation rate and tool traverse speed. Corrosion behavior was characterized using potentiodynamic polarization measurements and the free corroding potential response with respect to time. In addition, a galvanostatic technique was applied to estimate the pit nucleation and pit repassivation potential of processed alloy samples. The fine grain microstructure, obtained using FSP, exhibited improved corrosion response vs. the base material. Overall corrosion response is presented on a process map.

12:35 PM

Evaluation of Rotational Speed and Post Annealing Effect on the Microstructural Homogeneity of Friction Stir Processed 5083 Aluminum Alloy: *Chun-Yi Lin*¹; Truan-Sheng Lui¹; Li-Hui Chen¹; ¹National Cheng Kung University

The effect of rotational speed and post annealing on the microstructural homogeneity of friction stir processed 5083 aluminum alloy was evaluated. In the stir zone grain size increased with the rotational speed from 450 to 850 rpm. While the rotational speed further arising up to 1650 rpm, the grain size was almost invariant. With a rotational speed of 450 rpm grains grew up to extremely large size and occupied nearly half area in SZ. Before 850 rpm increasing rotational speed could reduce extreme grain growth in post annealing. However, the post annealed microstructure of the specimens 850-1650 rpm was similar, in which the survived initial fine grains occupied about 60% area of SZ. The effect of stored energy induced by the different rotational speeds on the microstructural homogeneity of post annealed FSPed specimens was also discussed in this study.

Furnace Efficiency – Energy and Throughput: Session I

Sponsored by: The Minerals, Metals and Materials Society, TMS Light Metals Division, TMS: Energy Committee *Program Organizers:* Thomas Niehoff, Linde Gas; Cynthia Belt, Consultant; Russell Hewertson, Air Products and Chemicals Inc; Robert Voyer, Hatch

Wednesday AM	Room: 4
March 2, 2011	Location: San Diego Conv. Ctr

Session Chairs: Russell Hewertson, Air Products and Chemicals, Inc.; Thomas Niehoff, Linde Gas

8:30 AM

Furnaces Designed for Fuel Efficiency: *David White*¹; ¹The Schaefer Group, Inc.

This presentation will discuss the optimum furnace designs, Why they work and what you can do as purchasers to enhance that efficiency. Topics include refractory selection, circulation, preheat hearths, heat exchangers and operating procedures. Mainly large wet bath reverberatory furnaces will be presented with some information on tilters and immersion element melters and holders. Actual case studies will be presented of the energy savings.

8:50 AM

Latest Trends in Post Consumer and Light Gauge Scrap Processing to Include Problematic Processing Material such as UBC, Edge Trimmings and Loose Swarf: *Franz Niedermair*¹; Guenther Wimroither¹; ¹Hertwich Engineering

Melting of Post Consumer Aluminum Scrap is a challenging issue, with ever increasing requirements in terms of efficiency and environmental impact. In today's competitive world the following topics are of particular importance: Highest possible metal yield; Low energy/fuel consumption; Reduction of residues and emissions;Safe working and operational conditions. Hertwich Engineering, Braunau, Austria, a member of the SMS group, has recently developed a remelt furnace type for the processing of such scrap. The "HE-Ecomelt" furnace series is designed to accept a wide range of post consumer and light gauge scrap and to efficiently recycle the product into molten metal. Integrated high efficiency preheating and delaquering, thermal reclamation of organics and the applied submerge melting process ensure the best recoveries and lowest fuel consumption in the industry. At the same time, the ever increasing emission constraints in industrialized countries are easily met.

9:10 AM

Investigation of Heat Transfer Conditions in a Reverberatory Melting Furnace by Numerical Modeling: *Andreas Buchholz*¹; John Rødseth²; ¹Hydro Aluminium Rolled Products GmbH; ²Hydro Aluminium as

A numerical model based on the commercial software Fluent was used to analyze the heat transfer conditions in an industrial reverberatory melting furnace. The model comprises different physical phenomenon as gas f low, chemical reactions, i.e. combustion, conduction, radiation and latent heat release in the metal. The gas circulation was analyzed for different metal loads and burner arrangements. The melting process inside the furnace is inherently time-dependent, and a complete transient analysis is very timeconsuming. To study the impact of varied burner positions on the energy utilization, stationary solutions were applied, where the effect of melting heat was approximated by artificial heat sinks inside the metal. The results of the stationary solutions were compared with fully transient results to guarantee the transferability of the cost-efficient steady state calculations. The results stress the dominant effect of radiative heat transfer in the melting process.

9:30 AM

Oxyfuel Optimization Using CFD Modeling: *Thomas Niehoff*¹; Sreenivas Viyyuri¹; ¹Linde Gas

Before converting production furnaces to different combustion technologies it is essential to understand all related changes and side effects. An experienced team will be able to successfully conclude a conversion like this. However, CFD Modeling will enable to make informed decisions in terms of effort and results of furnace retrofitting with new combustion equipment. This paper will give insight of how Oxyfuel together with CFD can impact energy balance and productivity of production furnaces.

9:50 AM

Operational Efficiency Improvements Resulting from Monitoring and Trim of Industrial Combustion Systems: Jim Oakes¹; ¹Super Systems Inc

Combustion is the exothermic chemical reaction (a reaction in which heat is given off) of hydrogen and carbon atoms contained in fuels with oxygen. Excess O_2 makes heating inefficient, thus requiring more gas for the same results. In addition, excess air also allows for the formation of pollutants such as Nitrous Oxide (NO) and Nitrogen Dioxide (NO₂). It is estimated that precise control of air to fuel ratio will yield 5 to 25% or more savings in heat generation. The air gas ratio can be determined by analyzing the flue gas and the mixture for combustion can be altered to produce the most clean and efficient heat for the process. Periodic checking and resetting of air-fuel ratios is one of the simplest ways to get maximum efficiency out of fuel-fired process heating equipment. In heat treatment facilities, the customer would find potential efficiency improvements on generators, radiant tubes, furnaces, ovens, heaters, and boilers.

10:10 AM Break

10:30 AM

50% Reduction of Energy and CO2 Emission in Metallurgical Furnaces by Burners: Michael Potesser¹; B. Holleis²; M. Demuth²; D. Spoljaric²; J. Zauner³; ¹Superior Industries International; ²MESSER AUSTRIA GmbH; ³University of Leoben

The efficiency of industrial combustion processes can be raised in two ways, either by preheating the fuel and combustion air or by oxyfuel. The most important issue of the usage of oxygen burners is the substantially increasing melting rate by lowering the specific production costs because of the higher combustion efficiency. The flameless combustion (internal offgas recirculation) and the external offgas recirculation solves the problem with the high flame temperature and leads to cold combustion and lower dross formation or alloying elements combustion. The Oxipyr®-Air combines the technology of diluted combustion during air and oxygen usage decreasing the emission of pollutants. Constitutive of the Oxipyr®-Air development a fuel-oxygen-burner, Oxipyr®-Flex, was designed for a maximum of flexibility for the customer. The Oxipyr®-Air and Oxipyr®-Flex have been developed for the specific needs of melting and recycling companies for all non ferrous metals. The paper shows the theory, practical installations and economical outlook.

10:50 AM

New Technology for Electromagnetic Stirring of Aluminum Reverberatory Furnaces: James Herbert¹; *Alan Peel*²; ¹Altek LLC; ²Altek Europe Ltd.

The benefits of circulation in aluminum reverberatory furnaces are well documented and include higher productivity, and reduced fuel consumption and dross generation. One popular method to achieve the benefits of circulation is electromagnetic stirring. That said, this technology has certain drawbacks preventing its universal acceptance: high capital cost, high operating cost (especially power consumption and maintenance of water cooled copper tubes), reluctance to use water in close proximity to molten metal, and in some cases the inability to operate through full thickness refractory hearths. This paper describes a technology which amounts to the reinvention of traditional electromagnetic stirring devices, effectively addressing all of the above negative aspects of traditional systems. In this paper we will describe how these issues are addressed and results documented in recent installations

11:10 AM

Evaluation of Effects of Stirring in a Melting Furnace for Aluminum: *Kunio Matsuzaki*¹; Steve Iijima²; ¹National Institute of Advanced Industrial Science and Technology, Japan; ²Zmag America, Ltd.

The purpose of this paper is to investigate commercialization of an integrated melting furnace and stirrer for molten aluminum. The concept was tested via installation of a new type of permanent magnet stirrer to an existing furnace. The end goal is to improve the quality of aluminum through bath temperature homogenization and to reduce energy usage and dross generation while providing a reduction in melt loss. Traditionally, molten aluminum has been mechanically or electromagnetically stirred; however the former is both inefficient and can be dangerous, and the latter requires excessive energy and complicated components. In this research, molten aluminum was stirred by setting a permanent magnet circuit beside a furnace. This report also incorporates thoughts on more effective shapes of furnaces, compared to ordinary furnaces.

11:30 AM

Business Analysis of Total Refractory Costs: *Cynthia Belt*¹; ¹Consultant Refractory is a critical component of a furnace. Both planned and unplanned downtime due to refractory wear or failure can detrimentally affect production. Refractory materials, design, and maintenance can improve or degrade energy efficiency and melt rate. In addition, the cost of refractory is typically the largest maintenance expense of a melt or hold furnace. Total refractory costs include refractory materials, installation, energy, and downtime. Many attempts have been made by companies to hold down these costs in various ways. This paper compares several methods and gives relative cost savings based on a benchmark furnace.

11:50 AM

Improved Furnace Efficiency through the Use of Refractory Materials: James Hemrick¹; Angela Rodrigues-Schroer²; Dominick Colavito²; Jeffrey Smith³; ¹Oak Ridge National Laboratory; ²MINTEQ International, Inc.; ³Missouri University of Science and Technology

This paper will describe efforts performed at Oak Ridge National Laboratory (ORNL), in collaboration with industrial refractory manufacturers, refractory users, and academic institutions, to improve energy efficiency of U.S. industry through increased furnace efficiency brought about by the employment of novel refractory systems and techniques. Work in furnace applications related to aluminum, gasification, and lime will be discussed. The energy savings strategies discussed are achieved through reduction of chemical reactions, elimination of mechanical degradation caused by the service environment, reduction of temperature limitations of materials, and elimination of costly installation and repair needs. Key results of several case studies resulting from US Department of Energy (DOE) funded research programs will be discussed with emphasis on applicability of these results to high temperature furnace applications.

12:10 PM

Study on the Energy-Saving Technology of Chinese Shaft Calciners: Guanghui Lang¹; Chongai Bao¹; Shoulei Gao¹; *Ronald Logan*¹; Yan Li¹; Jingou Wu¹; ¹Sunstone

Shaft calcining technology is widely used in China for the calcination of green petroleum coke. It has the advantages of lower energy consumption and lower carbon burning loss compared to the rotary kilns. In this paper, a method of further reducing carbon burning loss using integrated technology is discussed.

Hume-Rothery Symposium Thermodynamics and Diffusion Coupling in Alloys - Application Driven Science: Diffusion and Phase-Field Simulations

Sponsored by: The Minerals, Metals and Materials Society, TMS Electronic, Magnetic, and Photonic Materials Division, TMS: Alloy Phases Committee

Program Organizers: Zi-Kui Liu, The Pennsylvania State University; Larry Kaufman, CALPHAD, Inc.; Annika Borgenstam, Royal Institute of Technology; Carelyn Campbell, NIST

Wednesday AM	Room: 31A
March 2, 2011	Location: San Diego Conv. Ctr

Session Chairs: Katsuyo Thornton, University of Michigan; Ingo Steinbach, Ruhr-University

8:30 AM Invited

Thermodynamics and Ionic/Electronic Transport in Oxides: Ye Cao¹; Saswata Bhattacharya¹; Jie Shen²; Clive Randall¹; *Long Qing Chen*¹; ¹Pennsylvania State University; ²Purdue University

Ionic and electronic transport is an important process that can influence the applications of many oxides. For example, one of the primary limiting factors for the life time of multi-layer dielectric capacitors is long-term resistance degradation. It is characterized by slowly increasing leakage currents under a constant voltage stress. In this presentation, a general thermodynamic formulation for the total free energy of an inhomogeneous system containing both electronic and ionic species as well as microstructures will be described within the phase-field formulation. The ionic/electronic transport equations as well as the electrostatic Poisson equation and the elasticity equation are then derived from the thermodynamic free energy. Implementation of spectral methods to solving the systems of equations under non-periodic boundary conditions will be presented. Application of the set of transport

equations to resistance degradation behavior of ferroelectric dielectrics and domain/defect interactions will be discussed.

9:00 AM Invited

Stress Induced Diffusion of Voids and Interstitials in Solids: *Ingo Steinbach*¹; ¹Ruhr-University

Diffusion in solids is caused not only by gradients in the local concentration, but also by gradients in the local stress distribution in the microstructure if the material exhibits a non negligible influence of its volume on the compostion. A multi-phase-field model is developed to account for the effect of concentration on volume in Vegard's approximation. The model is applied to diffusion of carbon in the austenite phase in a pearlitic steel grade and to diffusion of voids in a in a multi-grain structure. It is demonstrated, how stress driven diffusion in steel determines the growth kinetics of pearlite. In polycrystalline material it is shown how void diffusion controls grain growth for nano-sized structures. It is highlighted that the contribution of stress to diffusion in solids is crucial for the quantitative understanding of microstructure evolution.

9:30 AM Invited

Modeling Displacive-Diffusional Coupling in Phase Transformation and Plastic Deformation: *Yunzhi Wang*¹; Ju Li²; ¹Ohio State University; ²University of Pennsylvania

Microstructural evolution in materials often involves coupled displacive and diffusional processes. For example, structural phase transformations often involve coupled lattice shear, shuffle, and diffusion, while creep deformation often involves coupled dislocation glide, climb and atom diffusion. Mechanistic studies of these mechano-chemically coupled processes require modeling capabilities at micrometer, nanometer and even atomistic length scales but diffusional time scales. In this presentation, recent efforts in developing multi-scale modeling approaches by integrating ab initio calculations and atomic potentials into continuum phase field method at all length scales will be reviewed. Examples will be given to demonstrate quantitative aspects of the approaches in (a) predicting defect size and energy, and thermally activated processes of defect nucleation and migration, utilizing directly ab initio information as model input, (b) studying deformation/transformation mechanisms at atomic resolution but at diffusion time scales, and (c) identifying and incorporating transformation and deformation mechanisms in combination with advanced experimental characterizations.

10:00 AM Break

10:20 AM Invited

Diffuse Interface Modeling and Simulations: Conventional and Rigorous Treatments of Diffusion Accompanied by the Kirkendall Effect: Hui-Chia Yu¹; *Katsuyo Thornton*²; ¹University of Michigan - Department of Material Science & Engineering; ²University of Michigan - Department of Material Science & Eng.

The Kirkendall effect arises in substitutional alloys when various atomic species exchange with vacancies at different rates. Vacancies that facilitate diffusion are generated and eliminated at their sources and sinks, resulting in lattice shifts and deformations. The conventional model of the Kirkendall effect assumes that vacancy sources and sinks are distributed uniformly and thus the vacancy concentration remains at its equilibrium value throughout We simulate interdiffusion and Kirkendall-effect-induced the solid. deformation based on the conventional interdiffusion equation using the Smoothed Boundary Method. Bulging, grooving and bending due to the Kirkendall effect are studied. In a more rigorous model, free surfaces and grain boundaries are treated as the dominant vacancy sources and sinks, such that vacancy concentration remains at its equilibrium value only at these locations. We investigate the interdiffusion process, void growth, and deformation using simulations based on this rigorous model, again using the Smoothed Boundary Method.

10:50 AM Invited

Evaluation of Ordering Mobility from Antiphase Domain Growth Rate in Fe₃Al Using Phase-Field Simulation: *Yuichiro Koizumi*¹; Samuel Allen²; Masayuki Ouchi³; Yoritoshi Minamino³; ¹Tohoku University; ²Massachusetts Institute of Technology; ³Osaka University

The phase-field method (PFM) is becoming the premier method for predicting the microstructural evolution. For accurate prediction, reliable data of free energy and mobility are required. Although the free energies for major alloys are available in thermodynamic databases; the mobility for solute-atoms are derived from diffusivity data, the mobility for phase transformations is unavailable in many cases. In this study, the mobilities for ordering transformation in Fe3Al have been evaluated by comparing the rates of experimentally measured antiphase domains (APDs) growth and that simulated by PFM. The apparent ordering mobility experimentally evaluated for Fe-24at%Al alloy was approximately one half of that for Fe-26at%Al alloy. The difference was ascribed to the solute-drag by the PFM [Koizumi et al. Acta Mater. 2009;57:3039.]; the ordering mobilities re-evaluated by taking the solute-drag into account were in good agreement. This suggests that PFM is useful to extract underlying intrinsic mobility from experimentally measured extrinsic mobility.

11:20 AM

Phase Field Modeling of Beta to Alpha Transformations in Ti-6Al-4V: *Rongpei Shi*¹; Ning Zhou¹; Ning Ma²; Yunzhi Wang¹; ¹The Ohio State University; ²ExxonMobil Research & Engineering Company

Microstructure evolution during beta to alpha transformation in Ti-6Al-4V is investigated using a quantitative 3D phase field modeling. The model takes into account crystallography of the BCC to HCP transformation, misfit dislocations at the alpha/beta interfaces, and coherency stresses. In addition, model inputs are linked directly to available thermodynamic and mobility databases. Effects of local stress, existing precipitate and grain boundary on variant selection during nucleation and growth of alpha phase are studies. The spatial distribution of different variants of the alpha phase is found to correlate strongly with local stress, existing precipitate and grain boundary in a pre-existing microstructure. Various morphologies of intersecting alpha plates captured during their growth are compared with experimental observations.

11:50 AM

Thermotransport in γ(bcc) U-Zr Alloys: A Phase-field Model Study: Rashmi Mohanty¹; *Joshua Bush*¹; Maria Okuniewski²; Yongho Sohn¹; ¹University of Central Florida; ²Idaho National Laboratory

Atomic transport in the presence of temperature gradient or the thermotransport phenomenon was simulated for U-Zr alloys using a phase-field model derived from irreversible thermodynamics. The free energy of the system was directly incorporated from the available thermodynamic database, and the kinetic parameters such as atomic mobility and heat of transport terms were obtained from experimental values reported in the literature. The model was applied to a single-phase (bcc- γ phase) alloy and to a diffusion couple consisting of two single-phase (γ) alloys of different compositions, both subjected to a constant temperature gradient. An enrichment of Zr at the hot end of the single-phase alloy, with a corresponding depletion of U, was observed from an initially homogeneous single-phase alloy. A similar atomic transport was observed in the diffusion couple, where the magnitude and direction of the final composition gradient was dictated by a combination of atomic mobility and heat of transport.

Magnesium Technology 2011: Deformation Mechanisms I

Sponsored by: The Minerals, Metals and Materials Society, TMS Light Metals Division, TMS: Magnesium Committee Program Organizers: Wim Sillekens, TNO Science and Industry; Sean Agnew, University of Virginia; Suveen Mathaudhu, US Army Research Laboratory; Neale Neelameggham, US Magnesium LLC

Wednesday AM	Room: 6F
March 2, 2011	Location: San Diego Conv. Ctr

Session Chairs: Carlos Caceres, University of Queensland; Eric Nyberg, Pacific Northwest National Laboratory

8:30 AM

Crystal Plasticity Analysis on Compressive Loading of Magnesium with Suppression of Twinning: *Tsuyoshi Mayama*¹; Tetsuya Ohashi²; Kenji Higashida³; Yoshihito Kawamura¹; ¹Kumamoto university; ²Kitami Institute of Technology; ³Kyushu University

In this study, the compressive loading behavior of single crystals and bicrystals of magnesium without consideration of deformation twinning has been investigated by crystal plasticity finite element analysis method with the aim of fundamental understanding of kink band formation in magnesium alloys with long period stacking ordered structure (LPSO) phase. First, the basal plane of the single crystal model is set to be parallel to the compressive direction. For this analysis model, the effects of grain boundary, slight change of loading direction and heterogeneity of the initial dislocation density have been studied. Secondly, the analysis to clarify the influence of the angle between basal plane and the loading axis is performed. The results of the analysis are discussed in terms of active slip system and heterogeneity of deformation.

8:50 AM

Crystal Plasticity Modeling of Pure Magnesium Considering Volume Fraction of Deformation Twinning: Yuichi Tadano¹; ¹Saga University

In this study, a novel crystal plasticity model for pure magnesium involving the deformation twinning is presented. The deformation twinning is an important deformation mechanism of magnesium and other HCP metals. The deformation twinning has two important issues: first, large rotation of crystal lattice caused by twinning occurs. Second, in the crystalline scale, twinned and untwinned regions may simultaneously exist in a grain. Therefore, a crystal plasticity analysis of magnesium should introduce both of them, and the present framework takes into account these two key features. To represent the second issue, the volume fraction of deformation twinning is considered, and a material behavior of a grain is described as mixed state of twinned and untwinned regions. This paper provides some numerical examples with the present model, and it is shown that a smooth transition from untwinned to twinned states can be represented.

9:10 AM

Nucleation Mechanism for Shuffling Dominated Twinning in Magnesium: *Sungho Kim*¹; Haitham Kadiri¹; Mark Horstemeyer¹; ¹Center for Advanced Vehicular Systems

We observed for the first time spontaneous nucleation of $\{10-12\}$ twinning under tensile loading in magnesium crystal using atomistic molecular dynamic simulation. The system is a rectangular rod and rod axis is normal to basal plane of Mg crystal. The tensile deformation in c-axis nucleates $\{10-12\}$ twinning starting at the cornner of square of cross section of the rod. The twin boundary is spherical at the beginning and become a linear boundary in $\{10-12\}$ planes as time goes by. The twinning and shuffling processes are described. The nucleation mechanism of the shuffling dominated twinning is explained.

TMS2011 140th Annual Meeting & Exhibition

9:30 AM

On the Impact of Second Phase Particles on Twinning in Magnesium Alloys: Matthew Barnett¹; ¹Deakin University

Deformation twinning is an important deformation mode in magnesium alloys. Despite this, little is known on the extent to which the stress for twinning can be altered by a dispersion of second phase particles. The current paper presents a series of findings on the role of differently shaped particles on both the stress required for twinning and the characteristics of the twins that form. It is shown that plate shaped particles are, as one might expect, an effective strengthener to {10-12} twinning. When precipitate plates form on the basal planes, the relative hardening of basal slip is minor in comparison to that seen for twinning. This provides opportunity for the alloy designer to control the apparent critical resolved shear stresses (CRSS) for the different deformation modes. Possible sources for the hardening of twins are discussed.

9:50 AM

Influence of Crystallographic Orientation on Twin Nucleation in Single Crystal Magnesium: Christopher Barrett¹; *Mark Tschopp*¹; Haitham El Kadiri¹; Bin Li¹; ¹Mississippi State University

Deformation twinning plays a vital role in the mechanical behavior of polycrystalline magnesium alloys. To understand twinning in complex polycrystals, we need to first understand twinning phenomena in single crystals and bicrystals. This project studies twinning nucleation and propagation at the atomic scale for magnesium under various loading conditions. We used molecular dynamics to study the effect of loading orientation (in single crystals) and grain boundary structure on twinning or slip nucleation. We ran simulations at various strain rates, temperatures, and simulation cell sizes. The mechanisms are coupled with the stressstrain response and initial conditions to fully comprehend twinning nucleation. A better understanding of twin nucleation can elucidate how twinning phenomena occurs in more complex polycrystalline magnesium microstructures for inclusion in macroscopic constitutive models.

10:10 AM

Twinning Multiplicity in an AM30 Magnesium Alloy under Uniaxial Compression: *Q. Ma*¹; H. El Kadiri¹; A.L. Oppedal¹; J.C. Baird¹; M.F. Horstemeyer¹; ¹Mississippi State University

Twinning under compression along two perpendicular directions of an AM30 alloy with a {10-10} fiber texture was investigated. The primary extension {10-12} twinning occurred for both compression normal to the fiber and compression parallel to the fiber. These primary extension twins took the forms of fully residual twins parallel to the fiber and "stopped elastic" twins normal to the fiber. Both the {10-11}-{10-12} and {10-13}-{10-12} double twinning occurred in the matrix grains at the last stage of compression normal or parallel to the fiber, but as the "combined two shears mode" of the double twinning. Another time-sequence type of {10-11}-{10-12} double twin also activated early normal to the fiber. The primary extension twinning and contraction twinning seem to obey the Schmid law according to the texture evolution.

10:30 AM Break

10:50 AM

Inhomogeneous Deformation of AZ31 Magnesium Sheet in Uniaxial Tension: *Jidong Kang*¹; David Wilkinson¹; Raja Mishra²; ¹McMaster University; ²General Motors R&D

Inhomogeneous plastic deformation during uniaxial tensile test of AZ31 magnesium sheet has been studied using digital image correlation and electron backscatter diffraction. Simultaneous examination of the strain distributions on both the flat and the through thickness surfaces of the sample loaded along the rolling direction reveals very little deformation in the thickness direction and strain gradients on the sheet surface parallel and perpendicular to the loading direction. The lack of thinning leads to the abrupt fracture right after a premature but profound diffuse necking without transitioning to localized necking. Such inhomogeneous deformation arises from the strong basal texture and the resultant high critical resolved shear stress for slip as well as

the need for contraction and double twinning. The strain distribution on the sheet surface evolves nonlinearly with strain, impacting the measurement of the r-value. The relationship between the inhomogeneity of deformation and the deformation mechanism will be presented.

11:10 AM

Limitation of Current Hardening Models in Predicting Anisotropy by Twinning in hcp Metals: Application to a Rod-Textured AM30 Magnesium Alloy: Andrew Oppedal¹; Haitham El Kadiri¹; Carlos Tomé²; James Baird¹; Sven Vogel²; Mark Horstemeyer¹; ¹Mississippi State University; ²Los Alamos National Laboratory

When a strongly textured hexagonal close packed (HCP) metal is loaded under an orientation causing profuse twinning or detwinning, the stress-strain curve is sigmoidal in shape and inflects at some threshold. Authors have largely attributed the dramatic stress increase in the lower-bound vicinity of the inflection point to a combined effect of a Hall-Petch mechanism correlated to grain refinement by twinning, and twinning-induced reorientation requiring activation of hard slip modes. We experimentally and numerically demonstrate that these two mechanisms alone are unable to reproduce the stress-strain behaviors obtained under intermediate loading orientations correlated to in-between profuse twinning and nominal twinning. We argue based on adopting various mechanistic approaches in hardening model correlations from the literature. We used both a physics dislocation based model and a phenomenological Voce hardening model. The HCP material is exemplified by an extruded AM30 magnesium alloy with a <10-10>-fiber parallel to the extrusion direction.

11:30 AM

Deformation Behavior of Mg from Micromechanics to Engineering Applications: Erica Lilleodden¹; Jörn Mosler²; Malek Homayonifar²; Mintesnot Nebebe²; Gyu Kim²; *Norbert Huber*²; ¹GKSS-Research Centre; ²Helmholtz-Zentrum Geesthacht

We have investigated the influence of the underlying microstucture of Mg on the macroscopic deformation behavior. Using microcompression experiments on Mg single crystals, we have identified the orientation dependent deformation slip and twinning systems. These have aided the development of an energy based crystal plasticity model for the twinning in polycrystals. This model has been applied to representative volume elements to identify the flow surface for a macroscopic model, which is used to predict the forming limit diagram. Validation of the results has been realised through Nakazima tests. Additionally an outlook will be given on the prediction of the forming behavior of laser beam welded Mg sheets and its dependence on welding direction.

11:50 AM

Effect of Substituted Aluminum in Magnesium Tension Twin: Kiran Solanki¹; Amitava Moitra¹; Mehul Bhatia¹; ¹Mississippi State University

Atomistic simulations are performed in order to study the Aluminum substitution effect on Magnesium twinning mechanism. Multiple twin boundaries are found in pure Mg single crystal under tensile loading condition involving {10-12} twinning plane. However, no twinning has occurred under compression loading. Al substitution has been done for 2, 5, 7, and 10% doping. For 2 and 5% Al substitution, number of twins increase when the system is monitored under tensile loading. On the other hand, for 7 and 10% Al doping under tensile loading, no twin has been found. We found that dislocation-twin and dislocation-dislocation interaction are majorly responsible for this behavior and it is important that which one is prevalent.

12:10 PM

Influence of Solute Cerium on the Deformation Behavior of an Mg-0.5wt.%Ce Alloy: Lan Jiang¹; John Jonas¹; Raj Mishra²; ¹McGill University; ²General Motors

Some researchers have found that the nucleation of recrystallization at shear bands plays a role in the formation of the RE texture component. In steel rolling, it is well known that the formation of shear bands is favored by increasing the amount of solute carbon and rolling at temperatures where dynamic strain aging (DSA) occurs, leading to flow localization. The question therefore arises whether Ce in solution can play a similar role in Mg alloys. Compression tests were therefore performed on samples taken from extruded bars of Mg-0.5 wt.% Ce. It was found that the effect of DSA on increasing the flow stress was stronger than that of extension twinning. The occurrence of DSA also led to a decrease in the ductility. In addition, after heat treatment and conventional cooling, the supersaturation of Ce resulting from such cooling increases the strength of the DSA effect during subsequent deformation.

Magnetic Materials for Energy Applications: Amorphous and Nanostructured Magnetocaloric Materials

Sponsored by: TMS Electronic, Magnetic, and Photonic Materials Division, TMS: Energy Conversion and Storage Committee, TMS: Magnetic Materials Committee; JSPS 147th Committee on Amorphous and Nanocrystalline Materials; Lake Shore Cyrotronics, Inc.; AMT&C

Program Organizers: Victorino Franco, Sevilla University; Oliver Gutfleisch, IFW Dresden; Kazuhiro Hono, National Institute for Materials Science; Paul Ohodnicki, National Energy Technology Laboratory

Wednesday AM	Room: 11A
March 2, 2011	Location: San Diego Conv. Ctr

Session Chair: Victorino Franco, Sevilla University

8:30 AM Invited

Effect of Magnetic Cluster Size on the Magnetocaloric Effect in a Magnetic Spin Glass: Eric Lass¹; Virgil Provenzano¹; *Robert Shull*¹; ¹National Institute of Standards and Technology

A number of years ago, it was predicted and subsequently demonstrated that the magnetocaloric effect of a material could be enhanced when the material's independent magnetic spins were replaced by groups of magnetic spins. At that time, a paramagnetic garnet, $Gd_5Ga_3O_{12}$, was modified by the addition of Fe to transform the garnet into a superparamagnet. This magnetic state transformation occurred because the Fe atoms enabled a magnetic superexchange interaction between the Gd spins. As a consequence, the magnetocaloric effect of the material increased by a factor of 4-5. As a test of how generic this effect is, we have investigated a classic spin glass material, Cr-Fe, sequentially aged to grow larger magnetic clusters in the material. Here, a review of the origins of the enhancement will be presented along with a report on the response of the magnetocaloric effect in such a material as the cluster size is sequentially changed.

8:55 AM Invited

Nanostructured Materials for Magnetic Refrigeration: Christian Binek¹; Tathagata Mukherjee¹; Ralph Skomski¹; David Sellmyer¹; Steven Michalski¹; Renat Sabirianov²; ¹University of Nebraska-Lincoln; ²University of Nebraska-Omaha

Alternatives to conventional cooling technology harnessing the electrocaloric or magnetocaloric effect (MCE) will play an important role in energy-efficient and environmentally-friendly technologies of the future. We focus on magnetocaloric materials which are cost-effective, stable, environmentally-friendly, and maximize the MCE in the vicinity of room-temperature while minimizing hysteretic losses. We use nanotechnology to harness the MCE of simple magnetic materials by tailoring interactions in and between ultra-thin films or particles. As an example, Co/Cr superlattices are realized by molecular beam epitaxial growth where finite-size scaling effects tailor the T_c of Co and RKKY inter-layer coupling is tuned via Cr thickness into antiferromagnetic coupling between Co layers. Isothermal entropy changes are deduced from the temperature and field dependence of the magnetization using the Maxwell and Clausius-Clapeyron relations. The experimental results are discussed in the light of our theoretical findings.

Future improved nanostructures are discussed.Support by NRI, Career-DMR0547887, and MRSEC-0820521.

9:20 AM Invited

Magnetocaloric Effect in Oxide Nanostructures: Hariharan Srikanth¹; Manh-Huong Phan¹; ¹University of South Florida

A grand challenge in magnetic refrigeration is to fabricate refrigerant materials as thin films and nanostructures preserving their magnetocaloric properties. We will discuss the magnetocaloric effect (MCE) in oxide magnetic nanostructures from the spinel (Fe₃O₄, CoFe₂O₄, NiFe₂O₄), garnet (Gd₃Fe₃O₁₂) and perovskite (La,Pr,Ca)MnO₃ families. We will demonstrate that particle size distribution and interparticle interactions lead to broadening of MCE over a wide temperature range thus offering the potential to enhance refrigeration capacity (RC). While blocking is detrimental to achieving large magnitude in MCE, surface spin disorder enhances the effect under high applied fields. We also show that the interesting coupling between the magnetic, structural and electronic degrees of freedom in manganites plays a critical role in enhancing the MCE in nanostructures. Our observations provide strong evidence for control of the surface spin ordering as a viable route to increase the MCE and RC in nanostructured materials.
br>Supported by DoE and ARO.

9:45 AM Invited

Ordered Arrays of Magnetic CoNi-Base Nanowires and Nanodots: Magnetization and Transport: *Manuel Vazquez*¹; Laura Vivas¹; Victor Prida²; Victor Vega²; ¹Spanish Council for Research; ²University of Oviedo

The magnetic behaviour of ordered arrays of magnetic nanowires is of general interest for the development of new generation of functional nanostructures, with properties for magnetocaloric effect, sensing devices or magnetic storage media [1]. Hexagonally-ordered arrays of magnetic nanopilars are prepared by electrochemical route filling self-assembled pores of anodic alumina templates. We introduce last achievements on ordered arrays of such CoNi-base single and multilayer nanowire arrays (20-80 nm diameter, 65 nm interwire distance, and 120 to 2,000 nm long). Magnetization and magnetic transport properties are studied as a function of geometry parameters and composition. The magnetic anisotropy is particularly investigated in view of its decisive role in all magnetic behavior including magnetic and energy related effects. [1] V. Franco, K. Pirota et al. Phys. Rev. B 77 (2008) 104434; K. Pirota, M. Vázquez et al. "Magnetic Nanowires", Handbook of Nanoscience and Nanotechnology, Ed. A. Narlikar, Oxford Un. Press (2010) 772.

10:10 AM

Magnetocaloric Effect in Gd-Based Thin Film Heterostructures: *Casey Miller*¹; Christopher Bauer¹; Daryl Williams¹; Brian Kirby²; ¹University of South Florida; ²NIST Center for Neutron Research

To understand the impact of nanostructuring on the magnetocaloric effect, we have investigated W(300Å)/Gd(2000Å)/W(300Å) and [W(50Å)/Gd(400Å)]_8/W(50Å). The samples were sputtered onto MgO(001) at 300K. Post-deposition annealing was performed sequentially from 150°C to 600°C, with structural and magnetic characterization between each step. For the 2000Å Gd film, the entropy peak shifts from about 276K in the as-deposited film to the bulk value by 450°C; further annealing to 600°C improves the magnitude to ~4.4J/kg-K for a 0-4T field change. Differences with bulk behavior will be discussed in terms of grain size and strain. The multilayer sample's entropy peak is significantly broadened relative to bulk Gd. Polarized neutron reflectometry results indicate a suppression of Tc at the W-Gd interface, which is the likely the cause of the peak broadening. Supported by AFOSR-YIP; use of the Center for Nanoscale Materials for magnetometry was supported by the US DOE under Contract No. DE-AC02-06CH11357.

10:25 AM Break

10:55 AM

Optimization of the Refrigerant Capacity in Multiphase Magnetocaloric Materials: *Rafael Caballero-Flores*¹; Victorino Franco¹; Alejandro Conde¹;

K. Knipling²; M. Willard²; ¹Sevilla University; ²U.S. Naval Research Laboratory

One of the key parameters for enhancing the performance of magnetocaloric materials is the refrigerant capacity, RC, i.e. the heat that can be transferred between the cold and hot reservoirs. In order to optimize it, two strategies are possible: either to look for new materials with large RC, or to use known materials as building blocks of composites for achieving a large RC. In this work we will present numerical simulations which prove that there exist optimal values of Curie temperatures, fractions of phases and applied field values which can enlarge RC with respect to the starting phases as much as ~90%. As a proof of concept, it will be shown that the combination of experimental data of two FeCoNiZrBCu alloys produces an enhancement in RC of ~37%, making it ~92% larger than that of the Fe-doped GdSiGe.

11:10 AM

The Magnetocaloric Effect of Fe-B-Cr-Gd Amorphous Alloys: J Law¹; *Raju Ramanujan*¹; V Franco²; ¹Nanyang Technological University; ²Universidad de Sevilla

The magnetocaloric effect of Fe80-xB12Cr8Gdx (x = 1 to 11) amorphous alloys was studied by magnetometry, TEM, DSC and XRD techniques. Gd addition can be used to tune the Curie temperature, addition of Gd also increases the crystallization temperature. A linear relationship between the magnetic entropy change and the magnetic moment of the alloys was observed. The experimental values of magnetic field dependence of the magnetic entropy change were consistent with a phenomenological universal curve. The maximum magnetic entropy change, for x = 1, was ~33% larger than Fe80B12Cr8, the refrigerant capacity (RC) is ~29% larger than Gd5Si2Ge1.9Fe0.1 and within 10% of Fe82.5Zr7B4Co2.75Ni2.75Cu1, which is one of the best Fe-based amorphous magnetocaloric material. The tunable Curie temperature can be used to increase RC and the temperature span of layered multi-composition magnetocaloric regenerators. These results as well as the development of a novel active transient cooling magnetocaloric system will be presented.

11:25 AM

Tuneable Magnetocaloric Properties of Gd-Based Metallic Glasses: Charlotte Mayer¹; Stéphane Gorsse²; Bernard Chevalier¹; ¹ICMCB/CNRS Bordeaux 1 University; ²ICMCB/CNRS IPB

Since the recent discovery of large second-order paramagnetic to ferromagnetic transitions upon cooling in rare earth and transition metal (TM) based amorphous alloys; magnetocaloric effect (MCE) and refrigeration capacity (RC) of Gd-rich metallic glasses has been intensively studied. They have shown that, additions and/or substitutions of alloying elements (mainly TM) to Gd, have a great influence on MCE properties of these materials. To have a better understanding of this tuning ability, we have synthesised a series of amorphous ribbons of compositions Gd₆₀TM₃₀In₁₀ and Gd₆₀TM_{30-x}TM²_xIn₁₀, with TM or TM² = Mn, Fe, Co, Ni, Cu. This family of metallic glasses gives impressive results: a huge range of accessible Curie temperatures (87 K < T_c < 220 K) and a magnetic entropy change peak value (ΔS_M^{Peak}) that can go to double. Finally, adequate TM and TM² mixing leads to the enlargement of the magnetic transition thus increasing the RC of the material.

11:40 AM

Magnetocaloric Studies in Binary Gd-X (X = B, Ga, & Mn) Alloys: *Tanjore Jayaraman*¹; Laura Langemeier¹; Mark Koten¹; Jeffrey Shield¹; ¹University of Nebraska

Magnetic refrigeration based on the magnetocaloric effect has attracted attention as it is energy efficient and a "greener" alternative to the existing vapor-compression refrigeration technology. Gd as a room temperature magnetic refrigerant has a narrow working temperature region. Indentifying suitable alloying additions and processing techniques that can alter the Curie temperature (T_c), improve near-room temperature magnetocaloric properties and extend the useful range of Gd-based alloys is of significant importance. This paper reports the variation of T_c , peak value of $\Delta S_M (|\Delta S_M|_{max})$, refrigerant capacity (q) and relative cooling power (RCP) on a series of Gd_{100-y}X_y (X = B, Ga and Mn; 0 = y = 20 at.%) alloys prepared by conventional melting and melt spinning. The T_c and $|\Delta S_M|_{max}$ for these alloys were controllable by alloying and processing. Improvement in $|\Delta S_M|_{max}$, q and RCP for these alloys over Gd suggests their potential application as room temperature magnetic refrigerants.

11:55 AM

Magnetocaloric Effect and Enhanced Refrigeration Efficiency in (La_{0,7}Sr_{0,3}MnO₃/SrRuO₃) Superlattices: *Qiang Zhang*¹; S. Thota¹; F. Guillou¹; P. Padhan¹; V. Hardy¹; A. Wahl¹; W. Prellier¹; ¹CRISMAT

Currently, the search for the magnetocaloric materials was limited mainly to polycrystalline systems or superparamagnetic nanoparticles. In this work, we reported the magnetic and magnetocaloric effect in a series of (La_{0.7}Sr_{0.3}MnO₃/SrRuO₃) superlattices where the SrRuO3(SRO) layer thickness is varying. Compared with the polycrystalline La_{0.7}Sr_{0.3}MnO₃ (LSMO) compound, the TC of different ($La_{0.7}Sr_{0.3}MnO_3/SrRuO_3$) superlattices is decreased to 325 K due to the finite size effect and the magnetization is significantly enhanced, leading to remarkable MCE modulated by the SRO layers. While the working temperature ranges are enlarged, $\Delta S(Max \text{ to } Min)$ values retain comparable with the values in polycrystalline La_{0.7}Sr_{0.3}MnO₃. As a consequence, the relative cooling powers (RCP) are significantly improved, the microscopic mechanism of which is related to the effect of the interfaces at La_{0.7}Sr_{0.3}MnO₃/SrRuO₃ and higher nanostructural disorder. These studies indicate that artificial oxide superlattices/multilayers may provide an alternative pathway in searching for efficient room-temperature magnetic refrigerators for (nano)microscale systems.

Material Science Advances Using Test Reactor Facilities: Session I

Sponsored by: The Minerals, Metals and Materials Society, TMS Structural Materials Division, TMS/ASM: Nuclear Materials Committee

Program Organizer: Todd Allen, University of Wisconsin-Madison

Wednesday AM	Room: 3
March 2, 2011	Location: San Diego Conv. Ctr

Session Chair: Todd Allen, University of Wisconsin

8:30 AM Introductory Comments

8:40 AM

In-Reactor Oxidation of Zircaloy and Surface-Modified Zircaloy in Water Vapor at Low Partial Pressures: *David Senor*¹; Stan Pitman¹; Mitch Cunningham¹; Clark Carlson¹; Walter Luscher¹; Kevin Clayton²; Glen Longhurst³; ¹Pacific Northwest National Laboratory; ²Idaho National Laboratory; ³Southern Utah University

The TMIST-1 irradiation experiment at the Advanced Test Reactor evaluated oxidation and nascent hydrogen uptake of Zircaloy-2, Zircaloy-4, and surface-modified Zircaloy-4. Zircaloy-4 specimens with two different microstructural textures, resulting from different manufacturing processes, were included in the experiment. The surface-modified material consisted of Zircaloy-4 that was coated on one surface with electroplated Ni in four different thicknesses, followed by heat treatment to fully react the Ni with the substrate, forming a layered surface of Zr-Ni intermetallics. The specimens were exposed to a flowing oxidant consisting of He carrier gas with D_2O at either 300 or 1000 Pa partial pressure. Exposure temperatures were either 330 or 370°C, and the exposure continued for approximately 131 days at temperature. Duplicate sets of specimens were exposed to the same conditions in-reactor and ex-reactor. Post-irradiation examination included dosimetry, mass gain measurements, Fourier-transform infrared spectroscopic measurement of oxide thickness, deuterium assay, optical microscopy, and SEM/EDS.

9:00 AM

Effect of Neutron Radiation on Mechanical Properties of Nanograin Structured Copper: *Walid Mohamed*¹; Korukonda Murty¹; Jacob Eapen¹; ¹North Carolina State University

With the abundance of interfaces and grain boundaries, materials with nanograin structures are expected to be relatively more radiation resistant than their conventional (micrometer) grain sized counterparts. We report here some preliminary results on conventional grained (38 micrometers) and nanocrystalline (28 nm) copper following neutron irradiation in PULSTAR reactor at the NCSU to relatively low fluence of 6x1017 n/cm2 corresponding to 0.34 dpa. While radiation hardening and decreased ductility were noted in conventional Cu, nano-Cu revealed softening and ductility increase following radiation. Microstructural observations in nano-Cu revealed in-reactor grain growth accompanied by dislocation and twin structures. Grain size dependence of strength followed Hall-Petch relation. Materials irradiated in ATR to higher neutron fluences corresponding to a maximum 2 dpa are being tested and the results to-date will be presented. This work is supported by ATR/NSUF program and we acknowledge the encouragement and support by Drs. Mitch Meyer and Todd Allen.

9:20 AM

Program for Irradiation of Reactor Structural Materials at the ATR-National Scientific User Facility: *Heather MacLean Chichester*¹; Kumar Sridharan²; Ramprashad Prabhakaran¹; Yong Yang²; Peng Xu²; Todd Allen²; ¹Idaho National Laboratory; ²University of Wisconsin-Madison

Under the University of Wisconsin Pilot Project, neutron irradiation experiments have been designed to understand the irradiation performance of structural materials for advanced nuclear power systems. Twenty-six materials are being irradiated in the ATR, including ferrtic/martensitic steels, HT-9, T91, NF616, HCM12A, 9% Cr ODS steel, Fe-Cr binary alloys, and austenitic alloys 800H, D9, NF709, super 304 stainless steel and HT-UPS-AX-6 alloy. Additionally, grain boundary engineered alloys, SiC and MgO-ZrO2 ceramics, as well as Fe-Cr-B amorphous alloys are also being irradiated. The samples are mostly 3 mm diameter TEM disks, but for some alloys miniature tensile samples are also being irradiated. Targeted temperatures are 300°C to 700°C, and doses are 3 and 6 dpa. Issues pertaining to irradiating such a large matrix of sample materials, geometries, and irradiation conditions will be discussed. Post-irradiation examination will include tensile, microhardness, and shear punch testing, along with transmission electron microscopy.

9:40 AM

MAX Ceramics for Nuclear Applications: A New Material for a New Generation of Power: *Darin Tallman*¹; Elizabeth Hoffman²; Dennis Vinson²; Robert Sindelar²; Gordon Kohse³; Michel Barsoum¹; ¹Department of Materials Science and Engineering, Drexel University; ²Savannah River National Laboratory; ³Department of Nuclear Engineering, Massachusetts Institute of Technology

Gen IV nuclear reactors need materials that can withstand harsher environments than in current reactors. The Mn+1AXn (MAX) phases are a group of layered machinable ternary compounds, where M is an early transition metal, A is a group 13 to 16 element, and X is C and/or N. These compounds possess mechanical properties atypical for ceramics. Data about their irradiated properties are required to fully realize their potential. Research is thus ongoing to characterize their irradiated properties. The pre-irradiated characterization, as well as neutron activation of several MAX compounds exposed to fast and thermal spectra will be presented. The specific activities of Ti3SiC2, Ti3AlC2 and Ti2AlC were similar to SiC and three orders of magnitude less than Alloy 617 for three activation times in both fast and thermal spectra. Like SiC, the main radioisotopes, after a decay period of 10 years are tritium and C14.

10:00 AM Break

10:30 AM

Status of UCSB ATR-1 and ATR-2 Experiments: *Takuya Yamamoto*¹; G. Robert Odette¹; Douglas Klingensmith¹; David Gragg¹; Ben Sams¹; Mitchell Meyer²; Gregg Wachs²; Julie Foster²; James Cole²; Dan Ogden²; Michael Sprenger²; Thomas Maddock²; Paul Murray²; Joseph Nielsen²; Randy Nanstad³; William Server⁴; ¹Univ. California Santa Barbara; ²Idaho National Laboratory; ³Oak Ridge National Laboratory; ⁴ATI Consulting

Two UCSB ATR irradiation experiments are described. About 1400 specimens for a large alloy matrix were irradiated up to 6 dpa at 8 temperatures from 300 to 750 °C in the UCSB ATR-1, experiment. An innovative passive capsule thermal design minimized irradiation temperatures uncertainties, which were evaluated by SiC monitors. UCSB ATR-1 will provide a specimen lending library for studies of irradiation hardening/softening, embrittlement, microstructural evolutions and basic mechanisms, including helium injection and diffusion multiple experiments. UCSB ATR-1 will support the development of irradiation effects models for advanced fission and fusion applications. The UCSB ATR-2 experiment will be carried out in an instrumented capsule at a lower flux location in ATR. It is aimed at providing a similar database on irradiation embrittlement for a large matrix of RPV steels at temperatures from 250 to 310°C up to extended life doses of 0.15 dpa.

10:50 AM

In-Situ Measurement of Tritium Permeation Through Stainless Steel: David Senor¹; Walter Luscher¹; Mitch Cunningham¹; Clark Carlson¹; Kevin Clayton²; Glen Longhurst³; ¹Pacific Northwest National Laboratory; ²Idaho National Laboratory; ³Southern Utah University

The TMIST-2 irradiation experiment at the Advanced Test Reactor evaluated tritium permeation through Type 316 stainless steel. The interior of the cylindrical test specimen was exposed to a He carrier gas with T_2 at 0.1, 5, or 50 Pa partial pressure. Extraneous permeation was minimized from the ends of the test specimen by temperature control and Al coatings. The active length of the test specimen was approximately 10 cm, and temperature in this region was maintained at either 292 or 330°C. Temperature and tritium concentration changes were made online during the test. Tritium permeation was measured in-situ by sweeping the outside surface of the test specimen with a He/Ne mixture that was carried out of the reactor vessel in Cu tubing to ion chambers and bubblers for scintillation counting. Post-irradiation examination included dosimetry, Auger spectroscopy of the stainless steel surface, residual He-3 assay, and optical and scanning electron microscopy.

11:10 AM

Target Development Initiatives at SINQ Applying Neutron Techniques: *Werner Wagner*¹; Peter Vontobel¹; Yong Dai¹; Michael Wohlmuther¹; ¹Paul Scherrer Institut

SINQ is a continuous spallation neutron source, driven by PSI's 590 MeV proton accelerator which routinely delivers 2.2 mA of proton beam (of which SINQ receives 1.5 mA), making SINQ a Megawatt-class spallation source. The neutron production target at SINQ is a stationary solid so-called 'cannelloni' type target, i.e. it consists of an array of steel or Zircaloy tubes filled with lead, cooled by heavy water. Target development towards optimized neutron production efficiency for the neutron users always was a primary endeavour of PSI. One of the mayor tools to investigate the target rods before and after service is neutron imaging, done at the SINQ radiography station NEUTRA, which is equipped to investigate highly radioactive samples. These investigations turned out to be indispensable for assessing the condition and integrity of the target rods after service, in support of further improvements and for the sake of radiological safety and lifetime prediction.



11:30 AM Invited

Criticality Validation and Reactor Physics Experiment for the Advanced Test Reactor (ATR) National Scientific User Facility (NSUF): *Kimberly Clark*¹; Denis Beller¹; John Bess²; ¹Univ. of Nevada, Las Vegas; ²Idaho National Laborotory

The ATR Critical facility at the Idaho National Laboratory (INL) provides a criticality experiment capability that has not been certified in the International Criticality Safety Benchmark Evaluation Project (ICSBEP). The qualification of the ATRC would be highly desirable as a generalpurpose thermal-spectrum facility to complement other U.S. facilities for nuclear criticality safety experiments. In the project described herein, University of Nevada, Las Vegas faculty and students and INL personnel are collaborating in an ATR NSUF project to develop, evaluate, and validate a physically accurate radiation transport model of the ATRC in accordance with guidelines of the ICSBEP. To validate the radiation transport modeling effort, which is in progress, and to provide data for the International Reactor Physics Experiment Evaluation Project, a series of experiments will be conducted using a cassette containing one to eight precision aluminum bars. The design, fabrication, and status of the experiment will be described.

11:50 AM Concluding Comments

Materials in Clean Power Systems VI: Clean Coal-, Hydrogen Based-Technologies, and Fuel Cells: SOFC II

Sponsored by: The Minerals, Metals and Materials Society, TMS Electronic, Magnetic, and Photonic Materials Division, TMS Structural Materials Division, TMS/ASM: Corrosion and Environmental Effects Committee, TMS: Energy Conversion and Storage Committee, TMS: High Temperature Alloys Committee *Program Organizers:* Xingbo Liu, West Virginia University; Zhenguo "Gary" Yang, Pacific Northwest National Laboratory; Jeffrey Hawk, U.S. Department of Energy, National Energy Technology Laboratory; Teruhisa Horita, AIST; Zi-Kui Liu, The Pennsylvania State University

Wednesday AM	Room: 33C
March 2, 2011	Location: San Diego Conv. Ctr

Session Chairs: Teruhisa Horita, AIST; Kathy Lu, Virginia Tech

8:30 AM

The Growth of the Oxide Scale on Alloy Interconnects under Electrical Current Supply: *Kenichi Kawamura*¹; Mitsutoshi Ueda¹; Toshio Maruyama¹; ¹Tokyo Institute of Technology

The usage of alloy interconnects differ from general usage of high temperature alloy. That is, the alloy interconnects must conduct an electrical current. The electrical conductivity is decreased by the formation of oxide scale on the surface of alloy. Since the oxide scale, generally Cr2O3 scale, is grown by diffusion of ionic species, the growth of oxide scale is influenced by the electrical current. In this study, we demonstrate the oxidation behavior of Fe-Cr alloy with or without electrical current supply, and analyzed quantitatively. This study was supported by New Energy and Industrial Technology Research Development Organization (NEDO).

8:55 AM

Oxidation Behavior of (CoMn)3O4 Coatings on Preoxidized 441HP Stainless Steel: *Kathryn Hoyl*¹; Paul Gannon¹; Preston White¹; Rukiye Tortop¹; ¹Montana State University

Ceramic coatings are being explored to extend the lifetime of the stainless steel interconnects in planar Solid Oxide Fuel Cells (SOFC). One promising coating is CoMn oxide, (CoMn)3O4, which is deposited in various ways. In this study, stainless steel 441HP samples were subjected to four levels of preoxidation prior to coating with magnetron sputtered metallic CoMn, and subsequently annealed to (CoMn)3O4 in 800°C air for various times. The oxidation behavior and electrical resistance were evaluated as a function of these exposures. Preoxidation was found to inhibit Fe transport from the

stainless steel into the coating. Preoxidized samples maintained a slightly lower area specific resistance (ASR) after 1650 hours compared to nonpreoxidized samples. Oxidation behaviors and possible implications for SOFC interconnects are presented and discussed.

9:15 AM

Influence of CeO₂ Coating on Fe-Cr Base Alloys for SOFC Interconnect Applications: *Keeyoung Jung*¹; Nazik Yanar¹; Frederick Pettit¹; Gerald Meier¹; ¹University of Pittsburgh

A model Fe-13.5Cr and a commercial Fe-26Cr-1Mo alloy were coated with CeO₂ via pulsed laser deposition (PLD) and sol-gel coating technique in order to suppress the growth kinetics of the thermally-grown chromia and to avoid chromia evaporation. The coated alloys were isothermally exposed at 800°C in dry air up to 500h and their oxidation characteristics were compared with those of uncoated alloys. It was found that fine-grained Ce-rich oxides were formed on the surface whereas a pure coarser-grained chromia scale was formed on the uncoated alloys. Overall growth kinetics of the thermal oxides were decreased, in the presence of a CeO₂ layer, by up to 50% in specific mass changes depending on oxidation time. Other microstructural features and a proposed mechanism to explain the difference in the observations will be discussed.

9:35 AM

Advanced Conductive Spinel Coating on SOFC Interconnect Frames with One-Step Heat Treatment: Jung Pyung Choi¹; Jeffry Stevenson¹; Matt Chou¹; Josh Templeton¹; Gordon Xia¹; ¹Pacific Northwest National Laboratory

Low-cost, chromia-forming ferritic stainless steels are usually used for making interconnect plates in planar SOFCs. However, volatile Cr-containing species, which originate from the steel's oxide scale, can poison the cathode material in the cells and subsequently cause power degradation in the device. A conductive MnCo spinel coating has been developed for preventing cathode materials poisoning. However, this coating is not compatible with the formation of hermetic seals between interconnect frame components and the ceramic cell. Thus, a new aluminizing process has been developed to enable durable sealing, prevent Cr evaporation, and maintain electrical insulation between stack repeat units. However, the coating processes for the conductive and non-conductive material are very different. Therefore, it is challenging to fabricate these two coatings at the same time. The authors have previously reported success in preparing simultaneous coatings. However, to reduce cost and time, additional modifications are under development.

9:55 AM

Fabrication of Metal-Supported Micro-SOFC: Gyeong Man Choi¹; Younki Lee¹; Sunwoong Kim¹; ¹POSTECH

Micro-SOFC, fabricated with thin film processes, is being developed for supplying electrical power for portable electronics. Lithography and etching processes are generally used for the miniaturization of the cell. As the cell components become thinner with reduced size, the cell becomes mechanically weaker. The use of metal support for micro-SOFC is one of the solutions to improve mechanical strength. In this study, we will review the status of micro-SOFC fabrication and our approach for the fabrication process. We have fabricated micro-SOFC on Ni support using simple fabrication process. A porous metal film was fabricated either in free-standing form or on top of glass substrate. Electrolyte film was further deposited on the porous metal. Details of fabrication procedure will be discussed.

10:15 AM Break

10:25 AM Invited

Search and Study of a Solid Oxide Fuel Cell Seal Material: Kathy Lu¹; ¹Virginia Tech

Solid oxide fuel cells are electrochemical devices that convert chemical energy into electric power. High temperature hermetic seal is essential for utilizing the full potentials of planar solid oxide fuel. In this talk, seal requirements will be first discussed from thermal, chemical, mechanical, and electrical property point of view. Based on these considerations, our glass composition design approaches will be explained in search of the best seal glass that can offer all the desired sealing properties and thermal stabilities. A boron-free SrO-La2O3-Al2O3-SiO2 seal glass will be specifically discussed because it has met all the thermal and chemical properties along with high thermal and chemical stabilities. Long-term thermochemical stability and interfacial compatibility of the seal glass with Crofer 22 APU and AISI441 interconnects will be analyzed. The results show excellent thermal stability and interface compatibility of the SrO-La2O3-Al2O3-SiO2 glass with the Crofer 22APU interconnect.

10:50 AM

In-Situ Neutron Diffraction Study of Porous NiO-YSZ Composite under Uniaxial Loading: *Ling Yang*¹; Ke An¹; Alexandru Stoica¹; Harley Skorpenske¹; Xunli Wang¹; ¹Oak Ridge National Laboratory

Porous cermet composites consisting of Ni and Y2O3-stabilized ZrO2 (YSZ) are commonly used as anode in solid oxide fuel cells (SOFCs). This type of anode-supported SOFCs has many advantages such as high electrical conductivity, low operating temperature, compatible thermal expansion behavior and reliable mechanical properties. The pores in the composite are essential to the integrity of SOFCs as they provide the diffusion path to the fuel and reaction products as well as the triple phase boundary where the charge transfer occurs, but the existence of pores can also weaken the mechanical properties due to local stress concentration. In this study, we performed insitu neutron diffraction measurement on NiO-YSZ composites of various porosity ratios under uniaxial loading at the engineering diffractometer VULCAN. With in-situ neutron diffraction, the deformation mechanisms at micro-structural level of each single phase, inter-phase lattice strain/stress evolution and the impact of porosities are characterized and discussed.

11:10 AM

Design on Elevated-Temperature and Methanol-Blocking Proton Exchange Membrane for Fuel Cell Application: Yan Xiang¹; ¹Beihang University

In the filed high temperature proton exchange membrane fuel cells, we successfully explored a series of Elevated-Temperature proton exchange membranes with high performance based on engineering plastics. The ET-PEMs show high proton conductivity (rang from $0.05 \sim 0.15$ S/cm) and good mechanical strength (tensile strength > 5MPa) under high temperature operation conditions of 110° C~200°C. Single HT-PEMFC based on this HT-PEM show excellence out-put performance, and the maximum power density of 500mW/cm² can be obtained at 160°C, which is comparable to the similar products of BASF. For the issue of Methanol permeability of DMFC, we invented both surface modification and in-situ structural modification for Nafion membrane, HPW and bacteriorhodopsin were involved as methanol-blocking agents using LBL techniques and bulk modification. The methanol crossover could be deduced more than 70%, meanwhile, the power density of single cell has improved.

11:30 AM

Magnetic Analysis of Nickel Nano-Particles in Solid Oxide Fuel Cell Materials: James O'Brien¹; ²; ¹Quantum Design; ²UCSD

Reaction sintering can reduce large-scale production costs of SOFC material 8YSZ. Addition of 1%NiO lowers the temperature for rapid yttria diffusion into zirconia, but leaves dissolved Ni2+ ions. During operation of the fuel cell in reducing environments, nickel particle formation occurs. This process does not alter the level of ionic conduction when 10YSZ is adopted. Magnetic analysis will determine Ni2+ ion solubility limits, monitor rate of reduction and characterize the formation of metallic nano-particles. Super-paramagnetic properties confirm one synthesis technique yields roughly 3 nm Ni particles. The temperature and DC field dependence of SQUID based AC susceptibility will establish particle size distribution on the bulk scale. Infusion of metallic nano-particles into environmentally robust, stable oxide host lattices could impact many areas, from electronic component design to catalysis.

11:50 AM

Investigation of 5 MOL% YSZ Electrolyte for SOFC: *Nilufer Evcimen*¹; Ahmet Ekerim¹; 'Yildiz Technical University

To investigate the performance of electrolyte for intermediate temperature SOFC, commercially available 5 mol% YSZ powder was used. Average particle size was measured as 0.3 μ m by using TEM. The sintering attitude of the powder was studied on pellets with conventional ceramic processing methods by means of mixing, pressing (110 MPa) and sintering. Sintering temperatures were determined as 1200, 1300 and 1400 °C for 3 h. Density measurements were done by using Archimedes technique. Sintered samples were observed via SEM and AFM and the best sintering temperature was selected as 1400 °C. Electrical property of YSZ pellets were measured after coating with platinum paste onto surface of the samples sintered at 1400 °C to serve as electrode. After that, pellets were heated at 800 °C for 1 h. This process was repeated for the other side. The ionic conductivity was measured by impedance spectroscopy in air between 500-900 °C.

Neutron and X-Ray Studies of Advanced Materials IV: Resolving Time

Sponsored by: The Minerals, Metals and Materials Society, TMS Structural Materials Division, TMS/ASM: Mechanical Behavior of Materials Committee, TMS: Chemistry and Physics of Materials Committee

Program Organizers: Rozaliya Barabash, Oak Ridge National Laboratory; Xun-Li Wang, Oak Ridge National Laboratory; Jaimie Tiley, Air Force Research Laboratory; Peter Liaw, The University of Tennessee; Erica Lilleodden, GKSS Research Center; Brent Fultz, California Institute of Technology; Y-D Wang, Northeastern University

Wednesday AM	Room: 10
March 2, 2011	Location: San Diego Conv. Ctr

Session Chairs: Erica Lilleoden, GKSS Research Center; Zahir Islam, APS

8:30 AM Keynote

Time-Resolved X-Ray Scattering Techniques for Sub-picosecond to Millisecond Investigation of The Dynamics of Atomic Displacement Cascades*: *Bennett Larson*¹; Jon Tischler¹; Roger Stoller¹; Matthew Perkins²; ¹Oak Ridge National Laboratory; ²Oak Ridge High School

Information on the dynamics of atomic displacement cascades, formed by the direct collision of fast neutrons or energetic ions with lattice atoms, has until now been obtained entirely from molecular dynamics simulations. In this talk, x-ray diffuse scattering techniques to be used for the first experimental measurements of the dynamical structure of energetic-ion induced cascades on sub-picosecond to millisecond time-scales using the Linac Coherent Light Source (LCLS) and the Advanced Photon source (APS) will be discussed. Methods for analyzing time-resolved diffuse scattering measurements from cascades using molecular dynamics simulations and numerical x-ray diffuse scattering calculations will be presented for cascades in iron and copper. Methods for measurements and simulations of cascade evolution in the nanosecond to millisecond regimes will be considered. *Research supported by the US DOE, Office of Basic Energy Sciences within the Center for Defect Physics Energy Frontier Research Center, and the DOE Academies Creating Teacher Scientists (ACTS) program (MPP).

8:55 AM

Three-Dimensional Reciprocal Space Mapping of Martensitic Transformations in Bulk Single Crystals by In-Situ High-Energy Synchrotron X-Ray Diffraction: Yu Wang¹; Xin Zhao¹; Tian-Le Cheng¹; Yang Ren²; ¹Michigan Tech; ²Argonne National Laboratory

Martensitic transformations in bulk single crystals of NiMnGa magnetic shape memory alloys are studied by in-situ X-ray diffraction at Argonne National Laboratory. High-energy X-ray beam of Advance Photon Source provides the required penetration depth for probing structural transformations in bulk specimens. 3D reciprocal space mappings of various



phases along transformation paths (temperature, stress) are constructed from sequences of 2D diffraction patterns at in-situ incremental specimen rotation. 2D experiment by in-situ specimen rocking is also performed, which reduces data collection time from hours for 3D diffraction at each experimental condition to seconds, thus enabling detailed studies along phase transformation paths. Combining 3D and 2D diffraction techniques allows accurate interpretation of diffraction data and provides detailed information of martensitic transformations in bulk single crystals. The observed diffraction features are further explained in light of recent observation by high-resolution transmission electron microscopy as well as theoretical modeling and computation of nanotwin microstructure refinement.

9:10 AM Invited

In-Situ X-Ray Diffraction Observations of Silver-Nanoink Sintering and High Temperature Eutectic Reaction with Copper: John Elmer¹; Eliot Specht²; ¹LLNL; ²ORNL

Nanoinks contain nm sized metallic particles suspended in an organic dispersant fluid and are finding numerous microelectronic applications. These nanoinks sinter at much lower temperatures then their conventional counterparts due to their high surface area to volume ratio and small radius of curvature that reduces their melting points drastically below their bulk values. The unusually low melting and sintering temperatures have great potential for materials joining since their melting points increase dramatically after initial sintering. In this presentation, Ag nanoink is studied using insitu synchrotron based x-ray diffraction to follow the kinetics of the initial sintering step, and to directly observe their high remelt temperature. Ag nanoink is further explored as a possible eutectic bonding medium with copper by tracking phase transformations to high temperatures using in-situ x-ray diffraction, and is demonstrated as a less expensive bonding medium than alternative physical vapor deposition or electroplating methods.

9:30 AM Invited

In-Situ Neutron and Synchrotron X-Ray Diffraction for the Investigation of Thermo Mechanical Processes in Materials Science: *Klaus-Dieter Liss*¹; ¹ANSTO

Physical thermo-mechanical simulation is widely used to evaluate microstructural changes in metals as they occur in production, manufacturing or application processes. Neutron radiation bears the advantage to average over larger sample volumes and therefore provide a good powder average, as needed for quantitative phase analysis and the determination of global texture. Synchrotron high energy X-rays around 100 keV allow to investigate the local structure of the specimen. Large and fast two-dimensional detectors are employed for a multi-dimensional exploitation of the diffraction patterns. The different scattering lengths between the two types of radiation can be used to enhance the contribution of particular species of atoms and, in some cases, be particularly sensitive to atomic order and disorder. Selected metallic systems are presented undergoing thermo-mechanical load. Features like grain correlations upon phase transformations, grain refinement, subgrain formation, grain rotation, dynamic recovery, dynamic recrystallization, grain growth and the evolution of texture are revealed.

9:50 AM Invited

Using In-Situ Neutron Diffraction and Mesoscale Modeling to Understand Texture Evolution during Recrystallization of Metallic Polycrystals Simulate Texture Evolution during Recrystallization of Metallic Polycrystals: Bala Radhakrishnan¹; Grigoreta Stoica¹; Govindarajan Muralidharan¹; Sarma Gorti¹; Xun-Li Wang¹; ¹Oak Ridge National Laboratory

Structural and functional materials often derive their unique properties through crystallographic texture that evolves during thermo-mechanical processing. Despite years of research, a comprehensive understanding of texture evolution during recrystallization has been elusive. Even with the availability of the most sophisticated computers and simulation tools, a direct dislocation level simulation of recrystallization is nearly impossible. The proposed research exploits the unique features of the VULCAN diffractometer at SNS, ORNL, to perform in-situ neutron diffraction investigation of the nucleation and growth steps associated with recrystallization. The texture data in conjunction with advanced microstructure evolution modeling are used to develop an integrated, predictive, tool for texture evolution in structural materials. The application of the tool to develop lightweight materials for the energy and automotive sectors will be discussed.

10:10 AM Invited

In-Situ High-Energy X-Ray Study of Advanced Materials for Energy Storage: *Yang Ren*¹; Zonghai Chen¹; Yugang Sun¹; Tu Truong¹; Jian Xie²; ¹Argonne National Laboratory; ²IUPUI

The increasing demand in safer and higher performance rechargeable batteries for broad applications has led to global efforts to develop advanced electrode materials, electrolyte components and additives, and other cell components. There is a critical need in understanding key material issues in batteries under realistic conditions and in real time. We will present here a recent application of synchrotron high-energy x-ray diffraction (HEXRD) for in-situ structural characterization of advanced battery materials. Our experimental work includes in-situ HEXRD studies of cathode materials during solid-state synthesis, time-resolved measurements during hybrid pulse characteristic test (HPPC) of a full battery, in-situ study of Si-Li interaction and nondestructive material characterization of commercial 18650 cells during cycling and long term aging tests. Our results provide important property-structure-performance information for in-depth understanding of advanced energy materials and the safety and performance of batteries. (Use of APS was supported by the U.S. DOE under Contract No. DE-AC02-06CH11357.)

10:30 AM

A Study of the Deformation Modes in B2 Intermetallics CoTi and CoZr Using In-Situ Neutron Diffraction and Electron Backscattered Diffraction: *Rupalee Mulay*¹; Sean Agnew¹; ¹University of Virginia

Many B2 compounds, like NiAl, are known to exhibit slip primarily on the <001>{110} slip systems, which provide only 3 independent slip systems and, hence, fail to satisfy the von Mises criterion for polycrystalline ductility. B2 CoTi and CoZr have been examined by in-situ neutron diffraction and the results reiterate that the primary slip systems are <001>{110}. In spite of the apparent violation of the von Mises criterion, CoZr and CoTi have shown significant ductility. Neutron diffraction also exposed a transition in strain hardening and possible explanations for the anomalous ductility include the slip of <110> or <111> dislocations and the formation of kink bands. The present study makes use of a combination of in-situ neutron diffraction, crystal plasticity modeling, slip trace analysis, and electron backscattered diffraction (to determine both the orientation of the grains and the in-grain misorientation axes) to establish the active deformation modes in these alloys.

10:40 AM Break

10:50 AM Invited

In Situ Studies of Engineering Processes with Synchrotron Radiation and Neutrons: Andreas Schreyer¹; Torben Fischer¹; Jorge Dos Santos¹; Andreas Stark¹; Robert Gerstenberger²; Peter Staron¹; Martin Müller¹; Florian Pyczak¹; Walter Reimers²; Norbert Huber¹; ¹GKSS Research Center; ²TU Berlin

High-energy X-rays and neutrons offer the large penetration depths that often are required for determination of bulk properties in engineering materials research. In addition, new sources provide very high intensities on the sample which can be used not only for high spatial resolution using very small beams, but also for high time resolution in combination with a fast detector. This opens up possibilities for a wide range of engineering specific in situ experiments. Typical examples that are already widely used are heating or tensile testing in the beam. However, there are also more challenging in situ experiments in the field of engineering materials research like e.g. friction stir welding, dilatometry, or cutting. Selected examples of such experiments will be presented.

11:10 AM Invited

Energy Research on the HIPPO Beam-Line at LANSCE: Sven Vogel¹; Yusheng Zhao¹; ¹Los Alamos National Laboratory

The HIPPO beam-line at LANSCE is a general purpose neutron diffractometer and in this presentation we provide an overview of energy-related research. We will present our recently commissioned battery cell nSEC for in situ studies of anode, cathode and electrolyte materials as well as studies of charge and discharge behaviour of commercial Li-ion battery cells. HIPPO's high neutron flux allows for time-resolved studies and we will present recent results of chemical segregation in U-10wt.% Mo fuel foils during simulated bonding cycles, where a temporal resolution of one minute was achieved on two 250 μ m foils as samples. We will briefly touch upon our research in hydrogen storage materials and present results from high pressure investigations of ammonia borane and on the high pressure behaviour of a metal-organic framework structure as a function of pressure medium.

11:30 AM Invited

In-Situ Intergranular Strains in Extrusion Textured 304L Stainless Steel: 18 Students¹; Harley Skorpenske¹; Ke An¹; Sheng Cheng²; Ercan Cakmak²; *Thomas Holden*¹; Hahn Choo²; Peter Liaw²; Xun-Li Wang¹; ¹Oak Ridge National Laboratory; ²University of Tennessee

Many measurements have been reported of intergranular strains in austenitic stainless steel alloys, but none for the case of extruded material nor for 304 stainless steel. This case serves to emphasize how the crystallographic texture can affect which grain orientations [hkl] in the material show non-zero intergranular strains. The measurements were made on the new VULCAN engineering diffractometer at the Spallation Neutron Source at Oak Ridge National Laboratory as part of the "National Neutron and X-ray School" to demonstrate to 18 students the capabilities of the instrument. The texture was a cylindrically symmetric extrusion texture and there were already residual strains in the material prior to subjecting the samples to tensile strains between 1 and 5.5%. The experimental results are compared with an elasto-plastic self-consistent model taking into account the texture and the {111}<10> slip system operating in austenitic alloys.

11:50 AM

In-Situ Study of Plastic Deformation in 316LN Stainless Steel by Fast Neutron Diffraction: *Alexandru Stoica*¹; Sheng Cheng¹; Ke An¹; Harley Skorpenske¹; Xun-Li Wang¹; ¹ORNL

A novel data acquisition system based on event mode data storage is currently implemented at SNS. By using time-of-flight diffractometer VULCAN, this data acquisition system provides exquisite capabilities to observe fast structural changes in materials subjected to plastic deformation. Unlike the conventional holding approach, the diffraction data are collected continuously during constant strain rate deformation tests. This new approach allows adjustable data histograming and stroboscopic data processing. We report the evolution of lattice strain during tensile and cyclic deformation of 316LN stainless steel. The intergranular (type II) strains are unambiguously separated from the elastic macroscopic contribution. By monitoring the broadening of the diffraction peaks we were also able to observe the accumulation of intragranular (type III) strains. The density of residual dislocations induced by plastic deformation was estimated from these data. Under deep plastic deformation we observed characteristic grain orientation changes, which influence the residual intergranular strains.

12:05 PM

In-situ Phase Transformation Studies of High Strength Beta Titanium Alloys: *Xinjiang Hao*¹; Nicholas Wain¹; Chao Yang¹; Xinhua Wu¹; ¹University of Birmingham

The addition of C to beta Ti alloys has a significant effect on the phase transformations and leads to homogeneous and fine microstructures and to better mechanical properties, but at present the mechanisms underlying these effects are not understood, partly because only limited dynamic observations of the phase transformations have been made. This work, using in-situ high temperature synchrotron diffraction experiments, is aimed at identifying the mechanisms underlying the effect of C through direct observations of the

influence of C on the transformations so that a less empirical approach can be developed for the improvement of the properties of Ti alloys.

12:20 PM Invited

Texture Evolution and Phase Transformation in Titanium Investigated by In-Situ Neutron Diffraction: *Dong Ma*¹; A.D. Stoica¹; K. An¹; L. Yang¹; H. Bei¹; R.A. Mills¹; H. Skorpenske¹; X.-L. Wang¹; ¹ORNL

In-situ neutron diffraction has been carried out to study texture evolution and the α (hcp)<-> β (bcc) phase transformation in titanium upon continuous heating and cooling. It was found that the recrystallization of α resulted in the development of a new texture component, which facilitated the texture formation in β in the beginning of the α > β transformation. However, surprisingly, the transformation-induced texture started to diminish upon completion of the transformation. This new observation is explained in terms of competitive β -grain growth. The texture changes upon the β > α transformation during cooling will be also discussed.

Pb-Free Solders and Other Materials for Emerging Interconnect and Packaging Technologies: Thermo-Mechanical Behavior II

Sponsored by: The Minerals, Metals and Materials Society, TMS Electronic, Magnetic, and Photonic Materials Division, TMS: Electronic Packaging and Interconnection Materials Committee *Program Organizers*: Indranath Dutta, Washington State University; Darrel Frear, Freescale Semiconductor; Sung Kang, IBM; Eric Cotts, SUNY Binghamton; Laura Turbini, Research in Motion; Rajen Sidhu, Intel Corporation; John Osenbach, LSI Corporation; Albert Wu, National Central Univ, Taiwan; Tae-Kyu Lee, Cisco Systems

Wednesday AM R March 2, 2011 L

Room: 7B Location: San Diego Conv. Ctr

Session Chair: Sung Kang, IBM Corporation

8:30 AM Invited

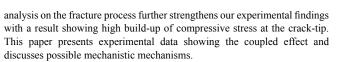
Local Mechanical Properties of Microstructural Constituents in Pb-Free Solders by Micropillar Compression: Ling Jiang¹; *Nikhilesh Chawla*¹; ¹Arizona State University

Micropillar compression using a nanoindenter is a unique technique for probing the local mechanical properties of microconstituents in Pbfree solders. This methodology was used to perform uniaxial compression experiments on Sn, Sn-Ag3Sn eutectic, and Cu6Sn5. Focused Ion beam (FIB) was employed to mill the microconstituents. The pillars were tested using a nanoindenter with a flat tip in compression, to determine the stressstrain behavior. The effect of aspect ratio and taper of pillars on mechanical properties will be discussed. The crystallographic orientation of pillars was examined using electron back-scattered diffraction. The relationship between orientation and mechanical properties of pillars will be discussed. A knowledge of local microconstituent behavior can be used to develop "composite models" that predict the behavior of the solder as a whole.

8:55 AM Invited

Coupled Effect of Electric and Mechanical Load on the Fracture Behavior of Lead-Free Solder Joint: *Choong-Un Kim*¹; Woong Ho Bang¹; Hong-Tao Ma²; Tae-Kyu Lee²; Kuo-Chuan Liu²; ¹University of Texas Arlington; ²Cisco Systems, Inc.

Mechanical reliability of solder joint has been a subject of extensive studies in recent years. These studies have addressed various contributing factors to the fracture reliability such as thermo-mechanical load conditions, and microstructural evolutions due to aging and electromigration. However, all these studies have failed to consider the most critical aspect of solder reliability, that is the fact that mechanical load is combined with electrical load in real solder joint. Our recent investigation on this subject reveals that the current and mechanical load (and thus fracture) couples in completely unexpected manner. Specifically, it is found that there exists a condition where high density electric current can retard the joint failure. Our theoretical



9:20 AM Invited

Effects of Aging on Pb-Free Solder Properties in Long Term Service: *Peter Borgesen*¹; Babak Arfaei¹; Tariq Tashtoush¹; Younis Jaradat¹; Awni Qasaimeh¹; ¹Binghamton University

Practical SnAgCu solder joint microstructures are inherently unstable, and resulting properties have been shown to keep changing over periods of years. In the absence of loading, this is primarily a result of ongoing coarsening of the secondary precipitates. The sensitivity to this varies with alloy composition, including the addition of Pb in so-called backward compatible assembly, and solder pad finishes as do dependencies on aging temperature. This is further complicated by systematic dependencies on solder volume and reflow parameters. Comparisons between alternatives by accelerated testing may, therefore, easily be misleading. Effects on life in long-term service are, however, not easily simulated by accelerated preconditioning. In addition, cyclic loading leads to pile-up of dislocations between precipitates, providing for particularly rapid diffusion paths and, thus, both faster coarsening and different temperature dependencies. Finally, recrystallization and subsequent crack growth are affected strongly by the coarsening. Consequences for long term reliability are discussed.

9:45 AM Invited

Electromigration-Enhanced Stress Relaxation of Sn and Sn-Ag-Cu Alloy: H. Liu¹; Q. Zhu¹; Z. Wang¹; J. Shang²; ¹Institute of Metal Research; ²University of Illinois

Solder interconnects are often subject to both electric and mechanical forces which may combine to cause device failures. In this study, the mechanisms of electromigration-induced softening of solder interconnects were investigated by examining the electromigration damage and the stress relaxation behavior in Sn and Sn-Ag-Cu solder joints. With pure Sn, electromigration favored the grain boundary processes such as grain rotations and grain boundary sliding so that the dominant mechanism of stress relaxation changed from dislocation climb to grain boundary diffusion. For Sn-Ag-Cu, electromigration produced excess vacancies and numerous hillocks on the alloy surface. The interaction of excess vacancies with dislocations led to enhanced stress relaxation in the solder joint.

10:10 AM Break

10:20 AM

Time-Dependent Mechanical Properties of Thermomechanically Fatigued Pb-Free Solder Joints: *Andre Lee*¹; K. Subramanian¹; ¹Michigan State University

Evolution of microstructures and the cyclic mechanical loading attributed to thermal expansion coefficient mismatches of various entities presence in electronic interconnects are some of the known factors that affect the service reliability of Pb-free electronic solder joints. Residual mechanical property evaluation invariably destroys the specimens, without providing any means for following the progress of damage accumulation within the same solder joint. Time-dependent stress relaxation behavior in such joints will be highly sensitive to the internal changes. Small-amplitude oscillatory shear stress relaxation measurements can provide means to continuously characterize the damage accumulation resulting from thermomechanical fatigue (TMF). Studies based on series of strain-controlled experiments at different temperature regimes were used to evaluate time-dependent mechanical properties of Pb-free solder joints exposed to varying extents of TMF. Results from these experiments are used to address some critical issues in the accelerated tests employed for long-term service reliability of Pb-free solders.

10:40 AM

140th Annual Meeting & Exhibition

Life Prediction of Sn-3.0Ag-0.5Cu/ENIG and OSP Pb-Free Solder Joints of Chip Scale Package for Automotive Electronics: *Won Sik Hong*¹; Chulmin Oh¹; ¹Korea Electronics Technology Institute

Due to ELV (End-of-Life Vehicle) banning, it is necessary to use Pb-free solder in car electronics. Therefore, in this study, we have predicted solder joints life of chip scale package (CSP) for automotive cabin electronics. For the experiment, 84 ball CSP was soldered with Sn-3.0Ag-0.5Cu on OSP and ENIG finish PCB. To investigate the fracture time of solder joints, we have conducted three kinds test under thermal shock conditions: -40~110, -25~125, -40~140 deg.C. Also, we continuously monitored the resistance of daisy-chained CSP solder joints. Failure criterion was 300 ohms of loop resistance. From these results, we have analyzed fracture mechanism and interfacial reaction of CSP solder joints. Finally, using the Norris-Landzberg modification of the Coffin-Manson equation, we have estimated solder joint life due to thermo-mechanical fracture of automotive electronics.

11:00 AM

Lead-Free Solder Joint Reliability under Wide Range of Thermal Cycling Conditions: *Hongtao Ma*¹; Mudasir Ahmad¹; Kuo-Chuan Liu¹; ¹Cisco Systems, Inc.

In lead-free solder joints reliabilities, there is a common understanding that the different temperature range of temperature cycle test may result into different results, especially the failure modes. Unfortunately, the differences in failure modes for lead-free packages across these different test conditions have not been fully studied and documented. In this study, a comprehensive set of tests was performed on test vehicles with different package types, sizes, pitches, and solder joints metallurgies. Accelerated Thermal Cycling (ATC) testing was performed using four different thermal cycling profiles: 0-100 °C, -40-125 °C, -55-125 °C, and -60-150 °C. Data from the tests were analyzed for failure mode and failure rate using Weibull statistics, and the characterized life for each test condition was determined and analyzed. The data will help quantify discrepancies due to test condition variations and will also provide valuable guidance on effects of package types, size, pitches, and solder joints metallurgies.

11:20 AM

Microstructural and Damage Evolution in Thermally Cycled Sn-3.5Ag Solder Joints: *Govindarajan Muralidharan*¹; Kanth Kurumaddali¹; Andrew Kercher¹; Larry Walker¹; Scott Leslie²; ¹Oak Ridge National Laboratory; ²Powerex Inc

There is a significant need for next-generation, high-performance power electronic packages and systems with wide band gap devices that operate at high temperatures in automotive and electric grid applications. Sn-3.5Ag solder is a candidate for use in such packages with potential operating temperatures up to 200°C. However, there is a need to understand thermal cycling reliability of Sn-3.5Ag solders. Damage evolution occurring in large area Sn-3.5Ag solder joints between silicon dies and Direct Bonded Copper (DBC) substrates subject to thermal cycling between 200°C and 5°C was followed using high resolution X-ray radiography techniques. This study will highlight the effect of thermal cycling conditions and stress state on damage evolution in these solder joints. *Research was sponsored by the U. S. Department of Energy, Office of Electricity Delivery and Energy Reliability, and by the Assistant Secretary for Energy Efficiency and Renewable Energy, Propulsion Materials Program, Office of Vehicle Technologies.

11:40 AM

Effects of Reflow Parameters and Aging on Fracture Toughness of a Lead-Free Solder Joint under Dynamic Loading Conditions: *Zhe Huang*¹; Praveen Kumar¹; Indranath Dutta¹; Rajen Sidhu²; Mukur Renavikar²; Ravi Mahajan²; ¹Washington State University; ²Intel Corp.

The fracture behavior of solders at high strain rates is a critical design parameter for the reliability of microelectronic packages as solder joints are prone to failure during drop. A methodology for measuring mixed-mode fracture toughness of Sn3.5Ag0.7Cu solder/Cu joints under dynamic loading conditions was developed. This method was applied to investigate the effect of reflow parameters (dwell time and cooling rate) and aging on the fracture



toughness of solder joints at different strain rates (0.1 to 100 s-1) and at various loading angles (0 – 75° at an interval of 15°). The results show that critical strain energy release rate, GC, decreased with an increase in the strain rate, dwell time and the cooling rate. A fracture mechanism map was developed to describe the correlation between the yield strength (dependent on the microstructure of solder), the IMC morphology, the mode mixity and the fracture toughness.

Phase Stability, Phase Transformations, and Reactive Phase Formation in Electronic Materials X: Interfacial Reactions of the Pb-Free Solder Joints

Sponsored by: The Minerals, Metals and Materials Society, TMS Electronic, Magnetic, and Photonic Materials Division, TMS: Alloy Phases Committee

Program Organizers: Chih-Ming Chen, National Chung Hsing University; Hans Flandorfer, University of Vienna; Sinn-Wen Chen, National Tsing Hua University; Jae-ho Lee, Hongik University; Yee-Wen Yen, National Taiwan Univ of Science & Tech; Clemens Schmetterer, TU Bergakademie Freiberg; Ikuo Ohnuma, Tohoku University; Chao-Hong Wang, National Chung Cheng University

Wednesday AM	Room: 7A
March 2, 2011	Location: San Diego Conv. Ctr

Session Chairs: Sinn-Wen Chen, National Tsing Hua University; Yee-Wen Yen, National Taiwan Univ. of Sci. & Tec.

8:30 AM Invited

Effect of Ag on Growth Behavior of Cu6Sn5 Formed between Molten Sn-xAg-0.5Cu Solders and Cu UBMs: Moon Gi Cho¹; Sun-Kyoung Seo¹; *Hyuck Mo Lee*²; ¹Samsung Electronics; ²KAIST

Cu6Sn5 intermetallic compounds (IMCs) formed at the interface of Sn-3.0Ag-0.5Cu solders with Cu exhibit much smaller grains, but their thickness is not substantially different from that of IMCs formed in Sn-0.5Cu and Sn-1.0Ag-0.5Cu solders with Cu. More specifically, the ripening growth of Cu6Sn5 grains during reflow is reduced by the addition of 3.0 wt% Ag into Sn-rich solders. The measurement of the angles of two neighboring Cu6Sn5 grains indicates that the interfacial energy of Cu6Sn5/molten solders in Sn-3.0Ag-0.5Cu is much smaller than that of Sn-0.5Cu and Sn-1.0Ag-0.5Cu, respectively. The Cu6Sn5 IMCs formed at the interface of Sn-3.0Ag-0.5Cu with Cu during reflow retain small grain size even after aging for 500 h, and the small Cu6Sn5 grains induce slower growth of Cu3Sn IMCs during aging.

8:55 AM Invited

Influence of Alloying Elements on Solid-State Reactive Diffusion at Interconnection between Sn and Pd: Masanori Kajihara¹; ¹Tokyo Institute of Technology

Tin-base solders are widely used in the electronics industry. If a multilayer Pd/Ni/Cu conductor is interconnected with the Sn-base solder, Pd-Sn compounds are formed by reactive diffusion at the interconnection during soldering and then gradually grow during energization heating at solid-state temperatures. However, the Pd-Sn compounds are brittle and possess high electrical resistivities. Thus, the growth of the compounds deteriorates the electrical and mechanical properties of the interconnection. In order to inhibit the deterioration of the interconnection, influence of various alloying elements on the growth behavior of the compounds during the solid-state reactive diffusion was experimentally observed at temperatures of T = 433-473 K in the present study. According to the observation, the addition of Ag into Pd decelerates the growth. For the addition of Ni into Sn, however, the deceleration works at T < 473 K but not at T = 473 K.

9:20 AM

Solid-Solid Reaction between Sn3Ag0.5Cu Alloy and Au/Pd/Ni(P) Metallization Pad with Various Pd Thicknesses: *Wei-Hsiang Wu*¹; Yen-Chen Lin¹; Cheng-Shiuan Lin¹; Cheng-En Ho¹; ¹Yuan Ze University

In the past ten years, there has been a growing concern over "black pad" in the electroless nickel/immersion gold [Ni(P)/Au] surface finishing applications. In order to diminish such reliability concern, the deposition of a protective layer of Pd [or Pd(P)] between the Ni(P) and Au has gained a great attention and was readapted very recently. The thickness of Pd layer is customarily deposited within a range of 0.05 - 0.3 micron based on the cost-effective consideration. However, the effect of Pd thickness on the solderability has not been well established yet. In this study, the solid-solid reaction between 96.5 wt.% Sn – 3 wt.% Sn – 0.5 wt.% Cu (SAC305) alloy and the Au/Pd/Ni(P) with various Pd thickness (0, 0.1, 0.25 micron) was investigated. The growth kinetics of the reaction product(s) and the mechanical reliability in response of the different Au/Pd/Ni(P) will be presented in this talk.

9:35 AM

Phase Equilibria of the Sn-Fe-Ni Ternary System and Interfacial Reactions at the Sn/Fe-xNi Alloys Couples: Yee-wen Yen¹; Hsien-Ming Hsiao¹; Shih-Wei Lin¹; Chen-Kuan Lin¹; Chiapying Lee¹; ¹National Taiwan University of Science and Technology

In this study, the phase equilubria of the Sn-Fe-Ni ternary system and interfacial reactions in Sn/Fe-Ni alloys couples were experimentally investigated. The experiment indicated that the isothermal section of the Fe-Ni-Sn ternary system at 270° had eight tie triangles, seventeen two-phase regions, ten single-phase regions and without any ternary intermetallic compounds (IMCs).One FeSn2 phase was formed at the Sn/Fe-xNi interface, when the Ni concentration was less 60 at.%. When the Ni content was between 80-90 at.%, both the FeSn2 and Ni3Sn4 phases were formed on the interface. When the Ni content in the Fe-Ni alloy was up to 95 at.%, only the thick layer of the Ni3Sn4 phase could be found. The IMC growth mechanism of the Sn/Alloy 42 and Sn/Fe-60 at.%Ni couples was diffusion-controlled. The reaction path of the Sn/Fe-80at.%N couple was Sn/Sn+FeSn2/Ni3Sn4/Fe-80 at.%Ni.

9:50 AM

Modeling of Alternating Reaction Phases in Sn/Ni-V Couples: Chun-Chong Fu¹; *Chih-chi Chen*¹; ¹Chung Yuan Christian University

Ni-V alloys are barrier materials in flip chip technology, and Sn is the primary constituent of Pb-free solders. It is demonstrated that unusual alternating reaction phases, T/Ni3Sn4/T/Ni3Sn4, are formed in solid/solid Sn/Ni-V couples. T phase is an amorphous Sn-Ni-V ternary phase. In this study, a mathematical model was formulated to describe the alternating phenomenon. The basic assumption of the model is that Sn is the dominant diffusion species, and that V is immobile. The parameters of the model were determined by the least square method, and the correlation coefficient (R2) demonstrated a good agreement between the experimental and calculated results. The differential equations can be solved by using some assumptions. The alternating phenomenon is represented by the none-zero imaginary part of the eigen value, which is caused by the relative high mobility difference between Sn and V in the diffusion zone.

10:05 AM Break

10:25 AM Invited

Phase Evolution and Growth at the Interface of Sn/Cu-xZn under Liquid and Solid Reaction: Chi-Yang Yu¹; Jenq-Gong Duh¹; ¹National Tsing Hua University

Cu-Zn is a potential substrate material to improve the reliability of solder/ Cu-Zn solder joints. In this study, three kinds of solder joints, i.e. Sn/Cu, Sn/ Cu-15Zn, and Sn/Cu-30Zn (wt.%), were fabricated to probe the formation mechanism of intermetallic compounds (IMCs). At the Sn/Cu interface, thick Cu6Sn5 and Cu3Sn grew rapidly during liquid and solid reaction. Kirkendall voids formed between Cu3Sn and Cu substrate after solid state aging. In contrast, no void was observed at these Sn/Cu-Zn interfaces. The



Sn/Cu-15Zn and Sn/Cu-30Zn solder joints revealed slow growth rate of interfacial IMCs, and the formation of Cu3Sn was evidently suppressed. Cu6(Sn,Zn)5, Cu(Zn,Sn), and CuZn were the dominant IMCs. The phase evolution is attributed to the atomic diffusion and elemental re-distribution at the Sn/Cu-xZn interfaces under liquid and solid reaction. With regards to the thickness variation of interfacial IMCs, the growth mechanisms of IMC and related phases are proposed.

10:50 AM

Metallurgical Reaction in Sn-Cu-Ni Solder Alloys: Han-wen Lin¹; Chih Chen¹; ¹National Chiao Tung University

Sn-Pb alloys have used in packaging industry due to its favorable physical, mechanical and metallurgical properties. However, since the RoHS was adopted in 2003 and it took effect in 2006, new Pb-free alloys, such as Sn-Ag, Sn-Cu, Sn-Ag-Cu, have been developed. Among these systems, Sn-Ag and Sn-Ag-Cu are the most common candidates as Pb-free solder materials in packaging industry. However, as the bumps get smaller and smaller, the brittle intermetallic compounds of tin and silver, Ag3Sn, might become a fatal factor to joints. Therefore, alloy system of Sn-Cu-Ni is proposed. In this paper, different composition of Sn-Cu-Ni are prepared, including SnCu2Ni1, SnCu3Ni1.5, SnCu4Ni2 (weight percent). The metallurgical reactions of the solder alloys with Ni and Cu foils will be investigated.

11:05 AM

Microstructure Effect of Electroplated Cu Foils on Interfacial Reaction with Pb-Free Sn-Based Solders: T. S. Huang¹; *Cheng Yi Liu*¹; ¹National Central University

The interfacial reaction between Pb-free Sn-based solders and Cu substrate has been studied for decades. Yet, how does the microstructure of Cu affect the interfacial reaction is still an issue to be understood. In this study, we will investigate the correlation between the microstructure of Cu substrate and the interfacial reaction. Cu substrates with different orientations are prepared by electroplating. Then, reflowing solder balls on the electroplated Cu substrates and aging the Sn/Cu solder joint samples under 150°. The aged Sn/Cu samples were examined by the metallurgical the examination, XRD and FIB analysis to investigate (1) the grain morphology and preferred orientation of electroplated Cu substrates. (2) Cu-Sn compound layers and Kirkendall voids distribution at the joint interfaces. The results indicate that the growth kinetics of the interfacial Cu₂Sn and Cu₂Sn₅ layer strongly depends on the prefer-orientation of the electroplated Cu substrates, i.e., (111) and (220). In addition, the detail growth kinetics of the Cu-Sn intermediate phases, (Cu3Sn and Cu6Sn5) layers are modeled by analyzing the three interfaces (Cu/Cu3Sn, Cu3Sn/Cu6Sn5, and Cu6Sn5/Sn) movement. The detail kinetics would be presented in this talk.

Physical and Mechanical Metallurgy of Shape Memory Alloys for Actuator Applications: Alloy Design and Development

Sponsored by: The Minerals, Metals and Materials Society Program Organizers: S. Raj, NASA Glenn Research Center; Raj Vaidyanathan, University of Central Florida; Ibrahim Karaman, Texas A&M University; Ronald Noebe, NASA Glenn Research Center; Frederick Calkins, The Boeing Company; Shuichi Miyazaki, Institute of Materials Science, University of Tsukuba

Wednesday AM	Room: 11B
March 2, 2011	Location: San Diego Conv. Ctr

Session Chairs: Sebastian Fähler, IFW Dresden; Petr Sittner, Institute of Physics of the Academy of Sciences

8:30 AM Introductory Comments

8:35 AM Plenary

New Experimental Results on the Role of Alloy Composition and Microstructure on Thermodynamic and Mechanical Properties of NiTi Shape Memory Alloys: Gunther Eggeler¹; ¹Ruhr-Universitat Bochum

NiTi shape memory alloys are well known for many years. They show fascinating properties like the one way effect (1-WE) and pseudoelasticity (PE) which are technically exploited in different areas of engineering and medical technology. These properties rely on thermally or stress induced martensitic transformations as has been reported on many occasions. However, a number of open issues remain which hamper the breakthrough of these high potential functional materials. Thus, there are no precise data on the concentration dependence of the phase transition temperatures in the binary alloy. The elementary processes which govern the formation of microstructure during ingot metallurgy processing routes are only poorly understood. And the role of dislocations during the martensitic transformation and their effect on functional fatigue remains unclear. Moreover, basic micro mechanical aspects like crack propagation and the stress induced formation of R-phase have not been fully rationalized. The brief overview reports on progress in these areas made by the collaborative research center on shape memory technology (SFB 459) funded by the German research foundation (DFG) at the Ruhr-Universität Bochum in the last two years. Areas in need of further research are outlined.

9:05 AM Invited

Characteristic Features of Ni- and Fe-Based Magnetic Shape Memory Alloys: Ryosuke Kainuma¹; ¹Tohoku University

In the past decade, many kinds of Ni-based magnetic shape memory alloys, such as Ni-Co-Al[1], Ni-Fe-Ga[2], Ni-Co-Mn-In[3], besides the Ni-Mn-Ga alloy have been reported. Very recently, our research group has found new magnetic shape memory alloys in ferrous alloy systems, Fe-Mn-Ga[4] and Fe-Ni-Co-Al[5]. In the presentation, characteristic features on magnetic, martensitic and mechanical properties for these advanced Ni- and Fe-based magnetic shape memory alloys are reviewed and their ability for actuator applications will be discussed. (References) [1] K. Oikawa et al., Appl. Phys. Lett., 79 (2001) 3290. [2] K. Oikawa et al., Appl. Phys. Lett., 81(2002) 5201. [3] R. Kainuma et al., Nature, 439 (2006) 957. [4] T. Omori et al., Appl. Phys. Lett., 95 (2009) 082508. [5] Y. Tanaka et al., Science, 327 (2010)1488.

9:25 AM Invited

Design of Ferromagnetic Shape Memory Alloy (FSMA) Composites: *Minoru Taya*¹; ¹University of Washington

I will discuss the design of a set of new FSMA composites based on "hybrid mechanism of actuation" under magnetic field gradient. Originally, we discovered this Hybrid Mechanism based on FePd. Due to its higher cost, we is now designing lower-cost FSMA composites made of Ferromagnetic (soft magnetic) material and Superelastic SMA, which can exhibit larger strain at faster speed under the applied magnetic field gradient. I will discuss several cases of such FSMA composite actuators following first the fundamental hybrid mechanism which includes both modeling, processing and characterization.

9:45 AM

Thermoelastic and Non-Thermoelastic Martensitic Transformations in Fe-Mn-Al and Fe-Mn-Ga bcc Alloys: *Toshihiro Omori*¹; Ikuo Ohnuma¹; Kiyohito Ishida¹; Ryosuke Kainuma¹; ¹Tohoku University

Martensitic transformations (MTs) from the γ -fcc parent phase to the α '-bcc or -bct martensite phase are commonly recognized in Fe-based alloys. Recently, we have reported that MTs from the α -bcc phase occur in Fe-Mn-Al and Fe-Mn-Ga systems, and that these transformations are thermodynamically reasonable. In the Fe-Mn-Al system, the α phase has a disordered A2 structure and the MT is non-thermoelastic, in which the martensite phase has a fcc structure. On the other hand, the Fe-Mn-Ga alloy has a L2₁ ordered structure, showing thermoelastic MT to a fct structure. It is interesting to note that these two alloy systems show opposite magnetic properties. Those parent and martensite phases are ferromagnetic and weak magnetic (probably antiferromagnetic) in Fe-Mn-Al alloy, but ferromagnetic and paramagnetic in Fe-Mn-Ga alloy, respectively. Stress- and magnetic field induced properties will also be presented.

10:00 AM Break

10:10 AM

Phase Transformation and Shape Memory Effect of Ti(Pt, Ir): Yoko Yamabe-Mitarai¹; Toru Hara¹; Seiji Miura²; Hideki Hosoda³; ¹National Institute for Materials Science; ²Hokkaido University; ³Tokyo Institute of Technology

We have focused on the alloys combining with Ti and platinum group metals such as TiPt or Ti(Pt, Ir) as high-temperature shape memory alloys due to their high martensitic transformation temperature above 1273 K. In the previous study, phase transformation and shape memory effect were investigated in the alloy with 50at% of Ti. The 2% of the strain recovery was found in ternary compounds by heating above Af after compression test. In this study, phase boundary of the B2 phase was first investigated in Ti-Pt-Ir ternary system. Based on the obtained phase boundary, several alloys with Ti-rich composition were prepared. Composition dependence of phase transformation and shape recovery effect was investigated in Ti-Pt-Ir with a variety of composition.

10:25 AM

New Ferrous Polycrystalline Shape Memory Alloy Showing Huge Superelasticity: *Yuuki Tanaka*¹; Toshihiro Omori¹; Ryosuke Kainuma¹; Yuji Sutou¹; Kiyohito Ishida¹; ¹Tohoku University

Recently, we have developed a pollicrystalline Fe-Ni-Co-Al based alloy exhibiting a large superelasticity of about 13% due to a thermoelastic \Box (fcc) / α ' (bct) transformation, which is almost twice than that of the Ni-Ti-based shape memory alloys. This ferrous alloy shows a very large mechanical damping capacity about 5 times larger than that in the Ni-Ti alloy and exhibits some unique properties, such as a large reversible change in magnetization during tensile loading and unloading and a magnetic-induced strain of about 1% at room temperature[1]. In this presentation, details on the alloy design and the fundamental physical properties of the Fe-Ni-Co-Al-based alloys are introduced. [1] Y. Tanaka, Y. Himuro, R. Kainuma, Y. Sutou, T. Omori, K. Ishida, Science, 327 (2010) 1488.

10:40 AM

The Effect of Aluminum Additions on the Shape Memory Behavior in NiTiZr Alloys: Derek Hsen Dai Hsu¹; Taisuke Sasaki²; Gregory Thompson²; *Michele Manuel*¹; ¹University of Florida; ²The University of Alabama

The NiTiZr shape memory alloy system is of interest due to zirconium's ability to significantly change transformation temperatures as a function of composition. The addition of aluminum to this system provides the opportunity to form coherent Heusler phase precipitates. The present work reports the change in the thermomechanical, transformation, and microstructural behavior of the alloy system with the addition of aluminum as a quaternary alloying element to NiTiZr alloy with zirconium contents up

to 20 at.%. An overview of NiTiZr and NiTiAl alloys is provided and the results will be used to develop a new thermodynamic framework for alloy design. The authors would like to acknowledge support from the National Science Foundation under award number CMMI-0824352.

10:55 AM

Characterization of New Phases in the Ti-Pt System Relevant to High Temperature Shape Memory Alloys: *Karem Tello*¹; Scott Cochran¹; Jacob Neuchterlein¹; Keith Roman¹; Dana Drake¹; Heather Rosin¹; Anita Garg²; Ronald Noebe²; Michael Kaufman¹; ¹Colorado School of Mines; ²NASA Glenn Research Center

Nitinol (Ni-Ti) shape memory alloys (SMAs) are used widely in superelastic and shape memory applications near ambient temperatures. Platinum increases the martensitic transformation temperatures responsible for the shape memory properties and makes them potentially attractive as high temperature SMAs (HTSMAs). Unfortunately, the Ti-Pt phase diagram is poorly understood in the range 30-50 at. % Pt making the development of HTSMAs difficult. In this investigation, alloys in this range cast and heat treated and characterized using DTA, SEM and TEM methods. The alloys frequently contained more than two phases even after equilibration treatments; since this violates the phase rule, it was concluded that interstitial contamination must be complicating matters. Furthermore, one of the new phases of approximate composition Ti5Pt3, which appears to be interstitially stabilized, is related structurally to what appears to be a complex, lower-symmetry and equilibrium Ti4Pt3 phase. The results will be examined and a modified phase diagram proposed.

11:10 AM

Influence of Precipitation on the Phase Transformation Temperatures of High Temperature Shape Memory NiMnColn Films: Steven Rios¹; Ibrahim Karaman¹; Xinghang Zhang¹; ¹Texas A&M University

Amorphous Ni_{s0}Mn₃₈Co₆In₆ films 20 μ m in thickness were fabricated using DC magnetron sputtering. Films crystallized during annealing in a differential scanning calorimeter (DSC). Crystallized films retained a nonmodulated L1₀ martensite structure at room temperature. DSC studies were used to determine the crystallization activation energy and showed that as the annealing temperature increased, the martensitic phase transformation temperature decreased substantially. The formation of precipitates and evolution of grain size are investigated by scanning transmission electron microscopy. Mechanisms that lead to the reduction of phase transformation temperature are discussed.

11:25 AM

Phase Transformation and Microstructure Evolution in Rapidly Solidified Co-Ni-Ga Ferromagnetic Shape Memory Alloys: Haamun Kalaantari¹; Reza Abbaschian¹; ¹University of California, Riverside (UCR)

Co-Ni-Ga ternary alloys are good candidates as Ferromagnetic Shape Memory Alloys (FSMAs) for modern applications such as sensing and actuating devices. The alloys have magnetic properties similar to Ni-Mn-Ga system, but with improved ductility since these Co and Ni based alloys generally consist of dual-phase structure with the phase imparting enhanced room temperature ductility significantly. In this investigation, Electromagnetic Levitation (EML) technique is applied to explore the effects of rapid solidification and bulk supercooling in a Co2NiGa and some of its off stoichiometric alloys. The effects of these solidification processing variables on the phase transformation, microstructure and FSM properties will be discussed.

11:40 AM

Plasticity Enhanced Martensite Transformation in Ni-Ti Shape Memory Alloys: *Harshad Paranjape*¹; Sivom Manchiraju¹; Peter Anderson¹; ¹The Ohio State University

The response of polycrystalline shape memory actuators depends in part on the internal stress state that is induced by plastic deformation. This deformation may occur during preprocessing or during subsequent operation of the actuator. This work uses a recently developed finite element approach to study how plasticity in the austenite (B2) phase affects transformation



during both pseudoelastic and load-biased thermal cycling conditions for a solutionized Ti-50.9at.%Ni polycrystal. An outcome is that plasticity may be viewed as "good" or "bad", depending on whether it enhances or suppresses martensite formation. The particular outcome at a grain level depends on the local texture. This knowledge is used to synthesize model polycrystals that manipulate the nature of plasticity in an effort to optimize actuator performance.

11:55 AM End of Session

Polycrystal Modelling with Experimental Integration: A Symposium Honoring Carlos Tome: Dislocation Dynamics, Geomaterials, Nanoscale

Sponsored by: The Minerals, Metals and Materials Society, TMS Structural Materials Division, TMS Materials Processing and Manufacturing Division, ASM-MSCTS: Texture and Anisotropy Committee, TMS/ASM: Mechanical Behavior of Materials Committee, TMS/ASM: Computational Materials Science and Engineering Committee

Program Organizers: Ricardo Lebensohn, Los Alamos National Laboratory; Sean Agnew, University of Virginia; Mark Daymond, Queens's University

Wednesday AM	Room: 6C
March 2, 2011	Location: San Diego Conv. Ctr

Session Chairs: Laurent Capolungo, Georgia Tech; Amit Misra, Los Alamos National Laboratory; Olivier Castelnau, ENSAM

8:30 AM Invited

Scaling Laws for Dislocation Microstructures in Cyclic Deformation: Ladislas Kubin¹; Sauzay Maxime²; ¹CNRS; ²CEA

The dislocation microstructures formed during the monotonic deformation of fcc crystals follow two well-known scaling laws. These laws relate the flow stress to the square root of the mean dislocation density and to the inverse of the wavelength of dislocation patterns. A compilation of literature results on the cyclic deformation of fcc single and polycrystals shows that these scaling laws also apply to persistent slip bands (PSBs) and dislocation cell structures. The two scaling constants are, however, three times smaller than in monotonic deformation. This result seems to arise from the partial reversibility of cyclic plastic flow, as modeled by Essmann in the 1980's. The saturation stress for PSBs and the critical stress for the onset of dynamic recovery in monotonic deformation appear to exhibit very similar temperature dependencies. This shows that the two stresses are governed by the same mechanism, specifically the mutual annihilation of screw dislocations by cross-slip.

8:55 AM Invited

Dislocation Dynamics Enhanced Single Crystal Constitutive Law: *Laurent Capolungo*¹; Carlos Tome²; irene Beyerlein²; ¹Georgia Institute of Technology; ²Los Alamos National Laboratory

Hexagonal closed packed (hcp) metals deform plastically via the simultaneous activation of several different deformation modes (i.e. twinning, slip). As in the case of cubic crystals, interactions between slip systems, which translate into latent hardening or softening at the macroscopic scale, are of particular interest. Indeed, these slip system interactions control microstructure development- and in particular the magnitude and strength of strain gradients. In order to precisely quantify the effects of such dislocation interactions, a new constitutive model is developed. The model is directly informed with results obtained from discrete dislocation dynamics simulations of the strength and chance of junction for each junction type. Mobile, statistically stored and geometrically necessary dislocations evolutions are accounted for as well as their directionality. Latent hardening between different slip modes are captured via the introduction of a new dislocation storage model

9:20 AM

Experimental and Simulation Study of Grain Boundary Influence on Dislocation Mean Free Path: *Gael Daveau*¹; Benoit Devincre²; Thierry Hoc³; Odile Robach⁴; ¹LEM (CNRS-ONERA) / MSSMAT (ECP); ²LEM (CNRS-ONERA); ³LTDS (EC-Lyon); ⁴CEA-Grenoble DSM/INAC/SP2M/ NRS

In this study, a dislocation density based model [1] initially developed for fcc single crystal is extended to strain hardening in polycrystal. The early stages of plastic deformation in a Cu tri-crystal are investigated as an ideal validation test.Crystal rotation and elastic strain are measured by Laue microdiffraction in the vicinity of grain boundaries (GBs). In addition, the storage of GND density induced by the existence of GBs is evaluated at increasing deformation. The corresponding profiles are used to test predictions made with DD simulation. From that comparison, a decrease of the dislocation mean free path is determined as a function of GB distances. Following a multiscale modeling approach, this information is finally included in a "storage-recovery" constitutive law part of a crystal plasticity code. The latter is used to simulate deformations at larger scale. [1] Devincre, Hoc, Kubin, Science, 320 (2008) p 1745–1748.

9:40 AM Invited

Slip Systems Interactions in Ice Single Crystals: Benoit Devincre1; 1CNRS

With dislocation dynamics simulation we examine the nature and the strength of slip systems interactions in ice single crystals. As an hcp material with plastic deformation dominated by basal slip, focus is on basal-basal, basal-pyramidal and basal-prismatic slip interactions. Based on the results of large-scale 3D simulations of latent hardening tests, an interaction matrix is proposed for crystal plasticity modelling.

10:05 AM Break

10:20 AM Invited

Polycrystal Plasticity: Linking the Microscopic and Macroscopic Scale: *Hans-Rudolf Wenk*¹; ¹University of California

Material scientists are generally concerned about deformation of objects meters in size and over time spans of hours. Similar processes take place in the Earth but on a much larger scale of thousands of kilometers and lasting for millions of years. We will illustrate how the visco-plastic self-consistent theory successfully predicts texture development in the lower mantle that are compatible with seismic observations of anisotropy. While modeling of flow in the deep Earth is on a large scale, it requires information about deformation mechanisms in the phases perovskite, postperovskite and magnesiowuestite that can only be determined at the microscopic (micron) level with diamond anvil experiments. Also here VPSC is needed to interpret active slip systems from experimental textures of these phases which are unstable at ambient conditions. This micro-macro linking has attracted materials researchers such as Gilles Canova and later Carlos Tomé to engage in geophysical research.

10:45 AM Invited

The Transient Creep of Polycrystalline Ice Inferred from Theoretical, Numerical, and Experimental Micromechanical Approaches: *Olivier Castelnau*¹; Claudiu Badulescu²; Renald Brenner³; Paul Duval⁴; Fanny Grennerat⁴; Noel lahellec²; Maurine Montagnat⁴; Hervé Moulinec²; Pierre Suquet²; Quoc Huy Vu³; ¹PIMM-CNRS; ²LMA-CNRS; ³LPMTM-CNRS; ⁴LGGE-CNRS

The significant overall hardening occurring during the transient creep of polycrystalline ice strongly depends on the elastic and viscoplastic behaviors at the grain scale but also on dislocation processes at the slip system level. The local viscoplastic anisotropy, which is particularly large for ice crystals, plays a crucial role in the development of intra- and inter-granular stress and strain field heterogeneities. One difficulty for the description of transient creep behavior comes from the coupling between elastic and viscoplastic responses, and the subsequent memory effect that has to be considered. We will present our ongoing work on the topic in which full-field modeling (based on a FFT approach), mean-field modeling (homogenization), and experimental characterization of intragranular strain heterogeneities (image

correlation) on 2-D specimens, are compared with each other. Presented results will focus on the link between local grain microstructures, strain heterogeneities, and effective behavior.

11:10 AM

Rheologic Anisotropy Associated with Flow-Induced Texturing of Earth's Mantle: Donna Blackman¹; Olivier Castelnau²; ¹UCSD; ²CNRS

We investigate feedbacks between upper mantle flow and associated texturing of polycrystalline mineral aggregates. A multi-scale (nanometer-100's km), linked numerical procedure allows us to assess local rheological anisotropy that could alter the mantle flow. Results to date use an 'intermediate coupling' approach. Mantle flow is computed assuming isotropic viscosity. Anisotropic rheology due to flow-induced textures is determined at local positions throughout the model space. These local viscosity tensors update the stiffness matrix and a new steady-state flow-field is solved. In low gradient areas, deviation from isotropic results is small. In high strain-rate gradient areas, notable rheologic anisotropy is predicted. Differences in flow velocities reach ~25% of the spreading rate in these regions of this interim case. We expect to report results for successive iterative runs, where updated viscosity tensors are computed at each step and introduced to the subsequent flow model calculation.

11:30 AM Invited

Studying the Mechanical Response of Regions within Grains and near Grain Boundaries Using Spherical Nanoindentation: Siddhartha Pathak¹; *Surya Kalidindi*²; ¹Mechanics of Materials and Nanostructures Laboratory, EMPA; ²Drexel University

We discuss the capabilities of spherical nanoindentation stressstrain curves, extracted from the measured load-displacement dataset, in characterizing the local mechanical behavior within individual grains and near grain boundaries of polycrystalline samples. Since nanoindentation length scales are smaller than the typical grain sizes in polycrystalline samples, this technique is an ideal tool for detailed characterization of the microscale heterogeneities present in these materials and their evolution during various metal shaping/working operations. Using a series of examples, we demonstrate the tremendous capabilities of our data analyses procedures in a) characterizing the local indentation yield strengths in individual grains of deformed polycrystalline metallic samples and relating them to increases in the local slip resistances, b) correlating the stored energy differences of individual grains to their Taylor factors as a function of imposed cold work, and c) understanding the role of interfaces such as grain boundaries in the deformation of a multi-phase polycrystalline sample.

11:55 AM

Ab-Initio Based Study of the Elastic Properties of Dual-Phase Ti-Nb Polycrystalline Composites: *Martin Friak*¹; Benedikt Sander¹; Duancheng Ma¹; William Counts¹; Dierk Raabe¹; Joerg Neugebauer¹; ¹Max Planck Institute for Iron Research

We present a scale-bridging approach for modeling the integral elastic response of polycrystalline composites that is based on a multiphysics combination of (i) parameter-free first-principles calculations of thermodynamic phase stability and single-crystal elastic stiffness, and (ii) homogenization schemes developed for polycrystalline aggregates and composites. The modeling is used as a theory-guided bottom-up materials design strategy and applied to Ti-Nb alloys as a promising candidate for biomedical implant applications. The theoretical results (i) show an excellent agreement with experimental data and (ii) reveal a decisive influence of the multi-phase character of the polycrystalline composites on their integral elastic properties. The study shows that the results based on the density-functional-theory calculations at the atomistic level can be directly used for predictions at the macroscopic scale, effectively scale-jumping several orders of magnitude without using any empirical parameters (see e.g. Raabe et al., Acta Materialia, vol. 55, 4475, (2007)).

12:15 PM

Plasticity of Metallic Nanolayered Composites: Shrinking Tomé to Nanoscales: *Amit Misra*¹; ¹Los Alamos National Laboratory

Metallic nanolayered composites synthesized via physical vapor deposition possess ultra-high strengths. Although the individual layer thickness is on the order of nanometers, foils with total thickness on the order of a few tens to a hundred micrometers can be readily produced and deformed to large plastic strains via room temperature rolling. A symmetric slip model will be presented to account for preservation of the initial crystallographic relations after large strain deformation. The VPSC model developed by Carlos Tomé was used to model texture evolution in Cu-Nb nanolayered composites. At this length scale, the model accounts for the interface between Cu and Nb layers by computing the aggregate response of composite grains using a visco-plastic self-consistent scheme. The model was later extended to interpret similar observations of preservation of initial out-of-plane textures at nanoscales in other nanolayered systems such as nanotwinned Cu and Cumetallic glass composites.

12:35 PM

Assessment of the Hertzian Estimate of Dislocation Nucleation Stresses from Nanoindentation Experiments: Li Ma¹; Dylan Morris²; Stefhanni Jennerjohn³; David Bahr³; Lyle Levine¹; ¹NIST; ²Michelin North America; ³Washington State University

The dislocation nucleation stress of crystalline materials is frequently estimated from the maximum shear stress assuming Hertzian contact up to the first "pop-in" event, which is a sudden displacement burst during loadcontrolled nanoindentation. However, the irregular indenter tip shape will significantly change the stress distribution, and therefore the maximum shear stress from Hertzian estimation. In this work, the near-apex shape of two real Berkovich indenters, one lightly and another heavily used, were measured by SPM and directly input into FEA models for "virtual" nanoindentation experiments on <100>-oriented single-crystal tungsten. Simultaneously, experiments were carried out using the same indenters. The load-displacement curves from FEA simulation show good agreement with those from the experiments. However the discrepancies between Hertzian and FEA estimates of the shear stresses are larger than 30%. This indicates that small irregularities of indentor tips may cause significant deviations from Hertzian estimation of dislocation nucleation stress from nanoindentation experiments.

Processing and Properties of Powder-Based Materials: Powder and Laser Processing

Sponsored by: The Minerals, Metals and Materials Society, TMS Materials Processing and Manufacturing Division, TMS: Powder Materials Committee

Program Organizers: K. Morsi, San Diego State University; Ahmed El-Desouky, San Diego State University

Wednesday AM	Room: 33A
March 2, 2011	Location: San Diego Conv. Ctr

Session Chair: David Bourell, University of Texas-Austin

8:30 AM Introductory Comments

8:35 AM

Effect of Heat Diffusion in Interparticle Micro-Welding for 3-D Particle Assembly: *Kenta Takagi*¹; Kimihiro Ozaki¹; Keizo Kobayashi¹; ¹National Institute of Advanced Industrial Science and Tecnology

We have developed a particle assembly method to build up arbitrary 3-D structures for novel functional materials and devices. The key technique in this method was interparticle bonding in terms of accurate locating of particles. Micro-laser and resistance weldings would be preferred approaches because both of good connectivity and spot heating. The welding tests to single point were conducted using monosized micro-particles of



various materials. Highly thermal conductive materials were hard to be bonded without distortion, because local melting at the contact point could not be attained due to fast heat diffusion. FEM analysis revealed that the thermal problem became more serious in multipoint bonding. As a result, the materials with the conductivity smaller than several tens W/mK were found to be adequately bonded. Eventually, 3-D structures with diamond lattice were successfully assembled using the lowly thermal conductive particles such as Bi alloy and polymer by the developed method.

8:55 AM

Thermal Characterization of Powder-Based Selective Laser Sintering of Nylon-12: *Tim Diller*¹; Rameshwar Sreenivasan¹; David Bourell¹; Joseph Beaman¹; ¹University of Texas

Precise thermal control of selective laser sintering (SLS) is desirable for improving geometric accuracy, mechanical properties, and surface finish of nylon parts. A measurement system was set up to monitor thermal aspects. A SinterStation 2500 SLS machine was the test-bed for studying part builds made of Duraform(tm) nylon-12 powder. Thermal characterization included resistance temperature detectors embedded in the part bed powder to monitor the temperature during the build process. Part bed surface temperature was measured with an infrared camera aimed through the front window. A two-part, macro-scale, time-dependent multi-physics computational thermal model was developed. Boundary conditions were chosen to match the observed conditions in the test-bed machine. In this presentation, initial results are shared, including insights into the material properties and their evolution during the build and the importance of tight control of the preheating process. This research was funded by the Department of Defense under Grant Number GRT00015778.

9:15 AM

Characterization of Al-Ni Composites Produced by Ultrasonic Powder

Consolidation: Dinc Erdeniz¹; Teiichi Ando¹; ¹Northeastern University

Reactive composites, applicable to localized heating applications, were produced from Al and Ni powders by ultrasonic powder consolidation (UPC) at temperatures = 573K in 1 s. The composites exhibited a fully dense microstructure consisting of a metallurgically bonded Al matrix and nearly undeformed Ni particles distributed in the Al matrix. No indications of reactions were noted between the elements. Differential scanning calorimetry (DSC) revealed two exothermic and one endothermic peaks. The phase evolution during DSC was investigated by X-ray diffraction (XRD). The first exothermic peak initiated at 830 K was due to solid-state formation of Al₃Ni and Al₃Ni₂. At 913 K, an endothermic peak formed due to eutectic melting of Al₃Ni and Al which triggered ignition, producing the second exothermic peak at 925 K. The final reacted materials consisted of Al₃Ni, Al₃Ni₂, AlNi and unreacted Ni.

9:35 AM

Comparison of the Effect of Particle Size on the Compressive Strength of Sintered Wollastonite - And Chemically Bonded Phosphate - Ceramics: *H. A. Colorado*¹; J. Juanri¹; Clem Hiel²; H. T. Hahn¹; J-M Yang¹; ¹University of California, Los Angeles; ²Composite Support and Solutions Inc

The effects of different wollastonite powders size distributions on the compressive strength of both sintered and chemically bonded phosphate ceramics (CBPC) is currently being investigated. Wollastonite powder samples were compressed at 5000lb and then sintered at 1050°C for 30h. Compression tests were conducted to evaluate the effectiveness of the sintering treatment. For comparison proposes, CBPCs were fabricated by mixing a phosphoric acid formulation (from CS&S) with different wollastonite powders size. Curing and compression tests were conducted for the CBPCs to evaluate the powder processing effects on their final mechanical properties. The micro-structure in all cases was studied with Scanning Electron Microscopy.

9:55 AM

Laser Cladding of Functional Coatings for Biomedical Applications: Shaodong Wang¹; Lijue Xue¹; ¹National Research Council Canada

Surface coating can be used to enhance and/or optimize the functionalities of medical implants and devices. Blown powder laser cladding, a material additive technology, has a potential to apply various functional coatings on the metallic materials for biomedical applications. Two laser clad coatings have been investigated for medical implant applications: (1) Ti-6Al-4V alloy coating laser-clad on porous titanium foams; and (2) Composite coating of Ti-6Al-4V combined with Co-Cr-Mo alloy laser-clad on Ti-6Al-4V substrates. The microstructure of the laser-clad coating was examined by optical microscope (OM) and SEM. Micro-hardness was measured in the laser-clad coating. Sliding wear testing was particularly performed to evaluate the wear resistance of (Ti-6Al-4V + Co-Cr-Mo) composite coating using pin-on-disc wear testing. Initial results show that laser-clad Ti-6Al-4V coating on porous titanium foams is dense and crack-free. The addition of a small fraction of Co-Cr-Mo alloy will significantly increase the wear resistance of the Ti-6Al-4V composite coating.

10:15 AM Break

10:25 AM

Millimeter-Wave Beam Sintering of Ceramic Laser Host Materials: Arne Fliflet¹; Steven Gold¹; Spencer Miller²; M. Imam¹; C. Feng¹; ¹Naval Research Laboratory; ²Directed Energy Professional Society Scholar

Millimeter-wave beam sintering of ceramic laser host materials such as neodymium-doped yttrium aluminum garnet (Nd:YAG) and ytterbiumdoped yttria (Yb:Y₂O₃) has been under investigation at the Naval Research Laboratory (NRL) for high-energy laser (HEL) applications. Compacts pressed from high-purity micron and submicron grain-size powders are placed in closed insulating caskets and heated by an 83 GHz beam to temperatures of 1600-1800°C using a combination of direct and indirect heating. Over 99% theoretical density has been achieved with moderate grain growth; however, imperfections in the sintered compact microstructure have as yet prevented full transparency. As an aid to designing insulating caskets with low thermal gradients and consistent processing temperatures, we have compared temperature profile calculations based on an inhomogeneous slab model for millimeter-wave beam heating of the casket/work-piece system with experimental measurements. The implications of these calculations and measurements for improving the millimeter-wave sintering process will be discussed.

10:45 AM

Characterization of Particle-Interface Structure and Its Effect on Tensile Fracture in Bulk Copper Produced by Cold Gas Dynamic Spray Processing: *Paul Eason*¹; Phillip Brooke¹; Timothy Eden²; Gerald Bourne³; Michael Kaufman⁴; ¹University of North Florida; ²Pennsylvania State University; ³University of Florida; ⁴Colorado School Of Mines

Cold gas dynamic spray processing is employed as a coating technology in many alloy systems. It has been proposed that improved control over process variables could permit the freeform fabrication of bulk parts. In this investigation, bulk copper samples were sprayed using either nitrogen or helium process gas, allowing comparison of the effects of particle velocities. The helium sprayed samples exhibit recrystallized grains smaller than 100 nm in diameter in regions adjacent to prior particle boundaries. These regions are the subject of investigation into the mechanisms of bonding resulting from high velocity impact. Tensile specimens were produced from samples in the as-sprayed and annealed condition. Field-emission scanning electron microscopy was performed to relate the fracture response to the presence and extent of interfacial bonding. Focused ion beam sectioning and transmission electron microscopy were also employed to establish the extent of interfacial mixing/bonding by examining the fracture path.

11:05 AM

A Feasibility Study of Multi-Pass Cladding Using High-Power Direct Diode Laser: Soundarapandian Santhanakrishnan¹; Radovan Kovacevic¹; ¹Southern Methodist University

In this study, a multi-pass cladding by high power direct diode laser (HPDDL)is performed to study the hardness uniformity in the clad to the substrate. A 2-kW HPDDL of 808 nm in wavelength is used to clad the tool steel H13 on the substrate of AISI 4140 steel. A number of experiments are carried out by changing the laser power and scanning speeds while keeping a constant powder feed rate and the size of overlap to produce different sizes of clad. A coupled thermo-kinetic (TK) hardening model is developed to predict the temperature history, rates of heating and cooling, temperature gradient, rate of solidification and the hardness. The study of microstructure, energy dispersive X-ray spectroscopy (EDX), and hardness measurements are performed to quantify the effect of process parameters on the variation of solidification and the change of hardness.

Properties, Processing, and Performance of Steels and Ni-Based Alloys for Advanced Steam Conditions: Mechanical Behavior and Physical Metallurgy

Sponsored by: The Minerals, Metals and Materials Society, TMS Structural Materials Division, TMS/ASM: Corrosion and Environmental Effects Committee, TMS: High Temperature Alloys Committee

Program Organizers: Peter Tortorelli, Oak Ridge National Laboratory; Bruce Pint, Oak Ridge National Laboratory; Paul Jablonski, National Energy Technology Laboratory; Xingbo Liu, West Virginia University

Wednesday AM	Room: 33B
March 2, 2011	Location: San Diego Conv. Ctr

Session Chair: Paul Jablonski, National Energy Technology Laboratory

8:30 AM

Creep Properties of Fe-20Cr-30Ni-2Nb Austenitic Heat Resistant Steels Strengthened by Intermetallics Designed for A-USC Power Plant: *Masao Takeyama*¹; Imanuel Tarigan²; Naoya Kanno²; ¹Tokyo Institute of Technology, Consortium of the Japan Research and Development Center for Materials (JRCM); ²Tokyo Institute of Technology

Carbon free Fe-20Cr-30Ni-2Nb (at%) austenitic steels newly designed for A-USC power plant exhibit excellent creep properties at 973 K. The creep rupture strength is twice as high as that of SUH 347 steel and could meet the requirement of 10^{5} -hour creep rupture strength higher than 100 MPa at 973 K. In these steels, two types of intermetallic phases of Ni₃Nb (GCP) and Fe₂Nb Laves (TCP) precipitate with different kinetics and morphology; the former precipitates homogeneously within grain interiors in short-time range, whereas the latter mainly at grain boundaries in long-term range. The higher the grain-boundary area fraction of the Laves phase, the lower the creep rate, and the creep rate decreases continuously even though the GCP phase coarsens. Thus, the superior long-term creep strength is attributed to the Laves phase at grain boundaries. The novel strengthening mechanism called "*Grain-boundary precipitation strengthening* (GBPS)" will be given.

8:50 AM

Development and Evaluation of High Mn Containing Alumina-Forming Austenitic Stainless Steel Alloys for Advanced Steam Conditions: *Yukinori Yamamoto*¹; Michael Santella¹; Michael Brady¹; Neal Evans²; Philip Maziasz¹; ¹Oak Ridge National Laboratory; ²University of Tennessee

A series of alumina-forming austenitic (AFA) stainless steel alloys, based on Fe-(12-14)Cr-(2.5-4)Al-(10-25)Ni-(2-10)Mn-(0.6-2.5)Nb-(0.05-0.1)C, wt%, are currently under development for use at 600-900°C. The alloys exhibit superior oxidation resistance to chromia-forming stainless steel alloys, in water-vapor containing environments. This presentation focuses on the development of a low-cost grade of AFA alloys utilizing Mn substituting for Ni to both stabilize the austenite matrix relative to the ferrite phase and reduce raw material costs. Preliminary results indicated that alloys based on Fe-14Cr-2.5Al-(5-10)Mn-(10-12)Ni exhibited a good combination of oxidation resistance at 650°C in air with 10% water vapor and creep resistance at 750°C/100MPa comparable to that of type 347 stainless steel (Fe-18Cr-12Ni base). Details of microstructure, creep, and oxidation resistance will be presented. This research is sponsored by the U.S. DOE, Office of EERE Industrial Technologies Program, and the LDRD Program of Oak Ridge National Laboratory, under contract DE-AC05-00OR22725 with UT-Battelle, LLC.

9:10 AM

New Ferritic Steels with Combined Optimal Creep Resistance and Ductility Designed by Coupling Thermodynamic Calculations with Focused Experiments: *Zhenke Teng*¹; Fan Zhang²; Michael Miller³; Chain Liu⁴; Austin Chang²; Shenyan Huang¹; Robert Tien⁵; Ye Chou⁵; Peter Liaw¹; ¹University of Tennessee, Knoxville; ²CompuTherm LLC; ³ Oak Ridge National Laboratory; ⁴Hong Kong Polytechnic University; ⁵Multi-Phase Services Inc.

Two critical issues restricting the applications of NiAl precipitatestrengthened ferritic steels are their poor room temperature ductility and insufficient creep resistance at temperatures higher than 600°C. In this study, thermodynamic modeling approach is integrated with focused experiments to investigate the ductility and creep resistance of steel alloys based on the Fe-Ni-Al-Cr-Mo system. The mechanical property studies showed that the creep resistance increases with increasing the volume fraction of B2-ordered precipitates, while the opposite trend was observed for the ductility. Low solubility of Al in the Fe matrix was found to favor a ductility increase. Thermodynamic calculations were used to predict the volume fraction of B2-ordered precipitates and the elemental partitioning to guide the selection of alloy compositions which may exhibit the balanced creep resistance and ductility. Key experiments were then conducted to validate the prediction. This integrated approach was found to be very effective in the alloy design and development.

9:30 AM

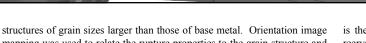
Alloy 740 Weld Strength Optimization: *John deBarbadillo*¹; Brian Baker¹; ¹Special Metals Corporation

If the goals of the USA A-USC project are to be met, age hardened nickel-base alloys will be required for a number of welded components such as headers and reheaters. These alloys pose new issues for large pressure containing systems because their homogenization temperatures are too high to permit full heat treatment of weldments in the field. Extensive testing has shown that age hardened alloys have reduced creep strength, described by the term "weld strength reduction factor" (WSRF). The WSRF is on the order of 0.7-0.8 for nickel-base alloys. This loss of strength can be compensated for in some joints, but not in others. There are several active programs underway in the USA to address this issue. This paper reviews microstructural information and relates it to the predicted cast structure, computed thermal cycles and the phase stability for alloy 740. Potential solutions are proposed and initial results presented.

9:50 AM

Creep Rupture Testing of InconelTM 740 Weldments: *Michael Santella*¹; John Shingledecker²; Oleg Barabash¹; ¹Oak Ridge National Laboratory; ²EPRI

Creep-rupture testing at 750 and 800°C was performed on cross-weld specimens of gas-tungsten-arc welded InconelTM 740 tubes. In one case, the weldments were given a post-weld heat treat-ment of 800°C for 4 h. For fixed time conditions, these specimens failed in the weld deposits at rupture times averaging near 75% of those for base metal, i.e., the average weld strength factor was about 0.75. In the second case, before testing, the weldments were solution treated at 1120°C for 1 h and then aged at 800°C for 4 h. Failures in these specimens occurred in base metal at rupture times near those of unwelded base metal. Solution treatment caused the original dendritic microstructures of the weld deposits to recrystallize into equiaxed



140th Annual Meeting & Exhibition

mapping was used to relate the rupture properties to the grain structure and crystallographic orientation.

10:10 AM Break

10:30 AM

Effect of Steam Exposure on the Creep Properties of Ni-Based Alloys: Sebastien Dryepondt¹; Bruce Pint¹; Edgar Lara-Curzio¹; ¹ornl

Advanced coal-fired ultrasupercritical steam conditions of 760°C and 350 bar have been targeted to meet the future demand for high-efficiency, low emission power generation. This is a dramatic increase compared to the current targets of 600-625°C and ~245 bar. The durability of current candidate Fe- and Ni-based alloys under such harsh conditions needs to be determined and creep testing in air as well as oxidation testing in steam is being conducted. Lifetime models based on these tests cannot accurately integrate the effect of steam exposure on the alloy creep resistance, or the influence of stress on the material oxidation rate. To estimate the effect of steam environment on creep properties, Ni-based specimens have been exposed from 2000 to 5000 h in steam or inert gas prior to creep testing in air. These results were compared to creep data from a new environmental creep rig that allows testing in steam.

10:50 AM

High Temperature Fatigue Life of Coated and Uncoated Valve Materials: *Jeffrey Evans*¹; Seth Farrington¹; Sebastien Dryepondt²; Bruce Pint²; ¹University of Alabama in Huntsville; ²Oak Ridge National Laboratory

In many power generation applications, the search for higher system efficiency has resulted in a progressive increase in operating temperatures. A direct consequence is a decrease of some components' durability due to the appearance of new types of failure. In the case of exhaust valves in natural-gas fired reciprocating engines, high temperature oxidation assisted cracking has been suggested as a rupture mechanism. The presence of water vapor in the exhaust gas accelerates the depletion of Cr from the valve material. The Ni-based alloy 31V is currently one material used in this application, however, its fatigue life has not been reported in the open literature. Aluminide coatings have demonstrated their ability to protect Ni-based alloys from high temperature corrosion, but their impact on the substrate mechanical properties needs to be assessed. This study evaluates the fatigue life of coated and uncoated samples of alloy 31V when tested at elevated temperature.

11:10 AM

A Study on Constitutive Model for Alloy IC10: *Hongjian Zhang*¹; Weidong Wen¹; Haitao Cui¹; ¹Nanjing University of Aeronautics and Astronautics

Alloy IC10, a newly developed Ni3Al-based superalloy, is a typical multiphase alloy with about 65% volume fraction of Gama' phase. As IC10 exhibit unusual thermo-mechanical flow behaviors, a constitutive model was developed to describe the features of IC10. It is well known that the deformation mechanism of different phase is different. So, two assumes are proposed in this model: (i) the contributions to the yield and hardening of different phases are different; (ii) the yield and hardening is the effect of obstacles opposing the motion of mobile dislocations. The flow stress of IC10 can be calculated by building the relationships between the contributions and the evolution of the mobile dislocation density in different experiment conditions. The results show that it is valid.

11:30 AM

A Study on Constitutive Model for the Recrystallization Behaviors of Alloy IC10: *Hongjian Zhang*¹; Weidong Wen¹; Haitao Cui¹; Ying Xu¹; ¹Nanjing University of Aeronautics and Astronautics

IC10 is a newly developed Ni3Al-based superalloy, with its nominal composition (wt %): .07-0.12%C 11.5-12.5%Co 6.5-7.5%Cr 5.6-6.2%Al 4.8-5.2%W 1.0-2.0%Mo 6.5-7.5%Ta1.3-1.7%Hf0.01-0.02%B and Bal. Ni. As IC10 shows typical dynamic recrystallization behaviors above 1173k, a mechanism-based constitutive model was developed to describe the recrystallization features of IC10. It is well known that the deformation

is the results of the movement of mobile dislocations. In this paper, the recrystallization behaviors can be described by building evolution of mobile dislocations. The model is used to simulate recrystallization behaviors of IC10 under different experiment conditions. The results show that it is valid.

Refractory Metals 2011: Tungsten-Based Alloys *Sponsored by:* The Minerals, Metals and Materials Society, TMS Structural Materials Division, TMS: Refractory Metals Committee *Program Organizers:* Omer Dogan, DOE National Energy Technology Laboratory; Jim Ciulik, University of Texas, Austin

Wednesday AM	Room: 19
March 2, 2011	Location: San Diego Conv. Ctr

Session Chairs: Gary Rozak, H.C. Starck, Inc.; John Shields, Pentamet Associated, LLC

8:30 AM

New Refractory High-Entropy Alloys: *Oleg Senkov*¹; Garth Wilks¹; Daniel Miracle¹; C. (Andrew) Chuang²; Peter Liaw²; ¹Air Force Research Laboratory; ²University of Tennessee

Microstructure and properties of two refractory high entropy alloys, $W_{25}Ta_{25}Mo_{25}Nb_{25}$ and $W_{20}Ta_{20}Mo_{20}Nb_{20}V_{20}$, are reported. The alloys were produced by vacuum arc-melting. Despite containing many constituents both alloys have a single-phase body-centered cubic (BCC) structure. The lattice parameters a = 3.2134(3) Å for the quaternary alloy and a = 3.1832(2) Å for the quinternary alloy were determined with high-energy X-ray diffraction using a scattering vector length range from 0.7 to 20 Å⁻¹. The alloy density and Vickers microhardness were $\rho = 13.75$ g/cm³ and H_v = 4455 MPa for the $W_{25}Ta_{25}Mo_{25}Nb_{25}$ alloy and $\rho = 12.36$ g/cm³ and H_v = 5250 MPa for the $W_{20}Ta_{20}Mo_{20}Nb_{20}V_{20}$ alloy. The exceptional microhardness in these alloys is greater than that of the individual constituents, suggesting the operation of a solid-solution-like strengthening mechanism.

8:50 AM

Mechanical Properties of Refractory High-Entropy Alloys: *Oleg Senkov*¹; Garth Wilks¹; Daniel Miracle¹; ¹Air Force Research Laboratory

Compression properties of two refractory high entropy alloys, $W_{25}Ta_{25}Mo_{25}Nb_{25}$ and $W_{20}Ta_{20}Mo_{20}Nb_{20}V_{20}$, determined in the temperature range from 20°C to 1600°C, are reported. The alloys were produced by vacuum arc-melting and had a single phase bcc crystal structure. Compression test samples were 3 mm in diameter and 6 mm in length. The compression tests were conducted in vacuum using a constant strain rate of 0.001 s⁻¹. The room temperature yield strength of the four-component alloy was 1050 MPa and it slowly decreased from 560 MPa to 405 MPa in the temperature range of 600 to 1600°C. The addition of V increased the yield strength by ~200 MPa in this temperature range. The compression strain of the alloys was ~5% at 20°C and above 20% in the temperature range of 600°C – 1600°C. The very high elevated temperature yield strength was suggested to be controlled by a solid-solution-like strengthening mechanism.

9:10 AM

Creep, Oxidation and Intermetallic Phase Formation: Assessing the High Temperature Performance of a Tungsten-Stainless Steel Hybrid: Ben Reyngoud¹; Milo Kral¹; ¹University of Canterbury

The purpose of this study was to investigate the feasibility of a hybrid material comprised of stainless steel reinforced with tungsten wire. The single greatest threat to the success of this composite is the volatile oxidation behaviour of tungsten. Various strategies to protect the tungsten from oxidation were investigated, while simultaneously assessing if there was sufficient ductility and durability to manage thermal cycling and mismatches in thermal expansion coefficients. Creep tests were conducted under isothermal and cyclic conditions at temperatures as high as 1100°C. SEM, EDS, EBSD and TEM were utilized to characterize the formation of cracks, voids, intermetallic phases and oxides.

9:30 AM

WC(100) Surface and Co/WC(100) Interface: Spin-Polarized Ab Initio Study: *Victor Zavodinsky*¹; ¹Russian Academy of Sciences

Ab initio methods of the density functional theory and pseudopotentials were used to study the clean WC(100) surface and the formation of the Co/WC(100) interface. It has been found that the first Co monolayer repeats the geometry of the WC(100) surface with the same value of the lattice constant. The second Co monolayer also repeats the fcc-cubic WC geometry, however the distance between the first and second Co layers is rather less than the distance between planes in the WC cubic crystal. The binding energy grows but the separation energy decreases with transfer from 1ML to 2 ML cobalt covering. The density of states for the WC/Co system looks like the superposition of DOSes for bulk fcc-WC and Co layers. All Co layers are ferromagnetic, however, the magnetization does not influence essentially on their energetics and geometry.

9:50 AM Break

10:10 AM

A Bimodal Distribution of W Grain Size in a Mechanically Alloyed Bulk Tungsten Heavy Alloy: *Andrew Zeagler*¹; Alex Aning²; ¹Virginia Polytechnic Institute and State University; ² Virginia Polytechnic Institute and State University

A tungsten heavy alloy (W–4wt.%Ni) was mechanically alloyed by SPEX mill for various milling times. Cold isostatically pressed powders were solid-state sintered for 1 hour at 1200°C, yielding densities 90–95% of the theoretical value. Scanning electron microscopy revealed a bimodal distribution of W grain size; grains 1–3 μ m in diameter are observed to surround regions of submicron grains. Subsequent sets of samples were mechanically alloyed with 2 and 6 wt.% Ni, and the effects of Ni content and milling time on the composition, grain size and volume fraction of each region were analyzed by microscopy and energy dispersive x-ray spectroscopy.

10:30 AM

Spark Plasma Sintering of Tungsten-Rhenium Alloys for Very High Temperature Nuclear Reactor Applications: *Cory Sparks*¹; John Youngsman¹; Jonathan Webb²; Steve Howe²; Indrajit Charit³; Megan Frary¹; Darryl Butt¹; ¹Boise State University; ²Idaho National Laboratory; ³University of Idaho

Very high temperature nuclear reactors require materials capable of withstanding elevated temperatures. Refractory alloys, such as tungstenrhenium, have been identified as suitable materials due to their excellent high temperature capabilities, but difficulties associated with conventional processing techniques have limited their development. In this study, the tungsten-rhenium microstructure was optimized using alternative techniques such as high energy ball milling and spark plasma sintering, which can control initial particle size and subsequent grain growth. The microstructure and thermo-mechanical properties of the sintered samples were characterized and the results compared to traditionally consolidated alloy data. This comparison illustrates the advantages of using spark plasma sintering to process tungsten-rhenium alloys for very high temperature nuclear applications.

10:50 AM

Physical and Mechanical Properties of Tungsten-Rhenium Alloys Produced Via Spark Plasma Sintering: *Jonathan Webb*¹; Indrajit Charit²; Cory Sparks³; Darryl Butt³; Megan Frary³; Mark Carroll⁴; ¹Center for Space Nuclear Research; ²University of Idaho; ³Boise State University; ⁴Idaho National Laboratory

Future fast spectrum fission reactors used in both terrestrial and space applications will require materials with very high melting temperatures such as tungsten and tungsten-rhenium alloys. In order to support refractory alloy development for fission reactors, tungsten-rhenium alloys of varying rhenium compositions were mechanically alloyed via high energy ball milling technique. The mechanically alloyed tungsten-rhenium powders were then spark plasma sintered at 1600 K and 1700 K for 20 minutes to

produce W-Re alloys with high bulk density (92-97% of theoretical density). The specific heat, thermal conductivity, thermal expansion coefficient, and creep properties of these materials are tested at temperatures ranging from 300 K to 1300 K. The research is supported by the US Nuclear Energy University Program (NE-UP).

11:10 AM

Characterization and Sintering of Open-Cell Ceramic Foams Infiltrated with Tungsten Powder: *Eric Faierson*¹; Kathryn Logan¹; ¹Virginia Polytechnic Institute and State University

Extreme environments require materials that retain adequate mechanical properties at elevated temperatures, and in other hostile conditions such as radiation. Tungsten has a high melting point (3422° C), and retains good mechanical properties at elevated temperatures. This study investigates the use of open-cell ceramic foams to provide a continuous network of reinforcement in a composite material. Silicon carbide and tantalum carbide foams with reticulated vitreous carbon (RVC) cores were infiltrated with tungsten powder by applying vibration, vacuum, and/or isostatic pressure. The infiltrated foam was densified through vacuum sintering. Microstructural analysis was conducted on the foam prior to infiltration and after densification. Mechanical tests were conducted to determine the influence of foam pore and ligament size on the strength and fracture behavior of the foams. Measurements of neutron transmittance through the foam were also conducted.

11:30 AM

Comparative Study of Grain Boundary Impurity Effects in Tantalum and Tungsten Based on First-Principles Calculations: Zhiliang Pan¹; Laszlo Kecskes²; *Qiuming Wei*¹; ¹University of North Carolina Charlotte; ²U. S. Army Research Laboratory

We used density functional theory to systematically calculate the separation energy of symmetric tilt S3(111) GBs of tungsten and tantalum, with and without impurity atoms (H, B, C, N, O, F, Al, Si, P, S, Cl, Fe). We found that although the effects of various interstitial impurity atoms on the specific GB are different, the influence of certain impurity atoms on the GBs is similar. Boron and carbon both enhance the GBs, whereas oxygen, sulfur and silicon etc, weaken the GBs. More importantly, despite the existence of interstitial impurities, GB separation energy of tungsten is always higher than that of tantalum given similar atomic configurations. These findings suggest that it is not yet convincing to attribute the poor ductility of tungsten only to the decreased GB separation energy. We need to consider the competition between brittle deformation mechanisms such as GB separation and plastic deformation mechanisms such as dislocation activities.

11:50 AM

Atomistic Modelling of Complex Phases in Refractory Alloys: *Thomas Hammerschmidt*¹; Bernhard Seiser²; Ralf Drautz¹; David Pettifor²; ¹ICAMS Ruhr-Universität Bochum; ²University of Oxford

The group of topologically close-packed (TCP) phases plays an important role in modern alloys and steels. While their precipitation in single-crystal Ni-based superalloys has a detrimental effect on the mechanical properties, the TCP phases are desirable in precipitation-hardened steels. The formation of the TCP phases is attributed to high local concentrations of refractory elements. We discuss that the trend of the structural stability of TCP phases in refractory elements is captured by a simple tight-binding model. We carried out extensive density-functional theory calculations of the tcp phases A15, C14, C15, C36, mu, sigma, and chi in binary refractory alloys and summarize the influence of band-filling and atomic size on TCP phase stability.



Shape Casting IV: Light Metals Division Symposium in Honor of Prof. John T. Berry: **Properties**

Sponsored by: The Minerals, Metals and Materials Society, TMS Light Metals Division, TMS: Aluminum Processing Committee, TMS: Solidification Committee

Program Organizers: Murat Tirvakioglu, University of North Florida; Paul Crepeau, General Motors Corporation; John Campbell, University of Birmingham

Wednesday AM	Room: 15B
March 2, 2011	Location: San Diego Conv. Ctr

Session Chairs: Glenn Byczynski, Nemak Europe; Sergio Felicelli, Mississippi State Univ

8:30 AM Introductory Comments

8:40 AM

On Faceted Fatigue Fracture in Castings: Murat Tiryakioglu¹; John Campbell2; 1University of North Florida; 2University of Birmingham

Facets are intriguing features observed on the fracture surfaces in some high-cycle fatigue specimens. There exist several hypotheses on their formation and how they contribute to the fatigue failure. An extensive literature survey on faceted fatigue fracture in castings is presented in this study. A new hypothesis is proposed based on the experimental observations presented in the literature, which states that facets form as a result of casting defects. The implications on the true fatigue life potential of castings are discussed in the paper.

9:00 AM

Effect of Holding Time before Solidification on Double-Oxide Film Defects and Mechanical Properties of Aluminium Alloys: Mahmoud El-Sayed¹; Hanadi Salem²; Abdel-Razik Kandeil¹; William Griffiths³; ¹Arab Academy for Science, Technology & Maritime Transport; ²American University Cairo; 3University of Birmingham

Double oxide films (bifilms) have been held responsible for the variability in the mechanical properties of aluminium castings. It has been suggested that the air entrapped inside the bifilm reacts with the surrounding melt leading to its consumption, which might improve the mechanical properties of the castings. In this work, the effect of the holding time of the melt before solidification on the entrained double oxide films for different aluminium alloys was investigated. The Weibull moduli of the plate castings were determined under tensile conditions, and their fracture surfaces examined for evidence of oxide films. The results suggested the occurrence of two competing mechanisms during the holding treatment. The consumption of air inside the bifilms due to reaction with the surrounding molten metal improves the mechanical properties, but this may be followed by hydrogen passing into the bifilms, which has a deleterious effect on properties.

9:20 AM

Weibull Analysis of Thin A356 Plates Cast with an Electromagnetic Pump Green Sand Process: Ratessiea Lett¹; Sergio Felicelli¹; John Berry¹; Rafael Cuesta²; Jose Maroto²; Ruth San Jose²; ¹Mississippi State University; ²CIDAUT

Four multiple gated configurations were utilized with an electromagnetic pump green sand process in order to produce quiescently-filled thin A356 plates that minimize melt surface damage during casting and defect formation during solidification. Eight cast plates were examined, two from each gating design. The method of four point bend testing was used to obtain information about the mechanical properties of the castings, as this method produces a uniform distribution of the bending stress within the central span. From these results, a Weibull statistical analysis was performed in order to quantify specimen failure rate for each of the configurations. The specimen fracture surfaces were then examined using Scanning Electron Microscopy in order to locate possible locations of failure initiation as well as the presence of oxide bifilms. This project is funded by the National Science Foundation (NSF) under the International Research and Education in Engineering (IREE) program.

9:40 AM

Guidelines for 2-Parameter Weibull Analysis for Castings: Murat Tiryakioglu1; 1University of North Florida

Mechanical properties of castings have been analyzed generally by using the two-parameter Weibull distribution for more than a decade. The statistics of this Weibull analysis has received much attention recently. These recent results will be summarized and a step-by-step procedure will be introduced to conduct a proper Weibull analysis for castings. The use of the procedure will be demonstrated on actual datasets.

10:00 AM

Melt Cleanliness, Hydrogen Content and Tensile Properties of A356: Derya Dispinar¹; Arne Nordmark¹; Freddy Syvertsen¹; ¹SINTEF

Degassing of aluminium melts is one of the most important stages in a casting operation. Main reason for this treatment is the removal of hydrogen from the melt, and thereby the ultimate goal is the achievement of a pore-free casting. However, it was shown that the interaction between the bifilms and the hydrogen plays a significant role on pore formation. Therefore, series of degassing experiments were carried out with commercially available A356. Two melts were prepared and one melt was upgassed gradually and the other was degassed gradually. Tensile samples were collected and bifilm index measurements were compared at each treatment sequences. Weibull analysis was used and it was found that the turbulence and vortex (increase in bifilm index) during rotary degassing caused an increase in the scatter irrespective of the hydrogen content.

10:20 AM Break

10:40 AM

The Origin of Griffith Cracks: John Campbell¹; ¹University of Birmingham

The presence any pre-existing Griffith crack or a pore is not necessarily to be expected in solidified metals as a result of the extremely high interatomic forces. It seems likely that pores and cracks may not be created intrinsically by the atomic mechanisms involved in the formation of a solid by solidification from liquid, or condensation from vapor phases nor, probably, by mechanisms of plastic deformation. It is proposed here that initiation sites for pores and cracks for most, if not all failures of metals, can only be introduced into metals via extrinsic (entrainment) mechanisms resulting from production processes, particularly melting and casting, but also spraying and powder metallurgy processes. It seems probable that only entrainment processes can create unbonded interfaces that can explain microstructures containing cracked (apparently 'brittle') intermetallics and decohered phases, and the initiation of tensile fracture and fatigue.

11:00 AM

The Use of the Weibull Statistical Method to Assess the Reliability of Cast Aluminum Engine Blocks made from Different Casting Processes: Glenn Byczynski1; Robert Mackay1; 1Nemak Canada

The use of aluminum cast engine blocks has grown considerably within the automotive industry due to their lighter weight when compared to traditional materials such as cast iron. In this investigation, three aluminum cast engine block processes: High Pressure Die Cast, Precision Sand Cast Process-Zircon and Precision Sand Cast Process-Silica/Chill are evaluated in terms of reliability (Weibull Plots) of the mechanical strength determined from tensile test samples extracted from the bulkhead region. Metallographic analysis was performed on the tensile test samples to provide interpretative feedback on the statistical analysis of the mechanical test results.

11:20 AM

Ultra-High Strength Sand Castings from Aluminum Alloy 7042: O. Senkov1; Alan Druschitz2; S. Senkova1; K. Kendig1; J. Griffin2; 1Air Force Research Laboratory; ²University of Alabama Birmingham

Ultra-high strength, aluminum alloy castings with very good ductility have been successfully produced using the combination of chemically bonded sand molds, an Al-Zn-Mg-Cu-Sc alloy (aluminum alloy 7042) and solidification under pressure. In the T6 condition, castings had the following mechanical properties: 585-595 MPa ultimate tensile strength, 505-520 MPa yield strength and 5-10% elongation. HIP'ing slightly increased the tensile strength (to 590-610 MPa) and increased the elongation (to 8-12%). In the T4 condition, castings had the following mechanical properties: 490-540 MPa ultimate tensile strength, 340-360 MPa yield strength and 10-13% elongation.

11:40 AM

Relationship between Structures and Properties of Al-Cu Alloys: Alicia Ares¹; Liliana Gassa¹; Carlos Schvezov¹; ¹CONICET

The objective of the present research consist on studying the type of structure (columnar, equiaxed or with columnar to equiaxed transition, CET) using parameters of the solidification process and electrochemical parameters in Al, Cu and Al-Cu alloys with different concentrations. In order to obtain columnar, equiaxed and CET structures, the alloys were directionally solidified upwards in an experimental set up with a set of thermocouples in the samples which permit to determine the time dependent profiles during the process. From these profiles and the location of thermocouples it was possible to calculate the cooling rates, growth velocities and temperature gradients along the samples. The electrochemical studies of the samples were realized by using an electrochemical impedance spectroscopy (EIS) technique and potentio-dynamic polarization curves immersed in 3% NaCl solution at room temperature. It was found a higher susceptibility to the corrosion as the Cu content increased in the alloy.

12:00 PM

Microstructure Characterization of Magnesium Control Arm Castings: Liang Wang¹; Ratessiea Lett²; Sergio Felicelli²; John Berry²; ¹Mississippi State University ; ²Mississippi State University

Microstructural and mechanical property data were generated from several control arm castings of Mg alloy AZ91 produced for the High Integrity Magnesium Automotive Components (HIMAC) project. The castings were made by four different processes: squeeze cast, low pressure permanent mold, T-Mag, and Ablation. Ten control arms were examined from each of the four casting groups. The microstructure, grain size, pore fraction, and pore size were measured with optical microscopy and image analyzer. Different types of defects are identified to evaluate the four casting processes. In order to explore the presence of oxide films, a series of four-point bend (FPB) tests were performed, and the maximum load was measured. The mechanical properties of the castings were quantitatively evaluated for reliability using a two-parameter Weilbull distribution function. A detailed metallographic analysis of the fracture surfaces of FPB samples was performed using SEM. This project was sponsored by the United States Automotive Materials Partnership (USAMP).

Size Effects in Mechanical Behavior: Indentation Size Effects

Sponsored by: The Minerals, Metals and Materials Society, Not Applicable, TMS: Nanomechanical Materials Behavior Committee *Program Organizers:* Erica Lilleodden, GKSS Research Center; Amit Misra, Los Alamos National Laboratory; Thomas Buchheit, Sandia National Laboratories; Andrew Minor, UC Berkeley & LBL

Wednesday AM	Room: 2
March 2, 2011	Location: San Diego Conv. Ctr

Session Chairs: Erica Lilleodden, GKSS Research Center; Khalid Hattar, Sandia National Laboratories

8:30 AM

Stress-Strain Responses from Spherical Nano-Indentation and Micro-Pillar Compression Experiments: A Comparative Study: *Siddhartha Pathak*¹; Rejin Koodakal²; Surya Kalidindi³; Johann Michler²; ¹California Institute of Technology; ²EMPA - Swiss Federal Laboratories for Materials Testing and Research; ³Drexel University

Spherical nano-indentation and micro-pillar compression experiments were conducted on individual grains (grain size ~mm) of varying orientations in two sets of Fe-3%Si (BCC) polycrystalline samples of different deformation levels - as-cast and 30% deformed. The local indentation loading modulus and yield strength values, as well as certain aspects of post-yield strain hardening behavior, were obtained by transforming the raw load-displacement data obtained using spherical indenters of two different radii (1 and 13.5 μ m) into indentation stress-strain curves. Micro-pillars of varying diameters were FIB machined on the same grains and compressed in-situ SEM to identify their uniaxial elastic modulus, yield strength and strain hardening behavior. The advantages and limitations of each technique in capturing the effects of lattice orientation and the level of plastic deformation in their respective stress-strain responses are discussed. An analysis on the similarities, as well as individual insights from each of the two techniques, is also presented.

8:50 AM

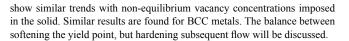
Nanoscale Behavior of Ta Single Crystals – Temperature and Orientation Dependence: Zhi-Chao Duan¹; Juergen Biener²; Monika Biener²; Andrea Hodge¹; ¹University of Southern California; ²Lawrence Livermore National Laboratory

The study of Ta at elevated temperatures presents new insights into the nanoscale flow behavior of BCC materials. Here we will report on the deformation behavior of BCC single crystals Ta (100), (111) and (110) studied by a combination of nanoindentation and atomic force microscopy. Nanoindentation at temperatures ranging from $25 - 200^{\circ}$ C was used to study the plastic flow behavior of Ta. For all three crystal orientations the onset of plasticity is marked by a discontinuity in the load displacement curve, which is most pronounced on the (100) surface. We will discuss the origin of the "pop-in" event, as well as the atomistic mechanism of the deformation process during nanoindentation. Most notably, we find that the shape of the load displacement curves changes with increasing temperature and multiple pop-ins separated by elastic reloading segments were observed at 200° C.

9:10 AM

The Effect of Point Defects on the Nucleation Plasticity in Small Volumes: *David Bahr*¹; Veronica Perez¹; Iman Salehinia¹; Marc Weber¹; ¹Washington State University

In small structures, the chances that relatively defect free volumes control the mechanical performance of materials increases. Nanoindentation has been used to measure the onset of plasticity in Ni single crystals with differing point defect (vacancy and hydrogen impurities) concentrations. The effect of increased vacancy concentration is to statistically lower the yield point, similar to the effects of increasing sampled volume by changing the probe tip radius. Hydrogen also appears to slightly lower the yield point in these materials. These results are compared to EAM simulations which



9:30 AM

Length Scale Effect on the Mechanical Properties of Irradiated Metals: *Khalid Hattar*¹; Thomas Buchheit¹; Brad Boyce¹; Luke Brewer²; ¹Sandia National Laboratories; ²Naval Postgraduate School

Length scale effect on mechanical properties is important in the development of a validation technique to simulate end of life irradiation damage in metals relevant to nuclear reactors. This technique utilizes heavy-ion irradiation to generate extensive damage, but is limited in volume. Nanoindentation and micropillar compression is implemented to elucidate the change in properties as a function of irradiated microstructure produced. The nanoindentation work investigates the geometric effect through the comparison of pyramidal and spherical indentations. Finite element modeling of various tip geometries and implantation conditions provides assistance in distinguishing between a perceived increased hardness of the irradiated region and the classic indentation size effect. The effect of length scale testing is also observed in the mechanical response of irradiated micropillars. Both measurements are susceptible to geometrically driven size effects and methods to distinguish between geometrical influences and radiation damage on will be discussed.

9:50 AM

Plastic Flattening of a Sinusoidal Surface: Fengwei Sun¹; Erik Van der Giessen²; *Lucia Nicola*¹; ¹Delft University of Technology; ²University of Groningen

When two rough surfaces are pressed into contact, plastic deformation occurs at rather small loads. During further loading, the forces between contacting asperities, as well as the true contact area, evolve in a non trivial way. This evolution is not properly calculated by the current statistical contact models, like Persson's and Mueser's, since in those models the plastic behavior of the asperities is neglected. Other studies focus instead on an accurate description of the material behavior, but are limited to a single deforming contact. The aim of this work is to extend those studies to a collection of asperities. The numerical technique used is discrete dislocation plasticity, which has proven successful to capture size dependent plastic behavior of isolated contacts, as well as arrays of flat contacts. The description of the surface is kept simple; the roughness is represented by a sinusoidal wave of varying amplitude and period.

10:10 AM Break

10:40 AM Invited

Statistical Effects in Nanoindentation and Nanopillar Compression: James Morris¹; Hongbin Bei¹; Easo George¹; ¹Oak Ridge National Laboratory

Experimental probes such as nanoindentation, or nanopillar compression, only stress a small volume. When this highly stressed region is comparable to the density of defects, the number and arrangement of defects in the region is highly variable, and the response of the material is similarly stochastic. Simple statistical models are formulated to describe these distributions of behavior. In the case of nanoindentation, close agreement between the model and experiment is shown using only the defect density and a single defect strength. Scaling behavior of the results is observed, breaking down when pop-in is primarily determined by the theoretical strength of the material. For nanopillar deformation, the distribution of defect strengths becomes important. Thus, experiments on different geometries may provide complementary information on both defect densities and defect strength distribution. This research was sponsored by the Division of Materials Sciences and Engineering, U.S. Department of Energy, Office of Basic Energy Sciences.

11:10 AM

Size Effects in Yield Instabilities: *William Gerberich*¹; ¹University of Minnesota

Plastic instability in indentation has been studied via decades of research. Load control produces displacement excursions, and displacement control produces load drops. The magnitude of the plastic instability, e.g. the displacement jump to arrest, depends on the driving force when indenting single crystals. But does it also depend on the indenter tip shape or contact radius? Similarly, the magnitude of the plastic instability occurring in the compression of nanopillars also depends on the driving force. But does this also depend on size through the pillar diameter? The role of back stress, if any, is explored to demonstrate differences and similarities between indentation and pillar compression. Size effects aware demonstrate in FCC, BCC, and HCP systems. Generally, increasing size of indentation contact diameters or compressed pillar diameters produce increased instabilities. Caveats associated with the stochastic nature of nucleation sites are emphasized as well.

11:30 AM

140th Annual Meeting & Exhibition

Time-Dependent Plasticity in the Small-Scale: Influence of Initial Strain: Byung-Gil Yoo¹; In-Chul Choi¹; Kyu-Sik Kim¹; Jun-Hak Oh¹; Yong-Jae Kim¹; *Jae-il Jang*¹; ¹Hanyang University

Recently, many nanomechanical studies have reported that the mechanical responses of materials can be significantly dependent on both the size and time of deformation. One more interesting finding is that in some materials, e.g. nanocrystalline materials and amorphous alloys, the time-dependent deformation (often simply referred to as "creep") can occur even at room temperature. Analyzing the creep in the small-scale can be valuable not only for solving scientific curiosity, but also for obtaining practical engineering information, e.g. life-time and reliability of BMG-based MEMS. In this talk we would like to report our recent observations that the initial strain at the onset of creep does seriously affect the small-scale time-dependent deformation in a somewhat interesting way.

Surfaces and Heterostructures at Nano- or Micro-Scale and Their Characterization, Properties, and Applications: Energy and Catalysis Technologies II - and - Biological Applications

Sponsored by: TMS Electronic, Magnetic, and Photonic Materials Division, TMS Materials Processing and Manufacturing Division, TMS: Nanomaterials Committee, TMS: Surface Engineering Committee

Program Organizers: Nitin Chopra, The University of Alabama; Ramana Reddy, The University of Alabama; Jiyoung Kim, Univ of Texas; Arvind Agarwal, Florida International Univ; Sandip Harimkar, Oklahoma State University

Wednesday AM	Room: 31B
March 2, 2011	Location: San Diego Conv. Ctr

Session Chairs: Ramana Reddy, The University of Alabama; Arvind Agarwal, Florida International University; Nitin Chopra, The University of Alabama

8:30 AM

Silicon-Coated Carbon Nanotube Anodes for Lithium-Ion Batteries: *Michelle Gaines*¹; Samuel Karpowicz¹; Deborah Williams²; ¹Georgia Institute of Technology; ²DM Therrell School for Technology, Engineering, Math, and Science

Current rechargeable lithium-ion batteries contain graphite anodes. Although adequate for powering small, portable electronics, graphite anodes don't possess enough storage capacity to power larger devices. Silicon has a much higher storage capacity, providing the potential for much more energy storage during charging. The only challenge with using silicon lies in its resulting pulverized structure after repeated charge/discharge cycles. In this work, multi-walled carbon nanotubes (MWCNT) were used as mechanical reinforcements for amorphous silicon. MWCNT were grown using thermal CVD on copper foil. Two catalyst systems were compared: 1) Iron(III) p-toluenesulfunate, reduced to form iron nanoparticles on the surface and 2) metal tri- and bi- diffusion layers with an iron coating on top. Amorphous silicon was deposited on top of the carbon nanotubes using plasma enhanced chemical vapor deposition. Full and half cells were constructed from commercially available cathodes, and electrical impedance and galvanic cycling were performed.

8:45 AM

Fundamental Studies on Morphological Evolution of Multi-Functional Carbon Nanotubes-Nickel/Nickel Oxide Core/Shell Nanoparticle Heterostructures: Wenwu Shi¹; Anshuman Bansal²; *Nitin Chopra*¹; ¹The University of Alabama; ²Alabama School of Fine Arts

A simple and facile method was utilized to fabricate carbon nanotubesnickel/nickel oxide core-shell nanoparticles (CNC) heterostructures. Nickel nanoparticles from thermal decomposition of nickel salt were nucleated on well-dispersed carbon nanotubes to form heterostructures. Various chemical synthesis parameters, post-fabrication processing, and carbon nanotube surface chemistries were studied to manipulate nanoparticle coverage density, size, shape, oxide shell thickness, and magnetic properties. Alignment of these heterostructures on a large area substrate was also achieved. Such a patterning of heterostructures is of great importance for magnetic devices, supercapacitors, and 3-D nanoarchitectures.

9:00 AM Break

9:10 AM Introductory Comments for Biological Applications

9:15 AM Invited

Cytokine Nanotechnology: *Venkat Sharma*¹; ¹University of West Alabama Therapeutic usage of cytokines has been widely established in the medical field. Cytokines are a group of proteins that elicit their biological effects similar to hormones and serve as intercellular messenger molecules of the immune system. Therefore, cytokines and their receptors are increasingly considered as therapeutic drug targets. Although usage of cytokines is theoretically ideal, an obstacle in the way of treatment is due to its characteristics; therefore, actual treatment with cytokines needs more improvement over its delivery system and prolongation of cytokine life span. Combination of cytokine to nanotechnology techniques might accomplish what would otherwise be impossible in drug delivery. By manipulating nanoparticle surface characteristics, it is theorized that cytokines can efficiently be delivered to the target place. In this presentation, I will survey the variety of applications of formulating therapeutic agents with nanotechnology and further provide a survey of the actual effect of nanoparticles on cytokine secretion.

9:45 AM Invited

Surface Modification of Microneedles for Antimicrobial Activity: *Roger Narayan*¹; Shaun Gittard¹; Boris Chichkov²; Aleksandr Ovsianikov²; Shane Stafslien³; Bret Chisholm³; ¹University of North Carolina & North Carolina State University; ²Laser Zentrum Hannover; ³North Dakota State University

Microneedles with antimicrobial properties may be prepared by coating microneedles with materials that exhibit antimicrobial activity. Silver exhibits broad-spectrum activity against bacteria; this activity is attributed to disruption of electron transport, as well as interruption of deoxyribonucleic acid replication. In this study, silver thin films were deposited on the surfaces of polymer microneedles at room temperature using pulsed laser deposition. We fabricated silver-coated microneedles using a two-step process, which involved two photon polymerization-micromolding and pulsed laser deposition. In the first step, solid microneedle arrays were prepared using organically-modified ceramic material by means of two photon polymerization-micromolding. In the second step, pulsed laser deposition was used to deposit silver thin films on these microneedle arrays. An absence of S. aureus growth was noted beneath the silver-coated microneedle array. In addition, inhibited growth was observed in the region surrounding the microneedle array, which suggested that silver was released into the agar.

10:15 AM Invited

Functionalized Quantum Dots for Molecular Profiling of Cancer Biomarkers: Peter Searson¹; ¹Johns Hopkins University

Quantum dots have received considerable attention for applications in biomedicine, particularly in imaging and sensing. In contrast, cellular targeting using quantum dots has remained challenging. Quantum dots exhibit high quantum yield, narrow emission peak, broad excitation range, and are resistant to photobleaching. We report on different surface modification schemes and show how surface modification is key to producing stable suspensions of quantum dots in water. We show results for profiling of cancer biomarkers using quantum dots conjugated with targeting antibodies.

10:45 AM Invited

Autonomous Nano/Microscale Motion through Catalysis: Ayusman Sen¹; ¹Pennsylvania State University

Self-powered nano and microscale moving systems are currently the subject of intense interest due in part to their potential applications in nanomachinery, nanoscale assembly, robotics, fluidics, and chemical/biochemical sensing. We will demonstrate that one can build nanomotors that mimic biological motors by using catalytic reactions to create forces based on chemical gradients. These motors are autonomous in that they do not require external fields as energy sources. Instead, the input energy is supplied locally and chemically. By appropriate design, the chemical gradients can be translated into anisotropic body and/or surface forces. Depending on the shape of the object and the placement of the catalyst, different kinds of motion can be achieved. The resulting nanomotors can be tethered or coupled to other objects to act as the "engines" of nanoscale assemblies. It is also possible to control the movement of nanomotors by: (a) chemotaxis, (b) phototaxis, and (c) magnetic steering.

11:15 AM

Precipitation and Crystallization of Hydroxyapatite on Boron Nitride Nanotubes Immersed in Simulated Body Fluid: *Debrupa Lahiri*¹; Virendra Singh²; Anup Keshri¹; Sudipta Seal²; Arvind Agarwal¹; ¹Florida International University; ²University of Central Florida

Success of Boron Nitride Nanotubes (BNNT) as reinforcement in orthopedic implant/scaffold or structural mimic of collagen in bone repair depends on mineralization and integration of hydroxyapatite (HA) on BNNT surface to form an integrated bone-like structure. Present study investigates precipitation and crystallization-ability of HA on BNNT, immersed in simulated body fluid (SBF) for 7, 14 and 28 days. Presence of phosphate peak of HA in Raman Spectrum proves the formation of HA precipitate on BNNTs immersed in SBF. The SEM and EDS results reveal linear increase in calcium content on BNNT between 7 -28 days. The quantitative EDS results suggest an initial threshold period for starting the precipitation. HRTEM study shows amorphous HA covering the BNNT surface initially (7 days), which forms well defined crystal structure with increasing time (28 days). Analysis of lattice images at interface provides further insight into the crystallographic arrangement of HA crystals on BNNT surface.

11:35 AM

Synthesis of Magnetic and Fluorescent Bifunctional Nanoparticles: Yaolin Xu¹; Soubantika Palchoudhury¹; *Yuping Bao*¹; ¹The University of Alabama

Magnetic nanoparticles (MNP) have significantly advanced cancer treatments through targeted drug delivery and localized therapy. MNPs further make simultaneous therapy and diagnosis possible as magnetic resonant imaging (MRI) contrast agents. Unfortunately, the studies of simultaneous therapy and diagnosis of MNPs are limited by the expensive MRI equipment. Currently, fluorescence imaging remains the primary choice for bio-imaging because of its high sensitivity. Here, we reported magneticfluorescent integrated nanoparticles using iron oxide as the magnetic component and metallic nanoclusters as the fluorescent component. Iron oxide nanoparticles were synthesized using a modified co-precipitation method by introducing a capping molecule during synthesis. Subsequently, these iron oxide nanoparticles were used as seeds for the synthesis of Ag metallic nanoclusters. Around 10 nm iron oxide nanoparticles were successfully produced, followed by attachment of fluorescent clusters with a broad emission in the range of 600 -650 nm. This work is funded by NSF-DMR 0907204



11:50 AM

Synthesis of Multiple Platinum Attached Iron Oxide Nanoparticles: Soubantika Palchoudhury¹; Yaolin Xu¹; Yuping Bao¹; ¹The University of Alabama

We report the synthesis and detailed structural analysis of multiple Pt attached iron oxide nanoparticles (NPs). Two different routes were carried out to obtain water soluble, Pt attached iron oxide NPs. First, Pt NPs were attached onto iron oxide NP surfaces in organic solvent followed by a phase transfer process; second, a surfactant exchange process was performed first, prior to the deposition of Pt NPs. The presence of Pt NPs is evident based on the contrast in the transmission electron microscopy images. High-angle annular dark field (HAADF) and energy dispersive x-ray (EDX) analysis were further performed to confirm the presence of Pt.

12:05 PM

Colloid-Chemical Nanoprocesses and Nanotechnologies on the Basis of Oxyhydrate Systems of Rare-Earth Elements: *Tatiana Prolubnikova*¹; Yuri Sucharev¹; Tatiana Ukolkina¹; Konstantin Nosov¹; ¹Chelyabinsk State University

Research of oxyhydrate gel systems of rare-earth elements showed that the processes of structure formation are nonlinear dynamic processes. Oxyhydrates have emission-wave duality behavior. Due to this fact, you can discover and understand colloid-chemical phenomena occurring in the gels. It was researched pulsating spontaneous splashes of oxyhydrate gel's nanocurrent. It was proved antimicrobial activity of these currents in a wide range of microorganisms. The reason for current ripple is self-organization gel over time. Research of rheological properties of oxyhydrates from the position Nonlinear Dynamics discovered anomaly viscosity and the possibility of establishing nanomicroscopy for monitoring structural changes during ageing. We have a digital phase molecular microscope to examine colloid chemical state of oxyhydrate systems based on stochastic coherent resonance. Nanodimension of colloid oxyhydrate structures proved studies of their optical density. Consecutive kinetic experiments give maximum size of nanocluster, which are registered in the system at different wavelengths.

12:20 PM Concluding Comments

2011 Functional and Structural Nanomaterials: Fabrication, Properties, Applications and Implications: Characterizations of Nanomaterials and Session in Honor of Prof. T. Kang

Sponsored by: The Minerals, Metals and Materials Society, TMS Electronic, Magnetic, and Photonic Materials Division, TMS: Nanomaterials Committee

Program Organizers: Jiyoung Kim, Univ of Texas; David Stollberg, Georgia Tech Research Institute; Seong Jin Koh, University of Texas at Arlington; Nitin Chopra, The University of Alabama; Suveen Mathaudhu, U.S. Army Research Office

Wednesday PM	Room: 8
March 2, 2011	Location: San Diego Conv. Ctr

Session Chairs: Jiyoung Kim, University of Texas at Dallas; Seung Kang, Qualcomm

2:00 PM Introductory Comments

2:05 PM Invited

Tailored Fabrication and Characterization of Nanostructures: *Moon Kim*¹; ¹University of Texas at Dallas

As the scaling of silicon integrated circuits continues, the future of electronics will rely on both top-down and bottom-up approaches. In addressing both of these approaches, nanoscale fabrication, manipulation, and characterization become ever more important. The electron beam lithography approach for nanowire fabrication provides a top-down method that allows us to control their orientation and size. In the same manner, future

nanowires can be fabricated from different materials such as Ge and GaAs. This will allow us to explore these materials' properties when scaled down to the quantum regime. This talk will present our recent research efforts on several key electronic material systems of current and future interests including lithographically defined Si nanowires and nanodots and insitu manipulation and characterization of graphene sheets and functional nanostructured devices. Single CMOS and HEMT transistors were also characterized by in-situ TEM with nanometer scale spatial resolution.

2:35 PM

Scanning Tunneling Microscopic Characterization of Electron Transport in Pi-Conjugated Organic Self-Assembled Monolayer: *Govind Mallick*¹; Shashi Karna¹; ¹Army Research Laboratory

Surface topology and electron transport properties of self-assembled monolayer (SAM) of an engineered molecule 4,4'-[1,4-phenylenebis(me thylidynenitrilo)]bisbenzenethiol (PMNBT), 1-dodecanethiol (dDT) and 1-hexadecanethiol (hDT) adsorbed on Au substrates have been investigated by scanning tunneling microscopy (STM) under ambient condition. The estimated differential conductance, (dI/dV)v=0.75 = 123.91nS for PMNBT, is over an order of magnitude larger than the corresponding value (7.15nS) for dDT and two order of magnitude larger (0.078nS) than hDT. The tunneling current (I) as a function of the applied bias (V) between STM tip and SAM of PMNBT exhibits asymmetric behavior. A combination of electronic and geometrical effects in the molecule and at the molecule-metal interface is proposed to be responsible for the observed asymmetric I-V characteristics. The increased conductance in PMNBT is also explained in terms of its nearest available electronic states.

2:50 PM

Tunneling Spectroscopy with Near Zero Line-Width Broadening: Ramkumar Subramanian¹; *Pradeep Bhadrachalam*¹; Taejoo Park²; Jiyoung Kim²; Seong Jin Koh¹; ¹University of Texas at Arlington; ²University of Texas at Dallas

For practical application of nanoparticles/quantum dots in the field of energy harvesting, bio-labeling and treatment, in opto-electronic devices and in photonic crystals it is imperative to know their electronic structure. Currently available tunneling spectroscopic techniques, however, are accompanied by a large linewidth broadening, typically ~100meV even at cryogenic temperatures(~5K). We present a novel tunneling spectroscopy technique in which electronic structure of individual quantum dots can be directly measured with extremely small linewidth broadening even at room temperature. The spectroscopic measurement units are composed of doublebarrier tunneling junctions and were fabricated using CMOS-compatible processes. Using the lock-in technique, direct differential conductance measurements were carried out to obtain the electronic structure of 6nm and 7nm CdSe quantum dots. The spectroscopic measurements were done at 77K, 150K, 225K and room temperature. Clear peaks were observed even at room temperature with a linewidth(FWHM) of ~20meV. At 77K, the FWHM linewidth was only ~3meV.

3:05 PM

Sub-Nanometer Resolution 3D Mapping of Isotopically Modulated Si Multilayers by Atom-Probe Tomography: *Oussama Moutanabbir*¹; Dieter Isheim²; Yoko Kawamura³; Kohei Itoh³; David Seidman²; ¹Max Planck institute of Microstructure Physics; ²Department of Materials Science and Engineering, Northwestern University; ³School of Fundamental Science and Technology, Keio University

The introduction of enriched and stable semiconductor isotopes as an additional degree of complexity in nanofabrication processes provides a wealth of opportunities in the manipulation of the properties of the emerging nanomaterials. In spite of the crucial information it could provide, there are only a few theoretical studies on the influence of the isotopic content on the physical properties of nanoscale systems. Tackling this promising area requires characterization techniques that are sensitive to one of the isotopic effects besides having the spatial resolution needed to probe nanoscale structures. In this work, we demonstrate that UV-laser assisted local-electrode atom-probe tomography is an unique instrument capable of

achieving an atomic resolution and having a detectability of <10 atomic ppm for each isotope. As a model system, we used isotopically modulated Si layers of 28Si and 30Si isotopes having a thickness below 10 nm. 3D atomby-atom isotopic maps with sharp interfaces are achieved.

3:20 PM

Electronic Structure of Bimetallic Nanowires and Implications for Catalytic Activity: Regina Ragan¹; ¹University of California, Irvine

Self-organization of atomic ensembles on surfaces using atomic structure on nanowire templates is used to fabricate metal nanoassemblies having feature size and atomically controlled interfaces that are typically unattainable using lithographic technique. Core-shell nanowires consisting of an outer layer of Au coating a rare earth disilicide nanowire have unique electronic structure that is very promising for various applications such as nanocatalysis. Using synergistic first principles and scanning probe techniques, we have characterized atomic and electronic properties of Au-disilicide core-shell nanowires on Si(100) substrates. Calculations of electronic structure predict that electrons deplete from Au adatoms on disilicide nanowire surfaces; Scanning Kelvin probe force microscopy measures a reduced work function for Au on disilicide nanowires in agreement with electron depletion on the surface. The chemical properties of Au-disilicide anostructures will also be discussed in terms of charge density, density of states and adsorption energy of CO molecules.

3:35 PM Break

3:50 PM Introductory Comments

3:55 PM Invited

Nano-Scale Multilayer Mask for EUV Lithography Applications and Its Extendability: *Jinho Ahn*¹; Tak Kang²; ¹Hanyang University; ²Seoul National University

Extreme ultra violet lithography (EUVL) using 13.5nm wavelength is an extreme technology in the point of optical material preparation, which consists of nano-scale multilayer structure for EUV Bragg reflection. This is expected to be the most promising patterning process for 22nm half pitch and below. To extend the patterning capability below 16nm, a phase shift concept might be required to improve the image contrast with a thinner absorber stack. However, there are many fabricating issues to be solved before it can be applied to manufacturing. In this paper, we suggest an optimal attenuated phase shift mask (PSM) structure. The changes of phase shift and reflectivity depending on the structure were studied using aerial image simulation. In addition, the lithographic performances of manufactured attenuated PSM were investigated using coherent scattering microscopy (CSM).

4:25 PM Invited

Aminosilane Monolayer-Assisted Patterning of Conductive Poly(3,4-Ethylenedioxythiophene) PEDOT Source/Drain Electrodes for Bottom Contact Pentacene Thin Film Transistors, and the Effects of the Surface Morphology of PEDOT on the Electrical Performance: Kyunghoon Jeong¹; Hyunjung Shin¹; Jaegab Lee²; ¹Kookmin University; ²Center for Materials and Processes of Self-Assembly

Organic thin film transistors (OTFTs) with conducting poly(3,4ethylenedioxythiophene)(PEDOT) electrodes have been fabricated using a bottom-up process consisting of the selective growth of PEDOT on a prepatterned (3-aminopropyl)trimethoxysilane (APS) monolayer. The newly developed bottom-up process produced strongly adherent, selectively and uniformly patterned PEDOT films on oxidized substrates. In addition, the PEDOT/APS double structure showed an approximately one order of magnitude lower leakage current and contact resistance than the Au/ Ti electrodes. Furthermore, smooth PEDOT films produced well-oriented pentacene islands while rough PEDOT films randomly oriented islands. In addition, PEDOT electrodes provided morphological continuity at the electrode-channel interface, making the accumulation channel of the pentacene formed on the electrodes a main contributor to the contact resistance. As a result, the smooth PEDOT surface yielded the low contact resistance, approximately half of that obtained with the rough surface.

4:55 PM

Electrochemical Characterization of CdSe and CdTe Electrodeposits: *Jae-Ho Lee*¹; Ju-Young Lee¹; ¹Hongik University

The electrodeposition in acidic aqueous electrolyte bath of cadmium selenide and cadmium telluride on gold electrodes has been studied by electrochemical analysis. Conventional cyclic voltammetry using potentiostat is considered as a reliable method to study electrochemical behavior of electrodeposition of CdSe and CdTe. The mechanism of CdSe and CdTe deposition and its cyclic voltammetry were studied in the Se and Te ion concentration, temperature, potential, scan rate and also we investigated changing surface morphology and atomic composition of Se and Te by EDS(energy dispersive spectroscopy) were varied with Se and Te ion in electrolyte. Check surface morphology by FeSEM. Structure information about those materials was obtained by X-ray diffraction

5:10 PM

Electrochemical Migration of Cu on Printed Circuit Board; Mechanism and Sn Surface Finish Effect: *Young-Chang Joo*¹; Min-Suk Jung¹; Shin-Bok Lee¹; Ho-Young Lee¹; Tak Kang¹; ¹Seoul National University

Electrochemical migration (ECM) phenomenon, defined as the formation of conducting filaments under an applied voltage, high temperature and humidity, leads to short-circuit failure of electronic devices. To secure the disadvantages of Cu, which is the most widely used for metal electrode, Sn coating was introduced because Sn has stronger corrosion resistance compared to Cu and forms inter-metallic compounds (IMCs). Results revealed that time to failure (TTF) increased dramatically in the sample with Sn coating and 160 nm-thick Sn coating was more effective than 90 nmthick coating in terms of increasing the TTF from water drop test (WDT). By anodic polarization test, it was found that IMCs, formed between Sn and Cu layers, enhanced the corrosion resistance with passivity behavior. By introducing WDT and anodic polarization test, it was understood that dissolution step controlled entire ECM process corresponding to the rate determining step in ECM.

5:25 PM

Biosensor Applications of Functionalized Singular TiO2 Nanotubes: *Mingun Lee*¹; Jie Huang¹; Moon Kim¹; Hyunjung Shin²; Jiyoung Kim¹; ¹University of Texas at Dallas; ²Kookmin University

Nanotubular structures are highly regarded in biological sensor applications for the high detection sensitivity stemming from their inherently high surface area per volume. Most notably, TiO2 nanotubes have an added benefit of nontoxicity, making them an invaluable candidate. In this study, we have evaluated TiO2 nanotube functionalization for specific chemical detection. To accommodate selectivity for streptavidin, the surface was treated with biotin; selective binding between the two chemicals ensures excellent results. Precise control over the nanotube wall thickness is critical in fine-tuning performance parameters of the resulting biosensor, hence ALD was employed in nanotube fabrication. Finally, singular nanotubes rather than nanotube bundles were selected for study, as the former has a brighter prospect in miniaturization and multichannel device application. This research was supported by a grant (code #:2010K000351) from 'Center for Nanostructured Materials Technology' under '21st Century Frontier R&D Programs' of the Ministry of Education, Science and Technology, Korea.

5:40 PM Concluding Comments

2nd International Symposium on High-Temperature Metallurgical Processing: Raw Materials Processing

Sponsored by: The Minerals, Metals and Materials Society, TMS Extraction and Processing Division, TMS: Pyrometallurgy Committee, TMS: Energy Committee *Program Organizers:* Jiann-Yang Hwang, Michigan Technological University; Jerome Downey, Montana Tech; Jaroslaw Drelich,

Michigan Technological University; Tao Jiang, Central South University; Mark Cooksey, CSIRO

Wednesday PM	Room: 18
March 2, 2011	Location: San Diego Conv. Ctr

Session Chairs: Ismail Duman, Istanbul Technical University; Wei Li, Kunming University of Science and Technology

2:00 PM

An Innovative Process on Beneficiation of Superfine Low Grade Hematite Ore: *Deqing Zhu*¹; Yongzhong Xiao¹; Tiejun Chun¹; Jian Pan¹; ¹Central South University

In this paper, an innovative process of reverse floatation-direct reductionlow intensity magnetic separation was developed to effectively beneficiate the superfine run-of-mine (ROM) ore mined from Hunan Province, China. Mineralogy was measured that the ROM ore is of superfine low grade hematite ore type, assaying 27.23%Fetotal and with main valuable minerals of hematite occurring at size between 3~5µm. The upgrading results show that the final iron concentrate, assaying 88.31%Fe total and 94.45% metallization degree was obtained at an overall iron recovery of 69.92% under the following conditions: rough concentration by grinding of ROM up to 88.72% passing 0.074mm and reverse flotation at pH=9.4, 100g/t starch and 200g/t dodecylamine(DDA), and coal reducing the rough concentrate pellets containing 12% calcium containing complex additive at 1200° for 120min and 2.5 coal-to-pellet mass ratio, and finally magnetic separation of the reduced pellets by grinding up to 89.20% passing 0.043mm at 0.08T field intensity.

2:20 PM

Calcination Behavior of Sivrihisar Laterite Ores of Turkey: Ender Keskinkilic¹; Saeid Pournaderi²; Ahmet Geveci²; Yavuz A. Topkaya²; ¹Atilim University; ²Middle East Technical University

This study investigated calcination behavior of one of the Turkish laterite deposits, which was recently found in Sivrihisar region. Representative limonitic laterite samples (1.26% Ni) taken from Yunusemre Karasivritepe and Kucuksivritepe location were first subjected to drying. Removal of chemically bound water and other volatiles were then studied, in detail. In the calcination experiments, temperature and time were the main experimental variables. Thermal treatment was conducted at the specific temperatures in 250°C - 800°C range. The weight losses due to elimination of chemically bound water and other volatiles were reported to be approximately 10 per cent of the weight of the ore. For the particle size used in the current work, 700°C and 40 minutes were determined to be the optimum calcination temperature and time, respectively.

2:40 PM

Function of High Pressure Roll Grinding in Producing Magnetite Oxidized Pellets: Yu-feng Guo¹; Hai-zheng Hao¹; Tao Jiang¹; Jan-jun Fan¹; ¹Central south University

Function of High Pressure Roll Grinding(HPRG) was systematically studied in producing oxidized pellets by using magnetite concentrate as raw material, with results that the bentonite dosage was massively reduced, when specific surface area of magnetite concentrate pretreated by HPRG was controlled at 2553.41 cm2.g-1 approximately, the bentonite dosage was decreased to 0.8% compared with 1.3% without pretreating. The green ball quality was also obviously improved, due to the marked increase of specific surface area and fine particles content of pretreated material ,as well as the

improvement of granulometric distribution and the static pelletizability index of pelletfeed. With decrease of pellte porosity and increase of pellet compactness, the primary solid phase reaction and oxidation reaction were accelerated, which made the pellets surface form compaction layer which handicappes the diffusion and migration of oxigyen, promoting the double layer structure of pellet forming, consequently, the compression of preheated and roasted pellets was not markedly improved by HPRG.

3:00 PM

140th Annual Meeting & Exhibition

Magnetic and Floatability Behaviors of Nonstoichiometric Pyrrhotites: Vladimir Luganov¹; Shinibai Baiysbekov¹; *Tatyana Chepushtanova*¹; Viktor Ermolayev¹; ¹The K.I. Satpayev Kazakh National Technical University

Using Faraday method of magnetic scale, it was found that magnetic pyrrhotites are formed in the result of roasting. When temperature increasing up to 220°C, magnetic permeability of pyrrhotites Fe0,855S, Fe0,888S, Fe0,909S dramatically increases, then falls to zero at temperatures of 310-320°C. At temperatures above Curie point (till 570°C) an abrupt drop of magnetic permeability had been observed, followed by consistent increases in magnetic permeability until reaching its peak at Fe0,855S = 3,75; Fe0,888S = 5,43; Fe0,909S = 2,18 point CI at 700-800°C. Curie temperature depends on pyrrhotites composition. Temperature hysteresis of magnetic properties has been observed within the temperature interval of up to 240°C. Results of investigations show that electro kinetic potentials of the pyrrhotites increases with pH rising within the interval 5-13, and decreases with reduction of sulfur content from 52,1 mV for pyrrhotite Fe0,85S till ~ 40,8 mV for pyrrhotites Fe0,89S.

3:20 PM

Improving the Pelletization of Fluxed Hematite Pellets by Hydrated Lime: *Deqing Zhu*¹; Wei Yu¹; Tiejun Chun¹; Jian Pan¹; ¹Central South University

In this paper, the technology of producing fluxed pellets by using hydrated lime as binder instead of bentonite was carried out. The results show that the drop numbers of 4.8 to 5.0 times/0.5m, compressive strength of 19.7 to 24.2 Newton per pellet and thermal shock temperature of 280 to 385°C for green balls with 0.8% bentonite and green balls containing 2% hydrated lime were obtained under the same conditions of 8.5% moisture, 1.45 basicity and balling for 10min in disc pelletizer. Comparing with bentonite as binder, the compressive strength of fired pellets with hydrated lime is elevated by 13.82% and climbs up to 3113 Newton per pellet under the following conditions: preheating at 1050°C for 15min and firing at 1300°C for 15min. The hydrated lime also improves the metallurgical performance of fired pellets, the reduction index being enhanced from 68.55% to 70.58%, RDI+3.15 increased from 90.12% to 98.79% and reduction swelling index dropped from 22.35% to 7.39%, respectively.

3:40 PM

Microwave Assisted Breakage of Metallic Sulfide Bearing Ore: Matthew Andriese¹; ¹Michigan Technological University

An mafic ore body contains high concentrations of nickel and copper chiefly occurring in the minerals pyrrhotite, chalcopyrite, and pentlandite. Refractory ore bodies are difficult to treat by conventional mineral processing methods thus it is of interest to find other processing methods that increase metallic-particle/host rock liberation. One such proposed method to improve particle liberation is microwave-pretreatment of the ore. Differential heating properties of the constituent mineral phases produce cracks in ore particles by tension. Preliminary experiments have shown the ore particles heat rapidly when exposed to 1000W microwave power for short durations of time (30, 60, 90s). SEM imaging shows fracture occurring along grain boundaries and throughout host rock matrix. Preliminary ball milling experiments show promising results for increased grindability of the ore. Further work would be to investigate the effect microwave treatment has on the work index and washability of the ore after the grinding stage.

4:00 PM Break

4:10 PM

Research on the Ball Milling and Followed by Microwave Reduction of Panzhihua Low Grade Ilmenite Concentrate: Ying Lei¹; Yu Li¹; *Jinhui Peng*¹; Libo Zhang¹; Shenghui Guo¹; Wei Li¹; ¹Key Laboratory of Unconventional Metallurgy, Ministry of Education

In this work, the Panzhihua low grade ilmenite and graphite were milled for 1, 2, 4 and 8 h firstly, then the temperature rising behavior of milled sample in microwave field were studied. The average heating rate of samples milled for 1, 2, 4, 8 h were 1.86, 4.08, 2.82, and 2.32 K/s; Before optimize the microwave reduction process, several experiments were conducted in order to confirm the parameters range. After milled for 4 or 8 h and reduced above 930°, the Fe metallization are higher than 90%; Then the optimization was investigated by using response surface methodology (RSM), the significance of predict model and each terms were analyzed, and the optimization parameters were given as: milling time is 4 h; reduction temperature is 1001 or 1070° ; the holding time is 37.5 or 26.9 min. Under these conditions, the Fe metallization given by predict model is 91 or 92 %.

4:30 PM

Research on the Recovery of Vanadium from Low-Grade Vanadium Slag by the Calcium Roasting Process: Xiaojun Li¹; ¹Chongqing University

The recovery of vanadium from low-grade vanadium slag (V2O3 8%) by means of calcium roasting and acid leaching was investigated. XRD analysis shown that there are three different of calcium vanadate formed during roasting process. The acid leaching of the roasted slag indicated that the content of CaO in roasted slag plays an important role in the roasting process, vanadium extraction ratio was increased from 55.3% to 69.2% when CaO/V2O3 increased from 0.5 to 1.125, but the ratio would be decreased when CaO/V2O3 exceed 1.125. When the roasting temperature was increased from 750° to 825°, vanadium extraction ratio would be increased from 56.3% to 69.7%. However, the slag would be sintered when the roasting temperature is higher than 825°, which would lead to the decrease of vanadium extraction ratio.

4:50 PM

Study of Strengthen Pelletization of Nickel Laterite: *Jian Pan*¹; Xian Zhou¹; De Zhu¹; Guo Zheng¹; ¹Central South University

In ferronickel production, it is one economical and efficient technology that the nickel oxide and part of the iron oxide are reduced to metal by agglomeration and smelting in blast furnace. Due to the physical and chemical properties of the laterite ores, a large fraction of fines is generated during the pre-treatment stages and the strength of agglomeration is weakened, which results in low productivity and bad quality. In this paper, the process of pelletization of nickel laterite was developed firstly, and some parameters to strengthen the pelletization of nickel laterite has been optimized. The result showed that the compressive strength of fired nickel laterite pellet can reach over 2000 Newton per pellet while firing at the temperature of 1220° ~ 1250° and induration for 12min under the optimization conditions, and the product pellet can be used as high-quality burden for blast furnace to manufacture ferronickel.

5:10 PM

Waste to Wealth: Production of Fe-Ni from Lateritic Ore/ Chromite over Burden of Sukinda Deposite in Orissa, India: *Bhagyadhar Bhoi*¹; Chitta Mishra²; Hara Mishra³; ¹Institute of Minerals and Materials Technology; ²Natinal Aluminium Company Ltd.; ³Industrial Promotion and Investment Corporation of Orissa Ltd.(IPICOL)

In the Sukinda Valley of Orissa, India, the total quantity of nickel ore reserves comprising of both lateritic and overburden have been estimated at around 231 million tonnes containg 0.3 to 0.9 % Ni. While mining of one tonne of Chromite ore, around 6-7 tonnes of chromite over burden are removed. These overburden materials are disposed off as waste materials causing lot of environmental hazards and ecological imbalance. India imports a large amount of nickel and ferro-nickel to meet its growing demands in various sectors. For import substitution, efforts have been made to produce

ferro nickel from the lean deposits of nickel bearing lateritic ores / chromite overburden materials by reduction roasting followed by magnetic separation and then the nickel rich magnetic fraction is smelted to produce ferro-nickel. It has been possible to produce ferro-nickel of grade varying from 4-25% nickel.

5:30 PM

Mineralization Behavior of Fluxes during Iron Ore Sintering: Min Gan¹; *Xiaohui Fan*¹; Tao Jiang¹; ¹Central South University

The mineralization behavior of common fluxes is studied by investigating the microstructures with optical microscope. The results show that the reactions start between iron ore and lime, small particle limestone, which form the primary liquid. Then coarse limestone, dolomite and serpentine take part in reaction under the action of primary liquid. Limestone is the easiest to mineralization, then dolomite, and the last one is serpentine. In order to mineralize dolomite and serpentine completely, either the basicity of sinter should be increased or the size of them should be reduced.

Advances in Mechanics of One-Dimensional Micro/ Nano Materials: Nanomechanics: Size Scale and Theory

Sponsored by: The Minerals, Metals and Materials Society, TMS Materials Processing and Manufacturing Division, TMS Electronic, Magnetic, and Photonic Materials Division, TMS: Nanomechanical Materials Behavior Committee

Program Organizers: Reza Shahbazian-Yassar, Michigan Technological University; Seung Min Han, Korea Advanced Institute of Science and Technology; Katerina Aifantis, Aristotle University

Wednesday PM	Room: 1B
March 2, 2011	Location: San Diego Conv. Ctr

Session Chairs: Xiaodong Li, University of South Carolina; Julia Greer, California Institute of Technology

2:00 PM Invited

Measurement of Size-Scale Effects in Pure Ni: Effect of Initial Dislocation Density: Jaafar El-Awady¹; Paul Shade²; Sang-Lan Kim³; *Michael Uchic*⁴; Satish Rao³; Dennis Dimiduk⁴; Chris Woodward⁴; ¹Johns Hopkins University; ²Universal Technology Corporation; ³UES, Inc.; ⁴Air Force Research Laboratory

The importance of the initial dislocation density on the mechanical response of microcrystals has been the subject of both recent experimental and simulation-based studies. However, there is little experimental examination of the changes to either the size-dependent flow response or the observed strain intermittency in pure FCC metals as a function of the initial dislocation density. We have performed long annealing treatments that have reduced the initial dislocation density in pure Ni single crystals to extremely low levels, approaching 10^8 m^2 . These low dislocation density crystals enabled studies of size-scale effects in pure FCC metals that contain essentially no grown-in dislocations. Furthermore, we have pre-deformed <110> oriented crystals to selected stages of substructure development: Stage II, the transition between Stage II-to-III, and Stage III. The talk presents experimental measurements from these crystals to characterize the effect that the starting substructure has on size-affected flow response as well as plastic intermittency.

2:25 PM Invited

3:00 PM

Atomistic Simulations of the Strength of Gold Nanowires: Christopher Weinberger¹; ¹Sandia National Labs

Molecular dynamics simulations of nanostructures can be used to estimate strength but are limited by the timescale resolution. To overcome this, we use energy barrier calculations of dislocation nucleation to estimate the strength of gold nanowires. Crystal orientation, size and surface termination



types are included in this study to predict strengths, which can be compared to experiments.

2:50 PM Invited

Gradient Theory for One-Dimensional Configurations and Objects: *Elias Aifantis*¹; ¹Aristotle University of Thessaloniki

Various forms of gradient theory are used to discuss one-dimensional configurations and objects. They include interfaces, layers, fibers, nanowires and nanotubes.

3:15 PM

Size Effects on Strength and Plasticity of Vanadium Nanopillars: Seung Min Han¹; Tara Bozorg-Grayeli²; James Groves²; Yi Cui²; William Nix²; ¹Korea Advanced Institute of Science and Technology; ²Stanford University

A size effect study was conducted on vanadium BCC nanopillars that were synthesized from both the thin film and the bulk crystal in (100) orientations. Our results indicate that the size dependent deformation behavior exists for V; the smaller nanopillars displayed discrete bursts and higher stresses during deformation. The size effect exponent was calculated to be -0.79, and our results were compared with the previous reports on Nb, Ta, Mo and W. Our V results reported a higher size effect exponent compared to those of Ta, Mo, and W, and this trend is in agreement with the critical temperature dependent size effect theory. V poses a unique opportunity in conducting insitu TEM deformation study due to its high electron transparency. Our report on both ex-situ and in-situ studies will be discussed.

3:30 PM Invited

Size Dependent Deformation Mechanism Transition in a Titanium Alloy: Zhiwei Shan¹; ¹Xi'an Jiaotong University

Using micro-compression and in situ nano-compression experiments, we find that the stress required for deformation twinning (DT) increases drastically with decreasing sample dimension (d) of a titanium alloy single crystal, until d is reduced to a critical value(~ 1 micrometer), below which the DT is overtaken altogether by less correlated, ordinary dislocation plasticity (ODP). Accompanying the transition in deformation mechanism, the maximum flow stress of the submicron-sized pillars was observed to saturate at a value close to titanium's ideal strength. A "stimulated slip" model is developed to explain the strong size dependence of DT. The large sample size in transition is easily accessible in experiments, making our understanding of size dependence highly significant for applications (Q. Yu, Z. W. Shan, J. Li, X. X. Huang, L. Xiao, J. Sun and E. Ma, Nature 463, 335-338, 2010).

3:55 PM Break

4:10 PM Invited

Size Matters: Size-Dependent Mechanical Properties of Metallic Systems: *Julia Greer*¹; Dongchan Jang¹; Andrew Jennings¹; Ju-Young Kim¹; ¹California Institute of Technology

When microstructural (intrinsic) or external material dimensions are reduced to nano-scale, they exhibit unique behaviors. We fabricate nanopillars with different initial microstructures ranging from 50 nm to 1 micron by using Focused Ion Beam and E-beam lithography/electroplating approaches. Their strengths in uniaxial compression and tension are subsequently measured in in-situ mechanical deformation instrument, SEMentor. We discuss nano-mechanical behavior in four distinct metallic systems: single crystals, nano-crystalline metals, nano-twinned metals, and metallic glasses. We observe SMALLER is STRONGER phenomenon in single crystals while nano-crystalline metals exhibit SMALLER is SOFTER trend. Metallic glasses show strength increase and ductility when reduced to nano-scale. Unlike in bulk, nano-scale materials exhibit discretized stressstrain relationships. We attribute these dissimilarities to free surface effects, leading to unique dislocation interactions with internal interfaces (grain and twin boundaries) in the presence of free surfaces and shear transformation zones in metallic glasses, serving as fundamental reason for observed deformation mechanisms.

4:35 PM Invited

Environmental Effects on the Mechanical Behavior and Function Performance of Nanostructures: Xiaodong Li¹; ¹University of South Carolina

Nanostructures are often mechanically tested and/or functionally operated in various severe environments, such as at high humidity levels and electron beam radiation conditions. We found that humidity and electron beam radiation remarkably affect the mechanical behavior and function performance of nanostructures. The mechanical properties such as elastic modulus vary significantly at different humidity levels and electron beam radiations, in turn affecting the function performance of the nanostructures which utilize the elastic modulus as the function base. We also found that functions of the mechanically damaged nanostructures can be recovered by self healing in the nanostructures in situ over a period of time.

5:00 PM Invited

Transition from Deterministic to Stochastic Deformation: *Alfonso Ngan*¹; ¹University of Hong Kong

The deformation of small material volumes is often jerky, with discrete strain jumps occurring in a stochastic manner. In this paper, the condition for the stochastic model of deformation is analyzed theoretically. The model used considers a large ensemble of macroscopically identical but microscopically different experiments each of which emits bursts randomly according to a rate law that depends on the history of emission and the instantaneous stress. The model predicts that if burst sources get depleted on continuous emission, the stress-strain behavior will be stochastic, and if burst sources get multiplied on continuous emission, the stress-strain behavior will be deterministic. The strength at the same strain in the stochastic regime is also higher than in the deterministic regime. The condition for sources getting depleted on continuous emission corresponds to "dislocation starvation", and so the model predicts that dislocation starvation is always accompanied by the stochastic mode of deformation.

5:25 PM Invited

Structural Transformations in Bulk Nanocrystalline Materials, Nanorods, and Nanoparticles Triggered by Disclinations: *Alexey Romanov*¹; Anna Kolesnikova²; Leonid Dorogin³; Ilmar Kink³; Elias Aifantis⁴; ¹Ioffe Physical-Technical Institute RAS; ²Institute of Problems of Mechnical Engineering; ³University of Tartu; ⁴Aristotle University of Thessaloniki

Present talk gives the analysis of structural transformations caused by disclinations and leading to grain refinement in bulk nanocrystalline materials (BNCMs), emerging 1D nanowhiskers (NWs), and structural changes in pentagonal nanorods (PNRs) and nanoparticles. The model developed for BNCMs qualitatively and quantitatively describes the effect of grain size diminishing in the course of plastic deformation and explains the peculiarities of the flow stress dependence on the grain size. A new model of NW formation operates with prismatic dislocation loops that condensate on the disclination defect placed in the triple junction of grain boundaries of a polycrystal. To understand the transformations in nanoparticles and PNRs their internal organization is explained in terms of disclinations. It is demonstrated that initial multiple twinned structure of particles or PNRs is unstable with respect to dislocation formation above a certain critical diameter of a particle or radial phase separation in case of two-phase PNR.

5:50 PM

Vibration Analysis of Nano-Structures Using Wavelets and Gradient Theory: Avraam Konstantinidis¹; ¹Aristotle University of Thessaloniki

The vibration of cantilevers used in nano-electromechanical systems (NEMs) is studied using gradient theory, first proposed by Aifantis and co-workers in 1984. Wavelets are then proposed to extract the noise from the vibration signals. The same is sought for the vibration of single walled carbon nanotubes (SWCNTs).

Alumina and Bauxite: Energy and Environment

Sponsored by: The Minerals, Metals and Materials Society, TMS Light Metals Division, TMS: Aluminum Committee, TMS: Aluminum Processing Committee

Program Örganizers: James Metson, University of Auckland; Carlos Suarez, Hatch Associates Consultants Inc

Wednesday PMRoom: 17AMarch 2, 2011Location: San Diego Conv. Ctr

Session Chair: To Be Announced

2:00 PM

Perspective on Bayer Process Energy: Don Donaldson¹; ¹Alumina Consultant

The three most important cost items in the production of alumina are bauxite, caustic soda and energy. Alumina energy cost will rise more than other costs as energy prices increase and energy related environmental issues impact alumina production. Many refineries will need to adjust process to maintain or improve their position on the world cost curve. The Bayer Process is simple but the use of energy in the process can be complex. The uses of energy in the Bayer process and their interrelationship will be discussed.

2:20 PM

Optimization of Heat Recovery from the Precipitation Circuit: *Rashmi Singh*¹; Sushant Hial¹; Michael Simpson¹; ¹Vedanta Aluminium Ltd.

In the Bayer process, temperature profile across the precipitation circuit plays a major role to maximize the precipitation yield while maintaining product quality. For this reason, plate heat exchangers are used both at inlet to Precipitation and in between precipitation stages at Vedanta Aluminium's Lanjigarh alumina refinery. For the Heat Interchange Department (HID), cooling media is spent liquor while for the Interstage Coolers (ISCs) of Precipitation both spent liquor and cooling water are used. A simple model was built using existing heat exchanger performance data along with heat and mass balances across Heat Interchange Department (HID) and Precipitation. This was then used to determine feasible modifications for improving heat recovery in the Precipitation circuit. The results obtained have indicated process steam reduction of 3 % can be achieved with minor modifications.

2:40 PM

Alunorte Global Energy Efficiency: Arthur Monteiro¹; Reiner Wischnewski²; *Cleto Azevedo*¹; Emerson Moraes¹; ¹Alumina do Norte do Brasil S.A.; ²Hydro Aluminium AS

Alunorte is the largest alumina refinery in the world with a production capacity of 6.3 Mtpy. The plant has a specific energy consumption of less than 8 GJ per ton of alumina which defines the world-wide benchmark for energy efficiency in alumina production. The high energy efficiency is achieved by taking advantage of a good process design, the utilization of state-of-the-art technologies, good operation and the processing of high quality bauxite. The technologies which are applied in Alunorte to contribute to the global energy efficiency of the plant are reviewed and its heat integration and its water balance are discussed.

3:00 PM

Opportunities for Improved Environmental Control in the Alumina Industry: *Richard Mimna*¹; John Kildea²; Everett Phillips¹; Wayne Carlson¹; Bruce Keiser¹; ¹Nalco Company; ²Nalco Australia

Alumina production from bauxite offers a unique set of environmental concerns that affect air, water, and solids. Governments and industry have recognized that reductions in plant emissions and environmental impacts are necessary. The alumina industry is not the only industry that has been subjected to, and responded to, such regulatory scrutiny over the past decade. A number of industry sectors are actively developing innovative ways to control a broad range of potential environmental hazards. A number of these technologies may have direct application in alumina refineries. Methods to significantly reduce mercury emissions in both air and water have recently

been developed for use in a range of industries. In addition, powerhouse emissions of NOx, SOx, and particulate matter can now be significantly reduced. This paper reviews a number of these new technologies now in commercial use in non-alumina plants and considers how they may be applicable within the alumina industry.

3:20 PM

Alumina Refinery Water Management: When Zero Discharge Just Isn't Feasible....: Lucy Martin¹; Steven Howard¹; ¹Bechtel

Management and treatment of liquid effluents are determinant considerations in the design of alumina refineries. Rainfall, evaporation rate, proximity to the coast, process design and layout, ore mineralogy, the local environment, and potential impact on contiguous communities are all integral to the development of an appropriate refinery water management strategy. The goal is to achieve zero discharge of liquid effluent to the environment. However this is not always the most feasible solution under the extreme rainfall conditions in tropical and subtropical locations. This paper will explore the following issues for both inland and coastal refineries: •Methods to reduce and control refinery discharges •Treatment design criteria •Socioeconomic aspects relating to surface water use in settlements adjacent to the refinery.

3:40 PM Break

3:50 PM

High Purity Alumina Powders Extracted from Aluminum Dross by the Calcining—Leaching Process: *Liu Qingsheng*¹; ¹Jiangxi University of Science and Technology

A new calcining-leaching process was used to extract high purity alumina(A1203)powders from aluminum dross in this study. The aluminum dross was mixed with soda(Na2CO3)and calcined at 900°C to yield soluble aluminates. Subsequently the calcined dross was leached with sulfuric acid (H2SO4) to produce a solution containing aluminum. The unwanted metal ions including Fe3+and Na+ were removed by ethylene diamine tetraacetic acid(EDTA)and water washing. Then added the proper dispersant,controlling the crystallization of aluminum trihydroxide precipitation, and the drying and calcining process was carried out, resulting in ultra fine Al2O3 powders with high purity. The characteristics of the Al2O3 powders were examined by means of XRD, TEM and Brunauer-Emmet-Teller (BET) surface analysis method. The extraction efficiency of Al2O3 can surpass 98% by optimization of the calcination and lixiviation processes. Well-dispersed fibriform Al2O3 powders were obtained by calcining at 800°C and the purity of the ultra fine Al2O3 powders was more than 99.6%.

4:10 PM

Effect of Calcium/Aluminium Ratio on MgO Containing Calcium Aluminate Slags: *Wang Bo*¹; Sun huilan¹; Guo Dong¹; Bi Shiwen²; ¹Hebei University of Science and Technology; ²Northeastern University

MgO is the main impurity in calcium aluminate slag. The existence of MgO will change the occurrence state of alumina and decrease the alumina leaching property of slag. In order to remove or reduce the negative effect of MgO, the method of changing C/A of calcium aluminate slag was studied and the effect mechanism was also analyzed. The results showed that the formation of quaternary compound 20CaO•13Al₂O₃•3MgO•3SiO₂ ($C_{20}A_{13}M_3S_3$) would be inhibited with the increasing of C/A of calcium aluminate slag, and the MgO crystallized in the form of periclase independently under this condition. There is an optimal C/A to improve the alumina leaching property of calcium aluminate slag. The increase of C/A could not remove the negative effect of MgO on calcium aluminate slag completely, and the optimal C/A of slag will increase with the increase of MgO content.

4:30 PM

Study on Extracting Aluminum Hydroxide from Reduction Slag of Magnesium Smelting by Vacuum Aluminothermic Reduction: *Wang Yaowu*¹; Feng Naixiang¹; You Jing¹; Hu Wenxin¹; Peng Jianping¹; Di Yuezhong¹; Wang Zhihui¹; ¹Northeastern University

Feng Naixiang invent a new producing magnesium method, which mainly include two steps, the first step is producing magnesium with vacuum



aluminothermic reduction, the second step is extracting aluminum hydroxide from reduction slag. In the reduction slag, the alumina is more than 65% and it is mainly in the form of CaO • 2Al2O3. The process of producing aluminum hydroxide from the slag leached by the mixture solution of sodium hydroxide and sodium carbonate was studied. It showed that the leaching rate of alumina is more than 85% when leaching temperature is 85°, L/S is 5 and leaching time is 2h. The magnesia-alumina spinel which generated in the reduction process and 3CaO•Al2O3•6H2O which generated in the leaching process are the two main ways caused loss of alumina. The chemical composition of aluminum hydroxide products which obtained after desiliconisation and carbonation precipitation can meet the quality standard of the alumina plant.

4:50 PM

Application of Thermo-Gravimetric Analysis for Estimation of Tri-Hydrate Alumina in Central Indian Bauxites --- An Alternative for Classical Techniques: Yarlagadda Ramana¹; Rajesh Patnaik¹; ¹Vedanta Aluminium Limited

Tri-hydrate alumina (Al2O3.3H2O) content in bauxite is a fundamental quality parameter in Bayer alumina process using low temperature digestion. Classical techniques available for its estimation are mainly time consuming and prone to standard and non-standard sources of error. Extensive studies on analysis of samples from Central Indian bauxite sources using thermo-gravimetry at varied temperature ranges and comparing it with that of the data obtained from classical techniques have revealed that loss of molecular water at different temperatures in thermo-gravimetry provides a meaningful tool to correlate with tri-hydrate alumina content by applying relevant correction factors derived from the experimental data at different concentrations of tri-hydrate alumina. The studies also have found that the thermo-gravimetric analysis can be used as a very fast and dependable technique with higher levels of accuracy over classical methods and free from other interferences. The accuracy levels of the method developed were checked using reference standards.

5:10 PM

Determination of Oxalate Ion in Bayer Liquor Using Electrochemical Method: Seval Turhan¹; Betül Usta¹; Yücel Sahin²; Oktay Uysal³; ¹ENTEKNO Industrial Technological and Nano Materials Ltd.& Anadolu University, Faculty of Science, Department of Chemistry; ²Anadolu University, Faculty of Science, Department of Chemistry; ³ENTEKNO Industrial Technological and Nano Materials Ltd

The Bayer process can be summarized as the digestion of bauxite with caustic liquor and the subsequent precipitation of hydrated alumina [1]. Most bauxite contains organic compounds in various amounts. Depending upon the digestion conditions, 5–10% of the organic carbon is converted to sodiumoxalate [2]. When sodiumoxalate, if not controlled in Bayer process, builds up to a certain level of supersaturation, it precipitates out in the hydrate precipitator tank. This co-precipitation affects the quality of alumina [3]. In this study, we investigated the electrochemical determination of oxalate ion by using differential puls voltammetry in Bayer liquor. A linear relationship between oxalate concentration and current response was obtained with good reproducibility of the current. [1] T.G. Pearson, The chemical background of the aluminium industry, Monograph No. 5, Royal Institute of Chemistry, London, UK, 137-143, 1955. [2] G. Lever, Travaux, 13, 335 (1983). [3] R. Calalo, T. Tran, Light Metals, 125(1993).

Aluminum Alloys: Fabrication, Characterization and Applications: Emerging Technologies

Sponsored by: The Minerals, Metals and Materials Society, TMS Light Metals Division, TMS: Aluminum Processing Committee *Program Organizers:* Subodh Das, Phinix LLC; Zhengdong Long, Kaiser Aluminum; Tongguang Zhai, University of Kentucky

Wednesday PM	Room: 14A
March 2, 2011	Location: San Diego Conv. Ctr

Session Chair: Subodh Das, Phinix LLc

2:00 PM

Microstructure Evolution Of Cryomilled Nanostructured Light Weight Al 5083 During SPS: *Yuhong Xiong*¹; Dongming Liu¹; Ying Li¹; Baolong Zheng¹; Troy Topping¹; Yizhang Zhou¹; Deepak Kapoor²; Chris Haines²; Joseph Paras²; Darold Martin²; Julie Schoenung¹; Enrique Lavernia¹; ¹University of California; ²US Army

Al alloys are widely used because they provide the combination of light weight and high strength. In recent years, spark plasma sintering (SPS) technology has emerged as a viable approach to sinter materials due to its rapid heating and high pressure application features. In this study, SPS was chosen to produce dense ultrafine-grained bulk samples using cryomilled nanostructured powder. A bimodal microstructure and banded structures were observed through TEM investigation. The evolution of such microstructures can be attributed to the starting powder and the process conditions, which are associated with the thermal, electrical and pressure fields present during SPS. A finite element method (FEM) was also applied to investigate distributions in temperature, current and stress between metallic powder particles. The FEM results reveal that the localized heating, deformation and thermal activation occurring at inter-particle regions are associated with the formation of the special microstructure.

2:20 PM

Design and Optimization of Innovative High Performance Aluminum Sandwich Structures: Antonio Valente¹; *Edward Chen*²; ¹PLY Engenharia, Lda; ²Transition45 Technologies, Inc.

An innovative technique to manufacture high performance aluminum sandwich structures has been developed. A sheet metal is cut and bent to form the skin and the core of the sandwich. This element is joined to the plain sheet to form the panel. With intelligent layout the new solution can outperform traditional metal sandwich structures in specific stiffness and provide multi-functionality. This presentation describes the evolution of the OpencellTM concept from an idea, to a product, and then software implementation that meets a variety of requirements for the preliminary design of structures. Manufacturing aspects served as design drivers and numerical simulations by Finite Element Analysis (FEA) were used to improve mechanical performance. The panel bending and out-of-plane shear stiffness were used as design objectives to start. A variety of panel configurations were optimized, by integrating commercial FEA code in a process integration and design optimization environment, for the most effective use of material.

2:40 PM

Effects of Spark Plasma Sintering (SPS) on Cryomilled Nanostructured Al 5083 Alloy: *Dongming Liu*¹; Yuhong Xiong¹; Troy Topping¹; Yizhang Zhou¹; Chris Haines²; Joseph Paras²; Deepak Kapoor²; Darold Martin²; Julie Schoenung¹; Enrique Lavernia¹; ¹UC Davis; ²US Army, RDECOM-ARDEC, Picatinny Arsenal, NJ 07806, USA

Fundamental studies have been conducted to investigate the influence of SPS processing variables on densification behaviors for cryomilled nanostructured Al 5083 powders and the mechanical properties of the subsequent compacts. It has been found that: pressure-loading mode has a significant effect on mechanical properties and bonding between powders: in comparison with that loaded at room temperature, pressure loaded at target sintering temperature can enhance bonding between particles and thus improve the mechanical properties; surface activation at pores and other interfaces can help break up the oxide layers existing on particle surfaces and release absorbed gases; grain size as well as powder size play important roles in shrinkage of samples; pulse pattern shows an insignificant influence on the consolidation of SPS processed samples unless using a pulse pattern with on:off ratio less than one; the cryomilled powder is more easily consolidated than the atomized one.

3:00 PM

Microstructural and Electrochemical Characterization of Anodic Oxide Films Formed on Spray-Deposited Al-Si Alloys: *Hector Herrera*¹; Manuel Palomar¹; Mario Romero¹; Jose Juárez²; ¹Metropolitan Autonomous University (UAM); ²Centro Nacional de Metrología (CENAM)

In this research, aluminum oxide films were grown on one spraydeposited Al-Si alloy and its extrudate product using an anodizing treatment. The electrochemical behavior of the oxide-films was investigated by electrochemical impedance spectroscopy (EIS) technique and potentiodynamic polarization measurements in chloride media. The surface morphology was examined by scanning electron microscopy (SEM). Anodizing was performed in H2SO4 by means of standard procedures and sealed in either boiling water, or potassium dichromate. Finally, the effect of the anodic-surface modification by immersion in boiling CeCl3 for 2 hours on the pitting corrosion resistance was also investigated. The results of the electrochemical characterization demonstrate that anodizing followed by a simple hot water sealing was less effective, so pits were detected on the anodic oxide film in less than 2 days, as denoted by characteristic changes in the EIS spectra at the lowest frequencies. Improved results were achieved with the hot cerium surface modification.

3:20 PM

Preparation of Al - Li Alloys for Lithium-Air Secondary Battery by Solid Diffusion Method: Tao Cheng¹; Zijian Lv¹; *Xiujing Zhai*¹; Mingjie Zhang¹; Ganfeng Tu¹; ¹Northeastern University

In present work, Al-Li alloys used as lithium-air battery anode material were prepared by solid diffusion method. In the system of molten LiCl-KCl-LiF with molar compositions of 55%-45%-5%, electrolytic reduction of Liion on solid aluminum plate was conducted; And Al-Li alloys were formed by the diffusion of metal Li into the plate. The effects of influencing factors, such as electrolysis time, cell voltage and current density, were all studied. The characteristics of Al-Li alloys were analyzed by X-ray diffraction and scanning electron microscopy. It was found that the lithium content of 15%wt. in Al-Li alloys can be obtained by solid diffusion method for 4.0 h with the current density of 0.125 A.cm⁻² at 480 \176C; and the phase compositions of the Al-Li alloys were alpha- and beta-aluminum lithium from X-ray diffraction analysis.

3:40 PM Break

3:55 PM

Effects of Process Parameters on Rolled Precursor of Aluminum Foam Sandwich Panel: *Binna Song*¹; Guangchun Yao¹; Guoyin Zu¹; Lei Wang¹; Zhihao Guan¹; ¹Northeastern University

The small size preforms of aluminum foams sandwich panel were prepared by a powder rolling method using the powders of AlSi12 alloy, Mg and TiH2 as raw materials. Effects of foaming temperature and time on rolled foamable sandwich panel were investigated in details using SEM, OM analysis and a scanner at a resolution of 300 dpi. The results show that deformation of Al face sheet of the aluminum foams sandwich panel completely disappears. Furthermore, the local melting of Al face sheet can also be hardly found. The bonding between Al face sheet and foam core is good. No macro and micro defects exist in the cell structures and 225% of the expansion rate is achieved. The metallurgical bonding between Al face sheet and foam core can be absolutely obtained as the optimum foaming process of the small size preforms are guaranteed, viz., foaming temperature is 700° and the range of foaming time is between 90 and 120 seconds.

4:15 PM

Preparation and Characterization of Short Carbon Fiber Reinforced Aluminium Matrix Composites: Pengfei Yan¹; Guangchun Yao¹; Jianchao Shi¹; Xiaolan Sun¹; *Hongjie Luo*¹; ¹School of Materials & Metallurgy, Northeastern University

Aluminium matrix composites reinforced by short carbon fibers were prepared through stir casting process. The carbon fibers coated with copper by using electrolysis plating were characterized by using scanning electron microscopy (SEM). The composites with different levels of carbon fibers were prepared through stir casting method. The microstructure and mechanical properties of composites were evaluated. The microstructure results showed that the carbon fibers were reasonably uniformly distributed within the aluminium matrix and exhibited good interfacial bonding with the matrix. The mechanical properties testing results indicated that the tensile strength and hardness increases with the increase of carbon fiber level. The results demonstrated that the stir casting is a promising method to prepare aluminium matrix composites.

4:35 PM

Preparation of Aluminum Foam Using a Novel Gas-Generating Agent: Deng-Wei Huo¹; *Xiang-yang Zhou*¹; Tai-kang Zhang¹; Jin Qin¹; Jie Li¹; Huan Zhao¹; ¹School of Metallurgical Science and Engineering, Central South University

The thermal decomposition behavior of a novel gas-generating agent (NA) and its effect on the viscosity of aluminum melt were investigated, as well as the preparation technology of aluminum foam by using NA as foaming agent and viscosifier was presented. The results show that NA has a wide decomposition temperature range and a gentle decomposition rate, and NA can effectively increase the viscosity of aluminum melt, as a result, the dric-metal foaming agents such as TiH2 and ZrH2 can be replaced by NA and an extra viscosifier such as Ca is unnecessary during preparation process of aluminium foam by melt foaming method. The aluminum foam with porosity of 60%-85% can be prepared while the additive amount of fine NA powder as viscosifier is in the range from 0.6wt% to 1.0wt%, and the additive amount of coarse NA powder as foaming agent is in the range from 1.6wt% to 2.2wt%.

4:55 PM

High Temperature Dry Sliding Wear Behaviour of Aluminium-Silicon/ Graphite Composite Processed by Stir Casting: G. Rajaram¹; S. Kumaran¹; ¹National Institute of Technology Tiruchirappalli

Aluminum metal matrix composites are extensively used for tribological applications due to excellent wear resistance especially during sliding under dry, wet and high temperature environments. In this present study, aluminum silicon alloy and aluminum silicon alloy /graphite (3 wt.%) composite were prepared by stir casting method and their dry sliding wear behaviour was investigated by using Pin on Disc wear tester with temperatures up to 350°C in air. Incorporation of graphite and its distribution was confirmed with optical microscopy. Wear rate of alloy and composite was decreased with increasing temperature due to formation of oxide and glazing layers on the sliding surfaces. However, the wear behaviour of composite is better than that of alloy for all temperature conditions due to formation of rich tribo film between sliding surfaces by smeared graphite particulates. The worn surfaces of alloy and composite were characterized by scanning electron microscope to understand the wear mechanism.



Aluminum Reduction Technology: Improvement in Cell Equipment and Design

Sponsored by: The Minerals, Metals and Materials Society, TMS Light Metals Division, TMS: Aluminum Committee, TMS: Aluminum Processing Committee

Program Organizers: Mohd Mahmood, Aluminium Bahrain; Abdulla Ahmed, Aluminium Bahrain (Alba); Charles Mark Read, Bechtel Corporation; Stephen Lindsay, Alcoa, Inc.

Wednesday PM	Room: 17B
March 2, 2011	Location: San Diego Conv. Ctr

Session Chair: Stephan Broek, Hatch Ltd

2:00 PM

Retrofit of a Combined Breaker Feeder with a Chisel Bath Contact Detection System to Reduce Anode Effect Frequency in a Potroom: *Jonathan Verreault*¹; René Gariépy¹; Bernard Desgroseilliers¹; Claude Simard¹; Xavier Delcorde²; Christophe Turpain²; ¹Rio tinto Alcan; ²ECL

Chisel bath contact detection is a feedback system provided on aluminium reduction cell alumina point feeders to ensure that the crust breaker (or chisel) contacts liquid bath. The benefits of chisel bath contact detection on anode effect reduction are well known on AP technologyTM operating with a separate system of breaker and feeder. The present paper describes the technology adaptation for a safe hot change installation of chisel bath contact detection applied to the combined breaker/feeder in a P-155 cell while at the same time introducing a longer pneumatic cylinder stroke. Mechanical modifications allowing the reuse of most of the existing breaker/feeder parts as well as the results obtained on four experimental cells during the development phase are presented. The retrofit procedure is also described in the context of a hot change while controlling HSE related aspects. *AP technology*TM is trade-mark of Rio Tinto Innovations Ltd.

2:20 PM

Anode Dusting from a Potroom Perspective at Nordural And Correlation with Anode Properties: *Halldor Gudmundsson*¹; ¹Century - Nordural

Anode performance in the cells is ultimately the most important measure of the anode quality and is not always reflected in the quality certificates. Nordural has through the years developed some tools to measure anode performance in the cells to use as feedback to anode suppliers so that they may improve the anode performance. Anode dusting in the cells leading to anode spikes and loss of current efficiency can be the biggest issue in the supplier - customer relationship. This paper shows some examples of anode dusting excursions experienced with three anonymous anode suppliers, how it was measured in the cells and how it was reduced or resolved in cooperation with the suppliers.

2:40 PM

The Application of Continuous Improvement to Aluminium Potline Design and Equipment: *William Paul*¹; ¹Rio Tinto Alcan

The design and supply of technologies to a large number of aluminium smelter projects, over the last two decades, has provided a unique opportunity to benefit from continuous improvement. This improvement process starts with feedback from customers and suppliers, combined with input from R&D and internal reviews, to identify, validate and then incorporate experiences and innovation from many areas. The process can be described as systematic continuous improvement and the results are superior technology packages that incorporate the latest enhancements and better meet clients' needs. This paper describes the methodology used to manage the continuous improvement of technology packages. It includes examples of improvements, including ancillary equipment redesign to improve safety and reduce forklift truck usage. Also discussed are the challenges and opportunities of working with potline equipment suppliers. Effective cooperation enables the development of fit for purpose solutions that minimise potline commissioning issues and maximise pot performance.

3:00 PM

Alcoa STARprobe: Xiangwen Wang¹; Bob Hosler¹; Gary Tarcy¹; ¹Alcoa, Inc.

Alcoa STARprobe is a probe device/system used to measure cryolitic bath properties including Superheat, Temperature, Alumina concentration, and cryolite Ratio (acidity), STAR, all together in real time for active pot control. The patented measurement principle is based on differential thermal analysis (DTA). This paper shows the fundamentals of operation along with the correlation of all the analysis with the accepted methods (XRD and pyrotitration for acidity, thermal couples for Bath Temperature and LECO and XRF analysis for alumina). The timing of the measurement will be shown to be equal to the traditional methods and the reliability (including reusable use of the probes) will also be described.

3:20 PM Break

3:30 PM

Active Pot Control Using Alcoa STARprobe: Xiangwen Wang¹; *Gary Tarcy*¹; Eliezer Batista¹; ¹Alcoa, Inc.

To run an aluminum smelting cell, routine bath sampling and subsequent chemistry analysis are required along with pot temperature measurement. The sampling and analytical process is lengthy and tedious and very often, results are delayed as long as 24 hours. In addition the results are not coupled to the other critical information (e.g, noise, automatic resistance adjustments etc) at the time of the sample. Alcoa STARprobeTM, which was previously described, corrects these deficiencies while providing a means to more efficiently and effectively control a smelting pot. This paper presents the background philosophy for an advanced control that has been enabled by the new measurement technique. The control method has been applied in multiple plants and demonstration of improved performance will be shown.

3:50 PM

Applications of New Structure Reduction Cell Technology in Chalco's Smelters: *Fengqin Liu*¹; Songqing Gu¹; Jiangmin Wang¹; ¹Chalco

A new generation of key energy saving technology for aluminum reduction – the new structure aluminum reduction cell technology has been successfully developed by Chalco and widely applied in Chalco's smelters, which includes such key technologies, as the new specially designed cathode installation, heat preservation lining and low voltage operation control system. The molten metal fluctuation driven by the great magnetic field is greatly restrained in the cells, based on which reducing ACD without any loss of current efficiency is realized for lower energy consumption and less emission. The industrial tests and applications of this technology have been carried out successfully in the various scale aluminum reduction cells in Chalco's smelters and about 12000 kWh of DC consumption per ton of aluminum and 3.70 V of cell voltage have been achieved.

4:10 PM

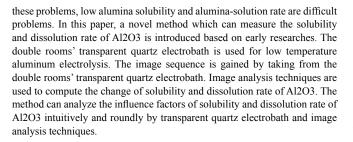
Transport Numbers in the Molten System NaF-KF-AlF3-Al2O3: Pavel Fellner¹; *Jan Hiveš*¹; Jomar Thonstad²; ¹Slovak University of Technology in Bratislava; ²NTNU

Transport numbers in the molten system NaF – KF – AlF3 (Al2O3, CaF2) were investigated by the Hittorf method. It was confirmed that in molten cryolite, Na3AlF6, 1010 °C, the current is transported almost exclusively by the Na+ cations (t(Na+) = 0.99). When AlF3 is added to a Na3AlF6 melt, the transport number of sodium cations decreases to 0.74 at the composition corresponding to NaAlF4. In molten K3AlF6 the transport number of K+ cations equals 0.836 at 1005 °C. In melts containing both Na+ and K+, the cations contribute to the charge transport approximately in the ratio of the squares of their ionic radii.

4:30 PM

Study on Solution of Al2O3 in Low Temperature Aluminum Electrolyte: Hongmin Kan¹; Ning Zhang¹; Xiaoyang Wang¹; ¹Shenyang University

Current efficiency can be increased and energy consumption can be lowered by low temperature aluminum electrolysis. However, many problems will occur, such as low electrical conductivity, cathode shell, low alumina solubility and alumina-solution rates if the temperature is too low. Of



Biological Materials Science: Mechanical Behavior of Biological Materials II

Sponsored by: The Minerals, Metals and Materials Society, TMS Electronic, Magnetic, and Photonic Materials Division, TMS Structural Materials Division, TMS: Biomaterials Committee *Program Organizers:* Jamie Kruzic, Oregon State University; Nima Rahbar, University of Massachusetts, Dartmouth; Po-Yu Chen, University of California, San Diego; Candan Tamerler, University of Washington

Wednesday PM	Room: 15A
March 2, 2011	Location: San Diego Conv. Ctr

Session Chairs: Dwayne Arola, University of Maryland Baltimore County; Ryan Roeder, University of Notre Dame

2:00 PM Invited

Energy Absorption in Natural Materials: *Joanna McKittrick*¹; Po-Yu Chen¹; Ekaterina Novitskaya¹; Maria Lopez¹; Irene Chen¹; Marc Meyers¹; ¹University of California, San Diego

Some of the most remarkable materials in terms of energy absorption and impact resistance are not found through human processing but in nature. Solutions to the continuing problems of improved composite technologies may lie in replicating naturally occurring systems. In this presentation, several mammalian structural materials: bones (bovine femur, elk antler), teeth and tusks from various taxa, armadillo and turtle carapaces, horns from the desert big horn sheep, and equine hooves are examined. The relationships between structural and mechanical properties for these materials, with an emphasis on energy absorption mechanisms are established. Energy absorbing strategies utilized in these materials will be identified. Implementation of these bioinspired design strategies can serve as a basis for the design of new energy absorbent synthetic composite materials. This research is supported by NSF Grant (Ceramics and Biomaterials Program) 1006931.

2:30 PM Invited

High Performance Impact-Tolerant and Abrasion-Resistant Materials: Lessons from Nature: *David Kisailus*¹; Qianqian Wang¹; Michiko Nemoto¹; Dongsheng Li¹; Brian Weden¹; ¹University of California at Riverside

Chitons are marine mollusks found worldwide in the intertidal or subtidal zones of cold water as well as in tropical waters. These organisms have evolved an amazing feeding structure called a Radula. The Radula is a ribbonlike structure that consists of abrasion resistant teeth anchored to a flexible stylus that the organism uses to abrade rocky substrates to reach algae. We investigate the structure and mineralization process in Cryptochiton stelleri, the largest of the chitons. Using various microscopy and spectroscopy techniques as well as synchrotron analyses, we have uncovered critical structure-function relationships in the mineralized teeth and insights into the mineralization processes in these unique structures. Investigation of the mechanical properties of the fully mineralized teeth have revealed that the combination of ultrahard minerals and templating organics, architected in a unique microstructure, lead to a damage tolerant composite that is of the hardest known biominerals known in nature.

3:00 PM

Anatomic Variability in the Elastic Anisotropy of Human Cortical Bone Tissue is Governed by the Orientation Distribution of Apatite Crystals: Justin Deuerling¹; David Rudy¹; *Ryan Roeder*¹; ¹University of Notre Dame

Computational models commonly account for elastic inhomogeneity in cortical bone using power-law scaling relationships with tissue or mineral density, and assume elastic isotropy or homogeneous anisotropy due to inadequate experimental data. Therefore, the objectives of this work were to characterize anatomic variation in the elastic anisotropy of human cortical bone and identify the governing structural parameters. Elastic constant magnitudes decreased and anisotropy increased from the mid-diaphysis toward the epiphyses of human femora. Tissue exhibited orthotropy toward the epiphyses, but was reasonably approximated as transversely isotropic near the mid-diaphysis. A specimen-specific micromechanical model accounting for seven structural parameters across multiple length scales identified the apatite crystal volume fraction and orientation distribution to be the most influential structural parameters governing the elastic constant magnitude and anisotropy, respectively. Model results were verified by experimental measurements of the elastic anisotropy, mineral density, tissue porosity, and apatite orientation distribution on the same tissue specimens.

3:20 PM

Ab Initio Study of Thermodynamic, Structural, and Elastic Properties of Mg-Substituted Crystalline Calcite: *Martin Friak*¹; Pavlina Elstnerova¹; Liverios Lymperakis¹; Michal Petrov¹; Tilmann Hickel¹; Helge Fabritius¹; Andreas Zigler²; Svetoslav Nikolov³; Sabine Hild⁴; Dierk Raabe¹; Joerg Neugebauer¹; ¹Max Planck Institute for Iron Research; ²University of Ulm; ³Bulgarian Academy of Sciences; ⁴Johannes Kepler University Linz

Arthropoda, that represent nearly 80 % of all known animal species, are protected by an exoskeleton formed by their cuticle. The cuticle represents a hierarchically structured multifunctional bio-composite based on chitin and proteins. Some groups like Crustacea reinforce the load-bearing parts of their cuticle with calcite. As the calcite sometimes contains Mg it was speculated that Mg may have a stiffening impact on the mechanical properties of the cuticle. We present a theoretical parameter-free quantum-mechanical study of phase stability and structural and elastic properties of Mg-substituted calcite. Our results show that substituting Ca by Mg causes an almost linear decrease in the crystal volume with Mg concentration and of substituted crystals. As a consequence the calcite crystals become stiffer giving rise e.g. to substantially increased bulk moduli.

3:40 PM Break

3:50 PM

Crack Propagation in Biocomposites: A Phase Field Study: *Murali Palla*¹; Tanmay Bhandakkar²; Wei Cheah³; Mark Jhon¹; Huajian Gao²; Rajeev Ahluwalia¹; ¹Institute of High Perform. Computing; ²Brown University; ³Institute of Materials Research and Engineering

We investigate, using a phase field approach, the crack propagation in systems akin to biological composites which have layered microstructures of stiff mineral and a soft organic phase. We find crack bifurcation at the interfaces of the soft phase, which is distinct from the usual dynamic crack branching. The crack tip shape shows extensive blunting due to the presence of the soft strip. We also find a significant increase in the fracture toughness due to the presence of the thin layer of soft material. The effect of geometrical distribution of the soft and stiff phases on the crack propagation behavior is of interest and extrinsic mechanisms that enhance the toughness would be investigated using phase field approach.

4:10 PM

Fracture Behaviour of Whole Teeth and Dentine at Different Hierarchical Levels: *Claudia Fleck*¹; Tania Traykova¹; Paul Zaslansky²; Anke Maerten²; ¹Technische Universitaet Berlin; ²Max-Planck-Institute of Colloids and Interfaces

We investigated the interaction of cracking and damage with the microstructure of dentine on different hierarchical levels. Micro-tomography and histological sectioning of compression loaded whole premolars served



to characterise failure patterns in different dentine areas on the whole tooth level. Cracks developed in the dentine and in the enamel even though the teeth were not visibly broken. Bending and notch tensile tests on wet bar-like specimens were performed to better understand the material properties of dentine itself. ESEM and XRD showed profound differences in the spatial strain distribution round the tip of advancing cracks. The observation of crack propagation during fracture of dentine revealed differences in the strain distribution within the microstructural elements of the hierarchical levels. We believe that similar strain fields, modified by the graded structure of dentine and the layered structure of the tooth, are responsible for crack initiation and propagation in dentine in the whole tooth.

4:30 PM

Depth, Tubule Density and the Fatigue Crack Growth Resistance of Dentin: *Juliana Ivancik*¹; Dwayne Arola¹; ¹University of Maryland Baltimore County

Dentin is a complex hierarchical mineralized tissue that occupies the majority of the human tooth by both weight and volume. The most distinct structural feature of this tissue is the dentin tubules, which is a system of microscopic channels extending in almost a radial arrangement from the pulp. The number, orientation and size of the tubules varies as a function of depth within the tooth. In this experimental investigation contribution from the tubule characteristics, including geometry and density, on the fatigue crack growth properties of dentin were characterized. There was a significant correlation between the tubule density and the relative resistance to fatigue crack initiation and growth; decreasing resistance was associated with greater depths. Overall, there was nearly a 1000 times increase in the incremental fatigue crack growth rate over the depth of tissue examined. This behavior appears attributed to the mechanisms in which crack extension occurs from adjacent tubules.

4:50 PM

Nanoscopic Dynamic Mechanical Properties of a Mineralized Tissue: Human Dentin: Dwayne Arola¹; *Heonjune Ryou*¹; ¹University of Maryland Baltimore County

In this study intertubular and peritubular components of dentin were evaluated by Dynamic Mechanical Analysis (DMA) using nanoindentation. The complex (E), loss (E"), and storage (E') modulii of intertubular and peritubular dentin were measured using a Hysitron Triboindenter over a range of dynamic frequencies (1 to 100 Hz). As expected, the storage modulus of the peritubular cuff (22.19 GPa<E'<34.71 GPa) was significantly greater (p<0.001) than for the intertubular dentin (16.08 GPa<E'<22.79 GPa) over the range of frequencies, due to the higher relative mineral content. The loss modulus of the intertubular cuffs (0.70 GPa<E'<1.60 GPa), but the differences were not significant (p>0.05). While the modulii increased with loading frequency they were not dependent on the mean load. The intertubular and peritubular dentin exhibit significant differences in the time-dependent aspects of mechanical behavior when measured using a dynamic mechanical analysis.

5:10 PM

The Effects of High Doses of Irradiation on the Fracture Behavior of Human Cortical Bone: *Holly Barth*¹; Maximilien Launey²; Robert Ritchie¹; ¹UC Berkeley; ²Lawrence Berkeley National Laboratory

Human bone is exposed to irradiation for a wide range of medical and scientific reasons. In the medical community bones are sterilized through irradiation for bone allograft surgery. For scientific studies the effects of irradiation is a concern with experiments that use *in situ* testing with high–energy synchrotron radiation diffraction and tomography imaging. Bone's mechanical behavior is a function of its' multi-dimensional hierarchical nature. To better predict the effects of irradiation on bone's fracture behavior it is important to investigate changes at each significant size scale. The findings in this study show that bone exposed to high levels of irradiation can cause serious deleterious effects to the collagen which leads to drastic losses in strength, ductility and toughness. It was shown that the plasticity in

bone was suppressed after as little as 70 kGy and the fracture toughness was decreased by a factor of 5 after 210 kGy of irradiation.

5:30 PM

Quantitative and Qualitative Changes in the Structure and Properties of Demineralized and Deproteinated Compact Bone: *Ekaterina Novitskaya*¹; Joshua Vasquez¹; Robert Urbaniak¹; Steve Lee¹; Po-Yu Chen¹; Ana Castro²; Gustavo Hirata²; Joanna McKittrick¹; ¹UCSD; ²Centro de Investigación Científica y de Educación Superior de Ensenada

Bone loss (osteoporosis) and demineralization occur as bones age and are major causes of bone fractures. The mineral/collagen interaction is important for understanding how this affects the bone fracture. A method of partial demineralization of bone was established through aging in 0.6N hydrochloric acid (HCl), monitored by inductively coupled plasma optical emission spectroscopy on the acid solution. Compression and bending mechanical tests of partially demineralized, completely deproteinated and untreated bovine femur bone were investigated with different strain rates. Fracture surfaces were analyzed by optical microscopy, scanning electron microscopy, micro-CT scanning, and atomic force microscopy. Compression tests showed that the sum of the stress-strain curves for completely demineralized and completely deproteinated bone was far lower than that of the untreated bone, indicating a strong molecular interaction between a collagen matrix and a mineral phase. This research is supported by the National Science Foundation grant DMR 0510138 and UC-MEXUS 2009 grant.

Bridging Microstructure, Properties and Processing of Polymer Based Advanced Materials: Session II

Sponsored by: The Minerals, Metals and Materials Society, TMS Extraction and Processing Division, TMS Materials Processing and Manufacturing Division, TMS: Materials Characterization Committee, TMS: Shaping and Forming Committee, ASM-MSCTS: Texture and Anisotrophy Committee

Program Organizers: Dongsheng Li, Pacific Northwest National Laboratory; Said Ahzi, University of Strasburg; Moe Kahleel, Pacific Northwest National Laboratory

Wednesday PM	Room: 32B
March 2, 2011	Location: San Diego Conv. Ctr

Session Chairs: Dongsheng Li, Pacific Northwest National Laboratory; Frédéric Addiego, CRP Henri Tudor

2:00 PM Keynote

Amorphous and Semi-Crystalline Blends of Poly(Vinylidene Fluoride) and Poly(Methyl Methacrylate): Characterization and Modeling of the Mechanical Behavior: Jean Halary¹; ¹ESPCI ParisTech

After extensive studies in the 1970s in relation to miscibility and piezoelectric properties, the blends of poly(methyl methacrylate) (PMMA) and poly(vinylidene fluoride) (PVDF) have been revisited with the aim of assessing their mechanical behavior. Depending on the amount of PVDF, either amorphous or semi-crystalline blends are produced: typically, the blends remain amorphous when their PVDF content does not exceed 50 wt%. Emphasis is put on the low deformation range covering the anelastic and plastic behaviors. The reported data depend, as expected, on temperature and strain rate and also, markedly, on blend composition and degree of crystallinity. Molecular arguments, based on the contributions of the glass transition motions and of the PMMA motions associated by the secondary relaxation are proposed to account for the observed features. Thanks to this understanding of the phenomena on the molecular level, accurate models can be selected in the view of stress-strain curve modeling.

2:30 PM

Mechanical Behavior of Melt Mixing Polypropylene Organoclay Nanocomposites: Said Ahzi¹; Nadia Bahloui¹; Kui Wang¹; Rodrigue Matadi¹; Rene Muller¹; ¹University of Strasbourg

This work aims to investigate the mechanical behavior of polypropylene organoclay nanocomposites uder quasiststaic and dynamic loading conditions. The nanocomposite was obtained by mixing the polypropylene matrix with a master bach of polypropylene modified anhydrid maleic and montmorillonite organoclay (pp-nanocor). The obtained nanocomposite exhibits a good dispersion and an exfoliated morphology. To study the effect of the nanocomposite dispersion and morphology, another nanocomposite was prepared by melt mixing of polypropylene and a modified montmorillonite (dellite) (pp-dellite). The dynamic behaviour was investigated by using a split Hopkinson pressure bars, at different strain rates and different temperatures. The obtained results for pp-nanocor, showed an ncrease of both Young's modulus and yield stress with the increasing organoclay concentration. However pp-dellite nanocomposites presented poor mechanical properties compared to those of pp-nanocor.

2:50 PM

Microstructural Characterization of Plastic-Bonded Explosives: *John Yeager*¹; Daniel Hooks¹; David Bahr²; ¹Los Alamos National Laboratory; ²Washington State University

Plastic-bonded explosives (PBX's) consist of hard, anisotropic molecular crystals in a polymer matrix. Historical studies have shown PBX's fail prematurely via crack propagation along the crystal-polymer interface. Characterization of the interface is therefore important for the development of predictive failure models. Additionally, study of the interface reveals the importance of wetting and dewetting phenomena which relate mechanical and explosive properties to the manufacturing process. Here, the interface is characterized using several methods. The adhesion of the crystal to several polymers has been characterized by surface energy measurements and a novel mechanical test, revealing that the practical adhesion is orders of magnitude higher than the calculated work of adhesion. The physical nature of the interface has been probed with atomic force microscopy and nanoindentation and is compared to pristine crystal surfaces. The interfacial chemistry has been analyzed with neutron reflectometry, differentiating between a clean interface and a compositionally graded interphase region.

3:10 PM

An Electron Microscopy Study of Nanoscale Surface and Sub-Surface Deformation Response of Polymer Nanocomposites: *Qiang Yuan*¹; Devesh Misra¹; ¹University of Louisiana at Lafayette

The objective of the presentation is to elucidate the nanoscale surface and sub-surface deformation response of polymer nanocomposites. The commonality in surface deformation behavior between nano- and microscale deformation is studied in order to reinforce the underlying fundamental principles governing surface deformation. An understanding of mechanics of surface deformation is accomplished via electron microscopy analysis of scratch damage at and beneath the surface in conjunction with physical and mechanical properties.

3:30 PM Break

3:50 PM

Investigation on Modified Humic Substances Based Binders for Iron Ore Agglomeration: *Tao Jiang*¹; Guihong Han¹; Yuanbo Zhang¹; Yanfang Huang¹; Guanghui Li¹; ¹School of Minerals Processing & Bioengineering, Central South University

Characterization of modified humic substances based binders for iron ore agglomeration was examined by chemical analysis, optical density, FTIR and TG-DSC. Chemical analysis displays the proportion of fulvic acid (FA) to humic acid (HA) in the binders is 1:10. Compared with the HA, the FA possesses more functional groups. Meantime, optical density ratio analysis shows that molecular weight and aromatization degree of the FA are smaller than those of the HA. FTIR spectra further confirm aromatic and aliphatic fractions are associated with various types of oxygen-rich groups including carboxyl and hydroxyl groups. TG-DSC and chemical analysis indicate structural changes of the binder including thermal decomposition, dehydroxylation and/or decarboxylation are caused during heating. The structural characterization of the binder ensures its good performance in the field of iron ore agglomeration.

4:10 PM

Triple Shape Memory Polymers Based on Self-Complimentary Hydrogen Bonding: *Taylor Ware*¹; Keith Hearon²; Duncan Maitland²; Walter Voit¹; ¹The University of Texas at Dallas; ²Texas A&M University

Triple-shape polymers (TSPs) are a growing subset of a class of smart materials known as shape memory polymers. TSPs can store one permanent and two metastable shapes. We describe a novel TSP system, comprised of both permanent covalent crosslinks and reconfigurable hydrogen bonding crosslinks, which enables broad and independent control of both glass transition temperature (Tg) and crosslink density. Triple shape properties arise from the combination of (meth)acrylate copolymers and the dissociation of self-complimentary hydrogen bonding moieties. Specifically, ureidopyrimidone methacrylate and a novel monomer, ureidopyrimidone acrylate, were copolymerized with methyl acrylate, butyl acrylate and bisphenol a ethoxylate diacrylate. Control of Tg from 10-70°C was demonstrated; concentration of hydrogen bonding moieties was varied from 0-40mol%; concentration of the diacrylate was varied from 0-20mol%. The effects of varying concentration of each crosslink type were observed through changes in shape-memory characteristics including stress-strain response and changes in modulus as a function of temperature.

4:30 PM

Thermomechanical Properties of Epoxy Nanocomposites Using Surface Functionalized Silica Nanoparticles: *Muhammad Sajjad*¹; Bernhard Feichtenschlager¹; Silvia Pabisch²; Thomas Koch¹; Sabine Seidler¹; Herwig Peterlik²; Guido Kickelbick³; ¹TU wien; ²University of Vienna,; ³Saarland University.

Surface functionalized silica nanoparticles have been utilized in order to enhance better interaction with the epoxy matrix to produce homogenous nanocomposite films of epoxy. The resulting nanocomposites were characterized by DSC, DMA, TGA and micro hardness techniques. The dispersibility of the particles in organic media and within the polymer matrix was investigated by transmission electron microscopy (TEM) and SAXS. Diglycidylether of Bisphenol F epoxy matrix was embedded with two sized silica nanoparticles (big and small which were prepared by in situ polymerization (via Stoeber process). Silica nanoparticles (one fraction in the lower nanoscale "small" and one in the higher nanorange "big") have been surface functionalized with 3 glycidylpropyltrimethoxysilane (Gly-C3-TMeOS). Due to the surface modification of the silica nanoparticles better dispersibility was achieved throughout the whole matrix which resulted in homogenous and transparent films even at higher nanoparticle loadings. SAXS results confirmed the better structural properties with both sized particles. The mechanical properties of the resulting nanocomposites were generally superior to the pure epoxy matrix. The prepared nanocomposite films showed increase in micro hardness and higher elastic moduli. On the other hand, incorporation of the modified nanoparticles was responsible for some decrease in the glass transition temperature as was evidenced during DSC study and thermal degradation behaviour was almost unaffected by even the use of modified particles.

4:50 PM

Electrospun Polymer Nanofiber Composite as Thermal Neutron Scintillators: *Stephen Young*¹; Indraneel Sen¹; Dayakar Penumadu¹; ¹University of Tennessee, Knoxville

Electrospun polymer nanofibers are attractive due to their volume-tospace, chemical, electrical and unique optical properties. Homeland security has great interest in applications with polymeric scintillation detectors that directly discriminate between neutron and gamma radiations using manufacturing techniques that are inexpensive and which can be effectively implemented to produce large area detectors. Lithium-6 isotope has a significant thermal neutron cross-section and produces high energy charged



particles on thermal neutron absorption. In this research, lithium-6 fluoride (⁶LiF) loaded polymer composite was successfully spun onto a stationary aluminum target creating a thermal neutron scintillator made of randomly oriented fibers. Fiber mats thus obtained were characterized for morphology, optical properties, polymeric properties like glass transition and response to thermal neutrons, alpha, beta and gamma radiation. Fiber matrix was made out of an aryl vinyl polymer and a wavelength shifting fluor with efficient resonant energy transfer characteristics.

5:10 PM

Environmental Reliability Anlysis of Mobile Phone Based on Active Disassembly Using Smart Materials: Liu Zhifeng¹; *Zhao Liuxian*¹; Li Xinyu¹; ¹Hefei University of Technology

Active disassembly using smart material (ADSM) is a method using shape memory material to replace fastener, when it is heated to the stimulated temperature, the product can be disassembled actively. ADSM can enhance the disassembly efficiency greatly; therefore, it gets more and more attention. When the method of ADSM is applied to practical electronic products, such as mobile phone, we need to conduct environmental reliability analysis of the product before it is put into market. This paper is about the environmental reliability analysis of mobile phone based on active disassembly using smart materials. Firstly, establishing the active disassembly model of mobile phone. Then analyzing the impacts of temperature, vibration and collision on the mobile phone. Finally, modifying the structure of mobile phone rationally by analysis.

5:30 PM

Epitaxial and Confinement Effects in Hybrid Organic-Inorganic Nanostructured Composites: *Qiang Yuan*¹; Devesh Misra¹; ¹University of Louisiana at Lafayette

We described here the fundamental mechanisms underlying nucleation and growth of polymer crystals in polymer-carbon nanotube composites. The periodic patterning of polymer lamellar crystals decorated along the carbon nanotube axis is discussed in terms of epitaxial and nanoparticle confinement effect. Furthermore, the dependence of crystallization conditions including pressure and temperature on this novel structure is investigated. As a result, by controlling pressure and crystallization temperature, a high degree of structural control may be achievable, which has profound effect on mechanical properties.

5:50 PM Keynote

Bio-Based Nanocomposites Formed by Nanoparticle-Catalyzed Polymerization of Furfuryl Alcohol: *Rina Tannenbaum*¹; ¹Georgia Institute of Technology, School of Materials Science and Engineering

Bio-based polyfurfuryl alcohol (PFA) matrix nanocomposites have been fabricated by in-situ polymerization of furfuryl alcohol (FA), using montmorillonite nanoclays (MMT) or cellulose whiskers (CW) both as catalysts and matrix modifiers, to enhance thermal performance. The present work describes the polymerization of FA in the presence of MMT and CW and the resulting structure-property relationships. Fabricated nanocomposites were characterized by FTIR and TGA. Both nanocomposites afford a notable increase in the onset of degradation temperature compared to pure PFA. CW-PFA nanocomposites show improved mechanical toughness over previously reported PFA systems. To realize MMT-PFA nanocomposites with increased thermal stability, organomodified MMT clay must be selected. These results also highlight the importance of investigating both the non-oxidative and oxidative degradation behavior of a given material.

Bulk Metallic Glasses VIII: Simulation and Modeling

Sponsored by: The Minerals, Metals and Materials Society, TMS Structural Materials Division, TMS/ASM: Mechanical Behavior of Materials Committee

Program Organizers: Gongyao Wang, University of Tennessee; Peter Liaw, Univ of Tennessee; Hahn Choo, Univ of Tennessee; Yanfei Gao, Univ of Tennessee

Wednesday PM	Room: 6D
March 2, 2011	Location: San Diego Conv. Ctr

Session Chairs: Dan Miracle, AF Research Laboratory; Ju Li, University of Pennsylvania

2:00 PM Invited

Partial Coordination Numbers in Solute-Rich Glasses: *Dan Miracle*¹; Oleg Senkov²; Garth Wilks³; ¹AF Research Laboratory; ²UES, Inc.; ³General Dynamics

A clear description of the atoms in the first coordination shell surrounding each constituent atom is essential for a structural description of metallic glasses. Only limited experimental data are available for these partial coordination numbers. The efficient cluster packing (ECP) model enables prediction of partial coordination numbers, but this has only been developed for solute-lean glasses. The most stable metallic glasses are generally soluterich, so that the first coordination shells around solute and solvent sites are expected to contain both solute and solvent atoms. We extend the earlier model to enable prediction of partial coordination numbers in solute-rich binary glasses. Results from predictions of this new model are compared with available experimental data. This analysis enables bond counting and packing efficiencies to be estimated. Results from these calculations will be presented and discussed with regard to the recent topological fluctuation theory (TFT) of metallic glasses.

2:20 PM

Atomic-Scale Modeling of Chemical Effects on the Glass-Forming Ability of Metallic Glass Alloys: *Logan Ward*¹; Katharine Flores¹; Wolfgang Windl¹; ¹The Ohio State University

Atomic size ratio, number of constituents, and enthalpy of mixing are well-known rules for selecting constituents for metallic glasses. The role of atomic size ratio in the glass-forming ability has been examined through several experimental and computational studies. However, there has been little research into other aspects of atomic interactions, such as bond energy and the curvature of the potential well. In this research, the influence of these interactions on glass-forming ability was studied through molecular dynamics simulations. A method for determining the fragility of a supercooled metallic liquid was developed to indicate glass-forming ability. These methods were then applied to systems with modified potentials to determine the effects of curvature and bond energy changes. A major goal of this work is to develop new rules for constituent selection, as the bond energy and well shape can be directly linked to many thermal and elastic properties of the constituent materials.

2:30 PM Invited

Cold Versus Hot Shear Banding in Metallic Glass: A Stick-Slip Model Compared with Experiments: Evan Ma¹; ¹Johns Hopkins University

Recent experiments (e.g., by T.G. Nieh et al., Y. Li et al., F. Dalla Torre et al.) have revealed that for some BMGs, the serrations in the compressive stress-strain curve correspond to the sliding of a single shear band in a stop-and-go fashion. The details of the serration (e.g., the step size of the growing shear offset and the stability of the shear) depend on the sample size and machine stiffness. Here we illustrate a stick-slip model to explain the origin of the serration and the effects of sample size and machine stiffness. The model also predicts the regime where the shear band becomes hot and unstable from the get-go. The predicted striation spacing, size of the shear offset, sliding speed, as well as the temperature reached and the duration

of the shear band stop-and-go cycle, all quantitatively agree with the experimental observations.

2:50 PM

Condensed Bond Enthalpies in Metal-Nonmetal and Metal-Semimetal Compounds: *Amanda Dahlman*¹; Daniel Miracle¹; Garth Wilks¹; ¹Air Force Research Laboratory

Bond enthalpies are widely used measures of the energy contained in a bond between atoms in molecular gases and have recently been extended to metallic systems in the condensed state. The further extension of this concept to metal-semimetal and metal-nonmetal compounds is performed using readily available thermodynamic and crystallographic data. These determined values will be critically examined by exploring trends and relationships between compounds.

3:00 PM Invited

Effects of the Potential Landscape on Metallic Liquids and Alloys: James Morris¹; ¹Oak Ridge National Laboratory

One approach to understanding the transition between the liquid and glass states has been through the concept of the potential landscape, which has been used to demonstrate that there are three distinct temperature regimes: the high-temperature liquid, the low-temperature glass, and an intermediate "potential dominated" regime. This will be reviewed, with a particular emphasis on recent simulation results on metallic glasses. We demonstrate that there are experimentally measureable signatures of the associated transition from the high temperature regime to the intermediate regime, which show up in simulations of both model systems and more realistic potentials. The different regions show different diffusive, structural and thermodynamic signatures. The fragility of the liquid is shown to be correlated with the Poisson ratio of the glass phase, in accordance with recent experimental and theoretical results. This research was sponsored by the Division of Materials Sciences and Engineering, U.S. Department of Energy, Office of Basic Energy Sciences.

3:20 PM

Continuum Modeling of Bulk Metallic Glasses and Composites: *Fadi Abdeljawad*¹; Max Fontus²; Lisa Manning¹; Mikko Haataja¹; ¹Princeton University; ²Prairie View A&M University

At low temperatures, monolithic bulk metallic glasses (BMGs) exhibit high strength and large elasticity limits. On the other hand, BMGs lack overall ductility due to highly localized deformation mechanisms. Recent experimental findings suggest that the problem of catastrophic failure by shear band propagation in BMGs can be mitigated by tailoring microstructural features at different length scales to promote more homogeneous plastic deformation. Herein, based on a continuum approach capable of capturing strain softening, we present a quantitative analysis of the effects of microstructure on the deformation behavior of monolithic BMGs and BMG composites. In particular, simulations highlight the importance of short-ranged structural correlations on ductility in monolithic BMGs and demonstrate that ductile phase morphology and its associated length scales control the ductility of BMG composites. In broader terms, our results provide new avenues for further improvements to the mechanical properties of BMGs.

3:30 PM Break

3:40 PM Invited

Stress and Fracture Analyses of Bulk Metallic Glasses under Compressive Loading: Leon Keer¹; Xiaoqing Jin¹; Gongyao Wang²; Oleg Senkov³; Daniel Miracle³; Peter Liaw²; Jules Raphael⁴; ¹Northwestern University; ²The University of Tennessee, Knoxville; ³Air Force Research Laboratory; ⁴Columbus McKinnon Corporation

Fracture under compressive loading exhibits distinct behaviors than that under tensile loading. Various crack-propagation modes have been identified for compression failure of bulk metallic glasses (BMGs). Experiments on Ca-based BMG under uniaxial compression indicate that cracks initiate from micro porosity and propagate in a direction generally parallel to the loading axis. Micromechanical stress analysis shows that pores cause axial tensile splitting microcracks emanating from the pore. A simplified computational model based on the linear elastic fracture mechanics (LEFM) is proposed to investigate the crack-extension behaviors under compressive load. The stable crack length is characterized by a dimensionless fracture-mechanics quantity required to attain the associated crack length. The stability of crack growth is examined based on the stress-intensity-factor (SIF) calculation, and its dependence on the loading and geometric conditions is discussed in this study. The present modeling provides heuristic insights into the different failure modes under compression.

4:00 PM Invited

Deformation and Failure of Glasses at Nanoscale: *Ju Li*¹; ¹University of Pennsylvania

Recent experiments on nanoscale amorphous materials have suggested interesting ductility - size scale dependencies (PNAS 104, 11155; PRB 77, 155419). Such size effect may shed light on the connection between plastic deformation and underlying spatio-temporal hierarchies of structural flow defects, the smallest of which is a single shear transformation zone ~1nm^3. A mesoscale computational model on the same level as discrete dislocation dynamics for crystalline materials is constructed, which utilizes detailed statistical information about shear transformations, damage accumulations and damage repairs from atomistic simulations.

4:20 PM

Correlation between Elastic Modulus and Intrinsic Plasticity of Metallic Glass: The Roles of Atomic Configuration and Alloy Composition: *Yongqiang Cheng*¹; Ajing Cao¹; Evan Ma¹; ¹Johns Hopkins University

Recent experiments revealed intriguing correlations between elastic modulus and plasticity of MGs. The shear modulus (G) to bulk modulus (B) ratio G/B was found to be a useful indicator of the intrinsic plasticity. We will discuss how the structural order (atomic configuration) and the composition (constituent elements) influence the intrinsic mechanical properties of monolithic MGs, and what common basis underlies the apparent property correlations. Using computer simulation, it is found that B is primarily determined by the constituent elements and the composition, while G is more sensitive to the degree of structural order. Using more ductile metals (in its crystalline form) and/or creating more disordered structure would therefore result in a lower G/B ratio of the MG, as well as less strain localization (enhanced intrinsic plasticity). Such a microscopic picture for the macroscopic property correlation is expected to facilitate the search of MGs with desired properties.

4:30 PM Invited

Equation of State of Metallic Glasses: Mo Li¹; ¹Georgia Institute of Technology

Equation of state (EOS) relates pressure, volume and other thermodynamic variables in a material system under hydrostatic loading. The EOS of metallic glasses exhibits marked features that are different from those of many crystalline phases: a softer regime at low pressure and a harder regime at high pressure, and a hysteresis loop. There are also reports of polymorphic transitions between different amorphous phases. In this talk, I will present our recent work using both atomistic and analytical work on EOS in model metallic glasses. We show that the EOS is closely related to the topological packing of the glassy phases and the physical properties of constituent alloy elements; there exist two regimes under hydrostatic pressure, which are connected by a topological phase transition. We will discuss and put forward a measure for the transition. The EOS from the atomistic simulation and those from various models will be compared and discussed.

4:50 PM Invited

Molecular Dynamics Simulations of Metallic Glasses under Cyclic Loading: *Yunfeng Shi*¹; Despina Louca²; Gongyao Wang³; Peter Liaw³; ¹Rensselaer Polytechnic Institute; ²University of Virginia; ³The University of Tennessee

We present a molecular dynamics study of cyclic loading tests on model metallic-glass nanowires. Both compression-compression and tension-tension cyclic loading are imposed on the testing sample up to 100 cycles.



The maximum strain is chosen to be 4 %, which is above the linear elastic regime but without shear band formation. The cyclic-loaded samples exhibit spatially uncorrelated shear band formation, which indicates the absence of accumulated structural damages. Upon compression-compression cyclic loading, it was found that the metallic-glass nanowire hardens in compression tests, while softens in tensile tests. However, upon tension-tension cyclic loading, it was found that the metallic-glass nanowire softens in compression tests, while hardens in tensile tests. Such asymmetric hardening behavior can be explained in terms of anisotropic distribution of icosahedral pairs, which evolves during cyclic loading.

5:10 PM

Phase-Field Modeling of Phase Transformations in Glass Forming Alloys: *Tao Wang*¹; Ralph Napolitano²; ¹Ames Lab; ²Ames Lab & Iowa State University

A phase-field model is presented for phase transformations in glass forming alloys. The competitions among stable and metastable phases are simulated for Cu-Zr alloys. The free-energy density is developed from atomistic calculations and thermodynamic modeling and some kinetic properties are extracted from molecular dynamics simulations. The simulation results provide a better understanding of the influences of the underlying thermodynamic and kinetic factors.

5:20 PM Invited

Molecular Dynamics Studies of Cu-Zr-Al Metallic Glasses in Connection with In-Situ Synchrotron Experiment: *Yunche Wang*¹; Chun-Yi Wu¹; Feng Jiang²; Jinn Chu³; Peter Liaw²; ¹National Cheng Kung University; ²The University of Tennessee; ³National Taiwan University of Science and Technology

Cu-Zr-Al glass-forming alloys have received increased attentions due to minor changes in the aluminium content drastically affecting the plasticity of the metallic glass. Molecular dynamics (MD) thin-film models of the alloys have been constructed by sputter-deposition simulation with argon as working gas on substrate. The simulated, as-deposited films were amorphous. Results from uniaxial loading/unloading MD simulations were compared with data from in-situ synchrotron experiments on radial distribution functions, Young's modulus and Poisson's ratio of the (Cu50Zr50)100-xAlx (in atomic percent, at%) amorphous alloys with x less than 12. Young's modulus and Poisson's ratio of the cube samples were calculated from the MD simulations, and they were found to be in agreement with experimental data. Strong correlations between the loose-packing local structures and the plasticity of the glass-forming alloys were found. Atomic structures at short and medium range orders of the alloys will be discussed.

5:40 PM

Correlations between Local Stresses and Moduli in Model Metallic Glasses: Karimi Kamran¹; *Craig Maloney*¹; ¹Carnegie Mellon University / Civil & Environmental Engineering

Molecular dynamics (MD) simulations of sheared model metallic glasses have long shown evidence for localized flow emph{events}. However, meaningful ways for defining flow emph{defects} where the system has a propensity to yield have been elusive. We present results of MD simulations of slowly sheared Lennard-Jones glasses. We show that the deviatoric component of the coarse grained stress tensor shows a non-trivial power-law decay with coarse-graining size refelecting a scale-invariant local anisotropy. We furthermore discuss how these scalings of the stress field are related to similar scalings in the elastic moduli. The results call into question the naive use of the stress field to identify defective regions in a glass.

5:50 PM Invited

Local Atomic Structure of Ca-Mg-Zn Bulk Metallic Glasses: Oleg Senkov¹; Emma Barney²; Yongqiang Cheng³; Daniel Miracle¹; Evan Ma³; Alex Hannon²; ¹Air Force Research Laboratory; ²ISIS, Rutherford Appleton Laboratory; ³John Hopkins University

Amorphous structure of ternary $Ca_{60}Mg_XZn_{40,X}$ metallic glasses (X = 10, 15, 20, and 25 at.%) was modeled by Reverse Monte Carlo (RMC) and *ab initio* Molecular Dynamics (MD) techniques. The RMC and MD modeled

structures were statistically the same and consistent with experimental neutron and X-ray diffraction data. The amorphous structure was described as a mixture of Mg and Zn centered atomic clusters, with Ca dominating in the first shell. A coordination number (CN) of 10 (with about 7 Ca and 3 (Mg+Zn) atoms) was most common for the Zn-centered clusters. CN = 11 and 12 (with about 7-8 Ca and 4 (Mg+Zn) atoms) were most common for Mg-centered clusters. Analysis of the neighbor environment and bond angle distributions suggested near-equilateral triangles and pentagonal bipyramids to be the most common nearest atom configurations. The results were compared with recently proposed cluster packing models.

6:10 PM

Predicting the Properties of High Entropy Alloys from Electronic Structure: *Andrew Cunliffe*¹; Colin Freeman¹; Iain Todd¹; ¹University of Sheffield

The electronic structures of the High Entropy Alloys (HEAs); CoCrFeNiAl (bcc) and CoCrFeNiTi (fcc) have been modelled using Density Functional Theory (DFT). The Fermi energy and free electron density from the model have been used to predict mechanical and physical properties of the alloys. This approach has allowed prediction of resistivity, heat capacity, thermal expansion coefficient and bulk modulus of the alloys. The predicted bulk modulii for CoCrFeNiAl and CoCrFeNiTi are 58.7 GPa and 41.36 GPa respectively. The adoption of different crystal symmetries is also explained in terms of the different free electron densities of the alloys. The properties of HEAs are difficult to predict, as they have no obvious base metal to extrapolate from. The use of DFT modelling in the treatment of HEAs allows the prediction of properties from composition and gives a better understanding of the behaviour of these novel materials.

6:20 PM Invited

Predicating the Bulk Elastic Modulus and Density of Metallic Glasses by First Principles Calculation: *X. Hui*¹; *Z. P. Lu*¹; G. L. Chen¹; Z. K. Liu²; ¹University of Science and Technology Beijing; ²The Pennsylvania State University

Metallic glasses are generally regarded as elastically isotropic, and they behave as an elastic continuum at low temperatures. Here we present a new way for the predication of bulk moduli and densities of metallic glasses by ab initio molecular dynamics and first principles calculation. Using this approach, we obtained the bulk moduli and densities for Zr-, Cu-, Co, and Ti based bulk metallic glasses, and found that the predicated results are in good agreement with the experimental data. Additionally, some other physical properties can be also deduced from this work.

Cast Shop for Aluminum Production: Grain Refinement, Alloying, Solidification and Casting

Sponsored by: The Minerals, Metals and Materials Society, TMS Light Metals Division, TMS: Aluminum Committee, TMS: Aluminum Processing Committee

Program Örganizers: Geoffrey Brooks, Swinburne University of Technology; John Grandfield, Grandfield Technology Pty Ltd

Wednesday PM	Room: 16A
March 2, 2011	Location: San Diego Conv. Ctr

Session Chairs: Peter Schumacher, University of Leoben; Arild Hakonsen, Hydo Alusminium Hycast a.s.

2:00 PM Introductory Comments

2:05 PM

Hycast Gas Cushion (GC) Billet Casting System: Idar Steen¹; Arild Hakonsen; ¹Hydro Aluminium

The Hycast GC Billet Casting System for casting of extrusion billets has been in use in Hydro Aluminium casthouses (both primary and remelt) for more than 20 years. The technology is based on a patented mould construction utilizing dual graphite rings for optimal distribution of oil

3:45 PM Break

3:55 PM

Modification and Grain Refinement of Eutectics to Improve Performance of Al-Si Castings: *Milan Felberbaum*¹; Arne Dahle; ¹The University of Oueensland

The formulation of alloy compositions for aluminium castings has not changed significantly for decades. Strontium (Sr) modification is commonly used to obtain a refined fibrous morphology of eutectic in Al-Si foundry alloys, and grain refinement can be used to refine the primary Al dendrites. Compared to the coarse plate-like unmodified silicon morphology, the refined fibrous eutectic structure can substantively improve the mechanical properties particularly ductility and fatigue. However, a problem often associated with Sr modification is a change in porosity - distribution and amount. A new alloy technology has been developed to produce castings combining a well-modified eutectic with reduced porosity. This can be achieved by providing effective substrates for the nucleation and growth of eutectic cells. Further, the additions do not change the overall alloy specification, ie. they involve trace level additions. This paper will present the current status in the development and commercialisation of the new eutectic grain refiner and modifier.

4:20 PM

Production of Al-Ti-C Grain Refiners with the Addition of Elemental Carbon and K2TiF6: *Fatih Toptan*¹; Isil Kerti¹; Sibel Daglilar¹; Ahmet Sagin¹; Omer Faruk Karadeniz¹; Aysin Ambarkutuk¹; ¹Yildiz Technical University

Al–Ti–B grain refiners are widely used as aluminium grain refiners despite the problems in application Al–Ti–C refiners have an increasing demand in recent years. In the present work, Al-Ti-C grain refiners with different Ti:C ratios were produced by in-situ method with the addition of elemental carbon into the Al-Ti master alloy and addition of K2TiF6 and elemental carbon powder mixture into the commercially pure aluminium. Microstructures were characterised by optic microscope and scanning electron microscope equipped with energy dispersive spectroscopy. The effects of production method and Ti:C ratio on the grain refinement process was investigated with Alcoa Coldfinger Test and optimum conditions were determined. Commercial Al-Ti-B grain refiners also tested with Alcoa Coldfinger Test in identical conditions and it has been stated that, insitu Al–Ti–C refiners are more effective than commercial Al-Ti-B grain refiners in grain refining.

4:45 PM

Effect of Mechanical Vibrations on Microstructure Refinement of Al-7Mass% Si Alloys: *Takuya Tamura*¹; Toshiro Matsuki²; Kenji Miwa¹; ¹National Institute of Advanced Industrial Science and Technology (AIST); ²Yamagata Research Institute of Technology

Mechanical vibration treatment is known to induce microstructure refinement. However, it is not completely understood which factor of vibrations is important for microstructure refinement. Factors of vibrations include frequency, acceleration, velocity and amplitude. Thus, this study aims to investigate effect of mechanical vibrations on microstructure refinement of Al-7mass%Si alloys by a systematic study. As a result, it was found that velocity of vibrations is important factor for primary crystals refinement. The square of the velocity corresponds to the energy of mechanical vibrations. Thus, the energy of mechanical vibrations promotes microstructure refinement during solidification. Moreover, it was found that primary crystal particles become rosette-like and fine when the mechanical vibrations are applied to the melt from about 923K to 888K (liquidus - 2K). This result is considered to indicate that the mechanical vibrations promote heterogeneous nucleation.

5:10 PM

Predicting the Response of Aluminum Casting Alloys to Heat Treatment: *Chang-Kai Wu*¹; Makhlouf Makhlouf¹; ¹Worcester Polytechnic Institute

The mechanical properties of aluminum alloy castings can be greatly improved by a precipitation hardening. Typically, this heat treatment consists of three steps: (1) solutionizing, (2) quenching, and (3) aging; and is

and gas into the mould. Annual production capacity in existing casthouses equipped with Hycast GC is more than 2 million tons /year. The diameter range is from 152mm up to 405mm (6"-16"). The Hycast GC casting system produces excellent and consistent metal quality in combination with high productivity, excellent metal recovery and low maintenance cost. The technology is now available for the aluminium industry also outside Hydro Aluminium. This paper describes the main technical achievements of the technology with focus on operational issues as HES, metal recovery, metal quality and productivity.

2:30 PM

Studies of Fluid Flow and Meniscus Behavior during Horizontal Single Belt Casting (HSBC) of Thin Metallic Strips: *Donghui Li*¹; Jaspreet Gill¹; Mihaiela Isac¹; Roderick Guthrie¹; ¹McGill Metals Processing Centre

Horizontal Single Belt Casting (HSBC) of strips is a green strip casting technology potentially capable of replacing current slab caster operations. As-cast strip bottom surface quality is a key factor for near-net shape casting operations. The meniscus behavior at the triple point of gas, substrate, and liquid metal when the melt first touches the moving belt is important to surface quality, as is the way in which the melt is in subsequent contact with the chill substrate. In this paper, meniscus behavior and fluid flow mechanisms were analyzed and predicted through mathematical modeling, using ANSYS Fluent software. The mathematical modeling of meniscus behavior and fluid flow was further supported by physical water modeling, and was validated through HSBC simulator tests using aluminum alloys.

2:55 PM

Development of Alba High Speed Alloy: Abdulla Ahmed¹; *Jalal Hassan*¹; ¹Aluminium Bahrain (Alba)

Aluminium Bahrain has developed inhouse an alloy called "ALBA HIGH SPEED 6063.10", which is a variant of alloy AA 6063. The driving force behind this has been, the ever standing requirement of extruders to attain progressively higher extrusion speeds, thereby boosting productivity. Small and controlled amount of Mn and Mg addition to alloy 6063 was found to help in improving extrusion speeds and reduce die pick-up thereby improving the surface appearance. The reason was attributed to improved beta to alpha transformation rates at the microstructure level. This was achieved by having tight control of Mn addition to reduce the band from 0 - 0.10 % in normal 6063 alloy to 0.03% - 0.06% in 6063.10. In addition controlling the Mg addition to 0.45 % - 0.51 % in the new alloy, assisted in better distribution of Mg2Si precipitates in the matrix during the cooling process post soaking at 580C.

3:20 PM

Dissolution Studies of Si Metal in Liquid Al under Different Forced Convection Conditions: *Mehran Seyed Ahmadi*¹; Stavros Argyropoulos¹; Markus Bussmann¹; Don Doutre²; ¹University of Toronto; ²Novelis Global Technology Center

The dissolution of Silicon metal into liquid Aluminum is a very slow process. The main focus of this research is to develop procedures which contribute to speeding up the dissolution of Silicon metal into Aluminum bath.Experimental dissolution studies of Silicon metal in liquid Aluminum will be reported under natural and forced convection conditions. A unique Revolving Liquid Metal Tank (RLMT) is being used, capable of stirring approximately 50 kg of liquid Aluminum to create desired tangential velocities. In addition experimental work on Silicon dissolution in liquid Aluminum under conditions of two-phase flow, utilizing Nitrogen gas, in liquid Aluminum will also be reported. Silicon dissolution into liquid Aluminum under single-phase flow will be compared with results obtained in two-phase flow conditions. Finally, the commercial software FLOW-3D is being adapted to predict the various transport phenomena involved; comparisons will be presented between experimental and predicted results.

WEDNESDAY PM



performed by first heating the casting to and maintaining it at a temperature that is a few degrees lower than the solidus temperature of the alloy in order to form a single-phase solid solution. Then rapidly quenching the casting in a cold (or warm) fluid in order to form a supersaturated non-equilibrium solid solution; and finally, reheating the casting to the aging temperature where nucleation and growth of the strengthening precipitate(s) can occur. Obviously, these processing steps involve significant thermal changes that may be different from location to location in the casting. The objective of this project is to develop a finite element model and the necessary material database that allow predicting these physical and material property changes.

Characterization of Minerals, Metals and Materials: Nanomaterials, Nanotechniques and Thin Films

Sponsored by: The Minerals, Metals and Materials Society, TMS Extraction and Processing Division, TMS/ASM: Composite Materials Committee, TMS: Materials Characterization Committee *Program Organizer:* Sergio Monteiro, State University of the Northern Rio de Janeiro - UENF

Wednesday PM	Room: 14B
March 2, 2011	Location: San Diego Conv. Ctr

Session Chairs: Shadia Ikhmayies, Al Isra University; Jozef Zrnik, Comtes FHT, Inc.

2:00 PM

Microstructural Characterization of Nanomaterials Produced from Co-Products of the Ethanol Production (DDGS): Joner Alves¹; *Chuanwei Zhuo*²; Yiannis Levendis²; Jorge Tenório¹; ¹University of Sao Paulo; ²Northeastern University

Reduction of combustion-emitted greenhouse gases, which are associated with global warming, may be achieved by use of CO2-neutral alternative fuels, such as bio-ethanol. Distillers Dried Grains with Solubles (DDGS) are the main co-products of the corn-grain-based ethanol industries. In 2009, the North American production of ethanol from corn was about 38 billion liters, which generated approximately 31.5 million tons of DDGS. Samples of DDGS were pyrolysed at temperatures of 600-1000 °C in a two-stage laminar-flow horizontal furnace, and a catalyst system was used to synthesize nanomaterials. This work presents a microstructural characterization of these nanomaterials by scanning electron microscopy (SEM) and transmission electron microscopy (TEM). Results showed that the nanomaterials produced from pyrolysis of DDGS were in the form of long, entangled, rope-like structures with rugged walls, lengths in the tens of microns, and axially non-uniform diameters in the range of 100-300 nm.

2:15 PM

Photoluminescence of the Interface of SnO2:F/CdS:In/CdTe Thin Film Solar Cells Prepared Partially by the Spray Pyrolysis Technique: *Shadia Ikhmayies*¹; Riyad Ahmad-Bitar²; ¹Al Isra University; ²Al-Hussain Ben Talal University, Ma'an Jordan

CdS/CdTe solar cells were built by depositing a 200 nm layer of SnO2:F on glass substrates by the spray pyrolysis (SP) technique, a 500 nm CdS:In layer by the same technique and a 1-1.5 μ m CdTe layer by vacuum evaporation. The cells were CdCl2 heat-treated in nitrogen atmosphere for 30 minutes at 350°C. The photoluminescence (PL) spectra were measured at the CdS/CdTe interface for two cells with different values of the CdTe layer's thickness at temperature T = 60 K. A deconvolution peak fit was performed from which it is found that the peaks are characteristic of the solid solution CdSxTe1-x. The parabolic relation that relates the bandgap energy with the composition was used to estimate x, where x is [S]/([Te]+[S]) and [Te], [S] are the concentrations of Te and S atoms respectively. The results show that the interface is smooth and the change of the bandgap occurs gradually.

2:30 PM

Particle Size Analysis of Metallic Nanoparticles Using Ultra-High Resolution Mass Sensors: *Kerri-Ann Hue*¹; Ken Babcock²; Patrick O'Hagan¹; Larry Unger¹; ¹Particle Sizing Systems; ²Affinity Biosensors

Metallic nanoparticles exhibit properties that are significantly different from individual atoms or bulk materials. Their applications are diverse and have varying applications in areas such as cancer treatment, biochemical sensors, nanoelectronics, and drug delivery. For each of these applications extensive characterization must be performed in order to probe the unique properties of these nanoparticles. In this study, ultra-high resolution mass sensors consisting of MEMs-fabricated, suspended microchannel resonators were used to determine the size and concentration of metallic nanoparticles. With femtogram (10E-15 g) mass resolution, ultra-high resolution mass sensors can weigh individual particles suspended in fluid, and so measure their mass, density, and size. Particle size analysis with these sensors provides excellent accuracy and resolution compared to mature technologies such as light scattering. This technique also provides quantitative information via the ability count particles.

2:45 PM

Observation of Heterogeneous Deformation in Commercial Purity Ti Using Nano-Indentation: *Yiyi Yang*¹; Claudio Zambaldi²; Leyun Wang¹; Philip Eisenlohr²; Thomas Bieler¹; Martin Crimp¹; ¹Michigan State University; ²Max-Planck-Institut für Eisenforschung

Nano-indentation is widely applied to measure mechanical properties on a local scale, providing an opportunity to understand how the local structure, such as grain boundary and grain orientation is linked to observed local deformation behavior. In this work, a series of conical nano-indentations were performed on a patch of grains in polycrystalline titanium of commercial purity (and hexagonal lattice structure). Atomic force microscopy (AFM) was then used to observe the resulting surface topography due to the dislocation pile-up formation, which is heterogeneous in different grains. The driving mechanism for pile-ups is almost crystallographically dependent in that the influence of stress concentrations due to indenter shapes is negligible. The dependence of nanohardness and plastic zone size upon different grain orientation was studied. Support was provided by NSF grant DMR-0710570 and DFG grant EI 681/2-1.

3:00 PM

Production of CdS1-xTex Thin Films and Bandgap Investigation of the Produced Solid Solution: *Shadia Ikhmayies*¹; Riyad Ahmad-Bitar²; ¹Al Isra University; ²Al-Hussain Ben Talal University, Ma'an Jordan

CdS1-xTex thin films with $0 \le x \le 0.3$ were prepared on glass substrates by the annealing of CdS:In thin films produced by the spray pyrolysis technique. The annealing was performed in nitrogen atmosphere at 400°C in the presence of Te vapor. The compositions of the films were determined by energy dispersive X-ray detection (EDAX) measurements. Scanning electron microscopy (SEM) was used to investigate the morphology of the films. The transmittance of the films was measured at room temperature in the wavelength range 400-1100 nm and used to produce the absorbance of the films. The first derivative of the absorbance was used to estimate the optical bandgap energy Eg by using the minima in the first derivative. The relation between the bandgap energy and the fraction x was found to fit with a parabola and bandgaps in the range 2.196=Eg=2.480 eV were obtained. Urbach tailing in the bandgap was also investigated.

3:15 PM

Studying the Microstructural Evolution of Nanocrystalline Metals in Response to External Straining by Automated Acquisition and Indexing of Diffraction Patterns in the TEM: *Kai Zweiacker*¹; Andreas Kulovits¹; Jorg Wiezorek¹; ¹University of Pittsburgh

Nano-crystalline Ni with an average grain size of 40nm has been cold deformed at room temperature by rolling to thickness reductions of up to 85%. In this grain size regime plastic deformation is facilitated by dislocation activity. Dislocation–grain boundary interactions dominate during plastic flow, resulting in grain boundary character evolution and inducing grain coalescence. We used automated acquisition and indexing of precession

diffraction patterns and hollow-cone dark-field imaging in the transmission electron microscope to monitor the evolution of populations of grains orientations in these nanocrystalline aggregates. The high spatial resolution of the TEM allowed us to monitor these changes on the nanoscale, which was previously not possible with SEM based approaches. We acknowledge use of the facilities of the Materials Micro-Characterization Laboratory of the Department of Mechanical Engineering and Materials Science, University of Pittsburgh, and support by a grant from the National Science foundation NSF-CMS 0140317.

3:30 PM Break

3:45 PM Invited

An Investigation of the Photoluminescence and Transmittance of CdS1-xTex Thin Films: *Shadia Ikhmayies*¹; Riyad Ahmad-Bitar²; ¹Al Isra University; ²Al-Hussain Ben Talal University, Ma'an Jordan

CdS1-xTex thin films were prepared by first producing CdS:In thin films by the spray pyrolysis (SP) technique and then annealing the films in the presence of Te vapor in nitrogen atmosphere. X-Ray diffraction (XRD) measurements showed that the films are polycrystalline with the wurtzite structure. Transmittance measurements were recorded at room temperature in the wavelength range 400-900 nm and used to deduce the absorbance. The first derivative of the absorbance was calculated and used to find the values of the bandgap energy, where more than one bandgap was obtained for each film. These results show that the films are inhomogeneous or the composition differs with location. The photoluminescence (PL)was recorded at T = 60 K and a deconvolution peak fit was performed for each spectrum. The results of the PL spectra are consistent with those obtained from the first derivative and confirm the inhomogeneity of the films.

4:15 PM

Convergent Beam Electron Diffraction of Nanomaterials: Karen Henry¹; Richard Vanfleet²; *Gregory Thompson*¹; ¹University of Alabama; ²Brigham Young University

The most readily available technique for the determination of long-range order parameter S is X-ray diffraction. Experimentally, S is determined by measuring the total integrated peak intensities of the superlattice and fundamental reflections according to kinematical scattering theory. However, X-ray scattering from thin films and nanoparticles can be very small and difficult to measure with laboratory diffractometers. In contrast, electron scattering can be more amenable for diffraction studies of small volumes, though strong interaction of electrons with the material results in multiple scattering events. As a result, the scaling of the ratio of integrated intensities is no longer valid and S determination becomes more complex. To correctly account for multiple electron scattering events, a multislice simulation is necessary to predict the convergent beam electron diffraction (CBED) intensities for a given order parameter, orientation and thickness. This talk will address these techniques for thin films and nanoparticles.

4:30 PM

Measuring the Elastic Modulus of Polymers by Nanoindentation with an Atomic Force Microscope: Daniel Hoffman¹; Ibrahim Miskioglu¹; Katerina Aifantis²; *Jaroslaw Drelich*¹; ¹Michigan Technological University; ²Aristotle University of Thessaloniki

A new method to determine the elastic modulus of a material using the atomic force microscope (AFM) has been proposed by Pethica et al. (Nanotechnology 19, 2008, 495713). This method models the cantilever and the sample as two springs in a series. The ratio of the cantilever spring constant (k) to diameter of the tip (2a) is treated in the model as one parameter (α =k/2a). The value of \945:, along with the cantilever sensitivity, are determined on two reference samples with known mechanical properties and then used to find the elastic modulus of an unknown sample. To determine the reliability and accuracy of this technique it was tested on several polymers. Traditional depth-sensing nanoindentation was preformed for comparison. Using both methods, the elastic modulus of the polymers tested was calculated. The elastic modulus values from the AFM were within ±(5-20)% of the nanoindenter results.

4:45 PM

Microstructural Analysis of Nanomaterials Synthesized from Unserviceable Tires: Joner Alves¹; *Chuanwei Zhuo*²; Yiannis Levendis²; Jorge Tenório¹; ¹University of Sao Paulo; ²Northeastern University

The ever increasing number of automobiles and the consequential increase in consumption of tires have generated a pressing environmental issue, concerning the disposal of unserviceable tires. The worldwide disposed of waste tires is approximately 1 billion units per year and this amount is expected to increase by 2% each year. This work presents a microstructural characterization of nanomaterials synthesized in a catalyst system from the effluent of burning waste tire chips in a horizontal two-stage laminar-flow furnace. Controlled combustion of waste tire chips took place at temperatures of 900 or 1000°C, and stainless steel meshes were used to synthesize the nanomaterials at 1000°C. Produced materials were analyzed by scanning electron microscopy (SEM) and transmission electron microscopy (TEM). The catalyst meshes were covered by materials with diameters of 20 to 200 nm and lengths of about 40 μ m. They possessed structures similar to those of carbon nanotubes.

5:00 PM

Synthesis of Sr-Doped LaP₃O₉ Films in Phosphoric Acid Solutions and Their Proton Conduction Properties: *Takayuki Onishi*¹; Naoyuki Hatada¹; Kazuaki Toyoura¹; Yoshitaro Nose¹; Tetsuya Uda¹; ¹Kyoto University

Lanthanum polyphosphate, LaP₃O₉, is considered as a potential solid electrolyte in fuel cells. It exhibits relatively high proton conductivity when doped with alkaline earth metals such as Sr. For practical use, however, further enhancement of the conductivity is necessary while the proton conductivity mechanism has not been understood. For example, it is not clear whether the bulk conduction or grain boundary conduction is dominant. It is also unknown which crystallographic direction is the best for the proton conduction. To determine them, we aimed at measuring the proton conductivity of polycrystalline Sr-doped La₃O₉ with different grain sizes or specific crystallographic orientations. However it is difficult to obtain these samples by solid-state synthesis. In this study, therefore, we attempted to synthesize polycrystalline films of Sr-doped La₃O₉ in condensed phosphoric acid solutions. Then the grain size, crystallographic orientation, and the conductivity of the samples were analyzed and compared with previously reported values.

5:15 PM

Effects of Heat Treatment Schedule on the Crystallization Behavior and Thermal Expansion of a LiS₂ Based Glass-Ceramic: Onder Guney¹; Erdem Demirkesen¹; ¹Istanbul Technical University

In this study, the crystallization and thermal expansion coefficient behavior of a lithium disilicate (LiS₂) based glass-ceramic which is derived from SiO₂-LiO₂-Al₂O₃-K₂O-ZrO₂ system was investigated by using x-ray diffraction (XRD),high temperature x-ray diffraction (HTXRD), differential thermal analysis (DTA) and dilatometer techniques. Analytical reagent grade chemicals were used as raw materials for preparing glass batches. Nucleation and crystal growth heat treatments were planned according to DTA results. Amorphous and crystalline phases developed during the heat treatments, were determined by quantitative XRD. Applied heat treatments showed the formation of metastable lithium silicate (LS) and its transformation to stable LS₂. The thermal expansion coefficients of glass-ceramics were also measured depending on the applied heat treatments.

5:30 PM

Characterization of Nanocrystalline Silver Fabricated by Warm-Vacuum-Compaction Method: *Wei Liu*¹; Qionghua Zhou¹; ¹Henan University of Science and Technology

Nanocrystalline silver bulk material with average grain size of 20.3 nm was prepared by warm-vacuum-compaction method. The as-prepared nanocrystalline silver was characterized by X-ray diffraction (XRD), differential scanning calarmeutry analysis (DSC), thermogravimetric analysis (TG), and 6157 type Electrometer test, respectively. The experimental results show that the average grain size and microstrain of the nanocrystalline silver are 20.3 nm and 0.088%. The melting point and melting enthalpy are



955.7°C and 82.34 J/g, which are lower than that of coarse-grained silver by 6 K and 22.6J/g, respectively. The electrical resistivity of nanocrystlline silver increases with higher temperature when the range of temperature is between 233K and 293K. The electrical resistivity at 293 K is $1.475 \times 10-7$ O•m, which is higher than that of coarse-grained silver by a factor of 9.

Characterization of Nuclear Reactor Materials and Components with Neutron and Synchrotron Radiation: Development of Nuclear Energy Systems and Fuels

Sponsored by: The Minerals, Metals and Materials Society, TMS Structural Materials Division, TMS/ASM: Nuclear Materials Committee

Program Organizers: Matthew Kerr, US Nuclear Regulatory Commission; Meimei Li, Argonne National Lab; Jonathan Almer, Argonne National Laboratory; Donald Brown, Los Alamos National Lab

Wednesday PM	Room: 4
March 2, 2011	Location: San Diego Conv. Ctr

Session Chairs: Meimei Li, Argonne National Lab; Matthew Kerr, US Nuclear Regulatory Commission

2:00 PM Keynote

Using Synchrotron Radiation to Study Nuclear Energy Systems: Lynda Soderholm¹; ¹Argonne National Laboratory

The realization of advanced nuclear reactors as a national source of reliable energy awaits materials research on fuels, reactor components under extreme environments, and options for waste treatment and storage. As described in a recent workshop, [1] third generation synchrotrons such as the Advanced Photon Source (APS) provide a high-flux of coherent, variable-energy x-rays that can be used to probe in situ a wide range of chemical, physical, and materials problems of relevance to nuclear energy production. Experimental opportunities will be highlighted within the context of techniques that provide new information. Also presented will be guidance on how to access these techniques at the APS. This work was performed with the support of DOE-OBES, under contract number DE-AC02-06CH11357[1] Workshop on the Role of Synchrotron Radiation in Solving Scientific Challenges in Advanced Nuclear Energy Systems, 27-28 January 2010

2:30 PM Invited

Zirconium Alloy Oxide Structure Studied Using Microbeam Synchrotron Radiation Diffraction and Fluorescence: Arthur Motta¹; Aylin Kucuk²; Marcelo Gomes da Silva³; Robert Comstock⁴; Barry Lai⁵; Zhonghou Cai⁵; ¹Penn State University; ²EPRI; ³Universidade Federal do Ceara; ⁴Westinghouse Electric Co.; ⁵Argonne National Laboratory

Corrosion can often limit the service life of materials in nuclear power plants. To better understand the corrosion resistance of Zr-based alloys in light water reactors and in supercritical water reactors, techniques were developed to characterize oxide corrosion films using synchrotron radiation. Cross-sections of oxides formed in high temperature water or steam were probed by a microbeam (200 nanometers) of synchrotron radiation to provide both diffraction and fluorescence data. The diffraction data provided information on oxide phases, grain size, and crystallographic texture as a function of distance from the oxide-metal interface, while the fluorescence results provided chemical information at the ppm level. Results from the characterization of these oxides will be presented and linked to the protective or non-protective character of the oxide layers, thus highlighting the contributions made by the synchrotron radiation studies in improving our understanding of mechanisms of corrosion protection in these materials.

3:00 PM

Texture and Intergranular Stresses of Hydrides Precipitated in Zr-2.5%Nb and Zircaloy-4: *Javier Santisteban*¹; M A Vicente-Alvarez¹; Pablo Vizcaino²; A. D. Banchik²; Jon Almer³; ¹CONICET; ²Comision Nacional de Energia Atómica; ³Argonne National Laboratory

We have measured texture and intergranular stresses of hydrides precipitated in Zr-2.5%Nb pressure tube material and Zircaloy-4 plates of different microstructures by synchrotron X-Ray diffraction experiments. Results show large in-plane compressive stresses in hydride platelets precipitated in pressure tube material and in Zircaloy-4 of ~30 μ m grain size, whilst no stresses are observed for hydrides in Zircaloy-4 of ~100 μ m grain size. The origin of these stresses and the effect of tensile stress on hydride texture were investigated by performing in-situ hydride dissolution/ precipitation under external loads. Some of the loads were high enough to produce hydride reorientation as seen under the optical microscope. Small changes in hydride texture were observed for all loads, whilst clear differences in hydride intergranular stresses emerged only for samples presenting hydride reorientation. The observed stresses can be explained by the constraint imposed by grain boundaries to the planar growth of hydride platelets.

3:20 PM

A High Energy Synchrotron X-Ray Study of Biaxial Thermal Creep of AISI 316L Steel: *Hsiao-Ming Tung*¹; Kun Mo¹; Xiang Chen¹; Jonathan Almer²; Meimei Li²; James F. Stubbins¹; ¹University of Illinois; ²Argonne National Laboratory

A study of the thermal creep properties of Type 316L stainless steel was performed using pressurized tube specimens. Creep tubes of 8.12mm outside diameter (OD) by 0.25 mm wall thickness were subject to constant load generated with a high-pressure high-purity argon gas. Specimens were heated to 650 and 700\176C in an air environment. Macro-strain due to the change in OD was measured with a high-precision laser profilometer. To evaluate creep damage due to microstructural change of the creep tubes, high energy synchrotron X-ray diffraction was used to determine the lattice strains of the creep tube during deformation at the temperature of 650 and 700\176C. Fracture surface of the creep tubes was characterized using scanning electron microscopy (SEM). The grain boundaries with chromium-rich carbide precipitated are likely the path for crack propagation during fracture.

3:40 PM

Synchrotron X-Ray Characterization of the Oxide Structure Formed an Ferritic-Martensitic Alloys Exposed to 500°C Steam and Supercritical Water: *Jeremy Bischoff*¹; Arthur Motta¹; Guoping Cao²; Robert Comstock³; Zhonghou Cai⁴, ¹Penn State University; ²University of Wisconsin-Madison; ³Westinghouse Electric Co.; ⁴Argonne National Laboratory

The Supercritical Water Reactor (SCWR) is a Generation IV design envisioned for its high thermal efficiency and simplified core. One of the major materials issues for its development is the corrosion resistance of the cladding and structural materials when exposed to supercritical water at temperatures between 500°C and 600°C. Candidate alloys include ferritic and martensitic steel alloys and the protective oxide layers formed during corrosion determine the overall corrosion rate. In this study oxide layers formed on these alloys during exposure to 500°C steam and supercritical water were analyzed using microbeam synchrotron x-ray diffraction and fluorescence. This technique enables the examination of the oxide layer microstructure with a spatial resolution up to 0.2 μ m, with simultaneous acquisition of elemental and phase information. The results of these examinations in various alloys will be shown and compared to corrosion kinetics with a view to determining corrosion mechanisms.

4:00 PM Break

4:10 PM Keynote

Microbeam, Timing and Wavelength-Dispersive Studies of Nuclear Materials with Synchrotrons: *Gene Ice*¹; ¹Oak Ridge National Laboratory

Synchrotron sources allow for nondestructive 3D studies of materials structure and evolution at unprecedented time and length scales. These new

capabilities are essential to understand the underlying materials physics needed to make transformational materials with tailored physical properties. For activated samples, high-brilliance synchrotron sources are particularly important and will allow for small samples to be studied after doses that would make larger samples difficult to handle. We describe ongoing 3D x-ray microscopy studies of materials structure, and describe how these studies provide new insights into materials structure evolution, with direct ties to emerging models. We also describe emerging opportunities with sources of the future. Work sponsored by the U.S. Department of Energy (DOE), Office of Basic Energy Sciences, Division of Materials Sciences and Engineering. Experiments performed on Beamline 34-ID at the Advanced Photon Source Argonne II, supported by the DOE Office of Basic Energy Science, Division of User Facilities.

4:40 PM

Synchrotron Radiation Study of Hydride Reorientation in Zircaloy under In Situ Stress and Temperature Cycles: *Kimberly Colas*¹; Arthur Motta¹; Mark Daymond²; Jonathan Almer³; Zhonghou Cai³; ¹Pennsylvania State University; ²Queen's University; ³APS Argonne National Laboratory

Hydrogen ingress into zirconium alloy fuel cladding during operation in nuclear reactors can degrade cladding performance due to formation of brittle hydrides. At temperature and under stress, hydrogen redistribution and reorientation can occur, reducing cladding resistance to failure. Thus, it is crucial to understand the kinetics of hydride dissolution and reprecipitation under load and at temperature. In the current study we have used high energy synchrotron radiation diffraction to study the kinetics of hydride reorientation in previously hydrided Zircaloy-4 sheet. Micro-beam diffraction was performed on samples containing hydrides grown at stress concentrations such as crack tips to study their state of strain and their orientation relationship with the matrix. In addition the strain was measured in hydrides formed near the crack with a spatial resolution of 50 microns, to provide a map of hydride precipitation and straining. The results are discussed in terms of previous measurements in the literature.

5:00 PM

SAXS and ASAXS Studies of Nanoscale Features in Reactor Pressure Vessel Steels and Nanostructured Ferritic Alloys: *Takuya Yamamoto*¹; Nicholas Cunningham¹; G. Robert Odette¹; Carlo Segre²; Shanshan Liu²; Sonke Seifert³; ¹Univ. California Santa Barbara; ²Illinois Institute of Technology; ³Argonne National Laboratory

Small angle and anomalous small angle X-ray scattering (SAXS/ASAXS) measurements were on RPV steels and model alloys aged at 350°C for 13000 h as well as nanostructured ferritic alloys (NFA) at the ANL APS. Aging the RPV steels and model alloys resulted in precipitation of Cu(Mn-Ni-Si) rich nm-scale phases. The NFA contain nm-scale Y-Ti-O features. ASAXS was performed on \sim 15 µm samples near the K-edges of Mn, Fe, Ti and Y (depending on the alloy composition) while SAXS was performed at 18 keV on 50 µm thick specimens. Control specimens without NF were also measured. The data analysis is currently under way and has proven to be challenging, especially due to X-ray fluorescence. The size distribution of a RPV model alloy has been analyzed and is in good agreement with SANS results. The status of the analysis of the overall experimental matrix will be presented, along with lessons learned.

5:20 PM

Design of Materials Testing Capsule in PULSTAR Reactor for High Temperature Irradiations: *Santosh Sahoo*¹; Kalyan Chitrada¹; Jacob Eapen¹; Timothy Burchell²; K. Murty¹; ¹North Carolina State University; ²Oak Ridge National Laboratory

A limited number of thermo-mechanical experiments have been conducted in the past at high temperatures in a nuclear reactor. An irradiation capsule is currently being fabricated in the PULSTAR reactor at the North Carolina State University which is capable of conducting irradiations tests at temperatures in excess of 1000 deg.C. In this design, concentric alumina tubes separated by nitrogen gas enclose a tubular graphite electrical heater (in lieu of gamma heating) containing disk shaped materials samples. Extreme care is taken for maintaining thermal and electrical insulation as well as minimizing the activation from nuclear radiations. A pressurized inert gas environment is maintained inside the capsule to avoid the risk of graphite oxidation. We report the main features of the irradiation capsule design and results from thermal/stress analysis using the Finite Element software – ANSYS. We acknowledge financial support from the Department of Energy (DoE).

5:40 PM

Microtomographic Investigation of Damage in E911 Steel after Long Term Creep: Federico Sket¹; *Andras Borbely*²; Karl Maile³; Rudy Scheck³; ¹IMDEA Materials; ²Ecole des Mines de Saint-Etienne; ³Materialprüfungsanstalt Universität Stuttgart

Damage distribution in a notched hollow cylinder made of E911 steel and crept for 26,000 h under multi-axial stress state was assessed. Highresolution tomographic reconstructions allowed characterization of the size, shape and spatial distribution of cavities along the notch of the cylinder. Cross-correlation analysis between the corresponding distributions of cavities number density and different stress parameter indicate that the highest similarity is obtained for stress triaxiality. The maximum principal stress and the von Mises stress show also strong correlation with damage distribution. The analysis of the size distribution of non-coalesced cavities in terms of general power-law functions describing nucleation and growth, led to the conclusion that cavity growth in E911 steel is dominated by the constrained diffusion mechanism.

Coatings for Structural, Biological, and Electronic Applications II: Process-Property-Performance Correlations - II; Metallic, Semiconducting and Insulating Coatings

Sponsored by: The Minerals, Metals and Materials Society, TMS Electronic, Magnetic, and Photonic Materials Division, TMS: Thin Films and Interfaces Committee

Program Organizers: Nuggehalli Ravindra, New Jersey Institute of Technology; Choong Kim, University of Texas at Arlington; Nancy Michael, University of Texas at Arlington; Gregory Krumdick, Argonne National Laboratory; Roger Narayan, Univ of North Carolina & North Carolina State Univ

Wednesday PM	Room: 6E
March 2, 2011	Location: San Diego Conv. Ctr

Session Chairs: Gregory Krumdick, Argonne National Laboratory; Roger Narayan, Univ of North Carolina & North Carolina State Univ

2:00 PM

The Development of a Non-Destructive Multiple Partial Unloading Micro-Indentation Technique for Thermal Barrier Coating Spallation Prediction: *Jared Tannenbaum*¹; Kwangsoon Lee¹; Bruce Kang¹; Mary Anne Alvin²; ¹West Virginia University; ²National Energy Technology Laboratory

Failure of TBCs applied to gas turbine combustor components currently limits the maximum temperature at which these engines operate. In this research, a non-destructive load-based micro-indentation methodology for damage assessment of these coatings is presented. A multiple-loading/ partial- unloading evaluation procedure has been developed wherein stiffness responses of TBC coupons subjected to thermal loads have been analyzed. At various thermal cycles time-series color maps were developed correlating accumulated degradation to overall TBC residual stress states. Through this procedure regions having relatively higher stiffness are correlated to elevated out-of-plane tensile residual stress states. A high temperature exposure testing plan was conducted where after each thermal loading, microstructural analyses were carried out identifying damage accumulation. Results indicate this test methodology is capable of predicting spallation sites on TBCs before its occurrence. In addition, FEM analyses of interfacial stresses produced upon cooling has provided explanation to the experimentally observed failure patterns within this region.



2:15 PM Invited

Study of the Nanocomposites for Superalloy Thermal Barrier Coatings: *Shiqiang Qian*¹; ¹School of Materials Engineering, Shanghai University of Engineering Science

High temperature alloy can be plated on metal bonding coat layer, by magnetron sputtering or electrophoresis, and thermal barrier layer, by high-speed jet electrodeposition or electrophoresis. We can get nanocomposites on alloy by plating metal bonding coat layer first and then thermal barrier layer. The surface morphology,phase composition and element of these two layers can be observed through OM, XRD, SEM. We placed the K17 high temperature alloy into melting sodium chloride at 900° for 1h then air-cooled for 10 minutes and did 15 cycles hot corrosion test. For metal bonding coat layer, magnetron sputtering is better than electrophoresis while for thermal barrier, electrophoresis better than high-speed jet electrodeposition. We found that it has better anti-hot-corrosion performance for nanocomposites through plating NiCrCoAlY, a metal bonding coat layer, by magnetron sputtering and then YSZ, a thermal barrier layer, by electrophoresis on K17 alloy.

2:40 PM

Effect of Solubilizer on Low-Temperature Stability of Organic Solderability Preservative: *Zhongliang Xiao*¹; Yan Shi¹; Yu Ding¹; Daoxin Wu¹; Guojun Xu²; ¹Changsha University of Science and Technology; ²Shenzhen Yicheng Electronic Technology Co., Ltd

Organic solderability preservative(OSP) become more and more important in PCB producing process because of requirements on environment protection and reducing cost. An organic solderability preservative(OSP) against low temperature was prepared by adding a kind of solubilizer. The effect of the content of OSP solubilizer on the low-temperature stability of the OSP solution and OSP film thickness, OSP film hydrophobic, and Solderability. The results showed that the storage temperature of the OSP lower than the common OSP 10-15°C while the other properties have no obvious change.

2:55 PM

Failure Mechanisms of Strained Copper Films on Polyimide: Megan Cordill¹; Gerhard Dehm²; ¹University of Leoben; ²Erich Schimd Insitute of Materials Science

Mechanical properties and interfacial phenomena of thin films on compliant substrates are important to understand in order to design reliable flexible electronic devices. Thin films of Cu with an interlayer of Ti on polyimide substrates will be examined for their use as interconnects in flexible electronic devices. Using an in-situ tensile device inside a scanning electron microscope the mechanical behavior can be observed. With this technique, the initial fracture and buckling of the film can be observed and correlated to the strain. The strain of initial failure and subsequent delamination are observed to increase with film thickness. However, when the films are annealed the adhesion decreases as well as the fracture strain. The difference in mechanical behavior is examined using TEM, EBSD, and FIB to uncover the mechanisms defining the mechanical behavior of these films systems.

3:10 PM

High-Performance Organic-Inorganic Thin Film Structural Adhesive Interphases: *Jeffrey Yang*¹; Reinhold Dauskardt¹; ¹Stanford University

High-performance bonding plays an integral role in the reliability of thinfoil structural laminates. Novel organic-inorganic thin films with a throughthickness composition gradient have been developed to create complex metal / silane interphase regions engineered to form durable bonds between metal oxides and structural adhesive organic resins. Despite the efficacy of these hybrid films, much remains unknown about the fundamental processingnanostructure-property relationships that govern their performance and reliability. Strategies for forming strong adhesive bonds using a conditioned oxide, an optimized sol-gel layer and a high-performance epoxy resin are described. Micro and nanoscale mechanisms of interphase degradation and failure have been characterized under a range of loading and environmental conditions, revealing significant improvements in adhesion strength and enhanced resistance to moisture-assisted crack growth over traditional bonded joints. The influence of metal oxide isoelectric point and epoxy functionality on fracture energy and network connectivity will also be discussed.

3:25 PM

Effect of the Duty Cycle on the Microstructural, Mechanical and Tribological Properties of TiN Layers Deposited by PACVD: Mohammad Sadegh Mahdipoor¹; Mani Montazeri²; Mansour Soltanie²; Farzad Mahboubi¹; *Mohammad Hamed Habibi*³; Shahrokh Ahangarani⁴; ¹Amirkabir University of Technology; ²Iran University of Science and Technology; ³University of Tehran; ⁴Iranian Research Organization for Science and Technology

The PACVD process by pulsed-DC plasma in a TiCl4-N2-H2-Ar gas mixture to deposit TiN layer is investigated. The heat treatment of quench and temper carried out on hot work steel samples. Then TiN layers were deposited on all samples at 540 °C, 3-5 mbar pressure, and N2/H2= 0.22 gas flow ratio for 90 min. Deposition process were carried out under three different duty cycles, 40%, 50%, and 60%, to investigate the effect of this parameter on the microstructural, mechanical, and tribological properties of the coatings. Coatings properties were characterized using XRD, SEM, AFM, and Hardness tester with nano indenter and pin-on-disk wear test. The results indicate that by decreasing the duty cycle, the TiN layer shows an isotropic growth, smoother surface, more thickness and more surface hardness. As a result of wear tests, TiN coating deposited at 40% duty cycle showed the best wear resistant.

3:40 PM Break

3:50 PM

The Influence of Pre-Treatment Plasma Nitriding on Tribological Properties of TiN Coatings Produced by PACVD: Mohammad Sadegh Mahdipoor¹; Farzad Mahboubi¹; Mahdi Raoufi²; Hasan Elmkhah³; *Mohammad Hamed Habibi*⁴, ¹Amir Kabir university; ²Iran University of Science and Technology; ³Tarbiat Modarres University; ⁴University of Tehran

The aim of this study was to investigate the effect of pre-treatment plasma nitriding (PN) on mechanical and tribological behavior of TiN coatings deposited by plasma assisted chemical vapor deposition (PACVD). A group of hot work steel samples were plasma nitrided at 500 °C for 4 h. Then TiN layer was deposited on all of samples at 520 °C temperature, 8 kHz frequency and 33% duty cycle. The microstructural, mechanical and tribological properties of the coatings were investigated using SEM, WDS, AFM, microhardness tester and pin-on-disc wear test. The load of wear test was 10 N and the samples were worn against different pins, ball-bearing steel WC-Co. The results indicate that the difference of hardness between the samples with PN-TiN layer and those samples with only TiN layer without PN was 450 HV and the former samples showed a significant amount of wear resistance in comparison to the latter ones.

4:05 PM

The Effects of Annealing on the Charge-Discharge Characteristics of Al-Si Thin Film with Pre-Deposited Al Layer: *Chao-Han Wu*¹; Fei-Yi Hung²; Truan-Sheng Lui¹; Li-Hui Chen¹; ¹Department of Materials Science and Engineering, National Cheng Kung University; ²Institute of Nanotechnology and Microsystems Engineering, Center for Micro/Nano Science and Technology, National Cheng Kung University

In this study, radio frequency magnetron sputtering was used to prepare Al-Si film anodes and the effect of both pre-sputtered Al thin film and oxygen fraction($17 \sim 7$ at. %) within the Al-Si film on the charge-discharge capacity characteristics are discussed. The pre-sputtered 40nm Al thin film not only reduced the resistivity of the composite anode film, but also diffused to prevent peeling between the Al-Si films and Cu foils after annealing in the vacuum. Owing to the above reasons, the stability for the charge-discharge cycling life at high temperature (55°) was achieved. The reduction of oxygen fraction in the Al-Si film also led to an improvement on capacity of the anode.

4:20 PM Invited

Morphology Evolution during the Growth of Polycrystalline Thin Films: *Ramanathan Krishnamurthy*¹; Mikko Haataja²; ¹Purdue University; ²Princeton University

Growth models for polycrystalline films, commonly used in optoelectronic applications, ignore time-dependent lateral grain size effects. We address this through a thermodynamics-based method that incorporates both grain boundary grooving and lateral grain growth effects. In prior work, we studied the annealing of a film with polydisperse grain sizes, and sucessfully reproduced several experimental observations, including microscopic features (e.g. 'ghost' lines, groove asymmetry, grooving-grain growth interactions), and aggregate characteristics of the grains of the film (e.g. surface roughness evolution). Here, we study film growth / deposition. We demonstrate that film grooving / grain growth is considerably enhanced / impeded when a large deposition flux is employed, owing to the enhanced chemical potential driving grooving. We examine spatially varying fluxes, using physical vapor deposition & electrodeposition as examples, and find that film morphology evolution depends critically upon the ratio of length scales associated with growth instabilities and grain growth respectively.

4:45 PM

Characterization of Nanospherical ZnO: Al Films and ZnO: Al/p-Si Structure: *Nilgun Baydogan*¹; O. Karacasu²; H. Cimenoglu²; ¹Istanbul Technical University, Energy Institute; ²Istanbul Technical University, Metallurgical & Materials Engineering Department

Multilayer transparent conducting aluminium doped zinc oxide films have been deposited on p type silicon wafers by the sol-gel dip coating process to fabricate ZnO:Al/p-Si heterojunction. Each layer was pre-heated at 400 °C in a conventional furnace for 10 min. and the final films were annealed at different temperatures in oxygen, vacuum and nitrogen ambient. The surface of ZnO:Al films on p-Si substrates were characterized by using XRD, SEM and EDS analysis. Results showed that the films consist of almost spherical nanoparticles with a size range of 25-50 nm. The thickness measurements were performed by a surface profilometer(Dektak- 6M surface profilometer) at different parts of the films. The optical properties of nanospherical ZnO:Al thin films were performed by UV/VIS Spectrophotometer in the wavelength range from 192.5 to 950 nm. The resistivity of ZnO:Al the film on p-type silicon wafer was investigated by Dispensible Four Point Resistivity Probe with Mounting Stand (SIGNATONE).

Commonality of Phenomena in Composite Materials II: Understanding Composite Performance

Sponsored by: The Minerals, Metals and Materials Society, ASM International, TMS Structural Materials Division, TMS/ASM: Composite Materials Committee *Program Organizers:* Meisha Shofner, Georgia Institute of Technology; Carl Boehlert, Michigan State University

Wednesday PM	Room: 6A
March 2, 2011	Location: San Diego Conv. Ctr

Session Chair: Enrique Barrera, Rice University

2:00 PM Invited

Microstructural Optimization of Hybrid Materials for Multifunctional Performance: Jonathan Spowart¹; ¹Air Force Research Laboratory

Hybrid materials can be defined in various ways, including functional hybrids and structural hybrids. Often, the differences between these two definitions become blurred. Moreover, the microstructures of hybrid materials can range over many orders of magnitude in length scale - from the nanoscale at the interface, up to the macroscale at the structural component level. Microstructural characterization over multiple length scales therefore remains a challenge. In this presentation, we focus on optimizing the combination of different materials to provide new and improved

functionalities for the resulting hybrid. Methods for microstructural optimization from the literature and our own research are discussed, in the context of providing optimized multifunctional performance. Abstract Cleared for Public Release | Distribution Unlimited | 88ABW-2010-3965

2:40 PM

Stiffness Based Failure Predictions in Composite Structures: Chandra Veer Singh¹; ¹Cornell University

Presently, composite structures are designed against strength failure. The criteria used are often empirical and overly conservative, as recognized by recent world wide failure exercise (WWFE-III). Moreover, many applications involve design functions such as structural deflections, vibrations, etc., where critical performance is determined by material stiffness. Design of these structures with strength criteria alone is inaccurate as subcritical damage in form of ply cracking and interfacial debonding occurs well before ultimate failure. Here we present a siffness based failure criterion which accounts for progressive damage. Initiation and progression of damage is analyzed using a fracture mechanics based energy model. Subsequent stiffness reduction is computed using our newly developed synergistic damage mechanics. The structure fails when its stiffness properties reduce below a critical level. Above model is implemented in commercial FEA package ABAQUS via user subroutine. The model is then applied to practical problems and verified with available experimental data.

3:00 PM

Ablation Properties of Glass Ceramic Matrix/C and Glass Ceramic/Sic Matrix Composites during Oxyacetylene Torch Test: Julien Beaudet'; Jonathan Cormier¹; André Dragon¹; ¹PPRIME

The ablative properties of two laminated composites, having the same glass matrix and architecture with different kind of fibers, are evaluated and compared. Ablation tests are performed using an oxyacetylene torch on samples having two different thicknesses. Mass loss and ablation depth are measured after flame exposure. The results obtained shows that the decomposition of SiC fibres during thermal exposure has a significant impact on ablation behavior. The oxidation process of SiC produces a liquid SiO2 film at the top of the material during ablation. This leads to an improved ablation resistance compared to a glass ceramic / C composite, especially in case of successive flame exposures where the SiO2 film consumes a substantial fraction of the heat flow during its liquefaction.

3:20 PM

Higher-Order Micromechanics and Effective Elastic Moduli of Particle Reinforced Composites: *Keiji Yanase*¹; Jiann-Wen Ju²; ¹Fukuoka University; ²University of California, Los Angeles

A novel higher-order micromechanical formulation is proposed to predict the effective elastic moduli of particle reinforced composites. By considering the direct particle interactions, micromechanical field equation is systematically presented, and the near-field particle interactions are accounted for in the effective elastic moduli of spherical particle reinforced composites. Specifically, the focus is upon the effective elastic moduli of two-phase composites containing randomly distributed isotropic spherical particles. To demonstrate the predictive capability of the proposed micromechanical framework, comparisons between the theoretical predictions and the available experimental data on effective elastic moduli are rendered.

3:40 PM Break

4:00 PM Invited

Enhancing Performance, Durability and Properties of Engineering Resins through the Use of Nanotechnology: *Michael Meador*¹; ¹NASA Glenn Research Center

Future NASA missions will require materials with durability, properties and performance that far exceed that of today's materials. Developments in nanotechnology over the past decade have demonstrated that addition of nanoscale additives to engineering resins and composites can significantly enahnce their mechanical properties and durability. This paper will review NASA's plan for development of nanostructured materials and their potential use in NASA missions and recent results from research efforts in this area.



4:40 PM

Modelling Shear Fracture of Hybrid CFRP/Ti Laminates with Cohesive Elements; Effects of Geometry and Material Properties: *Parya Naghipour*¹; Marion Bartsch¹; Joachim Hausmann¹; Karola Schulze¹; ¹German Aerospace Research Center (DLR)

Hybrid laminates made of Carbon Fibre Reinforced Plastic (CFRP) and metal foil plies (e.g. titanium) have been investigated numerically and experimentally to be considered for applications in aerospace industry. The numerical FE model of the hybrid laminate, subjected to lap shear fracture, is composed of a CFRP core between two titanium layers with cohesive elements lying within CFRP/Ti interface. In the FE model, the CFRP laminate is assumed as an orthotropic homogenized continuum under plane stress, and titanium face sheets are modelled as an elastic-plastic continuum. The constitutive law for the quadratic CFRP/Ti interface elements, implemented as User Element in ABAQUS, is an exponentially decaying law representing the degrading behaviour of the interface. The influence of geometry (e.g. overlap length and total length), interface cohesive properties, and plastic deformation of the adherent metal foils on the lap shear fracture response are analyzed in detail in this study.

5:00 PM Invited

Deformation Mechanisms in Carbon Nanotube/Epoxy Composites: Scott Brownlow¹; Alexander Moravsky²; *Bhaskar Majumdar*¹; ¹New Mexico Tech; ²MER Corporation

This presentation will highlight our understanding of load transfer in double wall carbon nanotube/epoxy composites obtained by a combination of in situ FTIR and Raman measurements. Emphasis will be focused on FTIR measurements of spectral shifts of the epoxy matrix under mechanical load, and a theoretical basis for such stress induced shifts using recent quantum mechanical analysis of a modular epoxy-hardener molecule combination will be provided. Some of the problems of using Raman measurements to interpret load transfer in the randomly oriented nanotube reinforcement will be pointed out. The final part of the presentation will focus on application of carbon nanotubes in hybrid carbon-fiber-nanotube composites. The beneficial effect of interply nanotube layers on interlaminar fracture toughness and delamination damage resistance, and the associated failure mechanisms, will be discussed.

Computational Plasticity: Crystal Plasticity

Sponsored by: The Minerals, Metals and Materials Society, TMS Materials Processing and Manufacturing Division, TMS Structural Materials Division, TMS/ASM: Computational Materials Science and Engineering Committee, TMS: High Temperature Alloys Committee *Program Organizers:* Remi Dingreville, Polytechnic Institute of NYU; Koen Janssens, Paul Scherrer Institute

Wednesday PM	Room: 1A
March 2, 2011	Location: San Diego Conv. Ctr

Session Chair: To Be Announced

2:00 PM Invited

A Methodology for Simulating Microtexture Evolution in Deformed Aluminum and Titanium Polycrystals: *Paul Dawson*¹; Romain Quey¹; ¹Cornell University

Crystal plasticity models implemented in finite element formulations have been used successfully to predict the effects of plastic anisotropy on deformation and to predict the evolution of crystallographic texture. Currently, efforts are focussed on predicting the spatial variations in lattice orientations within individual grains (microtextures) that are observed experimentally in deformed samples. Several challenges arise in making such predictions accurately. Samples of sufficient size (number of crystals) and sufficient resolution (number of elements discretizing each crystal) must be instantiated and deformed to large strains. The results must be abstracted for comparison to experimental data. We discuss the simulation of microtexture evolution in metallic alloys, focusing on comparison of metrics that quantify microtextures: average lattice misorientations, crystallographic spread of misorientations, and its crystallographic dependence. We compare predicted trends to ones measured in deformed aluminum and contrast the behaviors of aluminum and titanium polycrystals.

2:30 PM Invited

A Modular Crystal Plasticity Framework Applicable from Component to Single Grain Scale: *Philip Eisenlohr*¹; Denny Tjahjanto¹; Christoph Kords¹; Franz Roters¹; Dierk Raabe¹; ¹Max-Planck-Institut für Eisenforschung

The solution of a continuum mechanical boundary value problem requires a constitutive response connecting deformation and stress at each material point. Such connection can be regarded as three separate hierarchical problems. First, partioning of the (mean) boundary values of the material point among its microstructural constituents and the associated homogenization of their response. Second, based on an elastoplastic decomposition of (finite strain) deformation, these responses follow from explicit or implicit time integration of the plastic deformation rate per constituent. Third, to establish the latter a state variable-based constitutive law needs to be interrogated and its state updated. We demonstrate the versatility of such framework, which has been implemented into finite element packages, by considering three scenarios. Component-scale forming simulations comparing different homogenization schemes, selective refinement of the constitutive material description within a single geometry, and gradient-dominated deformation of an oligocrystalline patch using a non-local constitutive law.

3:00 PM Invited

An Efficient Strategy to Take Texture-Induced Anisotropy Point-By-Point into Account during FE Simulations of Metal Forming Processes: Paul Van Houtte¹; Jerzy Gawad¹; Philip Eyckens¹; Bert Van Bael¹; Samaey Giovanni¹; Dirk Roose¹; ¹Katholieke Universiteit Leuven

Focus will be on the implementation of texture-induced plastic anisotropy in FE simulations of metal forming. The crystallographic texture can be introduced as a state variable in every integration point. A multi-scale model is then called to calculate the stress-strain response and the local texture evolution in every integration point and for every strain increment. Less calculation-intensive is to use anisotropic analytical constitutive models, identified in advance from mechanical tests. These can also be done in a "virtual" way, i. e. using measured texture data and a multi-scale model. However, texture evolution is then not taken into account. An adaptive scheme for updating the texture and the anisotropy has been developed recently. Texture and anisotropy were updated by the ALAMEL-model. Results for a cup drawing process will be shown. The calculation time was reduced from months to days. Predicted fields of plastic anisotropy and textures will discussed including experimental validation.

3:30 PM Invited

Crystal Plasticity Computations Using Real Grain Arrangements to Simulate Deformation and Fracture: *Henry Proudhon*¹; Samuel Forest¹; Wolfgang Ludwig², ¹MINES ParisTech; ²INSA Lyon

Progress with Finite Elements (FE) codes, more robust meshing algorithms and larger computer power make Crystal Plasticity FE simulations suitable to simulate the deformation and fracture of complete specimens. This becomes of primary interest when those specimens can also be characterized experimentally in the form of the 3D arrangement of their grain microstructure and damage evolution. Two examples of applications of those large scale simulations are described in this paper. In the first example, Crystal Plasticity simulations are conducted on sample imaged by Diffraction Contrast Tomography, which allows to resolve the 3D shape and orientation of the grains constituting the specimen. It is shown how to explicitly take into account the presence of a crack within the microstructure and its effect on the strain/stress distribution. The second example aims at simulating 3D coherent X-ray diffraction patterns in a polycrystalline gold sample to help interpreting the complex results obtained experimentally.

4:00 PM

A Rate-Dependent Polycrystal Model for Evaluation of the Creep Deformation in the Heat Affected Zone of the Modified 9Cr-1Mo Steels: *Mehdi Basirat*¹; Gabriel Potirniche¹; Triratna Shrestha¹; Indrajit Charit¹; Karl Rink¹; ¹University of Idaho

The high creep resistance at the elevated temperature has made the modified 9Cr-1Mo steels an excellent choice for power plant reactor pressure vessels. Modeling creep based on classical inelastic approaches is predominant in creep literature. While these efforts have a certain practical importance, they are essentially phenomenological in nature. In this paper a rate-dependent polycrystal plasticity model has been developed for computing the creep deformation of the modified 9Cr-1Mo steels in the weld heat affected zone. The constitutive behavior of tertiary creep at the crystal level has been modeled through evolution equations for three simultaneous degradation processes: (i) subgrain and dislocation network coarsening, (ii) a decrease in dislocation density, and (iii) solute depletion at the subgrain level. A user subroutine has been developed to compute the resulting creep strains; furthermore the numerical results have been validated experimentally. Finally a User MATerial Subroutine (UMAT) has been implemented in the ABAQUS software.

4:15 PM Break

4:30 PM Invited

Use of Spectral Databases for Crystal Plasticity Finite Element Simulations of Bulk Deformation Processing of Cubic Metals: Hamad Al-Harbi¹; Josh Shaffer¹; Surya Kalidindi¹; ¹Drexel University

In recent work, we have demonstrated the viability and computational advantages of DFT-based spectral databases for facilitating rigid-viscoplastic crystal plasticity solutions in cubic metals subjected to arbitrary deformation paths. In this paper, we report the first incorporation of our novel spectral crystal plasticity databases into a commercial finite element package for simulating bulk deformation processing operations on face centered and body centered cubic metals. The evolution of the underlying crystallographic texture in the work-piece and its associated macroscale anisotropic properties predicted from our new Spectral Crystal Plasticity Finite Element Approach (SCP-FEA) will be compared against the corresponding results from the conventional crystal plasticity finite element method. It will be shown that SCP-FEA produces excellent predictions with about two orders of magnitude savings in the computational time.

5:00 PM

Modeling Mesoscopic Plastic Flow Heterogeneities of 3D Polycrystalline Microstructures Using Crystal-Plasticity FEM and FFT-Based Viscoplastic Model: Yoon Suk Choi¹; Benjamin Anglin²; Michael Groeber³; Paul Shade⁴; Michael Uchic³; Christopher Woodward³; Dennis Dimiduk³; Anthony Rollett²; Ricardo Lebensohn⁵; Triplicane Parthasarathy¹; ¹UES, Inc.; ²Carnegie Mellon University; ³Air Force Research Laboratory; ⁴UTC; ⁵Los Alamos National Laboratory

The initiation and development of mesoscopic plastic flow heterogeneities have been the objective of numerous numerical studies because of their significance in understanding and identifying critical microstructural features for microscopic instability and damage initiation. Numerical approaches widely used for such studies include crystal plasticity FEM and the imagebased FFT-based viscoplastic model. However, there are few experimental validations of these numerical approaches in the 3D mesoscopic space. Recently, some of the authors obtained 3D microstructure data using EBSD mapping and FIB-based serial sectioning from micro-tension specimens of polycrystalline nickel. Elasto-viscoplastic FEM modeling and FFT-based viscoplastic modeling were performed for these real 3D microstructures. The heterogeneities that develop within simulations of plastic responses were analyzed using various statistical characterization techniques, and compared between the two numerical approaches. An effort was also made to compare simulated plastic flow heterogeneities to the limited 3D plasticity information obtained from micro-tension specimens.

5:20 PM Invited

Efficient Methodologies for Determining Temperature-Dependent Parameters of Crystal Viscoplasticity: Daniel Smith¹; *Richard Neu*¹; ¹Georgia Institute of Technology

The current limitations of widespread use of crystal viscoplasticity in industry for modeling complex thermomechanical loading are often tied to the difficulty in the calibration of the temperature-dependent material parameters. The conventional approach typically involves conducting multiple sets of isothermal deformation experiments at different temperatures. This is highly costly and time consuming, often requiring months to establish the parameters. This paper outlines protocols aimed at efficiently determining microstructure-sensitive temperature-dependent material parameters. These protocols include minimal, carefully planned calibration experiments and the judicious use of optimization software for identifying material parameters. The approach is demonstrated on Ni-base superalloys with application of modeling the influence of microstructure on the thermomechanical fatigue and creep-fatigue response of hot section components in gas turbines. ModelCenter is used along with some MATLAB intermediary routines to assist the user in determination of material parameters for a crystal viscoplasticity model that is coded as a UMAT for ABAOUS.

5:50 PM

A Dislocation Density Based Crystal Plasticity Model for a-Titanium: Alankar Alankar¹; Philip Eisenlohr¹; ¹Max-Planck Institute for Iron Research

A constitutive model for single crystal plasticity of hexagonal a-titanium is developed. In the model framework, pure edge and screw dislocation densities evolve on basal, prismatic <a>, and pyramidal <a> slip families. For non-basal slip systems, a spread out core is assumed for screw segments, leading to much higher mobility of edge compared to screw dislocations, similar to the behavior found in body-centered cubic crystals. This enables the model to reflect the observed transition of stress evolution from stage I to stage II in single crystals oriented for prismatic slip. The basal slip behavior is modeled as in face-centered cubic metals. Calibration of the model is done based on experimental results of titanium single crystals with varying commercial purity. Further, the model is employed for analysis of microstructure evolution in a multicrystal. A reasonable agreement is found between experimentally observed slip and twinning activity in different grains.

6:10 PM

Numerical Eulerian Modeling in Dynamic Crystal Plasticity: *Ioan Ionescu*¹; Oana Cazacu²; ¹University Paris 13; ²University of Florida

A robust numerical algorithm for an Eulerian rigid-visco-plastic crystal model that accounts for high-strain rates, large strains, and large material and lattice rotations, was developed. The viscoplastic law is obtained from Schmid law by using an overstress approach; the numerical instabilities associated to the classical power law are thus eliminated. To handle the non differentiability of the plastic terms an iterative decomposition-coordination formulation coupled with the augmented Lagrangian method was adopted. A mixed finite element-finite volume strategy was adopted: the equation for the velocity field is discretized using the finite element method while a finite volume method, with an upwind choice of the flux, is adopted for the hyperbolic equation related to the lattice orientation.Several two-dimensional boundary value problems are selected to analyze the robustness of the numerical algorithm. The grains interaction during channel die compression of a multi-crystal was analyzed using an ALE description.



Computational Thermodynamics and Kinetics: Thermodynamics, Phase Stability and Phase Transformations

Sponsored by: The Minerals, Metals and Materials Society, ASM International, TMS Electronic, Magnetic, and Photonic Materials Division, TMS Materials Processing and Manufacturing Division, TMS: Alloy Phases Committee, TMS: Chemistry and Physics of Materials Committee, TMS/ASM: Computational Materials Science and Engineering Committee, ASM: Alloy Phase Diagrams Committee *Program Organizers*: Raymundo Arroyave, Texas A & M University; James Morris, Oak Ridge National Laboratory; Mikko Haataja, Princeton University; Jeff Hoyt, McMaster University; Vidvuds Ozolins, University of California, Los Angeles; Xun-Li Wang, Oak Ridge National Laboratory

Wednesday PM	Room: 9
March 2, 2011	Location: San Diego Conv. Ctr

Session Chairs: Patrice Turchi, Lawrence Livermore National Laboratory; Michael Gao, National Energy Technology Lab/URS Corp

2:00 PM Invited

Thermomechanical Processing Design of Nanoprecipitate Strengthened Alloys Employing Genetic Algorithms: *Pedro Rivera-Diaz-del-Castillo*¹; ¹University of Cambrdige

A modelling strategy for designing nanoprecipitation strengthened alloys is presented here. This work summarises the application of a new thermokinetics approach wherein multiple design criteria are enforced: corrosion resistance and high strength combined with affordable thermomechanical processing schedules. The methodology presented here iteratively performs thermodynamic and kinetic calculations, these are aimed at determining the best precipitate nanostructures following multiple design objectives. A genetic algorithm is employed to more rapidly finding optimal alloy compositions and processing parameters consistent with the design objectives. It was possible to computationally design new alloys strengthened by Ni-based nanoprecipitates and carbides with yield strengths exceeding 1.6 GPa and good corrosion resistance. A major limitation in the methodology is the determination of optimum processing times, which require the computation of formation energies of non-equilibrium precipitates employing other techniques. A method to circumvent such limitation is discussed.

2:30 PM

Thermodynamic Assessment and Experimental Investigation of the Ternary Ti–Al–Cr System: *Mario Kriegel*¹; Damian Cupid¹; Olga Fabrichnaya¹; Dmytro Pavlyuchkov¹; Kostyantyn Korniyenko²; Vera Khorujaya²; Fereshteh Ebrahimi³; Hans Seifert¹; ¹Freiberg University of Mining and Technology; ²I.N. Frantsevich Institute for Problems of Materials Science; ³University of Florida

Titanium aluminides alloyed with Cr are promising materials for high temperature applications because of their expected improved processability and high temperature oxidation resistance in comparison to the non-alloyed titanium alumindes. A thermodynamic description for the Ti–Al–Cr system was developed using experimental data on phase stabilities and phase equilibria from the literature. The ternary 964_1 –Ti₁Cr_{0.32}Al_{2.68} phase was modelled as a stoichiometric phase for the first time, and ternary mixing parameters of the 946–bcc, 946_0 , 945–TiCr₂ and 946–TiCr₂, and the end-members and mixing parameters of the 947–Ti(Al,Cr)₂ were optimized. Using this dataset, the liquidus and solidus surfaces and several key isothermal sections were calculated. In order to assess the reliability of the calculated liquidus and solidus surfaces, several alloys in the Ti–Al–Cr system were arc-melted and the as-cast structures were evaluated using the techniques of SEM, XRD, and thermal analysis (DTA / DSC).

2:45 PM

First-Principles Prediction of Partitioning of Alloying Elements between Cementite and Ferrite: Chaitanya Krishna Ande¹; *Marcel Sluiter*²; ¹Materials Innovation Institute, Delft University of Technology; ²Delft University of Technology

At long tempering times in steels when both cementite (Fe\$_3\$C) and ferrite (bcc-Fe-rich solid solution) phases are present, alloying elements tend to segregate to either of the two phases. V, Cr, Mn, Mo and W are found to partition to the cementite phase while the elements Al, Si, P, Co, Ni and Cu partition to ferrite. We show that partitioning of alloying elements and cementite (de)stabilization by alloying in mixtures of bcc-Fe and cementite are intimately related through the introduction of a partitioning enthalpy. The formation enthalpy of alloying element substituted cementite is shown not to be a proper gauge for addressing these questions and that magnetism plays an important role in describing the partitioning correctly.

3:00 PM

Ab Initio Aided CALPHAD Thermodynamic Modeling of Ionic Systems: Application to La_{1-y}MnO_{3±8}: *Shih-kang Lin*¹; Dane Morgan¹; ¹University of Wisconsin-Madison

Defect concentrations vs. temperature and gas partial pressures play a fundamental role in the properties of ionic systems. Defect models can be constructed through the conventional CALculation of PHAse Diagram (CALPHAD) approach using the Compound Energy Formalism (CEF). However, determining the large number of model parameters in the CEF from typical experimental data sets requires many, often poorly justified, approximations. *Ab initio* energies offer a way to reduce the approximations used in applying the CEF to complex ionic systems. However, the required ab initio energies are often end-members that are not stable and can involve non-neutral cells. Here we discuss approaches to treat these problems to enable ab initio energetics to be applied in the CALPHAD CEF. Initial results for La_{1-y}MnO₃₂₅, a base oxide for many important cathode materials in SOFC and other applications, will be presented.

3:15 PM

Phase Formation in Actinide Alloys: Why Ab Initio?: *Patrice Turchi*¹; Alexander Landa¹; Larry Kaufman²; Per Söderlind¹; ¹Lawrence Livermore National Laboratory; ²CALPHAD, Inc.

Nuclear fuels for fast spectrum nuclear reactors raise challenging questions on the role of minor actinides and fission products and gases on properties and performance. Hence, prediction of phase stability trends and phase diagrams of complex actinide-based alloys is undoubtedly the Holy Grail of materials properties simulations. We show that CALPHAD, combined with appropriate first-principles electronic structure results, is a powerful tool to predict the thermodynamic properties of actinide-based multi-component alloys. For the sake of clarity the presentation focuses on {Am,Np,Pu,U,Zr} that are the basis for candidate metallic fuels. Since experiments on this class of alloys are costly and challenging, we show that ab initio input provides useful guidance for well-chosen experiments that can lead to full validation and verification of the thermodynamic driving force that is critically needed for subsequent work on materials evolution and performance. Work performed under the auspices of the U.S. DOE by LLNL under contract DE-AC52-07NA27344.

3:30 PM Break

3:40 PM Invited

Topological Modelling of Martensitic Transformations: Robert Pond¹; ¹University of Exeter

According to the topological model (TM), a martenstic interface exhibits a partially coherent structure where the coherent segments are bounded by disconnections (line defects having both step and dislocation character) and crystal defects (slip or twinning dislocations) [1]. In this way the coherency strains are removed at long range. The transformation strain arises from the motion of the interfacial defects, laterally along the interface in the case of the disconnections, and along glide or twin planes in the wake of the moving interface for the crystal defects. It can be demonstrated that this transformation mechanism is diffusionless. The orientation relationship (OR) between the adjacent crystals is determined by the superposition of the coherency strain and the elastic fields of the defects in the static interface. In general, the OR deviates by a small tilt and/or twist deviation from the reference OR of the coherent segments. Experimental evidence supporting this model is accumulating, particularly from TEM observations, and will be presented. In addition, the TM provides mechanistic insights, in contrast to the earlier phenomenological model (PM). For example, the TM distinguishes between the reversible plastic transformation strain and the elastic distortion field. Whereas the former is determined by purely geometrical parameters, the latter depends on the relative elastic moduli of the parent and product crystals. This analysis also shows why the PM provides a good first approximation to transformation crystallography in cases such as Ti alloys, but fails for other cases such as lath martensite in steel. In the former instance, small tilt deviations are present so the invariant line concept is approximately valid, but in the latter case small twists are present, violating the invariant plane notion.[1] R.C. Pond, X. Ma, Y.W. Chai and J.P. Hirth, in Dislocations in Solids, edited by F.R.N. Nabarro and J.P. Hirth, Vol. 13 (Elsevier, Amsterdam, 2007), p. 225.

4:10 PM Invited

Ginzburg-Landau Modeling of Martensitic and Multifunctional Materials: Avadh Saxena¹; ¹Los Alamos National Lab

Strain plays a central role in phase transformations in martensites, ferroelastics as well as multiunctional materials such as ferroelectrics, multiferroics and magnetoelectrics. A variety of microstructures observed in these materials can be systematically modeled and understood by means of a crystal symmetry based Landau free energy in relevant strain tensor components. Since the strain components are not independent, the elastic compatibility constraint provides an anisotropic long-range force which governs the microstructure. In multifunctinal materials lattice distortion (or strain) acts as an elastic template to which magnetization, polarization and other functionalities couple. The long range elastic force competes with other forces, e.g. polar (or magnetic) short range dipolar forces resulting in multiple competing states and a multiscale microstructure. The consequences of the resulting microstructure on various materials properties will be discussed.

4:40 PM

Simulation of Liquid/Solid Phase Transformations - How Thin Is a Sharp Interface?: Markus Rettenmayr¹; ¹Friedrich-Schiller-University Jena

Different techniques for simulating phase transformations as e.g. the Phase Field Method incorporate a finite width of the interface, which is said to correspond closely to a natural interface. In contrast, sharp interface models generally assume the interface to be mathematically sharp or infinitely thin. However, if interface kinetics such as trans-interface diffusion is considered, sharp interface models still define the interface position precisely, but for the kinetic processes through the interface a finite width is implicitly assumed. If interface kinetics is included in solid/liquid phase transformation models, both solidification and melting can be modeled for a wide range of parameters, and the asymmetry between the two types of phase transformations is accounted for. The implications of the interface width in such simulations are discussed.

4:55 PM

A Molecular Dynamics Study of the Austenite-Ferrite Interface Mobility in Pure Fe: *Huajing Song*¹; Jeff Hoyt¹; ¹Mcmaster University

Molecular dynamics (MD) simulations performed on two phase simulation cells were used to compute the FCC/BCC boundary mobility in pure Fe over the temperature range 400-1000K. An embedded atom method interatomic potential was used to model Fe and the driving force for interface motion is the free energy difference between the two phases, which was computed as a function of temperature using a thermodynamic integration technique. For low index FCC/BCC crystallographic orientations no interface motion is observed, but for slight misorientations steps are introduced at the interface and sufficient mobility is observed over MD time scales. The interface velocity can reach 2 m/s and the mobility at 1000K is approximately 0.001

mol-m/J-s. In agreement with previous MD studies of grain boundary mobility, we find that the activation energy for the austenite-ferrite boundary mobility is much lower than values found in experiment.

5:10 PM

Phase Stability of Fe-Nb-M (M=Cr, Mn, Si, Ti): A First Principles Approach: Michael Gao¹; Paul Jablonski¹; ¹NETL

Metallic interconnects are the cost enabling technological leap for solid oxide fuel cells. Presently, the ferritic steel 441ss is the alloy of choice for this application. What seems to distinguish this alloy from other medium level Cr stainless steels is that 441ss forms C14 Fe2Nb Laves phase (Pearson Symbol hP12, prototype MgZn2) that provides additional precipitate strengthening. Furthermore, solute (namely Cr, Mn, Si, and Ti) partitioning in the Laves phase is controversial. In this work, we use ab initio density functional theory calculations to predict the energies of substituting alloying elements in the ferritic steel 441ss for Fe or Nb in the Laves phase. Based on the energy calculations of this Laves alone, it is found that Si atoms favor substituting for the Fe sites while Ti atoms for the Nb site. In order to compare with experimental phase diagrams, we also calculate the energies of the Fe-Nb-M ternaries.

5:25 PM

Thermodynamic Modeling of the Cu-Hf System: Yu Zhong¹; Arkapol Saengdeejing¹; *Laszlo Kecskes*²; Zi-Kui Liu¹; ¹Pennsylavania State University; ²US Army Research Laboratory

The complete thermodynamic description of the Cu-Hf binary system is modeled using the CALPHAD approach that combines both first-principles calculations and experimental investigations. The enthalpy of formation for all the compounds in the system are calculated via first-principles calculations, based on density functional theory (DFT), using the Vienna Abinitio Simulation Package (VASP). The projector augmented-wave (PAW) method is used and the exchange and correlation energy are described with the supplied generalized gradient approximation pseudopotentials (PBE). In addition to the recent work between 38 to 60 at.% Hf[1], further experimental investigations, including differential thermal analysis and scanning electron microscopy, were used to extend and study the phase equilibrium between 13 to 40 at.% Hf. References: [1] R. H. Woodman, B. R. Klotz, and L. J. Kecskes, J. Phase Equilib. Diffus. 27, 477 (2006).

David Pope Honorary Symposium on Fundamentals of Deformation and Fracture of Advanced Metallic Materials: Grain Boundaries, Phase Transformations, and Steels

Sponsored by: The Minerals, Metals and Materials Society, TMS Materials Processing and Manufacturing Division, TMS Structural Materials Division, TMS: High Temperature Alloys Committee, TMS/ASM: Mechanical Behavior of Materials Committee, TMS: Nanomechanical Materials Behavior Committee *Program Organizers*: E. P. George, Oak Ridge National Laboratory; Haruyuki Inui, Kyoto University; C. T. Liu, The Hong Kong Polytechnic University

Wednesday PM	Room: 32A
March 2, 2011	Location: San Diego Conv. Ctr

Session Chairs: Michael Mills, The Ohio State University; Robert Mulford, Knolls Atomic Power Laboratory

2:00 PM Invited

Physical Metallurgy Insights into the Effects of Grain-Boundary Segregants on Ductility and Fracture: *E. P. George*¹; C. T. Liu²; D. P. Pope³; ¹Oak Ridge National Laboratory; ²Hong Kong Polytechnic University; ³University of Pennsylvania

Elements that segregate to grain boundaries in metals can be harmful, beneficial, or benign. Some of these effects are manifested at low temperatures, others at elevated temperatures. Some at slow strain rates,



others at high strain rates. Some act on their own while others act in concert with or to counteract the effects of other segregants. Because of the sheer number of different mechanisms by which grain boundary segregants act, simple physical metallurgy insights gleaned from clever experiments are needed to isolate the operative mechanisms. A more comprehensive understanding will have to wait until multiscale models of deformation and fracture can properly account for trace (ppm level) changes in alloy composition. In this talk we will use examples of trace elements that exhibit beneficial and harmful effects on the ductility and fracture behavior of hightemperature materials to highlight what we know and do not yet know about the underlying mechanisms.

2:30 PM

Study of Grain Boundary Strength in AA2198 Using Notched Micro-Beam Bending: Daniel Kupka¹; Erica Lilleodden¹; ¹GKSS Research Center

Al-Li alloys are of great interest due to their high strength and low specific weight. However, these alloys show complicated fracture behavior, motivating fundamental studies of grain boundary strength and its dependence on thermo-mechanical processing. In the present work, we have studied the fracture of grain boundaries in rolled AA2198 sheets in the T8 ("heat treated") and T351 ("as-rolled") conditions using microbeam bending experiments. Micron-scale cantilever beams were fabricated by focused ion beam (FIB) milling, with single grain boundaries aligned within a semicylindrical notch. The beams were then loaded using a nanoindenter, and finite element simulations were carried out to help in the analysis of the loaddisplacement data. Intergranular fracture was shown to occur at the grain boundaries positions within the notch, as expected. Significant differences in normalized load and fracture morphology were observed between the T8 and T351 samples.

2:45 PM

In Situ TEM Observations of Reverse Dislocation Motion upon Unloading of Ultrafine-Grained (UFG) Aluminium Strained in the Microyield Region: Daniel Caillard¹; Frederic Mompiou¹; Marc Legros¹; Hael Mughrabi²; ¹CNRS; ²University Erlangen-Nürnberg

When strained in the microyield region and subsequently unloaded, UFG materials exhibit unusually large inelastic reverse strains which are not observed in similarly strained material of conventional grain (CG) size. In situ experiments have been carried out to find the origin of such an effect. Sources emitting dislocations which interacted with adjacent grain boundaries (GBs) have been observed. Depending on the character of the dislocations emitted, different behaviours have been observed: i) intensive cross-slip and rapid insertions in GBs for screw and mixed dislocations, and ii) pile-up formation in front of GBs for pure edge dislocations. Upon unloading, the release of stress induces a substantial reverse motion of dislocation pile-ups in case ii), whereas in case (ii) only a relaxation of the source was observed. On the basis of these results, the origin of the inelastic behaviour in the bulk material and the possible role of dislocation pile-ups are discussed.

3:00 PM

Grain Boundary Based Plasticity: In-Situ TEM Experiments and Modelling: Frederic Mompiou¹; Marc Legros¹; Daniel Caillard¹; ¹CEMES-CNRS

Ultrafine grains (UFG) and nanocrystalline (nc) metals are unstable and tends to evolve by grain growth even at a relatively low temperature. This behaviour seems also favoured by the application of a mechanical stress. However few studies have been focused on the elementary mechanisms that promote this instability and on the role of grain growth in the overall deformation process. We present here the results of in situ TEM straining experiments on self standing nc Al films at room temperature and on UFG Al at moderate temperature. All the results show unambiguously fast grain boundary motion assisted by the applied stress. The associated deformation has been found to be in the range of few percents in UFG Al, in contradiction with the available shear-migration coupling models. A tentative geometrical model (SMIG model) based on atom shuffling in the core of interfacial stepdislocation has been tentatively proposed.

3:15 PM

Truncated Dislocation Sources in Nanometric Aluminum Crystals: A Molecular Dynamics Study: *Bulent Biner*¹; L. P. Kubin²; ¹Idaho National Laboratory; ²LEM CNRS/ONERA

In this study, the evolution behavior of truncated dislocation sources by free surfaces in small finite volumes is elucidated for aluminum using molecular dynamics simulations. Under zero stress and without dislocations, very large stress gradients arising from surface effects, of the order of several GPas, were observed. The formation of very large stacking faults due to the operation of partial dislocations and the development of full and helix dislocations were recorded during the evolution of the truncated dislocation loops under an applied shear strain. In addition, cross-slip by the Fleischer mechanism, twin formation and detwinning with two different mechanisms were identified. These dislocation mechanisms were strongly influenced by the initial configuration of the truncated dislocation loops and the geometry of the simulation cell.

3:30 PM

Geometrical Construction and Structure of Quasi-Periodic Grain Boundaries in Cubic Materials: Mohammad Shamsuzzoha¹; ¹University of Alabama

Geometrical construction and the structure of a special type of quasiperiodic boundary in cubic materials based on vector representation of lattice sites is proposed. The construction of these quasi-periodic crystals is achieved when mutual rotation of a unique vector termed as sigma generating vector and its square root counterpart found in identically oriented orthogonal lattice network of the participating crystals brings mutual superposition. Grain boundary in such quasi-crystals appears to comprise of structural units. Experimental evidences such as HREM images and double diffracted electron diffraction pattern supporting the existence of such structural units for a [001]45° twist quasi-periodic grain boundary are presented.

3:45 PM Break

4:00 PM

Mechanism of Creep Deformation in Alumina-Forming Stainless Steel Fe-25Ni-14Cr-3.5Al-2.5Nb-0.1wt%C: *Deepak Kumar*¹; Yukinori Yamamoto¹; Michael Santella¹; Michael Brady¹; Edgar Curzio¹; ¹Oak Ridge National Laboratory

Alloy Fe-25Ni-14Cr-3.5Al-2.5Nb-0.1wt%C belongs to a family of creep resistant, Al2O3 film forming austenitic stainless (AFA) steel with intended applications in the range of 600-900°C. Al, Nb, Cr, and Ni level was optimized to promote the formation of an adherent and slow growing alumina film in this alloy, which is expected to provide better oxidation resistance than conventional Cr2O3 film forming stainless steel and Ni-base alloys in water vapor, C, and/or S rich environments. Strengthening is achieved via stable nano-scale MC and intermetallic phases. In the present study creep deformation and rupture behavior of alloy OC4 were investigated at stresses between 100 and 170 MPa and temperatures between 650°C and 800°C, and the results were compared with those for other precipitation strengthened alloys. Norton's law was used to model the creep response of the alloy. Long term microstructure stability was evaluated via up to 5000h aging studies.

4:15 PM

Evaluation and Modeling for Fatigue Damage Initiation of Thermal-Mechanically Processed High-Strength Steel: Angelika Brueckner-Foit¹; Benjamin Bode¹; *Yibin Xue*²; ¹Kassel University; ²Utah State University

The fatigue damage initiation of a differential thermal-mechanical processed (DTMP) high strength, functionally graded steel was evaluated numerically by implementation of a crystal plasticity constitutive model to a series of representative realistic microstructures. Most of the high cycle fatigue life is spent in fatigue damage initiation, which is susceptible to the variations in microstructural features. In-situ fatigue experiments were conducted to evaluate the microstructure-fatigue damage incubation properties. A three-dimensional simulation model was developed based on the realistic microstructure of the newly developed steel that includes phases, textures, and residual stresses from the thermo-mechanical processing. A crystal

plasticity constitutive model is implemented to evaluate microplasticity for accessing fatigue damage incubation mechanisms and predict the cycles needed for incubation. The directly application of the model will reduce the need to evaluate each individual part of the graded alloy and enhances the design and application of the novel steel.

4:30 PM

Influences of Material and Process Parameters on Delayed Fracture in TRIP-Aided Austenitic Stainless Steels: *Xiaofei Guo*¹; Wolfgang Bleck¹; ¹RWTH Aachen University

The effects of material and process parameters on delayed fracture susceptibility of three AISI 301 steels have been studied by Slow Strain Rate Tests (SSRT) and Deep Drawing Tests (DDT). The parameterss of austenite stability, presence of prior martensite nuclei and hydrogen content have been evaluated through analyzing the tensile strength, ductility, time to fracture and fracture surface of hydrogen pre-charged SSRT and DDT specimens. Steels having prior martensite nuclei or more unstable austenite were found more sensitive to delayed fracture. Besides, the time to fracture declined with increasing diffusive hydrogen content in a power-law manner. In addition, delayed fracture in DDT specimens could be prohibited by raising the forming temperature and punch velocity, owning to the suppressed phase transformation and partial residual stress relief. Fractographic studies revealed the transition of fracture mode from ductile to quasi-cleavage/inter-granular fracture depending on hydrogen content and stress triaxility.

4:45 PM

In-Situ EBSD Study of Micromechanical Behavior of TRIP Steel: *Nan Li*¹; Yandong Wang¹; Xin Sun²; Guilin Wu¹; Kang Yuan¹; ¹Beijing Institute of Technology; ²Pacific Northwest National Laboratory

The deformation-induced martensitic transformation behaviors have been investigated for several decades, while the origin of plasticity enhancement is less understood so far. Transformation-induced-plasticity (TRIP) steels are a typical class of multiphase steels, of which contains metastable austenite transforming into martensite lately during deformation, offering an attractive combination of strength and plasticity. In this presentation, we will report the in-situ experimental investigations of micro-mechanical behavior of the TRIP steel using Electron Back-Scattered Diffraction (EBSD) technique, which accounts for the quantitative information on contribution of the transformation-induced plasticity to the total plasticity. EBSD orientation mapping of all phases at different applied strains provide not only the transformation kinetics from austenite to martensite, but martensitic transformation crystallography, grain rotation, and strain partitioning of individual grains as well. Our investigations are important for in-depth understanding the role of martensite variant selection in the TRIP effect during plastic flow in the alloys with metastable phase.

5:00 PM

Patterning of Alloy Precipitation through External Pressure: Jack Franklin¹; Jennifer Lues¹; ¹University of Pennsylvania

Industrial heat treating has been developed to optimize the selection of final microstructures, and therefore material properties, across products as a whole. However as engineering problems become more complex and require multi-functional solutions it is desirable to fabricate 'architectured' or designed components whose microstructure and properties may vary across the sample. In this talk, I present an innovative processing technique designed to control the location of formation and growth rate of precipitates within metallic alloys in order to create multiple patterned areas of unique microstructure within a single sample. Control over precipitation is achieved by an additional surface pressure applied to selected locations during precipitate heating. The applied pressure changes both the enthalpic and chemical potential landscapes, which in turn control the rate and directionality of atomic diffusion in regions close to the loaded surfaces. Experimental results displaying a dependence on quench rate and thermal history are presented.

Dynamic Behavior of Materials V: Dynamic Effects in Materials

Sponsored by: The Minerals, Metals and Materials Society, TMS Structural Materials Division, TMS/ASM: Mechanical Behavior of Materials Committee

Program Organizers: Marc Meyers, UCSD; Naresh Thadhani, Georgia Institute of Technology; George Gray, Los Alamos National Laboratory

Wednesday PM	Room: 5A
March 2, 2011	Location: San Diego Conv. Ctr

Session Chair: Ellen Cerreta, Los Alamos National Laboratory

2:00 PM Invited

The Use of Diagnostics in Determining the High-Rate Response of Granular and Porous Materials: *W.G. Proud*¹; D.J. Chapman¹; W. Neal¹; D. Eakins¹; ¹Cavendish Laboratory

Granular and porous materials are widely encountered in nature, industrial products and engineerings applications. These materials are often used for their lightweight or shock absorbing properties. Characterising them at highstrain rates is difficult due to a number of factors; they tend to have very low strengths in the initial part of their crushing behaviour resulting in low initial signals in most diagnostics when most of the compaction is occurring; they display a marked ramping effect on any mechanical stimulus, resulting in incomplete compaction during the loading pulse and a strongly variable mechanical impedance; they show relatively large movements before becoming compact producing marked strain for in-material diagnostics which then produce incorrect signal levels; as well as these diagnosticrelated issues, it has been found that in looking for trends in behaviour that while granular materials generally change their properties slowly over a large range of porosities they can manifest a step change in their behaviour when a critical porosity is reached. This paper will outline some of the difficulties in studying these materials, review progress made, discuss the use of mulliple diagnsotics to understand the fundamental processes in these materials.

2:30 PM

Determination of Bulk Modulus and Shear Modulus of Human Thoracic Organ Tissue and Biosimulants at High Strain Rates: Morgan Trexler¹; Andrew Lennon¹; Adam Maisano¹; Alexis Wickwire¹; Timothy Harrigan¹; Quang Luong¹; Andrew Merkle¹; ¹Johns Hopkins University Applied Physics Laboratory

Modeling human body response to dynamic loading events and developing human surrogates require accurate high rate material properties of organ tissues. This work describes characterization of dynamic mechanical behavior of human thoracic organ tissues, including liver, lung and spleen, as well as biosimulants. Modified split Hopkinson pressure bar techniques were developed for measuring bulk and shear moduli under hydrostatic pressure and shear loading, respectively. Hydrostatic pressure was achieved via use of a steel confinement cylinder around a disc-shaped specimen. Shear specimens were tested in a double lap shear configuration. Shear tests require establishment and maintenance of a uniform state of stress in the sample, which was achieved via pulse shaping and verified using piezoelectric quartz force gages on the input and output sides of the specimens. Results of bulk and shear tests of thoracic organ tissues and silicone-based biosimulant materials are reported. Comparisons are made between tissues and simulants.

2:45 PM

Electrically Driven Expanding Plasma as a Means to Drive High Velocity and High Strain Rate Experiments: *Anupam Vivek*¹; Jason Johnson¹; Gregg Fenton²; Geoff Taber¹; Glenn Daehn¹; ¹Ohio State University; ²Applied Research Associates

When directed properly, plasma created by rapid vaproization of a metallic wire or foil by passing a very high current through them is an efficient medium for converting electric energy into kinetic energy. This energy can



then be used to propel sheets, tubes etc. at very high speeds. This method can provide considerable simplification in the experimental system as compared to electromagnetic solenoid actuators, and the consumable component can be very inexpensive. In this work, copper and aluminum tubes are expanded using fast, capacitor bank driven, vaporization of coaxially placed wires. Diameter, length and material of wire are varied for optimization purposes. Pressure is calculated from the velocity-time measurements done by Photon Doppler Velocimetry. Currents and voltages are also recorded. The pressure, current and voltage data would be compared against a multi-physics numerical model. Applications of the method will be discussed as will design rules for efficient system design.

3:00 PM

Shear-Rate Dependence in Dislocation Pile-up Simulations at Asymmetric Tilt Boundaries in Aluminum: Steven Valone¹; Jian Wang¹; Richard Hoagland¹; Timothy Germann¹; ¹Los Alamos National Laboratory

Materials deformation processes are increasingly approachable through atomistic methods. In one deformation process, dislocation pile-up at a grain boundary, how dislocations transmit through grain boundaries is of intense interest. Here dislocation pile-ups in an aluminum bicrystal with an asymmetric sigma-11 tilt grain boundary are simulated. Dislocations are initially distributed according to linear elastic estimates from a far-field stress of 40 MPa. The system is propagated for different periods of time, representing different shear rates. Incremental loading occurs every 40 ps or every 80 ps. In spite of the factor of two difference in shear rate, differences in the events are quite marked. At the higher rate, dislocations are transmitted on both available slip systems. The entities transmitted are perfect dislocations. At the slower rate, transmission and reflection events consist of multiple Shockley partial dislocations, parallel to each other, on one of the slip planes.

3:15 PM

Thermal Stability of Commercially Pure Ultra-fine Grained Al at High Strain Rates: *Emily Huskins*¹; K Ramesh¹; ¹Johns Hopkins University

Materials with ultra-fine grained (UFG) nanostructures are of interest due to their improved strengthening over their coarse-grained counterparts. However, these materials also exhibit different strain rate sensitivity and deformation mechanisms, both of which affect the stability of plastic deformation and therefore ultimate failure. One such example is thermal stability of UFG materials. While the thermal stability of coarse grain Al is available in ASM Handbooks this data cannot be applied for UFG and nanocrystalline Al due to changes in deformation mechanisms as a result of grain size reduction. In addition, there are limited studies of either UFG or coarse grained materials at elevated temperatures and high strain rates. In this work an UFG commercially pure Al (obtained through ECAP) is tested under dynamic compression (10^3 s^{-1}) at elevated temperatures (298K – 573K). The thermal stability of this material is investigated and a physics-based internal variable constitutive model is presented.

3:30 PM

The Implications of Loading History on Grain Size Effects in Polycrystalline Copper Spallation Damage from Hydrocode Simulations: Davis Tonks¹; Ellen Cerreta¹; Darcie Dennis-Koller¹; John Bingert¹; Veronica Livescu¹; Curt Bronkhorst¹; ¹Los Alamos National Lab

New incipient damage spallation experiments are being done at LANL on polycrystalline copper exploring the effects of grain size and loading rate on incipient damage morphology. The emphasis is on metallurgical and tomographic examination of the damage state in recovered samples, supplemented by VISAR records of the free surface velocity. However, a full understanding of the recovered damage morphology and its evolution requires a knowledge of the stress and strain histories of the damage process which are not measured in the experiment but must be calculated. This work presents calculated stress and strain histories of the gas gun shots together with their implications about the damage structures. The calculations will include 1D hydrocode simulations and some FEM simulations with more detailed grain microstructure included. The 1D simulations will reveal spatially averaged loading histories while the FEM calculations will reveal crystal grain effects investigation.

3:45 PM

Dynamic Characterization of Cast and Wrought Uranium-Niobium Metals: *Carl Cady*¹; George Gray¹; Ellen Cerreta¹; Robert Aikin¹; Dan Thoma¹; Robert Field¹; ¹Los Alamos National Laboratory

A uranium-6wt% niobium alloy with different processing paths was investigated as a function of strain rate, temperature and stress state. The "wrought" material was produced by forging and forming and the second material was generated using direct cast methods. Characterization over a range of rates and temperatures was used to generate a constitutive material model and Taylor impact testing was used to validate the model. The yield and flow stresses of the U-Nb materials was found to exhibit a pronounced strain rate sensitivity, while the hardening rates were found to be insensitive to strain rate and temperature. Twin dominated deformation processes are seen in U-6Nb at low strain rates. High strain rate and shock loading can be dominated by twinning or phase transformation. Evaluation of explosively driven hemispheres will provide insight into the relative difference between the two processing paths and an interpretation of the test results will be presented.

4:00 PM Break

4:10 PM Invited

Characteristic Responses of Thick Ceramic Bodies to High-Velocity Impact: *Jerry LaSalvia*¹; James McCauley¹; Jeffrey Swab¹; Parimal Patel¹; ¹U.S. Army Research Laboratory

Characteristic responses of ceramics to high-velocity impact by hard and ductile projectiles have been the recent subject of investigation. Most investigations have focused on ballistic response by determining the penetration-depth history of the projectile through the ceramic as a function of impact velocity. This enables penetration onset velocity, penetration velocities, and dwell durations to be estimated. Other investigations included post-mortem examination of the ceramics. These have provided insight into the fundamental processes governing both ballistic and material responses of ceramics. Because high-velocity impact involves the generation of transient, large amplitude, spatially and temporally varying stresses, these responses are complex, involving processes that span macro-to-nano length-scales driven primarily by shear and tension. Mechanistically, macrocracking, microcracking, comminution and fragmentation, solid-state amorphization, shear localization, microplasticity, twinning, grain boundary slip, stacking faults, and phase transformations have been observed. The characteristic responses of ceramics to high-velocity impact by hard and ductile projectiles will be reviewed.

4:40 PM Invited

Effects of Strain Rate and Stacking-Fault Energy on Microstructures and Mechanical Properties of Deformed Cu and Cu-Al Alloys: Y. Zhang¹; N.R. Tao¹; K. Lu¹; ¹SYNL, Institute of Metal Res.

Pure Cu and Cu-Al alloys were subjected to quasi-static compression (QSC) and dynamic plastic deformation (DPD) in order to investigate the effects of strain rate and stacking fault energy (SFE) on the microstructures and mechanical properties. For low SFEs, deformation twinning occurs in the QSC samples, and the amount of twins increases with decreasing SFEs. The twin thickness and sizes of refined grains decrease with a reduction of SFEs. For the DPD samples, the amount of twins is insensitive to SFE. However, the twin thickness and grain sizes decrease significantly with smaller SFEs. The microstructure characteristics of DPD samples with different SFEs are determined including twin thickness, grain size, volume fraction of nanosclae twins, etc. Tensile strength and ductility of the QSC and DPD sample are analyzed in terms of their microstructure features.

5:10 PM

The Critical Role of Shock Melting in Ultrafast Laser Machining: *Ben Torralva*¹; S. Ma¹; A. Kumar¹; S. M. Yalisove¹; T. M. Pollock²; K. Thornton¹; ¹University of Michigan; ²University California, Santa Barbara

The interaction of ultrashort laser pulses (ULP) with materials holds fundamental importance. To understand the damage and the dynamic deformation behavior under theses unique conditions, we combine computational modeling and experimental characterization of the collateral damage in CMSX-4. Hydrodynamics modeling is employed to simulate the interaction of ULP with metals to gain understanding of the state of the material during deformation, and a combination of experimental techniques is used to characterize the damage. We observe that the dislocation distribution is confined to the region beneath the laser-irradiated region, unlike with nanosecond lasers. Moreover, the amount of damage injected can be dramatically enhanced or suppressed depending on laser fluence. We propose that the initiation of shock melting is the origin of the sharp transition in ablation efficiency and in the amount of damage injected into the bulk. The importance of d-state scattering in the electron thermal transport model will be discussed.

5:25 PM

Blast Wave Mitigation Using a Nanoporous Functionalized Liquid Materials: Yu Qiao¹; Douglas Giese²; ¹UCSD; ²AgileNano

The use of bombs and blasts are the number one threat to the U.S. troops in Iraq and Afghanistan. Recently, we developed a novel, nanoporous functionalized material, AgileZorb, that can react within microseconds to sufficiently affect a shock front. AgileZorb is formed by immersing nanoporous particles in a liquid phase. The inner nanopore surface is specially treated so that it is nonwettable to the liquid. Under ambient condition, due to the capillary effect, the nanopores remain empty. At a blast wave front, the local high pressure can rapidly compress the liquid into the nanopores, converting a significant amount of energy into heat as well as interfacial tension. Our experiments have shown encouraging results.

5:40 PM

Effects of Grain Size and Boundary Structure on the Dynamic Response of Polycrystalline Copper: *Juan Escobedo*¹; Ellen Cerreta¹; Darcie Dennis-Koller¹; Curt Bronkhorst¹; Benjamin Hansen¹; Ricardo Lebensohn¹; Davis Tonks¹; Brian Patterson¹; ¹Los Alamos National Laboratory

Plate-impact experiments were conducted to examine the effect of grain size (30, 60 and 200 \956m) on the dynamic tensile response of high purity copper samples. The preceding compressive stress was ~1.5 GPa for all tests, low enough to cause early stage incipient spall. The free-surface velocity histories show no significant effect of the grain size on the initial pull-back signal. The quantitative metallography of the recovered samples shows the volume fraction of voids to be 0.4% for all cases. Nevertheless, the void size distribution is different, with the void size increasing with increasing grain size. In the 200 \956m samples, void coalescence was observed along the grain boundaries, whereas in smaller grained specimens individual voids dominated the deformation. EBSD observations show that voids preferentially nucleate/grow at grain boundaries with high angle misorientation, while the boundaries corresponding to low angle (<5°) or (931 3 type were more resistant to damage.

Electrode Technology for Aluminium Production: Cathode Design and Operation

Sponsored by: The Minerals, Metals and Materials Society, TMS Light Metals Division, TMS: Aluminum Committee Program Organizers: Alan Tomsett, Rio Tinto Alcan; Ketil Rye, Alcoa Mosjøen; Barry Sadler, Net Carbon Consulting Pty Ltd

Wednesday PM	Room: 16B
March 2, 2011	Location: San Diego Conv. Ctr

Session Chair: Richard Jeltsch, Consultant

2:00 PM Introductory Comments

2:05 PM

Preheating Collector Bars and Cathode Blocks Prior to Rodding with Cast Iron by Passing an Ac Current through the Collector Bars: *Erik Jensen*¹; Hans Petter Bjørnstad²; Jan Hansen²; ¹EAJ Consulting; ²ALMEQ

Three basic methods for heating collector bars and cathode blocks prior to pouring cast iron are in use today; gas burners directly impinging on the collector bars, ovens for heating bars and blocks separately, and third, passing an alternating electrical current through the collector bars to heat bars and blocks simultaneously. This paper examines electrical heating using the collector bar as the heating element. Passing an alternating current through the collector bar produces an easily regulated and uniform temperature throughout the bar. Radiant energy from the bar heats the slot area of the cathode block. Temperature levels are adjusted by time and voltage selection. Electrically heating collector bar/cathode block assemblies uses less than 15% of the energy required for propane gas burner heating. The method is quiet, requires little or no supervision, has no products of combustion to exhaust, and temperatures are highly repeatable.

2:30 PM

Development and Application of an Energy Saving Technology for Aluminum Reduction Cells: *Peng Jianping*¹; Feng Naixiang¹; Feng Shaofeng²; Liu Jun³; Qi Xiquan⁴; ¹Northeastern University; ²Zhejiang Huadong Aluminum Corporation Ltd.; ³East Hope Baotou Xitu Aluminum Ltd.; ⁴Northeastern University Engineering & Research Institute Co. Ltd

An energy saving technology based on novel structure cathodes in aluminum reduction cells has got wide application and development in many smelters in recent years. Structure characteristic of the cells are described in this paper. Some details, such as lining structure and wear of cathodes, are discussed according to the present applications. And the effect of bath component on energy consumption is also studied.

2:55 PM

Study of Electromagnetic Field in 300kA Aluminium Reduction Cells with Innovation Cathode Structure: *Baokuan Li*¹; Xiaobo Zhang¹; Suirui Zhang¹; Fang Wang¹; Naixiang Feng¹; ¹Northeastern University

The flow field of molten aluminum is divided by the novel structure that there are twenty-six pairs of convex blocks on the innovation cathode surface, as thus, the flow velocity decreases significantly, which weaken effectively the effect of gravity waves of molten aluminum so as to reduce the volatility of molten aluminum. The novel cathode structure can make the current distribution in the molten aluminum more uniform, which can reduce the flow power of molten aluminum. Small current in horizontal direction come into being on the convex surfaces, the current force the molten aluminum to form a loop around the convex plates, which is not only to weaken the action of vertical wave in aluminium reduction cells, but also is conducive to the dissolution of alumina. The aluminium reduction cells with innovation cathode structures have smaller fluctuations, stronger stability and improve the current efficiency of aluminum reduction cells.

3:20 PM Break

3:30 PM

Evaluation of the Thermophysical Properties of Silicon Carbide, Graphitic and Graphitized Carbon Sidewall Lining Materials Used in Aluminium Reduction Cell in Function of Temperature: *Ayesha Khatun*¹; Martin Desilets¹; ¹University of Sherbrooke

The thermal properties of the sidewall lining materials are required to ensure good predictions of the dynamic thermal behavior of Hall-Heroult cells. A precise estimation of energy losses and location of the side freeze, are made possible when the sidewall lining materials are well characterized as a function of temperature. The present work uses transient characterization techniques to measure the thermal diffusivity, heat capacity and thermal conductivity of silicon carbide, graphitic and graphitized carbon materials. The thermal diffusivity and the heat capacity are measured by state-of-the-art transient laser flash analyzer and a differential scanning calorimeter respectively. The thermal conductivity is calculated by assuming a constant density. Finally, based on the calculations conducted with a 2-D numerical model, the effect of the temperature varying thermal properties of the sidewall materials on the dynamic behavior of a laboratory scale phase change reactor is presented.

3:55 PM

Advanced Numerical Simulation of the Thermo-Electro-Mechanical Behaviour of Hall-Héroult Cells under Electrical Preheating: Daniel Marceau¹; Simon Pilote¹; *Martin Désilets*²; Lyès Hacini³; Jean-François Bilodeau³; Yves Caratini³; ¹Université du Québec à Chicoutimi; ²Sherbrooke University; ³Rio Tinto Alcan

In today's context, aluminum producers strive to improve their position regarding energy consumption and production costs. To do so, mathematical modeling offers a good way to study the behavior of the cell during its life. This paper deals with the numerical simulation of the electrical preheating of a Hall-Héroult cell using a quarter model of the cell. The fully coupled thermo-electro-mechanical model includes material non linearities and multiphysical behavior at interfaces allowing accurate evaluation of the stress distribution in the cathode blocks and surrounding components. The baking of the ramming paste as well as the evolution of its thermo-electro-mechanical properties are updated via the baking index computed using a kinetic of reaction. The model is initially calibrated with in situ measurements and then used to estimate the effect of preheating on the behavior of the cell including temperature, current, deformations as well as the contact conditions at critical interfaces.

4:20 PM

Creep Behaviors of Industrial Graphitic and Graphitized Cathodes during Modified Rapoport Tests: *Wei Wang*¹; Jilai Xue¹; Jianqing Feng²; Qingsheng Liu²; Lei Zhan²; Hua He²; ¹Unversity of Science and Technology Beijing; ²Ningxia Qingtongxia Energy Aluminium Group, China Power Investment Corporation

Creep is of importance for reduction cell design and cathode construction. The purpose of this work is to obtain the creep data for various cathode products under the conditions close to the industrial operation in reduction cells. A modified Rapoport equipment was used for measuring the creep behaviors during aluminum electrolysis with CR=4.0 and at temperature of 965°. Testing samples were taken from industrial semi-graphitic, full graphitic and graphitized carbon products and characterized for their graphitized degree using XRD method. The values of d200 for all cathode samples were lowered after aluminum electrolysis, and the graphitized cathode made in an energy saving heat-treatment process still showed smaller creep deformation than those of semi-graphitic and full graphitic cathode samples. The obtained data will be useful for quality control of cathode product and improvement in cathode performance.

Friction Stir Welding and Processing VI: Process Modeling and Verification

Sponsored by: The Minerals, Metals and Materials Society, TMS Materials Processing and Manufacturing Division, TMS: Shaping and Forming Committee

Program Organizers: Rajiv Mishra, Missouri University of Science and Technology; Murray Mahoney, Retired from Rockwell Scientific; Yutaka Sato, Tohoku University; Yuri Hovanski, Pacific Northwest National Laboratory; Ravi Verma, General Motors

Wednesday PMRoom: 5BMarch 2, 2011Location: San Diego Conv. Ctr

Session Chairs: Guntram Wagner, University of Kaiserslautern; Carl Sorensen, Brigham Young University

2:00 PM

Effect of Plasticized Material Flow on the Tool Feedback Forces during Friction Stir Welding: *Enkhsaikhan Boldsaikhan*¹; Dwight Burford¹; Pedro Gimenez Britos¹; ¹Wichita State University

The goal of this study is to characterize the dynamic nature of the friction stir welding process by examining time series data of the tool feedback forces. The tool feedback forces are generated by the resistance of the material to deformation in direct response to the rotational and translational motion of the weld tool during the welding process. While traveling from the leading face to the trailing face of the weld tool, a "pulse" flow of plasticized material usually imposes dynamic shear stresses and normal stresses on the weld tool surfaces. These dynamic stresses constitute the resultant tool feedback forces and the spindle torque that can be captured during the process. In this study, a 2D model, based on a pseudo shear stress concept, is established to characterize oscillations of the feedback forces with the dynamics of the material flow, including erratic flow associated with flaw formation.

2:20 PM

Weld Flaw Analysis of High Speed Friction Stir Processed Magnesium AZ31: Leon Hütsch¹; Jorge dos Santos¹; Norbert Huber¹; ¹GKSS Forschungszentrum GmbH

In the present study processing parameters in a range of welding speeds varying from 1 to 10m/min have been investigated in combination with different vertical forces and tool rotational speeds. The welding has been carried out on 2mm thick rolled AZ31sheets employing a Tricept 805 robot. The tool consisted of a threaded shoulder and a pin with three flats. The obtained welds were analysed by optical and electron scanning microscopy. The results have been compiled in the form of correlations between welding speed and vertical force as well as rotational speed, whereby regions of defect-free and defective welds could be identified. These results allow the determination of a stable process window. The verification and further refinement of the process window has been performed based on hardness and tensile testing of the produced welds. Additionally, an artificial neural network was trained to correlate the processing parameters with the observed weld flaws.

2:40 PM

Developing an Alternative Heat Indexing Equation for FSW: Joseph Querin¹; Judy Schneider¹; ¹Mississippi State University

In friction stir welding (FSW), a non-consumable, rotating weld tool is used to impart large shear deformations under simultaneous compressive stress states to join the faying surfaces of a weld joint. As a result of the process, the workpiece material microstructure is altered due to heat and plastic deformation. The peak temperature experienced in the weldment is guided by the workpiece material, weld tool geometry, friction stir weld tooling, and process parameters. This temperature is believed to be an important parameter in determining the characteristics of the weld and resultant weld properties. As there are currently no reliable analytical methods for determining process parameters, an alternative heat indexing equation is formulated based on maintaining a constant peak temperature.

3:00 PM Invited

Finite Element Modeling of Friction Stir Welding: Paul Dawson¹; Donald Boyce¹; ¹Cornell University

Friction stir welding is a complex process that severely alters the microstructure as metal is deformed by the action of the probe. Modeling the mechanical response involves solving coupled equations for the plastic flow, heat transfer, and evolution of critical descriptors of the state, especially the strength and damage. We summarize the components of a three-dimensional formulation for friction stir welding that incorporates of these elements. It utilizes an Eulerian reference frame and is limited to a steady-state approximation, but provides fully-coupled solutions for the flow field, temperature distribution, and state variables for strength and porosity. Of particular importance is the choice of constitutive equations that represent the viscoplastic behavior of the metal including strain hardening and softening. We illustrate the formulation with simulations of the welding of a titanium alloy and conclude with a discussion of remaining challenges for robust and useful simulation capability for the welding community.

3:25 PM

Investigation of Methods to Control Friction Stir Weld Power with Spindle Speed Changes: Kenneth Ross¹; Carl Sorensen¹; ¹Brigham Young University

Process zone temperatures in FSW determine the properties of the resulting weld and dramatically effects tool life in PCBN tools. Therefore an active control system to control weld temperature is desirable. Spindle power is a key factor in temperature control because it is the primary power input to the stir zone. Temperature control is achieved by using an outer control loop to set the desired power based on temperature feedback and an inner loop to adjust spindle speed to achieve the desired power. The inner loop can be achieved using a power feedback PID loop. Alternatively torque feedback can be used to change spindle speed to achieve the desired power. The choice of control scheme will affect the ability to control the process temperature. This paper investigates the dynamics of power control using the different control schemes and describes the implications of the control scheme on the temperature control process.

3:45 PM

Materials Design for Joinable, High Performance Aluminum Alloys: *Ryan Glamm*¹; Greg Olson¹; ¹Northwestern University

A systems based approach is used to design an aluminum alloy which has compatibility with friction stir welding, sufficient strength, resistance to stress corrosion cracking, and low cost of processing. As part of the systems approach, quantitative models are used to enhance predictive capabilities. PrecipiCale software is used to model nucleation, growth, and coarsening to characterize the relationship between processing and structure. A strength model is utilized from previous literature to model the relationship between structure and properties. Prototype alloys are designed and then characterized using atom probe tomography. Modeling parameters are calibrated from atom probe characterization of isothermal aging treatments. Friction stir weld thermal cycles are input into PrecipiCale to gain insight on microstructural evolution during welding. The resulting microstructures are input into the strength model and compared to experimental hardness data. These predictions are validated by experimental friction stir welding timetemperature cycles and microhardness measurements.

4:05 PM

Transient Heat and Material Flow Modeling of Friction Stir Processing of Magnesium Alloy: *Zhenzhen Yu*¹; Hahn Choo¹; Wei Zhang²; Zhili Feng²; ¹University of Tennessee; ²Oak Ridge National Laboratory

A three-dimensional transient model with a threaded pin tool was developed to investigate material flow and heat transfer during friction stir processing (FSP) of AZ31B Mg plate. The material was considered as a non-Newtonian viscoplastic fluid, and constitutive law was employed to describe the dependence of viscosity on temperature and strain rate, with the material constants determined from compression test under a wide range of temperatures and strain rates. A dynamic mesh method, combining Lagrangian and Eulerian formulations, was used to capture the material flow induced by the stirring motion of the pin. Temperature profiles recorded from actual FSP experiments were used to validate simulation results. Furthermore, massless inert particles were embedded in the model to track the detailed material flow history. Finally, a model with a smooth pin surface was established as well, in order to compare the influence of thread on the simulated thermal history and material flow.

4:25 PM Break

4:35 PM

Approaches to In-Situ Data Monitoring of FSW Quality: Haley Doude¹; Judy Schneider¹; ¹Mississippi State University

Since the development of friction stir welding (FSW) in 1991, researchers have seen the need for ways to better understand and predict FSW results. Current practices use a trial and error method to develop weld parameters for new materials to the FSW process and thorough destructive and nondestructive testing to prove that the weld is acceptable. Because of the time and expense of testing, other ways of developing parameters and determining weld quality are necessary. One such area of research is processing of the output signals from the FSW machine. If successful, weld quality could be determined real time or post-weld without destructive testing of the weld panel. Process parameters could also be adjusted real time to improve the weld quality as the material is being welded. This paper evaluates current research approaches and their effectiveness in determining weld quality.

4:55 PM

A Comparison of Experimental Data and Model Predictions with Constitutive Laws Commonly Used to Model Friction Stir Welding: *Katherine Kuykendall*¹; Carl Sorensen¹; Tracy Nelson¹; ¹Brigham Young University

Numerical modeling of friction stir welding is dependent on the constitutive law used to determine flow stress as a function of strain rate, temperature, and strain. Commonly used constitutive laws include Sheppard and Wright, Johnson-Cook, and Kocks and Mecking. Material constants were determined for AA5083 for these laws from constant strain rate and temperature compression data found in the Atlas of Formability. Two-dimensional Lagrangian models of axial compression tests identical to source data tests were developed. The modeled stress-strain curves were compared with curves from the Atlas of Formability.The Sheppard and Wright law is capable of capturing saturation but incapable of capturing strain hardening, which can account for up to 20% plastic strain. The Johnson-Cook law is capable of capturing strain hardening; however, its inability to capture saturation causes overpredictions of stress at large strains. The Kocks and Mecking model is capable of capturing strain hardening and saturation.

5:15 PM

Long Range Oscillations in Friction Stir Welding Tool Travel Speed: Mike Brendel¹; Judith Schneider¹; ¹Mississippi State University

Oscillations in the weld travel speed were observed during Friction Stir Welding (FSW) of Al-Li 2195-O panels. These oscillations can be explained as a beat frequency occurring between the frequency of the inverse weld pitch and the frequency of feedback correction to the weld table travel speed to maintain the initial set-point. The frequency of table correction was found to be constant in the inverse distance domain, but not in the inverse time domain. Measurements of the spacing between individual tooling marks on the FSW surface confirm these travel speed oscillations. Measured forces during the welding process were also influenced by these travel speed oscillations. The changing of the tool rotation rate from 170 to 200 RPM at constant travel of 13 IPM shifted the wavelength of the oscillations such that the inverse weld pitch at 200 RPM closely matched the frequency of table correction.

5:35 PM

Tool Load and Torque Study for Portable Friction Stir Welding in Aluminum: *Scott Rose*¹; Murray Mahoney²; Tracy Nelson¹; Carl Sorensen¹; ¹Brigham Young University; ²Consultant

As Friction Stir Welding (FSW) broadens its applications, the need for portable equipment has arisen. Minimizing both loads and torques is



necessary to fabricate a truly versatile and portable FSW system. In order to do this, a tool study was done to find the minimal loads needed to achieve a feasible portable system. This study evaluated optimal loads, torque and surface temperature profiles in AA 5083 through the variation of RPM, IPM, and different pin and shoulder configurations of two-piece FSW tools. Plunge studies were also done to evaluate different approaches to further reduce the high loads typically seen during the plunging of an FSW tool. Typical consolidated welds in this study were produced with around 2000 lbs of load and 20 ft-lbs of torque. Results from these studies will be presented illustrating the optimum tool design and weld parameters to minimize the load requirements for a portable FSW system.

5:55 PM

Towards Process Control of Friction Stir Welding for Different Aluminum Alloys: Axel Fehrenbacher¹; *Edward Cole*¹; Michael Zinn¹; Nicola Ferrier¹; Neil Duffie¹; Frank Pfefferkorn¹; ¹Univ. Wisconsin-Madison

The real-time temperature measurement of aluminum alloy 6061-T6 friction stir welds (FSW) has shown that spindle speed has a greater influence on the tool-workpiece interface temperature than travel speed. This process knowledge allows for spindle speed to be used as a control method for maintaining weld temperature. However, spindle speed dominance has not been shown to be true for all aluminum alloys 2024-T3, 5083-H116, and 7075-T6, where alloy 5083 is the only alloy of which neither spindle speed or travel speed has a significant effect on the interface temperature. Among the alloys, not only does the average interface temperature vary, but also the amplitude in temperature change, depending on the alloy and chosen weld parameters (spindle or travel speed).

General Abstracts: Structural Materials Division: Applications

Sponsored by: The Minerals, Metals and Materials Society, TMS Structural Materials Division, TMS: Advanced Characterization, Testing, and Simulation Committee, TMS: Alloy Phases Committee, TMS: Biomaterials Committee, TMS: Chemistry and Physics of Materials Committee, TMS/ASM: Composite Materials Committee, TMS/ASM: Corrosion and Environmental Effects Committee, TMS: High Temperature Alloys Committee, TMS/ASM: Mechanical Behavior of Materials Committee, TMS/ASM: Nuclear Materials Committee, TMS: Refractory Metals Committee, TMS: Titanium Committee

Program Organizers: Roger Narayan, Univ of North Carolina & North Carolina State Univ; Judith Schneider, Mississippi State University

Wednesday PM March 2, 2011 Room: 31C Location: San Diego Conv. Ctr

Session Chair: To Be Announced

2:00 PM

Steel Design for Blast and Fragment Protection: Zechariah Feinberg¹; ¹Northwestern University

In light of the general increase in terrorist attacks, there is a pressing need to design high performance, blast resistant steels that are capable of withstanding high impact explosions. The ultimate goal of this research is develop a blast resistant steel from a materials science perspective by fully understanding the interrelation between the processing, structure, properties, and performance. In this project, a systems-based approach using predictive models has been implemented to design a high-performance transformationinduced plasticity (TRIP) steel. An experimental alloy called TRIP-120 has been designed, created, optimized, and experimentally tested to verify the predicted property objectives of high strength, high toughness, shear localization resistance, and high uniform ductility to maximize energy absorption and deliver maximum blast resistant performance. By combining computational tools with experimental data, predictive models have been used to design optimized steel alloys for high strain rate loading conditions for improved blast and fragment penetration resistance.

2:15 PM

Effects of Differential Oxygen Access on the Corrosion Behavior of Zinc Relevant to Mechanically Stabilized Earth Walls: Victor Padilla¹; Akram Alfantazi¹; ¹UBC

The purpose of this work is to study the effect of differential oxygen access on the corrosion performance of zinc, the most commonly used material used as protection system on Mechanically Stabilized Earth (MSE) walls. Uneven soil compaction creates differential oxygen access, which promotes corrosion macrocells. High purity zinc (99.6%) was immersed in solutions with varied concentration of Na2SO4 to simulate the conditions in soils and ground water, while the concentration of NaCl was kept at 3.5 wt%. Corrosion rates were measured using potentiodynamic anodic polarization method in different concentrations of oxygen. Scanning Electron Microscope (SEM), and X-Ray Diffraction (XRD) were used to characterize the corroded samples. The results indicate an increase on the corrosion rate with increasing amount of Na2SO4, as well as a potential difference between samples at different oxygen concentrations, which indicates the possibility for macrocell formation under the studied conditions.

2:30 PM

Analysis of Eutectically Soldered Silicon Chips on a Copper Flanges with Innovative "Ductile Layer" Technology: Pu Zhou¹; *Michael Zimmerman*¹; Anil Saigal¹; ¹Tufts University

Managing thermal performances of high power silicon devices is critical in assuring long term reliability. For LDMOS power transistors, thermal performance has traditionally been optimized using hard "AuSi" eutectic solder, whereas, the flange is made of copper. Copper is a much more thermally conductive material, but it has a CTE mismatch with the silicon die that can result in large stresses and potential cracking of the die. A "ductile layer" technology has been developed to mitigate this problem. This paper presents the finite element analysis of stresses and deformation of eutectically soldered silicon chips to a copper flange incorporating the ductile layer technology. In this study different geometric and material characteristics of the ductile layer are considered. The analysis shows that the stresses in the silicon chips are significantly reduced due to the existence of the ductile layer, and the stresses decrease even further as the thickness of the ductile layer increases.

2:45 PM

Influence of Sulfide on Internal-Fracture-Type Rolling Contact Fatigue Life of Bearing Steels: *Kazuya Hashimoto*¹; Kazuhiko Hiraoka¹; Katsuyuki Kida²; ¹Sanyo Special Steel; ²Kyushu University

Energy saving is an important driving force to reduce of the size and weight of bearing components. Since bearings are expected to stand higher loads, it is desirable to substantially improve rolling contact fatigue (RCF) life of bearing steels and to develop the techniques to predict RCF life accurately. Flaking failure in RCF under well-controlled lubrication is originated from non-metallic inclusions. The factors to control this type of RCF life have not been clarified, except inclusion size, due to the difficulties in visualization of RCF processes. The authors have investigated the RCF processes through experiments on artificial-cavity-bearing materials, stress simulation and the evaluation of oxide-caused failure. The influences of sulfides on crack initiation and propagation behavior, and RCF life was examined in this paper.

3:00 PM

Stress-Rupture Behavior of Single Crystal Superalloy M09A: *Qi Zheng*¹; Jinxia Yang¹; Hongyu Zhang¹; Xiaofeng Sun¹; Hengrong Guan¹; Zhuangqi Hu¹; ¹IMR

M09A, a nickel-base single crystal (SC) superalloy was lately developed by IMR, CAS. Its hot corrosion-resistance is equivalent to that of IN738 and the stress-rupture property reach the level of first generation SC superalloys. It does not contain precious elements so that it is cheaper and lighter. It is a candidate used for turbine blade material working in marine environment and advanced IGT. The excellent stress-rupture property of M09A as a hot corrosion-resistant superalloy is resulted from the alloy design combined with the solidification control and heat treatment processes. Higher level of alloying strengthening was realized to obtain higher volume fraction of Ni3Al phase and avoid TCP phase formation. The grain boundary is removed by SC process to further improve the stress-rupture property and the hot corrosion-resistance at high temperature. More uniform and finer Ni3Al precipitates were obtained by the heat treatment process in the alloy.

3:15 PM

Tensile Deformation Characteristics of a Ferrite/Austenite Two Phase Steel Containing the High Mn and Al Contents: *Kyung-Tae Park*¹; Si Woo Hwang²; Jung Hoon Ji¹; Sera Kim¹; Youngil Son³; ¹Hanbat National University; ²Steel Research Institute; ³Agency for Defense Development

High Mn austenitic steels usually exhibit an excellent combination of strength and ductility, mainly due to twinning induced plasticity (TWIP). In this study, in order to produce the steel grade with the reduced specific weight as well as a good combination of strength-ductility, Al was added to a high Mn steel and its tensile characteristics were examined. The steel (Fe-20Mn-9Al-0.6C (in wt.%)) consisted of austenite and ferrite in a wide range of annealing temperatures. A special focus was made on identifying the deformation mode of austenite in relation to the SFE. This is because austenite deformation is primarily determined by the SFE and Al significantly increases the SFE of austenite. The results showed that austenite deformation was dominated by dislocation planar glide rather than TWIP even with the high SFE. The planar glide with the high SFE was rationalized in terms of the Fisher interaction.

3:30 PM

Shear Capacity of Reinforced Concrete Beams Using Recycled Coarse

Aggregates: Efe Ewaen Ikponmwosa¹; Musbau Salau¹; ¹University of Lagos An investigation into the shear capacity of reinforced concrete beams using recycled coarse aggregate from crushed graded inorganic particles processed from used construction materials and demolition debris is reported. Eighty (80) beams 150 x 150mm cross-sectional area and 1000mm length and twelve (12) cubes were cast. The concrete mix adopted was 1:2:4 (cement: sand: granite/recycled aggregate) with w/c ratio of 0.55 by weight. The percentage replacement of normal coarse aggregate by recycled aggregate was 0% for forty (40) beams and 30% for the remaining forty (40) beams. Six (6) cubes for each mix were cast. The specimens are subjected to line loads to determine their failure behaviour, deflection, crack patterns and post-crack performance. The results showed that the average density and strength of recycled aggregate concrete were slightly lower than that of normal aggregate concrete as the recycled aggregate concrete cubes densities and strengths averaged 97.8% and 88.7% of that of normal aggregate concrete. Each test beam specimen exhibited initial flexural failure at mid span. Diagonal cracks also propagated from each of the supports to the point of the application of load, indicating shear failure. The failure mode of the test specimens varied with the shear span - effective depth ratio as well as the concrete mix type.

3:45 PM Break

4:00 PM

Hot Deformation Behavior of Ti-6Al-4V Alloy with a' Martensite Starting Microstructure: *Hiroaki Matsumoto*¹; Bin Liu¹; Sang-Hak Lee²; Yunping Li¹; Kazuhisa Sato¹; Yoshiki Ono²; Akihiko Chiba¹; ¹Institute for Materials Research, Tohoku university; ²NHK Spring Co., Ltd

Hot deformation behavior and microstructural evolution of Ti-6Al-4V alloy in case of a' martensite starting microstructure were examined by comparing the case in equilibrium $(a+\beta)$ starting microstructure. In compression test in temperature region of $(a+\beta)$, Equiaxed grained structure is exhibited for both starting microstructures of a' martensite and equilibrium $(a+\beta)$ after compression test. Then, distortion-less ultrafine grained microstructure is obtained in case of a' martensite starting microstructure after hot compression especially under conditions of higher Z (Zener-Hollomon parameter). The apparent activation energy of hot deformation in temperature region of $(a+\beta)$ is 395 kJ/mol for the case of a' martensite starting microstructure and 320 kJ/mol for the case of $(a+\beta)$ starting microstructure, respectively. This result indicates that hot deformation behavior in the cases of a' martensite- and $(a+\beta)$ starting microstructure is different.

4:15 PM

Hot Ductility of Near-Alpha and Alpha + Beta Titanium Alloys: *Jeff Rodelas*¹; John Lippold¹; ¹The Ohio State University

Titanium alloy 5111 (5AI-1Sn-1Zr-1V-0.8Mo [wt%]) is a near-a intermediate-strength Ti alloy with excellent fracture toughness and low-temperature creep resistance. Elevated temperature mechanical behavior (up to ~1620 °C) has not been studied in great detail and is of great interest to many applications such welding. The hot ductility of β -processed Ti-5111 was measured using a Gleeble thermomechanical simulator. Samples were tested at temperatures from 600-1620°C using thermal cycles representative of welding. Ti-5111 exhibited a significant decrease in ductility when tested at temperatures below the β transus temperature exhibiting mixed inter/transgranular fracture with some ductile features. The sharp decrease in ductility for Ti-5111 below β transus likely contributes to processing-related issues such the poor friction stir weldability. Hot ductility of Ti-5111 was also compared to β -processed Ti-6Al-4V a + β alloy.

4:30 PM

Influence of Heterogeneous Deformation on Microstructural Cracking in Alpha-Titanium Alloys: *Motoaki Morita*¹; Satoshi Moroka¹; Osamu Umezawa¹; ¹Yokohama National University

Subsurface crack initiation in high-cycle fatigue has been detected as a transgranular cracking in alpha-titanium alloys at and below room temperature. Strain incompatible due to heterogeneous deformation may cause the cracking and form a crystallographic facet. In the present study, both neutron diffraction and Taylor analyses under tension mode were adopted to discuss the influence of heterogeneous deformation on the cracking. The stress distribution on grains was clearly detected and divided into soft and hard grains. The lowest rate of plastic work appeared at tensile axis of between [-12-11] and [-12-12]. The movable slip systems were determined as {01-10}<11-20> and {0001}<11-20>. The grain in which the highest rate of plastic work was around tensile stress axis of <0001> was hardly relaxed, since the slip systems of {10-11}<11-23> were not in active at all. Thus the tensile stress was accumulated normal to (0001) plane, and may assist to the microstructual cracking.

4:45 PM

Deformation Behavior of Biomedical Co-Cr-Mo Alloy: *Hiroaki Matsumoto*¹; Shingo Kurosu¹; Byong-soo Lee¹; Yunping Li¹; Yuichiro Koizumi¹; Akihiko Chiba¹; ¹Institute for Materials Research, Tohoku university

Cobalt-chromium-molybdenum (Co-Cr-Mo)-based alloys have been used as many kinds of biomedical applications due to their excellent biocompatibility and mechanical properties. The deformation behaviors of Co-27Cr-5.5Mo-0.16N (in mass%) alloy consisting of ε phase (fcc) and Co-27Cr-5.5Mo (in mass%) alloy consisting of e phase (hcp) were summarized in this study. Stacking fault formation followed by evoluiton to e phase with increasing strain was dominant deformation mode in γ Co-27Cr-5.5Mo-0.16N alloy. Excellent tensile ductility at room temperature more than 20% was seen in e Co-27Cr-5.5Mo-0.16N alloy. However, fracture occurred under quasi-brittle manner. Then, crack propagated preferentially at interface between ε phase and strain induced e phase which is due to the highly-accumulated strain at the interface. While, in e Co-27Cr-5Mo alloy, simultaneous activation of basal <a> slip and prismatic <a> slip is dominant deformation mode, and fracture occurred dominantly by intergranular fracture.



5:00 PM

Cyclic Oxidation Of Co-Al-W-Based Alloys At 900°C And 1000°C: *Raghavendra Adharapurapu*¹; Sara Perez-Bergquist¹; Jennifer Dibbern¹; Akane Suzuki²; Tresa Pollock³; ¹University of Michigan; ²General Electric Global Research Center; ³University of California Santa Barbara

New Co-Al-W-based alloys containing γ^2 -Co₃(Al,W) have been developed with superior high-temperature strength. Effect of quaternary additions of X=Ta/Mo/V/Ni on the phase stability and oxidation properties of Co-Al-W-X alloys have been investigated. Alloys were subjected to cyclic oxidation to a maximum temperature of 900°C/1000°C in air and SEM and XRD investigations of the oxidation products at various stages of oxidation have been conducted. A duplex oxide layer consisting of outer porous cobalt-oxide above a metal-rich complex oxide Co-W-Al-X-O was observed in all alloys. Compared to the Ni-based superalloys, the cobalt-based alloys have inferior oxidation resistance since the cobalt-oxide is not protective like alumina in Ni-based alloys. Among the quaternary elements, cobalt alloys with Ni additions exhibited the best oxidation resistance. Additions of V/Mo led to extensive spallation due to the formation of W-rich CoWO₄-spinels. Protective coatings or alternative alloying strategies may be necessary to improve the oxidation resistance of Co-based alloys.

5:15 PM

Effects of Solution Temperatures on Creep Properties and Fracture Mechanism of FGH95 Nickel-Base Superalloy: Jun Xie¹; Sugui Tian¹; ¹Shenyang University of Technology

By means of the enduring properties measurement and microstructure observation, an investigation has been made into the influence of the microstructure on the enduring properties and fracture mechanism of FGH95 superalloy. After solution treated at 1150°C, the thicker γ' phase is distributed in wider boundary regions. When temperature raised to 1160°C, the thicker γ' phase is fully dissolved, and the particles of (Nb, Ti)C are discontinuously precipitated along the boundaries. After solution treated at 1165°C, the grain size grown up obviously, and carbide films are continuously precipitated along boundaries. The carbide particles which are discontinuously precipitated along boundary can effectively restrain boundaries sliding. As the creep goes on, the deformation characteristic of the alloy is single and double orientation slipping. the slipping trace on the sample surface increase to bring out the stress concentration, which result in the initiating and propagating of the micro-cracks along the boundaries up to rupture.

5:30 PM

Novel Opencell[™] Metal Sandwich Panels: Antonio Valente¹; Mika Sirén²; Jukka Säynäjäkangas³; Edward Chen⁴; ¹PLY Engenharia, Lda; ²VTT Technical Research Centre of Finland; ³Outokumpu Stainless Tornio Works; ⁴Transition45 Technologies, Inc.

All-metal sandwich panels offer numerous outstanding properties allowing the designer to develop lightweight and efficient structural configurations for diverse applications. The most established type of allmetal sandwich panels is using directional stiffeners between solid surface sheets. Characteristic of these panels, however, is the heterogeneity of strength and/or stiffness properties in longitudinal and transverse directions. Sandwich panel technology development towards lattice truss concepts has resulted in a completely new metal panel idea called OpencellTM. Instead of a conventional three constituent panel structure (sheet/core/sheet), a combination of cut-and-formed core and single solid sheet element is used, resulting in higher degree of design variables for tailored properties. Other key benefits of the OpencellTM technology are reduction of the number of elements, and hence manufacturing phases and eventually weight. This presentation describes the design and optimization of prototype OpencellTM panels, their manufacture, and test results from static and fatigue bending type tests.

5:45 PM

Effect of Hydrogen on Tensile Properties of a Ductile Cast Iron: *Hisao Matsunaga*¹; Kenshin Matsuno¹; Katsuya Hayashida²; ¹Fukuoka University; ²Toppan Printing Co., Ltd.

Effect of hydrogen-charging and strain rate was investigated on the tensile properties of a ductile cast iron having spheroidal graphite, pearlite and ferrite structures. Hydrogen-charging accelerated the crack-growth from graphite. The crack-growth acceleration resulted in a decrease in reduction of area (RA) by ~40%. In the uncharged specimens RA was nearly constant regardless of strain rate, whereas in the hydrogen-charged specimens RA was gradually decreased with a decrease in strain rate. Hydrogen microprint technique and thermal desorption spectroscopy revealed that most of the charged hydrogen was diffusive and segregated at the graphite and pearlite. Considering all the obtained results together, the hydrogen-induced degradation was attributed to the following three mechanisms: (i) hydrogen supply to the crack tip from the graphite/matrix interface, (ii) Hydrogen-enhanced pearlite cracking and (iii) hydrogen emission from the graphite and supply to the crack tip.

6:00 PM

Analysis of Sandwich Composite Chassis Using Multiscale Modeling Technique: Arslan Siddiqui¹; ¹Pakistan Navy Engineering College - NUST

Our aim was to design a vehicle chassis that provides an ideal balance between strength and weight. The analysis approach was based on the multiscale modeling technique. A unit cell of facesheet and core was modeled in detail; this unit cell was then arrayed as per adequate size to overcome the non-linear effects of the honeycomb geometry itself. The materials used for the core were Aluminum honeycomb that was bonded by woven glass fabric laminates. The sandwich was analyzed under different boundary conditions, to obtain the bulk properties of composite. These bulk properties were then applied to the chassis of the vehicle as homogenized solid properties. The variable that was given primary importance was the thickness of honeycomb core.

Hume-Rothery Symposium Thermodynamics and Diffusion Coupling in Alloys - Application Driven Science: Materials Design and Diffusional Simulations

Sponsored by: The Minerals, Metals and Materials Society, TMS Electronic, Magnetic, and Photonic Materials Division, TMS: Alloy Phases Committee

Program Organizers: Zi-Kui Liu, The Pennsylvania State University; Larry Kaufman, CALPHAD, Inc.; Annika Borgenstam, Royal Institute of Technology; Carelyn Campbell, NIST

Wednesday PM	Room: 31A
March 2, 2011	Location: San Diego Conv. Ctr

Session Chairs: Richard Sisson, Worcester Polytechnic Institute; Roger Reed, University of Birmingham

2:00 PM Invited

Thermodynamics-Based Materials Design: *Greg Olson*¹; ¹Northwestern University

The development of the Thermocalc/DICTRA toolset at KTH raised the accuracy of the CALPHAD method and its supporting databases to sufficient accuracy to enable an approach to materials design. Thermodynamics-based parametric materials design integrating materials science, applied mechanics and quantum physics within a systems engineering framework has brought a first generation of designer "cyberalloys" that have now entered successful commercial applications, and a new enterprise of commercial materials design services has steadily grown over the past decade. As the central engine of the AIM methodology for accelerated qualification, the PrecipiCalc microstructural simulator, built on the multicomponent Thermocalc/DICTRA platform, has demonstrated both accelerated thermal process optimization at



the component level and the effective forecast of manufacturing variation with efficient fusion of minimal datasets. Flight qualification of the computationally designed Ferrium S53 landing gear steel using the AIM methodology heralds a new era of Integrated Computational Materials Engineering grounded in accurate multicomponent thermodynamics.

2:30 PM Invited

New Nickel-Based Superalloys By CALPHAD-Driven Design Methods: Roger Reed¹; Nils Warnken¹; ¹University of Birmingham

New grades of superalloys are needed in the aerospace, power generation and oil/gas sectors. Design rules are proposed by which new compositions can be chosen systematically, using models for the most important characteristics: e.g. creep resistance, microstructural stability, castability, density and cost. Application of the rules allows the very large compositional space to be reduced to just a few ideal compositions, so that optimal ones for given applications can be isolated. Much depends upon the accuracy of the underlying sub-models; the ones based upon CALPHAD are critical developments and limitations of these are emphasised. It is demonstrated that the procedures have the potential to remove much of the traditional reliance upon empiricism and trial-and-error-based testing.

3:00 PM Invited

High-Throughput Measurements for Accelerated Establishment of Materials Databases: *Ji-Cheng Zhao*¹; Xuan Zheng²; David Cahill²; ¹The Ohio State University; ²University of Illinois

This talk will use recent examples to illustrate high-throughput measurements for fast establishment of materials databases. The methodology is based on a simple idea of taking advantage of the compositional gradients and phase formation in diffusion couples and diffusion multiples to perform localized property measurements. Such measurements require a new suite of materials property microscopy tools with micron-scale resolution, but would greatly accelerate the efficiency of data gathering as compared to traditional measurements on individual alloys. The local equilibrium at the phase interfaces allows fast evaluation of phase diagrams which are essential input to CALPHAD modeling. Micron-scale resolution tools were developed to measure thermal conductivity, elastic modulus, and coefficients of thermal expansion (CTE). These tools can be applied not only to accelerate the development of structural materials, but also to discover new multifunctional materials.

3:30 PM Break

3:50 PM Invited

Atomic Defects in Alloys and Compounds: The Effect of a Macroscopic State: *Pavel Korzhavyi*¹; Andrei Ruban¹; Oleg Gorbatov²; Yuri Gornostyrev²; Borje Johansson¹; ¹Royal Institute of Technology (KTH); ²Institute of Quantum Materials Science

Case ab-initio studies of atomic defects in concentrated metallic (Febased) alloys and compound semiconductors (GaAs- and ZnO-based alloys) are presented. The general picture emerging from these studies is quite interesting and complex: The microscopic parameters of point defects (such as the energies of their formation, interaction, and migration) are found to be strongly dependent upon the macroscopic state (i.e., the electronic and magnetic structure) of the host. For example, we show that the solute-solute and vacancy-solute interactions are quite different in the fully ordered ferromagnetic state and the completely disordered paramagnetic state of the Fe-based alloy matrix. Also, we show that by changing (through alloying) the electronic structure of a metallic alloy or a compound semiconductor one may "tune" the chemical and magnetic exchange interactions of point defects in these hosts. We discuss how these effects are treated within the existing atomistic (e.g., cluster expansion) and continuum (e.g., Calphad) approaches. Modeling the Microstructural Development during the Nitriding of Low Alloy Steels: Mei Yang¹; Danielle Belsito¹; *Richard Sisson*¹; ¹Worcester Polytechnic Institute, Center for Heat Treating Excellence

The microstructural development during the nitriding of quenched and tempered low alloy steels has been theoretically and experimentally investigated. These results will be compared with those of CALPHAD calculations from Thermo-Calc, which use thermodynamic data to predict multicomponent phase behavior during nitriding. Isopleths with nitrogen content will be presented for steels with and without added aluminum. Customized Lehrer diagrams will be developed to predict the relationship between the nitriding potential and the phase development at different temperatures. In addition, a computational model is being developed to predict the nitriding behavior. The methodology and preliminary results for this model will be presented and compared with experimental results.

4:50 PM

Phase Field and DICTRA Simulations of Type 3 Boundaries: *Xiaoqin Ke*¹; John Morral¹; Yunzhi Wang¹; ¹Ohio State University

Boundaries between layers that form in diffusion couples can be characterized by the number of phases that change on crossing the boundary. Accordingly a type 3 boundary is one in which 3 phases change. In the present work, attempts were made to simulate type 3 boundaries using both a phase field model and the newly available homogenization model in DICTRA. It was found that type 3 boundaries could not be successfully simulated with the homogenization model, because of problems that will be presented. However type 3 boundaries could be simulated with the phase field method. All simulations were performed on a prototype A-B-C ternary system in which elements A, B and C form regular solutions with each other.

5:20 PM

Thermodynamics Test of the Mixed Enthalpy TiCxOy System: Bo Jiang¹; Chengjun Gao¹; Zhanmin Cao¹; Kai Huang¹; *Hongmin Zhu*¹; ¹USTB

The combustion enthalpy ΔH , and Cp of the TiC,TiO and Ti2CO were investigated by the differential scanning calorimeter(DSC) method.And the effects of parameters such as the start combustion temperature, the flow rate of oxygen, the heating rate and the sample preparation were discussed in detail. It was found that the results of $\Delta HTiC$ and $\Delta HTiO$ have a good agreement with the JANAF data.The mixed enthalpy of the reaction TiO + TiC = Ti2CO was calculated in this article.Furthermore,the standard formation Gibbs free energy of the solid solution TiCxOy (x+y=1)were obtained from the basis of regular solution model.

Magnesium Technology 2011: Deformation Mechanisms II; Formability and Forming

Sponsored by: The Minerals, Metals and Materials Society, TMS Light Metals Division, TMS: Magnesium Committee Program Organizers: Wim Sillekens, TNO Science and Industry; Sean Agnew, University of Virginia; Suveen Mathaudhu, US Army Research Laboratory; Neale Neelameggham, US Magnesium LLC

Wednesday PM March 2, 2011 Room: 6F Location: San Diego Conv. Ctr

Session Chairs: Paul Krajewski, General Motors; Wim Sillekens, TNO Science and Industry

2:00 PM

Texture Weakening Effect of Y in Mg-Zn-Y System: Seyed Amir Farzadfar¹; Mehdi Sanjari¹; In-Ho Jung¹; Elhachmi Es-Sadiqi²; Steve Yue¹; ¹McGill University; ²CANMET- Materials Technology Laboratory

The CALPHAD (Calculation of Phase Diagram) method was successfully used in this study to select the alloys from Mg-Zn-Y system, aimed at determining the mechanism(s) of texture weakening in Y-containing Mg alloys: PSN (particle-stimulated nucleation of recrystallization) and/or solute



effects. The selected alloys are Mg-6Zn-1.2Y, Mg-5Zn-2Y, Mg-2.9Y and Mg-2.9Zn (in wt%). After heat treatment, the ternary alloys contain (nearly) the same amount of ternary intermetallics in equilibrium with a Mg at 350 °C, and the microstructure of the binary alloys is composed of a-Mg solid solution at 350 °C containing the same solute amount as that in the ternary alloys. The hot deformation and post-deformation annealing of these alloys at a constant temperature (i.e., 350 °C) showed that the texture weakening happens during growth of recrystallized grains in deformed and annealed samples where Y element is in a-Mg solid solution.

2:20 PM

In-Situ Scanning Electron Microscopy Comparison of Microstructure and Deformation Behavior between WE43-F and WE43-T5 Magnesium Alloys: *Tomoko Sano*¹; Jian Yu¹; Bruce Davis²; Richard DeLorme²; Kyu Cho¹; ¹US Army Research Laboratory; ²Magnesium Elektron North America

In-situ tensile testing in the scanning electron microscope was used to investigate the quasi-static deformation behavior and fracture mechanism of WE43 magnesium alloys. The in-situ tensile experiments were conducted at room temperature at a constant crosshead speed of 0.5 mm / min. One set of samples was a rolled and quenched F temper alloy and the other set was an artificially aged T5 temper alloy. The objective of this research was to determine the effect of tempering on precipitates chemistries, microstructure, and mechanical properties. The sample orientation is known to affect the tensile properties. Hence tensile specimens with different sample orientation were tested. The crystallographic orientations were characterized by electron backscattered diffraction. Strong textures were observed with rolling plane crystals indicating a basal plane orientation.

2:40 PM

A Molecular Dynamics Study of Fracture Behavior in Magnesium Single Crystal: *Tian Tang*¹; Sungho Kim¹; Mark F. Horstemeyer¹; Paul Wang¹; ¹Mississippi State University

The analysis of crack growth in magnesium crystals was performed using molecular dynamics simulation with Embedded Atom Method (EAM) potentials. Four specimens with increasing sizes were used to investigate the influences of material length scale on crack growth of magnesium single crystals. Furthermore, the effects of temperature, loading strain rate, and the size of the initial crack were also verified. The specimens were subjected to uniaxial tension strain up to the total strain level of 0.2 with a constant strain rate. In the simulation of each specimen, the uniaxial stress strain curve was monitored. The simulation results show that the specimen size, loading strain rate, temperature, and the size of initial crack have strong influences on the yield strength at which the twin nucleated followed by the crack growing. The initial slope of the uniaxial stress strain curve is independent of the loading strain rate and temperature. Moreover, the stress at the crack tip was released by the reorganization of atoms as a result of the high mobility of atoms caused by high temperature.

3:00 PM

Microstructural Relationship in the Damage Evolution Process of an AZ61 Magnesium Alloy: *Marcos Lugo*¹; J Jordon²; M Horstemeyer¹; M Tschopp¹; ¹Mississippi State University; ²The University of Alabama

The damage evolution process of magnesium AZ61 alloy under monotonic tensile loading conditions is investigated. Specimens that had been subjected to interrupted tensile loading were examined under optical microscopy to quantify the number density of cracked intermetallic particles as a function of applied strain. Digital image analysis of the optical images was employed to automatically quantify damage by separating cracked from non-cracked particles. Lastly, an internal state variable damage model was shown to adequately capture the experimentally-observed damage of intermetallic particles in the magnesium AZ61 alloy.

3:20 PM

Formability Enhancement in Hot Extruded Magnesium Alloys: *Raja Mishra*¹; Anil Gupta²; Rajiv Sikand³; Anil Sachdev¹; Li Jin⁴; ¹General Motors; ²Advanced Materials and Processes Research Institute; ³National Physical Laboratory; ⁴Shanghai Jiao Tong University

The effects of cerium (Ce), aluminum (Al) and manganese (Mn) additions on the microstructure and mechanical properties of hot extruded magnesium alloy rods have been investigated. Seven different compositions of Mg alloys - Pure Mg, Mg-0.2Ce, Mg-0.5Ce, AM30, AM50, Mg-3Al-0.2Ce and Mg-5Al-0.2Ce were hot extruded under optimized process conditions. Minor addition of Ce to Mg was found to enhance its ductility from <10% to >30% and 3 - 5% Al addition resulted in ~40% and 50% increase in strength respectively, compared to pure Mg. A combination of 5% Al and 0.2% Ce addition resulted in concurrent improvement in strength and ductility as a result of concurrent grain size refinement, texture randomization and solute strengthening.

3:40 PM

Deformation and Evolution of Microstructure and Texture during High Speed Heavy Rolling of AZ31 Magnesium Alloy Sheet: *Tetsuo Sakai*¹; Akinori Hashimoto¹; Go Hamada¹; Hiroshi Utsunomiya¹; ¹Osaka University

An AZ31 magnesium alloy sheet was rolled to 60% by one pass operation at 473K at a rolling speed of 500m/min. During rolling, the mill was suddenly stopped and the sheet was withdrawn from the work rolls. The evolution of microstructure and texture of the AZ31 magnesium alloy sheet during rolling deformation was revealed by observing microstructure and texture at the plane perpendicular to the transverse direction from the entry to the exit of the zone of deformation of the withdrawn sheet. Crystals aligned their 0001 planes oblique to the sheet plane preferentially deforms near the entry of the deformation zone. Dynamically recrystallized grains are observed in the deformation zone. The double peak texture developed during recrystallization.

4:00 PM Break

4:20 PM

Formability of Magnesium Sheet ZE10 and AZ31 with Respect to Initial Texture: *Lennart Stutz*¹; Jan Bohlen¹; Dietmar Letzig¹; Karl Ulrich Kainer¹; ¹GKSS Forschungszentrum Geesthacht GmbH

The commercial application of conventional magnesium alloy sheets is hindered by their low formability and therefore technological and economic constraints. Tailoring the texture has been identified as playing a major role in enhancing the formability of magnesium sheets. In this study, the formability of magnesium sheet ZE10 and AZ31 was investigated. While the texture of AZ31 is of unfavourable basal type, ZE10 shows a significantly different texture with the basal planes being randomly distributed. More basal planes are oriented favourably for basal slip, promising higher formability and thus, lower process temperature. Formability is assessed by means of forming limit diagrams as a representation of material response to various strain paths. Nakajima tests were carried out from room temperature to 250°C. Local strain data is correlated with the microstructural evolution. This study reveals a significant influence of texture on formability with ZE10 sheet showing superior formability compared to AZ31.

4:40 PM

Hot Workability of Alloy WE43 Examined using Hot Torsion Testing: *Frederick Polesak*¹; Bruce Davis²; Rick DeLorme²; Sean Agnew¹; ¹University of Virginia; ²Magnesium Elektron North America Inc.

While rare earth additions can impart a variety of property improvements in magnesium alloys, they can also limit the processing parameter window inside which the alloys may be successfully wrought in commercial production routes such as extrusion and rolling. In the present work, hot torsion testing is used to explore the temperature and rate sensitivity of the flow stress of the alloy WE43 in order to establish the boundaries of this processing window. Two mechanisms appear to be important from a fundamental perspective: first, dynamic recrystallization appears to be a prerequisite for significant plastic flow; second, serrated flow and negative strain rate sensitivity are observed at lower deformation temperatures (T ~ 150-250°C). The Sellars-Tegart model and simple power law, both of which have been successfully applied to describe the temperature/strain-rate/flow stress relationship in AZ31 and many other Mg alloys, are explored in the context of WE43.

5:00 PM

Enhancement of Superplastic Forming Limit of Magnesium Sheets by Counter-Pressurizing: Wonkyu Bang¹; Hyun-Seok Lee¹; Hyung-Lae Kim²; Young-Won Chang²; ¹RIST; ²POSTECH

As often reported in various metallic materials, fine-grained wrought magnesium can exhibit extensive superplasticity at the elevated temperature, which makes superplastic forming (SPF) of magnesium as a promising process for manifesting complex-shaped, lightweight thin-walled structural components. The superplastic tensile deformation of magnesium is commonly accompanied by substantial cavitation in its failure stage, which is also typical to quasi-single phase aluminum alloys. In this regard, a series of bulge test have been conducted with independent inflating/counter-pressure control setup. From the evaluation of superplastic forming limit along Limit Dome Height (LDH), considerable improvement was reproduced by counter-pressurized conditions. Constitutive modeling and microstructural analysis implies that it is mainly achieved by the retardation of nucleation and growth of cavities under hydrostatic stress.

5:20 PM

Microstructural Evolution during Roller Hemming of AZ31 Magnesium Sheet: Amanda Levinson1; Raja Mishra2; John Carsley2; Roger Doherty1; Surya Kalidindi1; 1Drexel University; 2General Motors

The evolution of microstructure and texture during multi-pass roller hemming (prehemming and flat hemming) of commercial grade AZ31-O sheet has been studied using electron backscatter diffraction (EBSD). The prehemming and hemming operations were performed with and without local heating using a laser source. Dynamic recrystallization (DRX) occurred on the outer and inner diameter of the hem at all temperatures up to 200°C, with the center of the sheet exhibiting no DRX. The texture in the outer and inner diameter regions are rotated by 90° in the hemmed sample. It is observed that samples prehemmed at room temperature could not be flat hemmed even after applying heat. The results suggest that the large stored energy in the roller hemmed sheet induces recrystallization at room temperature but the damage in this prehemmed sample leads to failure even if heat is applied during subsequent roller passes.

5:40 PM

The Warm Forming Performance of Mg Sheet Materials: Paul Krajewski1; Peter Friedman2; Jugraj Singh3; 1General Motors; 2Ford Motor Company; 3Chrysler Group, LLC

The warm forming performance of five different magnesium sheet materials was evaluated using a heated pan die. Forming maps were generated to determine the optimum temperature and die conditions for successful forming. All five materials exhibited excellent formability above 325C, with a robust forming window. Below 300C, significant differences in the materials were observed. Some materials could be formed into a pan at temperatures as low as 175C while others could not be formed below 300C. The differences in forming performance were investigated considering material properties, tribology, and microstructure. These trials included both continuously cast and direct chill cast materials, and demonstrated that the continuously cast materials can be successfully warm formed.

Magnetic Materials for Energy Applications: Nanocrystalline and Nanocomposite Nd-Fe-B Magnets

Sponsored by: TMS Electronic, Magnetic, and Photonic Materials Division, TMS: Energy Conversion and Storage Committee, TMS: Magnetic Materials Committee; JSPS 147th Committee on Amorphous and Nanocrystalline Materials; Lake Shore Cyrotronics, Inc.; AMT&C

Program Organizers: Victorino Franco, Sevilla University; Oliver Gutfleisch, IFW Dresden; Kazuhiro Hono, National Institute for Materials Science; Paul Ohodnicki, National Energy Technology Laboratory

Wednesday PM	Room: 11A
March 2, 2011	Location: San Diego Conv. Ctr

Session Chair: Kazuhiro Hono, National Institute for Materials Science

2:00 PM Keynote

High Performance Magnets for Energy Efficient Devices: George Hadjipanayis1; 1University of Delaware

For the past twenty years, the Magnetics Lab at the University of Delaware has been involved in the development of materials for high performance permanent magnets. These materials are currently used in a vast number of commercial and military applications. These include advanced motors, generation and distribution of electrical power, the automotive and aviation industry, the information storage industry, medical surgical and diagnostic equipment, bioengineering, and numerous military weapons, guidance and communications systems. In this talk, I will summarize our latest efforts to develop high performance nanocomposite magnets with much higher energy products ((BH)_{max}>60 MGOe)using the bottom-up approach. The high strength of these magnets will allow lighter, more compact, lower cost and more energy efficient devices to be developed which will help us to reduce our dependency on fossil fuels and enable "more electric" product commercialization. Supported by DOE ARPA-E DE-AR0000046

2:40 PM Invited

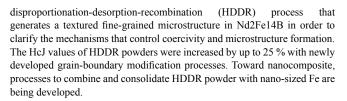
Coercivity Enhancement in Sintered Nd-Fe-B Magnets Annealed under High Magnetic Fields: Hiroaki Kato¹; Takahiro Akiya²; Kunihiro Koike¹; ¹Yamagata University; ²Tohoku University

The coercivity (H_{a}) mechanism in sintered Nd-Fe-B magnets is one of the most important issues in this research field with relation to a reduction of Dy usage for high-temperature applications. Although morphology of intergranular phases is thought to be strongly correlated with H_c values, there is no quantitative evidence for it. We found [1, 2] that a coercivity enhancement occurs by annealing the sintered Nd-Fe-B magnets under high magnetic fields at particular temperatures where a liquid phase appears in the grain boundary, which was confirmed by an endothermic anomaly in the DSC curve. In this presentation, we review our recent high-field experiments on a series of Nd-Fe-B-type sintered magnets with different values of Dy content and Cu additive concentration. [1] H. Kato, et al., J. Magn. Magn. Mater., 310 (2007) 2596. [2] T. Akiya, et al., IOP Conf. Series: Mater. Sci. & Eng. 1 (2009) 012034.

3:05 PM Invited

Toward Development of Anisotropic Nanocomposite Permanent Magnets: Satoshi Hirosawa1; 1Hitachi Metals, Limited

Researches aiming at realization of anisotropic nanocomposite permanent magnets on the basis of Nd2Fe14B have been facing a tremendous difficulty in obtaining a sizable coercivity (HcJ). One of approaches to possibly solve this problem is to develop a nanometer-sized internal microstructure in the hard magnetic Nd2Fe14B phase to hinder propagation of the magnetization reversal. Such a material with a built-in microstructure may be consolidated by itself to develop high-HcJ Nd-Fe-B magnets for the electric vehicle applications without relying on rare elements such as Dy. For these purposes, intensive researches are currently conducted on the hydrogenation-



3:30 PM Invited

Development of High Coercivity Nd-Fe-B Permanent Magnets: *Matahiro Komuro*¹; Yuichi Satsu¹; Hiroyuki Suzuki¹; Akira Nambu¹; Kazuhiro Ueda¹; Akira Sugawara¹; Hideyuki Matsuoka¹; ¹Hitachi, Ltd.

Nd-Fe-B permanent magnets are widely applied for various products including motors, generators and hard disk drives. Temperature resistant is especially demanded in the automotive application in various products. In order to get high temperature resistant, large amount of heavy rare-earth elements has been added in Nd-Fe-B magnets. Recently, effective processes for reducing the amount of heavy rare-earth elements have been developed to protect heavy rare-earth resources. In these new processes, heavy rare-earth elements which are supplied by vaporizing, slurry or solution are diffused along grain boundaries in Nd-Fe-B magnets. Among these processes, the effect of the magnetic properties improvement using the fluoride solution will be explained in detail. Segregation of the heavy rare-earth elements along grain boundaries with fluorine contributes to coercivity increase, leading to the great reduction of the heavy rare-earth elements consumption. The evaluation results for the motor with the high coercivity magnets will be introduced.

3:55 PM Invited

High Coercivity Nd-Fe-B Thin Films: *Toshiyuki Shima*¹; ¹Tohoku Gakuin University

Nd-Fe-B based permanent magnets have been used in a variety of applications such as sensors, actuators and motors because of their high magnetocrystalline anisotropy and high coercivity. In order to keep up with the recent trend of environmental and energy issues, a considerable number of magnets are adopted for the motors of electric and hybrid vehicles. However, it is well known that a practical value of coercivity in the Nd-Fe-B magnet is much smaller than that was predicted by the theory. In order to improve the hard magnetic properties of Nd-Fe-B magnet, understanding of the magnetization process is essential and important. We reported that the magnetic properties of Nd-Fe-B thin films were remarkably changed by the morphology and also by the addition of additive elements. In this talk, the recent studies of Nd-Fe-B thin films including in-field magnetic force microscope observation will be reviewed.

4:20 PM Invited

Current Status of Permanent Magnet Research and Market in China: *Aru Yan*¹; ¹Ningbo Institute of Material Technology and Engineering

The past decades have witnessed an impressive progress of permanent magnets in China. In 2008, China supplied 77.6% of Nd-Fe-B, 55.2% of ferrite and 55.3% of AlNiCo for global permanent magnets market. Financial crisis since 2008 has spurred Chinese magnet manufacturers to turn to products with high added value. This requirement further catalyzed the R&D on permanent magnets. Today both fundamental and application research have been carried out in China. New material systems including Nd-Fe-N and nanocrystalline composites were studied. Mechanisms were explored for the exchanged coupling between hard and soft nanocrystallines in composite magnet. Tranditional synthesis methods were improved and novel ones were developed. Especially, permanent magnet films attracted intense attention since their potential grand applications. Recently, Chinese government announced a plan to facilitate the popularization of electric vehicles and renewable wind power to reduce CO2 release, which provided a new large market for permanent magnets.

4:35 PM

140th Annual Meeting & Exhibition

Grain Refinement in Nd₂Fe₁₄**B Powders by High Hydrogen Pressure Reactive Milling and Desorption**: *Konrad Güth*¹; Julia Lyubina²; Ludwig Schultz¹; Oliver Gutfleisch¹; ¹IFW Dresden; ²Imperial College London

Recently, high performance permanent magnets undergo a renaissance in the scientific research. The magnetic properties, e. g. remanence, coercivity and consequently energy product, are strongly dependent on their microstructure and crystallographic orientation. One simple way to produce highly coercive powders for inexpensive Nd-Fe-B resin bonded magnets is the HDDR process (Hydrogenation Disproportionation Desorption Recombination). This process is carried out under carefully controlled hydrogen atmosphere at elevated temperature resulting in Nd₂Fe₁₄B crystallites with a size of about 300 nm well-oriented within micrometer-sized particles. A further increase in energy product of the HDDR powders may be achieved via inter-grain exchange coupling, which requires the decrease of grain size by one order of magnitude. Here, the combination of high pressure reactive milling (HPRM) technique prior to the hydrogen desorption and recombination process will be discussed on the basis of the structure and magnetic properties.

4:50 PM

CoercivityMechanisminHydrogenation-Disproportionation-Desorption-RecombinationProcessedNd-Fe-BBasePowders: T.Ohkubo¹;H. Sepehri-Amin¹;T. Nishiuchi²;S. Hirosawa²;K. Hono¹;¹National Institute for Materials Science;²Hitachi Metals Ltd

Since the grain size of Nd-Fe-B HDDR powders is close to the single domain size of Nd2Fe14B phase, coercivity values exceeding 20kOe should be achieved if grains can be magnetically decoupled. However, the coercivity of the HDDR powders is much lower for their ultrafine grain size. Hence, the aim of this work is to undesrtanding the reasons for the low coercivity of HDDR processed powders. The microstructure of HDDR processed Nd-Fe-B powders with different HD and DR times were studied using HRSEM, HRTEM and 3D atom probe. Based on the experimental results, we discuss the mechanims of the formation of ultrafine grained structure and the roles of microallyed elements like Ga. We also discuss the way to process fully dense high coercivity magnets from HDDR powders.

5:05 PM

Texture Investigation in Melt-Spun High Temperature Mixed Rare Earth-Iron-Boron Alloys: *Nathaniel Oster*¹; Iver Anderson²; Matthew Kramer²; R.W. McCallum²; Wei Tang²; Yaqiao Wu²; Kevin Dennis²; ¹Iowa State University; ²Ames Laboratory

To gain energy product and manufacturing efficiency, anisotropic polymer (PPS) bonded Nd-Fe-B (2-14-1) magnets have been identified for possible cost-effective use in automotive traction motors, especially if their operating temperature limit was raised to 200°C. Mixed rare earth (MRE) 2-14-1 alloy particulate for isotropic nanocrystalline bonded magnets was developed for 200°C, but translation to suitable anisotropic high temperature PPS bonded magnets remains a challenge. Modification of melt-spinning parameters and grain refining additions (such as TiC) are both possible methods to produce suitable directional growth. Thus, microstructure scale and degree of texturing were varied as a function of quench rate, temperature gradient, ribbon thickness, and alloy design. Analysis of results from scanning electron microscopy with orientation imaging, x-ray diffraction, and TEM of the resulting particulate will be presented, along with SOUID magnetometer characterization of aligned and unaligned magnets. Funding provided by DOE-EERE-FCVT Office through Ames Lab Contract No. DE-AC02-07CH11358.

5:20 PM

Structure and Magnetic Properties of Mechanically Milled Melt Spun Rare Earth-based Permanent Magnets: *Farhad Golkar*¹; Jeffrey Shield¹; ¹University of Nebraska-Lincoln

One challenge in developing "bulk" nanocomposite permanent magnets is increasing the soft magnetic phase fraction. One method is to utilize eutectic and near-eutectic compositions in the Sm-Co alloy system. The eutectic transformation naturally produces a two-phase structure with a ~ 0.21 soft magnetic phase fraction, and melt spinning results in a structural refinement

to 20-25 nm. Subsequent mechanical milling further reduced the scale, although the milled material retained crystallinity, as peaks characteristic of the TbCu₇-type structure were observed up to 6 h of milling. An increase in coercivity with milling time was observed. Annealing somewhat changed the phase distribution, leading to an increase in coercivity. Additionally, alloying elements resulted in the refinement of the microstructure during melt spinning, producing dramatic increases in coercivity to 5-10 kOe. These ternary and quaternary alloys were also mechanically milled in order to study the combined processing effects on the microstructures and magnetic properties.

5:35 PM

Effects of Cu Addition on Microstructures and Magnetic Properties of Nd-Fe(Co,Cu)-B Nanocomposite Magnets: Junhua You¹; ¹Shenyang University of Technology

The microstructure and magnetic properties of Nd4.5Fe73-xCo4CuxB18.5 (x=0,0.2,0.5,0.8,1.0) nanocomposite magnets prepared by melt spinning have been investigated by X-ray diffraction (XRD), differential thermal analysis (DTA), transmission electron microscope (TEM) and vibrating sample magnetometer (VSM). The results show that Cu can promote the nucleation rate of Fe3B phase, decrease the crystallizing temperature of Fe3B and Nd2Fe14B phases, refine the nanocomposite microstructure and enhance the magnetic properties. The optimum content of Cu is 0.2at%. The Nd4.5Fe72.8Co4Cu0.2B18.5 ribbon made at roll speed of 35 m/s obtained the better magnetic properties:Br=0.98 T, iHc =357 kA•m-1, (BH)max=89 kJ•m-3 after annealed at 690° for 10min.

5:50 PM

NdFeB Thick Films as Model Systems for Coercivity Analysis: Ciuta Georgeta¹; Fruchart Olivier¹; Zhang Yuepeng¹; Woodcock Thomas²; Gutfleisch Oliver²; Dempsey Nora¹; Givord Dominique¹; ¹CNRS/Institut Neel; 2IFW

The increasing demand for NdFeB-based permanent magnets for applications in electric vehicles and wind turbines combined with insecurity in sourcing of heavy rare earth elements has stimulated research into the development of Dy-free magnets. In this work, the preparation, characterization and analysis of Dy-free NdFeB films, which serve as model systems, will be described. The 5 µm thick films are deposited using high rate triode sputtering, in a two step process: deposition + annealing. Varying different processing parameters influences the microstructure, which in turn determines the coercivity. Strong out of plane texture and coercivity values as high as 2.8 T have been achieved. Magnetization reversal in low coercivity and high coercivity films has been studied using both global (vibrating sample magnetometry) and local (magnetic force microscopy) techniques. The understanding of magnetization reversal in these model systems should contribute to the development of Dy-free bulk magnets with the required properties.

Materials in Clean Power Systems VI: Clean Coal-, Hydrogen Based-Technologies, and Fuel Cells: Membranes and Materials for Renewable Energies Sponsored by: The Minerals, Metals and Materials Society, TMS Electronic, Magnetic, and Photonic Materials Division, TMS Structural Materials Division, TMS/ASM: Corrosion and Environmental Effects Committee, TMS: Energy Conversion and Storage Committee, TMS: High Temperature Alloys Committee Program Organizers: Xingbo Liu, West Virginia University; Zhenguo "Gary" Yang, Pacific Northwest National Laboratory; Jeffrey Hawk, U.S. Department of Energy, National Energy Technology Laboratory; Teruhisa Horita, AIST; Zi-Kui Liu, The Pennsylvania State University

Wednesday PM	Room: 33C
March 2, 2011	Location: San Diego Conv. Ctr

Session Chair: Yan Xiang, Beihang University

2:00 PM

w

Novel Metallic Membranes for Hydrogen Separation: Omer Dogan¹; ¹DOE National Energy Technology Laboratory

To reduce dependence on oil and emission of greenhouse gases, hydrogen is favored as an energy carrier for the near future. Hydrogen can be converted to electrical energy utilizing fuel cells and turbines. One way to produce hydrogen is to gasify coal which is abundant in the U.S. The coal gasification produces syngas from which hydrogen is then separated. Designing metallic alloys for hydrogen separation membranes which will work in a syngas environment poses significant challenges. In this presentation, a review of technical targets, metallic membrane development activities at NETL and challenges that are facing the development of new technologies will be given.

2:20 PM

Pd-Based Membrane Reactor for Simultaneous CO2 Sequestration and Hydrogen Production from Syngas Produced from IGCC: Yi Ma1; ¹Worcester polytechnic Institute

An integrated catalytic membrane reactor-separator process for producing pure hydrogen with high pressure CO2 for sequestration requires membranes with long-term chemical, thermal and mechanical stability at high temperatures and pressures. The basis of composite Pd and Pd/alloy membranes for hydrogen separations and productions will be discussed. Our patented technology for improving the long-term thermal stability of composite Pd- and Pd/alloy-porous-metallic-substrate membranes by the controlled in-situ oxidation of the substrate and bi-metal multi-layer (BMML) deposition to generate an intermetallic diffusion barrier layer will be demonstrated. Experimental results from a Pd-based catalytic membrane reactor for water gas shift (WGS) reaction using simulated Syngas composition from a coal gasifier showed superior performance exceeding thermodynamic equilibrium CO conversion, achieving 98% conversion at 450oC and clearly demonstrating the beneficial effects of a membrane reactor. A thinner membrane synthesized by the same technology showed a permeance exceeding the 2015 DOE target.

2:40 PM

Structure/Property Relations in Proton Conducting Ceramics of the Form SrCe0.95Yb0.05O3 With Applications in Membrane Separations: The Role of Microstructure and Second Phase Additions to Enhance Electronic Conductivity: Kyle Brinkman1; Frank Chen2; Kevin Huang2; Sung Gu Kang³; David Sholl³; ¹Savannah River National Laboratory (SRNL); ²University of South Carolina (USC); ³Georgia Institute of Technology

Membrane separations are a key enabling technology for future energy conversion devices. In this study, the model proton conducting system "SrCe0.95Yb0.05O3" was produced by conventional mixed oxide ceramic techniques and a chemical solution route to i) alter the microstructure and explore ii) second phase additions consisting of conductive oxide or metallic elements to enhance electronic conductivity. Microstructural modification was performed by using Spark Plasma Sintering (SPS) in order to densify



crystalline material without the grain growth associated with conventional sintering. Dual phase ionic and electronic conductive materials were fabricated from conventionally processed SrCe0.95Yb0.05O3 and metallic additions of noble metals palladium (Pd) and (Rh). In addition, calculations using Density Functional Theory (DFT) in model proton conducting ceramics were performed to understand the role of defects and structure on proton transport. The results obtained will be discussed in terms of applications as gas separation membranes in commercial and nuclear arenas.

3:00 PM

Ternary CuPdM Alloys for Hydrogen Separation Membranes: *Rongxiang Hu*¹; Michael Gao¹; Ömer Dogan²; Bret Howard²; Bryan Morreale²; ¹URS at National Energy Technology Laboratory; ²National Energy Technology Laboratory

CuPd alloys are among the most promising candidate materials for hydrogen separation membranes and membrane reactor applications due to their high hydrogen permeability. In order to reduce the Pd content and, therefore, the cost of the membrane materials, efforts have been initiated to develop CuPdM ternary alloys having a bcc structure. Searching for alloying elements is done using first principles electronic density functional theory calculations. Potential ternary alloys are synthesized via arc melting, followed by a homogenization heat treatment and equilibrium annealing. The phase stability and bcc phase boundary in Cu-Pd-M systems are investigated by microstructural observation (Optical microscopy and SEM), thermal analysis, and XRD. Finally, the hydrogen permeability of promising alloys is determined.

3:20 PM

Electrodeposition of ZnO Nanocrystallines on ITO Mesoporous Films and Application to Photoelectrochemical Cells: *Haining Chen*¹; Liqun Zhu¹; Weiping Li¹; Huicong Liu¹; ¹Beihang University, Key Laboratory of Aerospace Materials and Performance (Ministry of Education), School of Materials Science and Engineering

ZnO nanocrystallines doped indium-tin-oxide (ITO) mesoporous films were prepared by electrodepositing ZnO nanocrystallines on ITO mesoporous films in the electrolyte of 0.1 M Zn(NO3)2. To function as a photoelectrode, the CdS quantum dots as sensitizers were synthesized on the surface of ZnO nanocrystallines doped ITO mesoporous films. Both SEM and TEM images showed that ZnO nanocrystallines were successfully electrodeposited on the ITO mesoporous films. XRD pattern and selective area electron diffraction pattern revealed that the ZnO nanocrystallines were hexagonal (wurtzite) phase. The results of UV-Vis adsorption spectra analysis demonstrated that absorbance in visible region was enhanced with the deposition of ZnO and CdS on ITO mesoporous films. Photocurrent-voltage measurement results indicated that the ITO mesoporous film/ZnO/CdS photoelectrodes were efficient as a working electrode and its performance was superior to that of ITO mesoporous film/CdS photoelectrodes because of the suppression of recombination by ZnO coating.

3:40 PM Break

3:50 PM

Catalysts Decorated ZnO/Si Branched Nano-heterostructure Electrodes for Solar Water Splitting: *Ke Sun*¹; Kristian Madsen¹; Khaleda Banu¹; Deli Wang¹; ¹University of California, San Diego

Si is low-cost, abundant, and most broadly used for both electronics and photovoltaics. Nanostructure-enabled alternative renewable energy solutions promise high conversion efficiencies and low-cost, particularly for photoelectrochemical cells (H₂ generation from solar energy using semiconductor photoelectrodes). In this application, advantages, such as gigantic surface area-to-volume ratio and large solid/liquid interface, nanoscale hetero-epitaxy and band engineering, enhanced light absorption, etc, are exhibited from nanostructured photoelectrodes. We recently applied low-cost solution-based techniques to integrate ZnO nanowires (NW) to SiNW arrays forming a branched NW photocathode. This interesting structure provides improved performances for H₂ production compared to SiNW-based photoelectrode, mainly due to the increased absorption, enhanced charge generation, and improved electron transportation. In this work, additive photocatalysts including semiconductor quantum dots or metal nanoparticles, are applied to ZnO/SiNW heterostructures through a cost-effective scalable electrodeposition or a spray electropyrolysis method. Photocatalytic activities are investigated, targeting further enhancement of photoelectrochemical responses and suppression of corrosion.

4:10 PM

Competitive Adsorption of CO₂ from Binary Gas Mixtures in a Structurally Dynamic Porous Coordination Polymer: *Kristi Kauffman*¹; Jeffrey Culp²; Angela Goodman¹; Thomas Brown¹; Mark Bernardo¹; Russell Pancoast¹; Christopher Matranga¹; ¹National Energy Technology Laboratory; ²URS

Porous-Coordination-Polymers (PCPs), commonly referred to as Metal-Organic-Frameworks, are highly crystalline and exhibit large surface areas and pore volumes. They have attracted much attention for gas storage and separation applications. Yet, because measuring adsorption from mixtures is technologically challenging, most studies focus on single-component gases or simulations. Traditional gravimetric/volumetric methods cannot easily discriminate between gases in mixtures and are ineffective for evaluating gas selectivity. Here, we report a new method using Fourier-transform infrared spectroscopy (FTIR) and headspace Gas Chromatography (GC) to analyze adsorption from binary gas mixtures (CO₂/N₂, CO₂/CH₄, and CO₂/N₂O) in a flexible PCP, catena-bis(dibenzoylmethanato)-(4,4'-bipyridyl)nickel(II), (NiDBMBpy). We evaluated the isothermal adsorption of infrared-active gases into the NiDBMBpy sorbent bed at elevated pressures using FTIR. GC analysis was applied to determine the headspace composition following adsorption. NiDBMBpy preferentially adsorbs CO2 over N2 and CH4 but CO2 and N₂O are adsorbed equally. This trend is confirmed by both independent analytical techniques.

4:30 PM

Direct Deposition of Nanostructured Platinum Cluster on Gas Diffusion Layer for Highly Durable Polymer Electrode Membrane Fuel Cell (PEMFC: *Hyun-Jong Kim*¹; Ji-Eun Ahn¹; Ho Nyun Lee¹; Myung Keun Han¹; Hong Kee Lee¹; ¹Korea Institute of Industrial Technology

In this study, electrodeposition of platinum cluster was investigated, and especially the pulsed electro-deposition (PED) technique was found to be a versatile method for the preparation of nanostructured Pt depositis due to its simple operation, high purity of deposits, and improvement of energy density per volume. The pulse electro-deposition processes created the nanostructured Pt cluster directly on the surface of gas diffusion layer (GDL). By localizing platinum on the surface of a gas diffusion layer (GDL), it is possible to decrease the thickness of the catalyst layer and increase the efficiency of platinum usage. Experimentally, the Pt cluster was well dispersed in GDL and composed of Pt nanosheet. The growth mechanism was carefully monitored. By increasing the current density for pulse electrodeposition, the size of Pt cluster decreased, result in the enhancement of ESA. And, all showed very promising results.

4:50 PM

Optimization of the Concentrated V(IV)/V(V) Electrolytes in a Vanadium Redox Battery: *Feng Shi*¹; Huimin Lu¹; Yuan Yuan¹; ¹Beihang University

The higher vanadium concentration is required to reduce the size and weight of the battery and the main limitation for the vanadium electrolyte concentration is the precipitation of V(IV) ion. In this paper, the electrode process of concentrated V(IV) species has been studied at a Pt electrode using cyclic voltammetry and linear polarization techniques. The results have revealed that the solubility of VOSO4 decreases continuously with increasing H2SO4 concentration. In 2mol/l VOSO4 solution containing 3mol/l H2SO4, the V(IV) electrolyte has the highest peak current and the best reversibility. Adding alkali metal sulfates and organics, the additive effect on the electrolyte properties was discussed and the electrode process was investigated. The results indicate that the hydrophilic organics improve the stability of V(IV)/V(V)species, the alkali metal sulfates elevate the peak

current a little, and there is no adverse effect of the additives on the redox reaction in vanadium sulfate solution.

5:10 PM

Thermo-mechanical Reliability of Proton Exchange Membranes in Fuel Cells: *Ruiliang Jia*¹; Binghong Han¹; Takuya Hasegawa²; Jiping Ye³; Reinhold Dauskardt¹; ¹Stanford University; ²Nissan Motor Co., Ltd.; ³NISSAN ARC LTD.

Nafion perfluorosulfonic acid (PFSA) polymer thin films are currently the most popular material for proton exchange membranes in PEM fuel cells. A common failure mode that limits the operational life of fuel cells involves the mechanical degradation of the membranes. In the present work, we describe a number of thin film testing methods to characterize the mechanical and fracture properties of PFSA membranes under simulated fuel cell operational environments. Moreover, the role of the PFSA molecular structure together with selected composite forms made with the addition of oxide particles on mechanical and fracture behavior is demonstrated. The study not only reveals significant factors that influence the mechanical behavior and fracture properties of PFSA membranes in operation, such as water diffusion, foreign cation contamination and chemical degradation, but also investigates methods to improve thermo-mechanical reliability for fuel cell applications.

Microstructural Processes in Irradiated Materials: Nanostructured Alloys, Mechanical Properties

Sponsored by: The Minerals, Metals and Materials Society, TMS Structural Materials Division, TMS/ASM: Nuclear Materials Committee

Program Organizers: Gary Was, University of Michigan; Thak Sang Byun, Oak Ridge National Laboratory; Shenyang Hu, Pacific Northwest National Laboratory; Dane Morgan, UW Madison; Yasuyoshi Nagai, Tohoku University

Wednesday PM	Room: 3
March 2, 2011	Location: San Diego Conv. Ctr

Session Chairs: Robert Odette, University of California Santa Barbara; Peter Hosemann, University of California Berkeley

2:00 PM Invited

Radiation Response of Nanostructured Ferritic Steels to High Dose Ion Irradiation: *Michael Miller*¹; Yanwen Zhang¹; ¹Oak Ridge National Laboratory

The microstructures of a 14YWT nanostructured ferritic steel in the unirradiated state and after several high dose ion irradiations have been characterized by atom probe tomography in order to evaluate the radiation response of this material. The ultrafine Ti-, Y- and O-enriched nanoclusters were found to be present in the ferrite matrix in high number densities from doses between 3 and 450 displacements per atom (dpa). The microstructural changes that occur at these nanoclusters and at grain boundaries during ion irradiation will be discussed in detail with particular emphasis on the solute distributions in the vicinity of these microstructural features. This research was sponsored by the U.S. Department of Energy, Materials Sciences and Engineering Division. Research at the Oak Ridge National Laboratory SHaRE User Facility is sponsored by the Scientific User Facilities Division, Office of Basic Energy Sciences, U.S. Department of Energy.

2:40 PM

On the Stability of Nanofeatures in Nanostructured Ferritic Alloys – the Effects of Long Term High Temperature Thermal Aging and Friction Stir Welding: *Nicholas Cunningham*¹; Auriane Etienne¹; Yuan Wu¹; Doug Klingensmith¹; G. Robert Odette¹; Erin Haney¹; Erich Stergar¹; ¹UC Santa Barbara

Nano-structured ferritic alloys (NFAs) have high tensile and creep strength permitting service up to 800°C or more, manifest remarkable resistance to radiation damage and can manage high concentrations of helium. These outstanding properties derive from an ultrahigh density of Ti-Y-O enriched nano-features (NFs) that provide dispersion strengthening, help stabilize dislocation and fine grain structures, reduce excess concentrations of displacement defects by enhancing vacancy-self-interstitial recombination and trap helium in fine, and relatively harmless, bubbles. We present multi-technique characterization studies demonstrating the remarkable stability of the NFs during long-term thermal aging (e.g., for >19kh at 1000°C) and after severe plastic deformation experienced in friction stir welding (FSW). The characterization tools include atom probe tomography (APT), small angle neutron scattering (SANS), transmission electron microscopy (TEM), and micro-hardness. The various techniques are generally consistent with one another and with finite but modest decreases observed in microhardness of ~ 10% (aging) and 20% (FSW).

3:00 PM

Atomistic Studies on Y-Ti-O Nanoclusters in Ferritic Alloys: Lauren Marus¹; Hyon-Jee Voigt¹; Brian Wirth²; ¹University of California-Berkeley; ²University of Tennessee-Knoxville

Nanostructured ferritic alloys demonstrate high creep strength and irradiation resistance in high temperature irradiation environments of interest for advanced nuclear energy systems. The presence of a high number density of Y-Ti-O nanometer scale clusters (NCs) is responsible. However, the structure and composition of the NCs are not yet well understood. Through the systematic atomistic simulations we are beginning to understand and prioritize the effects of magnetism, strain energy, and vacancy and solute concentrations on the NCs. Interaction potentials are obtained by ab initio calculations of Fe-Y-Ti-O alloys. Lattice Monte Carlo (LMC) and off-lattice techniques have been used to simulate NC precipitation within the iron lattice. These results provide insight into features and necessary conditions for NC formation and are compared with available experimental data, although the modeling assumptions do have a substantial impact on the predicted NC structure.

3:20 PM

HRTEM Study of Oxide Nanoparticles in Fe-Cr MA/ODS Steels: Luke Hsiung¹; Micheal Fluss¹; ¹Lawrence Livermore National Laboratory

Structures of oxide nanoparticles in MA956, MA957, and K3 ODS steels produced by a mechanical alloying (MA) method have been studied using high-resolution transmission electron microscopy techniques to better understand the formation mechanism of oxide nanoparticles in ODS steels. Partially crystallized nanoparticles with a core/shell structure were frequently observed in all three ODS steels. While the crystalline nanoparticles in K3 and MA956 steels are mainly Y4A12O9, those in MA957 steel are mainly Y2TiO5 and Y2Ti2O7. HRTEM observations of crystalline nanoparticles larger than ~2 nm and amorphous or disordered cluster-domains smaller than ~2 nm provide us an insight into the formation mechanism of oxide nanoparticle in MA/ODS steels, which involves fragmentation, amorphization, and recrystallization. This work was performed under the auspices of the U.S. Department of Energy by Lawrence Livermore National Laboratory under Contract DE-AC52-07NA27344.

3:40 PM Break

4:00 PM

Radiation Response the Nanostructured Ferritic Alloy 14YWT to High Dose Irradiation: *Alicia Certain*¹; Jim Bentley¹; Shuttha Shutthanandan²; David Hoelzer³; Todd Allen¹; ¹University of Wisconsin-Madison; ²Pacific Northwest National Laboratory; ³Oak Ridge National Laboratory

Ferritic–martensitic (F/M) alloys are expected to play an important role as cladding or structural components in Generation IV and other advanced nuclear systems operating in the temperature range 350–700°C and to doses up to 200 displacements per atom (dpa). Nanostructured ferritic alloys (NFA) have been developed to operate at higher temperatures than traditional F/M steels. These steels contain nanometer-sized Y–Ti–O nanoclusters for additional strengthening. Heavy ion irradiations have been performed on 14YWT up to 100 dpa at two temperature 'extremes' (-75°C and 60 °C) in order to evaluate the stability of the nanoclusters at high doses. Energy-



filtered transmission electron microscopy (EFTEM) has been used to analyze the evolution of the nanoclusters post-irradiation.

4:20 PM

Microstructural Evolution by Helium Irradiation and Its Desorption in ODS Alloy: Jinsung Jang¹; *Yitao Yang*²; Hyung-Ha Jin¹; Suk-Hoon Kang¹; Chonghong Zhang²; ¹Korea Atomic Energy Research Institute; ²Institute of Modern Physics, CAS

Due to the superior thermal creep properties and the high resistance to neutron irradiation, oxide dispersion strengthened (ODS) steels are considered as potential candidate alloys for high temperature applications in advanced nuclear or fusion reactor. The accumulation of helium after neutron irradiation has a substantial influence on the mechanical properties and it would be of technical importance to understand the helium behavior and its consequences in the microstructure. In this work, lower energy helium ions are implanted into a commercial ODS alloy (MA956TM) samples with different fluences. Thermal helium desorption spectroscopy (THDS) and transmission electron microscopy (TEM) are used to study the helium irradiation and its release behavior, corresponding evolution of cavities, and surface morphology of the samples at different helium concentrations. For comparison, a high Cr steel will be also considered. * MA956TM is a trademark of SMC (Special Metals Corporation).

4:40 PM Invited

Nano-Mechanical Testing and Post Testing Investigation on Ion Beam Irradiated Single Crystal Cu: *Peter Hosemann*¹; Daniel Kiener²; Stuart Maloy³; Osman Anderoglu³; Eric Olivas³; Yongqiang Wang³; ¹UC Berkeley; ²University of Leoben; ³LANL

Ion beam irradiation is widely used to study the effects of radiation on structural materials. In this work we performed proton irradiation (1dpa, 150°C) on single crystal Cu. Before and after proton irradiation, in-situ nanoscale compression tests in a transmission electron microscope were performed to evaluate the mechanical properties of the irradiated material. It was found that the nano pillars changed their deformation behavior fundamentally after irradiation and behaved more bulk like The failure of the irradiated pillars was strongly localized. In addition, to gain bulk like data for comparison to the nano compression tests and to validate the method of crosssectional nano indentation on ion beam irradiated materials, nanoindentation experiments were carried out on 10μ m deep irradiated single crystal Cu . It was found that the hardness data fol-lowed the irradiation profile. Moreover, the deformed area underneath different indents was ex-amined using TEM.

5:20 PM

Point Defect Mediated Radiation Induced Creep in Nano-Crystalline Metal: *Yinon Ashkenazy*¹; Tai Kai-Ping¹; Pascal Bellon¹; Robert Averback¹; ¹University of Illinois at Urbana Champaign

Various mechanisms, such as Stress Induced Preferential Nucleation (SIPN) and Stress Induced Preferential Absorption (SIPA) have been proposed in the past to account for radiation induced creep (RIC). Here we consider a new mechanism of for RIC in irradiated nanocrystalline materials. The different time scales involved in creep and radiation damage present a challenge in simulating them in unison. We use a new simplified atomistic model or describing RIC. The model is based on introducing defects at grain boundaries and simulating short-time relaxations. A similar model was used successfully for simulating radiation induced viscous flow [PRL 90,055505(2003)]. We compare the resulting RIC rates for copper with those measured by a bulge test and show reasonable agreement. We further show that neither SIPN or SIPA are required. Using the same methods we explore the origins of lowered RIC rates caused by introducing of precipitates at quad-points.

5:40 PM

Stress, Temperature, and Dose Rate Dependence of Proton Irradiation Creep of Ferritic-Martensitic Steel T91: *Cheng Xu*¹; Gary Was¹; ¹University of Michigan

Developing an understanding of irradiation creep in ferritic martensitic steels has become a major objective for the fuel cladding and core internal design of the next generation sodium fast reactor. The in-situ irradiation creep apparatus at the Michigan Ion Beam Laboratory has been benchmarked against existing literature through thermal creep experiments. Through single variable change experiments, the dose rate dependence, stress dependence, and temperature dependence of irradiation creep for T91 were determined. Results show that the creep rate varies linearly with the dose rate, as expected. TEM was used to quantify the dislocation network and loop densities of T91 after irradiation creep of T91. Results of the creep experiments and the microstructure of the crept samples will be presented in the context of possible creep mechanisms.

Neutron and X-Ray Studies of Advanced Materials IV: Dislocations, Strains and Stresses II

Sponsored by: The Minerals, Metals and Materials Society, TMS Structural Materials Division, TMS/ASM: Mechanical Behavior of Materials Committee, TMS: Chemistry and Physics of Materials Committee

Program Organizers: Rozaliya Barabash, Oak Ridge National Laboratory; Xun-Li Wang, Oak Ridge National Laboratory; Jaimie Tiley, Air Force Research Laboratory; Peter Liaw, The University of Tennessee; Erica Lilleodden, GKSS Research Center; Brent Fultz, California Institute of Technology; Y-D Wang, Northeastern University

Wednesday PM March 2, 2011 Room: 10 Location: San Diego Conv. Ctr

Session Chairs: Karen Pantleon, Denmark Technical University; Phil Ryan, APS

2:00 PM Keynote

In-Situ Laue Diffraction of Deforming Mo Pillars: Helena Van Swygenhoven¹; Julien Zimmermann¹; Steven Van Petegem¹; Cecile Marichal¹; Daniel Grolimund¹; Hongbin Bei²; Hongbin Bei²; Michael Weisser¹; ¹Paul Scherrer Institut; ²Oak Ridge National Laboratory

In-situ Laue diffraction is applied during compression of bcc single crystals. Pillars of 1 micron diameter are obtained from a directionally solidified (DS) NiAl-Mo eutectic grown. DS Mo pillars in as-grown and prestrained conditions, as well as DS pillars treated with FIB are investigated. To obtain free standing single pillars for Laue analysis, a special specimen preparation procedure was developed [Scripta Mat. 62 (2010) 746]. Among the results presented will be the macroscopic yield stress in as-prepared DS, pre-deformed and FIBed pillars and its relation to the mobility of screw dislocations, the character of the activated slip planes i.e. (112) and (110) planes, the difference in initial dislocation structure between pillars obtained from a deformed composite and pillars that are compressed free standing starting from the DS pillars, the formation of substructures in pillars compressed till high strains and the influence of FIB on the deformation behavior.

2:25 PM Invited

Depth-Resolved Phase Identification and Internal Stress Analysis after High Temperature Corrosion in Power Plants: *Karen Pantleon*¹; ¹Technical University of Denmark

During long-term high temperature exposure of superheater tubes in power plants various oxides are formed on the inner side (steamside) of the tubes and oxide spallation is a serious problem, because it causes blockage of loops and, consequently, overheating and failure due to insufficient steam flow. Instead of laboratory studies just mimicking the actual conditions in the power plant for simplified sample geometries, rather the investigation of real plant exposed tubes is essential for understanding phase transformations and stress evolution as a function of operating conditions, material influences and real sample geometries. Although X-ray diffraction including grazing incidence and microdiffraction techniques on real industrial samples is not straightforward, the present work demonstrates the need of those measurements. Depth-resolved phase analysis and phase-dependent stress analysis in the inner side of superheater tubes considerably contributed to understanding high temperature corrosion in power plants and allow evaluation of the risk of oxide spallation.

2:45 PM Invited

Developing Links Between the Microstructure and Lattice Strain Uncertainties: Jay Schuren¹; *Matthew Miller*¹; Alexander Kazimirov¹; ¹Cornell University

Even though failure mechanisms such as yielding and fracture initiate on the scale of the individual crystal, most life prediction models for polycrystals continue to be formulated on macroscale. Enormous opportunities exist, therefore, in the area of micromechanical testing of engineering materials to close this gap. In conjunction with the Cornell High Energy Synchrotron Source, we have developed a method for measuring lattice strain pole figures on deforming samples using synchrotron x-rays. This talk describes recent efforts focused on quantifying the link between each lattice strain measurement and the material microstructure. In particular we have found that experimental uncertainty is intimately linked to microstructure. In addition, we present a method for using grain size, texture measurements, and the range of specimen orientations to design in-situ loading / high energy x-ray diffraction experiments. We demonstrate the method on monotonic and cyclic loading of AA7075 aluminum and nickel-base superalloys.

3:05 PM Invited

Full Local Elastic Strain Tensor from Laue Microdiffraction: A White-Beam Method to Measure the Lattice Expansion: *Odile Robach*¹; Jean-Sébastien Micha²; Olivier Ulrich¹; Patrice Gergaud³; ⁻¹CEA-Grenoble / INAC; ²CNRS / SPrAM UMR 5819; ³CEA-Grenoble / LETI

In sample-scanning Laue microdiffraction, the local crystal orientation and local deviatoric strain tensor are obtained by illuminating the polycrystalline sample with a broadband "white" (5-30 keV) x-ray microbeam, and analyzing the spot positions in the resulting local Laue pattern. Mapping local lattice expansion is usually slower, due to the need to alternate between white and variable-energy monochromatic microbeam. A method was developed to measure lattice expansion in the white beam mode. The energy of one of the "side" diffracted beams of the grain of interest is measured using an energy-resolved point detector, while recording the Laue pattern on the "top" 2D detector. The experimental peak energy, Eexp, is therefore measured simultaneously with Etheor(HKL), the theoretical peak energy for zero lattice expansion. In several cases, this leads to an improved accuracy on da/a = - (Eexp-Etheor)/Etheor compared to the monochromatic beam method, as incertitude on beam position is avoided.

3:25 PM Invited

X-Ray Diffraction Evaluation of the Hardening State of Various Cubic and Hexagonal Materials after Large Strains: *Brigitte Bacroix*¹; Thierry Chauveau¹; Guy Dirras¹; Olivier Castelnau²; Renald Brenner¹; Akrum Abdul-Latif³; Christophe Le Bourlot¹; Aurélie Wauthier¹; ¹CNRS - LPMTM; ²CNRS - PIMM; ³SUPMECA - LISMMA

A high resolution X-Ray Diffraction technique, developed in our laboratory, enables us to characterize in some details the deformed state and especially to estimate, from the shape of the peaks measured within individual texture components, the dislocation density as well as the size of the formed subgrains / dislocation cells as a function of plastic strain and orientation. Some data recently obtained on several materials (AI, Fe, Mg and Zr) after different loading paths (severe deformation or classical rolling process) are presented and analyzed in some details and the comparison of these data with some calculations performed with advances micromechanical models enables us to identify the hardening, softening and fragmentation mechanisms operating in each case.

3:45 PM Invited

Extending Line Profile Analysis to Neutron Diffraction: Tamás Ungár¹; ¹Eötvös University Budapest

X-ray line profile analysis is a powerful tool for characterizing the microstructure of crystalline materials in terms of (i) grain size, (ii)

dislocation structure and (iii) planar defects either in bulk polycrystalline samples or on the single grain level. The angular or spatial resolution of recently commissioned neutron beamlines at spallation neutron sources open up new scopes for the characterization of microstructures by the method of neutron line profile analysis. The challenges and possibilities provided by neutron line profile analysis will be discussed on the basis of first experimental results.

4:05 PM

Comprehensive Characterization of the Effects of Composition, Temperature, Flux and Fluence on the Evolution of Cu-Mn-Ni Precipitates in Reactor Pressure Vessel Steels: *G. Robert Odette*¹; Nicholas Cunningham¹; Brian Wirth²; Matthew Alinger³; Takuya Yamamoto¹; Doug Klingensmith¹; ¹UC Santa Barbara; ²UC Berkeley; ³GE Global Research

Irradiation embrittlement of RPV steels is caused by radiation enhanced solute diffusion driven accelerated evolution of Cu (CRPs) and Mn-Ni (MNPs) rich precipitates, along with defect-solute complexes. A large SANS database on the effects of metallurgical (Cu, Mn, Ni and P) and irradiation (temperature, flux and fluence) variables on the evolution of the precipitate size, number density, volume fraction and composition is presented. The volume fractions of the precipitates increase with the alloy Cu, Mn and Ni contents. At high Mn and Ni levels the precipitates contain more Mn and Ni than Cu; and Mn-Ni-Si precipitates can form even in Cu free steels. The number densities and volume fractions of precipitates generally decrease with increasing fluence and decreasing flux. The fluence dependence of the precipitation often manifests stages of nucleation, growth and coarsening. Increasing flux delays precipitation to higher fluence.

4:15 PM Invited

Study of Precipitate and Recrystallization in Ti-Added Low Carbon Steels by SANS: Baek Seok Seong¹; ¹KAERI

SANS is very powerful tool to understand the precipitation on the recrystallization behavior in low carbon steels. The recrystallization temperature of the higher Ti-added is higher than that of the lower Ti-added steel. SANS measurements were performed both for cold rolled samples and for annealed samples. The size distribution and the volume fraction of the nano-sized precipitates were determined using a direct model fitting with a sphere. SANS results revealed no additional carbo-nitrides precipitation during the recrystallization annealing procedure in the low Ti-added steel. However, in higher Ti-added steel, new TiC precipitates, with a size range of several nm to several tens of nms, form during the recrystallization annealing process. This dynamic interaction of the precipitation of fine TiC particles with the recovery of dislocations seems the primary source of the retardation of the recrystallization in the higher Ti-added low carbon steel.

4:35 PM Break

4:45 PM Invited

Nanostructure of Surrogate Nuclear-Reactor Pressure Vessel Steels: Davor Balzar¹; ¹University of Denver

It is believed that the embrittlement of ferritic steels used in nuclearreactor pressure vessels is caused by formation of small (1-2 nm) copper-rich precipitates (CRPs). Small CRPs are coherent with the bcc matrix, which causes local matrix strain and interaction with the dislocation strain fields, thus impeding dislocation mobility. As CRPs grow, at some critical size the bulk crystal structure of copper (fcc) is achieved, the CRPs are no longer coherent with the matrix, and the matrix strain is relieved. We prepared a series of surrogate low-alloy ferritic-steel specimens. SANS measurements showed that the precipitate size distribution broadens and shifts toward larger sizes as a function of annealing time. Diffraction line broadening analysis showed that the strain-related broadening dominated and correlated with mechanical hardness and precipitate volume fraction, as determined from the SANS measurements. A model of strain broadening was developed to explain these results.



5:05 PM

Microstructure of MgGeO₃ Post-Perovskite at 84 GPa Determined by 3D X-Ray Diffraction: *Gabor Ribarik*¹; Carole Nisr²; Tamás Ungár¹; Gavin Vaughan³; Patrick Cordier²; Sebastien Merkel²; ¹Eotvos Lorand University, Institute of Physics, Budapest, Hungary; ²Université Lille 1; ³European Synchrotron Research Facility

MgGeO3 post-perovskite is a lower pressure analogue of MgSiO₃, the major mineral in Earth's D" layer. Plastic deformation has an important role for convection in the Earth's mantle. Moreover, observations of seismic anisotropy are likely linked to anisotropic lattice defects, like dislocations. A recently developed 3D X-ray diffraction technique was used at the ID11 beamline of ESRF to extract the microstructure of individual grains in a polycrystalline aggregate of post-perovskite samples. A special geometry was used to measure high resolution single crystal peak profiles. The dislocation structure of MgGeO₃ was determined by X-ray line profile analysis. Our results suggest <110> glide in $\{110\}$ or (001) and [010](001) as the most probable slip systems for this material, with a smaller contribution of [100] and [001] dislocations types. The results are compared to the most probable slip systems based on the magnitude of the Peierls stress, determined by numerical simulations.

5:20 PM

Influence of Recrystallization Texture on Tensile Behavior of Friction Stir Processed Magnesium Alloy: *Zhenzhen Yu*¹; Hahn Choo¹; Zhili Feng²; Ke An²; ¹University of Tennessee; ²Oak Ridge National Laboratory

In order to investigate the influence of thermo-mechanical input during friction stir processing (FSP) on the resulting texture and tensile behavior in a AZ31B Mg alloy, a series of FSP were conducted by varying its key parameters, i.e., rotation and travel rates of the weld processing tool. Neutron diffraction texture measurements show that, with the systematic changes in the thermo-mechanical input factor, there is corresponding changes in crystallographic texture that correlates well with the expected changes in deformation and recrystallization mechanisms. In order to investigate the influence of texture changes on tensile behavior of the stir zone (SZ), in-situ neutron diffraction tensile test along the longitudinal direction of the Mg plate was conducted on subsize tensile samples machined from the SZ of FSP plates. Tensile behavior showed dramatic changes in the strength and ductility in a way consistent with the changes in the FSP textures and the dominant deformation mechanisms.

5:30 PM

Investigation of Microstrain near the Fracture Surface in the Tensile-Overloaded Corrosion Resistant Hastelloy C-2000 Alloy: Gabor Csiszar¹; Soo Yeol Lee²; *Tamas Ungar*¹; Peter K. Liaw²; Lee M. Pike³; ¹Eötvös University Budapest; ²The University of Tennessee; ³Haynes International, Inc.

Fatigue-crack-propagation experiments following a tensile overload were carried out on compact-tension specimens of the corrosion-resistant Hastelloy C-2000 alloy. After the tensile overload, a large crack-growth retardation phenomenon was observed. In this work, the fracture surfaces of the fatigue-tested samples were studied by high-resolution X-ray diffraction for the purpose of line profile analyses. The X-ray beam was the size of 0.2 x 2 mm enabling the spatial resolution with 0.5 micron step size. Electron microscopy reveals about 5 nm coherent precipitates producing large coherency strains. The coherency strains are given in terms of dislocation densities determined by line profile analyses. The results are discussed in light of the overloading effect on the fatigue-crack-growth behavior.

5:45 PM

Neutron Diffraction Studies of Intercritically Austempered Ductile Irons: *Alan Druschitz*¹; Ricardo Aristizabal¹; Edward Druschitz¹; Camden Hubbard²; Thomas Watkins²; Larry Walker²; Mel Ostrander³; ¹University of Alabama at Birmingham; ²Oak Ridge National Laboratory; ³Rex Heat Treat

Intercritically austempered ductile irons have a unique combination of excellent mechanical properties (particularly fatigue durability) and excellent manufacturing characteristics (excellent castability, low production energy requirements, reduced greenhouse gas emissions and excellent machinability). In the present study, four different ductile iron alloys were produced using manganese and nickel as the primary austenite-stabilizing elements. The intercritical austenitizing temperatures were experimentally determined and two different heat treatments were performed on each alloy to obtain different quantities of austenite in the final microstructure. This paper reports the microstructures, phases present and tensile properties of these alloys. Further, lattice strains and diffraction elastic constants in various crystallographic directions and the transformation characteristics of the austenite as a function of applied stress were determined using neutron diffraction at the NRSF2 at the High Flux Isotope Reactor (HFIR) at Oak Ridge National Laboratory.

5:55 PM

Analysis of the Initial Oxidation of Gamma-TiAl by Non-Destructive Ion Beam Analysis: Hans-Eberhard Zschau¹; Michael Schütze¹; ¹Dechema e. V.

The gamma-Titanium Aluminides are one of the most important materials in high temperature technology. This material can be protected against oxidation at high temperatures by a dense alumina scale using the so-called fluorine effect. The non-destructive ion beam analysis was applied to study the oxide layer composition of F-implanted gamma-TiAl during the heating process up to 1000°C. The depth profiles of O, Al and Ti obtained by the Rutherford Backscattering Spectrometry (RBS) show the formation of an initial thin (1 micometer) alumina scale already after oxidation of 1h/800°C/ air. The F-depth profiles measured with the Proton Induced Gamma-ray Emission (PIGE) reveal the F-loss during the heating process, whereas a relatively small amount of fluorine remains at the metal/oxide interface. The potential of both methods to establish a non-destructive quality assurance of the formed alumina scale is pointed out.

6:10 PM

Crack Trafficking across Borders: Imaging Fatigue Crack Propagation In Situ at Grain Boundaries with Synchrotron Radiation: *Naji Husseini*¹; Martina Zimmermann²; Clinique Brundidge¹; Jason Geathers¹; Christopher Torbet³; Wah-Keat Lee⁴; Tresa Pollock³; J Jones¹; Roy Clarke¹; ¹University of Michigan; ²Universität Siegen; ³University of California, Santa Barbara; ⁴Argonne National Laboratory

Grain boundaries can form during the growth of single-crystal, nickelbase superalloys, and they are omnipresent in polycrystalline materials. Synchrotron x rays can produce quasi-three-dimensional, in-situ radiographs that reveal the micron-scale evolution of fatigue cracks through such grain boundaries. With a custom-built ultrasonic fatigue instrument operating at 20 kHz, we imaged crack propagation in thin microfoils under tension. The crack morphology at bicrystal grain boundaries depended on the load amplitude: cracks deflected by intergranular misorientation angles to remain on {111} planes at high amplitudes but became pinned to the grain boundaries at low amplitudes. In polycrystalline metals, cracks grew through or along grain boundaries depending on the orientation with respect to the load axis. In all cases, the crack growth rate decelerated, and then accelerated, when traversing a grain boundary. Accumulation of dislocations at the grain boundaries, mapped with rocking curves about Bragg angles, contribute to this change in growth rate.

6:20 PM

Particle Size Analysis of Multimodal Gamma-Prime (γ') Distributions in an Advanced Polycrystalline Nickel-Base Superalloy by a Peak Broadening Approach: David Collins¹; Howard Stone¹; ¹University of Cambridge

Diffraction line profile analysis can yield information on the structure, microstructure or micromechanics of materials. However, analysis of line profiles from materials with complex microstructures and multiple phases, particularly those that contain overlapping diffraction patterns, can be non-trivial. This is true of materials containing superlattice structures such as nickel-base superalloys. A theoretical diffraction pattern has been constructed for a nickel-base superalloy, accounting for the γ matrix and a trimodal distribution of γ' precipitates. Each γ' distribution was modelled independently, accounting for the differences in composition and therefore lattice parameters, along with the peak broadening from the particle size within each distribution. With this model, it was demonstrated that multimodal precipitate size distributions in these alloys may not be reliably determined from diffraction line profile analysis. This was supported by measurements made of the nickel-base superalloy RR1000 using high resolution synchrotron X-ray diffraction.

Pb-Free Solders and Other Materials for Emerging Interconnect and Packaging Technologies: Interfaces and Electromigration

Sponsored by: The Minerals, Metals and Materials Society, TMS Electronic, Magnetic, and Photonic Materials Division, TMS: Electronic Packaging and Interconnection Materials Committee *Program Organizers:* Indranath Dutta, Washington State University; Darrel Frear, Freescale Semiconductor; Sung Kang, IBM; Eric Cotts, SUNY Binghamton; Laura Turbini, Research in Motion; Rajen Sidhu, Intel Corporation; John Osenbach, LSI Corporation; Albert Wu, National Central Univ, Taiwan; Tae-Kyu Lee, Cisco Systems

Wednesday PM	Room: 7B
March 2, 2011	Location: San Diego Conv. Ctr

Session Chairs: Laura Turbini, Research In Motion; Polina Snugovsky, Celestica

2:00 PM Invited

Interfacial Reactions in the Sn-(Pb)/Ni-7wt%V Couples: Sinn-wen Chen¹; Yu-ren Lin¹; Hsin-jay Wu¹; Hong-ming Lin²; ¹National Tsing Hua University; ²Tatung University

The interfacial reactions in the Sn-(Pb)/Ni-7.0wt%V couples are examined at temperatures varied from 210oC to 450oC, and the interfacial reaction mechanisms are proposed. Although Pb does not react with the Ni-7.0wt%V substrate, the Sn-(Pb)/Ni-7.0wt%V interfacial reactions are affected with the Pb addition. Unlike the reaction results in the Sn/Ni-7.0wt%V couples, the Ni3Sn4 phase is formed in the early stage and the T phase is formed later in the Sn-40.0wt%Pb/Ni-V and Sn-90.0wt%Pb/Ni-V couples reacted at 210oC to 250oC. The T phase is formed first in the Sn-10.0wt%Pb/Ni-V couples and the results are similar to those in the Sn/Ni-V couples. A two distinguishable regions are observed in the T phase layer in the Sn/Ni-V couple reacted at 250oC. It is also observed that the region in the T phase layer adjacent to the solder is Ni-depletion layer and is primarily composed of fine grains of V2Sn3 phase.

2:25 PM Invited

Fundamental Studies on Electromigration in Eutectic Sn-Based Solder Joints: *Fu Guo*¹; Guangchen Xu¹; Ruihong Zhang¹; Hongwen He¹; ¹Beijing University of Technology

Electromigration (EM) induced failures have become a great threat with the miniaturization trend in microelectronic products. In practice, failure mechanisms of EM are associated with many factors such as Joule heating effects, thermomigration, and interfacial reactions, etc., hence the real root cause cannot be easily detected and understood. Therefore, fundamental studies by decoupling the complex failure modes using simply eutectic solders have become a necessity in an effort to advance a better understanding of the mechanisms of EM. This talk will summarize our recent progress in such efforts and present a critical overview of the basis of microstructural evolution, temperature evolution, and electrical resistivity evolution during current stressing. In addition, materials modification by introducing the alloying elements and reinforcing phases into the conventional solder alloys will be discussed to demonstrate their potential roles on retarding the EM process.

2:50 PM Invited

Effect of the Cu Thickness in Ti/Ni(V)/Cu under Bump Metallization on Interfacial Reaction and Mechanical Test of Sn3.0Ag0.5Cu Solder Joint: I-Tai Wang¹; Kai-Jheng Wang¹; Chi-Yang Yu¹; *Jenq-Gong Duh*¹; ¹National Tsing Hua University

In the Ti/Ni(V)/Cu under bump metallization (UBM), the Sn-patch is observed in the Ni(V) layer after reflow and aging. The Sn-patch growth may cause the IMCs detaching from the interface of solder joint and then reduces the reliability. In this study, the Sn3.0Ag0.5Cu solder was reflowed on the Ti/Ni(V)/Cu UBM with various Cu thickness at 250 deg. C for 60 s, and then aged at 150 deg. C for various periods of duration. It was revealed that the Sn-patch growth could be controlled by increasing the Cu thickness in Ti/Ni(V)/Cu UBM. As a result, the mechanical property of SnAgCu solder joint with thick-Cu UBM was superior to that with thin-Cu UBM via a high-speed impact tester. The coupling factor in the Cu thickness of UBM and mechanical property of solder joint was discussed. Besides, the optimal Cu thickness in Ti/Ni(V)/Cu UBM was proposed.

3:15 PM

Electroless Fe-Ni under Bump Metallurgy for Solder Interconnects: H. Zhou¹; J. Guo¹; J. Shang²; ¹Institute of Metal Research; ²University of Illinois

Fe-Ni alloys are attractive Under Bump Metallurgy because of their excellent metallurgical stability against liquid and solid solder alloys. However, traditional Fe-Ni wrought alloys, such as Fe-42Ni, have shown poor wettability with liquid solders. In this study, electroless Fe-Ni alloys were prepared by overcoming the difference in the reduction potential between Fe2+ and Ni2+ and by preventing Fe2+ from early oxidation. Electroless deposition of Fe-Ni alloys with high Fe concentrations was achieved on the copper substrate. The electroless Fe-Ni alloys were found to have excellent wettability, very slow reaction rates with liquid and solid solders, and excellent oxidation resistance.

3:35 PM Break

3:45 PM

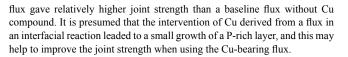
Effect of Solder Bump Heights on Cu Dissolution Rate in Pb-Free Flip Chip Solder Joints by Electromigration: *Fan-Yi Ouyang*¹, Pilin Liu¹; Matt Pharr², Kejie Zhao²; Zhigang Suo²; ¹Intel Corporation; ²Harvard University

Solder joint reliability has long been a concern in the microelectronic packaging industry. As microelectronic circuit dimensions continue to reduce, some reduction in package feature dimensions is also anticipated. To effectively use the limited space and meet the Z-height requirements in handheld devices, dramatic change in package design and shrinkage of solder bump dimensions is expected. With continuing reduction on the dimension of solder bump, the volume fraction of intermetallic compound (IMC) due to Cu-Sn reaction will increase. This will change the physical properties and diffusion behavior inside the solder bump, thus making it more important to understand the mechanism of Cu dissolution in Sn-based solder. The Cu dissolution in Pb-free solder joint under electromigration will be discussed here. We will focus on the role of solder bump height on Cu dissolution rate. A theory will also be proposed on relationship between Cu dissolution rate and solder bump height.

4:05 PM

Effects of Cu-Bearing Flux on Sn-3.5Ag Soldering with Electroless Ni-P/Au Surface Finish: Microstructure and Joint Reliability: *Hitoshi Sakurai*¹; Keun-Soo Kim¹; Youichi Kukimoto²; Katsuaki Suganuma¹; ¹Osaka University; ²Harima Chemicals, Inc.

The microstructure and joint reliability for Sn-3.5Ag soldering on an electroless Ni-P/Au surface finish by using the fluxes containing Cu(II) stearate were investigated. The content of the Cu compound in a flux varies from 0 wt.% to 40 wt.%. The study of the interfacial microstructure revealed that the thickness of a P-rich layer became thinner with increasing Cu content in a flux. According to the qualitative analysis of the joint interface, Cu was detected in the interfacial intermetallic layer formed by the use of the Cubearing flux. Additionally, joint strength tests showed that the Cu-bearing



140th Annual Meeting & Exhibition

4:25 PM

Effect of Cu Electroplating Process on the "Kirkendall Voiding" in SnAgCu-Cu Solder Joints: *Liang Yin*¹; Nikolay Dimitrov²; Peter Borgesen²; ¹Universal Instruments Corp; ²Binghamton University

Soldering to Cu surface finish with Sn-containing alloys usually leads to the formation of a layered interfacial Cu_3Sn/Cu_6Sn_5 structure. Frequently microscopic voids within Cu_3Sn have been observed to develop during extended thermal aging or current stressing. Excess impurity incorporation during Cu electroplating has been shown to cause this phenomenon. In this study, crystallographic orientation analysis by X-ray diffraction (XRD) was performed on samples plated by various electroplating additive combinations and plating process parameters. The results suggested that the level of impurity incorporation and the associated voiding propensity were greatly affected by applied over-potential and the texture of electroplated Cu films. A general picture was proposed, based on the parabolic adsorption behavior of organic molecules as a function of the applied over-potential.

4:45 PM

Correlations of Microstructure and Electromigation Behavior in Eutectic Sn-Pb Solder Joints: Andre Lee¹; Y. Lee¹; *K. Subramanian*¹; ¹Michigan State University

Atomic movements within a multi-phase alloy attributed to the directcurrent stressing will depend on size, shape and distribution of phases present. However, most of current stressing studies are carried out with solder joints possessing as-reflowed microstructures. To better understand the role of microstructure on materials movement resulting from direct current stressing, electromigration studies were carried out on eutectic Sn-Pb joints with coarsened microstructures produced by varying extents of isothermal aging treatments. These studies characterized the evolution of microstructural features at the bulk region of solder joints, as well as at the interface of solder/Cu substrates of anode and cathode. Results of this study indicate the electromigration behavior in a two-phase alloy is significantly influenced by the initial microstructure, evolution of microstructures and concentration gradients of moving atomic species under the influence of high current density. These events indirectly affect the type of interfacial intermetallic compounds formed at the solder/substrate interfaces.

5:05 PM

The Effect of Pd Thickness in the Interfacial Reaction between Sn-3.0Ag-0.5Cu Solder and Electroless Nickel/Electroless Palladium/Immersion Gold Surface Finish and Their Mechanical Properties: *Youngmin Kim*¹; Jin-Young Park¹; Young-Ho Kim¹; ¹Hanyang University

Electroless Nickel/immersion gold (ENIG) surface finish has been widely used in electronic packaging industries, however, ENIG easily causes black pad issue. Recently, electroless nickel/electroless palladium/immersion gold (ENEPIG) has been developed to overcome the weak solder joint by introducing a Pd between Ni and Au layer. Pd acts an efficient protector against corrosion in the Ni-P layer. ENEPIG offers an excellent solder joint even in higher thermal conditions. In this study, the thickness effect of Pd in the interfacial reaction between ENEPIG and Sn-3.0Ag-0.5Cu solder was investigated systematically by varying the thickness of Pd ranging from 0 to 0.5 μ m. In all specimens, (Cu, Ni)6Sn5 formed at the SAC/ENEPIG interfaces after reflow at 260°C. For Pd thickness of 0.5 μ m, monoclinic structure of (Pd, Ni)Sn4 formed over (Cu, Ni)6Sn5. The relationship between the interfacial reaction of SAC/ENEPIG with different thickness of Pd and their mechanical properties will be discussed.

Phase Stability, Phase Transformations, and Reactive Phase Formation in Electronic Materials X: Conductors, Dielectrics, Interconnects, Phase Change Memory, and Polymer Materials

Sponsored by: The Minerals, Metals and Materials Society, TMS Electronic, Magnetic, and Photonic Materials Division, TMS: Alloy Phases Committee

Program Organizers: Chih-Ming Chen, National Chung Hsing University; Hans Flandorfer, University of Vienna; Sinn-Wen Chen, National Tsing Hua University; Jae-ho Lee, Hongik University; Yee-Wen Yen, National Taiwan Univ of Science & Tech; Clemens Schmetterer, TU Bergakademie Freiberg; Ikuo Ohnuma, Tohoku University; Chao-Hong Wang, National Chung Cheng University

Wednesday PM	Room: 7A
March 2, 2011	Location: San Diego Conv. Ctr

Session Chairs: Alexandre Kodentsov, Eindhoven University of Technology; Jae-Ho Lee, Hongik University

2:00 PM Invited

Phase Transformation of PVP-Protected Noble Metallic Nanoparticle Deposits upon Heating in Air: *Jenn-Ming Song*¹; Guan-Di Chiou²; Wei-Ting Chen¹; Shih-Yun Chen²; Tzu-Hsuan Kao³; In-Gann Chen³; Hsin-Yi Lee⁴; ¹National Dong Hwa University; ²National Taiwan University of Science and Technology; ³National Cheng Kung University; ⁴National Synchrotron Radiation Research Center

By utilizing a proper deposition technique, e.g. drop-on-demand ink jet printing, inks containing noble metallic nanoparticles have been widely used to fabricate conductive lines and electrodes for electronic devices. For the transportation of power and signal, the nanoparticle deposits (NPDs) should be consolidated and well jointed with the contacts of the devices. This study prepared polyvinylpyrrolidone (PVP)-protected Ag and Au nanoparticles and observed their structural evolution upon heating using in-situ synchrotron radiation X-ray diffraction (SR-XRD). Due to the difficult desorption of the surfactant, low temperature melting of NPDs did not occur. Instead, particle coarsening and coalescence were verified by gradual intensification of the X-ray diffractions. This talk will also discuss the interactions between NPDs and the commonly used electronic metallic substrates, and how they influenced the phase transitions and oxidation of the NPDs, as well as the degree of thermal expansion.

2:25 PM

Synthesis of Ag Nanoparticles for the Fabrication of Highly Conductive Ink: Inyu Jung¹; Yun Hwan Jo¹; *Hyuck Mo Lee*¹; ¹KAIST

A various size of Ag nanoparticles were synthesized by using a thermal decomposition process for low temperature electronic devices. Monodispersed Ag nanoparticles with diameters of 6 nm, 8 nm and 12 nm were synthesized by incubation and ripening stages related with nucleation and growth. After Ag nanoparticles were made into ink with a proper solvent, the inkjet printing and thermal sintering methods were employed to form a metal thin film with thickness of 50nm. The electrical resistivity was examined by a 4-point probe system and compared with the resistivity of bulk Ag. As a result, the resistivity of the Ag film has reached around 50 μ O•cm, which is much higher than that of bulk Ag. To improve the electrical stability and properties, we applied surface treatment on the substrate and plasma ashing. Both treatments had the effect of diminishing the resistivity of the printed conductive films.

2:40 PM

Influence of Post Annealing Ambient on the Microstructure and Contact Resistance of Screen-Printed Silver Contacts of Silicon Solar Cells: *Sungbin Cho*¹; Jung-Woo Chun¹; Bo-Mook Chung¹; Joo-Youl Huh¹; Byung-Chul Lee²; Kuninori Okamoto²; ¹Korea University; ²Cheil Industries Inc.

Screen-printed Ag thick-film metallization is commonly used in photovoltaic industry for front-side emitter contacts of commercial Si solar

cells. During firing process, glass frit contained in Ag paste plays a crucial role in contact formation. In order to achieve good-quality ohmic contacts to Si emitters, thin glass layer formed in between Ag crystallites on Si surface and bulk Ag after firing must provide a certain path for current transport. Recently, it was shown that firing ambient has a strong influence on microstructure and contact resistance of fire-through contacts. In this study, we carried out post annealing treatments of fired contact samples at various temperatures above and below glass softening temperature under various ambient gases with different oxygen partial pressures. The precipitation of Ag particles in glass layer depending on annealing ambient was examined. In the presentation, we will discuss how the annealing ambient affects contact microstructure and thus contact resistance.

2:55 PM

Low Resistivity RuTaC Barrier for Cu Interconnection: Jau-Shiung Fang¹, J. Lin¹, B. Chen¹, G. Chen¹, T. Chin¹, ¹National Formosa University

Ultrathin Ru-Ta-C film on silicon substrate is evaluated as a barrier for copper metallization. The films were deposited by magnetron sputtering using Ru and TaC targets so that composition and structure can be adjusted by tuning the respective deposition power. The characterization of Ru-Ta-C and its barrier properties were elucidated by four-point probe measurement, x-ray diffractometry, field emission electron probe microanalysis, Auger electron spectroscopy (AES) and transmission electron microscopy. Structure of Ru-Ta-C films gradually changes from Ru₄Ta(C) to amorphous when increasing TaC. The failure temperatures are 800°C in a sandwiched scheme Si/Ru₈₂Ta₁₂C₅ (10 nm)/Cu and Si/Ru₇₇Ta₁₅C₇ (10 nm)/Si, and are at least 750°C for 5 nm Ru-Ta-C barriers. Because of its low resistivity (92 $\mu\Omega$ cm for Ru₈₂Ta₁₂C₅ film) and high thermal stability, the Ru-Ta-C film is promising as a barrier and capable of directly Cu electroplating without Cu seed.

3:10 PM Break

3:30 PM

Metal-Induced Crystallization and the Diffusion Behavior of Al/Ge Thin Film: Chao Nan Yeh¹; Kewin Yang¹; Albert T. Wu¹; ¹National Central University

Metal-induced crystallization (MIC) is a rapid process for crystallization in semiconductor materials, such as Si and Ge. In this paper, Al/Ge thin films were deposited by sputtering technique. Layer exchange and surface morphology evolution accompanied by MIC of Ge film induced by Al were investigated. Ge films were deposited on top of Al layer to avoid oxidation of Al. Complete layer exchange could be found after annealing at 300°C for 10 days. The interdiffusion coefficient of Al and Ge films that were annealed between 200°C to 400°C for various duration of time were calculated by Boltzmann-Matano analysis based on the ESCA depth profiling measurement. The diffusivities were in the range between the orders of 10^{-22-20} (m²/s) for heat treatment at different temperatures. From the SEM image, mushroom-shaped hillocks formed on the surfaces of the films at the annealing temperature at 400°C. We proposed a mechanism to explain the growth mechanism of the hillocks and discussed the phase stability after thermal treatment.

3:45 PM

Measurement of Warpage for Chips on Si Interposer: *Hsueh-Hsien Hsu*¹; Tao-Chih Chang²; Chih Chen³; Hsin-Yi Lee⁴; Albert T. Wu¹; ¹National Central University; ²Industrial Technology Research Institute; ³National Chiao Tung University; ⁴National Synchrotron Radiation Research Center

For the demand of electronic devices with high performance, 3D stacking IC in the vertical direction is a new trend for electronic packaging. 3D IC used Si as interposer. Due to the decreasing chip size, the thickness of the dies and the choices of underfill were critical to the mechanical properties of the chip. The test samples had microbump with the dimension of 25μ m. Both the dies and the substrates are Si. The samples were placed on a heating stage. The current was stressed at different temperatures while the chips were scanned by synchrotron radiation X-ray. The deformation of the dies was recorded in situ. The glass transition temperature, Tg, greatly affected the

warpage of the dies. Based on the out-of-plane strain, the deformation of the chips could be measured and the in-plane stress in the dies could be determined.

4:00 PM

Dynamic Transmission Electron Microscope Investigation of Coupled Laser Absorption, Phase Transformation, and Nanoscale Morphology in e₂Sb₂Te₅: Bryan Reed¹; Melissa Santala¹; Stefan Meister²; Thomas LaGrange¹; Geoffrey Campbell¹; Nigel Browning¹; ¹Lawrence Livermore National Laboratory; ²Stanford University

Morphology changes during cycling of phase change materials are detrimental to their stability as nanoscale memory systems. While x-ray and optical investigations can reveal much about the spatially-averaged kinetics, the Dynamic Transmission Electron Microscope provides complementary information because of its unique combination of abilities: single shot nanosecond/nanometer-scale real space imaging, in situ laser drive for direct, rapidly iterated before-during-after comparisons, and collection of diffraction data from very small volumes of material. We show that: (1) the amorphous phase shows some evolution of structure prior to obvious nucleation of the crystalline phase, (2) once crystal nucleation begins, the nucleation density is extremely high, and (3) while morphology changes are most pronounced when the material is partially melted for several microseconds, striations accumulate over a large number of laser shots below the threshold intensity for melting. This occurs at the same time as grain coarsening, so these processes may be coupled.

4:15 PM

Thermal Treatment of a Ni/Pt Bi-Layer Deposited on a Polyimide Film for Dye-Sensitized Solar Cells: *Sheng-Jye Cherng*¹; Chih-Ming Chen¹; ¹National Chung Hsing University

A Ni/Pt bi-layer coated on a polyimide (PI) film is prepared as an efficient counterelectrode for dye-sensitized solar cell (DSSC). Surface metallization of Ni/Pt on the PI film is carried out via a specific wet process, where the surface Pt is the catalyst and the bottom Ni is the conduction/light-reflection layer. Thermal treatment of the Ni/Pt bi-layer is performed to investigate the interaction between Ni and Pt. Surface morphology, interfacial microstructure, and phase evolution are studied using a scanning electron microscope, X-ray diffractometer, and transmission electron microscope. DSSCs employing the annealed Ni/Pt counterelectrodes are fabricated. Their photovoltaic performance and electrochemical impedance spectroscopy (EIS) are examined and the correlation between the thermal treatment of the Ni/Pt counterelectrode and the cell's performance is discussed.

4:30 PM

Synthesis of Carbon Nanomaterials from Paper Phenolic Board: Yu Ting Huang¹; YiWei Lin¹; Chih Ming Chen¹; ¹National Chung Hsing University

Due to the advantages of low cost and easy fabrication of printed circuit board (PCB), they have been widely used and manufactured in a variety of electronic products. The prototype of PCB is a bilayer copper (Cu)/polymer laminate, also named paper phenolic board. Two different methods are addressed to synthesize the carbon nanomaterials using the paper phenolic board as the carbon source. A patterned Cu trace is served as localized heating source. Thermal decomposition of the paper phenolic board takes place primarily near the Cu trace, and the products contain carbon nanosheets and tubular carbon nanofibers. Other than the above, we also use chemical vapor decomposition (CVD) method to synthesize the carbon nanomaterials. Tubular carbon nanofibers are successfully synthesized using different catalysts.

Physical and Mechanical Metallurgy of Shape Memory Alloys for Actuator Applications: Effect of Processing on the Properties of Shape Memory Alloys

Sponsored by: The Minerals, Metals and Materials Society Program Organizers: S. Raj, NASA Glenn Research Center; Raj Vaidyanathan, University of Central Florida; Ibrahim Karaman, Texas A&M University; Ronald Noebe, NASA Glenn Research Center; Frederick Calkins, The Boeing Company; Shuichi Miyazaki, Institute of Materials Science, University of Tsukuba

Wednesday PM	Room: 11B
March 2, 2011	Location: San Diego Conv. Cti

Session Chairs: Gunther Eggeler, Ruhr-Universität Bochum; Thomas Waitz, University of Vienna

2:00 PM Invited

On the Processes Involved in Shape Setting of SMA: *Petr Sittner*¹; J. Pilch¹; L. Heller¹; ¹Institute of Physics of the ASCR

Although shape setting of shape memory alloys has been performed for decades, the physical processes responsible for it are still not completely clear. The properly shape set SMA element displays functional properties (e.g. superelasticity) and, at the same time, its parent austenite shape is memorized. Both happens due to the microstructure changes brought about by thermomechanically driven processes at high temperatures and stress. Both cold worked and annealed SMAs can be shape set but strategies are different. In large extent, same processes as those involved in shape setting are responsible for degradation and strain drift of high temperature SMA actuators. In this work, results of recently performed in-situ experiments (thermomechanical, electrical resistivity, X-ray and TEM) during shape setting of NiTi wires by short DC electric pulses will be reviewed. Practical implications for industrial shape setting treatments as well as for optimization of high temperature actuation will be discussed.

2:20 PM

An In Situ Neutron Diffraction Study of Shape Setting NiTi: Othmane Benafan¹; Santo Padula²; Ronald Noebe²; Raj Vaidyanathan¹; ¹UCF; ²NASA GRC

A bulk polycrystalline NiTi shape memory alloy specimen was shape set while neutron diffraction spectra were simultaneously acquired. The temperature and shape of the specimen were controlled in a load frame while the stress exerted by the specimen on the grips was monitored during these in situ neutron diffraction experiments. The objective was to correlate internal stress, phase volume fraction, and texture measurements (determined from neutron diffraction spectra), with the macroscopic stress and shape changes (from a load cell and extensometry) during the shape setting procedure and subsequent shape recovery. Comparisons were made between the preshape set specimen and the post-shape set specimen, both with and without external constraints. Emphasis was placed on capturing the texture evolution in inverse pole figures and comparing the measured macroscopic blocking or actuation stress with direction dependent intergranular stresses determined from the neutron spectra.

2:35 PM Invited

The Effect of Inclusion Content on the Mechanical and Physical Properties of Binary NiTi Shape Memory Alloys: *Giorgio Vergani*¹; Frank Sczerzenie¹; Graeme Paul¹; ¹SAES Smart Materials

Binary nickel titanium alloys with transformation temperature in the range of 95 degrees centigrade are being used for several actuator applications. We have observed that higher transformation temperature binary alloys have larger inclusion size and greater area fraction of inclusions than superelastic alloys. Actuator performance is affected by the response to cyclic strain and by variations in strain recovery. Historically, higher inclusion content has been correlated to reductions in strain recovery. This paper will present new data on the structure, physical properties and mechanical behavior of standard 95 degrees centigrade alloy and alloy processed to minimize inclusion content. We will compare transformation temperature, active austenite finish temperature, static and cyclic mechanical properties and strain recovery of these materials.

2:55 PM

140th Annual Meeting & Exhibition

Characterization of Low Inclusions NiTi Shape Memory Wires for Industrial Applications: *Alberto Coda*¹; Luca Fumagalli¹; Giorgio Vergani²; Frank Sczerzenie²; ¹SAES Getters S.p.A.; ²SAES Smart Materials Inc.

Inclusions content is important for the mechanical behavior and performances of Nitinol wires particularly in fatigue rated devices. This includes high transformation temperature wires that are thermally or electrically actuated for industrial applications. Higher inclusions content has been correlated to reductions in strain recovery under thermomechanical cycling. Moreover, most fatigue fractures show inclusions at the initiation site. As lower the wire diameter is, as more important the size and concentration of inclusions become. Therefore, a general reduction of inclusions may have a beneficial effect in improving the shape memory properties of such devices. In this work, the functional behavior of standard 95°C binary NiTi wires and wires processed to minimize inclusion content will be compared. Possible explanations for the observed differences and their significance will be given and discussed.

3:10 PM

Study of the Influence of Inclusions on the Behavior of NiTi Shape-Memory Alloys in Thermal Cycling by Means of FEM: Marco Fabrizio Urbano¹; ¹SAES Getters

Despite the number of papers on the subject, the influence of inclusions on the behavior of Nitinol is still controversial. Numerical simulations can play a fundamental role in providing insight into this subject. As far as superelastic materials are concerned, other authors have shown by means of Finite Element simulations that, in wires loaded in rotary bending conditions, the presence of inclusions greatly increases the stress distribution in the cross section, and that the maximum stress increases as the distance between the inclusion and the neutral axis increases. In this work a similar approach is utilized to analyze the effect of inclusions on thermal cycles of wires loaded in tension. By means of a thermo mechanical constitutive model implemented in Ansys, the stress strain field in presence of a particle is computed. Both particle diameter and position are varied in the analysis. The influence on fatigue behavior is estimated.

3:25 PM Break

3:35 PM Invited

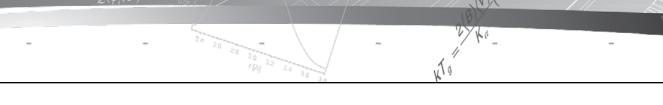
Shape Memory Alloy Cables: John Shaw¹; ¹The University of Michigan

Common structural cables (or wire ropes) are hierarchical constructions of straight and helical wire filaments and strands that have desirable mechanical properties as tension elements in terms of load carrying redundancy and increased bending compliance for spooling/packaging. Experiments on new cables made from NiTi shape memory alloy (SMA) wires show interesting thermomechanical phenomena as measured by infrared imaging and digital image correlation. Different mechanical responses and load-rate sensitivities are observed, depending on the particular construction and layup. SMA cables leverage the excellent properties of SMA wires in a scalable and tailorable form, and thus hold promise for new adaptive and enhanced structural properties over a broad range of applications.

3:55 PM Invited

Shape-Memory Nitinol with Micro-Channel Networks: Anselm J. Neurohr¹; *David Dunand*¹; ¹Northwestern University

NiTi powders containing parallel layers of steel wire meshes were densified into dense NiTi/steel composites. Subsequent electrochemical dissolution of the meshes results in parallel layers of orthogonally interconnected microchannels, with 24-34 vol.% and ~400 μ m diameters, exactly replicating the steel meshes. For low carbon steel wires, iron diffuses into the surrounding NiTi creating a Fe-enriched zone. For high carbon steel wires, TiC forms at the steel/NiTi interface thus inhibiting iron diffusion while also depleting



some titanium from the adjacent NiTi. In both cases, phase transformation characteristics of the NiTi regions near the micro-channels are altered, but not sufficiently to affect adversely the mechanical properties of porous NiTi which shows superelastic and shape-memory recovery. These NiTi structures with networks of micro-channels have potential as bone implants (where channels reduce stiffness and stress-shielding, while allowing bone ingrowth) and as actuators (where channels enable rapid heating and cooling, reducing actuation time.)

4:15 PM

Joining Strategies for Shape Memory Alloy Actuators: *Konstantin Lygin*¹; Sven Langbein¹; Tim Sadek¹; ¹Ruhr University Bochum

During the transformation from deformed to primal form shape memory alloys (SMA) display high forces. These forces are usable in actuators based on SMA technology. To transfer the actuating force of SMA elements it is necessary to connect them to the system environment. Basically three connection types are used: form locked, material bonded and friction locked. An example for a form locked connection is a SMA element sealed in a polymer matrix. With laser welding it is possible to create a material bonded connection. A force locked connection can be created by locking a SMA element with a screw. This paper presents the mentioned and several other connection methods for SMA components and categorizes those methods in terms of actuating forces, lifetime, interaction with system environment, geometry of actuating elements and joining elements. Finally SMA connection methods were recommended for different use cases with specific restrictions.

4:30 PM

Fabrication of Neck Ache Prevent Tool Applying Ti-Ni Superelastic Alloy: *Kazuhiro Kitamura*¹; Hiraku Tsuboi²; Katsuyoshi Chino³; Yu Takeuchi⁴; Kimio Satou⁵; ¹Aichi University of Education; ²Nagano Techno Foundation; ³C. K.Techno Co, Ltd.; ⁴Misuya Industry Co, Ltd.; ⁵Suzaka city

Ti-Ni alloy had excellent shape memory and superelastic effect. Especially, superelastic effect showed unique mechanical properties. We were developed the neck ache prevent tools applying Ti-Ni superelastic alloy. The superelastic wire was made from Ti-Ni wires of 1.5mm in diameter and 70mm in length. The components were arranged right and left side of the shoulder. The composition of this wire was Ti-50.8at%Ni. The transformation temperatures were measured by differential scanning calorimetry (DSC). From DSC measurement, this alloy showed the superelastic behavior at room temperature. The bending fatigue characteristics of superelastic wire were investigated by fatigue tester. Fatigue lives of the superelastic components were about 100,000 times at 1.8% strain.

4:45 PM

Severe Plastic Deformation of a Beta-Titanium Shape Memory Alloy: *Ji Ma*¹; Ibrahim Karaman¹; ¹Texas A&M University

Because of their biocompatibility and ease of cold working, β -titanium SMAs, such as Ti-Nb are being investigated as possible alternatives to the commonly-used Nitinol in biomedical applications. However, they suffer from low yield strength in the solution-treated condition. Equal Channel Angular Extrusion (ECAE) strengthens the alloy through grain refinement, increase in dislocation density, and possibly stress-induced precipitations of the β phase. After appropriate post-extrusion heat treatments, fully reversible shape memory effect and superelasticity were attained. Curiously, while the texture of cold-rolled specimens was similar to the expected BCC rolling texture, ECAE texture of the alloy was quite different from that expected for a typical BCC material undergoing ECAE. We suspect this discrepancy is related to stress-induced martensitic transformation taking place during processing, as well as the intermittent nature of cold rolling, where strain is applied incrementally throughout several passes, as opposed to ECAE, where all strain were applied at once.

5:00 PM

Self-Assembled Ti Nanowires on Single Crystal NiTi Shape Memory Alloys: *Xu Huang*¹; Yuriy Chumlyakov²; Ainissa Ramirez¹; ¹Yale University; ²Siberian Physical and Technical Institute

Self-assembled Ti nanowires were fabricated by electro-polishing a NiTi single crystal in a solution of 20% H2SO4-80% methanol at 1 A for 60 seconds. The resulting Ti nanowires were approximately 480X480 nm2 in cross section and 50 μ m in length. The nanowire orientations were determined and found to grow perpendicularly along the <110> and <100> planes of the single crystal substrate. Although most of them were oriented perpendicular to the surface, some presented an incline at a specific angle. Their composition was determined using microprobe methods and diffraction, and their electrical properties were investigated using four-point probe measurements. These methods for producing Ti nanowires could provide new routes for generating nanostructures.

5:15 PM End of Session

Polycrystal Modelling with Experimental Integration: A Symposium Honoring Carlos Tome: Steels, Damage

Sponsored by: The Minerals, Metals and Materials Society, TMS Structural Materials Division, TMS Materials Processing and Manufacturing Division, ASM-MSCTS: Texture and Anisotropy Committee, TMS/ASM: Mechanical Behavior of Materials Committee, TMS/ASM: Computational Materials Science and Engineering Committee

Program Organizers: Ricardo Lebensohn, Los Alamos National Laboratory; Sean Agnew, University of Virginia; Mark Daymond, Queens's University

Wednesday PM March 2, 2011 Room: 6C Location: San Diego Conv. Ctr

Session Chairs: Jose Gracio, Universidade de Aveiro; Thomas Bieler, Michigan State University; Chad Sinclair, University of British Columbia

2:00 PM Invited

Plastic Anisotropy in Multiphase Steels: Young Ung Jeong¹; *Frederic Barlat*¹; ¹Pohang University of Science and Technology

In advanced steels, which are mostly multiphase alloys, plastic anisotropy depends on many parameters, in particular crystallographic texture, slip properties and volume fraction of each phase. In this work, the stress-strain curves and flow anisotropy of multiphase steels are measured in uniaxial tension, in-plane biaxial tension and through-the-thickness disk compression. The yield loci are assessed using an in-plane biaxial tensile machine. For each material, the locus is determined at different amounts of plastic work. Continuum and simple crystal plasticity models are used to predict plastic properties. Because of the number of experiments conducted in this work, some data are used for constitutive model identification while others are used for validation purpose. The objective of this work is to compare the ability of simple continuum and crystal plasticity models to describe the plastic behavior of multiphase materials.

2:25 PM Invited

Effect of Asymmetric Rolling on the Mechanical Behavior of Low Carbon Steel under Shear Tests: A Simple Modelling Approach: Jose Gracio¹; ¹University of Aveiro

In this work we analyzed the mechanical behaviour of low carbon steel pre-deformed in conventional, continuous asymmetric and inverse asymmetric rolling and reloaded in simple shear at different orientations with respect to the previous rolling direction. In essence, the mechanical behavior in simple shear seems to be not strongly affected by the different rolling conditions imposed during pre-strain. The behavior was modelled with a simple approach based on the evolution of the dislocation microstructures. A



parameter which measures the amplitude of the strain path change as well as textural effects were incorporated in this approach.

2:50 PM

Comparison of Experimental and Computational Texture Evolution in Steel under Multi-Axial Loads: *Adam Creuziger*¹; Thomas Gnäupel-Herold¹; Lin Hu²; Anthony Rollett³; ¹National Institute of Standards and Technology; ²Carnegie Mellon University ; ³Carnegie Mellon University

In this study, as received High Strength Low Alloy (HSLA) and Transformation Induced Plasticity (TRIP) steel sheets are deformed under uniaxial, plane strain and balanced biaxial strain conditions. After deformation the texture evolution was investigated using neutron diffraction to determine both the phase fractions in the deformed material and how the crystallographic texture evolves as a function of strain for each deformation mode. Additionally, the texture evolution was modeled using a viscoplastic self-consistent (VPSC) model. Comparisons between the experimental and computational texture evolution show while there is good qualitative agreement, the VPSC model over predicts the amount of texture sharpness.

3:10 PM

Micromechanical Modelling of Strength and Deformation of Advanced High Strength Steels on the Grain Level: Christian Krempaszky¹; *Ewald Werner*²; Andreas Pichler³; Thomas Hebesberger³; ¹CD Laboratory of Material Mechanics of High Performance Alloys, TU-Munich; ²Technische Universität München; ³voestalpine Stahl Linz GmbH

A micromechanical model on the grain level is presented to describe the strength and deformational behaviour of advanced high strength steels based on microstructural and phase specific properties. The topology of the microstructure is modelled by Voronoï tessellation and appropriate coloring algorithms are presented to simulate the topology of the constituting phases ferrite, bainite and martensite. The effect of the geometrical arrangement of these phases in the microstructure and the strength ratio of the phases on formability is discussed in comparison with experimental results from tensile and hole expansion tests performed with industrially produced dual-phase and complex-phase steels. Special emphasis is placed on the comparison of two approaches, namely the finite element analysis and a discrete Fourier transform based algorithm.

3:30 PM Break

3:50 PM Invited

Roping of Ferritic Stainless Steels: Models and Experiments: *Chad Sinclair*¹; Guillaume Lefebvre¹; Ricardo Lebensohn²; Jean-Denis Mithieux³; ¹University of British Columbia; ²Los Alamos National Laboratory; ³ArcelorMittal

Roping of ferritic stainless steel sheet results in an anisotropic surface roughening parallel to the prior rolling direction. While this may appear to be a surface phenomenon, it is in fact a collective through thickness deformation pattern leading to a "corrugation" of the sheet. While many important factors associated with roping have been identified, many questions remain regarding what constitutes a "sufficient" set of conditions leading to "strong" or "weak" level of roping. At this time it is not possible, from experiment alone, to predict the severity of roping in a given material prior to testing it. This talk will review experimental and modelling efforts aimed at understanding the relationship between roping and local texture, grain (orientation) clustering and the collective deformation behaviour of groups of grains. Simulation results examining the morphological rotation of grains via 1-site and N-site viscoplastic model calculations will be discussed in relation to experimental observations.

4:15 PM Invited

Integrated Experimental and Crystal Plasticity Investigations of Heterogeneous Deformation and Damage Nucleation in Titanium: *Thomas Bieler*¹; Philip Eisenlohr²; Martin Crimp¹; Leyun Wang¹; A. Alankar²; Yiyi Yang¹, Rozaliya Barabash³; Gene Ice³; Wenjun Liu⁴, ¹Michigan State University; ²Max-Planck-Institut für Eisenforschung; ³Oak Ridge National Laboratory; ⁴Argonne National Laboratory

Predicting heterogeneous deformation and the likelihood of damage nucleation in polycrystalline metals requires knowledge of the history of slip system activity and its interaction with microstructural features such as interfaces. These processes are dependent on the strain path, which can be locally complex due to heterogeneous deformation arising from different orientations of neighboring grains, and effects of slip resistance and slip transfer across boundaries. To assess the ability of crystal plasticity finite element models to predict heterogeneous deformation, experimental characterization using several modern experimental characterization tools to quantify the activity of slip systems is used to directly compare with crystal plasticity finite element computational models. Comparisons between local and non-local models are used to identify where improvements in computational modeling are needed using illustrative microstructural patches from titanium and titanium alloys. Supported by NSF, DOE and DFG.

4:40 PM Invited

Role of Crystallographic Texture in the Delamination and Fracture of Al-Li Alloys: Armand Beaudoin¹; Rebecca Storer¹; Wesley Tayon²; Sean Hamel¹; Peter Kurath¹; ¹University of Illinois at Urbana-Champaign; ²NASA Langley

Driven by savings in weight, application of Aluminum-Lithium alloys in aerospace structures is increasing. Considering fracture of these alloys, the crack path may deviate from the Mode I direction toward the direction of elongated grain boundaries, a phenomena called delamination. Even in the absence of a "crack", uniaxial and cyclic failures are observed at elongated grain boundaries. To provide insight into fracture tolerant design, this work explores the relationship between crystallographic orientation and stress state about a primary crack. Coordinated use of experiment and modeling (crystal plasticity) are pursued to evaluate the contribution of anisotropy to the nucleation and propagation of delamination. In general, results indicate the key role of slip incompatibility: a grain oriented favorably for slip sharing a boundary with another 'less favorable' crystallographic orientation promotes the development of shear stress which sustains delamination. This work is supported by the NASA Marshall Flight Center through grant NNX09AN21G.

5:05 PM

Ductile Failure of Metals: The Initiation and Growth of Nanovoids: *Marc Meyers*¹; Eduardo Bringa²; Yizhe Tang¹; ¹UCSD; ²U. Nacional de Cuyo

It has been known since the 1940s that the ductile failure of metals proceeds by the initiation, growth, and coalescence of voids. In spite of the rigorous mechanical and metallurgical understanding of the processes involved gained in the past sixty years, the fundamental deformation mechanisms had not been understood. The postulation of special shear and prismatic dislocation loops to accomplish the outward matter transfer required for void formation, in 2004, has been followed by significant efforts, worldwide, in molecular dynamics. The generation and expansion of shear loops has been observed in simulations in copper and tantalum. A specific requirement is that the extremities of the dislocations have to remain attached to the void surface. In some cases these loops react and form prismatic loops which glide away from the void. In copper, partial dislocation loops generate extended stacking faults that impede cross slip. In tantalum, twinning can also occur, in some cases. We review our most recent research on the formation of these voids in both mono and nanocrystals.

5:30 PM

Roles of Stress and Strain in IG Cracking of Irradiated Stainless Steel in Supercritical Water: *Elaine West*¹; Gary Was¹; ¹University of Michigan

The Schmid factors of grains in irradiated 316L stainless steel were used as indicators of their deformation propensities to determine the role of stress

and strain on intergranular cracking in 400°C supercritical water. Variations in grain deformation propensities resulted in heterogeneous cracking that was promoted by strain incompatibilities, and ultimately determined by normal stress. The formation of cracks along grain boundaries perpendicular to the tensile axis and adjacent to grains with low Schmid factors indicated normal stress dependence. The Schmid-Modified Grain Boundary Stress Model was developed to evaluate the grain boundary normal stress as a function of the orientation of the grain boundary plane with respect to the tensile axis and Schmid factor. This model confirmed the normal stress dependence of intergranular cracking, and demonstrated that the Schmid factor dependence of the cracking could be predicted from the distribution of cracked grain boundary surface trace inclinations to the tensile axis.

5:50 PM

The Effect of Asymmetric Rolling on the Mechanical Properties of Interstitial Free Steel: *Saeed Tamimi*¹; Gabriela Vincze¹; Augusto Lopes²; Jose Gracio¹; Edgar Rauch³; Frédéric Barlat⁴; ¹TEMA; ²Departamento de Engenharia Ceramica e do Vidro; ³Génie Physique et Mécanique des MatériauxENSPG-INPG (ESA CNRS 5010); ⁴Graduate Institute of Ferrous Technology

Asymmetric rolling (ASR) of sheet metals has been used to improve the mechanical properties. Present work deals with the perspective of crystallographic texture and microstructure and their relevance with the mechanical properties of interstitial free steel using ASR. The effect of rolls velocity ratio on the properties of the samples was investigated. It was found that the speed ratio 1.5 can make better condition for shearing and consequently rising more shear texture. The samples were deformed for 60% strain and annealed in 550-700 °C for 1, 8 and 24 hours. The results indicate that 650 °C for one hour can be considerd as an optimum heat treatment condition for applied strain. Improvment in the mechanical respons and the texture evolution during ASR and conventional rolling are observed using numerical simulation of ideal texture based on a polycrystal plasticity model. The results were compared with the exprimental results.

6:10 PM

Simulations for Fatigue Damage Incubation Mechanisms of Textured Al Alloy Using Crystal Plasticity Model: *Yibin Xue*¹; Chong Teng¹; Tong Li¹; ¹Utah State University

The high-cycle fatigue life of a textured Al alloy is consumed primarily during fatigue damage formation or incubation stage. The vital fatigue damage forms at the micrometer-sized intermetallic particles located at or near the surfaces or the change of geometries, as commonly observed. In this paper, micromechanical simulations are implemented to assess the crystallographical textured effects on the fatigue-life critical damage formation, which are difficult or impossible to obtain experimentally. The representative unit cell (UC) models are set with an intermetallic particle located in typical grain orientations, sizes, and grain boundary mismatches of the textured 7075-T651 Al alloy. Crystal plasticity constitutive mode is applied to quantify the micronotch-root plasticity and such to quantify and classify the severity of texture effects to the fatigue damage incubation. Eventually, the uncertainty and statistical distribution of the fatigue incubation life induced by the texture are obtained.

Processing and Properties of Powder-Based Materials: Mechanical Alloying/Milling, Reactions and Consolidation

Sponsored by: The Minerals, Metals and Materials Society, TMS Materials Processing and Manufacturing Division, TMS: Powder Materials Committee

Program Organizers: K. Morsi, San Diego State University; Ahmed El-Desouky, San Diego State University

Wednesday PM	Room: 33A
March 2, 2011	Location: San Diego Conv. Ctr

Session Chair: K. Morsi, San Diego State University

2:00 PM Introductory Comments

2:05 PM

Effect of Milling Process on Mechanical Properties of Fully Consolidated Titanium and Titanium Alloy Powders Made by Armstrong Process[®] Technology: Yukinori Yamamoto¹; Wei Chen¹; Stephen Nunn¹; Jim Kiggans¹; Michael Clark¹; Sarma Gorti¹; Adrian Sabau¹; Ronald Swain¹; Craig Blue¹; Brian Fuller²; Kamal Akhtar²; ¹Oak Ridge National Laboratory; ²Cristal US, Inc./ International Titanium Powder

Press-and-sinter processing of new titanium and titanium alloy powders produced by the Armstrong Process[®] technology has been systematically investigated, in order to develop the optimized near-net-shape manufacturing process. This study focuses on the effect of different types of milling processes and the length of time the powder was milled on the mechanical properties and the chemistry after the consolidation process. Milling significantly improves the tap density and the density after sintering for both CP-Ti and Ti-6Al-4V powders when compared to un-milled powders. However, extended milling time tends to increase the oxygen and carbon contents in the powder which degrades the ductility of the consolidated materials. Effects of several different milling processes on the microstructure, the chemistry and the roomtemperature tensile properties will be discussed. This research is sponsored by the U.S. DOE, Office of EERE Industrial Technologies Program, under contract DE-AC05-000R22725 with UT-Battelle, LLC.

2:25 PM

Fabrication of Ultrafine-Grained Al-Mg Alloy via ECAP Consolidation of Nanostructured Powder: *Zhihui Zhang*¹; Xiaolin Wu²; Ying Li¹; Troy Topping¹; Wei Xu²; Yizhang Zhou¹; Kenong Xia²; Enrique Lavernia¹; ¹UC Davis; ²University of Melbourne

Nanostructured Al powder produced by cryomilling showed good microstructural stability against thermal exposure. However, the grain growth behavior in a stress/strain field during thermomechanical processing is less understood. In this work, the microstructure evolution in an Al-7.5Mg alloy was studied via direct ECAP consolidating the cryomilled powder with an average grain size of 25 nm. The ECAP was conducted at 200 and 325 °C and after 4 passes, the samples showed averaged grain sizes of 170 and 450 nm, respectively. However, the bulk sample by HIP consolidating the annealed (24 hrs at 400 °C) cryomilled powder at 400 °C only showed an average grain size of 100 nm, indicating that plastic strain introduced during ECAP may have played a role in grain growth. TEM examination revealed that grain rotation and coalescence contributed to the observed grain growth. Finally, the mechanical behavior of the ultrafine-grained Al-7.5 Mg alloys was discussed.

2:45 PM

Investigation of Mechanical Alloying Process Parameters on Fe-Mn-Si Based System: *A. Umut Soyler*¹; Burak Özkal¹; Leandru G. Bujoreanu²; ¹Istanbul Technical University; ²The "Gh. Asachi" Technical University

In this work, Fe-Mn-Si based powder mixture having shape memory alloy composition prepared by mechanical alloying and systematically studied with different milling conditions. Effect of ball to powder ratio (BPR), type and amount of binder addition and milling time were investigated as



process parameters. All mechanical alloying studies performed under argon atmosphere and stainless steel balls and vials were used as milling media. X-Ray diffraction (XRD), laser particle size analysis (LPSA), scanning electron microscopy (SEM) and optical microscopy (OM) techniques used to characterize the powders. Results were discussed to show that powder metallurgy can be an alternative technique to obtain Fe-Mn-Si based shape memory alloys with the required composition and microstructural homogeneity in contrast to classical metallurgy.

3:05 PM

The Effects of Boron Sources on the Mechanochemical Synthesis of AlB₂ from Chloride-Based Powders: *Duygu Agaogullari*¹; Hasan Gökçe¹; Ismail Duman¹; M. Lütfi Öveçoglu¹; ¹Istanbul Technical University

The mechanochemical process to synthesize aluminum diboride (AlB₂) powder from AlCl₃-B₂O₃-Mg and AlCl₃-B-Mg system at room temperature was investigated systematically in this study. The reaction was driven by high-energy ball milling of powder mixtures in Spex 8000 D Mixer/Mill performed at different durations. Milled powders were subsequently annealed in a tube furnace to obtain AlB₂ phases. After obtaining AlB₂, byproducts of the reaction i.e. MgO and MgCl₂, and impurities released by the milling vial (Fe, Ni, Cr) were removed by leaching and washing with distilled water and ethanol. The phases, morphologies and thermal properties of the milled, leached and annealed powders were characterized by X-ray diffraction (XRD), scanning electron microscope (SEM), differential thermal analyzer (DTA) and atomic absorption spectrometer (AAS).

3:25 PM Break

3:35 PM

Deformation-Induced Ductility in Cryomilled Nanostructured Nickel: *Yonghao Zhao*¹; Qian Zhan²; Troy Topping¹; Y. Li¹; Enrique Lavernia¹; ¹University of California, Davis, CA 95616, USA; ²University of Science and Technology Beijing, Beijing 100083, People's Republic of China

When bulk nanostructured (NS) materials are prepared via consolidation of individual particles, agglomerates or clusters, extraneous defects, such as porosity, and impurities are sometimes introduced leading to the degradation of ductility. In this study we propose to examine the hypothesis that deformation can be used to ameliorate negative effects of these artifacts on the ductility of NS alloys. The approach involved cryomilling and forging to synthesize bulk NS nickel with porosity (95.5% theoretical density) and nitrogen grain boundary (GB) segregation. The results demonstrate that cold rolling resulted in increased tensile ductility from 2 to ~4%, with slight decrease in yield strength from 1150 to 1050 MPa. Microstructural analyses suggest that the elimination of nano-porosity together with the physical breakdown of a continuous nitrogen layer at GBs during cold rolling are responsible for the observed ductility enhancement, and in the case of the latter phenomena, also a corresponding decrease in strength.

3:55 PM

The Effects of Ti Addition on the Microstructural and Physical Properties of Cu-SiC Composite Powders: *Ceren Dutdibi*¹; Hasan Gokce¹; A. Umut Soyler¹; M. Lutfi Ovecoglu¹; Burak Ozkal¹; ¹ITU

In this study, the effects of Ti addition on the microstructural properties and hardness values of the mechanically alloyed Cu-SiC based metal matrix composites were investigated. The Cu-SiC vol. % 20 matrix composites reinforced with different amounts of Ti such as 1, 2, 3, 5 vol. % were fabricated via mechanically alloying using a Spex Mixer/mill at room temperature. Powders were mechanically alloyed for 4 h using stainless steel milling media which closed under purified Argon atmosphere. Mechanically alloyed powders were characterized by using X-Ray diffractometer, Scanning Electron Microscope, Optical Microscope and Laser Particle Size Analyser. Moreover, micro-hardness measurements performed on the mechanical alloyed powders.

4:15 PM

The Effect of Ball-to-Powder Weight Ratio on the Synthesis of Aluminum Diboride: *Hasan Gökçe*¹; Duygu Agaogullari¹; Ismail Duman¹; M. Lütfi Öveçoglu¹; ¹Istanbul Technical University

In this study, AlB_2 powders were synthesized by using a combined method of mechanical alloying (MA) and annealing of elemental aluminum (Al) and boron (B) powders mixed in stoichiometric amounts. Mechanical alloying was performed up to 15 h under Ar atmosphere in a vibratory ball-mill (Fritsch Pulverisette 7 Premium Line) using hardened steel vial and balls. Subsequently, milled powders were annealed in a tube furnace under flowing Ar atmosphere at 650°C for 6 h. The effects of ball-to-powder weight ratios (BPR) on the synthesis of AlB_2 were examined in the experimental studies. Milled and annealed powders were characterized by using X-ray diffraction (XRD) technique, Scanning Electron Microscope (SEM) and Differential Thermal Analyzer (DTA).

4:35 PM

Investigation of Solid State Reaction Mechanism for Sodium Metaborate (NaBO2) Production: Aysel Kanturk Figen¹; Hatice Ergüven¹; Sabriye Piskin¹; ¹Yildiz Technical University

Sodium metaborate (NaBO2), is a compound derivative of borax, is used in the chemical industry as photographic and textile chemicals, detergents, cleansers, and adhesives. Literature on NaBO2 used as sources of boron in the production of the NaBH4 methods is available. Therefore, the use of anhydrous NaBO2 in the energy field and the importance of both commercial borates class are growing gradually. In this study, solid–state preparation of NaBO2 was investigated based on thermal analysis. Therefore, anhydrous borax (Na2B4O7) and sodium hydroxide (NaOH) were mixed at mole ratio of 1:2 and thermal analysis was performed at different heating rates. There were four endothermic peaks in the DTA plots, corresponding to four reactions that explain the solid state reaction stage as: diffusion stage, reaction stage, nucleation stage and growth stage.Keywords: Sodium metaborate; hydrogen; solid state; mechanism; thermal analysis

Properties, Processing, and Performance of Steels and Ni-Based Alloys for Advanced Steam Conditions: High Temperature Oxidation and Design for Resistance

Sponsored by: The Minerals, Metals and Materials Society, TMS Structural Materials Division, TMS/ASM: Corrosion and Environmental Effects Committee, TMS: High Temperature Alloys Committee

Program Organizers: Peter Tortorelli, Oak Ridge National Laboratory; Bruce Pint, Oak Ridge National Laboratory; Paul Jablonski, National Energy Technology Laboratory; Xingbo Liu, West Virginia University

Wednesday PM March 2, 2011 Room: 33B Location: San Diego Conv. Ctr

Session Chairs: Peter Tortorelli, Oak Ridge National Laboratory; Xingbo Liu, West Virginia University

2:00 PM

High Temperature Corrosion Resistance of Fe-Ni-Cr Alloys in CO2-H2O Atmospheres: Thomas Gheno¹; Jianqiang Zhang¹; *David Young*¹; ¹University of New South Wales

In the oxyfuel process, heat exchanger materials will be exposed to CO2/ H2O mixtures. The corrosion behaviour at 800oC of Fe-Ni-Cr alloys in these atmospheres has been investigated. Binary Fe-9Cr, Fe-20Cr and Fe-25Cr alloys, and ternary alloys containing 10 and 20 wt. % Ni were exposed to dry and wet Ar-CO2. Additions of Ni significantly slowed metal consumption rates for Fe-9Cr alloys, whereas the opposite effect was observed for high chromium alloys. Low chromium alloys formed iron-rich oxide scales, and underwent severe carburisation. Overall weight uptakes followed linear kinetics in dry CO2, but additions of H2O caused a transition to parabolic kinetics. In contrast, high chromium alloys formed a protective chromia layer in all atmospheres, although mild internal attack also took place. Resistance to corrosion was good, except for ternary alloys containing 10 wt.% Ni, which failed during long exposures. These observations are discussed in terms of reaction morphologies.

2:20 PM

Oxidation and Corrosion Resistance of Structural Alloys in Supercritical Water for Generation IV Reactor Systems: Peng Xu¹; Liang Zhao¹; Lizhen Tan¹; *Todd Allen*¹; ¹University of Wisconsin

The supercritical water reactor (SCWR) is considered to be one of the promising Generation IV nuclear reactor designs worldwide. The high outlet temperature (500-600C), high pressure (25 MPa), and a rather aggressive chemical environment in the SCWR require materials to be highly corrosion resistant. This paper reviews the oxidation and corrosion resistance of candidate alloy materials proposed for use in the SCWR environment, with a focus on grain boundary engineering. The talk will review how grain boundary engineering of the bulk metal dramatically changed the oxide formation in alloys 800H and 617. Additionally, recent work on grain boundary engineered Ni alloy 690 will be presented. Samples were tested at 500°C from 2 to 12 weeks. Selected samples were characterized using weight change, glance angle XRD, SEM, EDS, EBSD and TEM. The relationship between material chemistry, grain boundary character, and oxidation performance will be discussed.

2:40 PM

Steam Oxidation of Fe-20Cr-30Ni-2Nb Austenitic Steel at 973 K: *Toshio* Maruyama¹; Masakazu Yamashita¹; Mitsutoshi Ueda¹; Kenichi Kawamura¹; Masao Takeyama¹; ¹Tokyo Institute of Technology

Steam oxidation of Fe-20Cr-30Ni-2Nb austenitic steel which is a promising material for advanced power generation was examined at 973 K. Although oxidation in air provided a protective Cr2O3 scale, the duplex scale of magnetite and iron-chromium spinel was formed in steam oxidation. The microstructure of the steel which was varied by heat treatments of homogenization and aging affected the oxidation behavior.

3:00 PM

Austenitic Steel Oxidation in Steam: Alloy Composition and Surface Modification Solutions: *Bruce Pint*¹; ¹Oak Ridge National Laboratory

Oxidation in the presence of water vapor has become a major research topic in the past decade as material degradation has become a concern for current and future power generation systems. With or without free oxygen, the presence of water vapor has a dramatic effect on the oxidation behavior of both Fe- and Ni-base alloys. In current coal-fired systems, austenitic steel tubing can experience catastrophic scale spallation leading to blockages and tube failures. Potential solutions to this problem include (1) modifying initial service conditions to alter the spallation events, (2) using more expensive, higher-alloyed steels and (3) employing surface modifications such as coatings or shot peening. Current projects are evaluating the steam oxidation resistance of various commercial and model alloys as well as the durability of thin aluminide coatings on austentic steels. The viability of the potential solutions will be discussed.

3:20 PM

Moisture Effects on the Oxidation Behavior of Ni-Based Alloys: *Wei Zhao*¹; Brian Gleeson¹; ¹University of Pittsburgh

The effects of moisture on the 1000°C oxidation behavior of model Nibased alloys were studied using dry air and air + 30% water vapor ("wet air" in short) gas environments. It was found that the critical concentration of Al (N_{Al}^{*}) to form a continuous alumina scale on Ni-Al-Cr alloys increases when the environment is wet air. Further study also showed that the growth rate of NiO is enhanced, which was inferred to contribute to the NAl* increase. This enhanced NiO growth rate was the result of an increased amount of oxidation within the metal consumption zone. Internal oxidation experiments revealed that the increase in N_{Al}^{*} for wet air conditions could not be attributed to enhanced oxygen permeability. The presence of water vapor could also lead to instability of the NiO scale surface, which was found to be related to preferred oxide growth along certain crystallographic directions.

3:40 PM Break

4:00 PM

Oxidation Behavior of Alumina-Forming Austenitic Steel in Steam: Kinga Unocic¹; Michael Brady¹; Yukinori Yamamoto¹; Bruce Pint¹; ¹ORNL

Alumina-forming austenitic (AFA) stainless steels exhibit a unique combination of high temperature creep strength and corrosion resistance. By forming a protective alumina scale, AFA steels exhibit significantly better corrosion resistance than conventional, chromia-forming stainless steels and even Ni-base alloys. This improvement in oxidation resistance is a significant benefit for advanced steam applications where materials are often limited by their oxidation resistance rather than their creep resistance. Steam exposures have been conducted at several temperatures from 550\176-800\176C and the rate of oxidation is compared to conventional candidate alloys as well as model alumina-forming alloys. In addition, the reaction product on AFA steel has been characterized using a range of low- to high-resolution techniques. Research sponsored by the U. S. Department of Energy, Office of Energy Efficiency and Renewable Energy, Industrial Technologies Program.

4:20 PM

Hydrogen Ingress in Stainless Steels during High-Temperature Oxidation in Water Vapor: James Keiser¹; ¹Oak Ridge National Laboratory

High-temperature environments containing water vapor are encountered in energy production systems. Accelerated oxidation by water vapor is a limiting factor for stainless steels in these applications. It is well established that hydrogen derived from water vapor can penetrate oxidizing alloys. The complexities of tracking hydrogen species have hampered direct profiling and correlation of hydrogen ingress with the oxidized microstructure. Tracer studies were performed using SIMS in combination with XPS and TEM. Materials studied include Fe-20Cr, type 347 SS, and developmental alumina-forming austenitic SS which were exposed 24 h at 800°C in air + 10% D2O. The resultant D profiles were found to vary markedly among the alloys examined. Details of oxidized alloy microstructures and correlation of findings with alloy chemistry will be discussed. Research sponsored by the Laboratory Directed Research and Development Program of Oak Ridge National Laboratory, managed by UT-Battelle, LLC, for the U. S. Department of Energy.

4:40 PM

Steam Oxidation of New PVD Nano-Structured and Microstructured Coatings on P92 Steels: *Francisco Pérez Trujillo*¹; Maria Hierro¹; Maria Mato¹; Juan Sanchez¹; Marta Brizuela¹; ¹Universidad Complutense de Madrid

The steels with chromium contents between 9 and 12% wt are used for power plants with advanced steam oxidation conditions. In the last years numerous investigation in development of coatings has been realized with the aim the protected them against the oxidation in order to allow operation of steam turbines at 650°C. In this study, nano-structured coatings based in Cr-Al forming oxides were developed by PVD and deposited on P92 steel, have shown to be protective at 650°C under steam exposure under atmospheric pressure, comparing with the previously data reported in the literature on micro-structured coatings based in Fe-Al design. Experiment for 2.000 h exposure time shown a very promising application of nanostructured coatings for steam environments. Those coatings have similar corrosion rates than mico-structured, avoiding problems of inter-diffusion. Morphology and composition of coatings were characterized by different techniques, such as scanning electron microscopy will be shown.

5:00 PM

Characterization of Amorphous/Nanocrystalline Steel Coatings Developed by Different Thermal Spray Processes: *Vikram Varadaraajan*¹; Ramesh Kumar Guduru¹; Pravansu Mohanty¹; ¹Univ of Michigan

Amorphous/nanocrystalline coatings are very useful for wear and corrosion protection applications. Here, we report structure – property correlation of amorphous/nanocrystlline high performance steel coatings



developed by plasma, high velocity oxy fuel (HVOF), arc as well as a new hybrid spray process. The hybrid spray process combines the arc and HVOF techniques. Microstructural, mechanical, corrosion and tribological characterization of the coatings was done and compared. The mechanical testing data from shear punch and impact tests indicated that the amorphous coatings obtained via plasma and HVOF techniques had lower strength compared to the nanocrystalline hybrid and arc spray coatings. Corrosion properties revealed an influence of chemical composition of the coatings on the measured impedance and corrosion behavior. Tribology data showed similarities between the HVOF, plasma and hybrid coatings although the microstructure of hybrid coating was noticeably different from the other two. Arc coating showed higher coefficient of friction and weight loss.

Recycling General Session: Metals

Sponsored by: The Minerals, Metals and Materials Society, TMS Extraction and Processing Division, TMS Light Metals Division, TMS: Recycling and Environmental Technologies Committee *Program Organizer:* Joseph Pomykala, Argonne National Laboratory

Wednesday PM	Room: 12
March 2, 2011	Location: San Diego Conv. Ctr

Session Chair: Joseph Pomykala, Argonne National Laboratory

2:00 PM Introductory Comments

2:05 PM Keynote

2011 Vittorio de Nora Award Winner: Recycling of Contaminated Aluminium Scrap: Anne Kvithyld¹; ¹SINTEF

Recycling is important in the aluminum industry. Removal of contaminants such as the coat and organic materials- applied for protection and appearanceare the tail that wags the recycling dog. Successful removal of contaminants from scrap would ensure that more aluminum be recycled, minimize losses and prevent downgrading of the resource. Performing decoating in a closed system, efficient cleaning of the evolved gases and reuse of the energy is possible. Motivation for removal of contaminants on aluminium scrap will be presented. A sum up of fundamental studies will be given. De-coating may be described as two distinct regimes: Scission and Combustion, regardless of metal substrate and coating. This is studied by methods: (i) mass and enthalpy change together with the off-gas composition recorded simultaneously and (ii) hot stage microscope to give a visual record of the surface. In conclusion a more fundamental understanding of the decoating process should enable the metallurgical industry to process post consumer aluminium scrap in a more efficient and sustainable manner.

2:25 PM

Recycling and Material Price: An Exploration of the Effects of Secondary Substitutability on Price Stability: *Nathan Fleming*¹; Randolph Kirchain¹; Elisa Alonso¹; Richard Roth¹; Frank Field¹; ¹Massachusetts Institute of Technology

High material prices and price uncertainty can be harmful to manufacturing firms. Increased use of recycled materials, industry-wide, can lower both material prices and price variability; moreover, increased recycling decreases the use of primary material, which mitigates price increases due to scarcity effects. These stabilizing and price lowering effects are explored using an Aluminum industry model. We show that (a) increased recycling leads to smaller price fluctuations in the presence of a primary metal supply perturbation, and (b) that the more substitutable the secondary metal is for the primary metal, the lower the overall material price is.

2:45 PM

Increased Recycled Aluminum Content during Remelting by Incorporating Compositional Uncertainty: *Tracey Brommer*¹; Elsa Olivetti¹; Britt Elin Gihleengen²; Geir Øyen²; Hans Ole Riddervold²; Randolph Kirchain¹; ¹Massachusetts Institute of Technology; ²Norsk Hydro

Although significant environmental and economic gains result from remelting secondary materials during aluminum alloy production, high concentrations of alloying elements and compositional uncertainty limit their incorporation. Incorporation of secondary materials increases the likelihood a batch will not satisfy the compositional specifications of its intended final product. Such "batch errors" are inefficient and expensive prompting remelters to cautiously incorporate secondary materials, resulting in scrap underutilization and higher cost products. Remelters adopt deterministic batch planning algorithms to inform production portfolios, complementing manual batch planning by plant managers. Uncertainty-aware batch planning algorithms are an alternative to deterministic; potentially allowing remelters to simultaneously increase secondary material utilization and decrease batch errors by incorporating the compositional uncertainty of individual secondary materials into the optimization algorithm. This investigation characterizes the conditions under which uncertainty-aware batch planning algorithms outperform the deterministic and manual equivalents for a variety of remelting conditions in the context of interlinked production portfolios.

3:05 PM

On In-Process Separation of Zinc from EAF Dust: *Naiyang Ma*¹; ¹ArcelorMittal

EAF dust is categorized as a hazardous solid waste. EPA approves only two treatment methods: either sending the dust to zinc recycling facility, or stabilizing it first and then disposing it to a specially-lined landfill. Both treatment methods are costly to EAF steelmakers. In order to reduce the cost and even better to make profit from the dust, EAF steelmakers need to find a cost-effective technology to separate zinc from EAF dust. This paper is dedicated to discussion of a novel recycling strategy: in-process separation of zinc from EAF dust. The concept of in-process separation of zinc from EAF dust is first defined, and then a simple Zn concentration model is developed. From this model, two approaches of in-process separation of zinc from EAF dust are derived: (1) prematurely capturing dust at very high temperature when zinc is still in vapor status, (2) prematurely collecting dust immediately after quickly cooling EAF off-gas from high temperature to low temperature. Next, thermodynamic analysis is conducted to understand zinc behavior in EAF off-gas. It is demonstrated in theory that zinc is in vapor status while it exits from electric arc furnaces. At last, recycling routes and economics of in-process separation of zinc from EAF dust are discussed.

3:25 PM

The Removal of Nickel from Leachate of Galvanic Sludge with Titanium Dioxide: *Muge Sari Yilmaz*¹; Sibel Kasap¹; Ozgul Dere Ozdemir¹; Sabriye Piskin¹; ¹Yildiz Technical University

Galvanic sludge is generated at the end of the waste water treatment process of metal plating system. The waste sludge is one of the main hazardous solid wastes produced by metallurgical industries. It is caused the harm of human health and damage of the environment due to containing reasonable amounts of toxic metals (e.g., nickel, zinc, copper, chromium, iron, lead, cadmium, etc). The concentration of those toxic metals in the wastewater might reach 30% (w/w, dry weight) making their removal and recovery an interesting issue. In this study, synthesized titanium dioxide is used as adsorbent to remove nickel in leachate of galvanic sludge. The adsorption experiments were carried out isothermally at four different temperatures. The effects of pH, temperature, and contact time on nickel adsorption efficiency were investigated, and the optimum parameters were determined from the experimental studies. The experimental results indicated that pH, temperature, and contact time played a significant role on the adsorption capacity of nickel.

3:45 PM Break

3:55 PM

Recycling of High Quality Steel Scraps Directly in Electroslag Remelting Process (ESR): Burak Birol¹; Muhlis Saridede¹; ¹Yildiz Technical University

The scraps of high quality steels generally contain expensive alloying elements such as chromium, vanadium, nickel, etc. These scraps are melted in an induction or an electric arc furnace and refined in ESR (Electroslag Remelting) purification process. A significant amount of alloying elements are lost during these processes. In order to avoid these losses, scraps can be utilized directly in ESR by skipping the melting step. In this study, 316L stainless steel scraps were refined in ESR with selected synthetic slags. The products were analyzed by optic emission spectrometry and the effects of slag compositions on the alloying element losses were examined. According to the analysis of the scrap and the products, generally chromium, nickel and manganese losses were encountered. It was determined that the alloying element losses has no connection with electrical conductivity. The slag containing CaF2, Al2O3, and FeO gives the optimum Cr and Ni losses.

4:15 PM

Recycling of Wastes Generated during the Steelmaking Process: Victor Telles¹; Joner Alves¹; Denise Espinosa¹; Jorge Tenório¹; ¹University of Sao Paulo - USP

The world production of crude steel in 2009 reached 1.2 billion tons. For each ton of steel produced, 150 kg of steelmaking slag and 20 kg of steelmaking dust are generated. These are wastes with considerable production and limited applications, therefore this work studied the recovery of these wastes into useful sub-products. The slag was used as raw material in the production of mineral wools (a thermo-acoustic insulator) and the dust was inserted in the iron ore sintering process. Results showed that produced materials have exceptional proprieties, therefore the recovery of these wastes can contribute to decrease extraction of non-renewable resources, reduce the costs and impact of disposals, and aggregate value to the slag and dust.

4:35 PM

Differential Removal of Copper and Iron from Acidic Polymetallic Aqueous Solutions: *Jinhui Li*¹; Youjun Xiao¹; Daoling Xiong¹; Ruixiang Wang¹; Hao Chen¹; ¹Jiangxi University of Science and Technology

Leaching solution prepared from spent battery materials contains large quantities of valuable metals, such as Cu, Ni, Co, Mn and Fe. Therefore, recovery of valuable metals from acidic polymetallic aqueous solutions is of great importance for every plant. In this work, a method is introduced of recovery of Ni, Co and Mn from polymetallic solution prepared by leaching spent battery material. The basic concept includes copper was removed through replacement by iron powder followed by iron precipitation in goethite method. The experimental results show that Cu can be removed 99% at least through replacement by Fe powder, and the removal of Fe can achieve 99% by goethite method. At the same time, the loss of Ni, Co and Mn are about 2%, 3% and 2%, respectively. The purified solution which only contains Ni, Co and Mn can be used to prepare NixCoyMnz ternary system precursor.

4:55 PM

High Purity Alumina Powders Extracted from Aluminum Dross by the Calcining—Leaching Process: *Liu Qingsheng*¹; ¹Jiangxi University of Science and Technology

A new calcining-leaching process was used to extract high purity alumina (A1203) powders from aluminum dross in this study. The aluminum dross was mixed with soda (Na2CO3) and calcined at 900°C to yield soluble aluminates. Subsequently the calcined dross was leached with sulfuric acid (H2SO4) to produce a solution containing aluminum. The unwanted metal ions including Fe3+and Na+ were removed by ethylene diamine tetraacetic acid (EDTA) and water washing. Then added the proper dispersant, controlling the crystallization of aluminum trihydroxide precipitation and the drying and calcining process was carried out resulting in ultra fine Al2O3 powders with high purity. The characteristics of the Al2O3 powders were examined by means of XRD, TEM and Brunauer-Emmet-Teller (BET) surface analysis

method. The extraction efficiency of Al2O3 can surpass 98% by optimization of the calcination and lixiviation processes. Well-dispersed fibriform Al2O3 powders were obtained by calcining at 800°C and the purity of the ultra fine Al2O3 powders was more than 99.6%.

5:15 PM

Research on Effect of Recombination Action of Rare Earth Metals La,Ce and Y on Soil Enzymatic Activities: *Nie Jinxia*¹; Chen Yunnen¹; ¹Jiangxi University of Science and Technology

Rare earth resources are strategic and non-renewable resources. But disordered exploitation on rare earth metals leads to resources waste, environmental pollution and ecosystem destroyed. In this paper, soil collected from garden was cultured in thermostated incubator. Adding exogenous rare earth to the soil and the effects of recombination action of rare earth lanthanum, cerium and yttrium on soil enzymatic activities were sstudied. The results showed that single metal La and Ce can increase urease activity, but Y inhibits its. Coexist La/Y or La/Ce in soil inhibit the urease activity, coexist Y/Ce or coexist three metals promote its. Single metal La, Y and Ce can promote catalase activity, and that of coexist three metals. Pairwise coexist La, Y, Ce in soil inhibit catalase activity. With certain concentration of rare earth recombination action, urease activity in soil has been very significant direct proportion to ionic impulse, but catalase activity been insignificant inverse proportion to its.

Refractory Metals 2011: Refractory Metal-Based Composites I

Sponsored by: The Minerals, Metals and Materials Society, TMS Structural Materials Division, TMS: Refractory Metals Committee *Program Organizers:* Omer Dogan, DOE National Energy Technology Laboratory; Jim Ciulik, University of Texas, Austin

Wednesday PM	Room: 19
March 2, 2011	Location: San Diego Conv. Ctr

Session Chairs: James Ciulik, University of Texas at Austin; Michael Gao, URS at National Energy Technology Laboratory

2:00 PM Invited

Optimization of Mo-Ni-Al-X Alloys for High Temperature Oxidation: *Matthew Kramer*¹; Pratik Ray¹; Travis Brammer¹; Kevin Severs¹; Mufit Akine¹; ¹Iowa State University

Using a series of computational methodologies ranging from semiempirical methodologies to more accurate ab initio methods we have identified the Mo-Ni-Al system as a potential base alloy for high temperature applications. Of the a refractory metals, Mo appears to be the best candidate for combining a "skeleton" of a creep resistant metal with a high temperature intermetallic as a source of the oxidatively stable elements. Initial oxidation tests at 1150°C and above, while promising, shows that additional Platinum group metals, designated as X, are required to boost oxidation stability above 1300°C. Key to maintaining fracture toughness, creep strength and a prime-reliant oxidation protection will be synthesis methods to assemble the refractory metal and the oxidatively protective phases at the appropriate length scales. We are adopting a computational approach to optimize the Mo grain size and distribution in order to maximize the Mo fraction in the alloy without compromising oxidation stability.

2:20 PM Invited

Effect of Zr Micro-Alloying Additions on Microstructure and Mechanical Properties of Mo-Si(-B) Alloys: Martin Heilmaier¹; *Manja Krüger*²; Nelia Wanderka³; ¹Technische Universität Darmstadt; ²University of Magdeburg; ³Helmholtz Zentrum Berlin für Materialien und Energie GmbH

We review our current understanding of the effect of Zr-microalloying on the deformation behavior of mechanically alloyed Mo-Si(-B) alloys: addition of 0.5 and 1 at% Zr to Mo-Si solid solutions leads to both, an increase in bend strength and plastic deformability. Auger analyses yielded a change



in fracture mode from intercrystalline to transgranular failure indicating Si segregation to cause grain boundary embrittlement. Complementing atom probe tomography and transmission electron microscopy investigations, however, reveal the formation of nano-scale Mo₂Zr intermetallics decorating the grain boundaries was observed in ternary Mo-Si-Zr alloys, thereby suppressing the Mo₃Si₃ and Mo₃Si intermetallics found at grain boundaries in binary Mo-Si solid solutions. It is concluded that this phenomenon may be responsible for the observed decrease of the brittle-to-ductile transition temperature by Zr-addition in Mo-Si solid solutions as well as in complex 3-phase Mo-Si-B alloys.

2:40 PM

Fracture Behavior of Mo-Si-B Alloys at Elevated Temperatures in Air and Inert Atmospheres: *Joseph Lemberg*¹; Michael Middlemas²; Joseph Cochran²; Robert Ritchie¹; ¹University of California Berkeley; ²Georgia Institute of Technology

Refractory metal silicides, such as Mo-Si-B, have been proposed as possible successors to current nickel superalloys. These alloys have the potential to operate in temperatures greater than 1300°C. Two alloys (Mo-3Si-1B wt%) processed in vastly differing manners, but with similar "duplex" microstructures, are studied. A "duplex" microstructure couples the oxidation resistance of the intermetallic $Mo_5Si_3 \& Mo_5SiB_2$ (T2) phases with the fracture resistance of the ductile \945-Mo phase. Within the framework of fracture resistance, the effect of processing route is examined. In inert atmospheres at 1300°C both alloys exhibited initiation toughnesses more than four times higher than at room-temperature, though the reaction-synthesized material described by Middlemas and Cochran (JOM, 2008) is much more ductile above 1100°C. The influence of an oxidizing environment on the fracture resistance of these alloys, a relatively unexplored consideration, is also analyzed. The present results are compared to previously-reported behavior exhibited by much-coarser grained materials.

3:00 PM

Effect of Alloying on Phase Stability and Deformation Behavior of Mo-Si-B System: Oleg Kontsevoi¹; Arthur Freeman¹; ¹Northwestern University

Mo-base alloys are promising materials for ultra-high temperature applications (>1400 °C), while one of the main drawbacks is poor ductility. By means of density-functional theory calculations we investigated the effect of alloying with 3*d*, 4*d* and 5*d* metals on phase stability and deformation behavior of 3-phase system $T_1(Mo_sSi_3) - T_2(Mo_sSiB_2) - A15(Mo_3Si)$. We determine site preference, phase partitioning of alloying elements, and their effect on shear behavior and preferred deformation modes. We show that alloying with early 3*d* transition metals results in softening, while most 4*d* and 5*d* elements lead to hardening. The results are discussed in conjunction with possible pathways to ductility enhancement through alloying.

3:20 PM Break

3:40 PM

Molybdenum - Silicate Multiphase Composites: Mechanical Considerations: *Peter Marshall*¹; Joe Cochran¹; Will Daloz¹; ¹Georgia Institute of Technology

Multiphase, molybdenum based materials have received considerable attention for structural applications above 1150°C in oxidizing environments. In the MoSiB system a protective scale is accomplished by oxidation of molybdenum-silicides. However these composites suffer from poor fracture toughness at ambient temperatures due to the segregation of dissolved silicon to molybdenum grain boundaries and dislocations. In a novel approach presented here, the coating develops from a silicate glass phase present a priori in the composite. By avoiding a solid solution of silicon, the molybdenum matrix maintains ductility at room temperature. The glass is introduced through powder processing techniques as a fine, thermodynamically stable phase; taking care to minimize additional oxygen content. Additionally, powder processing allows for the introduction of other components to improve the high and low temperature mechanical properties. These include titanium and zirconium, commonly used in molybdenum alloys, as well as mullite, a refractory ceramic capable of pinning grain boundaries.

4:00 PM

Molybdenum-Silicate Multiphase Composites: Oxidation Concerns: William Daloz¹; Joe Cochran¹; Peter Marshall¹; ¹Georgia Institute of Technology

A new powder processing approach to produce oxidation resistant molybdenum alloys for high temperature is under development. Oxidation protection is provided by fine dispersion of silica glass particles within a molybdenum matrix. As the molybdenum oxidizes, the glass is exposed and melts to form a self-healing protective oxide coating. A third phase of homogeneously dispersed Mo2B provides boria which reduces glass viscosity so that the coating can be formed more rapidly at lower temperatures. Internal Mo2B also provides internal oxidation resistance. This is similar to the oxidation protection used in Mo-3Si-1B (wt%) systems; however embedding the glass directly into the Mo matrix and eliminating the Mo3Si (A15) provides the same volume of glass at lower volume fractions of brittle phases. Additionally the glass composition can be tailored for different applications and different temperatures beyond that achievable in Mo-Si-B based systems. A variety of microstructures for improved oxidation protection are explored.

4:20 PM

Microstructures and Oxidation Behavior of W Substituted Mo-Si-B Alloys: Pratik Ray¹; Mufit Akinc¹; Matthew Kramer¹; ¹Iowa State University

The drive for increased Carnot efficiencies requires the development of alloys that can withstand harsh environments. Mo-Si based alloys, with a multitude of high melting intermetallics, have attracted considerable attention as candidates for ultra-high temperature applications. Boron doped Mo5Si3 has been shown to have excellent oxidation resistance at high temperatures. The mechanical behavior of Mo5Si3 intermetallics is relatively poor. Hence, a microstructure containing Mo5Si3 along with Mo metal is thought to be more advantageous from the viewpoint of mechanical properties. Due to the nature of the Mo-Si-B phase diagram, co-existence of Mo, Mo5Si3 and Mo5SiB2 will require destabilization of Mo3Si, an intermetallic that has very low fracture toughness and poor oxidation resistance. Keeping this in mind, a combination of experimentation and computational techniques were used to determine optimal solute additions for destabilizing Mo3Si. The alloys thus designed were then tested for high temperature oxidative stability.

4:40 PM

Oxidation Performance of Mo-Si-B Alloys: Implications through Alloying and Pre-Treatment: *Steffen Burk*¹; Bronislava Gorr¹; Hans-Jürgen Christ¹; ¹Universität Siegen

Mo-Si-B alloys melt around 2000°C and exhibit good mechanical properties and oxidation resistance at very high temperatures. Mo-9Si-8B-X alloys show excellent oxidation behaviour between 900°C-1300°C as a consequence of a protective silica scale. Below 900°C, volatile Mo-oxide formation leads to catastrophic oxidation. A protective oxide layer is not formed as a consequence of simultaneous and competitive Mo- and Si-oxide formation. Implications through alloying additions as well as pre-treatment prior to oxidation in air were examined. Classical alloying with Cr is a suitable means for protective Cr-oxide scale formation at intermediate temperatures, whereas additions of small amounts of reactive elements was found to have a strong impact on the silica scale forming abilities. Furthermore, the oxidation behaviour can be controlled by selective oxidation of silica in oxygen-deficient atmospheres prior to operation in air. Sufficient oxidation protection for Mo-Si-B alloys from room temperature up to 1300°C requires a combination of these approaches.

5:00 PM

The Systematic Control of Polyhedral Mo Powder Formation with Different Particle Sizes: Xian Qin Wang¹; Fei Zhuang¹; Yuan Jun Sun¹; Jun Huai Liu¹; Jing Li¹; Hu Zhao¹; ¹Jin Dui Cheng (JDC) Molybdenum Group Co. Ltd.

The icositetrahedron molybdenum powder showed great advantage in high performance of molybdenum materials with the ultra-low oxygen

content, regular crystalline boundary and good flowability etc. Investigation indicated polyhedral Mo powder with different size should have unique property in alloying and catalyst application. The MoO3 decomposed from crystalline ADM was empolyed as start material. H2 dewpoint, flowrate and temperature profile, residence time combinatorially performed to achieve microstructure with different sub-particle size during MoO3-MoO2 reaction stage. In MoO2-Mo reaction stage, the MoO2 sub-particle size always could be inherited . However there was flexibility for large MoO2 sub-particles which could be seperated into samll Mo particles under the condition of slow reaction rate caused by low H2 flowrate , suitable H2O partial pressure and temperature with feeding rate. The growth regime of polyhedral Mo was discussed by bonding the experiment results with related theory to make the production progammed in future.

Sensors, Sampling, and Simulation for Process Control: Liquid Metal Sensing and Online Measurement

Sponsored by: The Minerals, Metals and Materials Society, TMS Extraction and Processing Division, TMS: Process Technology and Modeling Committee, TMS: Solidification Committee *Program Organizers:* Brian Thomas, University of Illinois at Urbana-Champaign; Andrew Campbell, WorleyParsons; Srinath Viswanathan, University of Alabama; Lifeng Zhang, Missouri University of Science and Technology; James Yurko, 22Ti LLC; Thomas Battle, Midrex Technologies

Wednesday PM	Room: 13
March 2, 2011	Location: San Diego Conv. Ctr

Session Chairs: Brian Thomas, University of Illinois at Urbana-Champaign; Lifeng Zhang, Missouri University

2:00 PM Introductory Comments

2:10 PM Keynote

In-Situ Sensors for Liquid Metal Quality: Roderick Guthrie¹; Mihaiela Isac¹; ¹McGill Metals Processing Centre

The development of effective methods for directly measuring liquid metal quality, prior to casting and final solidification, has been a goal for Process Metallurgists. Most techniques now in use either freeze a sample of the metal, or first concentrate the inclusions through filtering the metal through a porous frit, before then freezing the metal, and subjecting it to microscopic examination (e.g. PoDFA). The alternative method is to take a sample of metal, freeze it, and then dissolve the metal to release the particles (inclusions) through elutriation (The Slime Technique). The only true online, in-situ, methods are the Ultrasonic Liquid Metal Sensors (Mansfield Molten Metal Sensor), and the Electric Sensing Zone Approach (LiMCA and ESZ-pas). A brief history of the developments in these two approaches will be presented, and their long term prospects will be assessed versus other techniques.

2:40 PM Keynote

Sensors for On-Line Monitoring of Molten Metal Quality: Jeffrey Fergus¹; ¹Auburn University

The dissolution of gases in molten metals can lead to porosity and/or formation of inclusions in the resulting product. Real-time control of the process to minimize these defects requires information on the quality of the melt during processing. Electrochemical-based techniques can provide information on the chemical properties of the melt, while electromagneticor acoustic-based techniques are used for physical properties, such as the presence of inclusions. The aggressive environments in molten metals create challenges in the development of reliable sensors. In particular, materials that are stable and provide the needed transduction properties at these hightemperature reactive conditions must be identified or developed. In this paper, techniques for measuring dissolved gas and inclusion contents in molten metals are reviewed.

3:10 PM

Development of an Aqueous Particle Sensor (APSIII) System as a Research Tool for Studying the Behavior of Inclusions in Water Models of Tundish Operations: Mihaiela Isac¹; *Abhishek Chakraborty*¹; Luis Calzado¹; Roderick Guthrie¹; ¹McGill Metals Processing Centre

The control of liquid metal cleanliness during refining operations is an effective procedure used to improve the material properties of the final product. Low temperature simulation studies of inclusion behavior in steelmaking tundish operations have recently been carried out to develop techniques to float out as many inclusions as possible, prior to casting. The inclusions are simulated by glass microspheres submerged in water, and their behavior was studied with a new Aqueous Particle Sensor (APS III) recently constructed using digital based micro-computing technology. The working principle of the APS is identical to the well known Liquid Metal Cleanliness Analyzer (LiMCA) used worldwide for the detection of inclusion in molten aluminum. Both are based on the Resistive Pulse, or Electric Sensing Zone (ESZ) approach. The present "water LiMCA" has a wide particle size measurement capability, ranging between 25 to 170 microns, gathering online or off-line data with high accuracy.

3:35 PM Break

3:55 PM

Lorentz Force Velocimetry – A Contactless Technique for Flow Measurement in High-Temperature Melts: Andre Thess¹; Yurii Kolesnikov²; Christian Karcher¹; Rico Klein²; ¹Ilmenau University of Technology; ²Ilmenau University of Technology

We describe a non-contact technique for velocity measurement in electrically conducting fluids. The technique, which we term Lorentz force velocimetry (LFV), is based on exposing the fluid to a magnetic field and measuring the force acting upon the magnetic-field-generating system. We illustrate the physical principles of LFV and report results of comprehensive laboratory experiments which characterise the sensitivity of LFV. We then present results of an industrial test of the technique in the aluminium industry which demonstrates that LFV performs well under harsh industrial conditions. We finally outline some future developments and argue that LFV, if properly designed, has a wide range of potential metallurgical applications.

4:20 PM

The Development of a Sensor to Determine the Direction of Velocity in Liquid Aluminum: *Mitren Sukhram*¹; Stavros Argyropoulos¹; ¹University of Toronto

This paper shows that the temperature distribution within a cylindrical rod, while inserted into flowing liquid aluminum (Al), produces different heating profiles regarding the direction of flow. One can deduce the direction of velocity in the metal by understanding the heating pattern of the cylinder. Specifically, by being able to track the temperature as a function of spatial and temporal coordinates within the cylindrical rod, one can infer the direction of velocity. Experimental research work involving liquid Al has been conducted using this sensor in the Revolving Liquid Metal Tank (RLMT) at the University of Toronto. The RLMT is capable of melting approximately 50 kg of Al and imposing specified tangential velocities up to 0.35 m/s. It will be shown that our cylindrical rod sensor records different heating patterns under different fluid flow conditions. This temperature information is then used to infer the direction of velocity in the bath.

4:45 PM

New Sensors for the Velocity Measurement in Liquid Metal Processes: *Klaus Timmel*¹; Sven Eckert¹; Thomas Wondrak¹; Frank Stefani¹; Gunter Gerbeth¹; ¹Forschungszentrum Dresden-Rossendorf

In many technological processes involving liquid metals or semiconductor melts the velocity fields cannot be measured due to the lack of commercial measuring techniques for opaque melts. We present two measuring techniques which have proven recently as providing reliable velocity measurements in liquid metals, at least in the temperature range up to about 700°C: the ultrasonic Doppler Velocimetry (UDV) and the contactless inductive flow tomography (CIFT). UDV is capable of delivering velocity profiles along the



ultrasonic beam with a time-resolution of about 20 Hz. CIFT is based on the flow-induced modification of some externally applied magnetic field, which is measured by some array of magnetic field sensors outside of the melt. We present measurements with both techniques at the small-scale liquid metal model Mini-LIMMCAST of the continuous steel casting process. Both measuring methods give consistent results for the jets evolving from the nozzle outlets.

5:10 PM

Measurement of Molten Steel Surface Velocity with SVC and Nail Dipping during Continuous Casting Process: Joydeep Sengupta¹; Rui Liu²; Don Crosbie¹; S. Chung¹; M. Trinh¹; Brian Thomas²; ¹ArcelorMittal Dofasco; ²University of Illinois at Urbana Champaign

Surface velocity of the molten steel is critical to final product quality during continuous casting of steel. Plant experiments using two different new sensors, Sub-meniscus Velocity Control (SVC) devices and nail boards, are performed to evaluate their performance, and to quantify liquid steel velocities at locations 50 mm apart on the surface of ArcelorMittal Dofasco's No. 1 continuous caster under different casting conditions, including different throughputs, mold widths, Submerged Entry Nozzle (SEN) depths and SEN designs. A relation between the height difference of the solidified lump on the nail and surface velocity is confirmed and extended. Reasonable agreement between the two sensing methods of surface velocity is obtained, both in trends and magnitudes for both time-averaged velocity and transient flows. Correlations between surface velocity and throughput are developed using computational fluid dynamics (CFD) models and the performances for different casting conditions are compared and evaluated based on the velocity measurements.

5:35 PM

Measurement of Transient Meniscus Flow in Steel Continuous Casters and Effect of Electromagnetic Braking: Seong-Mook Cho1; Hyoung-Jun Lee1; Seon-Hyo Kim1; Rajneesh Chaudhary2; Brian Thomas2; Duck-Hee Lee3; Yong-Jin Kim3; Woong-Ryul Choi4; Sung-Kwang Kim4; Hui-Soo Kim4; 1Pohang University of Science and Technology; 2University of Illinois at Urbana Champaign; 3POSCO Gwangyang Steel Works; 4POSCO Gwangyang Works

Unstable meniscus flow leads to slab surface defects during continuous casting of steel, due to level fluctuations and vortex formation, which causes entrapment of argon bubbles and mold flux. Applying electromagnetic fields across the liquid steel pool, such as the "ruler" or "FC-mold" braking system, has been commercialized to stabilize meniscus flow. Plant measurements were performed using nail boards to quantify meniscus flow in a typical steel slab-casting mold with a slide gate system. Meniscus level shape, surface velocity, the direction of meniscus flow, and the variations of all of these parameters with time and location are all quantified by analyzing the shape of the skull of solidified steel that encases each dipped nail. The results reveal interesting time-variations in the flow pattern, which cannot and should not be detected with a standard mold-level sensor used for flow control. Finally, the effect of applying the electromagnetic field on the flow pattern is revealed.

Shape Casting IV: Light Metals Division Symposium in Honor of Prof. John T. Berry: **Methods and Systems**

Sponsored by: The Minerals, Metals and Materials Society, TMS Light Metals Division, TMS: Aluminum Processing Committee, TMS: Solidification Committee

Program Organizers: Murat Tirvakioglu, University of North Florida; Paul Crepeau, General Motors Corporation; John Campbell, University of Birmingham

Wednesday PM Room: 15B March 2, 2011 Location: San Diego Conv. Ctr

Session Chairs: Alan Druschitz, Univ of Alabama; Derya Dispinar,

2:00 PM Introductory Comments

2:10 PM

SINTEF

The Effect of Reducing the Molecular Weight of the Foam Pattern in the Lost Foam Casting Process: Kiavash Siavashi¹; Clare Topping²; William Griffiths³; ¹University of Birmingham; ²Isotron; ³University of Birmingham

In lost foam casting there can be a reduction in casting quality if the liquid polymer byproducts from the foam pattern become entrapped in the liquid metal. However, these are absorbed by the permeable pattern coating, once degradation has sufficiently reduced their molecular weight. This suggests that beginning with a lower molecular weight pattern may give higher quality castings, because less reduction in molecular weight will be required before absorption of the liquid polymer byproduct into the pattern coating. The initial molecular weight of expanded polymethylmethacrylate-polystyrene copolymer foam patterns was reduced by γ -radiation. The properties of castings made with these irradiated foam patterns, such as porosity, fluidity length, tensile and fatigue properties, (in the case of aluminium castings), and carbon pick up, (ferrous castings), were compared with the properties of castings made from unirradiated foam, to show the advantages of using the former.

2:30 PM

Classical Nondestructive Testing Techniques Do Not Correlate with Strength as Does Process Compensated Resonant Testing: Robert Nath¹; Marvin Johnson²; Clifford Grupke²; Chuck Leonard³; ¹Magnaflux Quasar; ²Retired/Consultant; ³Diversified Machine, Inc.

Process Compensated Resonant Inspection (PCRT) outperforms classical nondestructive testing (NDT) on aluminum parts based not just upon the significantly better results obtained from testing millions of automotive parts in production operations with achieved near-zero failures, but also insight gained from destructive testing and analysis. Several different destructive testing efforts were performed. Applicable classical NDT and PCRT were used. The PCRT relies on defining as "acceptable" those parts that are structurally acceptable, as measured by metallurgical, destructive and other nondestructive testing. Castings tested and accepted with classic NDT indications often have structural weakness and are accepted because their major defects are often the result of damaging thermal history or invisible oxide bifilms. Conversely, structurally acceptable castings are often rejected for negative classic NDT indications. Key previously assumed "facts" dealing with the parts and how they are accepted/rejected do not always stand up to more thorough destructive testing and analysis.

2:50 PM

Advanced Methoding Concepts for the Gravity Casting of Steel Alloys: Bob Puhakka1; 1Alloy Casting Industries

Wlodawer and Chvorinov provided invaluable early guidelines for the feeding of steel castings, but technology has moved on. This paper describes a new set of concepts that apply to the filling conditions for the entire family of steel casting alloys, from plain carbon to super duplex stainless steels. Application of the concepts is achieving new standards of quality together with reduced costs.

3:10 PM

Advanced Mold Design Technology of the LCS Waterjet (WJ) Entry Edge Casting Components Assisted by Flow, Solidification and Stress Modeling: Laurentiu Nastac1; John Romanelli1; 1Concurrent Technologies Corporation

In order to reduce cost, increase performance and ensure quality, this Navy Metalworking Center (NMC) project utilized an advanced casting simulation-based optimization approach to assist in the improvement of the mold design of LCS Waterjet (WJ) entry edge components. This approach helped to minimize mold filling and solidification related defects (misruns, coldshuts, shrinkage and porosity and hot tears), as well as post-solidification related defects (hot and cold cracks, distortion and residual stresses). The results of this optimization were used to more readily achieve first time quality on the geometrically challenging WJ components.

3:30 PM

Evaluation of the Distortion of a Hydro Turbine Blade during Heat Treatment Process: Jinwu Kang1; 1Tsinghua University

Hydro turbine blade castings are susceptible to distortion during heat treatment process for their thin and curved shapes. By the numerical simulation method, the distortion of the castings can be acquired. However, the distortion values depend on the selection of reference points which are selected only by experience. In this paper, a distortion evaluation method is presented, in which the normal direction change of local triangle areas with respect to the original shape is utilized. By this method, the distribution of distortion degree of the whole casting is obtained and the reference points are selected in the smallest distortion areas. Then, the dynamic distortion of the casting represented by the displacement values during heat treatment process is acquired. The distortion mainly concentrates on the two corners and the inner sides of root areas of the two corners are intensively cooled to avoid distortion. The simulated results show its validity.

3:50 PM Break

4.10 PM

The Capability Enhancement of Aluminium Casting Process by Application of the Novel CRIMSON Method: Xiaojun Dai¹; Mark Jolly¹; ¹University of Birmingham

The conventional foundry frequently uses the batch casting process where the aluminium alloys are melted and held in a furnace for a long time, sometimes as long as a complete shift. The long holding time increases the level of hydrogen absorption and the thickness of oxide films which are often the main reasons for casting defect generation. In this paper, a novel CRIMSON aluminium casting method is introduced which has a number of advantages. Instead of the batch casting method, it uses the single shot casting method to realize the rapid melting and rapid counter-gravity-filling mould operations, which reduce the contact time between the melt and environment, thus reducing the possibility of defect generation. Another advantage is the drastic reduction of energy consumption due to shortened melting and filling time. An actual case is used to compare the CRIMSON process and the conventional casting process.

4:30 PM

Optimization of the Process Parameters and Tooling Improvement for the Rheocasting of High Quality Aluminum Components Using the SEED Process: Chang-Qing Zheng¹; Ehab Samuel¹; Alain Simard¹; Florentin Laplume1; 1National Research Council Canada

The SEED (Swirled Enthalpy Equilibrium Device) rheocasting method, developed by Rio Tinto Alcan in collaboration with NRC Canada, was analyzed in an attempt to optimize parameters which affect the final casting quality. The SEED process has already proven successful in producing sound aluminum castings having an excellent combination of strength and ductility. However, in many of the existing semi-solid processes which make use of billets as feedstock, it is often found that the outer surface of the billets is contaminated. The use of such a contaminated billet can often result in an increased rejection rate of castings. To avoid the presence of a contaminated surface inside the casting, the paths along which the billet skin evolves must

be controlled during the filling stage. Simultaneously, there was an ongoing effort to enhance the mechanical properties of the aluminum alloys studied.

4:50 PM

Shaped Castings and Machining: John Wyatt¹; John Berry¹; ¹Mississippi State University

This paper will discuss three aspects of the machining of shaped castings: a) machinability, b) machining sequence, and c) residual stresses, the principal thrust being that of machinability. Currently, there is a growing movement to reconsider the whole process of machining from the standpoint of fracture mechanics. This has resulted from the groundbreaking work of Atkins at Reading University (UK), which is relevant to cast alloys and which, invariably, are multiphasic materials. Although secondary and tertiary phases have been blamed for tool wear, they are, in fact, intrinsically tied into the cutting process. The premise of Atkins is that ductile rupture takes place near the tool tip. These ductile tears manifest as dimples associated with the secondary and tertiary phases. Although some secondary phases will cleave (silicon particles in AlSi type alloys), some will decohere from the matrix leaving dimples. The authors will describe some experiments confirming the theories of Atkins.

5:10 PM

The Estimable Value of "Clever" Experiments: John Berry¹; ¹Mississippi State University

The inexorable growth of computational modeling in materials science and engineering has initiated a serious decline in the number of "clever", or genuinely useful experiments. Experimental evidence, if provided, is often second-hand and merely placed there to validate a model, thus not stimulating further study. Many established concepts in materials science have been overturned as a result of careful experiments. These experiments have often nucleated new concepts and have started a sequence of experiment pacing theory and vice-versa. In his long career, the writer has witnessed many examples of this pacing effect, some of which he lists. Several of these resulted in viable industrial processes. He describes unpublished work concerning the heat extractive capacity of molds, which is relevant to current processing developments. The experiments concerned spawned further analytical work providing examples of the said pacing effect.

5:35 PM Concluding Comments

Dr. Berry will have the opportunity to reflect on the symposium, metal casting and life.

Size Effects in Mechanical Behavior: Observing Size Effects Using the Microcompression Method Sponsored by: The Minerals, Metals and Materials Society, Not Applicable, TMS: Nanomechanical Materials Behavior Committee Program Organizers: Erica Lilleodden, GKSS Research Center; Amit Misra, Los Alamos National Laboratory; Thomas Buchheit,

Sandia National Laboratories; Andrew Minor, UC Berkeley & LBL

Wednesday PM	Room: 2
March 2, 2011	Location: San Diego Conv. Ctr

Session Chairs: Andrew Minor, UC Berkeley; Cynthia Byer, Johns Hopkins University

2:00 PM Invited

Achieving Ultra-High Strength and Strain-Hardening Rate by Trapping Dislocations in Small Material Volumes: Kwok-Sing Ng¹; Alfonso Ngan¹; ¹University of Hong Kong

The deformation of metallic micro-pillars is, in general, jerky and of a stochastic nature. The jerky flow is due to a source-depleted condition specific to small material volumes; therefore, confining the dislocations instead of allowing them to annihilate at free surfaces may change the deformation mode. In this work, a number of methods were used to confine



dislocations inside micro-sized aluminum pillars. First, the pillar was coated with a thin layer of tungsten by focused-ion-beam (FIB) induced, chemical vapor deposition (CVD) on its free surface. Secondly, a cavity was milled inside the pillar by FIB, and this was then filled with tungsten by FIB-CVD. The third method involved including a grain boundary inside the pillar to form a micro-bicrystal. In these cases, the coating, filling, or grain boundary was found to hold the dislocations inside the micro-specimen resulting in much smoother deformation with very high strength and strain-hardening rate.

2:30 PM Invited

Size Effects on Strength and Hardening in Cu Micropillars: P. J. Guruprasad¹; Daniel Kiener²; Gerhard Dehm²; Shyam Keralavarma³; *Amine Benzerga*³; ¹Ecole des Mines de Paris; ²Austrian Academy of Sciences; ³Texas A&M University

The stress-strain response under compression of single crystalline Cu micropillars is investigated. The crystals are oriented for double slip, and the size of the pillars studied fall in the range 0.4--10 microns. The experiments reveal a size effect on the crystal strength. The hardening rates are extracted from the experiments and compared with those from the simulations. A two-dimensional discrete dislocation dynamics framework is used to model the experiments with additional constitutive rules for junction formation and dynamic source operation. It is observed that the simulations using a relatively large initial density of Frank-Read sources yield good quantitative agreement with the experiments for all specimen sizes investigated. Moreover, the simulations predict the correct scaling of both the flow stress, as well as the strain hardening rate with the pillar size. Possible micro-mechanisms for the observed size effects are discussed in light of the DD simulations.

3:00 PM

Effect of Initial Dislocation Density on Microcompression Experiments of HCP Single-Crystal Magnesium: *Cynthia Byer*¹; K. T. Ramesh¹; ¹Johns Hopkins University

The size effects and orientation dependence of deformation mechanisms associated with single crystals under uniaxial compression are becoming an increasingly popular area of study. Microcompression literature shows that, for some materials, decreasing the diameters of these micro-scale pillars increases the yield stresses and strain hardening rates; however, many questions remain, especially for hexagonal close packed (hcp) materials. In this study, we focus on the impact of initial dislocation density on deformation mechanisms and size effects in single crystal magnesium. Microcompression experiments are conducted on micropillars (1-10 micrometers in diameter) fabricated using focused ion beam (FIB) milling on both chemically etched and unetched samples. Specimens are loaded along the [0001] c-axis and reveal that etched samples with lower initial dislocation densities fail at lower stresses than unetched micropillars. Post-mortem microscopy is used to examine the details of the deformation mechanisms that are involved.

3:20 PM

Size Effects in Slip and Twinning in Mg Single Crystals: *Erica Lilleodden*¹; Gyu Seok Kim¹; ¹GKSS Research Center

Microcompression testing has been performed on magnesium single crystals with [0001], [2-1-12], [10-11], [11-20] and [10-10] compression axes in order to investigate the slip and twinning mechanisms in Mg. In all cases a size effect in flow stress is observed, although the deformation mechanisms are varied between samples. While columns compressed along the [0001], [2-1-12], and [10-11] axes undergo dislocation plasticity, the columns compressed along the <11-20> and <10-10> axes are dominated by deformation twinning. While the basis for the size effect in the former cases can be explained by a finite volume effect on dislocation interactions, it is less clear why such a significant size effect occurs in the case of twinning. We will offer two possible explanations for the behavior, based on a mechanistic picture of the deformation behavior as revealed through SEM, EBSD and TEM characterizations.

3:40 PM Break

4:10 PM

Size Effects on Plasticity and Martensitic Transformation in Shape Memory Alloy Microcrystals: *Matthew Bowers*¹; Michael Mills¹; John Carpenter¹; Peter Anderson¹; Sivom Manchiraju¹; ¹The Ohio State University

The present study investigates the effects of crystal orientation and specimen size on the pseudoelasticity and shape memory response of Ni-Ti based shape memory alloys. Previous work has shown a dramatic increase in strength for pure nickel when reduced to micron and submicron test volumes, leading to the hypothesis that small sample sizes may influence dislocation plasticity. Experimental evidence exists which links residual strain caused by dislocation plasticity to degradation of the pseudoelastic effect in shape memory alloys. This suggests that enhancement of the pseudoelastic response with small sample dimensions may be possible. To investigate these size effects, FIB-machined single crystal micropillars are tested in compression and analyzed via mechanical response measurements and post-mortem TEM observations. An additional feature is that micropillar testing can activate specific martensite plates, allowing for the isolation and investigation of particular variants in the absence of interaction effects between competing plates.

4:30 PM

Anomalous Features of the Nanoscale Deformation of "Gum Metal": John Morris¹; Elizabeth Withey¹; Rohini Sankaran¹; Andrew Minor¹; Daryl Chrzan¹; Shigeru Kuramoto²; ¹University of California Berkeley; ²Toyota Central R&D Laboratory

The name "gum metal" has been given to a set of β -Ti alloys that, with appropriate preparation, appear to deform by a dislocation-free mechanism involving elastic instability at the limit of strength. We have studied the nanodeformation of these materials through nanoindentation and via instrumented, in situ compression in high resolution TEM. A number of unusual deformation mechanisms and patterns are observed. This paper will discuss three topics: (1) The initial deformation of nanopillars that yield at near ideal strength is local and nanoscaled, with the consequence that there is no significant size effect to the smallest sizes tested. (2) Nanopillar deformation sometimes involves the "shear bands" that dominate deformation at larger sizes, but these are secondary, post-yielding deformation features. (3) The material in the depths of nanoindentation pits contains no well-defined dislocations or other defects, but is rather deformed by continuous rotation about some preferential axis.

4:50 PM

A Microcompression Study of Gum Metal: Julia Hapke¹; Shigeru Kuramoto²; Erica Lilleodden¹; ¹GKSS-Research Center; ²Toyota Central R&D Laboratory

We have investigated a unique beta-Ti alloy called gum metal using microcompression testing. In the cold-worked state, this alloy has been reported to fail at its ideal strength without contribution of dislocation plasticity. In order to understand the effects of cold work on the deformation, a sample without cold working was also investigated. Microcompression specimens with diameters in the range of 300 nm to 10 μ m were fabricated within single crystalline volumes, where possible. In contrast to the non-worked sample displayed no clear grain structure. While the non-worked sample displayed a size effect in flow stress, no significant size effect was observed in the cold-worked sample. Both samples showed shear bands, but with significantly different shear band spacing. The resultant stress-strain responses and deformation morphologies will be further discussed in terms of the governing microstructural length scales.

5:10 PM

High Resolution Imaging of Gum Metal Defect Structure: *Rohini Sankaran*¹; Velimir Radmilovic²; Daryl Chrzan¹; Andrew Minor¹; John Morris¹; ¹University of California Berkeley; ²Lawrence Berkeley National Laboratory

Gum metal, a set of beta-Ti alloys, has remarkable mechanical properties that occur upon severe cold working, the most prominent being that it plastically deforms at its theorized ideal strength. Previous studies have indicated that plastic deformation is not achieved through conventional dislocation motion. However, the details of the precise mechanism to achieve this deformation are not yet well understood. Here, we aim to clarify the deformation mechanisms through high resolution TEM imaging of the defect structure in gum metal. The HRTEM images reveal a highly distorted lattice of non-discrete defects. Geometric phase analyses of the images reveal complex atomic displacements which may be indicative of an overlapping dislocation core structure in the cold worked gum metal. The relationship of these atomic displacements to theorized "nanodisturbances" as a possible deformation structure is discussed along with the atomic nature of possible dislocation pinning sites.

Waste Heat Recovery: Session I

Sponsored by: The Minerals, Metals and Materials Society, TMS Extraction and Processing Division, TMS Light Metals Division, TMS: Energy Committee

Program Organizers: Cynthia Belt, Consultant; Mark Jolly, University of Birmingham; Xingbo Liu, West Virginia University; Rachel DeLucas, H.C. Starck

Wednesday PM	Room: 31B
March 2, 2011	Location: San Diego Conv. Ctr

Session Chairs: Rachel De Lucas, HC Starck Inc; Xingbo Liu, West Virginia Univ

2:00 PM

Waste Heat Utilization to Increase Energy Efficiency in the Metals Industry: Elizabet Cruz¹; Maytinee Vatanakul¹; Rory Hynes¹; Jim Sarvinis¹; ¹Hatch

Energy efficiency improvements achieved using heat recovery processes offer benefits to both the business case and environmental impact of metallurgical facilities. Global demand drives the development of lower and lower grade ore bodies. This trend results in higher energy intensity and consequently increased waste heat. Waste heat boilers and Organic Rankine Cycle (ORC) processes are becoming cost competitive methods of utilizing this waste heat. This study analyzes heat recovery from available sources to produce power using: • High grade: waste heat boiler and steam turbine generator. This system will produce electricity, and/or process steam. • Low grade: ORC to produce electricity. The cycle is well adapted to low-moderate temperature heat sources. Processes from metallurgical plants, hot exhaust streams, cooling and condensers could benefit from application of these systems. The study demonstrates: • The energy and cost saving potential of waste heat recovery technologies• The environmental benefit

2:20 PM

Waste Heat Reduction and Recovery Options for Metals Industry: Arvind Thekdi¹; *Cynthia Belt*²; ¹E3M Inc.; ²Consultant

Waste heat from industrial operations in metals industry represents 20% to 50% of the total energy used in most manufacturing plants. Reduction and recovery of waste heat offers the most attractive and cost effective method of reducing energy intensity for an industrial plant to meet corporate energy saving goals. It is possible to reduce or recover 30% to 60% of the available waste heat by using conventional and readily available technologies. Projects to reduce or recover waste heat may offer less than 3 years payback to as short as a few months. This paper presents information on most commonly used methods for waste heat reduction and recovery in the metals industry

operations. It describes the methods and use of analysis tools that would allow a user to estimate energy savings, CO2 or GHG reduction potential, and economic benefit and includes appropriate case histories.

2:40 PM

Development of a Direct Evaporator for the Organic Rankine Cycle: *Donna Guillen*¹; Helge Klockow²; Matthew Lehar²; Sebastian Freund²; Jennifer Jackson²; ¹Idaho National Laboratory; ²General Electric Company

Research and development is currently underway to place the evaporator of an Organic Rankine Cycle (ORC) system directly in the path of a hot exhaust stream produced by a gas turbine engine. The main goal of this research effort is to improve cycle efficiency and cost by eliminating the usual secondary heat transfer loop. The project's technical objective is to eliminate the pumps, heat exchangers and all other added cost and complexity of the secondary loop by developing an evaporator that resides in the waste heat stream, yet virtually eliminates the risk of a working fluid leakage into the gaseous exhaust stream. The research team comprised of Idaho National Laboratory and General Electric Company engineers leverages previous research in advanced ORC technology to develop a new direct evaporator design that will reduce the ORC system cost by up to 15%, enabling the rapid adoption of ORCs for waste heat recovery.

3:00 PM

The Application of Industrial Waste Heat to ORC Waste Heat Generators: *Bob Miller*¹; ¹Calnetix, Inc.

The Organic Rankine Cycle (ORC) has been used for waste heat turbines to turn heat into electricity. The goal of this paper is to show as many practical applications of ORC technology to industrial waste heat streams. The cycle will be explained using a high speed radial expander along with discussion of heat exchangers and waste heat gas streams. Specific examples from chemical, petroleum, metals, and materials industries will be discussed. Project economics will be reviewed for industrial use.

3:20 PM

Topological Considerations for Thermoelectric Capture of Waste Heat: *Jan Beck*¹; David Nemir¹; Manuel Alvarado¹; ¹TXL Group, Inc.

Thermoelectric generation using special N-doped and P-doped semiconductors is well known as a means for direct heat energy to electrical energy conversion. However, while the technology is scalable and appropriate for energy capture from both small scale (milliwatt) and large scale (megawatt) heat streams, the choice of topology must be tailored to the power generation requirements. This paper describes a simulation study to define the optimal aspect ratios for the active thermoelements and the electrical interconnect. By using a finite element model that incorporates the intercoupled heat and electrical energy flows, a set of empirical rules is presented to guide successful generator deployments. A discussion is provided on using these rules for evaluating the costs and trade-offs in thermoelectric generator design.

3:40 PM

Waste Heat Recovery in the Aluminum Melting Furnaces: John W. Nortan¹; ¹Nortan Engineering, LLC

This presentation will cover the physical properties of waste heat recovery. It is a two part presentation. The first deals with actually recovering the heat with new state of the art heat exchangers and applying that heat to the furnace combustion and the second part will cover what other processes you can enhance with this "free" heat. It will also talk about converting it to steam, hot air or electricity to be used or sold back to the utility company. The economics of various schemes will be reviewed. A brief discussion on state and federal grants and subsidies will be presented.

4:00 PM

Energy Efficiency Improvement by Implementation of the Novel CRIMSON Aluminium Casting Process: *Mark Jolly*¹; Xiaojun Dai¹; ¹University of Birmingham

Foundry engineers in the traditional foundry usually regard the quality of casting component as the most important issue and leave the energy saving or energy efficiency as the subsidiary one. This frequently causes



disproportionate energy consumption as a result of the inefficient casting processes used and increases the production costs. This paper presents the novel CRIMSON aluminium casting process and compares its facility and melting process with traditional melt furnaces and aluminium alloy melting process. A real example is investigated to demonstrate quantitatively how the traditional foundry wastes energy and what the improvement of energy efficiency can be achieved using the novel CRIMSON method. The results of this investigation will help the foundry engineer recognize the importance of energy saving and demonstrate how to use this new technology to reduce production costs and carbon footprint without decreasing the quality of the cast component.

4:20 PM

Waste Heat Recovery Trial from Aluminum Reduction Cell Exhaust Gases: Hadi Fanisalek¹; Mohsen Bashiri¹; Reza Kamali¹; ¹Hormozal

Half of the input energy to aluminum reduction cell will be lost as waste heat which could be studied for possible recovery. Since the price of energy is increasing and the main production cost in primary aluminum industry is energy, waste heat recovery consideration will be interesting. One of the possible choices for recovery is from aluminum exhaust gases that need minimum modifications for reduction cell and has no influence on cell heat balance which is vital for the operation. By using heat exchangers with in-line and staggered tube arrangements placed before fume treatment plant (FTP) we will be able to recover enough amount of heat. The main challenging problem which is necessary to overcome will be the heat exchanger material and its design because of corrosive and dusty exhaust gases from potroom. In this paper, a desalination system with six effects of evaporator is proposed for producing distilled water by using recovered heat from hot exhaust gases. The calculated amount of produced distilled water is around 27,000 kg/hr in this specific suggested desalination plant. The suggested desalination plant is based on Hormozgan Aluminum Company data (Hormozal) in Bandar Abbas, Iran which is constructed by the Persian Gulf.

4:40 PM

The Study of Coal Gasification by Molten Blast Furnace Slag: *Peng Li*¹; Qingbo Yu¹; 'Northeastern University

A new heat recovery system is proposed. This system uses the endothermic heat of gasification reaction instead of sensible heat to recover the energy of molten blast furnace slag. The gasification technological parameter in molten blast furnace was calculated and the exergy of the system was analyzed. The gasification reactions were studied kinetically by the isothermal thermogravimetry using STA409PC thermal analyzer. The results showed that, according to different gasification agent, this system can produce syngas with different C-H ration. The exergy efficiency of this system is high and its internal exergy loss rate is about 5%. This method can bring huge economic and environmental benefits which are important to the survival and sustainable development of iron-steel enterprises. The molten BF slag acts as not only thermal media but also good catalyst. The kinetic parameters on gasification reaction with different types of coal used differ from each other, e.g.

5:00 PM

System for Recovering Waste Heat from High Temperature Molten Blast Furnace Slag: *Junxiang Liu*¹; Qingbo Yu¹; Qin Qin¹; ¹Northeastern University

Dry-granulation is a new process of molten blast furnace slag treatment and air is used as heat exchange medium. There are some shortages: poor effectiveness of granulation, high air-slag ratio and high energy consumption, which are the obstacles to popularize dry-granulation. Based on rotary cup atomization, the technique of recovering waste heat of molten blast furnace slag through waste heat boiler producing high pressure steam is exploited. The molten blast furnace slag is granulated to uniform small slag granules with high temperature, and slag granules pour into the waste heat boiler. It could produce steam, obtained in first row and second row tubes, when descending velocity of slag granules equaled 1.1mm/s and the Reynolds number equaled 7100. The application of the system for recovering waste heat from high temperature molten blast furnace slag has a significant meaning.

5:20 PM

Stability and Thermoelectric Properties of Transition Metal Silicides from First Principles Calculations: *Philippe Jund*¹; Xiaoma Tao¹; Romain Viennois¹; Catherine Colinet¹; Jean Claude Tédenac¹; ¹Université Montpellier 2 - ICGM

We report an ab-initio study of the stability and electronic properties of transition metal silicides in order to study their potential for high temperature thermoelectric applications. We focus on the family M5Si3 (M = Ta, W) which is stable up to about 2000 °C. We first investigate the structural stability of the two compounds and then determine the thermopower of the equilibrium structure using the electronic density of states and Mott's law. We find that W5Si3 has a relatively large thermopower but probably not sufficient enough for thermoelectric applications.